

A N N A L R E P O R T

1963

U. S. WATER CONSERVATION LABORATORY
Southwest Branch
Soil and Water Conservation Research Division
Agricultural Research Service
United States Department of Agriculture
Tempe, Arizona

ADMINISTRATIVELY CONFIDENTIAL

This report contains unpublished and confidential information concerning work in progress. The contents of this report may not be published or reproduced in any form without the prior consent of the research workers involved.

4772

LABORATORY STAFF

Professional:

Dr. H. Bower, Research Hydraulic Engineer
Mr. K. J. Brust, Agricultural Engineer
Dr. W. L. Ehrler, Research Plant Physiologist
Mr. L. J. Erie, Research Agricultural Engineer
Mr. G. W. Frasier, Agricultural Engineer
Dr. L. J. Fritschen, Research Meteorologist
Dr. R. D. Jackson, Research Physicist
Mr. C. L. Jenson, Agricultural Engineer
Mr. L. E. Myers, Research Hydraulic Engineer
Dr. F. S. Nakayama, Research Chemist
Mr. R. J. Reginato, Research Soil Scientist
Mr. J. A. Repogle, Research Agricultural Engineer
Mr. R. C. Rice, Agricultural Engineer
Dr. C. H. M. van Bavel, Research Physicist

Technicians:

R. M. Bula, Engineering Technician
E. J. Durban, Electrical Engineering Aid
E. D. Escarcega, Engineering Draftsman
O. F. French, Hydraulic Engineering Technician
J. R. Griggs, Physical Science Technician
L. E. Lisonbee, Physical Science Aid
J. L. MacIntyre, Physical Science Technician
J. B. Miller, Physical Science Technician
S. T. Mitchell, Physical Science Technician
K. G. Mullins, Physical Science Technician
B. A. Rasnick, Physical Science Technician
A. F. Sandecki, Physical Science Aid
D. R. Sowell, Physical Science Aid
B. W. Tilden, Soils Research Helper

Administrative, Clerical & Maintenance

O. J. Abeyta, Laborer
E. D. Bell, General Machinist
E. E. De La Rosa, Janitor
A. V. Figueroa, Laborer
B. E. Fisher, Library Assistant
D. S. Fry, Clerk-Stenographer
C. E. Hansen, Clerk-Stenographer
J. M. Hernandez, Laborer
C. G. Hiesel, General Machinist
N. A. Johnson, Administrative Assistant

Administrative, Clerical & Maintenance (Cont'd):

R. C. Klapper, Refrigeration & Air Conditioning Mechanic
J. M. R. Martinez, Laborer
R. S. Miller, Clerk-Stenographer
A. H. Morse, Clerk-Dictating Machine Transcriber
M. E. Olson, Clerk-Stenographer
M. A. Seiler, Clerk-Stenographer
M. F. Witcher, Clerk-Stenographer
M. M. Zamora, Laborer

CHANGES IN PERSONNEL

The Laboratory staff has been strengthened during 1963 by the addition of three new members. They are as follows:

J. R. Repogle, Research Agricultural Engineer
D. R. Sowell, Physical Science Aid
M. F. Witcher, Clerk-Stenographer

Also during 1963 there were five resignations. They are as follows:

R. M. Bula, Engineering Technician
E. J. Durban, Electrical Engineering Aid
J. M. Hernandez, Laborer
C. L. Jenson, Agricultural Engineer
N. A. Johnson, Administrative Assistant

The Laboratory staff is now essentially at full strength with one or two exceptions.

TABLE OF CONTENTS ^{1/}

<u>TITLE</u>	<u>SECTION</u>
Soil Moisture Conditions and Root Activity Distribution Patterns. F. S. Nakayama, C. H. M. van Bavel,.....	1
Dynamic Similarity in Elbow Flow Meters. L. E. Myers, K. J. Brust, J. A. Replogle.....	2
Soil Moisture Potentials and Water Uptake by Roots. F. S. Nakayama, R. D. Jackson, C. H. M. van Bavel.....	3
Calibration and Evaluation of Net Radiometers. Leo J. Fritschen.....	6
Soil Treatment to Reduce Infiltration and Increase Precipitation Runoff. L. E. Myers, G. W. Frasier.....	7
Reduction of Seepage Losses from Canals and Ponds. L. E. Myers, R. J. Reginato.....	8
Application of Hexadecanol-Octadecanol Monofilms to Small Ponds. L. E. Myers, G. W. Frasier.....	9
Measurement and Calculation of Unsaturated Conductivity and Soil-Water Diffusivity. R. D. Jackson, R. J. Reginato...	13
Field Application of Falling-Head Technique for Seepage Meters and of Double-Tube Method for Hydraulic Conductivity Measurement. H. Bouwer, R. C. Rice.....	14
Instrumentation for Turbulent Transfer Studies. Leo J. Fritschen.....	16
Surface Energy Balance and Evapotranspiration of Irrigated Alfalfa. L. J. Fritschen, C. H. M. van Bavel.....	17
Components of the Radiation Balance of Field Crops Under Irrigated Management. L. J. Fritschen.....	18
Development and Use of Gamma Transmission Equipment for the Measurement of Soil Density and Moisture Content. R. J. Reginato, C. H. M. van Bavel.....	20
The Use of Salty Well Water for the Pre-Planting Irrigation on Silty Clay Soils. L. J. Erie, O. F. French...	22

1/ Research outlines that have been terminated are not listed.

<u>TITLE</u>	<u>SECTION</u>
Consumptive Use of Water by Crops in Arizona. L. J. Erie, O. F. French	23
Theoretical Effect of Soil, Water Table, and Canal Conditions on Seepage from Canals. H. Bouwer	24
Measuring Horizontal and Vertical Hydraulic Conductivity of Soil with the Double-Tube Method. H. Bouwer, R. C. Rice..	25
Nondestructive Beta Ray Transmission Method for Measuring Water Content in Plants. F. S. Nakayama, W. L. Ehrler	26
Water Absorption, Transpiration, and Internal Water Balance of Cotton Plants as Affected by Changes in Evaporative Demands. W. L. Ehrler, C. H. M. van Bavel, F. S. Nakayama	29
Quantitative Measurement of Water Flow with Chemical Tracers. L. E. Myers, K. J. Brust, J. A. Replogle	30
Water Vapor Diffusion in Soils. R. D. Jackson	31
Direct Measurement of Evapotranspiration and the Energy Balance of Irrigated Crops. C. H. M. van Bavel, L. J. Fritschen	33
Exchange of Water Vapor with Plant Leaves and Its Relation to Stomatal Diffusive Resistance. F.S. Nakayama ...	34
Stomatal Behavior of Cotton Plants Under Controlled Environmental Conditions. F. S. Nakayama, W. L. Ehrler	34A
Appendix I, Analytical Laboratory	AI
Appendix II, Manuscripts Approved and Published during 1963..	AII

WORK AND LINE PROJECTS AND RESEARCH OUTLINES ^{1/}

<u>Work Project</u>	<u>Line Project</u>	<u>Research Outline Code No.</u> ^{2/}	<u>Title</u>
SWC-4		Ariz.-WCL	Conservation of Water Supplies for Agricultural Use.
	gG1		Measurement, Evaluation and Control of Seepage Losses.
		8	Reduction of Seepage Losses from Canals and Ponds. L. E. Myers, R. J. Reginato.
		14	Field Application of Falling-Head Technique for Seepage Meters and of Double-Tube Method for Hydraulic Conductivity Measurement. H. Bouwer, R. C. Rice.
		24	Theoretical Effect of Soil, Water Table, and Canal Conditions on Seepage from Canals. H. Bouwer,
		25	Measuring Horizontal and Vertical Hydraulic Conductivity of Soil with the Double-Tube Method. H. Bouwer, R. C. Rice.
	gG2		Atmospheric and Related Boundary Mechanisms in Water Vapor Losses from Plant, Soil and Water Surfaces.
		6	Calibration and Evaluation of Net Radiometers. L. J. Fritschen.
		9	Application of Hexadecanol-Octadecanol Monofilms to Small Ponds. L. E. Myers, G. W. Frasier
		16	Instrumentation for Turbulent Transfer Studies. L. J. Fritschen

1/ Research outlines that have been terminated are not listed.

2/ Research outline code number also indicates section number.

<u>Work Project</u>	<u>Line Project</u>	<u>Research Outline Code No.</u>	<u>Title</u>	
SWC-4	gG2	17	Surface Energy Balance and Evapotranspiration of Irrigated Alfalfa. L. J. Fritschen, C. H. M. van Bavel.	
		18	Components of the Radiation Balance of Field Crops Under Irrigated Management. L. J. Fritschen.	
		33	Direct Measurement of Evapotranspiration and the Energy Balance of Irrigated Crops. C. H. M. van Bavel, L. J. Fritschen.	
		gG3		Measurement, Evaluation and Control of Infiltration to Conserve Water.
			7	Soil Treatment to Reduce Infiltration and Increase Precipitation Runoff. L. E. Myers, G. W. Frasier.
			22	The Use of Salty Well Water for the Pre-Planting Irrigation on Silty Clay Soils. L. J. Erie, O. F. French.
		gG4		Physical Processes in the Soil Affecting Preventable Losses of Water by Surface Evaporation.
			13	Measurement and Calculation of Unsaturated Conductivity and Soil-Water Diffusivity. R. D. Jackson, R. J. Reginato.
			20	Development and Use of Gamma Transmission Equipment for the Measurement of Soil Density and Moisture Content. R. J. Reginato, C. H. M. van Bavel.
			31	Water Vapor Diffusion in Soils. R. D. Jackson
	gG5		Water Measurement and Control for Water Conservation.	
		2	Dynamic Similarity in Elbow Flow Meters. L. E. Myers, K. J. Brust, J. A. Replogle.	

<u>Work Project</u>	<u>Line Project</u>	<u>Research Outline Code No.</u>	<u>Title</u>
SWC-4	gG5	30	Quantitative Measurement of Water Flow with Chemical Tracers. L. E. Myers, J. A. Replogle, K. J. Brust.
SWC-11			Soil, Water, and Plant Relations as They Affect Use of Land and Water Resources.
	gG1		Uptake and Disposal of Water by Plants in an Arid Climate.
		1	Soil Moisture Conditions and Root Activity Distribution Patterns. F.S. Nakayama, C. H. M. van Bavel.
		3	Soil Moisture Potentials and Water Uptake by Roots. F. S. Nakayama, R. D. Jackson, C. H. M. van Bavel.
		23	Consumptive Use of Water by Crops in Arizona. L. J. Erie, O. F. French.
		26	Nondestructive Beta Ray Transmission Method for Measuring Water Content in Plants. F. S. Nakayama, W. L. Ehrler.
		29	Water Absorption, Transpiration, and Internal Water Balance of Cotton Plants as Affected by Changes in Evaporative Demands. W. L. Ehrler, C. H. M. van Bavel, F. S. Nakayama.
		34	Exchange of Water Vapor with Plant Leaves and its Relation to Stomatal Diffusive Resistance. F. S. Nakayama.
		34A	Stomatal Behavior of Cotton Plants Under Controlled Environmental Conditions. F. S. Nakayama, W. L. Ehrler.

TITLE: SOIL MOISTURE CONDITIONS AND ROOT ACTIVITY DISTRIBUTION PATTERNS

LINE PROJECT: SWC 11-gG1

CODE NO.: Ariz.-WCL-1

INTRODUCTION:

Essential materials are reported in the Annual Reports of 1960 and 1961.

TERMINAL REPORT:

The project was terminated. Although the major objectives of the investigation were achieved, the information was not directly applicable for use by other Laboratory projects, thus further expenditure of time, personnel, and equipment required for such an undertaking was deemed unnecessary at this time.

PERSONNEL: F. S. Nakayama, C. H. M. van Bavel

TITLE: DYNAMIC SIMILARITY IN ELBOW FLOW METERS

LINE PROJECT: SWC 4-gG5

CODE NO.: Ariz.-WCL-2

INTRODUCTION:

Thirty-seven commercial 90-degree elbows of 3-, 6-, 10-, and 12-inch diameter were calibrated as flow meters, and discharge coefficients were calculated from the calibration results. Theoretical discharge coefficients were computed from the dimensions of each elbow. The theoretical and calibration coefficients were then compared to determine if uncalibrated commercial elbows can be used as flow meters with reasonable accuracy.

PROCEDURE:

The thirty-seven elbows were calibrated as flow meters by measuring the flow rate and the pressure differential between two pressure taps located on the inside and outside bend radii at the midpoint of the bends. Calibration coefficients for the equation

$$Q = C (\Delta h)^{0.5} \quad [1]$$

were calculated for each elbow using the least-squares method, where Q is the flow rate in cfs, C is the calibration coefficient, and Δh is the pressure differential in feet of water. Reynolds numbers were computed for each calibration flow rate.

Theoretical coefficients, C_t , were also calculated from dimensions of each elbow using Lansford's equation

$$C_t = \left(\frac{R_c}{D} g \right)^{0.5} A \quad [2]$$

where R_c is the center-line radius of curvature, D is the elbow diameter, and A is the cross-sectional area of the elbow normal to the mean flow direction. These dimensions were determined by three different methods as described in "Annual Report of 1962."

Standard deviations of C were computed for each type and size elbow.

RESULTS AND DISCUSSION:

The calibration coefficients, difference between theoretical and calibration coefficients, and dimensions of the elbows are presented

in Tables 1 through 4. The calibration coefficients, C, as listed in Table 1, were found to be essentially independent of Reynolds numbers greater than 1×10^5 . At lower flow rates the calibration coefficient is not independent of Reynolds number and does not accurately describe the flow relation for Reynolds numbers lower than 1×10^5 . (This is equivalent to flow rates of about 0.2, 0.4, 0.6, and 0.8 cfs in 3-, 6-, 10-, and 12-inch diameter elbows, respectively.)

The average calibration coefficients and their standard deviation for each type and size of elbow are shown in Table 2. Standard deviation for the cast-iron elbows is primarily the result of non-uniformity in elbows of the same type and size because of the sand-molding process used for their manufacture.

Best results were obtained with the eight 3-inch, long radius elbows which had a standard deviation of 1.5 percent. The ten 3-inch, short radius elbows had a larger standard deviation of 2.4 percent, indicating the superiority of long radius elbows for use as flow meters. Standard deviation for the 6-, 10-, and 12-inch, short radius elbows ranged from 2.2 to 2.8 percent.

Die-cast, 3-inch, plastic elbows showed considerable promise with both short-turn and long-turn elbows having a standard deviation of only 0.8 percent with flow in one direction. Deviation increased when flow was reversed but the direction of flow can be specified for these elbows because of definite dimensional differences in the two legs of the elbows. Measurements following calibration showed that pressure taps had not been located uniformly from elbow to elbow and this could account for part of the already low deviation.

Dimensions used to calculate theoretical coefficients, C_t , are listed in Table 3. Considerable variation is shown for elbows of the same type, size, and manufacturer. This is to be expected for unmachined sand-molded castings. Manufacturer's dimensions for the plastic elbows are given in Table 4. Dimension measurements were not complete at the time of this report, but variations should be small because of the die-casting process used for their manufacture.

Percentage differences between calibration (C) and theoretical coefficients (C_t) are shown in Table 1. The largest differences occurred when manufacturer's dimensions were used to calculate C_t . These gave a maximum difference of 9.9 percent for the 3-inch, short radius cast-iron elbows which corresponds to the 10 percent error predicted for uncalibrated elbows by Lansford in 1936. Maximum difference for the 3-inch, long radius elbows was 6.6 percent using manufacturer's dimensions. Use of measured elbow dimensions reduced these maximum differences to 4.6 and 4.3 percent, respectively, for the short and long radius, 3-inch cast-iron elbows. The maximum difference between C and C_t was reduced by about one-half by using measured dimensions instead of manufacturer's dimensions. The internal measurement method produced slightly better values of C_t than the volume measurement method, but either measuring method provided C_t which varied from C by less than 5 percent.

Measured dimensions did not produce better values of C_t than manufacturer's dimensions for the 6- to 12-inch elbows. The reason is apparent from an examination of the measured dimensions presented in Table 3. C_t varies as $R^{0.5}$ and $D^{1.5}$ so that D is the most critical dimension. Measured D for the 3-inch cast-iron elbows ranged from 2.893 to 3.017 inches, with a variation in D equalling 4.13 percent of the nominal diameter. Similar variations for the 6-, 10-, and 12-inch elbows were only 1.25, 0.94, and 0.50 percent, respectively. Actual, as well as percentage, variation in D was less for the larger elbows than for the 3-inch size.

SUMMARY AND CONCLUSIONS:

Laboratory calibration of eight 3-inch diameter, long radius, cast-iron, commercial elbows showed that the coefficient C in the discharge equation $Q = C (\Delta h)^{0.5}$ had a standard deviation of only 1.5 percent. Q is the flow, in cfs, and Δh is the differential pressure, in feet of water, between the inside and outside of the elbow. Ten short-radius elbows of the same size and type had a standard deviation of 2.4 percent for C, indicating the superiority of long radius elbows

for use as flow meters. Standard deviation of C for thirteen 6-10-, and 12-inch diameter, short radius cast-iron elbows ranged from 2.2 to 2.8 percent.

Laboratory calibration of six die-cast, 3-inch, plastic elbows showed a standard deviation in C of only 0.8 percent for both long- and short-turn elbows. The long-turn plastic elbow has dimensions comparable to the short radius cast-iron elbow. This small deviation was for flow in one direction only, but flow direction can be specified for these elbows because of definite dimensional differences in the two legs of the elbows.

Theoretical coefficients C_t were computed for the elbow discharge equation $Q = C (\Delta h)^{0.5}$ from actual elbow dimensions and were compared to the calibration coefficient C obtained from flow measurements. Use of manufacturer's dimensions for calculating C_t resulted in a maximum error of 9.9 percent for the 3-inch, short radius, cast-iron elbow. Use of measured dimensions for the same elbows reduced the maximum error to 4.6 percent. Measured dimensions did not produce better values of C_t than manufacturer's dimensions for the 6- to 12-inch elbows. Elbow diameter, D, is the most critical dimension since C_t varies directly with $D^{1.5}$. Actual variation of D was less for the larger elbows than for the 3-inch elbows. Percentage variation in D was only 0.5 for the 12-inch elbows as compared to 4.1 for the 3-inch elbows.

These studies indicate that discharge coefficients obtained from laboratory calibration can be used with properly installed uncalibrated long radius, 3-inch diameter, cast-iron elbows to measure flow with an error of only 1.5 percent standard deviation. Similar measurement error for short radius cast-iron elbows of 3-, 6-, 10-, and 12-inch diameter would have a standard deviation ranging from 2.2 to 2.8 percent. Most of this deviation results from nonuniformity of the cast-iron elbows which are manufactured by a sand-molding process. Plastic elbows, which are die-cast, are quite uniform. Uncalibrated 3-inch diameter plastic elbows appear capable of measuring flow with a standard deviation of less than 1 percent.

PERSONNEL: L. E. Myers, K. J. Brust, J. A. Replogle

Table 1. Calibration coefficients, C, and percent difference, Δ , of theoretical coefficients, C_t from C for thirty-seven commercial, 90-degree elbows.

Elbow type	Diam.	No.	C ^{1/}	Δ_s ^{2/}	Δ_i	Δ_v
			in ft ^{5/2} sec ⁻¹	%	%	%
ASA class 125, flanged, cast iron (short radius)	3	1	0.329	6.4	-0.9	-0.3
			0.327	7.2	-0.3	0.4
		2	0.331	5.7	-1.2	
			0.330	6.0	-0.9	
		3	0.320	9.3	-3.8	-4.1
			0.319	9.9	-3.4	-3.8
		4	0.327	7.0	-4.6	-4.6
			0.320	9.4	-2.5	-2.5
		7	0.348	0.7	-2.3	-1.1
			0.345	1.5	-1.4	-0.3
		8	0.338	3.4	-2.4	-0.3
			0.339	3.2	-2.6	-0.6
		11	0.326	7.3	3.3	4.8
			0.331	5.8	1.8	3.4
		12	0.326	7.3	2.4	3.7
			0.325	7.5	2.8	4.0
		17	0.323	8.3	-1.2	-0.6
			0.329	6.5	-3.0	-2.4
18	0.329	6.5	-4.0	-3.3		
	0.324	7.9	-2.5	-1.8		
ASA class 125, flanged, cast iron (short radius)	6	20	1.138	5.6	4.0	4.5
			1.170	2.7	1.1	1.6
		21	1.201	0.1	-1.4	-0.2
			1.162	3.4	1.9	3.1
		22	1.205	-0.2	-3.6	-3.8
			1.154	4.2	0.7	0.4
		23	1.192	0.8	-1.0	-0.7
			1.205	-0.2	-2.1	-1.7

^{1/} Second value for each elbow number is for elbow in reversed position.

^{2/} Subscripts refer to method of determining dimensions used to calculate C, manufacturing specifications, s, internal measurements, i, and volume measurements, v. U.S. Water Conservation Laboratory

Table 1. Continued.

Elbow type	Diam.	No.	$C \frac{1/}{}$	$\Delta_s \frac{2/}{}$	Δ_i	Δ_v
	in		ft ^{5/2} sec ⁻¹	%	%	%
ASA class 125, flanged, cast iron (short radius)	10	30	3.048	-1.6	-3.1	-3.6
			3.048	-1.6	-3.1	-3.6
		31	3.176	-5.5	-2.6	-1.6
			3.070	-2.3	0.8	1.8
		32	3.175	-5.5	-2.8	-2.8
			2.958	1.4	4.3	4.3
33	2.944	1.9	-0.4	-0.6		
	3.148	-4.7	-6.7	-7.0		
34	3.151	-4.8	-5.0	-4.9		
	3.034	-1.1	-1.4	-1.2		
ASA class 125, flanged, cast iron (short radius)	12	40	4.205	0.2	-3.4	-3.7
			4.331	-2.7	-6.2	-6.5
		41	4.238	-0.6	-2.0	-2.2
			4.198	0.4	-1.1	-1.2
		42	3.969	6.2	2.3	2.3
			4.282	-1.6	-5.2	-5.2
43	4.217	-0.1	-1.3	-1.4		
	4.186	0.7	-0.5	-0.7		
ASA class 125, flanged, cast iron (long radius)	3	5	0.410	3.7	-1.5	-0.7
			0.407	4.4	-0.7	0.0
		6	0.407	4.4	-1.0	0.2
			0.401	6.0	0.5	1.7
		9	0.416	2.2	-1.0	0.0
			0.418	1.7	-1.4	-0.5
10	0.413	2.9	-0.2	0.2		
	0.409	3.9	0.7	1.2		

1/ Second value for each elbow number is for elbow in reversed position.

2/ Subscripts refer to method of determining dimensions used to calculate C_t , manufacturing specifications, s, internal measurements, i, and volume measurements, v.

Table 1. Continued.

Elbow type	Diam.	No.	C <u>1/</u>	Δ_s <u>2/</u>	Δ_i	Δ_v
			ft ^{5/2} sec ⁻¹	%	%	%
ASA clas 125, flanged, cast iron (long radius)		13	0.404	5.2	-3.0	-2.5
			0.401	6.0	-2.2	-1.7
		14	0.399	6.6	-2.0	-0.2
			0.399	6.6	-2.0	-0.2
		15	0.405	4.9	-2.2	-2.0
			0.410	3.7	-3.4	-3.2
		16	0.415	2.4	-4.3	-3.4
			0.406	4.7	-2.2	-1.2
Type 1, Bored end, ABS plastic (long turn)	3	P ₁	0.346	-5.8		
			0.336	-3.0		
		P ₂	0.340	-4.1		
			0.331	-1.5		
		P ₃	0.347	-6.0		
			0.333	-2.1		
Type 1, bored end, ABS plastic (short turn)	3	P ₄	0.300	-6.3		
			0.306	-8.2		
		P ₅	0.297	-5.4		
			0.295	-4.7		
		P ₆	0.302	-7.0		
			0.299	-6.0		

1/ Second value for each elbow number is for elbow in reversed position.

2/ Subscripts refer to method of determining dimensions used to calculate C_t , manufacturing specifications, s, internal measurements, i, and volume measurements, v.

Table 2. Average calibration coefficients and standard deviations for 37 commercial 90-degree elbows.

Elbow type	Nominal diam.	Number of elbows calibrated	Average calibration coefficient (C)	Standard deviation
	in		ft ^{5/2} sec ⁻¹	%
ASA class 125, flanged cast iron (short radius)	3	10	0.329	± 2.4
	6	4	1.178	2.2
	10	5	3.075	2.8
	12	4	4.206	2.5
(long radius)	3	8	0.407	1.5
Type 1, bored end ABS plastic (short turn)	3	3	0.300 (flow normal)	0.8
			0.300 (flow reversed)	1.9
(long turn)	3	3	0.344 (flow normal)	1.1
			0.333 (flow reversed)	0.8

Table 3. Measured and calculated dimensions for 31 commercial, 90-degree, flanged, cast iron, elbows.^{1/}

Elbow No.	Face diam.	Tangent length		Vol.	Face to center	Calculated radius of curvature		
		Inner bend	Outer bend			R _{cs} ^{2/}	R _{ci}	R _{cv}
	in	in	in	in ³	in	in	in	in
1	2.909	0.80	1.20	60.98	5.56	4 3/4	4.60	4.55
	2.893	0.80	1.20		5.55			
2	2.905	Not available			5.51	4 3/4		
	2.905				5.49			
3	2.997	1.80	2.20	66.67	5.49	4 3/4	3.65	3.67
	3.002	1.60	1.80		5.52			
4	3.017	1.60	2.00	67.52	5.54	4 3/4	3.72	3.71
	3.016	1.60	2.00		5.49			
7	2.979	0.80	1.20	65.16	5.56	4 3/4	4.66	4.55
	2.988	1.00	1.00		5.55			
8	2.967	1.00	1.20	63.30	5.41	4 3/4	4.54	4.42
	2.975	0.80	1.00		5.47			
11	3.014	0.80	1.40	67.28	5.59	4 3/4	4.51	4.37
	2.996	1.40	1.20		5.52			
12	3.001	1.20	1.10	67.14	5.65	4 3/4	4.43	4.31
	2.997	1.30	1.50		5.53			
17	2.983	1.20	1.40	65.59	5.54	4 3/4	4.07	4.03
	2.979	1.80	1.60		5.50			
18	2.989	1.60	1.60	66.11	5.59	4 3/4	3.99	3.94
	2.993	1.60	1.60		5.45			
20	5.960	0.54	1.63	370.1	8.06	7 ± 1/32	6.93	7.01
	5.948	0.53	1.87		8.08			
21	5.951	0.85	1.66	373.0	8.07	7 ± 1/32	6.96	7.13
	5.950	0.44	1.49		8.04			
22	5.876	0.66	1.42	355.9	8.04	7 ± 1/32	6.88	6.85
	5.918	0.49	1.97		7.99			
23	5.889	0.47	1.50	359.4	8.00	7 ± 1/32	7.08	7.14
	5.908	0.41	1.55		8.12			

^{1/} See "Annual Report, 1962" for explanation of dimensions referred to in this table.

^{2/} Subscripts refer to method of determining dimensions used to calculate R_c, manufacturing specifications, s, internal measurements, i, and volume measurements, v.

Table 3. Continued.

Elbow No.	Face diam. in	Tangent length		Vol. in ³	Face to center in	Calculated radius of curvature		
		Inner bend in	Outer bend in			R _{cs} ^{2/} in	R _{ci} in	R _{cv} in
30	9.932 9.964	1.38 1.66	1.81 2.17	1393	11.07 10.89	9 13/16 ± 1/32	9.25	9.17
31	9.918 9.907	0.63 0.48	0.52 1.50	1390	11.04 11.02	9 13/16 ± 1/32	10.27	10.47
32	9.990 10.001	1.52 0.52	1.05 1.19	1395	11.10 10.92	9 13/16 ± 1/32	9.96	9.96
33	9.930 9.940	1.67 1.68	1.99 1.91	1394	10.87 11.06	9 13/16 ± 1/32	9.15	9.14
34	9.994 9.994	0.96 1.36	1.88 2.13	1408	11.01 10.94	9 13/16 ± 1/32	9.39	9.41
40	12.014 11.964	1.84 1.88	1.79 2.58	2221	12.07 12.03	10 3/4 ± 1/16	10.02	9.95
41	11.960 11.938	0.64 0.47	2.29 2.45	2183	12.00 12.04	10 3/4 ± 1/16	10.56	10.53
42	11.999 12.016	1.53 1.93	1.95 2.64	2229	11.86 12.07	10 3/4 ± 1/16	9.96	9.97
43	11.956 11.982	1.24 1.23	1.55 1.72	2186	12.00 11.98	10 3/4 ± 1/16	10.55	10.53
5	2.972 2.981	1.28 1.31	1.31 1.40	90.52	7.76 7.83	7 ± 1/16	6.48	6.59
6	2.969 2.963	1.23 1.28	1.28 1.25	89.70	7.76 7.76	7 ± 1/16	6.50	6.66
9	3.001 2.996	1.28 1.25	1.28 1.26	92.31	7.91 7.83	7 ± 1/16	6.60	6.71
10	3.015 3.013	1.28 1.37	1.23 1.28	91.98	7.80 7.76	7 ± 1/16	6.49	6.56

1/ See "Annual Report, 1962" for explanation of dimensions referred to in this table.

2/ Subscripts refer to method of determining dimensions used to calculate R_c, manufacturing specifications, s, internal measurements, i, and volume measurements, v.

Table 3. Continued.

Elbow No.	Face diam.	Tangent length		Vol. in ³	Face to center in	Calculated radius of curvature		
		Inner bend in	Outer bend in			R _{cs} ^{2/} in	R _{ci} in	R _{cv} in
13	2.993	1.83	1.63	90.91	7.79	7 ± 1/16	6.08	6.12
	2.971	1.75	1.62		7.78			
14	2.963	1.62	1.67	90.40	7.72	7 ± 1/16	6.16	6.37
	2.963	1.40	1.53		7.73			
15	2.992	1.75	1.69	92.24	7.90	7 ± 1/16	6.15	6.18
	2.983	1.70	1.78		7.85			
16	2.987	1.50	1.59	91.73	7.78	7 ± 1/16	6.18	6.31
	2.986	1.66	1.59		7.77			

^{1/} See "Annual Report, 1962" for explanation of dimensions referred to in this table.

^{2/} Subscripts refer to method of determining dimensions used to calculate R_c, manufacturing specifications, s, internal measurements, i, and volume measurements, v.

2-11

Table 4. Manufacturing dimension specifications and calculated radius of curvature for commercial, 90-degree, bored end, ABS plastic elbows.

Elbow type	Diameter in	Tangent length in	Face to center in	Radius of curvature in
Long turn	3.068	1.716	5.562	3.85
Short turn	3.068	1.716	4.562	2.85

TITLE: SOIL MOISTURE POTENTIALS AND WATER UPTAKE BY ROOTS

LINE PROJECT: SWC 11-gG1

CODE NO.: Ariz.-WCL-3

INTRODUCTION:

The objectives, theory and techniques, and methods of analysis in this phase of the study have been discussed in the Annual Reports of 1960, 1961, and 1962.

I. DIFFUSION STUDIES WITH TRITIATED WATER.

PROCEDURE:

Simultaneous diffusion of THO and H₂O in relatively dry soils was determined. Three Adelanto soil columns, 40 cm long and sealed with vacuum wax, were placed in an exposure chamber in which air passing through a saturated K₂SO₄ solution and also containing THO (1 μc ml⁻¹) was recirculated past the open end of the columns. (See Figure 1 WCL-31 for experimental set-up.) The equipment was placed in an insulating chamber of styrofoam. The room temperature was maintained at 26 ± 1 C. The soil materials were exposed to the THO solution for 14 days. New solution was used every two days to maintain a constant THO concentration.

After the predetermined exposure periods, the soil columns were removed and cut into 1-cm sections. One column was analyzed for H₂O distribution, and another column was analyzed for THO distribution. In the third column, alternate 1-cm sections were used for analysis of THO and H₂O. Since the volume of THO that could be extracted was too small for analysis, 0.5 ml of H₂O was added to the soil sample and the water extracted from it. The H₂O content was determined gravimetrically by drying at 105 C and the THO analyzed by liquid scintillation technique. The distributions of THO and H₂O in the column were plotted, and the diffusion coefficients D_{THO} and D_θ determined graphically and by the use of the relation

$$D_{\theta v} = - \frac{1}{2t} \frac{dx}{d\theta} \int_{\theta_1}^{\theta} x d\theta \quad [1]$$

where t is the exposure time, θ_i is the initial water content, and θ is the water content at a distance x .

RESULTS AND DISCUSSION:

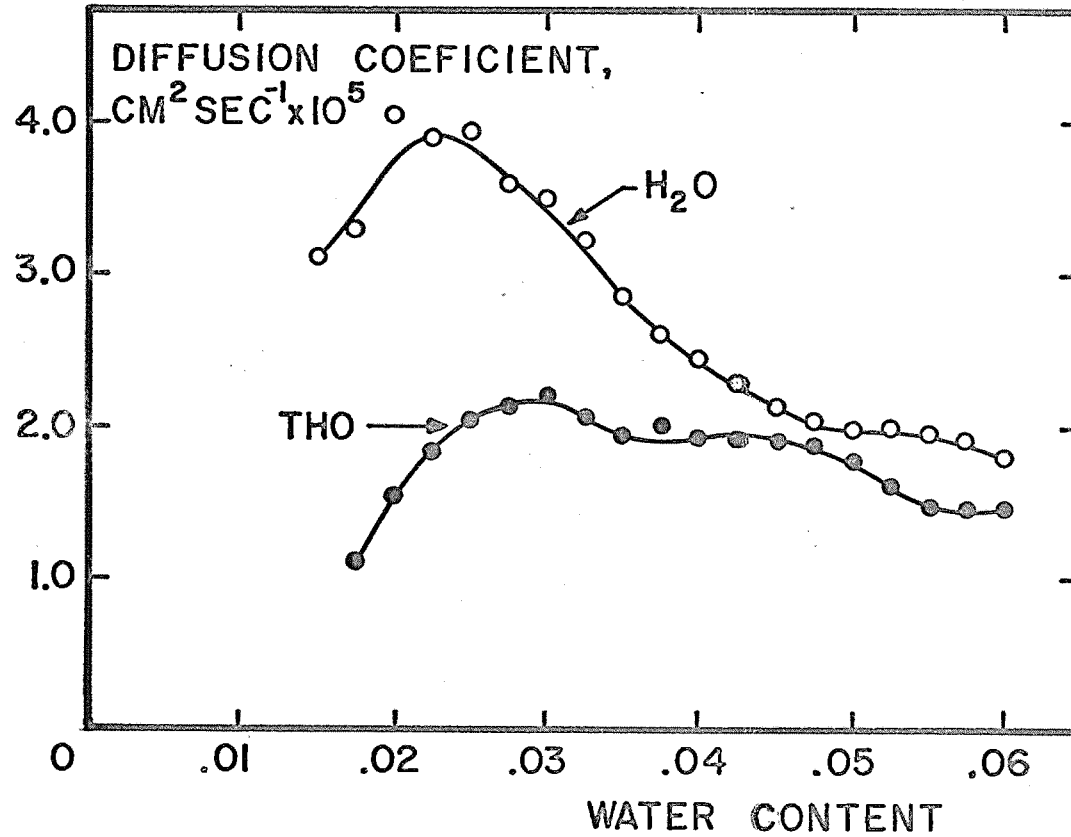
The diffusion coefficients of H_2O and THO at different water contents are compared in Figure 1. The diffusion coefficient of H_2O is consistently, but not proportionally, higher than that of THO. A maximum D value of $4 \times 10^{-5} \text{ cm}^2 \text{ sec}^{-1}$ was obtained at a fractional water content of approximately 0.02 for H_2O and $2 \times 10^{-5} \text{ cm}^2 \text{ sec}^{-1}$ at about 0.03 for THO. If the differences in D 's were strictly due to an isotope effect, it would be expected to be proportional. Furthermore, the magnitude of the difference is very much larger than that predictable from the difference in the diffusive masses of THO and H_2O . The lower D_{THO} values are apparently due to the exchange of the diffusing THO molecules with the H_2O adsorbed on the soil particle surfaces.

SUMMARY AND CONCLUSION:

The simultaneous diffusion of THO and H_2O in relatively dry Adelanto soils were measured. The diffusion coefficients of THO and H_2O were different, that of H_2O being consistently, but not proportionally, higher than that of THO at all water contents. A maximum D value of $4 \times 10^{-5} \text{ cm}^2 \text{ sec}^{-1}$ was measured at 2 percent water content for H_2O and $2 \times 10^{-5} \text{ cm}^2 \text{ sec}^{-1}$ at about 3.0% for THO. The differences are ascribed primarily to the exchange of the THO tracer molecule with the adsorbed H_2O molecule present on the soil surface.

The results reported here plus those presented in the 1962 Annual Report where it was reported that the THO vapor diffusion process was such that quantitative measurements of water absorption by roots using tagged water cannot be made in a plant-soil-water system led to the termination of this project.

PERSONNEL: F. S. Nakayama, R. D. Jackson, C. H. M. van Bavel



3-3

Figure 1. Diffusion coefficients of THO and H_2O in Adelanto soil at low water contents.

TITLE: CALIBRATION AND EVALUATION OF NET RADIOMETERS

LINE PROJECT: SWC 4-gG2

CODE NO.: Ariz.-WCL-6

INTRODUCTION:

During the past two years attempts have been made to measure the temperature of a surface radiometrically by placing an adapter on a miniature net radiometer. The adapter consists of a hemispherically shaped dome which may be attached to either side of the net radiometer. By knowing the temperature of the dome and the output of the transducer, and assuming that the dome and the surface of the transducer are in radiation equilibrium, total hemispherical radiation, and consequently the surface temperature, may be calculated.

The first attempt at measuring surface temperature was made using a modified version of the radiometer described in (1). The modification consisted of a transducer having an output in excess of $1.5 \text{ mv ly}^{-1} \text{ min}$. This transducer was constructed by winding 4-mil constantan wire on $1/16 \times 3/8 \times 3/4$ inch glass plates. Half of the coil was overlapped with copper so that the copper-constantan junctions are on the $3/8 \times 3/4$ inch surfaces. Two coils were connected in series and cast in epoxy to form a transducer, approximately 1-1/4 inches in diameter and 1/16 inch thick. The attempts to measure surface temperature with the adapter on the modified net radiometer failed due to internal reflection; that is, radiant energy passing around the sides of the transducer and reflecting internally off the dome and the transducer surface. To overcome this the two windings were cast in epoxy so that the diameter of the transducer was the same as the diameter of the mounting rings, 2.365 inches, and 1/16 inch thick. The transducer surfaces were painted black with a small white stripe to equalize long- and short-wave radiation absorption.

The second attempt at measuring temperatures was more successful than the first; however, it still was found to be lacking in that the temperature measured radiometrically was quite close to that measured with thermocouples at night when the temperatures were not

very large; however, during the daytime these two methods of temperature measurements disagreed considerably when the temperature in question was approximately 80C. The reasons for this disagreement were thought to be due to partial absorption of the long-wave radiation by the polystyrene domes, unequal absorption of radiant energy by the black paint, recording sensitivity, and a temperature coefficient of the transducer. Therefore, an improved radiometer was designed which would reduce these sources of error, and also, optimize a ± 5 -mv recording range by having both the recording accuracy and the sensitivity equivalent to $0.003 \text{ ly min}^{-1}$. The construction and calibration of the improved miniature net radiometer is to be discussed in detail.

Construction. The exploded view of the compensated net radiometer is shown in Figure 1. The assembly of this netradiometer is quite simple. All that is required is two hemispherically shaped polyethylene radiational windows, one on either side of the transducer, and two brass clamping rings. The lead wire is threaded through the stem on brass ring (A) and fastened into a 2-conductor cable-type connector. The connector is made waterproof by sealing the shell onto the stem and using a small O-ring between the connectors. The transducer is constructed by winding a 22-junction manganin-constantan thermopile around an epoxy bobbin, $0.125 \times 0.5 \times 1.0$ inches. This bobbin and a 10,000-ohm thermistor are then potted in epoxy to form a transducer 2.365 inches in diameter and 0.125 inches thick. The windings of the transducer are insulated by cementing a thin sheet of mica to either side; then 6-mil copper sheets, 1.5 inches in diameter, are symmetrically cemented onto each surface of the transducer. Both surfaces are painted with Parson's optical black paint. The three lead wires are threaded through the stem of brass ring (A), Figure 1, and soldered to a 1000-ohm microminiature trim pot, which is used as a voltage divider. The circuitry involved is shown in Figure 2.

Manganin and constantan was used to construct the transducer because both manganin and constantan have approximately the same

thermal conductivity of 0.052. The thermal conductivity of both are very much lower than that of copper, which is approximately 0.92. The resistance of copper changes over the range of use, while the resistance of manganin and constantan are practically constant. The thermal EMF of manganin-constantan is very similar to that of copper constantan, increasing from $38 \mu\text{v } ^\circ\text{C}^{-1}$ at 0C to $45 \mu\text{v } ^\circ\text{C}^{-1}$ at 70C. The thermistor and voltage-dividing circuit were used to compensate the temperature coefficient of the net radiometer. The micro-miniature trim pot does not have a temperature coefficient; however, care must be taken to avoid thermal EMF's arising from soldering the transducer copper lead wires to the gold-plated circuit pins of the trim pot. The copper sheets were cemented to each side of the transducer to increase the electrical output of the transducer. Parson's optical black lacquer was used to coat the transducer surfaces because of its uniform absorption properties throughout the wavelengths of solar and terrestrial radiation. Parson's optical black lacquer has an absorption factor of 0.985 in the visible, varying from 0.980 to 0.985 in the infrared in long-wave radiation. The radiational windows were constructed of 6-mil polyethylene, which is approximately 2-mil thick when the hemispherical radiation window is formed. Polyethylene was used because it has less absorption bands in the region of long-wave radiation, and the average transmission is more uniform throughout the region of solar and terrestrial radiation.

Method of calibration. The compensated net radiometer was calibrated in the calibration chamber described in (1). The method of calibration was slightly modified in that the three glass filters were removed and one Pyrex glass diffuser was used to cover the aperture on the upper brass plate. During calibration the net radiometer was supported in the middle of the calibration chamber by a 1/8-inch thick sheet of aluminum, painted black. Thus, the bottom half of the net radiometer would be subjected to long-wave radiation from the walls of the calibration chamber, while the top half of the net radiometer was subjected to the long-wave radiation

from the walls of the upper half of the calibration chamber, plus the short-wave radiation from the tungsten light source. The temperatures of the walls of the calibration chamber were measured and the long-wave flux calculated. After the temperature of the net radiometer transducer had reached equilibrium, three transducer outputs were measured. They consisted of the raw output, the divided signal, and the divided compensated signal. The net radiometer and aluminum sheet were then removed and replaced by an Eppley pyrhelimeter, model 15. The short-wave radiation from the bulb was measured by the Eppley pyrhelimeter. The walls of the calibrating chamber were controlled by pumping water of various temperatures through the walls. The radiational intensity of the light source was controlled and varied by regulating the line voltage and then transforming the line voltage from 90 volts to 160 volts.

RESULTS AND DISCUSSION:

The sum of the short-wave flux as measured by the Eppley pyrhelimeter and the long-wave flux calculated from the wall temperatures was plotted versus the output of the net radiometer for various transducer temperatures. The results obtained are shown in Figure 3, along with the compensated divided signal. It is quite apparent from these data that the transducer has an appreciable temperature coefficient at the greater radiational fluxes, the temperature of the transducer being very closely related to the wall temperature of the calibration chamber. By that I mean the transducer temperature of 28C at 1.05 ly min^{-1} was obtained when the wall temperatures were at 9C and the 60C transducer temperature was obtained when the wall temperatures were at 47C. Thus, the transducer temperature was 19C and 13C greater than the wall temperature, respectively.

The temperature coefficient of the transducer is more clearly depicted in Figure 4. The divided transducer signals were converted to $\text{mv ly}^{-1} \text{ min}$ and plotted versus the transducer temperature, along with the divided compensated signals. The relationship between the divided signal and temperature for the various radiational flux indicates a fairly linear relationship between flux and output at

a given temperature. The temperature coefficient of the divided signal amounts to 6.6 percent from 28C to 65C, which is the temperature range of interest in the Phoenix area. This means that if the transducer was calibrated at 25C, the transducer temperature would be approximately 47C. A 3 percent error would be evident if this transducer was subjected to radiant intensity of 1 ly min^{-1} at an ambient temperature of 47C and a -3 percent if the transducer was subjected to a radiant intensity of 1 ly min^{-1} at an ambient temperature of 9C. An additional error would be involved as the radiation intensity changes throughout the day. This error is difficult to evaluate other than by direct comparisons of the compensated and uncompensated net radiometers under field conditions.

The temperature coefficient of the transducer is due to the increasing thermal EMF per degree, which is partially offset by the decreasing temperature required per unit of net radiational flux as the temperature increases. Thus, the temperature coefficient for a given calibration constant would increase with the number of junctions in the thermal transducer. A similar calibration constant could be obtained with less junctions; however, the bobbin would have to be thicker, or a better insulating material used for the bobbin. J. P. Funk (2) stated that the heat transfer through the top hemisphere can be greater than that through the bottom hemisphere if the temperature gradient across the transducer is large. In order to maintain a high output and reduce this error due to convective heat transfer in the air spaces of the hemispherical radiation windows, Funk placed an aluminum heat sink through the center of the transducer.

Therefore, for a desired output, a compromise must be reached between the temperature coefficient due to number of thermocouple junctions and the possible convective heat transfer error due to the temperature gradient across the transducer. It was found that the transducers described in the introduction had a temperature coefficient of 0.07 percent per degree deviation above an ambient temperature of 20C. When the ambient temperature was at 40C and the net radiation

was at 1 ly min^{-1} , the temperature coefficient was equivalent to 1.4 percent, or 0.14 ly min^{-1} , which amounted to a radiational error of 14 percent. This transducer had 140 junctions and was wound on 1/16-inch glass, which had a very small temperature gradient across the transducer. This temperature coefficient is considerably larger than that of the manganin-constantan transducer having 22-junction thermopile. The use of a voltage-dividing circuit and a thermistor compensator practically eliminates the temperature coefficient over the range of interest in the Phoenix area. A different compensating circuit would have to be used for different ambient temperature ranges.

As of this writing, no attempt has been made to measure surface temperatures radiometrically with the compensated net radiometer.

SUMMARY:

During the past year attempts have been made to measure the temperature of a surface radiometrically by placing an adapter on a miniature net radiometer. The results of these attempts indicated that the net radiometers currently being used were not sufficiently accurate for this purpose. Possible sources of inaccuracy were thought to be due to the long-wave radiation absorption bands of the polystyrene domes, unequal absorption of radiant energy by the black paint, recording sensitivity, and the temperature coefficient of the transducer. Therefore, an improved net radiometer was designed which would reduce these sources of error and also optimize a ± 5 -mv recording range by having both the recording accuracy and sensitivity equivalent to $0.003 \text{ ly min}^{-1}$.

The improved net radiometer consists of five basic parts: a transducer, two clamping rings, and two polyethylene radiational windows. The transducer contains a 22-junction manganin-constantan thermopile and a thermistor which is used for temperature compensation. The temperature compensation is obtained by connecting the thermistor in parallel with the 900-ohm portion of a 1000-ohm voltage-dividing circuit. Preliminary results indicated that the noncompensated transducer had an error of 6 percent at 1 ly min^{-1} over the range

of 9C to 47C ambient. The compensator practically eliminated this error over the range of 20C to 47C ambient, which is a range of primary interest in the Phoenix area. However, an error of 1.6 percent exists from 9C to 20C. A different voltage-dividing system could be used to reduce the error at lower temperatures.

The temperature coefficients of shielded net radiometers have been overlooked in the past. This particular design with compensation appears to be of superior design to any shielded net radiometer in existence.

REFERENCES:

(1) Fritschen, Leo J.

1963. Construction and evaluation of a miniature net radiometer.
Jour. Appl. Met. 2: 165-172.

(2) Funk, J. P.

1962. Improvements in polythene shielded net radiometer.
Sym. Engin. Aspects of Environmental Control for
Plant Growth, Melbourne, Australia. Commonwealth
Scientific Industrial Research Organization.

PERSONNEL: Leo J. Fritschen

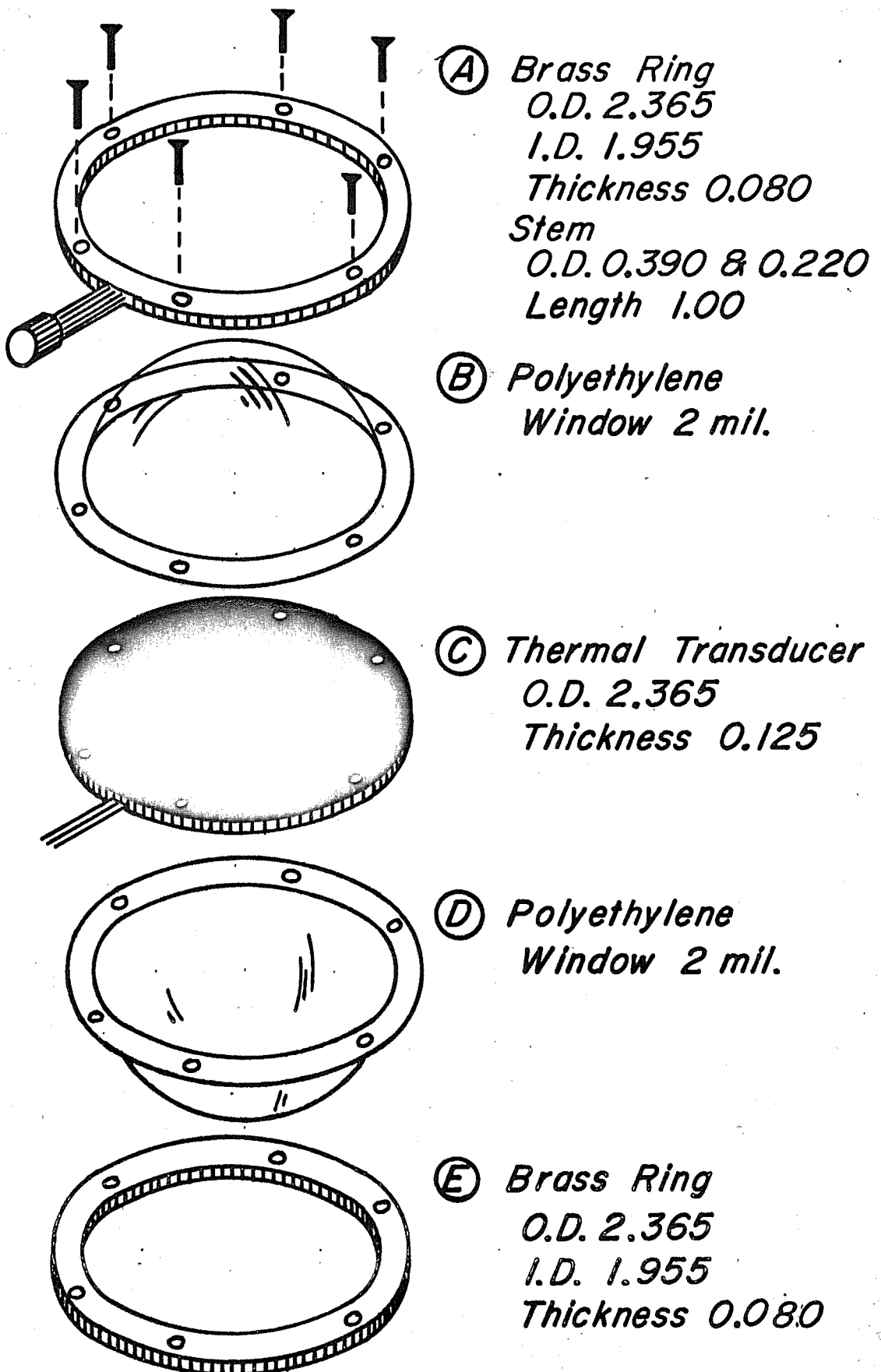


Figure 1. Exploded view of the compensated net radiometer.

6-9

A 22 Junction Manganin - Constantan Thermopile, Resistance 37.9 Ohms

B Fenwal Thermistor, 10 K Ohms, GB 41J1

C Bourns Microminiature Trimpot 3300P, 1000 Ohms

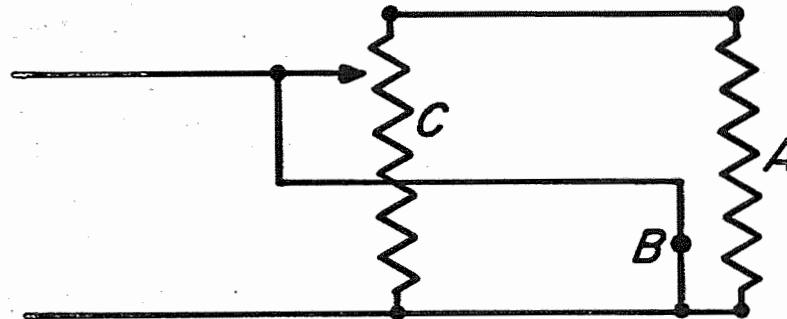


Figure 2. Circuitry of the compensated net radiometer.

6-10

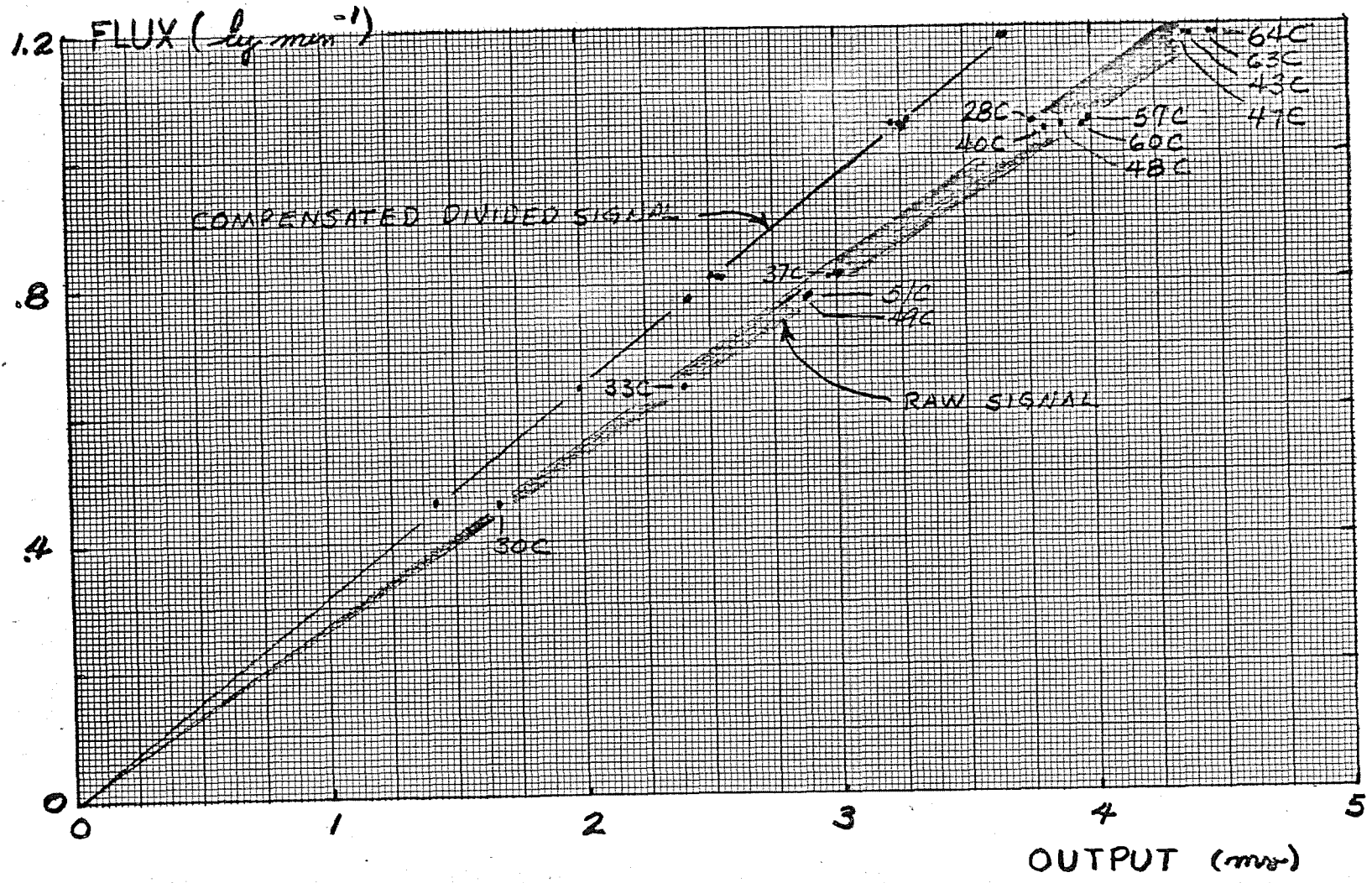


Figure 3. The relationship between flux and output at various transducer temperatures for a compensated and noncompensated net radiometer.

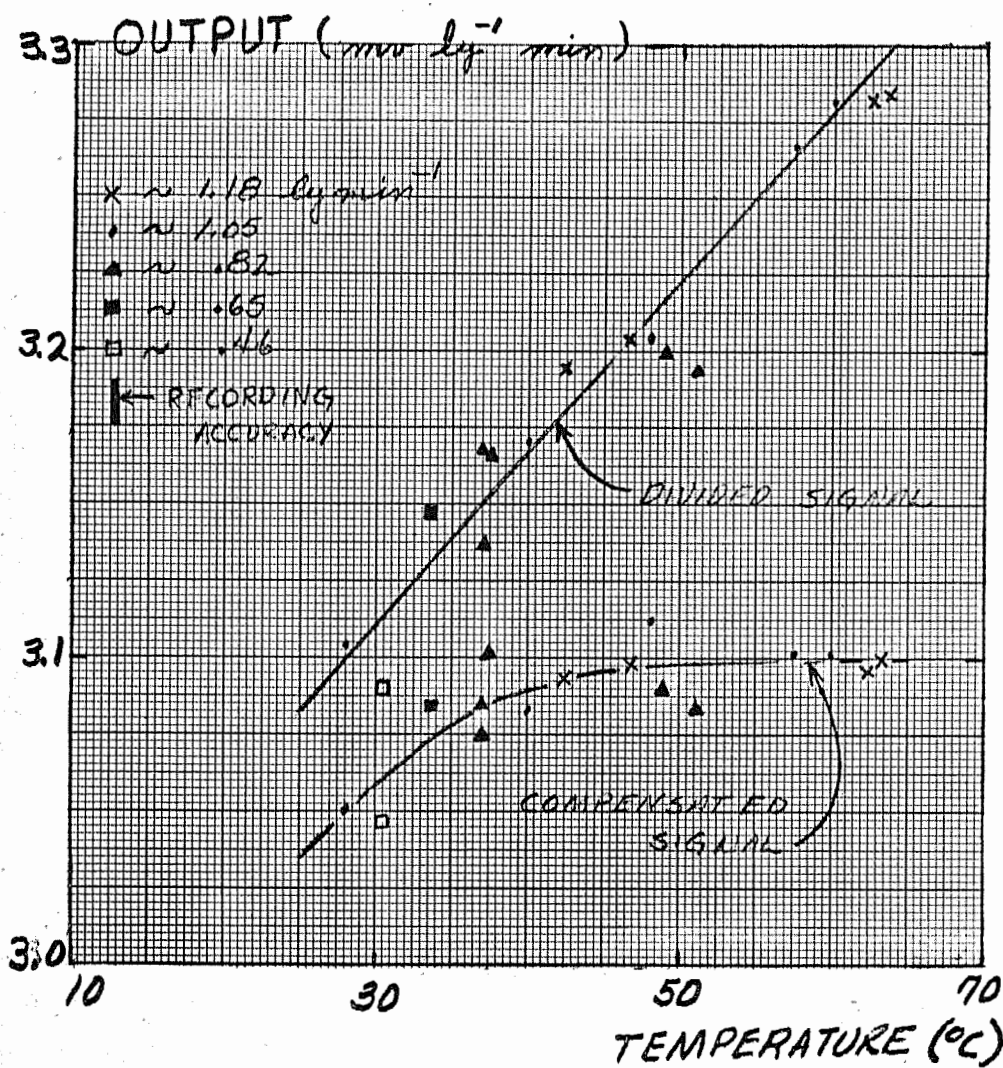


Figure 4. The relationship between output at 1 ly min⁻¹ and transducer temperature for a compensated and noncompensated net radiometer.

TITLE: SOIL TREATMENT TO REDUCE INFILTRATION AND INCREASE PRECIPITATION
RUNOFF

LINE PROJECT: SWC 4-gG3

CODE NO.: Ariz.-WCL-7

INTRODUCTION:

Recent laboratory studies have been concerned with investigations of materials which can be sprayed on the soil surface to create a reasonably strong pavement. These studies have shown that several asphaltic materials can be used for this purpose. Also the use of thin plastic films bonded to the soil is now being investigated.

The cooperative field program with the Bureau of Indian Affairs has progressed favorably during the past year with the installation of three new experimental operational water harvesting structures. This now gives a total of five cooperative water harvesting catchments on the Indian reservations in Arizona.

PROCEDURES:

Procedures were the same as outlined in the 1962 Annual Report with the following additions:

The bearing strength obtained from soil stabilizing compounds was measured in 37.8 cm × 12.1 cm × 5.1 cm soil trays constructed from 1.27 cm plywood. The soil was air dried and mixed with a sufficient quantity of water to obtain a moisture content of 10 percent by weight. The wetted soil was compacted into the trays in four increments of 700 grams each by dropping a 4.1 kg weight a distance of 61 cm 6 times on the center of a 37.5 cm × 11.1 cm × 1.9 cm plywood board reinforced to distribute the impact evenly. After compaction, the soil was dried for 48 hours in either a 50 C oven or air dried in the greenhouse as required. Treatments were sprayed on the dried soil surface, with the actual rate of application determined by weighing the trays before and after spraying, and the soil was dried for the specified number of days. The soil bearing strength was then determined by placing a 6.45 cm² compression foot on the treated soil surface and measuring with a dynamometer the force required to push the foot 0.635 cm into the soil at a traverse speed of 0.635 cm per minute. The soil bearing strength in each tray was

measured at three locations along the center line of the box with dynamometer readings taken at 5-second intervals up to 60 seconds, equivalent to 0.635 cm penetration of the foot.

The shear strength of compounds for bonding lap joints in plastic and aluminum sheets was evaluated in a testing machine. Five-cm lap joints were formed by spraying the ends of 10.2×60 cm strips of the sheet material and pressing the end of a second strip onto the compound about 2 minutes after spraying. After curing for the specified length of time, the strength of the lap joint was measured by pulling the joint to failure in shear in the testing machine at a traverse speed of 2.54 cm per minute and recording the force on a chart recorder.

Effective penetration of water repellents into soils was evaluated in 6.95 cm diameter infiltration cylinders. The soils were blended to a 15 percent moisture content and compacted into the cylinders in 8 separate 90-gram increments by dropping a 250-gram weight 6 times, a distance of 20 cm for each increment. The soil was then dried for 24 hours in a 50 C oven. After drying, the cylinders were treated and again dried for 48 hours in a 50 C oven. The effective depth of penetration was determined by removing successive 1.5 mm layers of soil and checking the water repellency of the exposed soil surface with drops of water.

Runoff from the 232.5 m^2 plots at Granite Reef is collected in 5300-liter steel tanks buried at the lower edge of each plot. Runoff from the small watersheds is collected in butyl lined reservoirs. After every rain the water collected in the tanks or reservoirs is pumped through a positive displacement type water meter calibrated in metric units. This procedure eliminates the errors which were occurring when the small water meters on the previous measuring systems were stopped by fine silt. The new system was installed on 23 April 1963. Results obtained from the plots before this date represent minimum values.

RESULTS AND DISCUSSION:

Soil stabilization. The soil stabilization studies were concerned with the relative effect of asphalt type, soil type, application rate

and curing time on the resulting soil bearing strength. Treatment and measurement data are presented in Table 1. Quantities of asphalt shown are in terms of actual asphalt. Asphalt materials used were a standard MC-70 cut-back, a low-viscosity cut-back available commercially as "Penepriime," and a cationic asphalt emulsion modified to obtain penetration into soil. Maximum bearing strength in kg/cm^2 obtained on loamy sand soil was: Penepriime - 60.2, MC-70 - 30.0, and modified S-1 - 19.7, untreated - 15.8. Treated and untreated strength of the sandy loam soil was considerably higher than the loamy sand. Higher application rates did not uniformly increase bearing strength. Asphalt in excess of the optimum rate reduces strength by acting as a lubricant. As would be expected, higher application rates generally required longer curing time to produce significant increases in strength.

These tests showed that it is possible to spray standard asphalt cut-backs on the soil to produce pavement with a bearing strength of 40 to 60 kg/cm^2 (500 to 800 psi). It should be pointed out that high bearing strength, although desirable, is not the only important factor in soil stabilization. Weathering characteristics, ductility and resistance to wetting are also of major importance and must be evaluated before final conclusions may be reached.

Soils stabilized with penetrating asphalts were still slightly porous and the application of a sealcoat was necessary. Testing machine measurements on soil trays showed that the 50-55 kg/cm^2 bearing strength of cured basecoats was reduced to 40-45 kg/cm^2 by the application of both cationic and anionic emulsion sealcoats. Sealcoats were applied at a rate of 0.490 kg actual asphalt per square meter and had cured for two weeks at the time of measurement. This reduction in bearing strength results from the application of additional asphalt which acts as a lubricant.

Preliminary bearing strength measurements were made on soils treated with a sprayable resin (S-2). The resin was applied to the soil surface at rates of 0.98 and 1.96 kg per square meter. After 30 days of curing in a greenhouse the resin produced maximum bearing

strengths of 31 kg/cm^2 on a loamy sand soil and 46 kg/cm^2 on a sandy loam soil. Treated soil was plastic and appeared capable of rehealing after damage.

Lap joint bonding. Asphalt-butyl compounds for bonding 5-cm lap joints of Tedlar and aluminum foil were investigated with the results shown in Table 2. An anionic emulsion (SS-2) and a cationic emulsion (S-1) were used with various amounts of butyl latex added to improve tack and bonding properties. All of the compounds required 10 or more days curing time to develop a lap joint in aluminum foil which was as strong as the foil itself. Maximum 2-hour strength was 0.08 kg/cm^2 . Full-strength joints were bonded on Tedlar after 1 day of curing and maximum 2-hour strength was 0.19 kg/cm^2 . Cationic emulsion was slightly better than anionic. Increasing the butyl content improved the bond strength. Development of full strength requires loss of water from the adhesives tested. This process is much too slow for aluminum foil and is borderline for the Tedlar. High wind can often occur shortly after an installation is made in the field and will destroy a weak lap joint.

Water repellents. The only water repellent studied was a silicone (R-9) which is heat resistant and will penetrate soils. The maximum effective penetration is influenced by the texture of the soil and the concentration of the applied solution. A maximum effective penetration of over 3 cm was obtained on a loamysand soil when the chemical was applied at 85 g/m^2 in a 2 percent solution. The same treatment on a sandy loam soil penetrated to 1.25 cm. Lower application rates give proportionately lower depths of chemical penetration. When the R-9 was applied at a concentration of 0.67 percent the soils were water repellent only on the soil surface, regardless of application rate, indicating that the reaction is concentration dependent. It was necessary to use a 3.3 percent concentration before the effective chemical penetration was equal to the total solution penetration. Typical penetration results are shown in Figure 1.

Two 9.3 m^2 plots at Granite Reef were treated on 30 May 1963. Plot 17 was treated at a rate of 28 g/m^2 and plot 18 was split into

two treatments with an application rate of 113 g/m^2 on the upper half and 57 g/m^2 on the lower half. During the period of 30 May to 31 Dec. 1963 plot 17 produced 51 percent runoff, plot 18 produced 78 percent runoff, and the untreated control, plot 4 produced 30 percent runoff from a total of 124 mm of rain. No erosion was observed on the treated plots which are on a 3 percent slope. Individual storm runoff values are presented in Table 4.

Observations of natural rainfall on soil treated with R-9 showed that the impact energy of the rain drops forced water into the pores of the treated soil layer. This phenomenon indicates that a water repellent soil cannot produce 100 percent runoff from rainfall.

Granite Reef field plots. Results during the year 1962 showed that the butyl and polyethylene sheetings on the 9.3 m^2 plots consistently collected more rainfall than was recorded in a weighing rain gage located nearby. On 6 Feb 1963 a second calibrated rain gage was installed at the test site about 150 meters from the first. Comparisons of the two rain gages have shown no measurable difference.

Several new treatments have been applied to the 9.3 m^2 plots. These are listed in Table 3. Runoff data are in Table 4. The oldest asphalt treatment, on plot 1, is now almost completely deteriorated, even with the protective coating of soil which has blown onto the plot. Plot 2, the butyl rubber, shows no sign of deterioration and has consistently given more runoff than the rain gages. The asphalt emulsion S-1 treatments, plots 3 and 5b, are showing serious deterioration due to weathering. Plot 5b was protected for approximately one year by a polyethylene sheeting listed in tables as plot 5a. Plot 6, treated with water repellent R-8, is still showing more runoff than the untreated control plot 4. Plot 7 was covered in January 1963 with an experimental low-cost artificial rubber sheeting. This sheeting had failed by the end of July and was subsequently removed at the end of August. Plots 17 and 18, treated with R-9, have previously been discussed. Plots 19, 20, and 21 treated with asphalt show a definite increase in runoff when a seal coat is applied.

Plot 19, which is a base coat alone, has shown a permeability to water and the runoff is decreasing with time as the coating deteriorates. The sealcoat, in addition to improving the runoff characteristics of the treatments, also protects the basecoat from deteriorating.

Treatments applied to the 232.5 m² plots are listed in Table 5 and the runoff results are presented in Table 6.

Plot 1 was resprayed at the end of 1962 with asphalt emulsion S-1. By July of 1962 the treatment had again deteriorated to an extent that runoff was low. The plot was then completely cleaned of all asphalt and a base stabilizing coat of Penepime applied at a rate of 1.470 kg asphalt/m². In October 1963, the plot was covered with 6-mil black polyethylene sheeting bonded to the soil with SS-2 asphalt emulsion modified with butyl latex.

The smoothed bare soil plot 2 is producing about 30 percent runoff with essentially no soil erosion.

Plot 3, the aluminum foil, is still in excellent condition and there appears to be no deterioration. This treatment has been giving about 80 percent runoff which is much lower than expected. Observations during a rainstorm have indicated that the impact of the rain drops is sufficient to form a mist which is blown from the catchment surface by wind. A vertical border 15.2 cm high placed around the plot on 12 Nov 1963 has failed to appreciably increase the runoff from this plot.

Plot 4, the butyl sheeting standard, has no observed deterioration and runoff is slightly more than 90 percent.

Plot 5, a two-phase asphalt treatment with modified S-1 asphalt as a basecoat and S-1 as a topcoat, is resulting in good runoff of nearly 90 percent and there has been no significant weathering deterioration since treatment.

Plot 6 is another two-phase treatment using Penepime as a basecoat with a split topcoat treatment, one-half of the plot is treated with S-1 modified with butyl latex (S-1B) and the other half of the plot is treated with SS-2 modified with butyl latex (SS-2B). This plot is also giving good runoff of about 95 percent and there has been no significant deterioration.

Runoff water from all asphalt plots has been colored. This coloring is believed to be oxidation by-products of the asphalt, but chemical analysis of the runoff water, including infrared and gas chromatography analyses, has failed to identify these products. Additional analyses will be made.

Hualapai Indian Reservation. The two catchments installed on the Hualapai Indian Reservation in 1962 did not collect much water because the areas experienced an exceptionally dry year. Even with no rain, useful information on field problems was obtained.

The Blue Mountain catchment initially installed in June 1962 was a split treatment with asphalt-fiberglass-aluminum foil on one half and 1.5-mil polyethylene bonded to the soil with asphalt on the other half. The half covered with the polyethylene was destroyed within a short period after installation by wind and was subsequently removed with this area being retreated in April 1963 with the two-phase asphalt treatment of Penepriime basecoat and SS-2B sealcoat. The half of the catchment with the aluminum foil-fiberglass appeared in excellent condition until September 1963 when a yucca plant growing underneath the sheeting raised a section of the sheeting free of the ground surface. Wind action progressively loosened more of the covering and finally over half of the aluminum foil-fiberglass was blown from the plot. Inadequate anchoring of the edges was also involved in the damage. The damaged area will be repaired in early 1964.

The Nelson road catchment, also installed in June 1962, was a split treatment with a surface coat of cationic S-1 on one half and asphalt--aluminum foil on the other half. The S-1 alone had deteriorated by the end of the first year. This area was retreated with Penepriime basecoat and SS-2B sealcoat during July 1963. The half of the plot which had been treated with the asphalt-aluminum foil was severely damaged during the winter by animals and wind. Bonding of the aluminum sheeting to the soil had been poor because a deteriorated asphalt emulsion was used in the application. This area was then cleaned and treated with Penepriime basecoat on 24 April 1963 and left for the summer to determine the weathering of the basecoat alone. By October 1963 this

basecoat had seriously deteriorated. The area was retreated in October 1963 with Penepime basecoat and divided into three subareas of 10.1×15.2 m for applications of different sealcoats. The upper 1/3 of the area was treated with S-1, the middle area was treated with SS-2, and the bottom area was treated with SS-2B. These areas will be observed to determine the relative weathering of the three sealcoats. The storage pit, which was lined with fiberglass and sprayed with asphalt emulsion, appears in excellent condition after 18 months. The fiberglass was given a new spraying of SS-2B in October 1963. A measurement of the evaporation and seepage losses from the pit over a 19-day period showed a loss less than 0.5 cm/day.

Fort Apache Indian Reservation. Two operational catchment areas were installed in cooperation with the Bureau of Indian Affairs on the Fort Apache Indian Reservation near White River, Arizona.

The Metate catchment area is $15.2 \text{ m} \times 61.0 \text{ m}$, constructed as a rectangle on a 4 percent slope with a $15.2 \times 15.2 \times 1.8$ m deep storage pit across the lower end. A pipe leads from the bottom of the storage pit to a metal watering tank where the water level is maintained by a float. The catchment and pit were sprayed with the two-phase asphalt treatment in May 1963 with Penepime as a basecoat and SS-2B as a sealcoat. In November 1963 the catchment was inspected with disappointing results. The treatment had failed to stabilize the soil and cracking and erosion had occurred. The soil is 36 percent clay, 26 percent silt, and 38 percent sand with 39.3 meq/g combined calcium and magnesium and 0.21 meq/g sodium on the soil complex. Laboratory studies are under way to determine methods and materials for stabilizing soils of this type. The soil sterilant which had been applied to the soil did not kill yucca and various shrubs which grow in the area.

The Cedar Mesa catchment area is a 30.5×30.5 m square which drains into a 189,000-liter steel tank. The area had originally been treated with a soil cement which had deteriorated. The soil cement covering was removed and a basecoat of Penepime was applied in October 1963. Two weeks later a 1-mil thick sheet of Tedlar was bonded to the

stabilized soil with SS-2B. To date the covering is satisfactory even though the basecoat had failed to penetrate the desired depth because of excessive soil moisture at the time of treatment.

Hopi Indian Reservation. An operational catchment area was treated in cooperation with the Bureau of Indian Affairs on the Hopi Indian Reservation near Keams Canyon, Arizona. This catchment is 48.8 m x 54.9 m and was originally covered with .635-cm thick asphalt planking which had been destroyed by wind of over 60 mph. Because of the high wind in the area it was decided to treat the area with the two-phase asphalt treatment of Peneprime basecoat and SS-2B sealcoat. Inspection 2 months after treatment showed satisfactory results even though it had been necessary to do additional hand killing of yucca which a pretreatment of soil sterilant had failed to kill.

Trick tank. This is a catchment area on the Kel Fox ranch which was constructed of roofing-type tar paper several years ago by the Forest Service with an excavated pit of approximately 760,000 liters at the lower side. The tar-paper had deteriorated rapidly. The area was cleaned up and sprayed with a two-phase basecoat and sealcoat asphalt treatment in August 1963. Observations of the plot in November 1963 were disappointing. The soil, which is similar to the Metate soil, had failed to stabilize satisfactorily and, even though there was no serious erosion, it is not expected to last through the winter.

Equipment. A heated tank trailer was constructed for use with materials which require heating for spray application. The pump and spray equipment was from the earlier spray boom trailer, as described in the 1962 Annual Report, with the addition of a four-speed transmission and friction clutch to facilitate starting and stopping. To date this unit has sprayed approximately 57,000 liters of asphalt with very satisfactory performance.

SUMMARY AND CONCLUSIONS:

Laboratory studies and field experience have shown that pavements with good bearing strength can be created by spraying asphaltic materials on the soil surface. Testing machine measurements on two different

soils, treated with three types of asphalt materials at various rates and curing times, showed that pavements with bearing strength of 40 to 60 kg/cm² (600 to 800 psi) could be produced. Cut-back asphalts produced higher strength than emulsion because of better distribution of asphalt within the soil. Higher strength was generally associated with longer curing time as expected. High bearing strength is desirable in soil stabilization treatments for water harvesting from the standpoint of reducing damage by animals and hopefully reducing costs by eliminating the need for fencing. Bearing strength is not the only criterion, however, and ductility and resistance to wetting must also be considered. The asphalt studies were supplemented by tests of a sprayable resin which produced bearing strengths of 30 to 45 kg/cm² (400 to 650 psi). Resin treated soils were quite ductile and appeared capable of self-healing.

Soils stabilized with cut-back asphalt are still porous and a sealcoat must be applied. Testing machine measurements showed that the 50 to 55 kg/cm² bearing strength of cured basecoats was reduced to 40 to 45 kg/cm² by application of asphalt emulsion sealcoats. The reduction in strength results from the application of additional asphalt which acts as a lubricant.

Lap joints in plastic film and aluminum foil installations can be destroyed if high velocity winds occur before the adhesive cures to form a strong bond. Testing machine measurements on lap joints made with butyl modified asphalt emulsions showed that 10 or more days curing time was required to develop a full-strength joint with aluminum foil. A full-strength joint has the same strength as the original sheet material. One day of curing produced full-strength joints on Tedlar plastic film. Development of full strength requires loss of water from the adhesives tested. This process is much too slow for aluminum foil and is borderline for Tedlar.

A heat resistant water repellent was evaluated in the laboratory to determine effectiveness in treating a layer of soil by spraying on the soil surface. Soil to a depth of 3 cm was successfully treated. Effective treatment depth was found to be a function of solution concentration, soil texture, and total application rate. Small plots

were treated at the Granite Reef testing site on 30 May 1963. Runoff was correlated to the quantity of repellent applied and ranged from 50 to 80 percent of the 124 mm total rainfall after treatment.

Rainfall measured from 9.3 m² plots of butyl and plastic films has consistently been higher than that measured in a recording rain gage. A second calibrated gage was installed 150 m from the first on 6 February 1963 and there has been no measurable difference in the catch of the two recording gages.

No deterioration has been observed on the 230 m² aluminum foil plot which was installed 19 January 1962 or on the 230 m² butyl sheet plot installed 30 November 1961. Runoff from the foil and butyl plots was 81.4 and 93.5 percent respectively of the 203.5 mm total rainfall during 1963. A 230 m² plot treated with cationic asphalt emulsion modified to achieve soil penetration has shown no measurable deterioration since installation on 21 December 1962 and has averaged 88 percent runoff. A similar plot with a cut-back asphalt basecoat and asphalt emulsion sealcoat has averaged 96 percent runoff since installation in August 1963.

Four operational catchments have been treated with apparent success in cooperation with the Bureau of Indian Affairs. Three were treated with a cut-back asphalt basecoat and an asphalt emulsion sealcoat. One was treated with white Tedlar plastic film bonded to the soil with asphalt. Two failures also occurred during 1963. An asphalt-fiberglass-aluminum foil treatment installed during June 1962 failed during September 1963 because of inadequate edge anchoring and a newly sprouting yucca plant which raised a section of the mat off the soil. Continued wind action on the loosened section progressively destroyed a 16 x 16 meter area of the treatment. Damage could have been prevented by better edge anchoring or by killing the yucca. A more serious failure occurred when the cut-back asphalt basecoat failed to stabilize a calcareous clay soil. This problem, now under laboratory investigation, must be solved before soils of this type can be successfully stabilized and sealed at low cost. In general

these experimental installations on operational sites have been encouraging and are providing valuable information concerning materials, application equipment and methods, and catchment design and construction.

PERSONNEL: L. E. Myers, G. W. Frasier

Table 1. Maximum bearing strength of two soils after surface spray applications of cut-back and emulsified asphalts.

Asphalt	Application rate	Drying time	Soil bearing strength	
			Loamy sand	Sandy loam
	kg/m ²	days	kg/cm ²	kg/cm ²
Untreated		2	15.8	
		4	14.1	27.5
MC-70	1.470	4	15.8	
		7	28.2	50.0
		14	28.2	
MC-70	2.452	4	17.2	
		7	15.8	47.9
		14	31.0	
Peneprime	1.470	4	18.3	
		7	36.6	>65.5 ^{1/}
		14	44.4	
Peneprime	2.452	4	15.8	
		7	15.8	50.7
		14	60.2	
Modified S-1	1.470	4	14.1	
		7	14.1	44.4
		14	15.8	
Modified S-1	2.452	4	7.7	
		7	17.6	38.0
		14	19.7	

^{1/} Dynamometer off scale.

Table 2. Average shearing strength of aluminum foil and Tedlar plastic film lap joints made with modified asphalt emulsions as the adhesive.

Elapsed time	Butyl content	Aluminum foil		Tedlar	
		SS-2	S-1	SS-2	S-1
	%	kg/cm ²	kg/cm ²	kg/cm ²	kg/cm ²
2 hrs	0	0.040	0.035	0.149	0.154
1 day		0.180	0.054	0.290 <u>1/</u>	0.172
10 days		0.237	0.139	0.251 <u>1/</u>	0.216 <u>1/</u>
30 days		0.264 <u>1/</u>	0.275 <u>1/</u>	0.235 <u>1/</u>	0.202 <u>1/</u>
2 hrs	3	0.063	0.081	0.112	0.127
1 day		0.099	0.054	0.269	0.276 <u>1/</u>
10 days		0.235	0.125	0.307 <u>1/</u>	0.218 <u>1/</u>
30 days		0.206 <u>1/</u>	0.229 <u>1/</u>	0.230 <u>1/</u>	0.220 <u>1/</u>
2 hrs	6	0.042		0.175	
1 day		0.120		0.248 <u>1/</u>	
10 days		0.260 <u>1/</u>			
30 days		0.246 <u>1/</u>			
2 hrs	12	0.027		0.187	
1 day		0.163		0.313 <u>1/</u>	
10 days		0.325 <u>1/</u>			
30 days		0.292 <u>1/</u>			

1/ Material failure.

Table 3. Treatments on 9.3 m² plots at the Granite Reef testing site.

Plot	Treatment date	Treatment
1	5 Jan 61	S-1 at .245 kg asphalt/m ² R-1 at 0.011 kg/m ²
	Retreated 25 Aug 61	R-1 at 0.011 kg/m ²
2	18 May 61	30-mil butyl rubber sheeting
3	15 Sept 61	S-1 at 0.490 kg asphalt/m ² upper half S-1 at 0.98 kg asphalt/m ² lower half
4	15 Sept 61	Untreated
5a	26 Jul 62	1.5-mil black polyethylene
5b	22 Sept 61	S-1 at 0.490 kg asphalt/m ² upper half S-1 at 0.245 kg asphalt/m ² lower half R-1 at 0.011 kg/m ² right half R-8 at 0.017 kg/m ² left half
6	22 Dec 61	R-8 at 0.028 kg/m ²
7	11 Jan 63	Polyisobutylene sheeting
17	30 May 63	R-9 at 0.028 kg/m ²
18	30 May 63	R-9 at 0.113 kg/m ² upper half R-9 at 0.057 kg/m ² lower half
19	7 May 63	Penepriime at 1.471 kg asphalt/m ²
20	Basecoat 7 May 63	Penepriime at 1.471 kg asphalt/m ²
	Topcoat 9 July 63	S-1 at 0.545 kg asphalt/m ² with 3% butyl latex
21	Basecoat 7 May 63	Penepriime at 1.471 kg asphalt/m ²
	Topcoat 26 Jun 63	SS-2 at 0.545 kg asphalt/m ² with 3% butyl latex

Table 4. Runoff results from rainfall on 9.3 m² plots at the Granite Reef testing site.

Date	Rainfall		Total	Plot No. 1		Plot No. 2		Plot No 3	
	Intensity			runoff		runoff		runoff	
	maximum	minimum		mm	%	mm	%	mm	%
1963	mm/hr	mm/hr	mm	mm	%	mm	%	mm	%
$\frac{3}{4}$ Jan	7.6	3.0	21.7	10.8	49.8	21.6	99.5	11.0	50.7
12 Jan	6.4	2.5	3.0	1.2	40.0	3.7	123.3	1.6	53.3
$\frac{10}{12}$ Feb	25.5	1.0	35.8	7.1	19.7	35.9	100.4	14.1	39.4
17 Mar	5.1	1.3	12.5	3.7	29.6	11.4	91.2	3.3	26.4
25 Apr	3.8	1.0	7.0	0.4	5.7	7.4	105.7	1.6	22.9
$\frac{4}{6}$ Aug	12.7	5.0	13.2	6.0	45.5	11.6	87.9	5.1	38.6
14 Aug	12.7	12.7	9.0	6.0	66.7	6.1 ^{1/}	67.8	3.3	36.7
16 Aug	25.0	5.0	29.0	15.5	53.4	29.7	102.4	12.6	43.4
24 Aug	63.5	12.7	13.4	6.5	48.5	13.5	100.7	4.9	36.6
18 Oct	25.4	5.1	23.0	9.8	42.6	24.5	106.5	11.8	51.3
2 Nov	2.5	2.5	7.2	2.9	40.3	9.8	136.1	2.7	37.5
$\frac{7}{8}$ Nov	10.2	6.0	11.7	3.3	28.2	11.4	97.4	4.1	35.0
21 Nov	50.8	25.0	17.0	2.9 ^{1/}	17.1	17.5	102.9	7.3	42.9
Total			203.5	76.1	37.4	204.1	100.3	83.4	41.0

- 1/ Drain trough plugged.
 2/ Storage reservoir leaking.
 3/ Lower edge of plot not sealed.

Table 4. Continued.

Date	Plot No. 4 runoff		Plot No. 5a runoff		Plot No. 5b runoff		Plot No. 6 runoff		Plot No. 7 runoff	
	mm	%	mm	%	mm	%	mm	%	mm	%
1963										
$\frac{3}{4}$ Jan	6.2	28.6	17.6	81.1			17.6	81.1	5.3	24.4
12 Jan	0.2	6.7	2.9	96.7			1.8	60.0	2.8	93.3
$\frac{10}{12}$ Feb	3.1	8.7	28.4	79.5			14.8	41.4	33.9	94.8
17 Mar	0.6	4.8	10.2	81.6			4.1	32.8	12.2	97.6
25 Apr	0.2	2.9	6.2	88.6			1.6	22.9	9.0	128.6
$\frac{4}{6}$ Aug	4.7	35.6			7.1	53.8	8.1	61.4	12.4	93.9
14 Aug	2.9	32.2			4.5	50.0	- $\frac{2}{1}$	-	8.4	93.3
16 Aug	12.3	42.4			18.7	64.5	- $\frac{2}{1}$	-	27.8	95.9
24 Aug	3.7	27.6			4.5	33.6	- $\frac{2}{1}$	-	12.6	94.0
18 Oct	4.9	21.3			9.8	42.6	- $\frac{2}{1}$	-		
2 Nov	0.8	11.1			4.9	68.1	- $\frac{2}{1}$	-		
$\frac{7}{8}$ Nov	2.4	20.5			3.3	28.2	- $\frac{2}{1}$	-		
21 Nov	<u>4.9</u>	<u>28.8</u>			<u>9.0</u>	<u>52.9</u>	<u>13.9</u>	<u>81.8</u>		
Total	46.9	23.0	65.3	81.6	61.8	50.0	61.9	56.2	124.4	86.0

$\frac{1}{1}$ Drain trough plugged.

$\frac{2}{2}$ Storage reservoir leaking.

$\frac{3}{3}$ Lower edge of plot not sealed.

7-17

Table 4. Continued

Date	Plot No. 17 runoff		Plot No. 18 runoff		Plot No. 19 runoff		Plot No. 20 runoff		Plot No. 21 runoff	
	mm	%								
1963										
$\frac{3}{4}$ Jan										
12 Jan										
$\frac{10}{12}$ Feb										
17 Mar										
25 Apr										
$\frac{4}{6}$ Aug	6.1	46.2	9.0	68.1	1.0 ^{3/}	7.6	0.4 ^{3/}	3.0	8.0 ^{3/}	60.6
$\frac{14}{16}$ Aug	22.2	58.4	31.4	82.6	25.8	67.9	27.7	72.9	29.3	77.1
24 Aug	7.8	58.2	11.0	82.1	9.4	70.1	7.0	52.2	11.0	82.1
18 Oct	11.8	51.3	18.3	79.6	12.6	54.8	19.1	83.0	20.4	88.7
2 Nov	2.0	27.8	5.4	75.0	3.3	45.8	6.7	93.1	6.1	84.7
$\frac{7}{8}$ Nov	5.3	45.3	8.6	73.5	4.5	38.5	9.8	83.8	10.2	87.2
21 Nov	<u>8.2</u>	<u>48.2</u>	<u>12.2</u>	<u>71.8</u>	<u>5.7</u>	<u>33.5</u>	<u>14.7</u>	<u>86.5</u>	<u>13.4</u>	<u>78.8</u>
Total	63.4	51.3	95.9	77.7	62.3	50.4	85.4	69.1	98.4	79.7

^{1/} Drain trough plugged.

^{2/} Storage reservoir leaking.

^{3/} Lower edge of plot not sealed.

Table 5. Treatments on 232.5 m² plots at the Granite Reef testing site.

Plot	Treatment date	Treatment
1 a	17 Jan 62	R-8 at 0.028 kg/m ² mixed with S-1 at 0.490 kg asphalt/m ²
	Resprayed 21 Dec 62	S-1 at 0.490 kg asphalt/m ²
1 b	30 Oct 63	6-mil black polyethylene
2	30 Nov 61	Smoothed untreated
3	19 Jan 62	1-mil aluminum foil
4	30 Nov 61	30-mil butyl rubber sheeting
5	Basecoat 18 Sept 62	Modified S-1 at 1.470 kg asphalt/m ²
	Topcoat 21 Dec 62	S-1 at 1.035 kg asphalt/m ²
6	Basecoat 19 Apr 63	Peneprime at 1.470 kg asphalt/m ²
	Topcoat south half 8 May 63	SS-2 at 0.654 kg asphalt/m ² with 3% butyl latex
	Topcoat north half 9 Jul 63	S-1 at 0.490 kg asphalt/m ² with 3% butyl latex

Table 6. Runoff results from rainfall on 232.5 m² plots at the Granite Reef testing site.

Date	Rainfall		Total	Plot No. 1 a		Plot No. 1 b		Plot No. 2	
	Intensity			runoff		runoff		runoff	
	maximum	minimum		mm	%	mm	%	mm	%
1963	mm/hr	mm/hr	mm	mm	%	mm	%	mm	%
3 Jan	7.6	3.8	20.1	- <u>1</u> /	-			6.97	34.7
4 Jan	7.6	1.3	1.6	- <u>1</u> /	-			0	0
12 Jan	6.4	2.5	3.0	2.49	83.0			0.97	32.3
<u>10</u> / <u>12</u> Feb	25.4	1.0	35.8	- <u>2</u> /	-			3.30	9.2
17 Mar	5.1	1.3	12.5	10.32	82.6			0.24	1.9
25 Apr	3.8	1.0	7.0	6.06	86.6			- <u>1</u> /	-
4 Aug	2.5	2.5	3.0	0.69	23.0			0	0
6 Aug	12.7	7.6	10.2	4.00	39.2			4.56	44.7
14 Aug	12.7	12.7	9.0	4.63	51.4			4.40	48.9
16 Aug	25.0	5.0	29.0	- <u>3</u> /	-			- <u>3</u> /	-
24 Aug	63.5	12.7	13.4	- <u>4</u> /	-			5.04	37.6
18 Oct	25.4	5.1	23.0			<u>3</u> /	-	12.33	53.6
2 Nov	2.5	2.5	7.2			6.77	<u>6</u> / 94.0	3.05	42.4
7 Nov	10.2	10.2	10.7			9.94	<u>6</u> / 92.9	3.98	37.2
8 Nov	1.3	1.3	1.0			0.77	<u>6</u> / 77.0	0	0
21 Nov	25.4	2.5	9.0			9.09	101.0	0.62	6.9
21 Nov	50.8	50.8	8.0			- <u>3</u> /	-	6.62	82.8
Total			203.5	28.19	63.1	26.57	95.2	52.08	31.5

1/ Catchment ditch not lined.
2/ Water meter not working correctly.
3/ Catchment tank overflowed.

4/ Changing plot treatment.
5/ Basecoat only.
6/ Lower edge of plot not sealed.

Table 6. Continued.

Date	Plot No. 3 runoff		Plot No. 4 runoff		Plot No. 5 runoff		Plot No. 6 runoff	
	mm	%	mm	%	mm	%	mm	%
1963								
3 Jan	16.04	79.8	20.01	99.6	18.02	89.9		
4 Jan	1.54	96.3	1.53	95.6	- <u>2/</u>	-		
12 Jan	2.72	90.7	2.94	98.0	2.58	86.0		
<u>10</u> <u>12</u> Feb	28.58	79.8	34.81	97.2	28.42	79.4		
11 Mar	10.02	80.2	7.84 <u>2/</u>	62.7	8.75	70.0		
25 Apr	6.60	94.3	6.13	87.6	6.14	87.7	4.18 <u>5/</u>	59.7
4 Aug	2.77	92.3	2.01	67.0	2.53	84.3	2.32	77.3
6 Aug	7.89	77.4	9.91	97.2	9.28	91.0	10.09	98.9
14 Aug	7.68	85.3	8.83	98.1	8.92	99.1	9.26	102.9
16 Aug	- <u>3/</u>	-	- <u>3/</u>	-	- <u>3/</u>	-	- <u>3/</u>	-
24 Aug	10.59	79.0	12.88	96.1	13.15	98.1	13.70	102.2
18 Oct	- <u>3/</u>	-	- <u>3/</u>	-	- <u>3/</u>	-	- <u>3/</u>	-
2 Nov	6.05	84.0	5.82 <u>2/</u>	80.8	7.06	98.1	6.78	94.2
7 Nov	8.71	81.4	10.23	95.6	10.24	95.7	10.57	98.8
8 Nov	0.55	55.0	1.10	110.0	1.01	101.0	0.91	91.0
21 Nov	6.28	69.8	8.12	90.2	8.73	97.0	10.22	113.6
21 Nov	7.24	90.5	9.43	117.9	6.91	86.4	7.45	93.1
Total	123.26	81.4	141.59	93.5	131.74	87.9	75.48	96.1

1/ Catchment ditch not lined.
2/ Water meter not working correctly.
3/ Catchment tank overflowed.

4/ Changing plot treatment.

5/ Basecoat only.

6/ Low Annual Report of the U.S. Water Conservation Laboratory

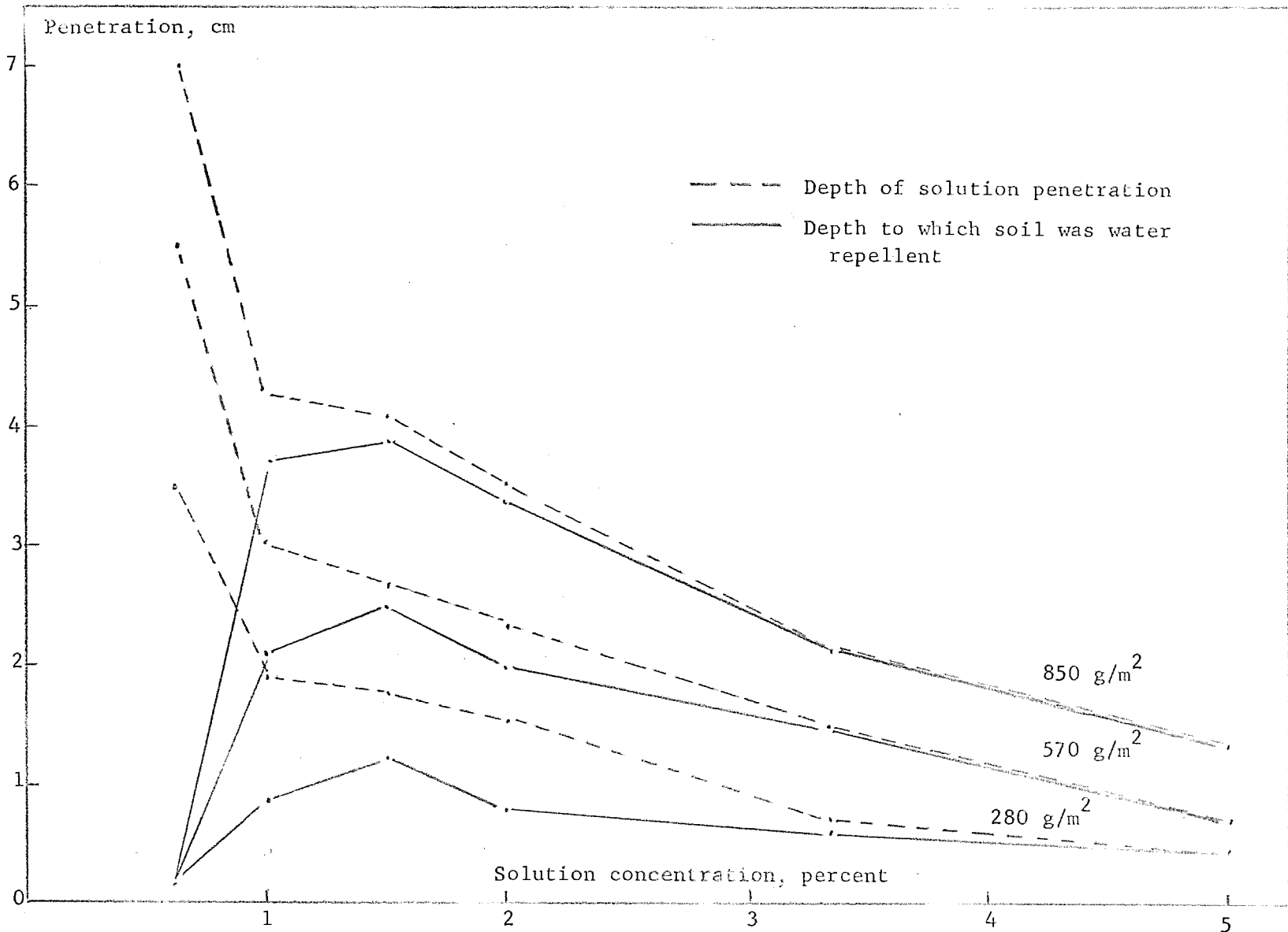


Figure 1. Depth of solution penetration and depth to which a loamy sand soil was water repellent following treatment with various rates and concentrations of a silicone compound.

TITLE: REDUCTION OF SEEPAGE LOSSES FROM CANALS AND PONDS

LINE PROJECT: SWC 4-gG1

CODE NO.: Ariz.-WCL-8

INTRODUCTION:

The use of dispersants for reducing seepage from earth stock tanks was tested at two sites in north-central Arizona.

Asphaltic compounds used as waterborne sealants for seepage reduction were investigated in two laboratory studies. The stability of low concentrations, 500 and 1,000 ppm, of asphalt emulsions in water was measured to indicate the feasibility of using low concentrations in ponding treatments. Adequate treatment of the sides of a pond or channel is dependent upon good stability. A preliminary study of the effect of seepage rate on the sealing process was also initiated. With high seepage rates the asphalt particles should be pulled into the soil pores and thus create an effective percentagewise reduction in seepage. With low seepage rates and low pressure gradients at the seeping surface, the asphalt particles may deposit in a porous layer and produce only a slight reduction in seepage.

Addition of herbicides to an asphalt cutback was tested in limited greenhouse studies to see if the procedure could prevent the growth of grasses through low-cost asphalt ditch linings.

Crack movement in concrete ditch linings was measured to obtain information concerning required performance standards for crack sealers. Satisfactory crack sealers must bond to concrete and must be sufficiently elastic to withstand crack movement due to temperature changes. Information concerning crack movement was not previously available.

The investigations mentioned above (dispersants, asphaltic compounds and crack movement) will each be discussed separately.

A. Dispersants.

1. Dick Mason Pond.

Procedure. On 31 August 1962, 1,000 lbs of TSP (tetra sodium pyrophosphate) was spread on this 6,500 ft² pond and disked into the top 3 or 4 inches of soil. Details of this treatment are found in the 1962 Annual Report.

Results. Spring runoff filled the pond to overflowing about 15 April 1963 and on 6 May 1963 samples of the water were taken. The water contained only 35 ppm sodium, indicating that dispersion of sodium from treated soil into the ponded water was not a problem. With the water surface about 1 ft below the spillway crest, the rate of loss was measured by the owner as about 0.3 inch per day whereas the pretreatment seepage rate was about 5 inches per day. These measurements indicate that the TSPP reduced rate of loss about 15 fold. The final seepage rate of approximately 0.3 inch per day can in part be accounted for by evaporation. The treatment is considered to be a success.

Future work on this pond will entail a detailed chemical and physical analysis of the soil at various locations in the pond.

2. House Mountain No. 1.

Procedure. House Mountain Tank No. 1, 15 miles southeast of Sedona, is a stock watering pond approximately 0.25 acre in size. A soil analysis of the pond bed showed that the amount of water-stable aggregated clay was approximately 3 percent. The mechanical analysis of the soil is: clay, 51 percent; silt, 47 percent; and sand, 2 percent with a textural designation of silty clay. A pretreatment seepage rate is not known except that the tank has never held water from the April runoff until the start of the grazing season in June. The 11,000 ft² pond was treated with 2,000 lbs of sodium carbonate. The salt was broadcast by hand and disked in to a depth of 3 to 4 inches on the pond bottom and 2 to 3 inches on the pond sides. The sodium carbonate treatment was designed to create an ESP (exchangeable sodium percentage) of 13 in the top 3 inches of soil.

Results. At this time there are no data available concerning posttreatment seepage rates and the site has not been visited since the treatment to obtain soil and water samples. However, the owner has advised us that the pond is now holding water. Future work will consist of posttreatment analyses of soil and water.

B. Asphalt Compounds.

1. Stability of dilute asphalt suspensions.

Procedure. Seven asphalt emulsions were diluted in tap water at two concentrations, 500 and 1,000 ppm, in 1,500 ml jars at a temperature of approximately 25 C. These emulsion concentrations correspond to actual asphalt concentrations of 250 and 500 ppm. An aliquot of suspension was then pipetted from a 10 cm depth at various time intervals and the amount of suspended asphalt was determined by drying and weighing.

Results. The types of asphalt emulsions used and the percent of asphalt remaining in suspension after 72 hours is shown in Table 1. The anionic emulsion is somewhat stable, but settling does occur. The nonionic emulsions were completely stable. From the table it is obvious that the four types of cationic emulsions give quite different results, ranging from 13 to 100 percent stable. These measurements show that it is possible to produce extremely stable suspensions of asphalt in water at concentrations of 500 and 1,000 ppm.

2. Effect of seepage rate on seepage reduction.

Procedure. Control soil and Granite Reef soil were tamped into 3-inch diameter cylinders. Water was added to saturate the soil and to continuously maintain a total head of about 16 inches of water above the soil surface. The seepage rate was then reduced by partially restricting the outlet tube of the soil cylinder to give a rate of 1 to 0.5 inches per hour. The two anionic and the cationic 1 asphalt emulsions mentioned in the stability tests were then added to produce concentrations of 500 and 1,000 ppm in the water ponded on the soil. Seepage rates were measured at intervals. Forty-eight hours after treating the cylinders, the outlet tube was opened fully and the unrestricted seepage rate determined. This test was intended to show what type of seal was effected by the treatment. If the asphalt actually plugged the pores, the seepage rate after opening the outlets would remain low.

If, however, the asphalt had deposited in a porous layer on the soil surface, a high seepage rate would be manifested.

Results. Test results were not conclusive because seepage rates gradually declined as partial air-locks developed in the outlet tubes. Despite this, the data indicate, as shown in Figure 1, a definite relationship between initial seepage rate and seepage reduction. When the initial, or restricted, seepage rate is very low the posttreatment unrestricted seepage rate is high, indicating that the asphalt did deposit as a porous layer on the soil surface. When the initial rate was high, the unrestricted rate was low. Data from previous tests show 99 percent seepage reduction when initial seepage rates were 10 to 20 inches per hour.

Improved techniques are now being used to clarify the relationship between initial seepage rate and the seepage reduction obtained with low concentrations of asphalt emulsions.

3. Asphalt herbicide evaluation.

Procedure. Johnsongrass rhizomes were planted 4 inches deep in 2-gallon ceramic crocks filled with control soil. Three different herbicides recommended for Johnsongrass control were mixed into a low-viscosity cutback asphalt commonly used as a soil stabilizer at the rate of 0.75 gal/yd². The herbicides were compatible with the asphalt and thorough mixing was easily accomplished. The asphalt-herbicide mixture was applied in quantity sufficient to penetrate 0.5 inch into the soil. Herbicide quantities applied were the rate recommended for normal application without asphalt. Treatments were duplicated and included: three asphalt-herbicide mixtures, asphalt alone, and untreated soil. The crocks were watered well after planting the rhizomes and before the treatments were applied.

Results. The Johnsongrass shoots penetrated all the asphalt and herbicide treatments as easily as they did the untreated surface. Except for tip browning and occasional slight distortion of a leaf, there appeared to be no ill effect on the grass from the herbicides.

Under the conditions of this study, herbicides mixed with cutback asphalt were not effective in inhibiting the growth of Johnsongrass through the stabilized soil.

C. Crack movement in concrete ditch linings.

Procedure. Small steel angles with faces machined flat were cemented to concrete ditch linings on each side of selected cracks. This was done for both north and south exposures on the ditches. Air and concrete surface temperatures were recorded at the time of measurement and the distance between the angles was measured by the use of sliding parallels and a micrometer. The method of measurement could be reproduced to 0.0002 inch.

Results. Minimum concrete temperatures coincided with minimum air temperatures and maximum joint opening. Maximum concrete temperatures were dependent on the angle of incidence of solar radiation as well as air temperature. The average maximum crack movement for a 14 ft section of a slipform ditch was 0.020 inch for cracks with northern exposure and 0.030 inch for southern exposure. The concrete temperature variation associated with this crack movement was 53 to 118 F for the southern exposure crack and 51 to 96 F for the northern exposure crack. Complete crack closure occurred at concrete surface temperatures of 75 F for northern exposure and 85 F for southern exposure. The amount of crack movement calculated from an equation using the coefficient of expansion for concrete is essentially the same as the measured movement. The data obtained indicate that under conditions of the above tests, a joint patching material for cracks in concrete must be flexible enough to withstand crack movement of at least 0.030 inch during a period of one day.

SUMMARY AND CONCLUSIONS:

Dispersants were successfully used to reduce seepage losses from two stock ponds that had previously never held water for use during the grazing season. Sodium salts were spread by hand and disked into the soil at rates designed to partially but not completely

break down the soil structure. Seepage was reduced from a pre-treatment rate of about 5 inches per day to a posttreatment rate of about 0.15 inch per day.

Stable, low-concentration suspensions of asphalt in water were studied in laboratory investigations of waterborne asphalt sealants for seepage control. Actual asphalt concentrations of 250 and 500 ppm in tap water were prepared which were completely stable for a 3-day period. Studies utilizing cylinders filled with soil indicated that seepage reduction obtained with asphalt suspensions is influenced by the initial seepage rate. High seepage rates result in movement of asphalt particles into the soil pores. When seepage rates are low, the asphalt apparently forms a porous layer on the soil surface.

Attempts to stop weed growth through sprayed asphalt ditch linings by incorporating herbicides in the asphalt were not successful in a controlled greenhouse experiment. Herbicides recommended for Johnsongrass control were easily incorporated in cutback asphalt used for soil stabilization but did not stop growth of the grass through soil sprayed with the asphalt-herbicide material.

Crack movement in concrete linings was measured to obtain information concerning required performance standards for crack sealers. With surface temperatures of concrete ranging from 51 to 118 F during the course of a day, the maximum crack movement was 0.020 to 0.030 inch for northern and southern exposure respectively. The cracks were completely closed at 75 F for northern exposure and 85 F for southern exposure. Crack sealers must be compounded to withstand this type of movement, bond strongly to the concrete (through silt and algae if necessary), remain durable for a long period of time, and be fairly inexpensive.

PERSONNEL: L. E. Myers, R. J. Reginato.

Table 1. Stability of dilute asphalt emulsions in tap water at 25 C.

Type of asphalt emulsion	Percent of asphalt remaining in suspension after 72 hours	
	500 ppm	1,000 ppm
Anionic 1	41	41
Nonionic 1	100	100
2	100	100
Cationic 1	100	90
2	33	13
3	60	53
4	23	55

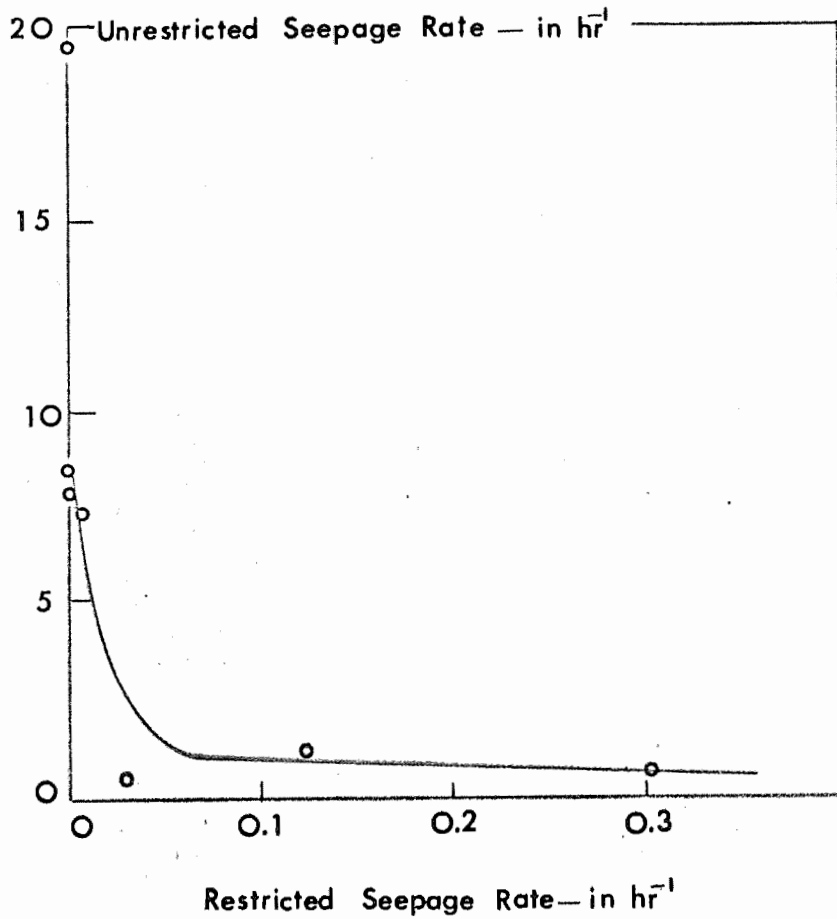


Figure 1. Effect of seepage rate on seepage reduction by dilute asphalt suspensions as indicated by the relationship between restricted seepage rate during treatment and unrestricted seepage rate after treatment.

TITLE: APPLICATION OF HEXADECANOL-OCTADECANOL MONOFILMS TO SMALL PONDS

LINE PROJECT: SWC 4-gG2

CODE NO.: Ariz.-WCL-9

INTRODUCTION:

See Annual Report 1962.

Studies of the long-chain fatty alcohol emulsion were conducted on large outdoor tanks. Preliminary studies were also made with floating powders which reduce evaporation by reflecting solar radiation and reducing the water temperature.

PROCEDURE:

Procedures were the same as outlined in the 1962 Annual Report with the following addition.

The evaporation control agents were evaluated on water surfaces in open top steel tanks buried in the ground. Four tanks, 274 cm diameter and 91 cm deep, were installed 40 cm apart with 8.0 cm of rim above the surrounding grassed surface. Each tank was connected to a stilling well where water surface elevation was recorded with water stage recorders which could be read to ± 0.5 mm. Supplemental point gage readings of the water surface elevations to ± 0.02 mm were made in the tanks every day.

Measurements of solar radiation and water temperatures were measured for selected 24-hour periods. Incoming short-wave radiation incident to and reflected by the water surfaces was measured with Kipp solarimeters and recorded on a strip-chart recorder at half-hour intervals. Temperature profiles were measured during the same 24-hour periods with thermocouples at 0, 2, 6, 15, 30, 63, and 80 cm below the water surface and recorded at half-hour intervals. Radiation and water temperature measurements were made simultaneously on treated and untreated tanks.

The long-chain alcohol emulsion (ECE No. 1) was applied continuously to the water surfaces, at a rate of approximately 1.1 g/m^2 per month, through a No. 22 hypodermic needle connected with flexible tubing to a constant head polyethylene bottle. Bottle height was adjusted to deliver the desired rate of flow. The needles tended to become plugged and some stoppages occurred. The floating powders were

hand sprinkled on the water surfaces to completely cover the surface with a white coating. Amounts applied were determined by weighing. Treatments were run in duplicate and effectiveness determined for 7-day periods by comparison of the evaporation losses from treated and untreated tanks.

RESULTS AND DISCUSSION:

A 1,000 ml sample of the ECE No. 1 prepared 16 March 1962 and stored in the laboratory, has shown no deterioration or separation to date.

Evaporation from all four untreated tanks was measured for 5 weeks. Maximum deviation of any tank from the average total of 173.2 mm for the period was 2.9 mm. Deliberately imposing a water level difference of 15 cm resulted in a maximum difference of 2.2 mm from the average total of 44.4 mm for one week. Differences among tanks never exceeded 5 percent of the average.

Evaporation reduction with emulsion. The ECE No. 1 emulsion reduced evaporation by 35 to 45 percent during February and March 1963 when daily untreated evaporation was 3 to 4 mm per day and treated water surface temperatures were 12 to 16 C. Reduction was 30 to 35 percent during May and June when treated surface water temperatures were 23 to 27 C and untreated evaporation was 7 to 8 mm per day. Typical data are presented in Table 1. Performance of the emulsion was good as long as the applicators remained operational. When a complete surface film of long-chain alcohol was present additional drops of emulsion floated as small beads just below the water surface. As the surface film pressure diminished the beads rose to the surface and replenished the film. This desirable phenomena provided a built-in reserve which compensated for temporary stoppages of the applicators. Complete stoppage of the applicators on several occasions emphasized the need for continuous maintenance of a film. Figure 1 shows the effect of losing the film after 4 days of treatment. Since the film reduces evaporation by physically interfering with the escape of water molecules, but not materially reducing absorption of incoming radiation, the net effect is an increase in water temperature

as shown in Figure 2. As a result of increased water temperature, evaporation following film loss exceeded the untreated rate. Net evaporation reduction for the week was only 21 percent despite a 40 percent reduction during the first 4 days of the week.

Effect of algae. During the period of 1 April to 8 April 1963 a heavy growth of algae was present in all tanks. On the treated tanks the monolayer film pressure compressed the algae into a space occupying approximately one-fourth of the water surface area, while on the untreated tanks the algae was evenly distributed over the entire surface. Evaporation reduction of 25 to 30 percent was obtained even though observations showed a considerable quantity of the emulsion was being dropped directly on the algae thereby reducing the amount which reached the water surface. To determine the effect of algae alone on evaporation, the two tanks which had been treated were cleaned, refilled, and treated with an algacide-emulsifier designated E-2. For a 7-day period the evaporation losses were: Tanks 1 and 3, cleaned, 39.6 mm and 38.6 mm, averaging 38.1 mm; and Tanks 2 and 4, algae, 36.5 and 37.9 mm, averaging 36.8 mm. This study indicated that algae alone did not materially influence the evaporation rate and showed that the presence of algae reduced but did not destroy the effectiveness of the long-chain alcohol emulsion.

Effect of excess emulsifier. In an effort to control the algae, E-2 algacide-emulsifier was applied to all tanks at a rate of 25 ppm of the total water. When the long-chain alcohol emulsion was subsequently applied to the water, evaporation reduction was less than 15 percent. Supplemental laboratory investigations showed that when E-2 was mixed with water at 25 ppm, the emulsifier formed a surface film which interfered with the formation of an alcohol film. The study also showed that, unfortunately, the emulsifier film does not reduce evaporation. Accordingly, the emulsions should be prepared with the minimum quantity of emulsifier which will produce a stable emulsion.

Evaporation reduction with floating powders. Floating powders for evaporation reduction were subjected to preliminary investigation during June and July 1963. A white, water-repellant powder with a

particle size of about 1 micron (ECP No. 1) reduced evaporation from 40 to 55 percent when applied at a rate of 230 g/m^2 . The powder was not self-spreading and attempts to apply lower rates of 77 g/m^2 resulted in nonuniform distribution and less effective evaporation reduction of 27 to 31 percent. A coarser water-repellent powder of about 15 micron size (ECP No. 2) reduced evaporation by about 20 percent. These data are presented in Table 2.

Incoming and reflected short-wave radiation was measured for a 24-hour period on 1 July 1963. Incoming radiation was 716 langley per day. Reflected radiation was 112 langley, or 15.5 percent, from the untreated water surface and 284 langley, or 39.7 percent, from the surface treated with ECP No. 1 at 230 g/m^2 . Water temperature profiles were measured during this same 24-hour period, as shown in Figures 3 and 4, but an energy balance could not be computed because of heat leakage from the sides and bottoms of the tanks. An indication of this heat loss is given in Figure 4 which shows a temperature wave moving downward from the water surface. Some indication of the temperature effect on evaporation is given in Figure 2 which shows surface temperatures on 28 June 1963 for untreated and treated tanks. Mean daily surface temperatures were: treated with long-chain alcohol (ECE No. 1) - 30.3 C ; untreated - 27.4 C (average); treated with white, water-repellant powder (ECP No. 1) - 25.0 C . This means that a loss of the powder treatment, by rain for example, would not result in the above normal evaporation which follows the loss of a long-chain alcohol film.

Laboratory studies were conducted to determine the amount of evaporation reduction attributed to ECP No. 1 as a vapor barrier as opposed to radiation reflection. Glass 600-ml beakers were treated with long-chain alcohol at 1.1 g/m^2 and with ECP No. 1 at 230 g/m^2 and evaporation was compared to untreated beakers. Treatments were triplicated and randomized and were exposed where incident radiant energy was negligible. Untreated evaporation was 31.2 mm in the 24-day period. Evaporation reduction by the alcohol was approximately 40 percent, comparable to field results, and by the ECP No. 1 was

approximately 5 percent. This study demonstrated that reflection of incident radiation is the primary mechanism for evaporation reduction by ECP No. 1.

SUMMARY AND CONCLUSIONS:

A long-chain fatty alcohol emulsion reduced evaporation from 274 cm diameter steel tanks by 35 to 45 percent when continuously applied at a rate of $1.1 \text{ g/m}^2/\text{month}$ (10 lbs/acre/month) and only small amounts of algae were present. Evaporation reduction was lowered to about 28 percent when one-fourth of the water surface was covered with algae. Mean daily water surface temperatures of alcohol treated tanks were about 3 C higher than in untreated tanks. During one test, when a film was applied for 4 days, evaporation from the treated tank during the second day after loss of the film exceeded the untreated rate by 33 percent. Net evaporation reduction for the week was only 22 percent despite the fact that reduction during the first 4 days averaged 40 percent. This same problem has been encountered by other investigators who applied the alcohol in solutions, powders, and flakes.

The emulsion has proven to be exceptionally stable and no separation or deterioration has occurred in a 1,000 ml sample stored in the laboratory for over 18 months. It has proven to be easy to apply and effective in reducing evaporation. There is a possibility that the bacteriocidal emulsifier will interfere with rumen activity in cattle. Although this is not expected to be a problem the question should be answered before the emulsion is recommended for use on stock ponds.

Floating white powders reduced evaporation from outdoor tanks by 40 to 55 percent by reflecting about 40 percent of the incoming solar radiation and lowering water temperatures. Laboratory studies showed that interference with vapor movement accounted for about 5 percent of the evaporation reduction. The powders are not self-spreading and can be dissipated by wind and rain. They may, however, be useful for reducing evaporation from uncovered water storage tanks in arid areas.

PERSONNEL: L. E. Myers, G. W. Frasier

Table 1. Reduction of evaporation from outdoor tanks treated with an emulsion of long-chain alcohol (ECE No. 1) at a rate of 1.1 g/m²/month.

Date		Untreated Evaporation	Tank 1		Tank 2	
From	To		Evaporation	Reduction	Evaporation	Reduction
1963	1963	mm	mm	percent	mm	percent
18 Feb	25 Feb	25.4	16.4	37.9	14.0	43.1
1 Mar	8 Mar	27.9	15.8	43.4	15.5	44.4
1 Apr	8 Apr	36.4	27.0	25.8	25.7	29.4 ^{1/}
18 Apr	25 Apr	38.3	36.1	5.1 ^{2/}	33.3	12.7 ^{2/}
30 Apr	6 May	43.5	34.2	21.4 ^{3/}	33.6	22.8 ^{3/}
20 May	27 May	53.8	35.3	34.4	36.6	32.0
25 Jun	2 Jul	55.1	35.9	34.9	-	-

^{1/} Algae covered one-fourth of tank area.

^{2/} Excess emulsifier in water.

^{3/} Film lost on 4 May 1963.

Table 2. Reduction of evaporation from outdoor tanks treated with floating powders ECP No. 1 and ECP No. 2.

Date		Untreated Evaporation	ECP No. 1		ECP No. 2	
From	To		Evaporation	Reduction	Evaporation	Reduction
1963	1963	mm	mm	percent	mm	percent
26 Jun	2 Jul	55.0	25.3	54.0 ^{1/}		
3 Jul	8 Jul	48.6	21.8	55.1		
10 Jul	16 Jul	51.5	26.0	49.5		
17 Jul	22 Jul	44.7	26.8	40.0		
19 Sep	26 Sep	36.7	26.8	27.0 ^{2/}	29.4	19.3 ^{3/}
27 Sep	4 Oct	46.0	31.9	30.7	36.2	21.3

^{1/} Treated at rate of 230 g/m².

^{2/} Treated at rate of 77 g/m².

^{3/} Treated at rate of 430 g/m².

9-7

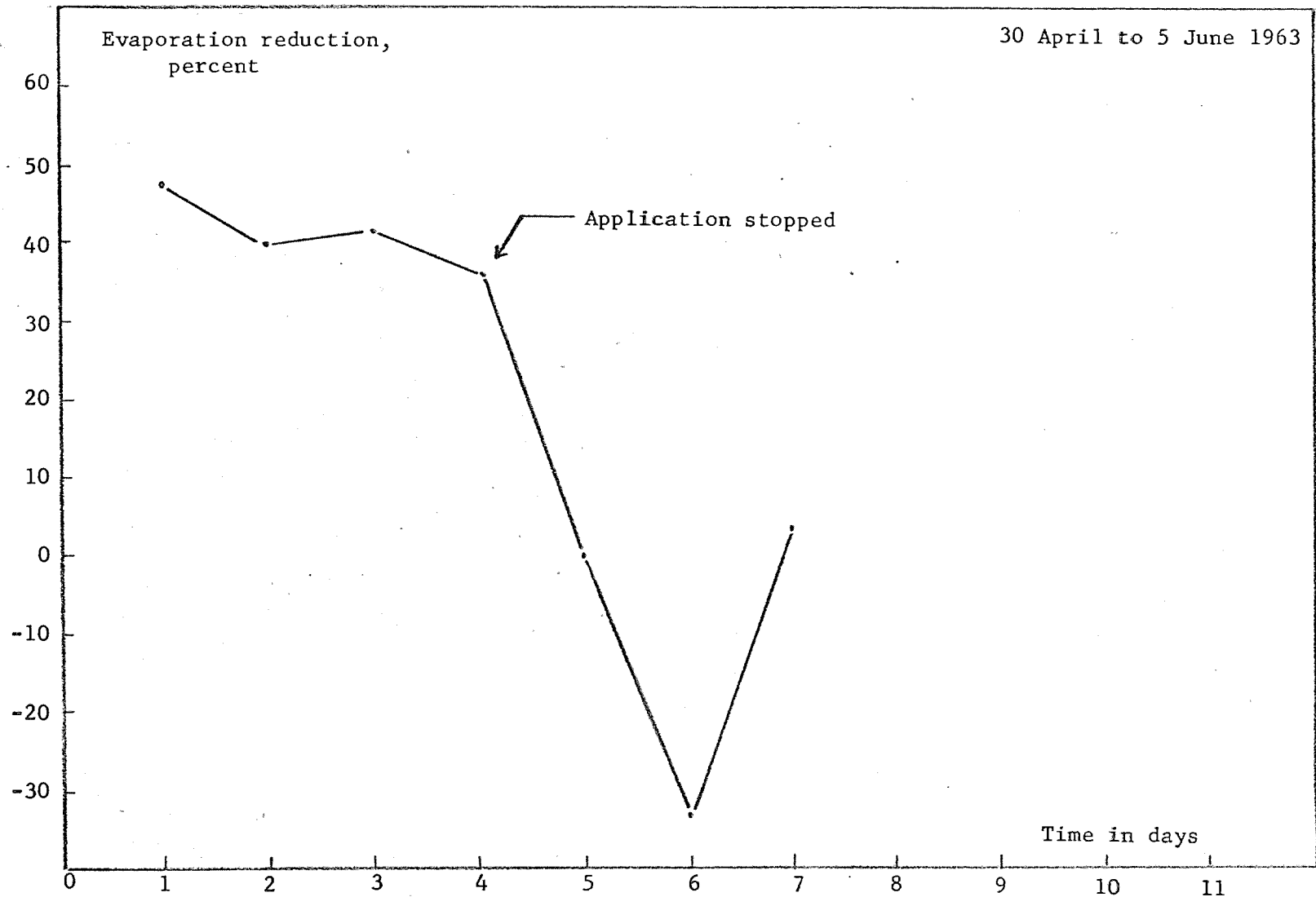


Figure 1. Reduction in evaporation for 7-day period from outdoor tank treated for 4 days with long-chain alcohol emulsion at a rate of $1.1 \text{ g/m}^2/\text{month}$. Reduction based on comparison with untreated tank.

Annual Report of the U.S. Water Conservation Laboratory

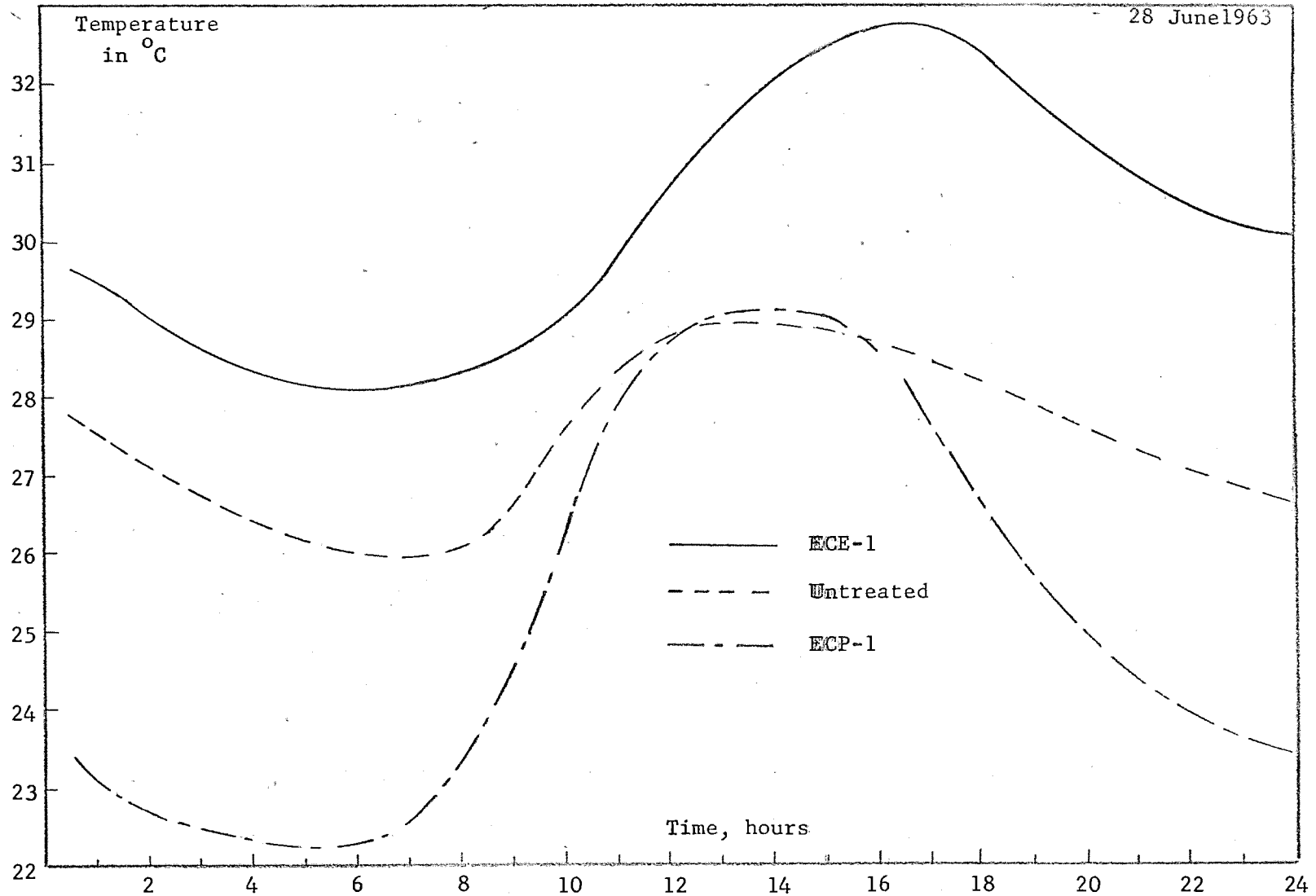


Figure 2. Water surface temperatures for 24-hour period in outdoor tanks treated with long-chain alcohol emulsion (ECE-1), floating white powder (ECP-1), and untreated. Annual Report of the U.S. Water Conservation Laboratory

9-11-6

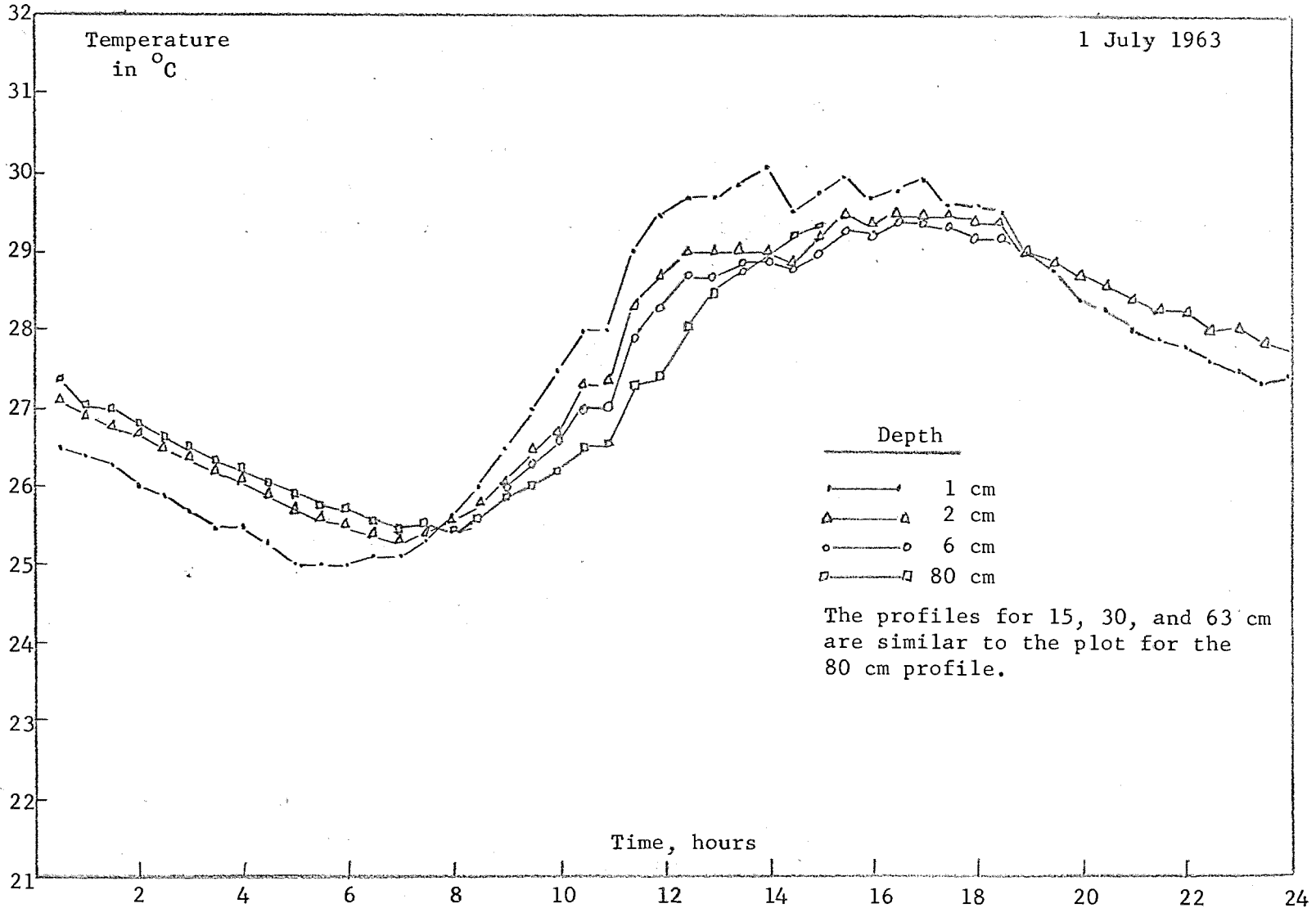


Figure 3. Water temperature for 24-hour period at selected depths in a unit used at the U.S. Water Conservation Laboratory tank.

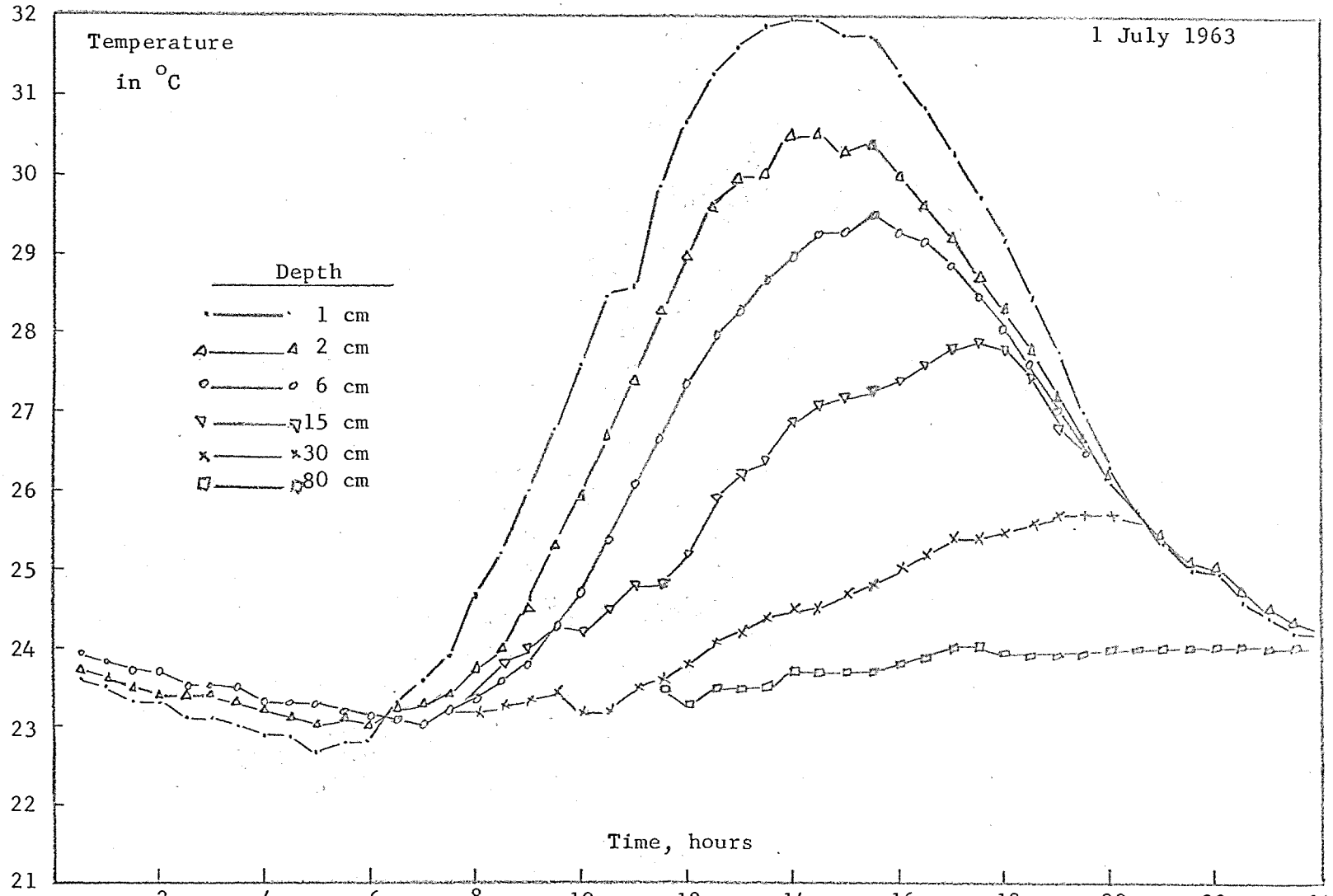


Figure 4. Water temperatures for 24-hour period at selected depths on 1 July 1963 with floating white powder (ECP-1) at 230 g/m².

TITLE: MEASUREMENT AND CALCULATION OF UNSATURATED CONDUCTIVITY AND
SOIL-WATER DIFFUSIVITY

LINE PROJECT: SWC 4-gG4

CODE NO.: Ariz.-WCL-13

INTRODUCTION:

The objectives and need for study for this project were reported in the 1961 Annual Report of the U. S. Water Conservation Laboratory. In the 1962 Annual Report the results of soil-water diffusivity measurements at several porosities and at several temperatures, and a theoretical and experimental examination of the pressure plate outflow method for measuring capillary conductivity were reported. Work done in 1963 consisted of measuring the unsaturated conductivity of a graded sand using a modification of the long column method of Childs (1), and calculating the unsaturated conductivity from water retention data using the method of Millington and Quirk (2).

PROCEDURE:

Unsaturated conductivity measurements. Air-dry 50-500 μ sand was packed into columns with the mechanized soil column packer. Three columns were joined together to form one column 101 cm long. The column consisted of 101 sections which could be separated for water content measurements. The size and construction of the plastic columns and the mechanized soil column packer have been described in the 1961 Annual Report, page 226. The 101-cm column was placed vertically on top of a 30-cm solid tube previously hand packed with the 50-500 μ sand. The solid portion provided a means of maintaining a water table at the bottom of the column. Beginning at about 28 cm above the water table, tensiometers (made by cementing porvic on a 1/4-inch o.d. plastic tube and connecting the plastic tube to a manometer) were inserted at 4-cm intervals for a portion of the column, then at 3-cm intervals at the region where drainage of the sand was expected. A total of 21 tensiometers were located within the column. Water from a constant head source was applied dropwise on the top of the column at a constant rate.

For desorption measurements, the column was saturated by allowing the inflow rate to be sufficiently high to essentially saturate the column. Subsequently the inflow rate was reduced and the water contents allowed to approach a dynamic equilibrium. When the pressure head readings on the manometer remained constant for a 24-hour period and the inflow and outflow was equal and constant, a final reading of the manometer and the flow rate was taken; the tensiometers removed from the column; and the column quickly sectioned into 2-cm sections from which the water content was obtained by drying the sample at 110 C for 24 hours. Plots were made of pressure head versus distance above the water table and volumetric water content versus distance above the water table. The water content at a particular pressure potential was obtained by comparison of the two graphs. The slope of pressure head versus distance, obtained graphically from the plot of pressure head versus distance above the water table, was divided into the flow rate per unit area to obtain the unsaturated conductivity of the sand. Slopes were taken at particular water contents from the water content-distance curve and the soil water diffusivity calculated at several water contents by dividing this slope into the unsaturated conductivity.

Calculation of conductivities from water retention data. The method of calculating unsaturated conductivity from water content retention data by the method of Millington and Quirk (2) consists of dividing the water content range into m equal parts, obtaining the pressure potential at the midpoint of each part, and calculating the conductivity using the following equation:

$$k = \frac{314 \theta_v^{4/3}}{m^2} \left[\frac{1}{\psi_1^2} + \frac{3}{\psi_2^2} + \frac{5}{\psi_3^2} + \dots + \frac{(2m-1)}{\psi_m^2} \right]$$

where ψ = pressure potential, θ_v = volumetric water content, k = unsaturated conductivity, and m = number of water content intervals. Reference is made to the original article and articles cited by Millington and Quirk for the derivation of this equation.

RESULTS AND DISCUSSION:

The modification of the long column method of Childs afforded a means of obtaining the capillary conductivity, the water retention curve, and, hence, the soil-water diffusivity from the same sample. This method works well for a coarse material having a gradation of pore sizes. For fine textured materials, very long columns are required, posing problems of uniform packing and other experimental difficulties. Coarse textured materials of uniform pore size have a sharp drainage point and, hence, a piston shaped head versus distance relation. This permits only one value for conductivity for each run to be obtained for materials of rather uniform pore size.

The 50-500 μ sand used in these experiments yielded head versus distance curves such as shown in Figure 1. From this curve the term $\Delta H/\Delta x$ can be obtained graphically at several points along the curve. Using Darcy's law, the conductivity k is obtained by dividing the flux per unit area q by $\Delta H/\Delta x$. In addition to head measurements at various x 's, water content was also determined as a function of x . Thus the k obtained from the slope measurement at, say, $x = 60$ in Figure 1 was related to the water content occurring at $x = 60$.

The results of k measurements made for desorption on four columns of 50-500 μ sand are shown in Figure 2. The agreement among the four replicates is excellent. The largest variation is at the higher water contents. This results from the inaccuracy of measuring the total head close to the water table (see Figure 1 for $x \approx 40$). One run was made for sorption. This will be discussed later.

From the plots of total head versus x and water content versus x the dynamic water retention curves for sorption and desorption were derived. These are shown in Figure 3. The dashed lines in Figure 3 represent data obtained from conventional pressure plate apparatus. Slopes of the retention curves at particular water contents were obtained graphically and divided into the conductivities to obtain the soil-water diffusivity curves shown in Figure 4. Note that the sorption and desorption diffusivities are nearly the same at the higher water contents with the desorption diffusivities being greater as the water content decreases.

From the water retention curves of Figure 3 the conductivities were calculated using the method of Millington and Quirk (2). The results of this computation are shown by the dashed lines in Figure 5. The solid lines represent experimental data. (The solid desorption line was taken from Figure 2. The solid sorption line is the result of one sorption conductivity measurement with the long column method.)

Figure 5 shows that the conductivities calculated from water retention data are higher than the experimental data. Also the calculated sorption conductivities are higher than desorption whereas the measured sorption conductivities are lower than the desorption conductivities. The ratio of measured to calculated saturated conductivities (sorption having a smaller ratio than desorption, because the theoretical value for sorption is greater than for desorption) was used as a matching factor. When this factor was applied to the above equation, the calculated curves fell reasonably close to the measured curves.

As a further check on the feasibility of calculating conductivities from retention data, conductivities were calculated for Adelanto loam. Soil-water diffusivity data (see 1962 Annual Report, page 210) and vapor diffusivities (see this report, project WCL-31) were available for this soil material. The saturated hydraulic conductivity for Adelanto loam was measured ($0.00271 \text{ cm min}^{-1}$ - average of 6 measurements) and used as a matching factor for the calculated conductivities. The adjusted conductivities were divided by slopes of the retention curve to obtain diffusivities. The results are shown in Figure 6 as x's. The Δ 's are measured soil-water diffusivities and the o's are vapor diffusivities. The agreement between measured and calculated values is reasonably good. This gives some justification for using calculated conductivities and diffusivities for filling in regions where direct measurement is difficult.

SUMMARY AND CONCLUSIONS:

The unsaturated conductivity of 50-500 μ sand was measured using a column 130 cm long and 3.18 cm in diameter. A constant inflow of water was maintained at the top of the column and the pressure was

measured at 21 locations within the column with tensiometers. When the outflow was constant and equal to the inflow the tensiometers were read and the flux recorded. The column was then separated into 2-cm sections and the water content determined. With these measurements the unsaturated conductivity and the water retention curve were obtained. Soil-water diffusivities were calculated from conductivities and slopes of the retention curve.

Theoretical conductivities, calculated from pore size distributions (estimated from water retention curves), were compared with measured values. Theoretical values agreed reasonably well with the measured values if a matching factor (the ratio of measured to computed saturated conductivities) was used to adjust the computed conductivities.

Theoretical conductivities were computed from a water retention curve for Adelanto loam and adjusted with a matching factor. The conductivities were divided by the slope of the water retention curve to obtain soil water diffusivities. The computed diffusivities were compared with measured soil water diffusivities and vapor diffusivities for this material. The computed values were in reasonable agreement with the measured values.

REFERENCES:

- (1) Childs, E. C.
1945. The water table, equipotentials, and streamlines in drained land. III. Soil Sci. 59:405-415.
- (2) Millington, R. J., and Quirk, J. P.
1963. Transport in porous media. 7th Internatl. Cong. of Soil Sci. Trans. pp. 97-106.

PERSONNEL: R. D. Jackson, R. J. Reginato

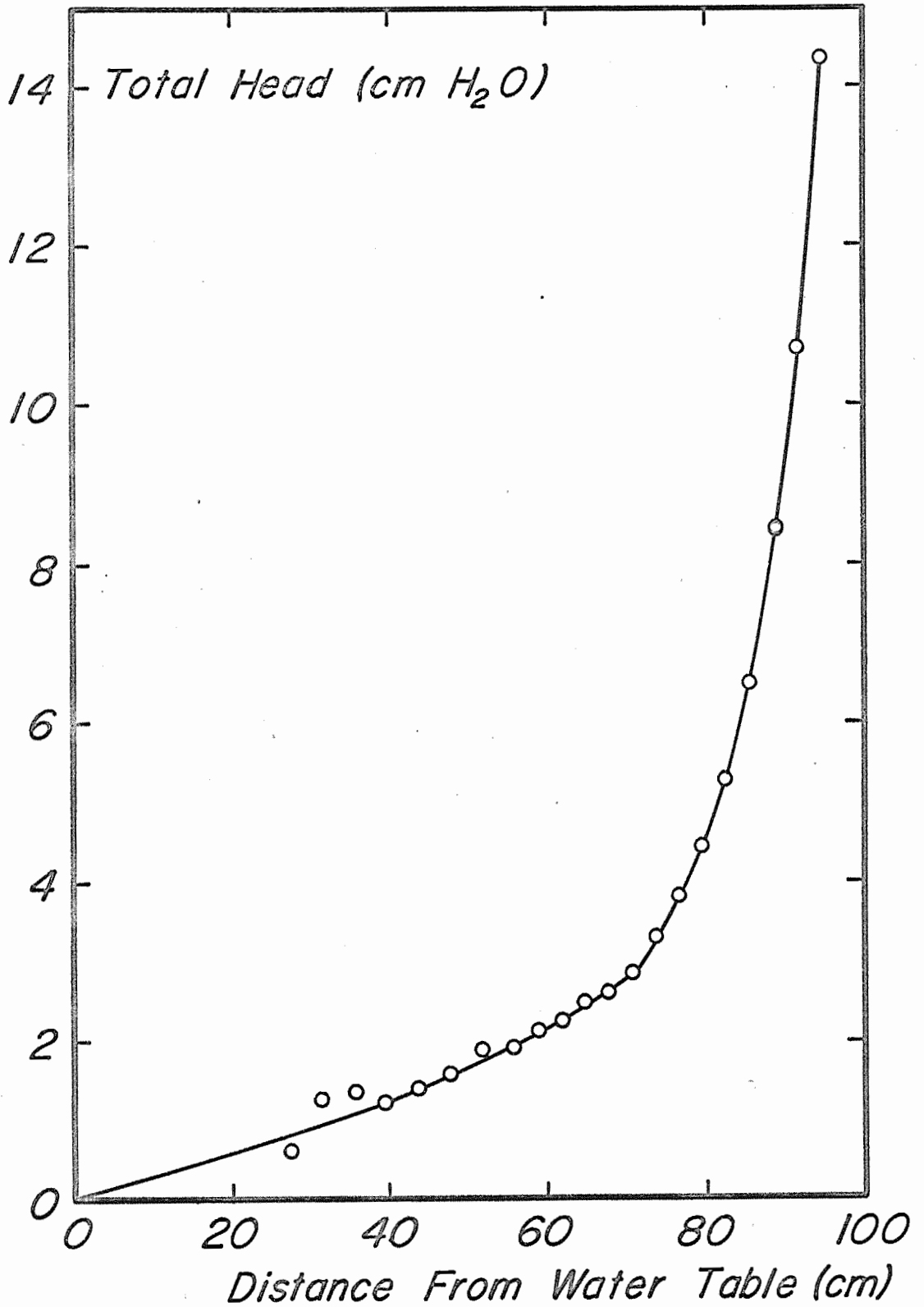


Figure 1. Total head versus distance from water table for desorption run on 50-500 μ sand.

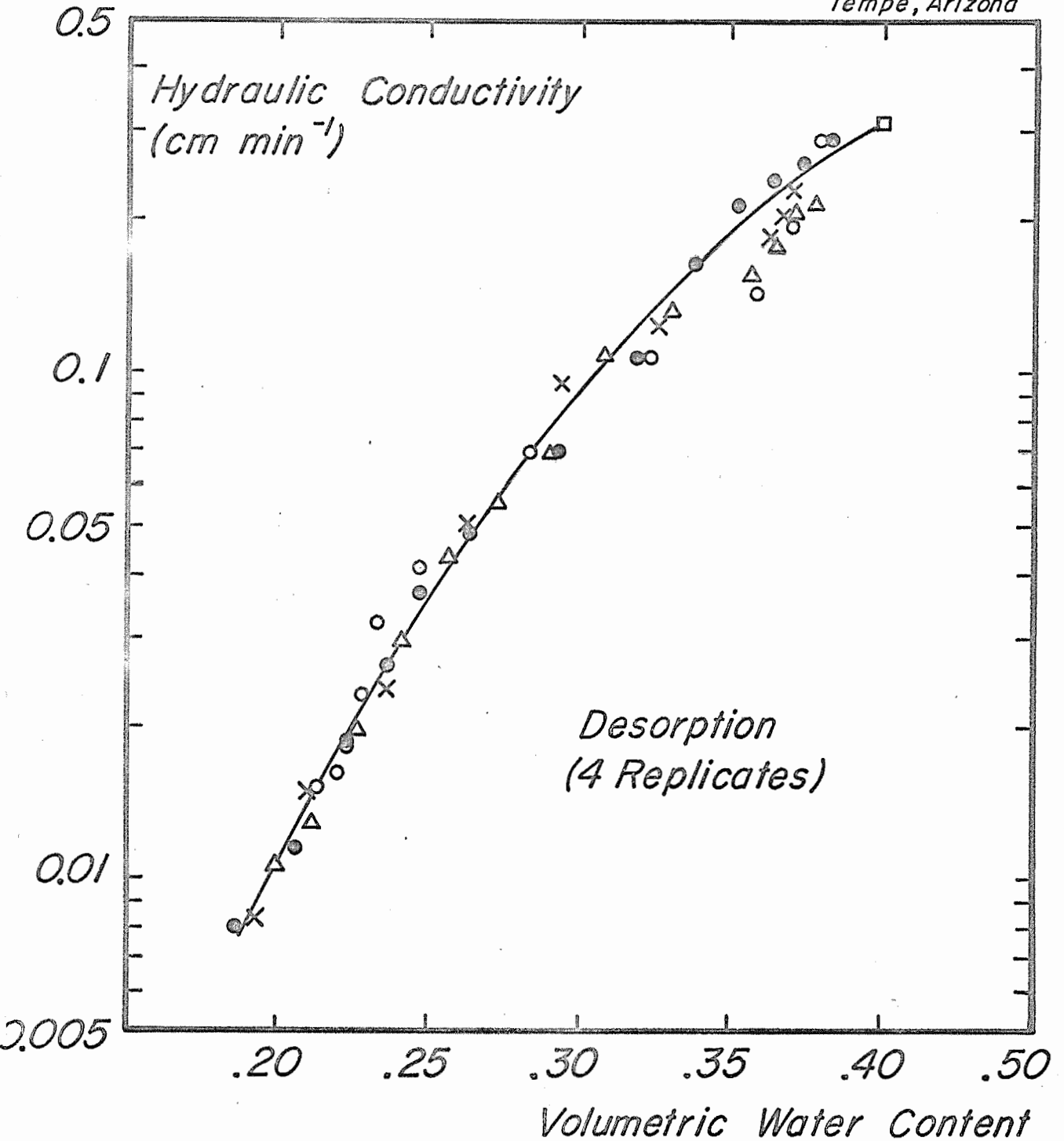


Figure 2. Hydraulic conductivity for unsaturated 50-500 μ sand.

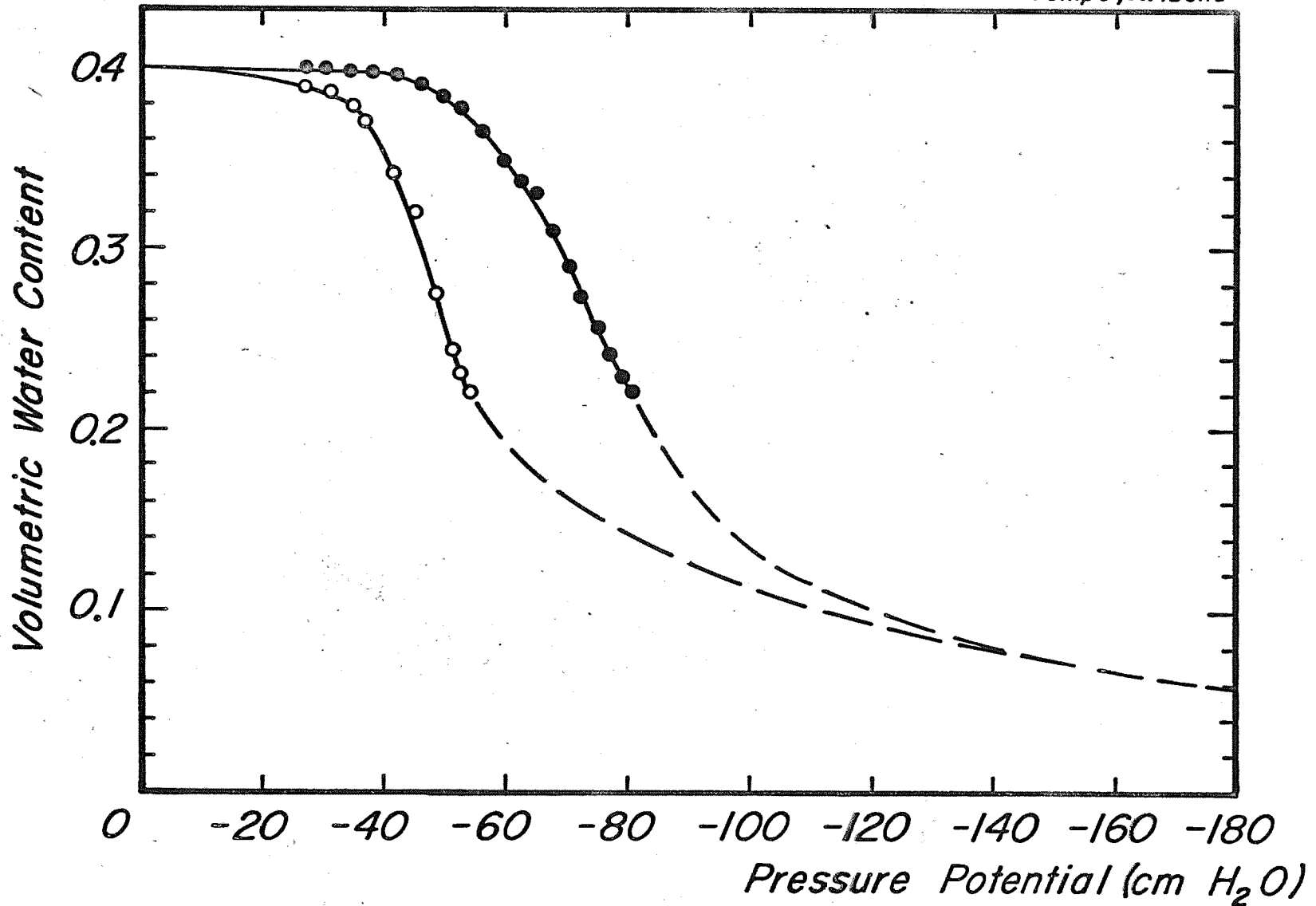


Figure 3. Water retention curves obtained from pressure and water content measurements of columns used to measure conductivities.

12-8

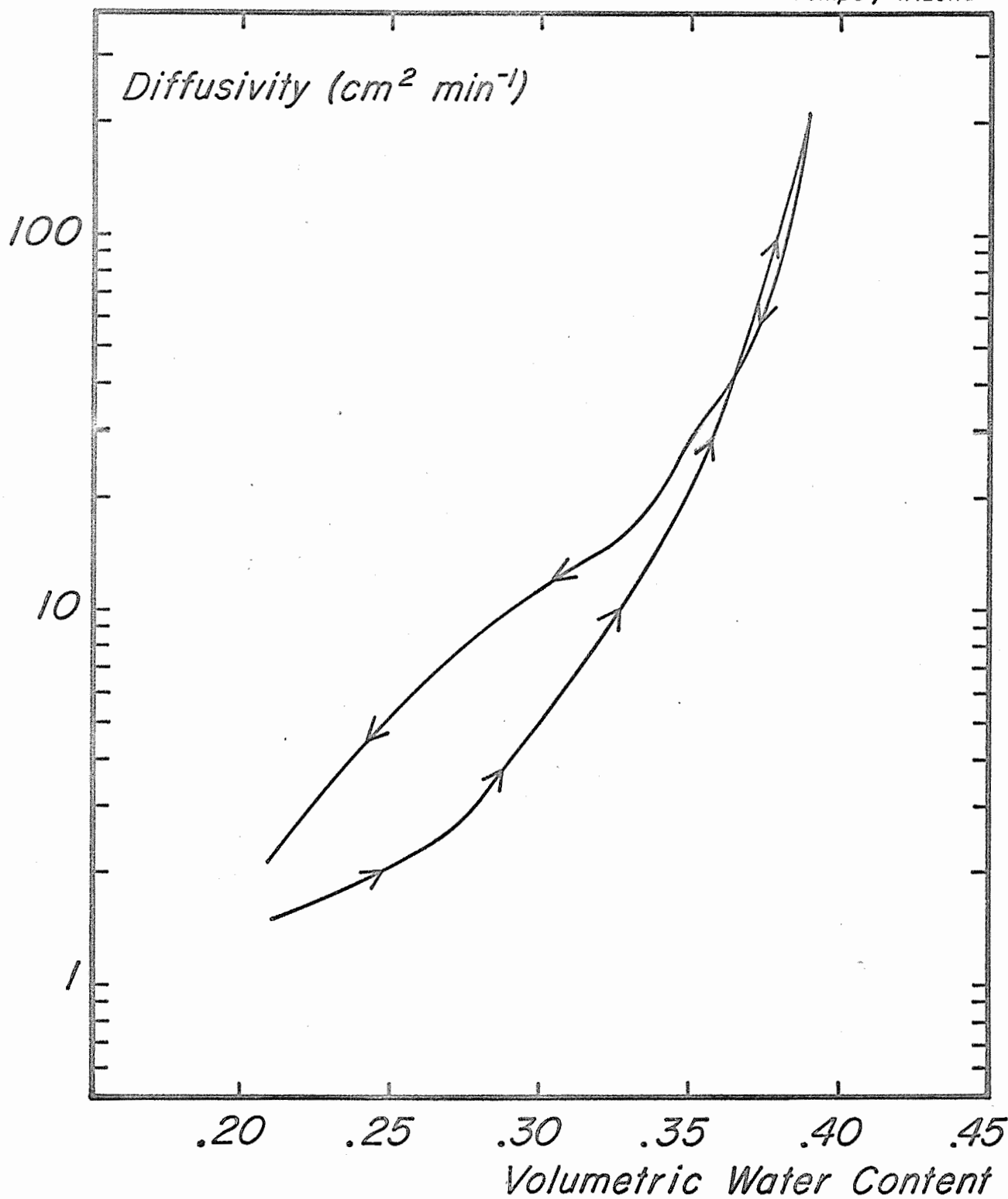


Figure 4. Diffusivities for 50-500 μ sand calculated from conductivities and slopes of the water retention curves.

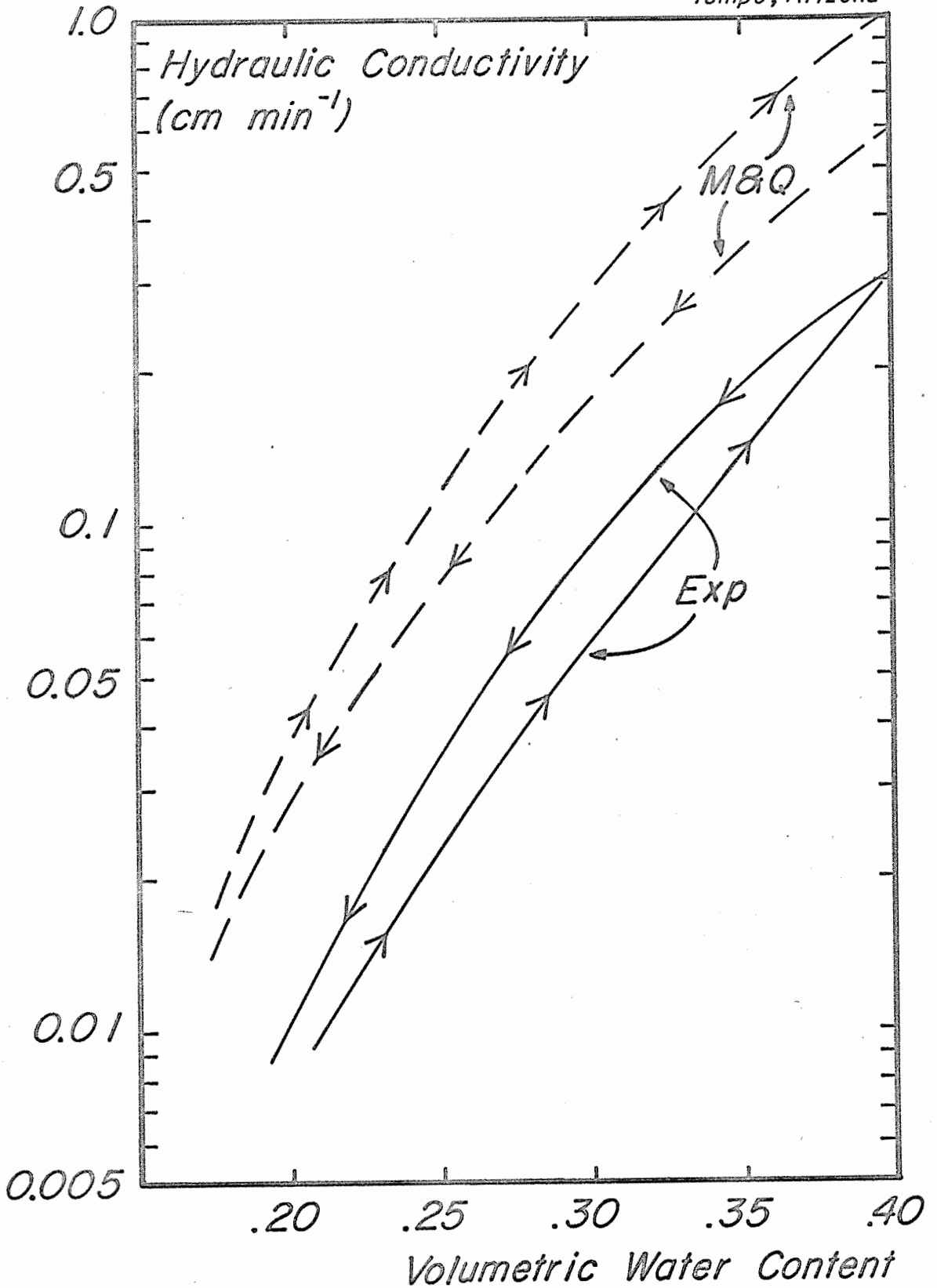


Figure 5. A comparison of theoretical (Millington and Quirk) and experimental conductivity for 50-500 μ sec. Annual Report of the U.S. Water Conservation Laboratory

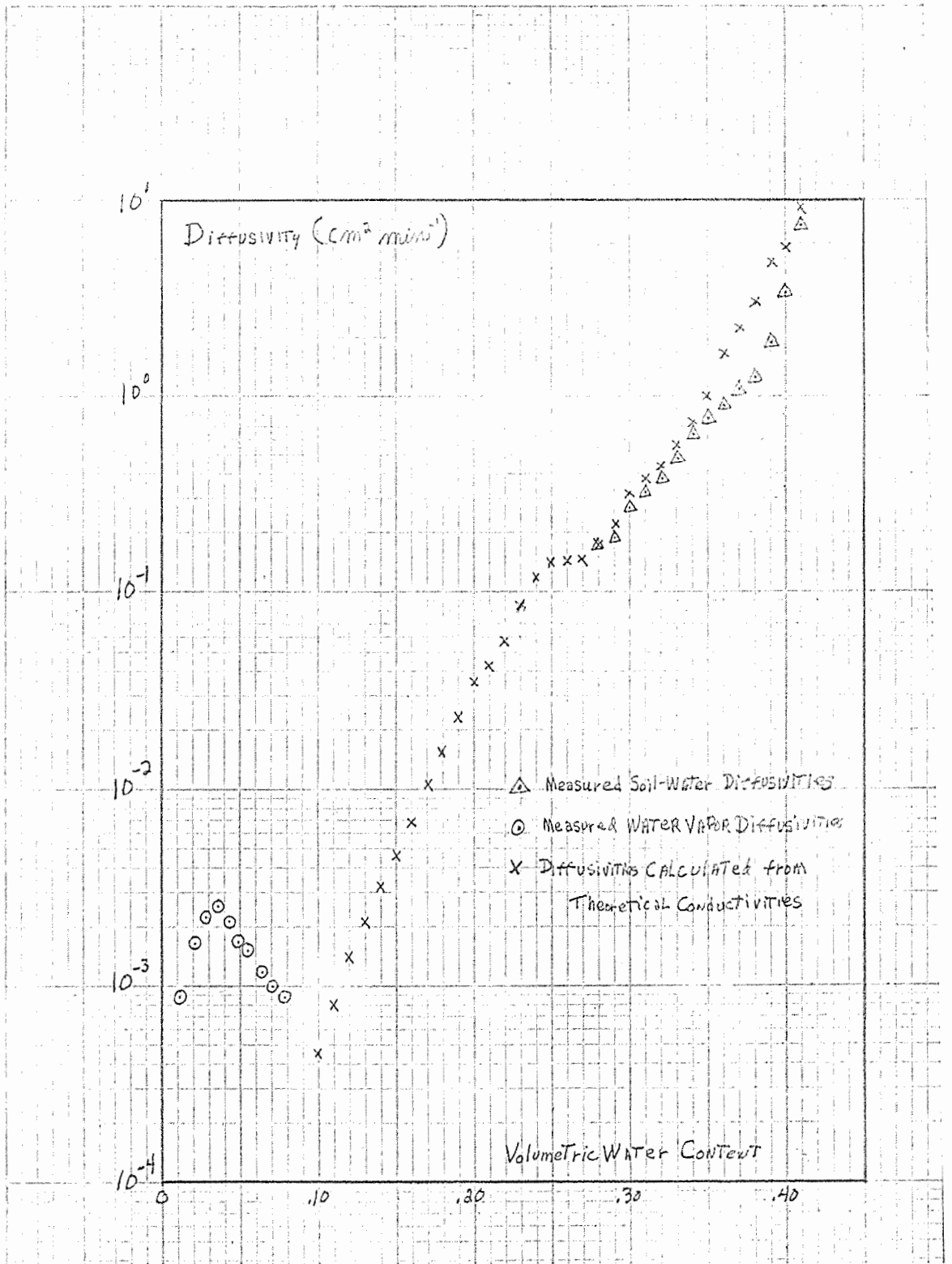


Figure 6. Soil-water diffusivities for Adelanto loam, measured and calculated. The calculated diffusivities were obtained from conductivities calculated using Millington and Quirk's method and a measured water retention curve.

TITLE: FIELD APPLICATION OF FALLING-HEAD TECHNIQUE FOR SEEPAGE METERS
AND OF DOUBLE-TUBE METHOD FOR HYDRAULIC CONDUCTIVITY MEASUREMENT

LINE PROJECT: SWC 4-gG1

CODE NO.: Ariz.-WCL-14

INTRODUCTION:

The falling-head seepage meter technique for measuring seepage and hydraulic conductivity of bottom material (see Annual Report 1962) was demonstrated before a group of engineers from the Soil Conservation Service. The demonstration was held in the Ferron area, Utah, July 22-25, 1963. A complete report of the studies, including copies of data sheets and graphs for processing the field data, was prepared. The results of the measurements with a brief discussion will be presented in this report.

Several modifications were made in the seepage meter equipment to permit more convenient and faster measurements and to increase the applicability of the method under unfavorable conditions such as hard soil, very shallow canals, or turbid water with no visibility.

A source of error with the seepage meter, which is difficult to evaluate, is the effect that disturbance of the bottom material, due to penetration of the meter, may have on seepage. To investigate this effect, seepage rates were measured while periodically increasing the depth of penetration of the meter. This study was performed in various ditches in the Salt River Valley. The study also yielded information regarding the reproducibility in time of the seepage rates.

PROCEDURE:

Demonstration of seepage meter in Utah. Falling-level measurements for the seepage meter tests were obtained with an inverted, vacuum U-tube manometer on the canal bank. In a number of cases, the seepage rates were very slow and the manometer tubes themselves were used as the falling-level reservoir. The locations of the seepage meter tests are described in Table 1. Seepage rates were calculated from graphs of the manometer readings versus time (see Annual Report 1961). Correction for velocity effects was significant in three cases (tests 3, 5, and 6, Table 1). For tests 3 and 6, the

value of the balanced flow differential head, H_b , after correction for velocity effect was so small that H_b was considered 0. The hydraulic conductivity of the bottom material was calculated according to the procedure in Annual Report 1962.

Modifications of seepage meter equipment. The three toggle bolts with wing nuts for fastening the lid of the seepage meter to the cylindrical part, were replaced by four toggle clamps. This eliminated the need for proper positioning of the lid and it will save considerable time and effort in installing the meter in turbid water with poor visibility.

A new falling-level reservoir was constructed which consisted of two five-inch long reservoirs with diameters of 2 and 4 inches. The 2-inch reservoir can further be reduced to an effectively smaller reservoir by the use of a cylindrical insert. The reservoirs are connected with a three-way plug valve to the tube leading to the seepage meter. One position of the valve connects the seepage meter with the small reservoir, another with the large reservoir, and a third position will shut the water supply off for measurement of the balanced-flow differential head, H_b , (see Annual Report 1962).

The conical top of the seepage meter was replaced by a flat lid. As regards the possibility of air accumulation in the seepage meter and the connecting tube to the falling level reservoir, most of the air will probably escape from the bottom material when the meter is pushed in. At that time, however, the lid is not yet installed, so that the air can escape. Thus, the advantages of a conical top are questionable. The flat lid is not only simpler but also more suitable for use of the seepage meter in shallow water. For this purpose also, the valve and connections of the falling-level reservoirs are mounted sideways instead of below the reservoirs.

To facilitate installing the meter in hard bottom materials, a driving device was constructed which, when in position, rests directly on the entire circumference of the cylindrical part of the meter.

Effect of meter penetration on seepage. Using the improved seepage meter equipment, seepage was measured at increasing depths of penetration, d , of the meter. The initial d was usually less than one inch. Seepage was then measured one, two, or three times at ten- to twenty-minute intervals. After that, the seepage meter lid was removed and the meter pushed in to a d of approximately 1-1/2 to 2 inches, etc. This procedure was repeated until three or four values of d had been obtained. With each seepage measurement, H_b was also determined. The tests were carried out at 11 different locations in the Salt River Valley. The canal locations were selected to include bottom material that consisted of uniform soil, fine soil over coarse soil, and vice versa.

RESULTS AND DISCUSSION:

Demonstration of seepage meter in Utah. The seepage rates (Table 2) were generally less than 0.5 ft/day. Seepage rates of a few feet per day were measured in only three cases. On one occasion (test 8) a negative seepage, or an inflow of ground water into the canal, was observed. The results confirmed conclusions from earlier seepage studies by the Soil Conservation Studies using inflow-outflow techniques, that the seepage rates in the area under investigation were low.

The results of the calculations of hydraulic conductivity of bottom material (Table 3) show that K is generally less than 0.5 ft/day. The bottom material is vertically fairly uniform for tests 1, 2, 16, 17, and 19 ($0.5 < I_s/K < 1.5$). Relatively coarse bottom material underlain by finer soil occurs for tests 3, 4, 5, 6, 11, 13, 15, and 18 ($I_s/K < 0.5$). The reverse, i. e., relatively fine bottom material overlying more permeable soil, occurs for tests 7, 9, 10, 12, and 14 ($I_s/K > 1.5$). For tests 12 and 14, the distance D_p of the more permeable soil below the channel bottom was calculated assuming the pressure below the slowly permeable surface material to be atmospheric. The high H_b -values for tests 7, 9 and 10 indicated the presence of a relatively thin, slowly permeable surface layer on the bottom. The hydraulic impedance, r_s , of this clogged surface layer

was determined according to the procedure described in Annual Report 1962. For tests 9 and 10, H_b exceeded the water depth, which indicated a sufficiently clogged surface layer to yield negative water pressures below it. These pressures are calculated in inches of water in the last column of Table 3.

Modifications of seepage meter equipment. Use of the modified seepage meter equipment in the studies of the effect of meter penetration on seepage demonstrated that the modifications accomplished the set goals of faster and more convenient measurement, and better adaptation to adverse canal conditions. A complete construction drawing of the improved seepage meter equipment was prepared.

Effect of meter penetration on seepage. The results of the studies on the effect of penetration of the seepage meter on the measured seepage and on H_b are shown in Table 4, where I_s and H_b are averages for the tests with two or three replicate measurements at each depth of penetration. Examples of complete data in graphical form are shown in Figures 1, 2, 3 and 4. For nine of the eleven tests, the change of seepage with increasing depth of penetration of the meter was less than 20%.

Depending on the soil conditions of the canal as reflected by H_b , the seepage I_s can be expected to increase, remain constant, or decrease with increasing d . If, for instance, a clogged surface layer is present, installing the seepage meter may disturb this layer along the circumference of the cylinder of the meter, and I_s may increase with increasing d . An example of this effect, which was only encountered in test 7, is shown in Figure 1. The continued increase in H_b until $d = 2$ inches in this test indicates that the thickness of the slowly permeable layer is approximately 2 inches. Examination of the bottom of the canal showed that there was a 1-1/4-inch layer of loose silt and organic material overlying hard sandy loam. The top 3/4-inch of the sandy loam was also slowly permeable as indicated by H_b in Figure 1.

An example of I_s decreasing with increasing d is shown in Figure 2 for test 11. The small H_b values indicated relatively

coarse material overlying finer material. Since H_b increased with d , the decrease in I_s can probably be attributed to compaction of the coarse material due to installation of the meter. If the finer underlying material had been compacted, H_b would have decreased with increasing d and this was contrary to what was observed. Another explanation for the change in I_s and H_b in Figure 2 could be that fines may settle in the "quiet" water inside the seepage meter. This effect, however, would be associated with time rather than with d .

In most tests, I_s remained relatively constant with increasing d , which also showed the reproducibility in time of the seepage data obtained with the technique. Constant I_s while H_b increased with increasing d was obtained for tests 1, 2, 3, 6, 8, 9, and 10. This indicated the presence of slowly permeable material near the surface of the canal bottom.

For tests 4 and 5, H_b was already relatively high for the smallest d , indicating that the slowly permeable layer had already been penetrated at the first measurement of I_s . For these two tests, subsequent pushing in of the seepage meter did not disturb the bottom material sufficiently to affect the measured seepage. Thus, if there were any disturbance caused by the installation of the meter, it must have happened while the meter was pushed in to the first value of d .

Figures 3 and 4 give examples of the trend that was most frequently observed.

SUMMARY AND CONCLUSIONS:

A demonstration of the falling-head seepage meter technique was held with and for the Soil Conservation Service in the Ferron area, Utah, in July 1963. Measurement of seepage and hydraulic conductivity of bottom material was made at 19 locations in various canals and ditches. For 15 locations, the seepage was less than 0.5 ft/day. The maximum seepage rate observed was 6 ft/day. Hydraulic conductivity of bottom material was less than 0.5 ft/day for 11 locations. The maximum hydraulic conductivity observed was 24 ft/day, which was in a sandy, gravelly deposit. The seepage at that location was measured as zero.

The balanced-flow differential heads indicated bottom conditions of uniform soil, relatively coarse soil over relatively fine soil and vice versa, and clogged surface layers. The occurrence of all four bottom conditions may be characteristic of old canals where erosion, sedimentation, and clogging have altered the original soil conditions.

The demonstrations clearly showed that the falling-head technique is suitable for routine use in seepage investigations. In general, measurement of seepage and balanced-flow differential head will be sufficient. The seepage is the quantity that is usually of most interest and its determination by means of a graph of the manometer readings is quite simple. The measurement of the balanced-flow differential head, which is also easy to carry out, makes it possible to draw qualitative conclusions regarding the conductivity characteristics of the bottom material (uniform soil, coarse material over fine material or vice versa, and clogged surface layers). The calculation of hydraulic conductivity will normally only be done for some specific purpose.

To increase the utility of the seepage meter for routine measurement, several changes were made in the equipment. The modifications consisted mainly of a flat lid fastened with toggle clamps to the cylindrical part of the meter, an improved falling-level reservoir assembly, and an improved driving device for installing the meter in hard bottom materials. These changes resulted in faster and more convenient measurement of seepage and improved adaptability of the meter to adverse canal conditions such as turbid and/or shallow water, or hard bottom material.

The effect of soil disturbance due to installation of the seepage meter on the measured seepage was studied by determining seepage rates while periodically increasing the depth of penetration, d , of the meter. A typical sequence of d was 1, 1.5, 2, and 2.5 in. For several tests, the seepage, I_s , and the balanced-flow differential head, H_p , were measured several times at 10 to 20 min intervals for each d . The tests were performed in ditches in the Salt River Valley for various conditions of bottom material. For 9 tests out

of a total of 11 completed so far, the variation of I_s with d was less than 20%. In one test, an increase of I_s with increasing d was observed. This increase was attributed to disturbance of a thin, clogged, surface layer. In another test, I_s decreased with d , probably due to compaction of the relatively coarse bottom material in which the meter was installed.

Since I_s can not be measured with the seepage meter for $d = 0$, the possibility must be considered that all disturbance and resulting effect on I_s takes place while the meter is pushed in to the first d -value. The general tendency of I_s to vary little with continued increases in d , even when H_b indicates continued presence of slowly permeable bottom material, supports the conclusion that bottom disturbance due to installation of the Tempe seepage meter has an insignificant effect on the seepage. Also, since some measurements were carried out for several hours per seepage meter installation, the study demonstrated that the results obtained with the falling-head seepage meter technique are reproducible in time. The study will be continued and more tests will be made.

PERSONNEL: Herman Bouwer and R. C. Rice.

Table 1. Location of seepage meter tests, Ferron, Utah.

Test No.	Date	Location
1	7-23	Ferron South, #1
2	7-23	Ferron South, #2
3	7-23	King Ditch, above 2nd main flume
4	7-23	Peterson Ditch, #1, Clyde Conover owner
5	7-24	Peterson Ditch, #2, Ellis Wild owner
6	7-24	Peterson Ditch, #3, Ellis Wild owner
7	7-24	Molen Ditch, #1, 100 yd below upper flume
8	7-24	Molen Ditch, #2, 100 yd below upper flume
9	7-24	Molen Ditch, #3, 1/4 mi below upper flume
10	7-24	Molen Ditch, #4, 3/8 mi below upper flume
11	7-24	Molen Ditch, #5, 3/8 mi below upper flume
12	7-24	Molen Ditch, #6, 3/8 mi below upper flume
13	7-24	Molen Ditch, #7, above Canyon Rd., 100 yd above upper flume
14	7-24	Molen Ditch, #8, above Canyon Rd., 100 yd above upper flume
15	7-25	Ferron North, #1, below bridge
16	7-25	Ferron North, #2, below bridge
17	7-25	Ferron North, #3, below bridge
18	7-25	Ferron North, #4, above bridge
19	7-25	Ferron North, #5, above bridge

Table 2. Calculation of seepage rates, Ferron, Utah

Test No.	Radius of seepage meter R_c , inches	Radius of reservoir R_v , inches	Fall in reservoir \bar{H} , in/min	Seepage $I_{s,o}$, ft/day
1	5	0.125	0.28	0.02
2	5	0.125	1.3	0.10
3	5	1.0	0	0
4	5	0.125	0	0
5	5	0.28	0.64	0.24
6	5	0.28	0	0
7	5	0.865	1.2	4.6
8	5	0.125	-0.74	-0.054
9	5	1.0	1.2	6.0
10	5	1.0	0.78	3.6
11	5	0.125	1.0	0.074
12	5	0.125	4.8	0.35
13	5	0.28	1.7	0.66
14	5	0.125	3.1	0.22
15	5	0.125	0	0
16	5	0.125	4.0	0.29
17	5	0.125	2.2	0.16
18	5	0.125	0	0
19	5	0.125	3.9	0.28

Table 3. Calculation of hydraulic conductivity information, Ferron, Utah.

Test No.	d in	H _w in	H _b in	F _f	K ft/day	$\frac{I_{s,o}}{K}$	D _p ft	r _s hr	p in
1	1.0	18	2.0	1.67	0.03	0.67			
2	1.75	19	5.3	1.27	0.07	1.5			
3	2.0	11	0	1.67	24.4	0			
4	1.5	12	0	1.37	0.58	0			
5	2.0	26	0.15	1.67	3.6	0.07			
6	2.5	30	0	1.05	4.8	0			
7	1.75	10	8.0	1.27				3.5	
8	2.0	18	-0.4	1.18	0.58	-0.09			
9	1.5	17	19.5	1.37				6.5	-1.0
10	1.25	14	17.0	1.50				9.5	-1.75
11	2.5	19	2.2	1.04	0.16	0.46			
12	2.0	15	7.9	1.32	0.11	3.3	0.55		
13	1.25	15	0.5	1.50	4.4	0.15			
14	1.0	11	4.5	1.67	0.12	1.8	1.1		
15	1.25	24	0	1.50	0.21	0			
16	2.0	14	4.4	1.18	0.28	1.0			
17	1.5	14	4.8	1.37	0.11	1.5			
18	1.25	18	0	1.50	0.11	0			
19	2.0	14	3.5	1.18	0.34	0.83			

Symbols:

d = depth of penetration of seepage meter

H_w = water depth in channel

H_b = balanced-flow differential head

F_f = flow factor

K = hydraulic conductivity

$I_{s,o}/K$ = hydraulic gradient

D_p = distance of more permeable material below canal bottom

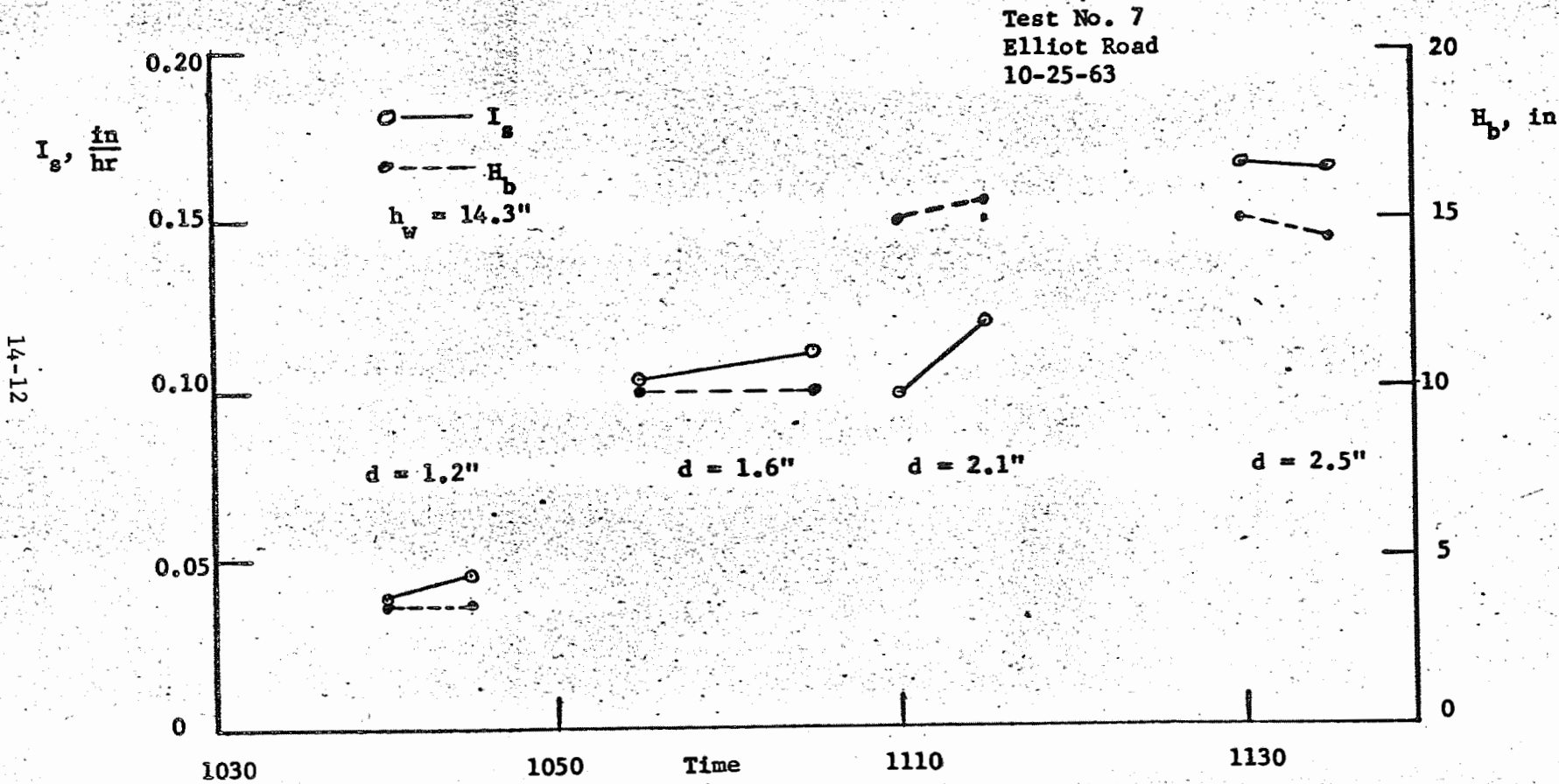
r_s = hydraulic impedance of clogged surface layer

p = pressure head of soil water below clogged layer

Table 4. Effect of depth of penetration of seepage meter on I_s and H_b .

Test and Duration	h_w in	d in	I_s $\frac{1}{}$ in/hr	H_b $\frac{1}{}$ in	Test and Duration	h_w in	d in	I_s $\frac{1}{}$ in/hr	H_b $\frac{1}{}$ in
No. 1 1.75 hr	10.5	1.5	0.55	1.3	No. 7 1.0 hr	14.3	1.2	0.042	3.7
		2.0	0.56	5.6			1.6	0.107	10.0
		2.75	0.62	7.6			2.1	0.105	15.3
			2.5	0.166			14.7		
No. 2 2.25 hr	21.5	1.25	0.31	0.8	No. 8 0.83 hr	11.3	1.0	1.44	7.5
		1.75	0.34	1.8			1.5	1.51	13.3
		2.25	0.28	4.6			2.0	1.54	16.2
		2.75	0.29	6.4					
No. 3 2.66 hr	22	1.0	0.29	2.2	No. 9 1.1 hr	11.4	1.0	0.71	1.5
		1.62	0.28	4.4			1.7	0.69	15.3
		2.0	0.30	5.9			2.1	0.64	15.0
		2.25	0.29	6.6			2.5	0.64	15.0
No. 4 2.83 hr	17	0.5	0.24	13.5	No. 10 0.75 hr	14.5	1.0	1.87	10.5
		0.8	0.25	14.7			1.5	1.76	17.8
		1.3	0.27	14.9			2.3	1.60	18.1
No. 5 1.0 hr	17	1.3	0.93	18.6	No. 11 0.4 hr	11.0	1.0	0.23	0.08
		1.8	0.92	21.4			1.4	0.21	0.15
		2.2	0.90	21.0			1.8	0.15	0.13
No. 6 0.5 hr	16	0.7	0.48	8.7					
		1.1	0.56	15.8					
		1.5	0.50	16.5					

$\frac{1}{}$ Average for each depth of penetration.



Annual Report of the U.S. Water Conservation Laboratory
Figure 1. Test showing I_s increasing with d .

14-13

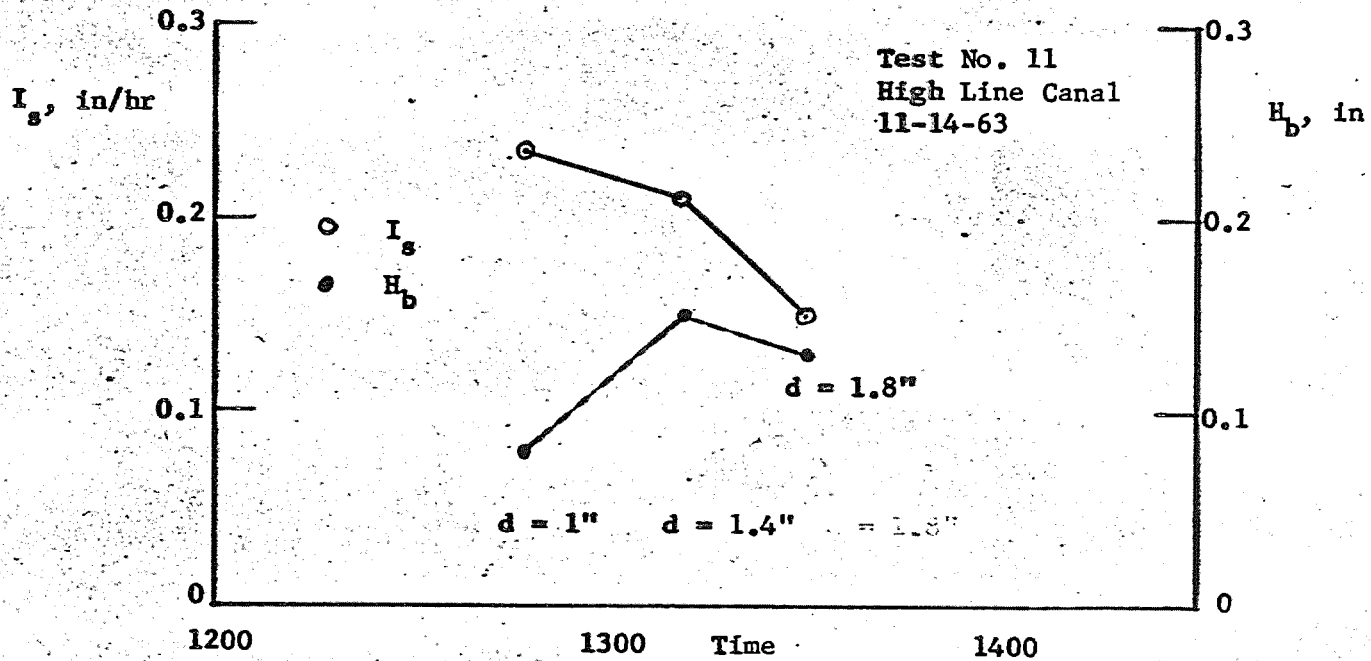


Figure 2. Test showing I_s decreasing with d .

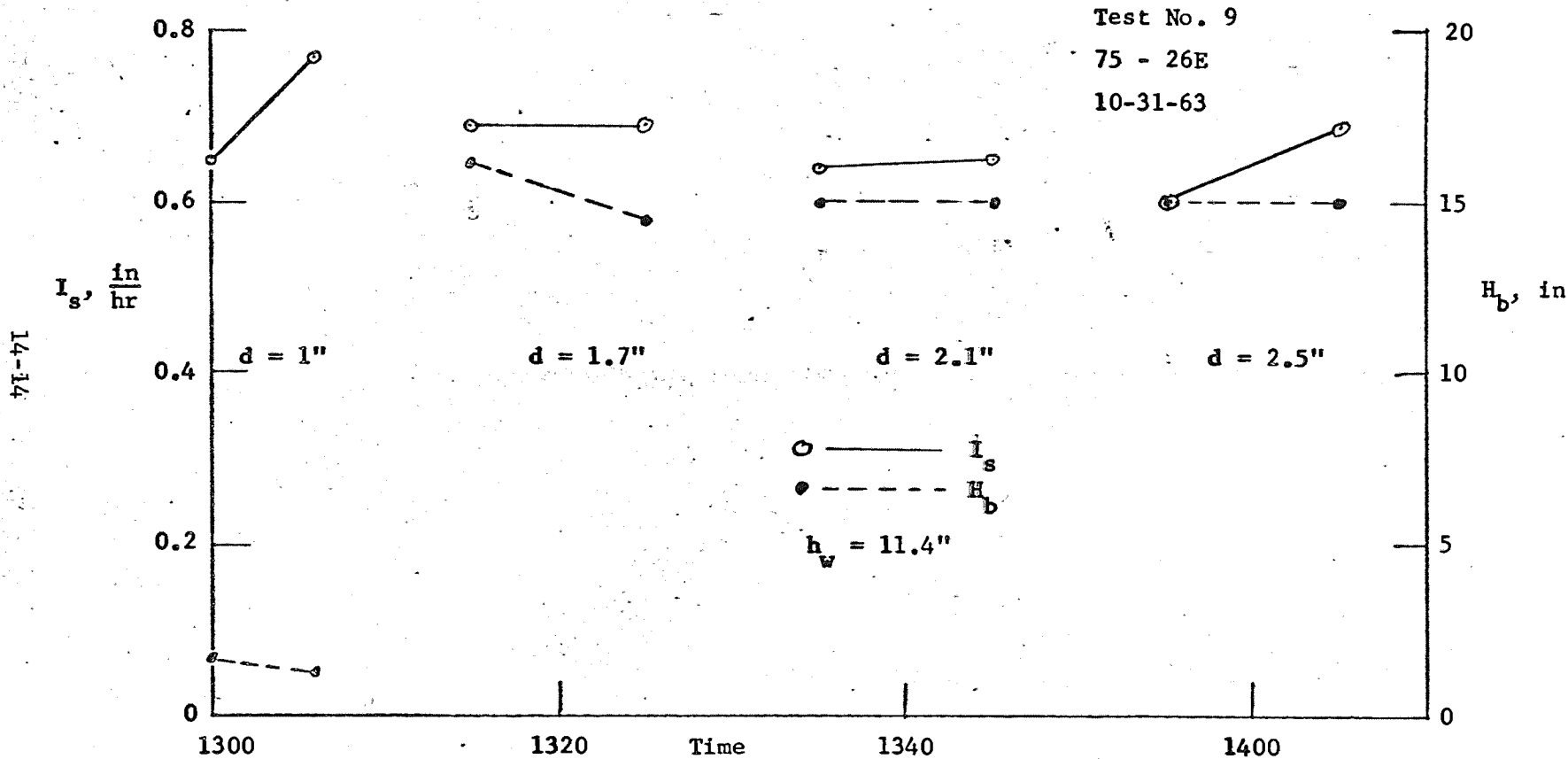


Figure 3. Test showing I_s essentially constant with d and H_b constant after the first increment of d .

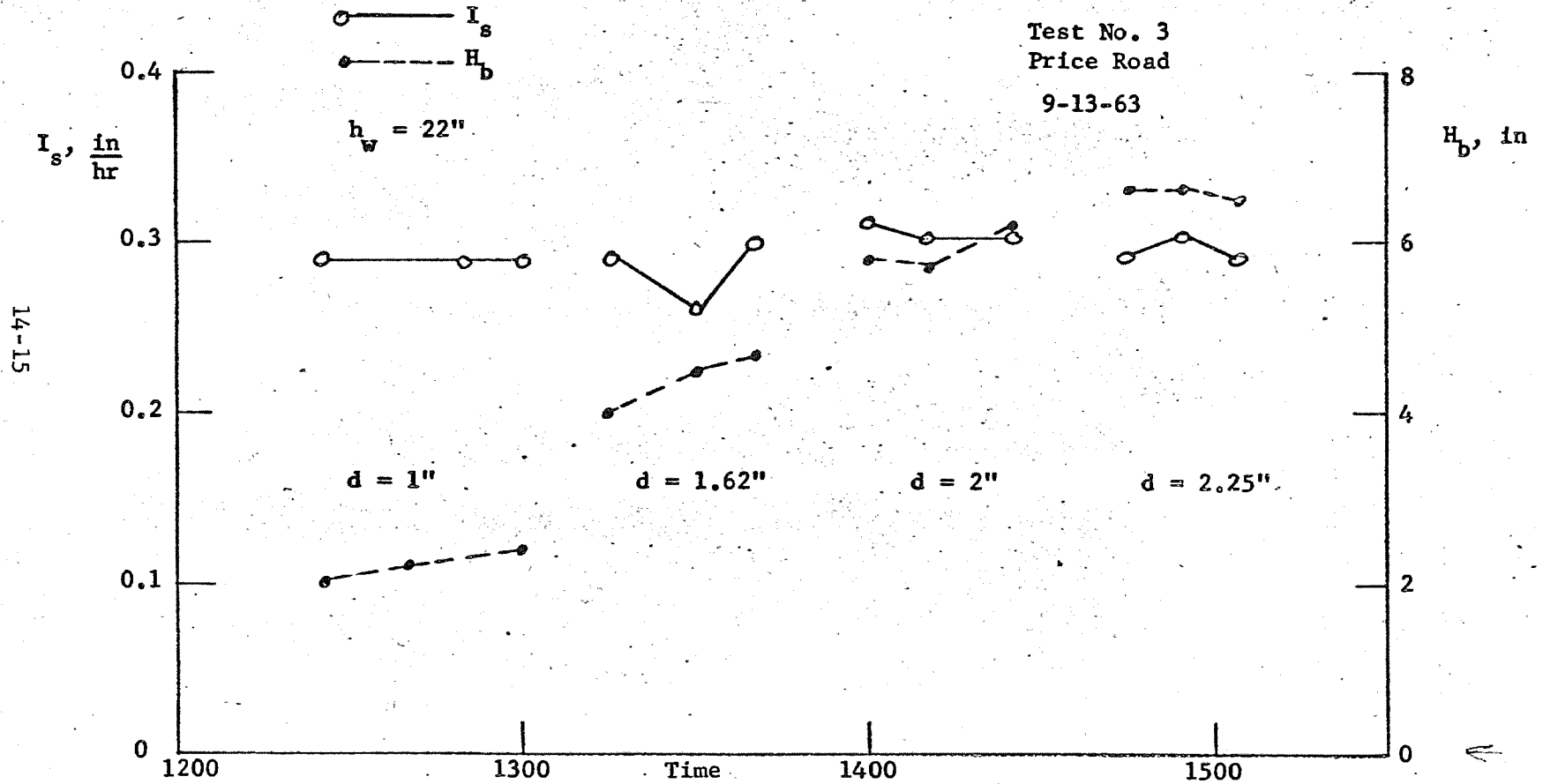


Figure 4. Test showing I_s constant and H_b increasing with d .
Annual Report of the U.S. Water Conservation Laboratory

TITLE: INSTRUMENTATION FOR TURBULENT TRANSFER STUDIES

LINE PROJECT: SWC 4-gG2

CODE NO.: Ariz.-WCL-16

INTRODUCTION:

Evaporation from the earth's surface accounts for the greatest loss of potentially available water. The evaporative process is primarily controlled by meteorological processes which supply the required energy and transport the water vapor. In order to control or reduce evaporative loss, a more complete understanding of the energy exchange and turbulent transport mechanisms and their complex interrelationship with the soil-plant continuum is required. This can be accomplished only by precise and extensive measurements of micrometeorological elements and evaporative flux so that a rational, physical correlation can be derived.

Several theories have been advanced for predicting the evaporative flux such as the eddy correlation, aerodynamic and energy balance techniques. None have been tested adequately under conditions of agricultural interest. Some require instrumentation which is difficult to maintain operational under field conditions. Previous studies (1) indicated that the Bowen equation provided satisfactory determinations of the evaporative flux from water and wet bare-soil surfaces for short periods of time. Tanner (2) has successfully used a modification of the Bowen equation over crop surfaces. This modification has not been tested for less than 1-day periods.

Preliminary testing at the U. S. Water Conservation Laboratory indicated that the modified version of the Bowen equation appeared most promising for determining short-period evaporative flux. Therefore, specialized instrumentation was developed for further testing of the method.

The modified version of the Bowen equation requires measurements of net radiation, soil heat flux, and gradients of air temperature and water vapor. Instrumentation is readily available for measuring net radiation and soil heat flow. Net radiometer improvements are still being made and will be reported under WCL-6. Instrumentation is not readily available for measuring air-temperature and vapor-pressure

gradients. These two elements should be sampled spatially and continually. The sampling and accuracy required limit the instrumentation that can be used. An air-sampling tower was developed for this purpose. The tower and the sensors are discussed, along with other instrumentation.

PROCEDURES:

(1) Air-sampling tower. During periods of light winds, vertical convection cells may exist; therefore, point-sampling of gradients of air temperature and water vapor may lead to erroneous results. The gradients must be sampled spatially. Spatial sampling imposes many problems, the foremost of which is the movement of low millivolt signal cables, vacuum lines, and water supplies through space. To accomplish this, a sampling tower was designed, tested, and redesigned. The complete tower now weighs 85 pounds; consequently, is considered quite mobile. The tower (shown in Figure 1) consists of a vertical post upon which a rotating head is placed. The head is driven by two 4-rpm Hurst synchronous reversible motors (Figure 2). The height of the head above the surface is adjustable from zero to 10 feet. To the head is attached a 10-foot horizontal boom which sweeps through space as the head rotates about the vertical post. Mounted on the end of the boom is the differential psychrometer.

The differential psychrometer with cover removed is shown in Figure 3. The two intakes (35-cm distance apart) sample air from the bottom - thus reducing the possibility of internal reflection of solar radiation, and dust and rain entering into the sensors. Located immediately behind the sensor intakes is a motorized 4-way valve. Behind the 4-wave valve and below the polarity reversing relay is located the differential air-temperature element. Behind the polarity reversing relay is located the water-supply control, and immediately beneath it is the differential psychrometer. The wick surrounding one of the two-junction thermopiles is shown in the figure. In practice, all that is required in way of measurements is the average wet-bulb temperature, the differential wet- and dry-bulb temperature. The differentials must be measured precisely.

The differential signals are connected to Speedomax-H Azar recorders, which have 1000-ohm transmitting slidewires (see Figure 4). The slidewires are connected to Royson Lectrocount II integrators. The output of the integrators consisting of contact closures is connected to two counters of the wind-register system. Thus, the integral of the differential temperatures is obtained during the period between printouts. After the micrometeorological data handling system prints out the integral in digital form, a reset command is given to the 4-way valve, which reverses the intakes relative to each psychrometer and also reverses the polarity of the differentials. While this is going on, the horizontal arm continually sweeps out a 180-degree arc, with one sweep requiring 10 minutes to complete. Investigation of divergence, edge effects, and direct comparison of different surfaces requires at least two air-sampling towers. The second tower is now nearing completion and should be operational in January of 1964.

(2) Dew probes. Measurement of the vapor-pressure gradients required for the modified Bowen equation is not easy under field conditions. Psychrometers are difficult to maintain operational. In an effort to utilize a simpler instrument, two Honeywell dew probes were tested. Several tests were made; however, only the final test is described. To measure the gradient very precisely, the instruments must be exchanged every readout. The instrument must have a time constant of less than 2 minutes if an integrated signal is to be obtained between printouts of the data handling systems.

Two Honeywell dew probes, No. SSP129Z005, were mounted in housings to be used under field conditions. The air flowing through each housing was measured with a Fisher flow meter. Moist air was passed through one dew probe, while the air passing through the other dew probe was first dried. The 66- and 95-percent time constant was determined at various flow rates along with the average temperature indicated by the dew probes. The results are shown in the attached Figure 5 where the equilibrium time and the average output time for the two dew probes are plotted as a function of the air flowing past each probe. At 20 liters min^{-1} the 95-percent change required 3 minutes,

while the 66-percent change required 1 minute and 20 seconds. The average millivolt output decreased from 0.78 mv at a flow rate of 4 liters min⁻¹ to 6.55 mv at a flow rate of 20 liters min⁻¹. The decrease in the average temperature amounted to 0.125 mv, or approximately 3C. From these data it was concluded that in order to achieve a time constant of approximately 1 minute, a very large flow rate would be required. The large flow rate would introduce an error in the dewpoint temperature measurement, consequently, would introduce an error in the measured vapor pressure; therefore, the Honeywell dew probes were not considered satisfactory when a small time constant is required. They would be satisfactory for measurement of profiles if the instruments were exchanged every 15 minutes and printed out at 15-minute intervals, the natural time constant of the instruments being approximately 12 minutes.

(3) Data analysis. Micrometeorological research requires frequent measurement of a large number of elements over an extended period of time. Consequently, considerable volume of data is rapidly acquired. It is desirable to be able to analyze the data quickly, efficiently, and economically. To achieve this objective, a program was written for the GE225 computer. This program contains the following generalized linear equation:

$$\text{Eq I} = \left\{ \left[(\text{Ch A} - \text{Ch B}) \cdot \text{C} + \text{Eq J} + \text{Eq K} + \text{D} \right] \left(\text{Eq L}^m \right) \right\} \text{E} \quad \text{F}_1, \text{F}_2 \quad [1]$$

Equation I is the equation to be solved. Channel A and channel B are inputs from the data handling system; C, D, and E are any constant. Equations J, K, and L are previous solutions at the same time printout, and m is any integer. F₁ and F₂ are flags. When flag F₁ is used, the computer will provide from memory the function of $\frac{\gamma}{\gamma + s}$ at eight different atmospheric pressures, will provide conversions from EMF to degrees centigrade using the National Bureau of Standards thermocouple conversion tables, will convert degrees of centigrade to σT^4 , and σT^4 to degrees of centigrade.

The use of the program requires identification of the variables in the generalized linear equation. As many as 100 Equation 1's can be solved in a run. The equations and the paper tape input are supplied to the processing center and are fed directly to the computer without consulting a programmer.

Samples of the types of solutions which can be obtained from the generalized linear program are given in Equations 2, 3, and 4:

$$LE = -(R_n + S + S') \left\{ 1 - \frac{\gamma}{\gamma + s} \left(\frac{\Delta T_a}{\Delta T_w} \right) \right\} \quad [2]$$

LE is the evaporative flux determined with the modified Bowen equation, R_n is the net radiation, S is soil heat flow, S' is the change in energy storage above the soil heat-flow transducer, $\frac{\gamma}{\gamma + s}$ is used to convert wet-bulb temperature gradients into vapor-pressure gradients, ΔT_a is the gradient of the air temperature, and ΔT_w is the gradient of the wet-bulb temperature.

$$S' = \frac{5 \times 0.5 \times 0.5}{\text{time sampled}} \left[(T_s + T_5)_b - (T_s + T_5)_e \right] \quad [3]$$

S' is the change in energy storage above the heat-flow transducer, T_s is the surface temperature, T_5 is the 5-cm temperature, and b and e represent the beginning and ending of the period.

$$T_r = \frac{1}{\epsilon \sigma} \left(C\epsilon T^4 - R_n - R_{su} \right)^{1/4} \quad [4]$$

T_r represents the temperature determined radiometrically, ϵ and σ represent the emissivity and the Stefan-Boltzmann constant, C is the calibration constant, T is the absolute temperature to the fourth power, R_n is net radiation, and R_{su} is the reflected solar radiation.

Utilizing this generalized linear equation, complete data analysis can be obtained on an overnight basis, and the cost of such analysis is very much less than would be required if the same amount of data was computed by hand. For example, in one experiment 39 channels of data were recorded every 15 minutes for two days. Eighty-two equations were used to analyze the 39 channels of data. A total of 15,744 basic calculations were made, 3936 hourly averages and 164 daily totals were computed, for a grand total of 19,844 usable calculations. The two days of data cost \$80 to analyze, or approximately \$0.004 cent per printed answer. All calculations are made with four-decimal-point accuracy. The answers are columnated by parameter with six columns per page, and three copies of each page are supplied. The generalized linear program has proven to be a very worthwhile tool in analyzing micrometeorological data rapidly and economically.

(4) Variable-resistance, millivolt source. In order to properly connect field sensors to the micrometeorological data handling systems, a variable-resistance millivolt source was deemed necessary for several reasons. The most important reasons are: first, to insure that the cables are connected to give the right polarity, connected to the proper channels, and to insure that stray millivolt signals are not being picked up; secondly, to adjust voltage dividers. The first reason is obvious. The second reason is not so obvious, and a further explanation is necessary. Since some of the micrometeorological sensors have outputs which exceed the range of the recorder, and since some have different calibration factors, it is necessary to scale the input voltage to match the recorder range so that the analog output is in terms of standard physical units or some easy multiple thereof. To accomplish this, a variable-resistance millivolt source which can generate a signal over a resistance comparable to that of the transducer is needed. For example, if a pyrliometer had a calibration constant of $10 \text{ mv ly}^{-1} \text{ min}$ and an internal resistance of 10 ohms, the millivolt source would be adjusted to yield a 10-millivolt output across a resistance of 10 ohms. The millivolt source is carried into the field, plugged

into the cable in place of the sensor, and the voltage is scaled down with a voltage divider located in the data handling system so that the analog output is equivalent to $500 \text{ digits ly}^{-1} \text{ min}$.

The schematic for the variable-resistance millivolt source is shown in Figure 6. Basically, it consists of a Mallory mercury battery, $3 \cdot 10^5$ ohm resistance steps, $9 \cdot 10^4$ ohm steps, and one 10-term potentiometer having a resistance 10^4 ohm. The output resistance is adjusted with a 10-term potentiometer having 100-ohm resistance. The variable-resistance millivolt source is capable of generating a millivolt signal ranging from 0.006 mv to 10 mv at 1 ohm to from 0.4 mv to 10 mv at 100-ohm source. The variable-resistance millivolt source has proven to be a very valuable tool.

(5) Wind register system. The wind register system described in the 1961 annual report, consisting of 9 Veeder-Root electromechanical counters, did not prove satisfactory in that the readout device of the counters required continual repair. Consequently, another wind register system was designed which utilized C. P. Clare type 210 stepping switches with 2 nonbridging levels, 10 points per level, 1 form C interrupter, and 1 form C off-normal contact assembly, furnished with oversized indicating wheel and base mounting brackets. Four switches were connected in series, forming one 4-digit counter.

The wind register system with the front panels removed is shown in Figure 7. Each row of stepping switches represents two counters. The counters are wired so that each unit switch has a load resistor in series with the coil to prevent overheating during periods of constant energization, and all contacts are protected with a capacitor-resistor spark suppressor. The counters are operated by intermediate Potter-Brumfield RS5D, 6-VDC relays, shown in lower right.

The operation mode is as follows: The counters count until the system begins to print out the lines, which include the counter data. The counting action is then interrupted, the counters are read out, and a reset command (approximately 10 seconds) is given by the system which causes the stepping switches in each counter to

reset sequentially. The counting action is then resumed. All counters may be turned on and off and may be connected to contact closures via banana plugs on the front panel. Two wind register systems have been built, one to be used with the micrometeorological data handling system located in the lysimeter room, the other to be used with the data handling system in the mobile micrometeorological laboratory.

(6) Determination of evaporation from a free-water surface using the modified Bowen equation. Four stock tanks, approximately 3 feet deep and 9 feet in diameter, are located at the U. S. Water Conservation Laboratory. These tanks had been used to study evaporation suppressants. Since these tanks were readily available, an experiment was conducted to determine if the modified Bowen equation would predict evaporation from a very small free-water surface.

Net radiation, solar radiation, reflected solar radiation, and total hemispherical radiation, both upward and downward, were measured over the tank. Water temperatures were measured at the surface and at 10, 20, 40, and 80 cm. The surface temperature was measured by fastening a thermocouple to a styrofoam block so that the thermocouple junction was just touching the surface of the water. The psychrometers were located at 5 and 40 cm above the water surface of the tank. Evaporation from the tank was measured using a point gage.

The experiment was conducted for only one day. Unfortunately, the day was not the most desirable. The sky was clear prior to 0700, becoming cloudy with showers occurring at 0800. Intermittent cloudiness prevailed the rest of the day. Results of this experiment are summarized:

	Flux, 21 August 1963 langleys day ⁻¹
Evaporation, measured (LE).....	-327
Evaporation, estimated with the modified Bowen equation (\hat{LE}).....	-265
Net radiation (R_n).....	150
Energy storage in the water (W).....	141
Sensible heat flux (A) over a water surface.....	36

Although these totals do not reflect the fact, the evaporation rates occurring during the night and the day are of comparable magnitude, with the energy supplied by the water within the tank for the nocturnal evaporation.

The geometry of the tanks is such that the change in energy of the water cannot be adequately measured; i.e., the area of the sides is large compared to that of the bottom. The diurnal heat wave penetrates to the bottom of the tank so the heat flow out the bottom of the tank must be measured; however, the heat flow out the sides of the tank cannot be neglected because of the large side area. Furthermore, the tanks are shallow enough that the radiant energy penetrates to the bottom of the tank and is converted into sensible heat at this point. This apparently causes convection currents within the tank, making evaluation of the energy storage in the tank very difficult from temperature measurements.

The conclusion can be drawn that the Bowen equation appeared to work over such a small surface area. However, the error in measurement of some 70 ly out of 320 is partially due to the inability to measure the energy storage in the water layer.

(7) Testing the modified Bowen equation. During the calendar year 1963, several tests were conducted to determine how closely the modified Bowen equation would estimate the evaporative and sensible heat flux. Basically, the Bowen ratio consists of a statement of the ratio of sensible heat to latent heat, as

$$\beta = \frac{A}{LE} ,$$

which is equal to

$$\frac{C_p K_H (\partial T / \partial Z)}{L K_w (\partial Q / \partial Z)} ,$$

where β is the Bowen ratio; A is the sensible heat flux; LE is the latent heat flux; C_p is specific heat of air at constant pressure; K_H is the transfer coefficient for sensible heat; T is temperature; Z is height; L is the energy required to vaporize one gram of water; K_w is the transfer

coefficient for latent heat; and Q is the specific humidity. When the gradients are measured over the same distance and an assumption is made that the ratio of the transfer of sensible heat coefficient to latent heat coefficient is one, β is equal to $\gamma\Delta T/\Delta Q$, where γ is the psychrometric constant. The Bowen ratio is then substituted in the energy balance equation

$$R_n + S + LE + \dots = 0 \quad ,$$

with the result that LE is equal to a $-(R_n + S) / (1 + \beta)$. If psychrometers are used to measure the vapor pressure instead of specific humidity, the equation may be rewritten in the form of

$$LE = -(R_n + S) \left[1 - \frac{\gamma}{P + s} \left(\frac{\Delta T_a}{\Delta T_w} \right) \right]$$

where γ is defined as the psychrometric constant and S is defined as 0.63 times the slope of the saturation vapor-pressure curve in the psychrometric tables over the atmospheric pressure (P). The last equation was used to test the modified Bowen equation. These data are summarized in Table 1.

In discussing these data by series, it is evident that the modified Bowen equation did not determine the actual evaporative flux with a reasonable degree of accuracy in Alfalfa 1. A comparison of daily and daylight totals indicates that the measurement of $R_n + S$ is not sensitive enough during the nocturnal hours. The gradients of temperature and wet bulb appear to have the right sign. It appears that the small error involved in measuring either net radiation or soil heat flow causes the sign of this term to be wrong, giving a positive sign for LE. Therefore, just the daylight data are to be discussed. Future investigations are to be conducted to determine the source error in measurement of both R_n and S during the nocturnal hours.

In discussing the daylight data for Alfalfa 1, it appears that the modified Bowen equation did not estimate the flux with a reasonable degree of accuracy. Even though the flux was small, the absolute error amounted to 60 ly for the daylight period. The gradients for these calculations were measured at 17 and 56 cm above the crop surface. These data were collected using a temporary psychrometer arrangement, with the psychrometer positions being manually interchanged every 30 minutes, while the data were collected automatically at 5-minute intervals. It appears that the gradients of air temperature and wet bulb were measured at too great a height above the crop surface; consequently, did not reflect the true gradients which regulate the flux of sensible and latent heat.

By 10 April in the Alfalfa 3 run, this temporary psychrometer arrangement had been replaced with an automatic device that was described in the 1962 Annual Report. Briefly, the sampling tower at this time consisted of a 10-foot horizontal arm mounted on a vertical support, the arm being motor-driven to sweep out a 180-degree arc in 10 minutes. Differential psychrometers were mounted on each end of a 60-inch arm which was attached at right angles to the horizontal arm. The horizontal arm was then motor-driven to interchange each sensor and height after the micrometeorological data handling system had printed out the data. This system did not prove satisfactory in that sometimes the horizontal arm did not rotate upon the command from the data handling system. Also, difficulty was encountered in keeping the psychrometer wicks wet. Therefore, the data presented are for periods when it appeared that everything was working. Using this tower in Alfalfa 3 on 10 April and a 5- and 40-cm gradient above the crop surface, an error of estimate of 4 percent - or in absolute terms, 9 ly - was obtained. Alfalfa 3 was a two-height study in which the area west of lysimeter 1 and lysimeter 2 were of the same height, being 13 cm, while the alfalfa on lysimeter 3 and the area east of the lysimeter was 35 cm.

In Alfalfa 4 on 22 April, the error of estimate was 1 percent or 2 ly. This was a three-height study in which the alfalfa west of

lysimeter 1 and lysimeter 1 was 10 cm; the alfalfa on lysimeter 2 was 30 cm, and the alfalfa on lysimeter 3 was 50 cm. On 23 April the error of estimate was a -1 percent, amounting to 3 ly.

During Alfalfa 7 the error of estimate increased to a -13 percent on both 3 and 4 July. In this case the 5- and 40-cm gradients were still used. The data were printed out at 5-minute intervals. This was a three-height study in which lysimeter 1 was 16 cm, lysimeter 2 was 20 cm, and lysimeter 3 was 49 cm. On both of these days, the sensible heat flux was quite large, over 200 ly day^{-1} , which may partially explain this underestimation of the latent heat flux by 13 percent. Another probable explanation is the fact that the areas treated similarly were only 15 meters wide, and the wind profile may not have adjusted to this new roughness.

In Alfalfa 6, 20 June, the entire field was treated similarly and the alfalfa was 30-cm tall. The modified Bowen equation underestimated the evaporative flux by 5 percent on 20 June, and by 8 percent on 21 June. The difference in the underestimation between 20 and 21 June may be due to the difference in advection. On the 20th of June with the average wind speed of 135 cm sec^{-1} , the sensible heat flux was 170 ly, while on the 21st of June with the average wind speed of 192 cm sec^{-1} , the sensible heat flux was nearly 300 ly.

In Alfalfa 9 the modified Bowen equation underestimated the flux again by 1, 5, and 17 percent on 25, 26, and 27 June, respectively. These data were collected over a dry stubble field where the evaporative flux was indeed small so the absolute errors were 1, 8, and 35 ly, respectively. Again we notice that the greater underestimation occurs with the greater wind speed; that is, the 17 percent was associated with an average wind speed of 225 cm sec^{-1} .

The data from Alfalfa 6 and Alfalfa 9 indicate that as wind speed increases above 150 cm sec^{-1} , the underestimation increases. This may be due to the fact that there is a considerable horizontal advection and that the upper sensor is not located with respect to the true gradient of transport.

In Alfalfa 10, 8 and 9 August, the average errors of estimate were 1 and 7 percent for the 8th and 9th, respectively. These errors represent 3 and 29 ly; again the greatest underestimation appears to be related to the stronger wind speed.

In summary, it appears that the modified Bowen equation can be used to determine the evaporative flux during periods of light wind (less than 100 cm sec^{-1}) with an error less than 5 percent. As the average wind speed increases to 150 cm sec^{-1} , the error of estimate is less than 10 percent. The error of estimate increases to less than 20 percent as the average wind speed approaches 200 cm sec^{-1} . Part of the error of estimate may be due to the size of the field. A parcel of air requires 23 seconds to move from the edge of the field to the sensing tower when the average wind speed is 200 cm sec^{-1} . In 23 seconds this parcel of air may not have been sufficiently changed to its new environment, thus top sensor may not reflect the true gradient of transfer. Another possibility is that the differential psychrometers were located approximately 60 inches apart; therefore, the gradients used may not be the true gradients. However, this error is expected to cancel out over a period of time with the sensors moving through space. The third possibility could be errors in actual measurements due to the types of sensors used. These errors are expected to be eliminated by using the differential psychrometer described in Section II.

SUMMARY AND CONCLUSIONS:

Accurate short-period determination of evaporation from various surfaces is of primary importance in water conservation to establish maximum rates of evaporation and to understand the complex dependence upon meteorological processes. Lysimetric measurement of soil-moisture depletion by weighing is undoubtedly the best method to routinely and accurately determine evapotranspiration for short periods. Lysimeters, however, do have limited use due to their immobility, time required for an installation, and the size required for certain plants. Micro-meteorological methods can be used to determine the evaporative flux for short periods of time and have several distinct advantages. They

do not require alteration of the surface, are not limited to a particular crop surface, and can be employed with a great deal of mobility. The main limitations are the instrumentation and the basic assumptions of the methods which may not be met under conditions of agricultural interest. Previous work (1) indicated that the modified Bowen equation appeared to be the most promising meteorological method to routinely determine short-period evaporation rates. Measurements were made during the past year to compare the evaporative flux determined by the modified Bowen equation with that obtained from the lysimeters. The results indicate that the modified Bowen equation can be used to determine evaporation during the daylight hours with an error of less than 5 percent when the average wind speed is less than 100 cm sec^{-1} . It appears that as the wind speed increases, the error of estimate also increases. These results were obtained while the instrumentation used was in a period of development, and therefore reflect some instrumental errors.

The results obtained with the modified Bowen equation during the nocturnal hours were generally of opposite sign to that determined by the lysimeters. The gradients of air temperature and vapor pressure have signs which are in agreement with the lysimetric flux. Therefore, it appears that small errors exist either in the measurement of net radiation or soil heat flux; the two parameters which determine the sign of the evaporative flux cause the evaporative flux to have the opposite sign. The nocturnal error is relatively small when daily totals are considered.

Instrumentation for the measurement of air-temperature and vapor-pressure gradients has been improved during the past year. The present air-sampling tower is a lightweight and fairly portable device, consisting of a vertical mast upon which a rotating head is mounted. Attached to the rotating head by a 10-foot horizontal boom is a box containing two small psychrometers, a 4-way switching valve, water-control mechanism, and a polarity reverser. Externally attached to the box are two air intakes. In operation the differential wet- and dry-bulb signals are fed through the polarity reverser to two integrators. These signals

are integrated until the data handling systems print out the data. A command from the data handling system causes the psychrometers to be reversed with respect to the air intakes, and causes the polarity of the differential signals to be reversed. The air-sampling tower with associated parts is quite an improvement over previous instrumentation in that the air-temperature and vapor-pressure gradients are sampled spatially, continuously, and sensor errors are cancelled by reversing the sensors with respect to the intakes.

Dew probes manufactured by Minneapolis-Honeywell were tested to determine the feasibility of their use for measuring vapor-pressure gradients. The dew probes were not considered satisfactory for the intended use because of their time constant. The purposed use required a time constant of less than 2 minutes -- preferably 1 minute. The dew probes have a time constant of approximately 3 minutes under the extreme ventilation rate of 20 liters min^{-1} . At this ventilation rate, the temperature of the dew probe appears to be 3C less than that in still air of the same moisture content.

Micrometeorological research requires complex analysis of a large number of data obtained from many sensors, which are frequently measured. Efficient analysis of these data requires the use of a computer and a very flexible program. To this end a program was written for the GE-225 computer. The fixed portion of the program allows the computer to accept the paper tape image obtained from the data handling system, allows these data to be processed with a generalized linear equation, and computes hourly averages and daily totals of the solutions of the linear equation. Using the program, a large number of calculations may be made on overnight service with a cost of approximately \$0.004 cent per calculation. The fixed portion of the program allows for the variables in the generalized linear equation to be identified by the personnel at the Laboratory, thus eliminating the need of consulting with a programmer. The program has proved to be a very valuable tool in micrometeorological research.

A variable-resistance millivolt source was constructed as an aid for wiring and calibrating portions of the micrometeorological data

handling systems. The millivolt source has proven to be a very valuable instrument because many scaling and wiring errors have been eliminated with its use.

The wind register system described in the 1961 Annual Report did not prove to be satisfactory in that the readout device of the counters required continual repair. Consequently, two additional wind register systems were designed and built using four 10-level stepping switches in tandem for each counter. The stepping switches have a more positive readout device than the Veeder-root counters used in the previous wind register system. These wind register systems have been tested and have been found capable of accurately counting at the rate of 1000 cpm. The total counts are read out in digital form by the data handling systems. The counters can be automatically or manually reset to zero.

An experiment was conducted to determine if the modified Bowen equation would determine the evaporative flux from one of four stock tanks located at the Laboratory. The results obtained indicated the geometry of the tanks was such as to preclude their use for this purpose largely because of the heat transfer through the walls. The results indicated that the evaporative rates at night were comparable to those obtained during the daylight periods on an intermittently cloudy day. Thus, 50 percent of the energy required for the evaporation was supplied by the water in the tank.

REFERENCES:

- (1) Fritschen, L. J., and Van Bavel, C. H. M.
1963. Experimental evaluation of models of latent and sensible heat transport over irrigated surfaces. Internatl. Assoc. Sci. Hydrol., Pub. No. 62, Com. for Evaporation, pp. 159-171.
- (2) Tanner, C. B.
1960. Energy balance approach to evapotranspiration from crops. Soil Sci. Soc. Amer. Proc. 24:1-9.

PERSONNEL; Leo J. Fritschen

Table 1. Solar radiation, average wind speed, evaporative flux determined with the modified Bowen equation and lysimeters for daily periods and daylight periods.

Date	Alfalfa Series	R_{sd}	\bar{U}	Lys	\widehat{LE}		LE		$\frac{\widehat{LE}-LE}{LE \times 100}$
					Total	Day	Total	Day	Day
		ly day ⁻¹	cm sec ⁻¹	← langley's →					
8 Feb	1	363	80	I	-222	-218	-189	-159	37
				II	-220	-217	-193	-171	27
				III	-229	-242	-176	-155	56
				Ave	-224	-226	-186	-161	40
10 Apr	3	418	135	II	-261	-236	-246	-227	4
22 Apr	4	698	107	II	-254	-356	-370	-354	1
23 Apr	4	705	118	II	-393	-397	-420	-400	-1
20 Jun	6	737	135	I	-522	-533	-590	-559	-5
				II	-449	-513	-572	-542	-5
				Ave	-448	-522	-581	-551	-5
21 Jun	6	762	192	I	-644	-660	-752	-710	-7
3 Jul	7	671	159	II	-212	-487	-625	-560	-13
4 Jul	7	694	144	II	-479	-492	-613	-568	-13
25 Jul	9	675	133	II	-164	-167	-187	-169	-1
26 Jul	9	640	142	II	-132	-152	-189	-160	-5
27 Jul	9	622	225	II	-144	-167	-246	-202	-17
8 Aug	10	603	75	I	-386	-383	-391	-373	3
				II	-320	-335	-388	-374	-10
				III	-400	-375	-376	-354	6
				Ave	-367	-364	-385	-367	-1
9 Aug	10	650	90	I	-	-402	-504	-427	-6
				II	-	-377	-493	-422	-11
				III	-	-402	-496	-421	-4
				Ave	-	-394	-498	-423	-7

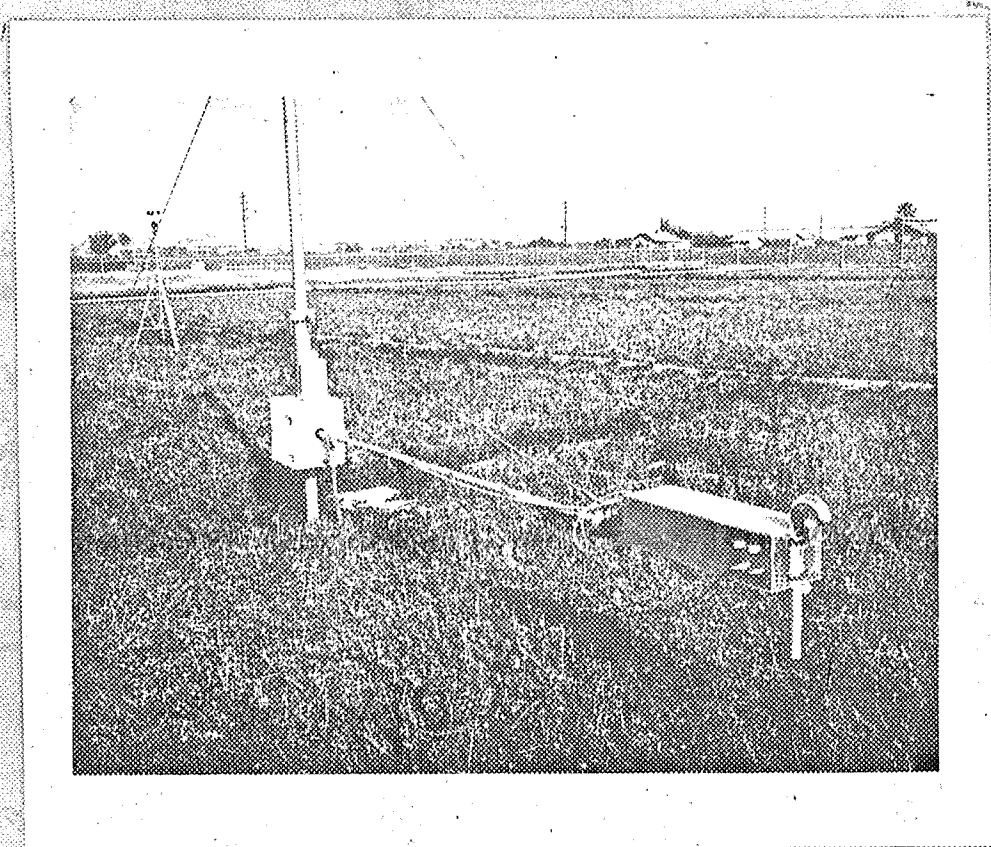


Figure 1. Air-sampling tower.

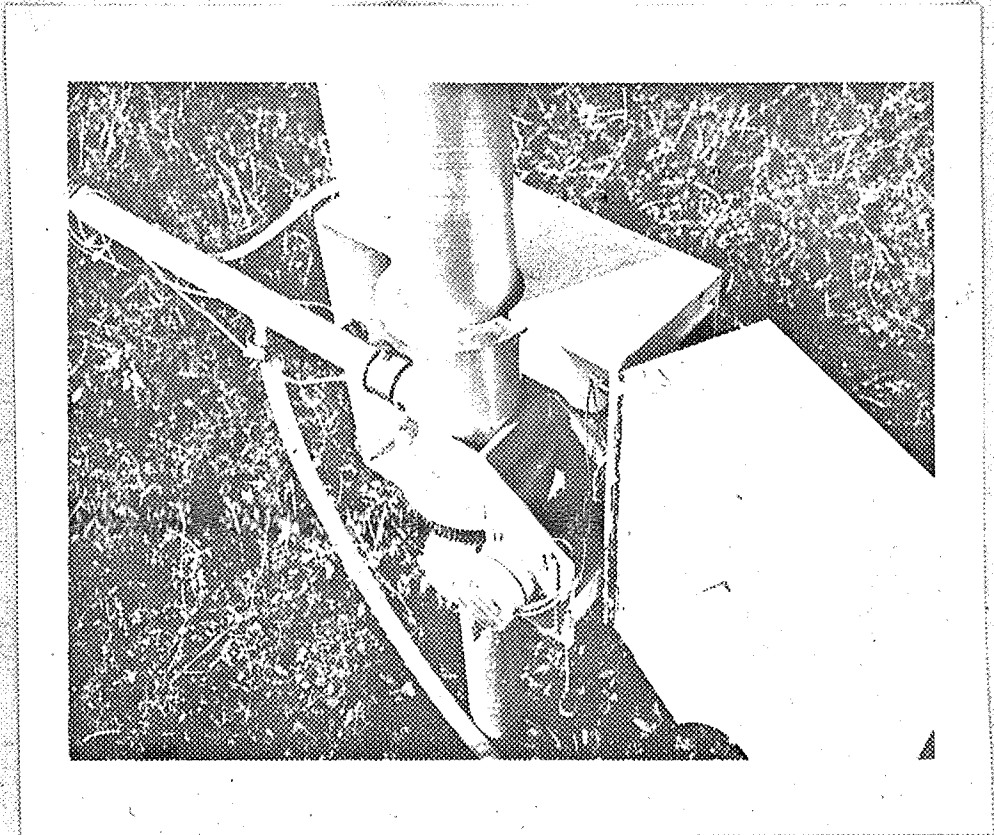
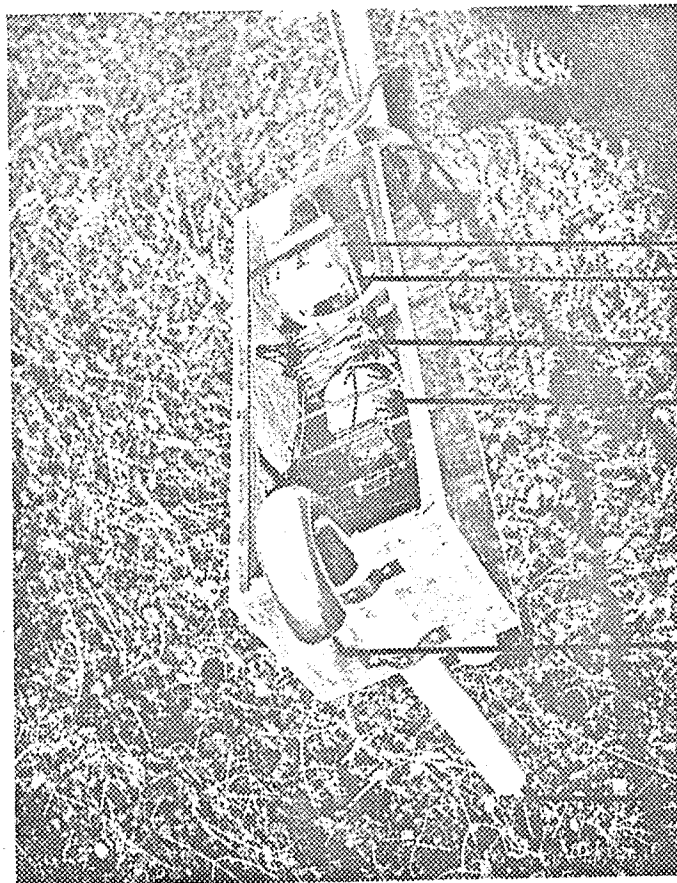


Figure 2. Closeup of the air-sampling tower drive mechanism.



- water supply control
- wick around the thermo-
pile of one psychrometer
- polarity reverser
- motorized 4-way valve
- upper intake
- lower intake

Figure 3. The differential psychrometer with housing removed.

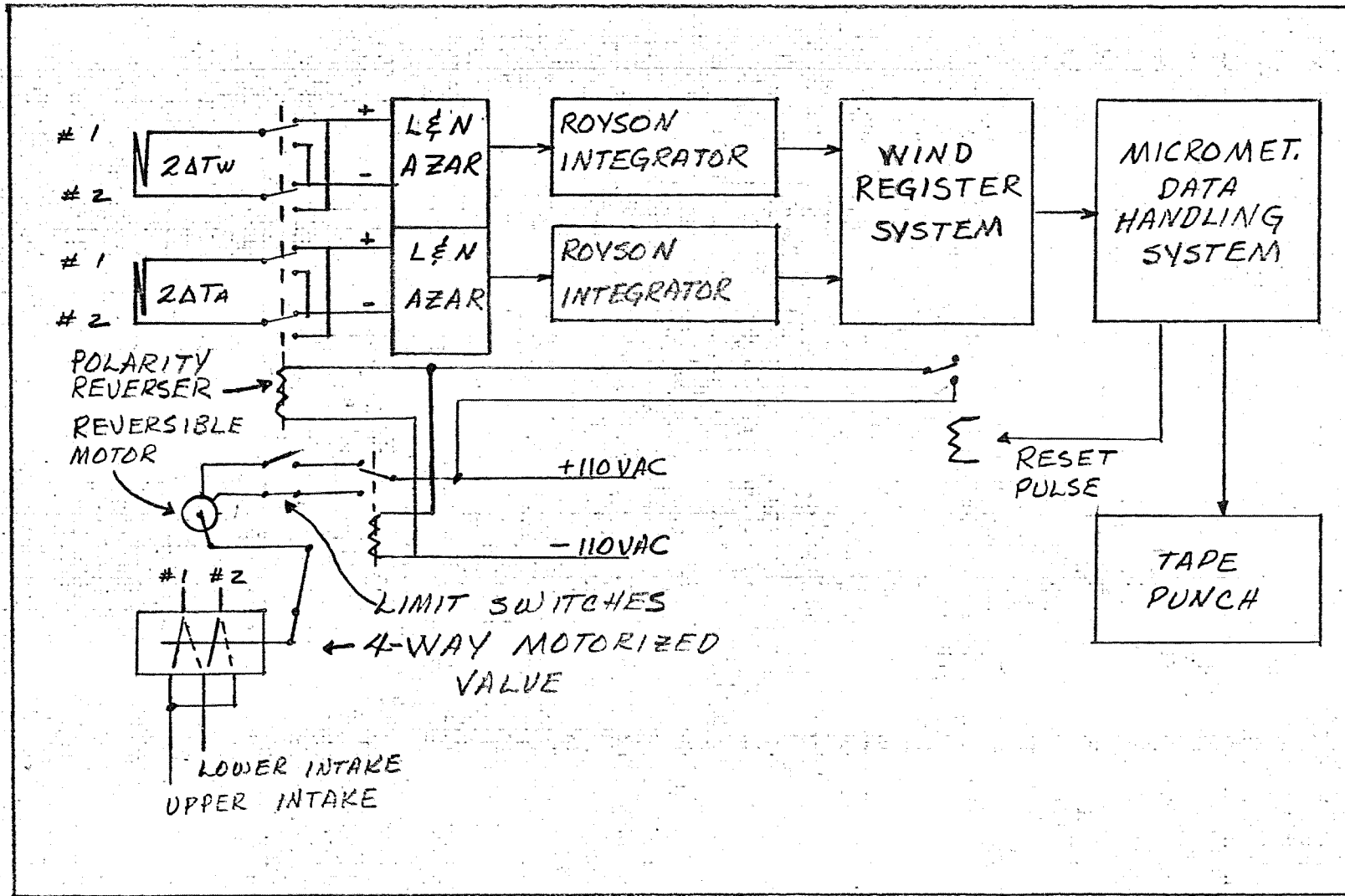


Figure 4. Functional diagram of the air-sampling tower and recording system. Annual Report of the U.S. Water Conservation Laboratory

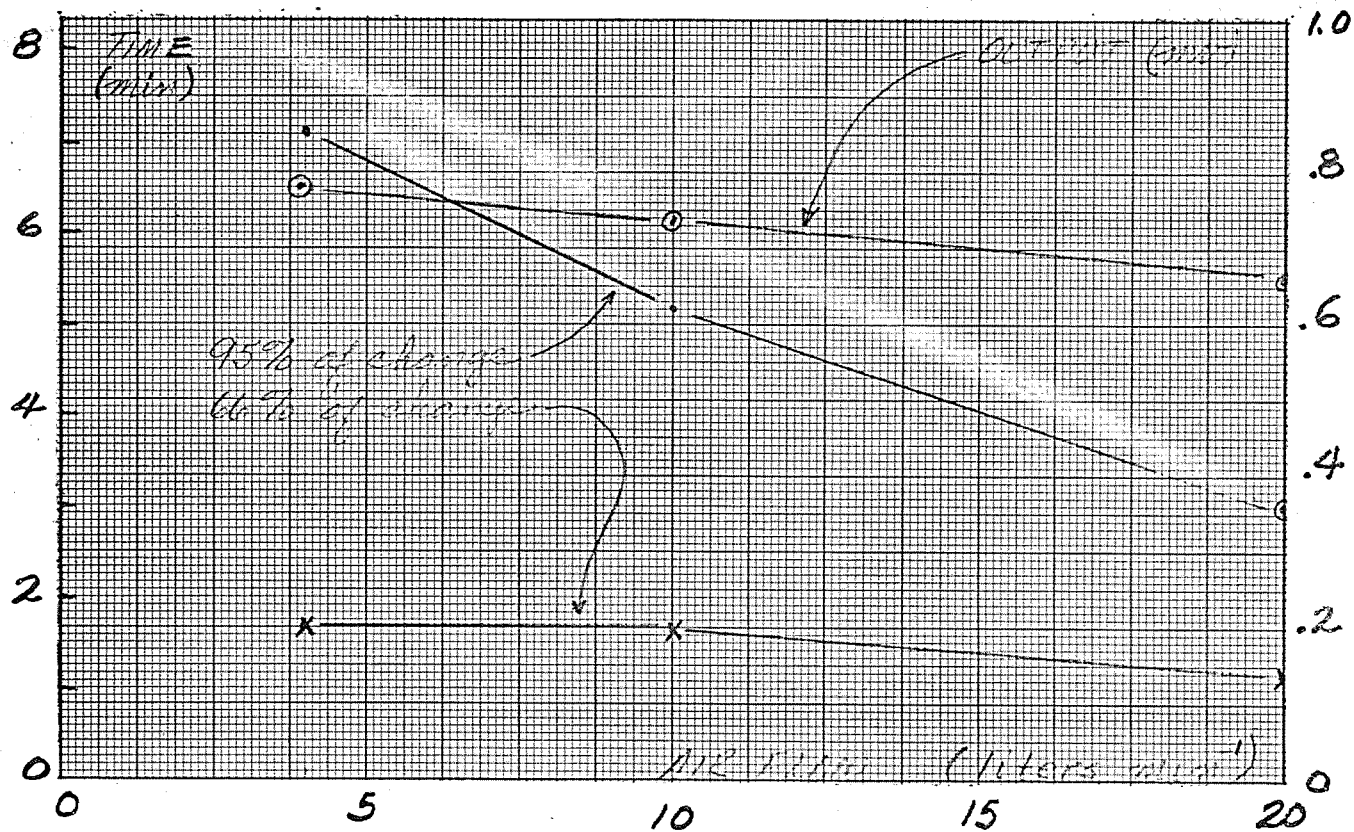


Figure 5. Equilibrium time and average output of two Honeywell dew probes, #SSP129Z005, as a function of air flowing past each probe. Annual Report of the U.S. Water Conservation Laboratory

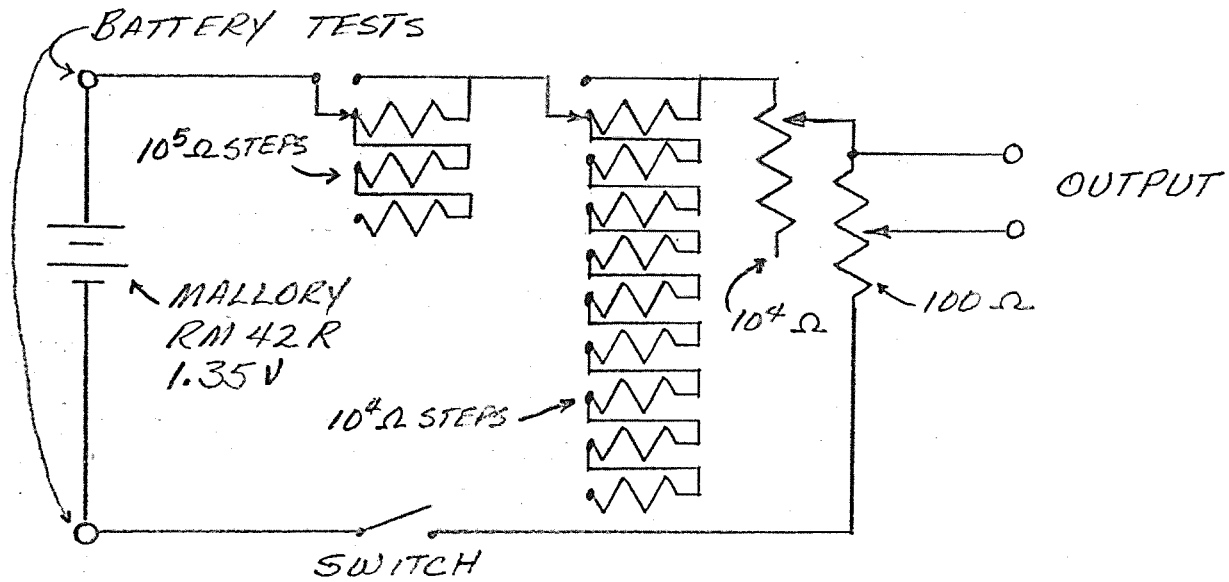


Figure 6. Variable-resistance millivolt source. Annual Report of the U.S. Water Conservation Laboratory

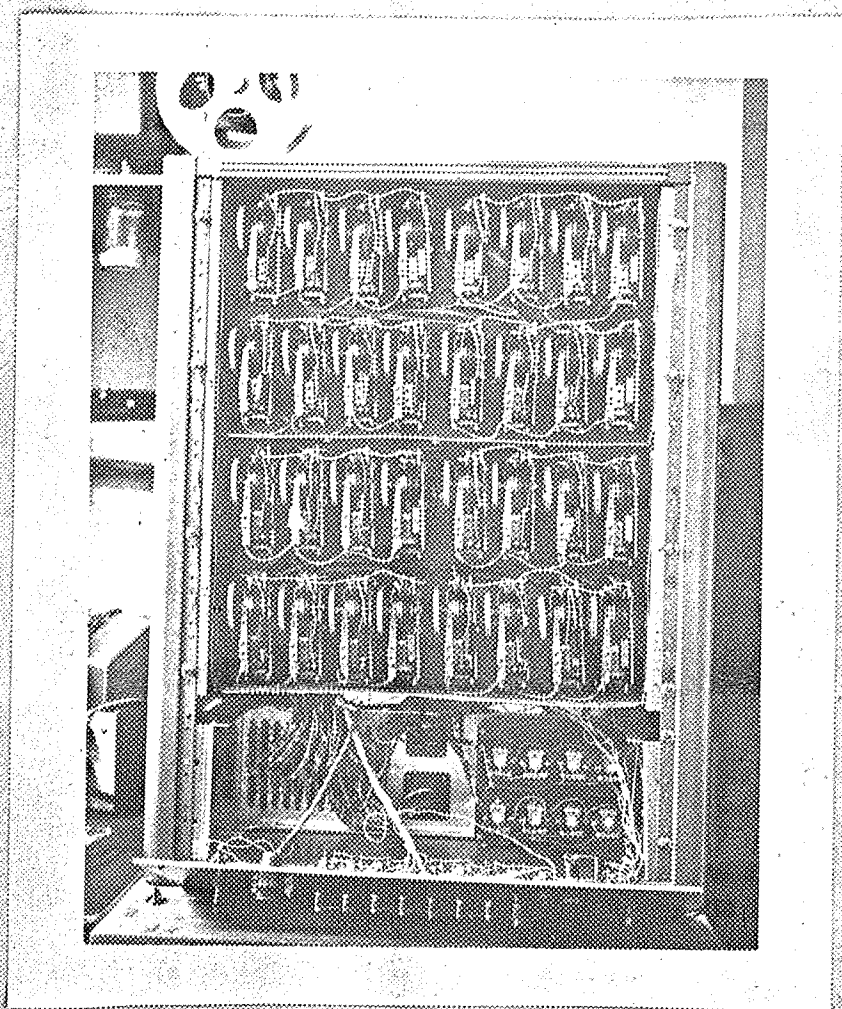


Figure 7. Wind register system with front panels removed.

TITLE: SURFACE ENERGY BALANCE AND EVAPOTRANSPIRATION
OF IRRIGATED ALFALFA

LINE PROJECT: SWC 4-gG2

CODE NO : Ariz. WCL-17

INTRODUCTION:

During the calendar year of 1963 investigations were carried out to determine the relationship between evapotranspiration and the surface energy balance for winter, spring, summer, and fall conditions, to determine the relationship between evapotranspiration and micrometeorological parameters over alfalfa of different heights, and over dry stubble, and also to determine how these relationships change as the soil moisture is depleted. A total of 30 days of data was recorded.

PROCEDURES:

The activities of the calendar year are summarized in Table 1. Net radiation was measured 1 meter above the crop with modified version of the net radiometer described in "Construction and evaluation of a miniature net radiometer" (see section on Papers Published in 1963). The modification consisted of replacing the two planar sheets of polystyrene and the transducer with a plate transducer the same size as the rings, having an output in excess of $1.5 \text{ mv ly}^{-1} \text{ min}$. Soil heat flow was measured at 5-cm depth with National Instruments Laboratory HF-2 heat-flow transducers. The surface soil temperature and the temperature at 5 cm were measured with single-junction thermocouples. The temperature at the surface and at 5 cm was used to calculate the change in energy storage of the layer of soil above the heat-flow transducer. This was then added to the heat flow measured at 5-cm depth, and is listed as $S + S'$. These basic elements were measured in and over each lysimeter in all the experiments with exception of Alfalfa 13 and 14 where lysimeters I and II were involved. Additional supporting data consisting of solar radiation, reflected solar radiation, wind direction and wind speed 80 cm to 1 meter above the crop, and air temperature were measured.

Frequency of recording. All the micrometeorological elements were recorded at 5-min intervals for Alfalfas 1, 2, 3, 4, 5, 6, 7, 8, and 9. The recording frequency was reduced to 15-min intervals for the remainder of the alfalfa experiments. Hourly averages were computed for all micrometeorological elements by forming an average of the values recorded at the beginning and end of each hour, plus the intervening printouts.

RESULTS AND DISCUSSION:

Energy balance series. Examples of the hourly distribution of the energy balance components for each of the four recordings – winter, spring, summer, and fall – are shown in Figures 1, 2, 3, and 4, respectively. The data presented are the average of three lysimeters, with the exception of Figure 3 which is lysimeter I. The days are quite comparable with respect to wind speed, with exception of Figure 3 which has a higher wind speed during the periods 1300 to 2000. The first three figures illustrate that net radiation increased as solar radiation increased. However, the ratio of net radiation to solar radiation increased from 0.48 on 8 February to 0.51 on 26 March to 0.61 on 21 June. After 21 June solar radiation decreased – so also did net radiation; however, the ratio of net to solar radiation remained at 0.62. The evaporative flux showed increases proportional to net radiation, with the ratio of net radiation to evaporative flux decreasing from 0.93 on 8 February to 0.88 on 26 March, 0.61 on 21 June and back to 0.81 on 9 August. It should be noted that the condition of the alfalfa in these four examples is not quite comparable in that the alfalfa was 12 cm, 20 cm, 30 cm, and 23 cm in height, respectively. The ability of the alfalfa to extract sensible heat from the air appears to increase with increasing height. A comparison can be made between 26 March and 9 August since the alfalfa was of similar height on these two days. Net radiation and evaporative flux being greater on 9 August, the ratio of net radiation to evaporative flux was 0.88 and 0.81, very comparable when considering that the alfalfa on the latter date was 3 cm taller. The ratio of sensible to latent heat flux increased from -0.07 on 8 February to -0.10 on 26 March to

-0.39 on 21 June and then decreased to -0.26 on 9 August. The 20th of June would be a better day for comparison because the average wind speed was more comparable to the other days. The ratio of sensible to latent heat flux was -0.29 on 20 June. The soil heat flux was negligible in the first three cases; however, a considerable amount of energy was used to heat the soil on 9 August. These results indicate a trend of increasing fluxes as the seasons progress from the winter to the summer months, with the exception of soil heat flux.

Daily totals of all of the data collected in the winter, spring, summer, and fall energy balance studies are listed in Table 2. The daily totals exhibit the same trends as were shown in Figures 1, 2, 3, and 4; however, comparison may be made between days within each series. For example, in Alfalfa 1, 8 February had a negative ratio of A/LE, while 13 and 14 February had positive ratios indicating that energy was used to heat the air. The difference in the sign of the ratios on 8 and 14 February, days of comparable solar radiation, may be explained by the difference in wind speed. The slightly larger average wind-speed movement on 8 February promoted more evaporation and caused energy to be extracted from the air. When the average wind was similar as on 13 and 14 February, differences in the energy balance components were directly related to the incoming radiation.

The most striking illustration of the influence of wind speed is shown in Alfalfa 6. The solar radiation differed by only 25 ly on these days, while the average wind speed differed by 57 cm sec⁻¹. The evaporative flux increased from 581 to 752 ly day⁻¹, the greater flux associated with the greater wind speed, thus causing more energy to be extracted from the air.

Influence of height of alfalfa upon the energy balance components.

Five different studies were conducted in which the influence of height of alfalfa upon the components of the energy balance equation was investigated. Unfortunately, cable trouble developed during these experiments and was not corrected until the last experiment; therefore, complete data are only available for two experiments, and partial data exist for the remaining three experiments.

The hourly distribution of the components of the energy balance equation for alfalfa of 10, 30, and 50 cm in height is shown in Figures 5, 6, and 7. Since these data were collected on the same day, the bulk meteorological elements would be similar for all three surfaces. The major difference lies in the evaporative flux, which increased with the increase in height of alfalfa. One could argue that the relationship between the evaporative flux and the height is directly related to leaf area, which is able to intercept both radiant and sensible heat. This appears to be partially true in that the leaf-area indices range from 2.4 for the 10-cm alfalfa to 2.8 for the 30-cm alfalfa to 4.0 for the 50-cm alfalfa. This appears to be a partial explanation of the differences; however, other differences exist also. Net radiation increases with increasing height and with increasing evaporative flux. This is as it should be. For a given energy input, more evaporation would cause a cooler underlying surface, and consequently, increase the net radiant balance. Other workers have noted similar effects (1, 2). The difference in evaporative flux may be due to the difference in roughness of the surfaces. Photographs taken at the time indicate that the 10- and 30-cm surfaces were quite smooth, as compared to the 50-cm surface. The final result of increased evaporation and increased net radiation with height is that 60 and 8 ly were used to heat the air over the 10-cm and 30-cm crops, while the 50-cm crop extracted 2 ly from the air.

Immediately after the recordings on 23 April, the area surrounding lysimeters II and III was mowed to the ground in an attempt to determine the maximum advected energy that would exist in this area at this time of the year. Unfortunately, before the mowed alfalfa was removed and the measurements made, 8.4 mm of rain occurred. By the 28th of April, regrowth had already started so that the data obtained do not represent the maximum advection that could be obtained. Cable trouble also developed; consequently, net radiation data from lysimeter I had to be disregarded. Even though the data obtained from lysimeters II and III cannot be compared

directly with the data from lysimeter I, these data are of interest and may be compared with the data of 22 April.

The hourly distribution of the energy balance components for lysimeter II and III only on 28 April are shown in Figures 8 and 9. The average wind speed was 38 cm sec^{-1} greater on the 28th of April than on the 22nd, indicating that if the net radiation were similar for both days, a larger evaporative flux would occur from the 10-cm crop on 28 April. This indeed is the case. The evaporative flux increased from 291 ly to 370 ly. If one assumes that the net radiation over lysimeter I was similar to that of the 22nd — namely, 370 ly — then the sensible heat flux would have been 51 ly. This can be compared with the sensible heat flux (shown in Figures 8 and 9) of 87 and 71 ly, respectively. The fact that less sensible heat flux occurred on lysimeter III than on lysimeter II may be explained by the rainstorm of the 25th, which tended to flatten the isolated alfalfa. Consequently, the surface was not as rough as previous. Isolation did not appear to increase the evaporative flux and the sensible heat flux. This is largely due to the regrowth of the alfalfa surrounding the lysimeters;

The daily totals of solar radiation, average wind speed, and the components of the energy balance equation for the height studies are given in Table 3. The influence of wind on the sensible heat flux for the three heights can be determined by examining the data of 22 and 23 April. Note the average wind speed on 22 April was at 80 and 40 cm on 23 April. An increase in wind speed decreased the export of sensible heat over lysimeter I, and caused sensible heat to be extracted from the air on lysimeters II and III. It is interesting to note that the maximum evaporative flux was recorded from 62-cm alfalfa on 17 July (809 ly). This is equivalent to 13.5 mm of water, and is very much in excess of the solar radiation on that day. If one assumes that net radiation was 400 ly, then the sensible heat flux would be equivalent to the net radiant flux.

The dry down series. A series of experiments were conducted to determine the components of the energy balance equation when the field

was irrigated, and the evaporative flux was determined by the meteorological factors, when the soil moisture was limiting and the evaporative flux was approximately one-half and one-fourth of net radiation. Data are shown in Figures 10, 11, and 12. Unfortunately, no direct comparison can be made between Figures 10, 11, and 12 because the time required for the soil moisture to become limiting was so great that the solar radiation – and consequently, the net radiant flux – decreased considerably. However, it is interesting to note that the ratio of net radiation to solar radiation remained fairly constant – 0.62, 0.61, and 0.60 – while the ratio of net radiation to evaporative flux increased from 0.81 to 1.28 and 2.62. As the soil moisture became limiting, the ratio of sensible to latent heat flux changed from a -0.26 to $+0.20$ to $+1.32$. Energy was stored in the soil in all three cases.

The daily totals collected in Alfalfa 10, 11, and 12 are shown in Table 4. Previously, we have noted that wind speed increased evaporative flux when soil moisture was not limiting. In Alfalfa 12, a 80 cm sec^{-1} increase in wind speed did not alter the evaporative or the sensible heat flux. In this case evaporation was already controlled by the plant and soil moisture, so that any change in the environmental conditions had very little influence on the evaporative flux.

Dry and irrigated stubble. Data were collected over dry and irrigated stubble, largely to test the Bowen equation for estimating evaporative flux under these conditions. The results are shown in Table 5. These data may be compared with the evaporation from bare soil reported in previous annual reports. One fact should be pointed out here however: even though the soil surface in Alfalfa 9 was quite dry, an increase in wind speed from 142 cm sec^{-1} to 225 cm sec^{-1} increased evaporative flux by 57 ly, and also increased the net radiant flux 27 ly by cooling the underlying surface. Consequently, less energy was utilized in heating the air. These results oppose those in Alfalfa 12 (Table 4), the difference being that the plant-root

system extracted moisture from greater depths; consequently, the soil profile was drier than during Alfalfa 9.

SUMMARY:

During the calendar year of 1963, investigations were carried out to determine the relationships between evapotranspiration and the surface energy balance for winter, spring, summer, and fall conditions, to determine the relationship between evapotranspiration and micrometeorological parameters over alfalfa of different heights and over dry stubble, and to determine how these relationships change as the soil moisture is depleted.

Data collected indicated that the ratio of net radiation to evaporative flux decreased from 0.93 on 8 February for the winter condition to 0.81 on 9 August for the fall condition, while the ratio of sensible to latent heat flux increased from a -0.07 on 8 February to -0.39 on 21 June and decreased to -0.26 on 9 August. The value of -0.39 cannot be compared directly with the others, since the alfalfa was some 10 cm taller at this time and was more capable of extracting sensible heat from the air. These results do, however, indicate that for alfalfa more and more energy was extracted from the air in the form of sensible heat as the seasons progressed from winter to fall, with the greatest amount of energy extractions associated with higher wind speeds.

Studies conducted on alfalfa surfaces of different heights indicate that the evaporative flux increases with the height of the surface; so also, does net radiation. The sensible heat flux was generally away from the transpiring surface for a 10-cm crop and to the transpiring surface for a 50-cm crop. The difference in transpiration rates of the three surfaces is partially explained by the difference in leaf-area index which ranges from 2.4 to 4.0 and to the roughness of the surface, the taller crop being more rough than the shorter crops.

The greatest evaporative flux measured (809 ly) was from a 62-cm alfalfa stand, which is equivalent to 13.5 mm of water. This is in

excess of the energy supplied by solar radiation and is two times as large as net radiation, which means that the amount of energy extracted from the air was equal to net radiation.

REFERENCES:

- (1) Decker, Wayne E.
1959. Variations in the net exchange of radiation from vegetation of different heights. Jour. Geophys. Res. 64:1617-1619.
- (2) Monteith, J. L., and Szeicz, G.
1962. Radiative temperature in the heat balance of the natural surfaces. Quart. Jour. Roy. Met. Soc. 88:496-507.

PERSONNEL: Leo J. Fritschen and C. H. M. van Bavel

Table 1. Activities - calendar year 1963.

Alfalfa Series	Date	Description	Height of alfalfa
1	8,13,14 Feb	Winter energy balance	12 cm on 3 lysimeters
2	26,27 March	Spring energy balance	20 cm on 3 lysimeters
6	20,21 June	Summer energy balance	30 cm on 3 lysimeters
10	8,9 August	Fall energy balance	23 cm on 3 lysimeters
3	10 April	Two-height study	13 cm on Lys I, II 35 cm on Lys III
4	22,23 April	Three-height study	10 cm on Lys I 30 cm on Lys II 50 cm on Lys III
5	28,29 April	Three-height study	10 cm on Lys I 30 cm on Lys II* 50 cm on Lys III*
7	3,4 July	Three-height study	15 cm on Lys I 20 cm on Lys II 37 cm on Lys III**
8	17,18 July	Three-height study	32 cm on Lys I 45 cm on Lys II 62 cm on Lys III***
9	25,26,27 July	Dry stubble	5 cm
13	15,16 Oct	Dry stubble	5 cm
14	18,19,20 Oct	Irrigated stubble	5 cm
10	8,9 August	Dry down series	23 cm on 3 lysimeters
11	12,13 Sept	Dry down series	35 cm on 3 lysimeters
12	24,25 Sept	Dry down series	36 cm on 3 lysimeters

* Lysimeters II and III isolated.

** 10 percent blossom.

*** About 50 percent blossom and was lodging.

Table 2. Daily totals of the energy balance components, solar radiation, and average wind speed for the winter, spring, summer, and fall energy balance studies.

Alfalfa Series	Lys	Date	R_{sd}	\bar{U}_{80}	R_n	S+S'	LE	A
			ly day ⁻¹	cm sec ⁻¹		ly day ⁻¹		
1	I	8 Feb			169	-3	-189	23
	II				159	0	-193	34
	<u>III</u>				<u>191</u>	<u>4</u>	<u>-176</u>	<u>-19</u>
	Ave		363	80	<u>173</u>	<u>0</u>	<u>-186</u>	<u>13</u>
1	I	13 Feb			201	21	-133	-89
	II				215	22	-148	-89
	<u>III</u>				<u>228</u>	<u>24</u>	<u>-141</u>	<u>-111</u>
	Ave		447	72	<u>215</u>	<u>22</u>	<u>-141</u>	<u>-96</u>
1	I	14 Feb			160	10	-124	-46
	II				161	4	-133	-32
	<u>III</u>				<u>173</u>	<u>11</u>	<u>-119</u>	<u>-65</u>
	Ave		358	72	<u>165</u>	<u>8</u>	<u>-125</u>	<u>-48</u>
2	I	26 March			248	4	-307	55
	II				268	8	-308	32
	<u>III</u>				<u>281</u>	<u>1</u>	<u>-287</u>	<u>5</u>
	Ave		513	110	<u>266</u>	<u>4</u>	<u>-301</u>	<u>31</u>
2	I	27 March			292	-15	-312	35
	II				302	-8	-322	28
	<u>III</u>				<u>321</u>	<u>-22</u>	<u>-303</u>	<u>4</u>
	Ave		563	112	<u>305</u>	<u>-15</u>	<u>-312</u>	<u>22</u>
6	I	20 June			440	-13	-590	163
	<u>II</u>				<u>440</u>	<u>-40</u>	<u>-572</u>	<u>172</u>
	Ave		737	135	<u>440</u>	<u>-27</u>	<u>-581</u>	<u>168</u>
6	I	21 June	762	192	461	-4	-752	295
10	I	8 August			380	-21	-391	32
	II				338	-32	-388	82
	<u>III</u>				<u>400</u>	<u>-41</u>	<u>-376</u>	<u>17</u>
	Ave		603	75	<u>373</u>	<u>-31</u>	<u>-385</u>	<u>43</u>
10	I	9 August			418	-44	-504	130
	II				374	-31	-493	150
	<u>III</u>				<u>424</u>	<u>-40</u>	<u>-496</u>	<u>112</u>
	Ave		650	80	<u>405</u>	<u>-38</u>	<u>-498</u>	<u>131</u>

Table 3. Daily totals of solar radiation, average wind speed, and the components of the energy balance equation for the height studies.

Alfalfa Series	Lys	Date	R_{sd}	\bar{U}_{80}	R_n	$S+S'$	LE	A
			ly day ⁻¹	cm sec ⁻¹		ly day ⁻¹		
3	I	10 April	418	135	200	12	-245	33
	II				207	17	-246	22
	III				238	34	-394	122
4	I	22 April	698	107**	369	-18	-291	-60
	II				383	-5	-370	-8
	III				453	-17	-438	2
4	I	23 April	705	118	374	-20	-331	-23
	II				384	-5	-420	41
	III				446	-16	-476	46
5	I	28 April	710	145	*	-51	-370	-
	II				386	-14	-459	87
	III				437	-33	-475	71
5	I	29 April	689	141	*	-61	-397	-
	II				380	-18	-514	152
	III				427	-33	-490	96
7	I	3 July	671	159	429	-24	-643	238
	II				421	*	-625	-
7	I	4 July	694	144	*	-26	-641	-
	II				421	-26	-613	218
	III				*	*	-763	-
8	I	17 July	679	97	*	-37	-654	-
	II				*	-1	-800	-
	III				*	-19	-809	-
8	I	18 July	677	101	*	-38	-678	-
	II				*	-17	-766	-
	III				*	*	-801	-

* Data missing due to cable trouble.

** Wind at 40 cm.

Table 4. Daily totals of solar radiation, average wind speed, and the components of the energy balance equation for the dry down series.

Alfalfa Series	Lys	Data	R_{sd}	\bar{U}_{80}	R_n	S+S'	LE	A
			ly day ⁻¹	cm sec ⁻¹	← ly day ⁻¹ →			
10	I	8 August			380	-21	-391	32
	II				338	-32	-388	82
	<u>III</u>				400	-41	-376	17
	Ave		603	75	373	-31	-385	43
10	I	9 August			418	-44	-504	130
	II				374	-31	-493	150
	<u>III</u>				424	-40	-496	112
	Ave		650	80	405	-38	-498	131
11	I	12 Sept			359	-25	-286	-66
	II				329	-17	-305	-7
	<u>III</u>				354	-21	-242	-91
	Ave		566	95	347	-21	-271	-55
11	I	13 Sept			189	-2	-244	57
	II				172	-5	-275	108
	<u>III</u>				189	-11	-229	51
	Ave		325	186	183	-6	-249	72
12	I	24 Sept			314	-38	-101	-175
	II				297	-27	-168	-102
	<u>III</u>				315	-39	-86	-190
	Ave		518	83	309	-35	-118	-156
12	I	25 Sept			313	-35	-103	-175
	II				290	-28	-176	-86
	<u>III</u>				321	-39	-88	-194
	Ave		518	164	308	-34	-122	-152

Table 5. Daily totals of solar radiation, average wind speed, net radiation, soil heat flux, evaporative flux, and sensible heat flux over dry and irrigated stubble.

Alfalfa Series	Lys	Date	R_{sd}	\bar{U}_{80}	R_n	S+S'	LE	A
			ly day ⁻¹	cm sec ⁻¹	← ly day ⁻¹ →			
9	II	25 July	675	133	357	-67	-187	-102
9	II	26 July	640	142	336	-62	-189	-85
9	II	27 July	622	225	363	-61	-246	-56
13	I	15 Oct	460	108	232	-11	-21	-200
	II				208	-14	-32	-162
13	I	16 Oct	412	201	224	-20	-35	-169
	II				221	-23	-48	-150
14	I	20 Oct	437	63	266	2	-157	-111

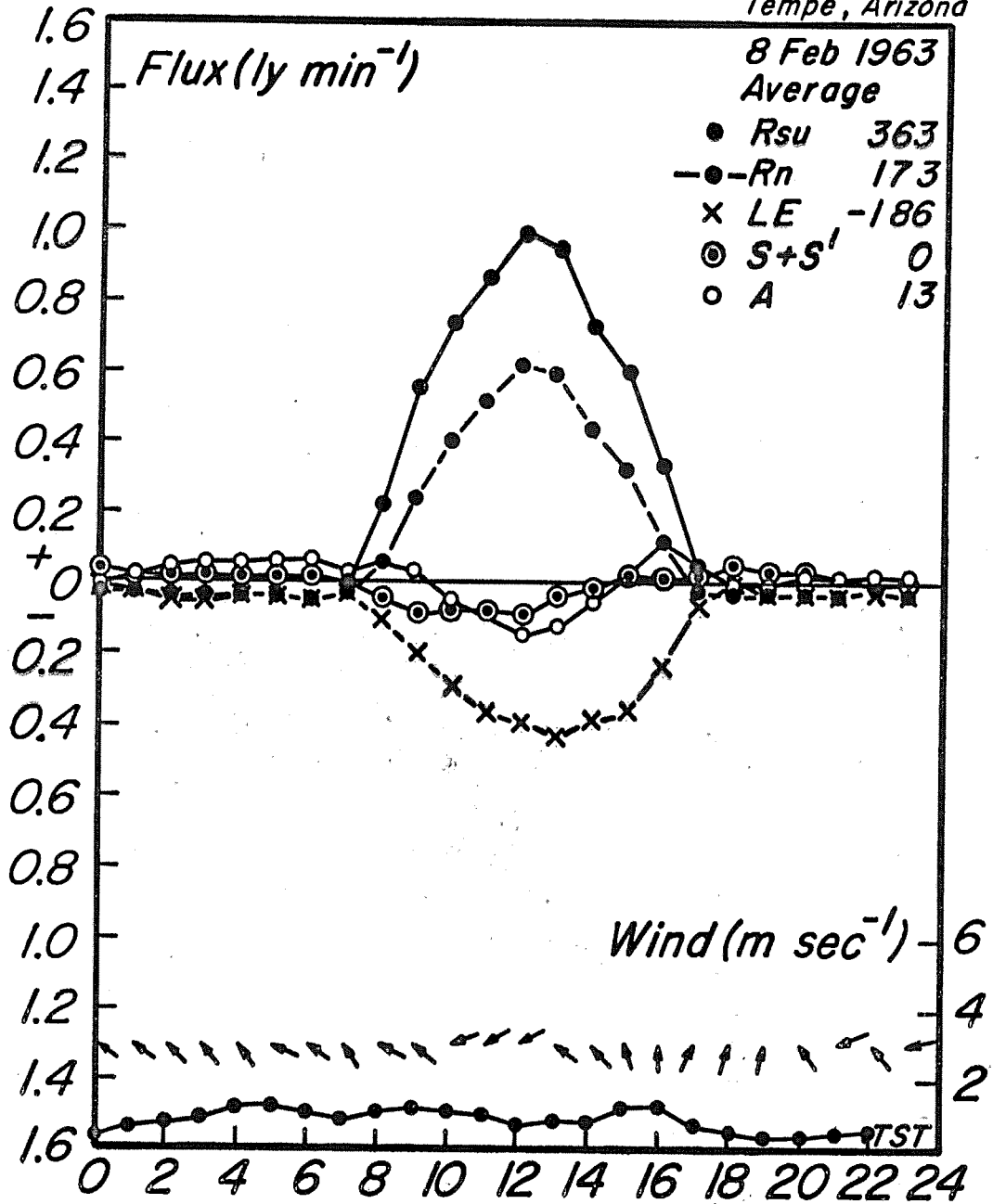


Figure 1. Hourly values of the components of the energy balance equation, solar radiation, wind speed and direction.

U.S. Water Conservation Laboratory,
Tempe, Arizona

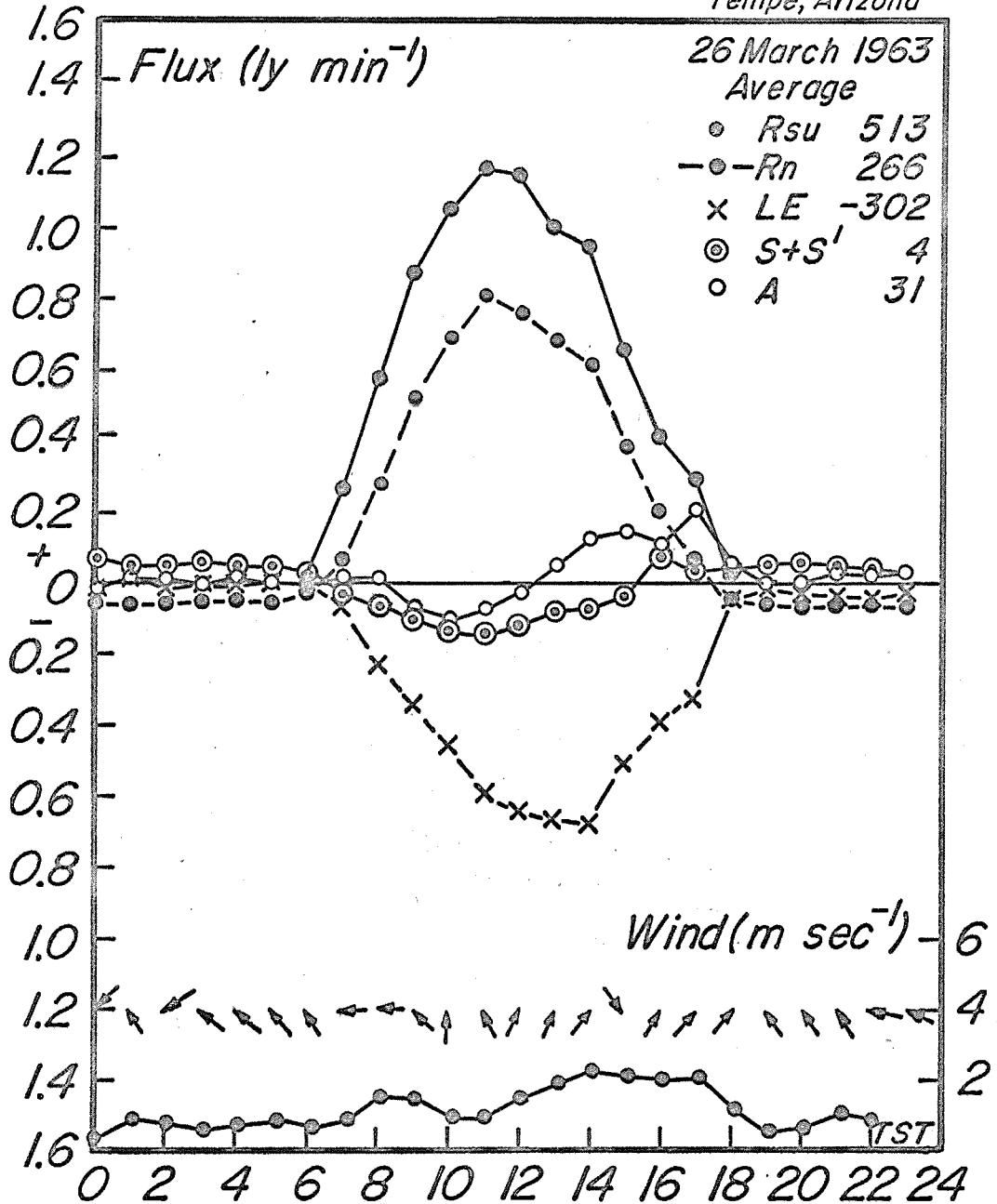


Figure 2. Hourly values of the components of the energy balance equation, solar radiation, wind speed and direction.

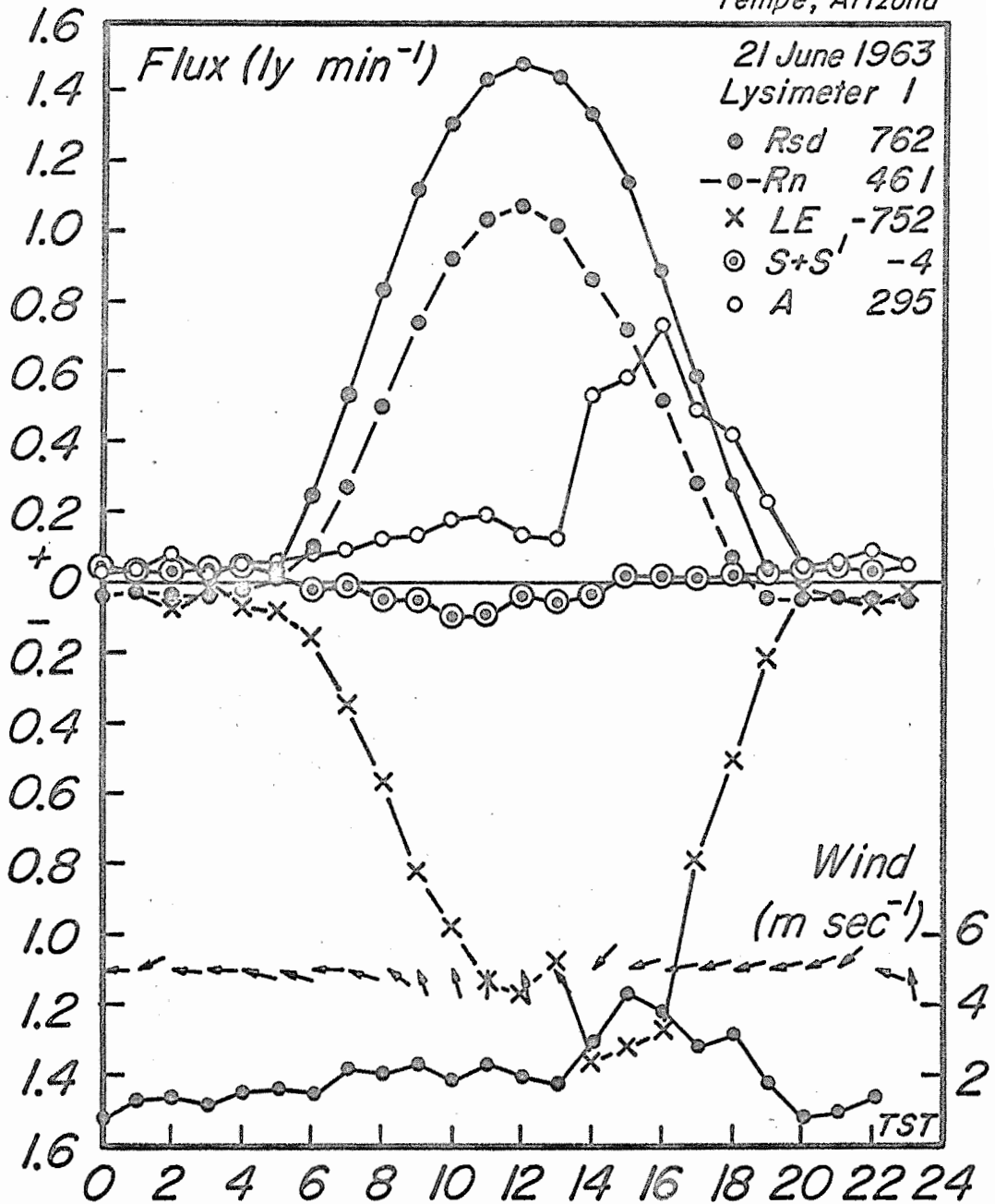


Figure 3. Hourly values of the components of the energy balance equation, solar radiation, wind speed and direction.

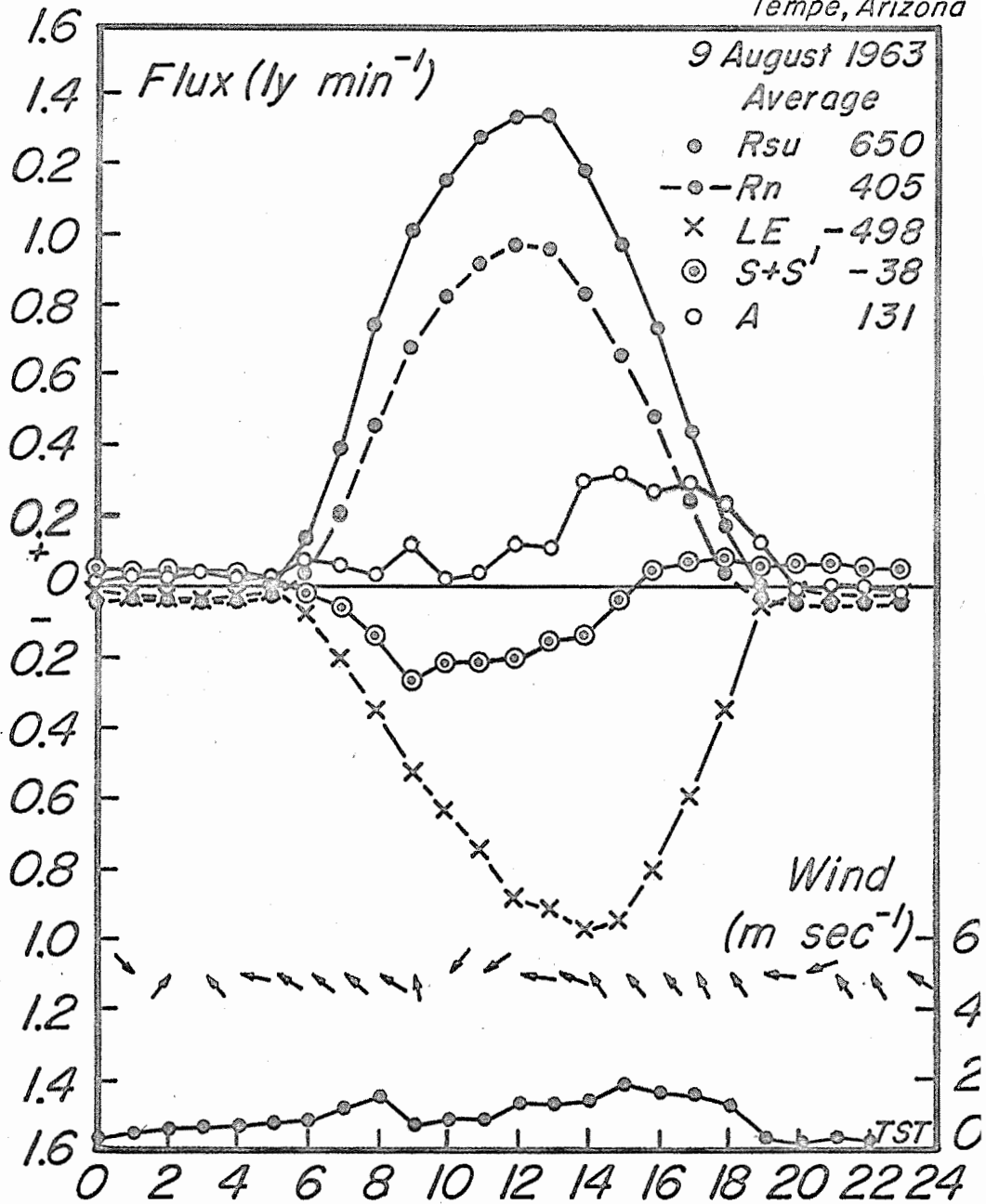


Figure 4. Hourly values of the components of the energy balance equation, solar radiation, wind speed and direction.

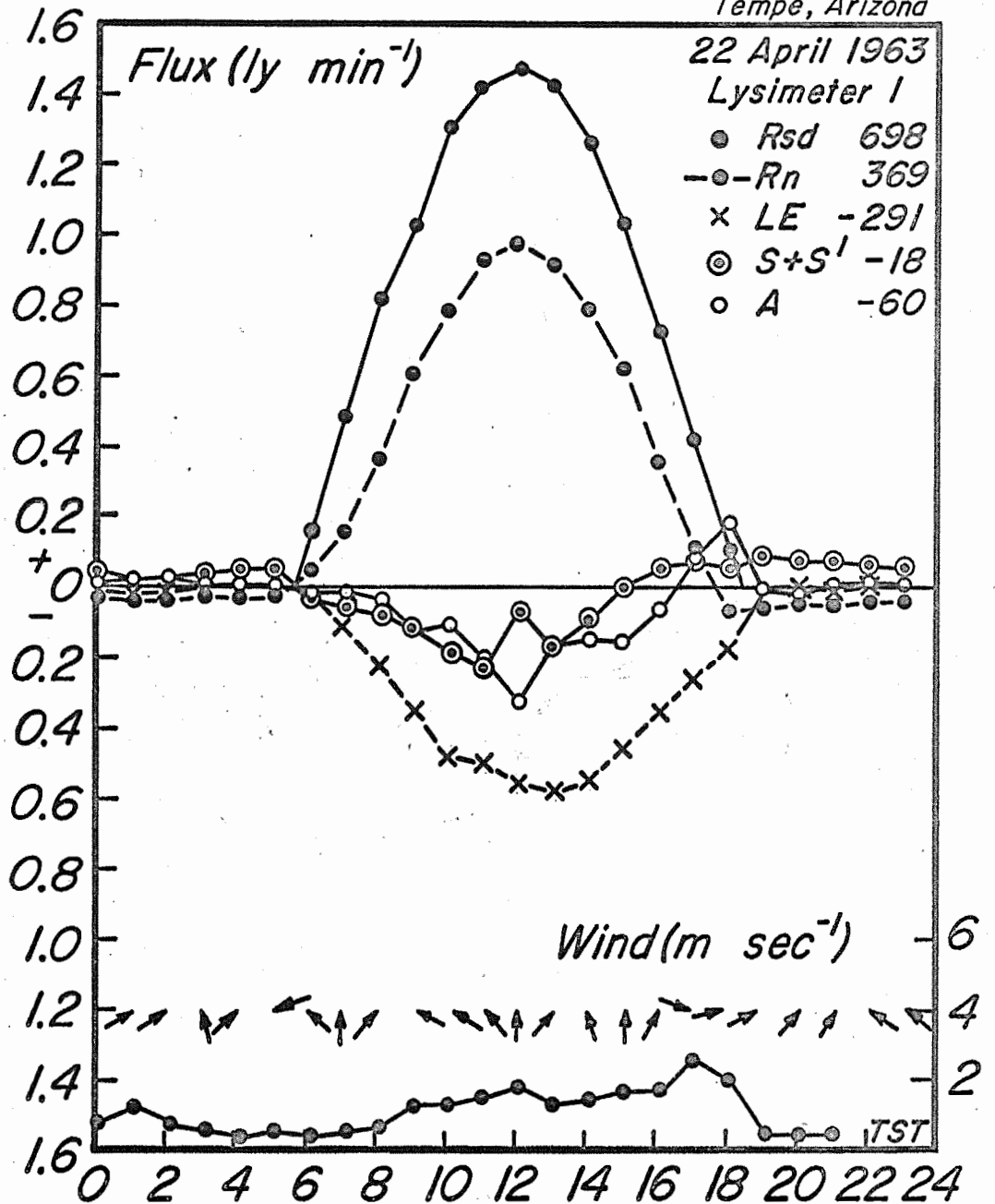


Figure 5. Hourly values of the components of the energy balance equation, solar radiation, wind speed and direction.

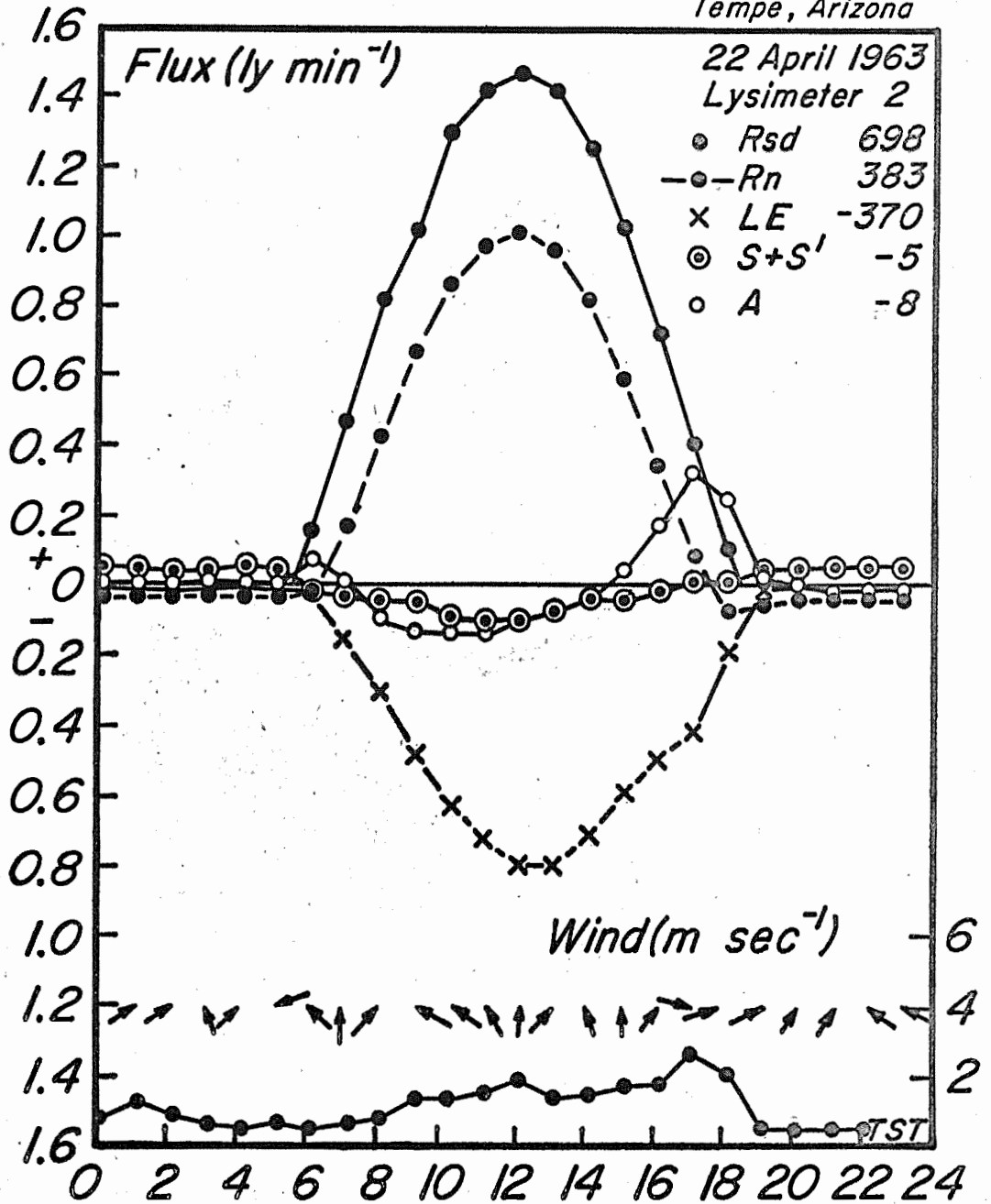


Figure 6. Hourly values of the components of the energy balance equation, solar radiation, wind speed and direction.

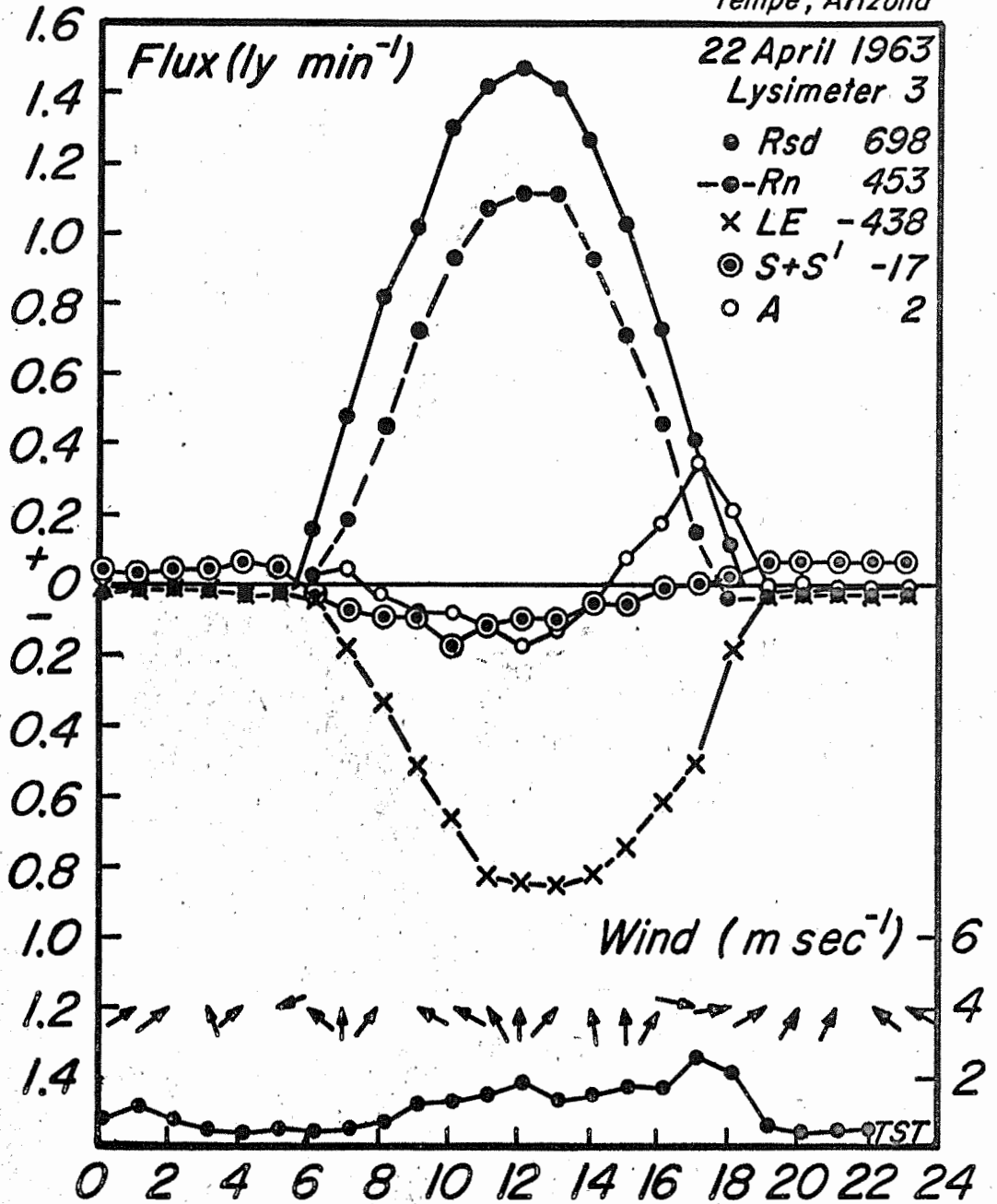


Figure 7. Hourly values of the components of the energy balance equation, solar radiation, wind speed and direction.

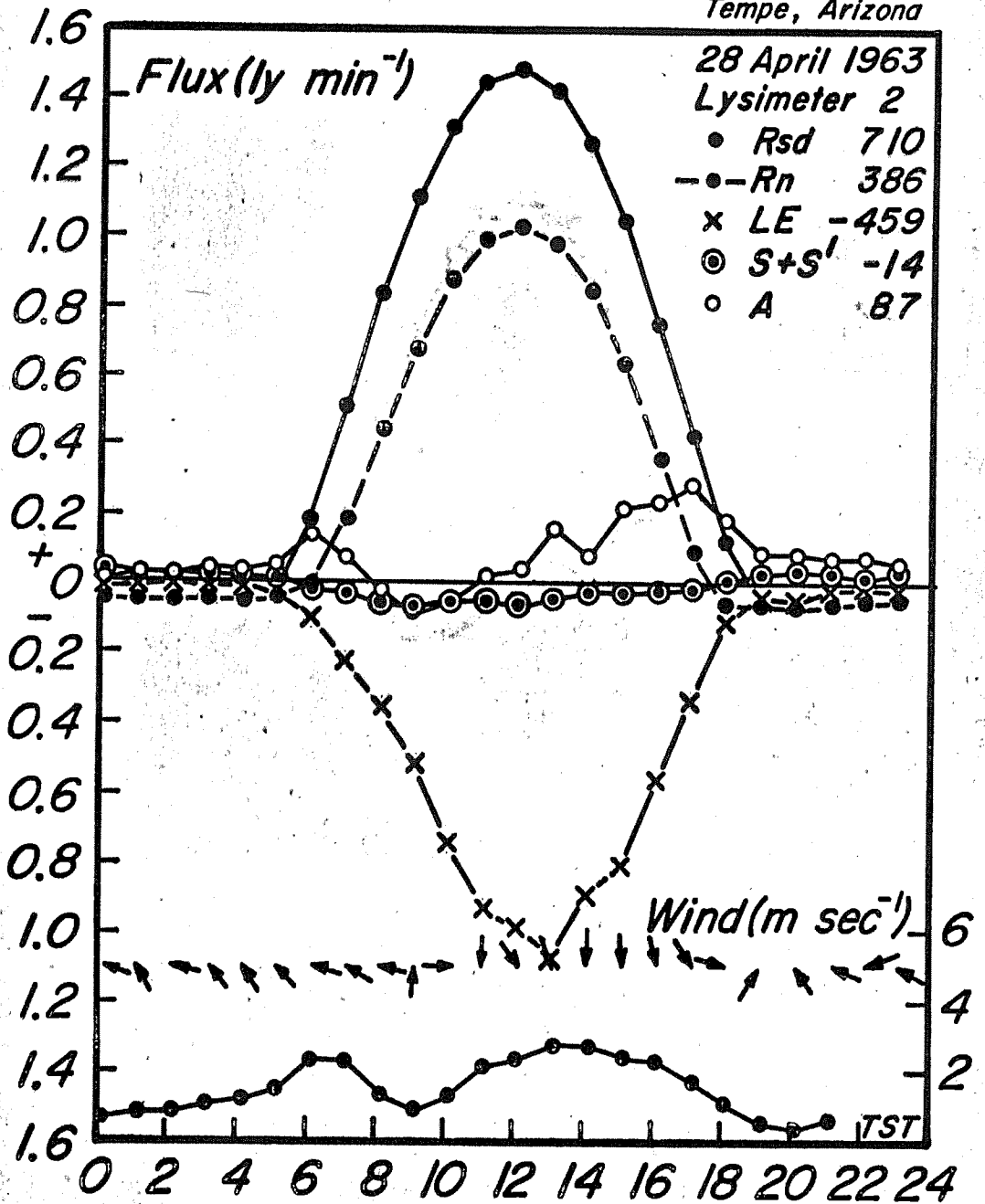


Figure 8. Hourly values of the components of the energy balance equation, solar radiation, wind speed and direction.

U.S. Water Conservation Laboratory,
Tempe, Arizona

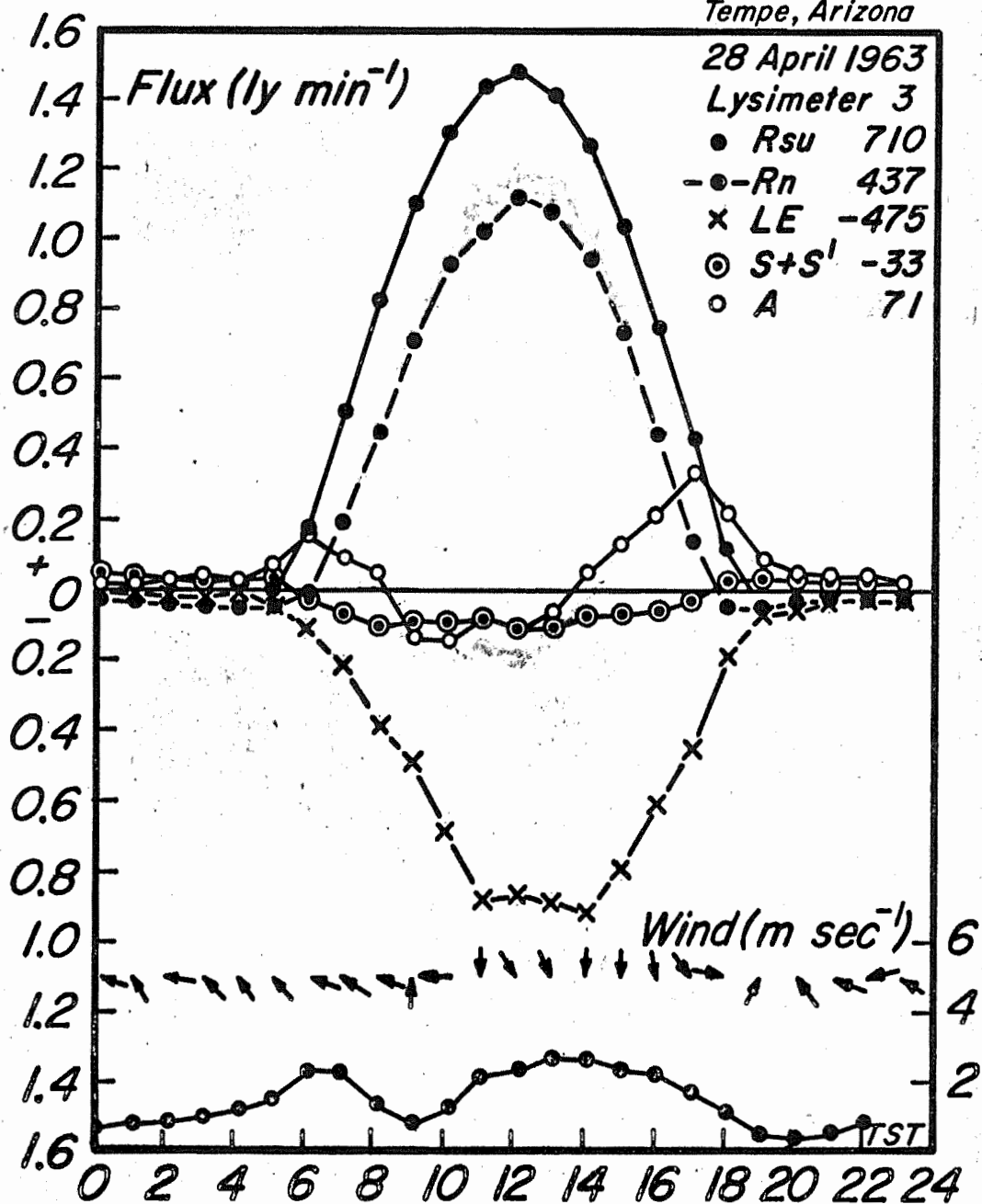


Figure 9. Hourly values of the components of the energy balance equation, solar radiation, wind speed and direction.

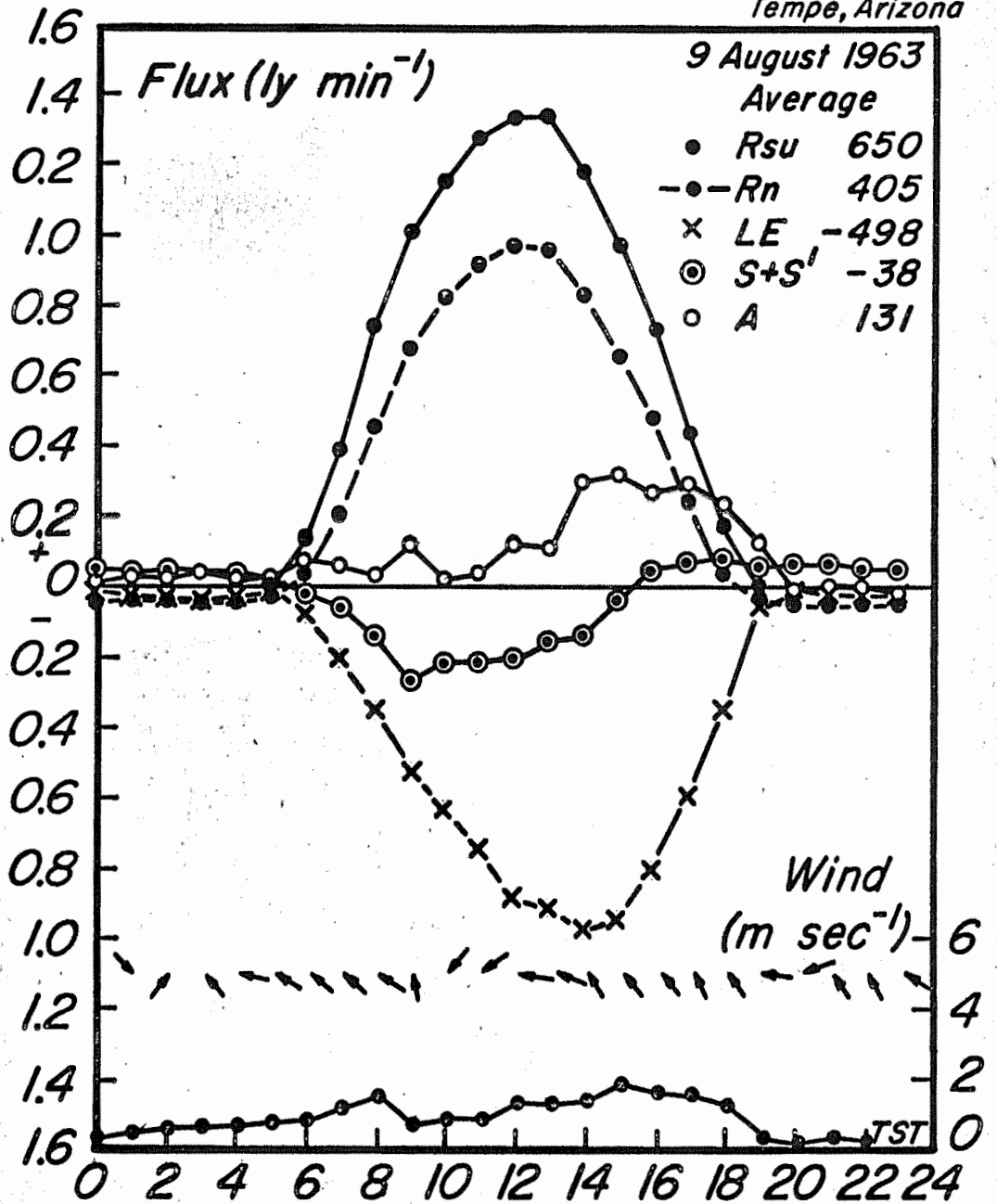


Figure 10. Hourly values of the components of the energy balance equation, solar radiation, wind speed and direction.

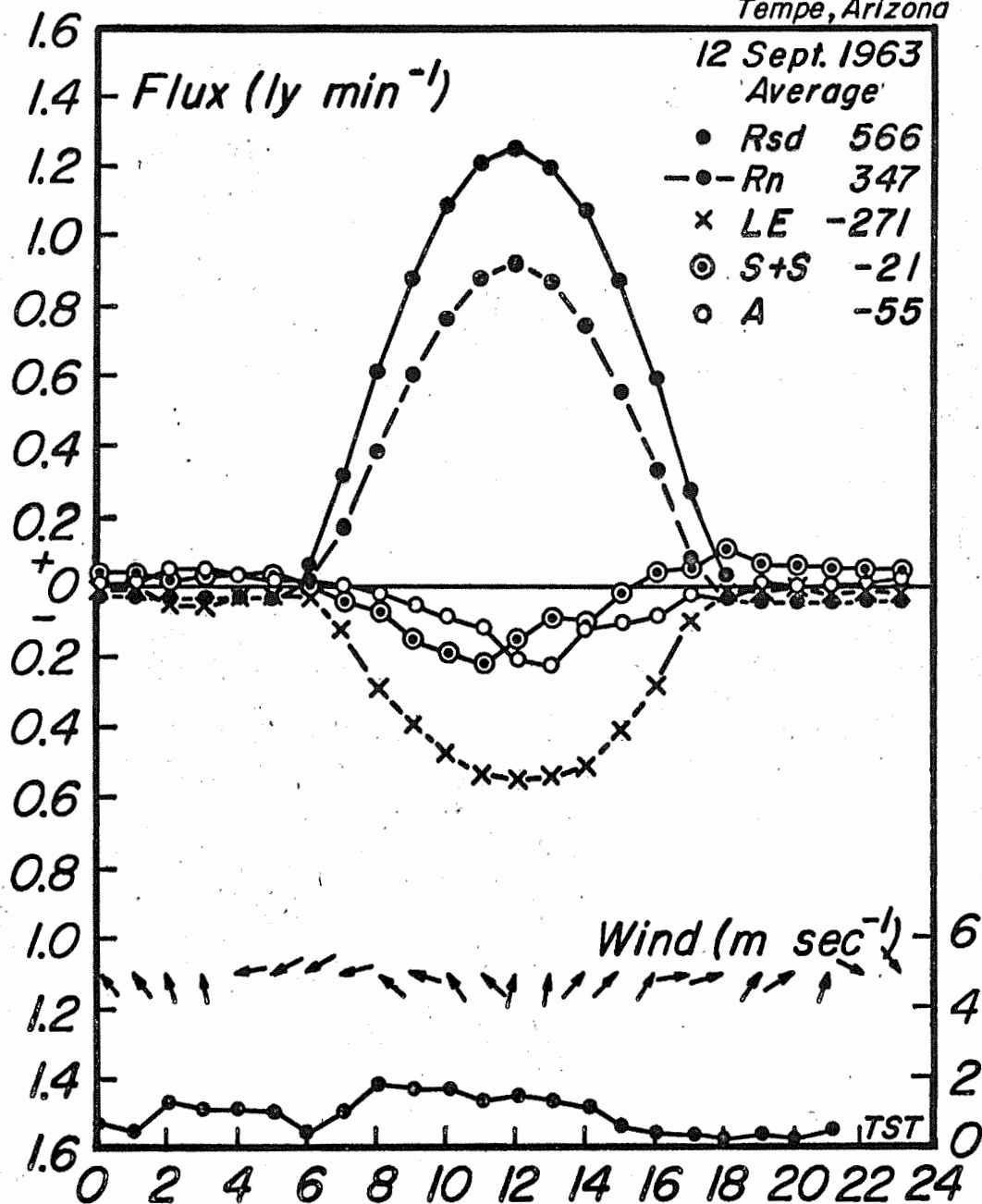


Figure 11. Hourly values of the components of the energy balance equation, solar radiation, wind speed and direction.

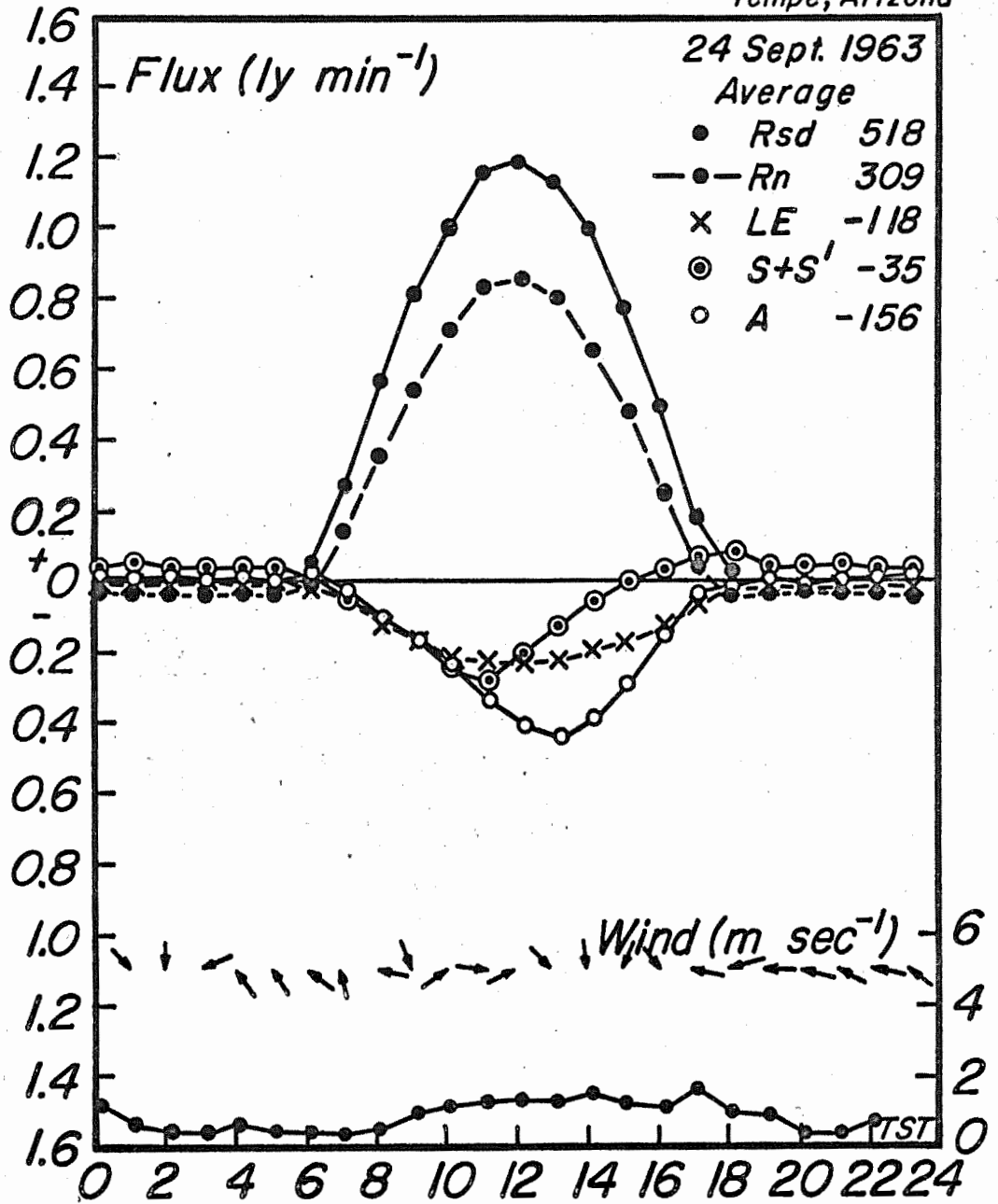


Figure 12. Hourly values of the components of the energy balance equation, solar radiation, wind speed and direction.

TITLE: COMPONENTS OF THE RADIATION BALANCE OF FIELD CROPS UNDER
IRRIGATED MANAGEMENT

LINE PROJECT: SWC 4-gG2

CODE NO.: Ariz.-WCL-18

INTRODUCTION:

Evaporation from a crop surface -- water not limiting -- is largely determined by the radiant and sensible heat fluxes. Of the incoming radiant flux, part is reflected and part is reradiated, thus reducing the amount of energy available for evaporation. Data were collected to determine if water could be conserved by management practices which would increase the reflected radiation.

RESULTS AND DISCUSSION:

Incoming and reflected solar radiation were measured over bare-soil surfaces both wet and dry, sudangrass from emergence to harvesting, and alfalfa at different stages of growth. These data were collected using solarimeters to measure incoming and reflected solar radiation. The data were sampled at various frequencies ranging from 5 to 30 minutes. Hourly averages and daily totals were computed for clear days. These data are summarized in Table 1. Data collected in November 1961 over dry bare soil indicated a reflection of 24 percent. Owing to the sun's altitude, the percentage reflection may be somewhat higher at this time of the year than would occur over dry bare soil during the summer months. However, the amount of energy reflected is still relatively low.

During the period from 17 February to 7 March, several days of data were collected which show the effect of drying soil upon the reflection coefficient. The soil was irrigated on 15 February so it was relatively wet on 17 February, and the reflection coefficient was 14 percent. As the soil dried the reflection coefficient increased, even though small amounts of rain fell on 19 February, 21 February, and 25 February, reaching a maximum of 26 percent on 7 March. The 7th of March, however, may not be representative due to the low solar radiation. Therefore, we should consider the 2nd of March to be the maximum value of 24 percent, which is the same as that measured in November of 1961.

During the period 24 March 1962 to 6 April 1962, data were collected which also illustrate the effect of a drying surface on a reflection coefficient. During this period the reflection increased from 15 percent for wet bare soil to 23 percent for a dry bare soil.

Sudangrass was planted in the experimental field in May 1962, so the data collected during the remainder of 1962 were over emerging and growing sudangrass. On 29 May the reflection coefficient was 13 percent; the sudangrass was beginning to emerge and was approximately 5 cm in height. The soil at this time was wet, being irrigated on the previous day. As the sudangrass grew and the soil surface was alternately wet and dry, the reflection coefficient increased to 22 percent by 11 June, and decreased to 19 percent on 21 June as a direct result of the clipping to 15-cm height on 12 June. As the sudangrass recovered from the clipping of 12 June, the reflection coefficient increased to 23 percent by 8 July and decreased to 22 percent by 13 July. The slight decrease in reflection coefficient from 8 to 13 July could be due to the fact that the sudangrass developed inflorescence during this period, thus provided a more ragged surface increasing internal reflection and thus, slightly decreasing the absolute amount of energy reflected. The difference is not significant. When the 140-cm sudangrass was mowed to 8-cm stubble and irrigated, the reflection coefficient dropped to 17 percent; and when the 100-cm sudangrass was mowed to 15 cm and irrigated, the reflection coefficient dropped to 20 percent. Again the reflection coefficient increased as the sudangrass grew developing more leaf area, becoming 21 percent on 18 August.

During 1963 the amount of solar energy reflected from alfalfa was monitored. On 13 February 1963, the reflection coefficient was 20 percent from 12-cm alfalfa. This remained fairly constant through March and April, while the alfalfa was maintained between 10 and 20 cm. During April three different heights were established - 10, 30, and 50 cm. The reflection coefficient appeared to be the highest, 23 percent, on the 30-cm alfalfa and slightly less, 22 percent, on the 50-cm alfalfa, with the 10-cm alfalfa having the lowest reflection.

Photographs tend to bear this out in that the 10-cm alfalfa was stocky without much leaf development, while the 30-cm alfalfa had a very smooth surface with adequate leaf development, and the 50-cm alfalfa had become aerodynamically rough and ragged.

On 25 July 1963, the alfalfa was mowed and not irrigated, so the surface was a dry stubble. The reflection coefficient from this surface was 22 percent.

During the latter part of August and September, the soil-moisture content in the alfalfa field was allowed to be depleted. During this period the reflection coefficient tended to drop from 20 percent to 19 percent.

On 15 October a dry-stubble surface existed. This stubble surface was different from that of 25 July in that the clippings were not removed. The reflection coefficient at this time was 25 percent, which is slightly higher than that of 25 July, partly due to the clippings and partly due to the lower sun altitude.

SUMMARY AND CONCLUSIONS:

Incoming and reflected solar radiation were measured over bare soil surfaces both wet and dry, sudangrass from emergence to harvest, and alfalfa at various stages of growth. The results from bare soil indicate that the reflection coefficient was approximately 14 percent when the soil was wet and increased to 24 percent as the soil dried.

The data obtained over the sudangrass indicated a 13-percent reflection coefficient over emerging sudangrass, increasing to 23 percent as the sudangrass grew and decreasing to 22 percent with the development of inflorescence. Mowing to 15-cm height tended to reduce the reflection coefficient from 22 percent to 18 or 19 percent, while mowing to 8-cm stubble reduced the reflection coefficient to 17 percent when the soil surface was wet.

The data collected over alfalfa indicated similar reflection coefficient to that obtained over sudangrass, with a 20-percent reflection coefficient over alfalfa recently trimmed to 10 cm, and a 23-percent reflection coefficient over 30-cm alfalfa having full leaf development and a smooth surface. As the alfalfa grew and the surface

became more rough, the reflection coefficient decreased to 22 percent. Dry alfalfa stubble had a reflection coefficient of 22 to 25 percent depending upon the amount of trash on the surface. Limiting soil moisture tended to decrease the reflection coefficient from 20 percent to 19 percent.

These results indicated that normal cultural practices do not alter the reflection coefficient greatly. Of course, the surfaces investigated were continuous bare soil and continuous crop. Row crops would be a combination thereof and the reflection coefficients resulting would depend largely on whether the soil surface was wet or dry during early stages of development and upon the raggedness of the cover during later stages of development. These data do not indicate a source of moisture conservation due to differing reflection coefficients as a result of management.

PERSONNEL: Leo J. Fritschen

Table 1. Incoming and reflected solar radiation, the ratio of reflected to incoming solar radiation, and description of the reflecting surface for 1961, 1962, and 1963.

Date	R_{sd}	R_{su}	R_{su} / R_{sd}	Surface condition
	$\leftarrow \text{ly day}^{-1} \rightarrow$			
19 Nov 61	376	91	.241	Dry bare soil
22 Nov 61	341	83	.244	Dry bare soil
17 Feb 62	450	64	.141	Wet bare soil, irrigated 15 Feb
18 Feb 62	464	67	.145	Drying soil
22 Feb 62	469	70	.150	4-mm rain on 19 Feb and 3-mm rain on 21 Feb
23 Feb 62	444	78	.176	Drying soil
27 Feb 62	494	95	.192	8-mm rain on 25 February
28 Feb 62	526	110	.209	Drying soil
1 Mar 62	518	118	.228	Drying soil
2 Mar 62	521	124	.237	Drying soil
7 Mar 62	119	31	.258	Dry bare soil
24 Mar 62	618	93	.150	Wet bare soil, irrigated 22 Mar
28 Mar 62	614	87	.142	Drying soil
5 Apr 62	622	102	.165	Drying soil
6 Apr 62	618	144	.234	Dry bare soil
29 May 62	720	96	.133	Emerging sudangrass, irrigated 28 May
5 Jun 62	746	162	.217	Growing sudangrass
11 Jun 62	747	166	.223	Growing sudangrass, irrigated 6 June
18 Jun 62	735	156	.213	Growing sudangrass, mowed to 15 cm and irrigated 12 June
21 Jun 62	728	137	.188	Growing sudangrass, irrigated 19 June

Table 1. Continued

1 Jul 62	731	147	.201	Growing sudangrass
8 Jul 62	700	161	.232	Growing sudangrass
13 Jul 62	740	160	.216	140 cm with inflorescence, irrigated 9 July
22 Jul 62	683	150	.219	100 cm starting inflorescence, irrigated 18 July
22 Jul 62	683	115	.169	8-cm stubble, irrigated 18 July
31 Jul 62	692	138	.199	Growing sudangrass, mowed 26 July, irrigated 29 July
9 Aug 62	633	127	.201	Growing sudangrass, irrigated 7 Aug
17 Aug 62	519	121	.233	Growing sudangrass, mowed 12 Aug, irrigated 15 August
18 Aug 62	652	139	.213	Growing sudangrass
13 Feb 63	491	98	.199	Alfalfa, 12 cm tall
27 Mar 63	625	126	.202	Alfalfa, 20 cm tall
23 Apr 63	710	138	.195	Alfalfa, 10 cm tall
23 Apr 63	710	166	.234	Alfalfa, 30 cm tall
23 Apr 63	710	158	.224	Alfalfa, 50 cm tall
21 Jun 63	762	160	.209	Alfalfa, 30 cm tall
4 Jul 63	694	124	.178	Alfalfa, 20 cm tall
25 Jul 63	675	147	.217	Dry stubble
9 Aug 63	650	130	.199	Alfalfa, 23-cm stubble
12 Sep 63	566	108	.190	Alfalfa, 35-cm stubble, soil moisture limiting
25 Sep 63	513	96	.187	Alfalfa, 36-cm stubble, soil moisture limiting
15 Oct 63	460	115	.250	Dry stubble

TITLE: DEVELOPMENT AND USE OF GAMMA TRANSMISSION EQUIPMENT FOR THE
MEASUREMENT OF SOIL DENSITY AND MOISTURE CONTENT.

LINE PROJECT: SWC 4-gG4

CODE NO.: Ariz.-WCL-20

INTRODUCTION:

See Annual Report for 1962.

General. The gamma-ray attenuation principle was used originally in soil for the measurement of dry density (bulk density). However, since the measurement is basically one of the total or wet density, it can also be used for measuring soil water content. The use of this technique for the laboratory study of the water content in soil columns followed quickly upon the establishment of general principles (4). Examples of such work are reported by Gurr (3) and Davidson, et al. (1).

When use is made of the counting of primary photons only, the method has a potentially high degree of resolution. This is accomplished in the laboratory by collimating both radiation source and detector and by electronically discriminating against secondary, scattered photons. The mass attenuation coefficients of the various soil constituents, with the exception of hydrogen, are not greatly different, thus permitting a general calibration of dry density versus beam intensity. However, under stringent laboratory conditions the method attains a sensitivity that may require an accounting for the numerical difference in the mass attenuation coefficient for water and for the soil solids.

Thus, Gurr (3) reported that from empirically obtained values for the above two coefficients, the water content of soil columns could be calculated from measurements of wet density in 1.25-cm increments with an average error of about .005 volume fraction. Similar work was done by Davidson, et al. (1), who reported a mass attenuation coefficient, using a Cs¹³⁷ source, of $0.0769 \pm 0.0012 \text{ cm}^2 \text{ g}^{-1}$ for a dry silt loam and of $0.0815 \pm 0.0008 \text{ cm}^2 \text{ g}^{-1}$ for water. A theoretical value of the latter is $0.0862 \text{ cm}^2 \text{ g}^{-1}$ (2). A standard error of .002 volume fraction for the calculated water content was indicated.

When the gamma attenuation method is to be used for measurements on soil in situ, the instrumental problem is much greater. Collimation

of the source and detector is not practical and one must rely entirely upon electronic discrimination. The question is whether under such conditions one must also account for the effect of chemical composition (i.e., primarily water content) upon the attenuation coefficient. In earlier work by Van Bavel (4) this matter was neglected and it seemed worthwhile to re-evaluate the validity of such a working assumption. For the purpose of the present study, all measurements were made with a geometry and apparatus that could be used in the field, except that the electronic recording equipment was of the laboratory category.

Theoretical. Information on the theoretical attenuation coefficients of important soil elements can be found in Grodstein (2). Its implications for measurements in soil, using Cs¹³⁷ as a gamma source, are briefly reviewed by Van Bavel (4) and further amplified in the following.

For any compound or mixture the mass attenuation coefficient is

$$u = u_1 f_1 + u_2 f_2 + \dots + u_n f_n$$

in which $u_1 \dots u_n$ are the mass attenuation coefficients of the elements involved and $f_1 \dots f_n$ their respective weight fractions. Theoretical attenuation coefficients at 0.662 mev for 9 representative oven-dry soils of the United States are computed in Table 1. The average value of the attenuation coefficient, μ_s , is $0.0775 \text{ cm}^2 \text{ g}^{-1}$ as compared with that of water, μ_w , which is $0.0862 \text{ cm}^2 \text{ g}^{-1}$.

The attenuation coefficient for a moist soil is then:

$$\mu = \frac{\mu_s \rho_s + \mu_w \rho_w}{\rho_s + \rho_w}$$

in which ρ_s is the dry density in g cm^{-3} and ρ_w the volumetric water content in g cm^{-3} . The effect of water content and density upon the total theoretical attenuation coefficient of moist soil can be seen in Table 2.

The figures of Table 2 show that, in theory, there is no universally applicable value of μ for moist soil and, thus, no unique relation between $(\rho_s + \rho_w)$, or wet density, and beam intensity. Rather, the following relation applies:

$$I = I_0 \exp(-(\rho_s \mu_s + \rho_w \mu_w)x) \quad [1]$$

in which I_0 is the unattenuated beam intensity, I the actual one and x the length of the attenuation path. To a much smaller extent one can say from Table 1 that the same conclusion pertains to the relation between ρ_s and gamma attenuation by the soil solids only.

Whether these theoretical distinctions warrant attention when measurement techniques are employed that are applicable to in situ measurement of soil moisture content, can be decided from the experimental data that follow.

PROCEDURE:

Equipment. The radiation source is a 5-mc Cs¹³⁷ capsule with a gamma-ray energy of 0.662 Mev. The source capsule, 1.270 cm in diameter and 1.905 cm long, is held in a positioning tube (OD 2.54 cm) provided with holes with a diameter of 0.3 cm, drilled 1.0 ± 0.1 cm apart vertically (Figure 1).

The detector is a 2.54-cm diameter by 1.27-cm thick NaI(Tl) scintillation crystal mounted on a DuMont K1780 multiplier phototube. The signal of the phototube goes through an emitter-follower with a gain of 5 to the counting system. A positioning tube for the detector (OD 4.13 cm) was built, similar to the one for the source capsule. Both positioning tubes move freely in the access tubes such as would be used for field measurements. All parts are made out of brass stock. See Appendix I for description of electronic circuitry.

To maintain the distance between the source and detector constant, an alignment jig was constructed as shown in Figure 2. The jig also allows access tubes to be placed parallel in the field.

All data reported here were obtained with laboratory type counting equipment. The signal from the emitter-follower is fed into a linear amplifier, through a single-channel pulse height analyzer, into a scaler with a precision timer. The resolution time of the electronic system is on the order of μ sec. All the electronic equipment had a common ground and was operated at 112 ± 0.3 VAC line voltage.

For future field measurements, count rates will be obtained with a slightly modified Tempe rate meter (6). Tests have indicated that its accuracy for the current application is equivalent to that of the laboratory-type counting equipment.

Standard. In order to check on the operation of the electronic system during the measurements, the count rate through a magnesium rod (density 1.773 g cm^{-3}) was taken periodically and adjusted electronically to give $3,000 \pm 35$ cpm, the deviation being equivalent to a density change of $\pm 0.003 \text{ g cm}^{-3}$. Two Mg rods were used; one in which the access tubes were placed in holes drilled through the rod and the other which was cut to just fit between the access tubes. There was no difference between the count rates obtained with either Mg rod. Before and after each measurement the count rate in the Mg standard was checked. During the course of any one day the discriminator level usually had to be adjusted ± 0.3 volt: with the level set at approximately 45 volts. This slight adjustment is necessary because of the drift in the electronic system.

The proper discrimination or pulse threshold level was found as follows. A block of aluminum, approximately 11 cm thick, was placed next to the source, halfway between the source and detector, and next to the detector. Count rates were obtained at these three positions at increasing threshold settings. When the count rates at the three locations were not significantly different from each other, the contribution of scattered radiation was considered negligible and the count rate in the Mg rod at this threshold setting was adopted as the standard.

The energy spectrum in air at a distance of 1 m and the integral count rate in the alignment jig through Mg are shown in Figure 3. The location of the threshold setting is indicated by the arrow.

Calibration. Calibration was required to find the values of I_0 , μ_s , and μ_w in equation [1], so that ρ_w could be calculated, given a direct measurement of ρ_s . Actually, the values of μ_{sx} and μ_{wx} were measured and used for the computation. To evaluate I_0 and μ_{sx} , a tray was constructed containing 20 stationary glass plates, each 0.6125 cm

thick, normal to the gamma beam. The tray was slotted so that the spaces between the plates could be filled with additional glass plates or with water (Figure 2).

I_0 represents the count rate of the unattenuated beam but this rate is too high for accurate counting. Therefore, the value of I_0 was obtained by extrapolating to zero density from the count rates obtained with the glass tray with various numbers of plates. The density of each glass plate was determined and the error varied from $\pm 0.001 \text{ g cm}^{-3}$ at 1.00 g cm^{-3} to $\pm 0.002 \text{ g cm}^{-3}$ at 2.000 g cm^{-3} .

The attenuation coefficient for oven-dry soil was obtained as follows: Oven-dry Adelanto loam was packed into a brass cylinder of 6.1 cm diameter and length such that it fitted snugly between the two access tubes. A mean count rate was determined by averaging the time in minutes for 20,000 counts at ten locations through the column. Knowing I_0 , the count rate, and the density of the oven-dry sample, the attenuation coefficient of dry soil was calculated.

The attenuation coefficient of water was obtained by filling the spaces in the glass tray, one at a time, with water. Each section corresponds to a definite water density which is equivalent to a volumetric water content and the count rate was determined for various combinations of water-filled sections.

Verification. In order to assess the applicability of equation [1] for a soil (Adelanto loam), 26 soil samples ranging from 0.014 to 0.381 volumetric water content were packed in brass cylinders. The time for 20,000 counts was recorded at each of ten locations through each cylinder and the average count rate and standard deviation were calculated. The volume of the cylinder, $886 \pm 1 \text{ cm}^3$, and the weight of the entire soil sample was used to determine the gravimetric moisture content and the dry density, both with an error of $\pm 0.003 \text{ g cm}^{-3}$. Errors reported here are computed at the 95% confidence level or roughly twice the standard error.

RESULTS AND DISCUSSION:

The plot of glass density versus count rate (Figure 4) yields the value of I_0 , $115,900 \pm 880 \text{ cpm}$. The linearity of the relation indicates

that the contribution of scattered radiation is negligible and that the use of equation [1] is valid.

With the value of I_0 and the measurement in dry soil, also shown in Figure 4, the attenuation coefficient of oven-dry soil was calculated to be $0.0699 \pm 0.0004 \text{ cm}^2 \text{ g}^{-1}$, slightly less than the values reported by Gurr (3) and Davidson, et al. (1). This value is based on assuming that $x = 30.3 \text{ cm}$.

From a plot of moisture content versus count rate from the glass-water system (Figure 5) the attenuation coefficient of water was calculated to be $0.0748 \pm 0.006 \text{ cm}^2 \text{ g}^{-1}$. Again the linearity of the data is quite evident.

Using the above values for I_0 , $\mu_s x$ and $\mu_w x$ in equation [1], a volumetric water content was calculated for each of the 26 soil samples as follows:

$$\rho'_w = \frac{\ln I_0 - \ln I - \rho_s \mu_s x}{\mu_w x} \quad [2]$$

A plot of the calculated versus measured water content is shown in Figure 6. The vertical line through each of the points is the standard deviation of that particular sample. This variation is chiefly due to the variation in the ten separate measurements of I . By linear regression analysis the slope of the line is equal to 1.0420 ± 0.0520 and the intercept -0.0064 ± 0.0018 . The dashed lines correspond to the confidence limits for these data, equal to ± 0.025 volume fraction. All but one of the points fall within the established confidence limits. Although the standard deviation is ± 0.025 volume fraction, the average deviation of calculated versus measured values for all 26 samples is ± 0.010 volume fraction.

The water content was also calculated, assuming that the difference in attenuation coefficient between water and soil could be neglected, as follows:

$$\rho''_w = \frac{\ln I_0 - \ln I}{\mu_s x} - \rho_s \quad [3]$$

Equation [3] requires one less variable than equation [2]. A plot was

then made of this calculated value versus the measured one in Figure 7. The standard deviations were omitted, but are equal to those in Figure 6. The slope of the line is equal to 1.1131 ± 0.0577 and the intercept equal to -0.0036 ± 0.0020 .

To establish whether or not equation [2] is equivalent to equation [3], and to eliminate the sampling error of I, a plot of the water contents calculated in both ways was made, shown in Figure 8. The slope of the line is 1.0688 ± 0.0037 and the intercept 0.005 ± 0.0005 .

With the type of equipment and procedures used the relation between water content and gamma attenuation is accurately described using the exponential-inverse square law. However, it is critical to determine and to maintain the correct threshold value for the discriminator setting (Figure 3). Once established, only minor adjustments are necessary to compensate for electronic drift.

Figures 4 and 5 show that a precise evaluation of the attenuation coefficients and of I_0 can be made with our equipment. However, the results show in Figure 8 that there is no advantage in the use of equation [2] over that of equation [3], thus eliminating the need for taking into account the value of μ_w . Actually, equation [3] is given by line 2 in Figure 4. Thus, $\rho_w + \rho_s$ can be read simply from a graph or from a table based on equation [3]. The routine use of equation [2] is more time-consuming.

The scatter of the data points in Figures 7 and 8 is in marked contrast with the quality of the data in Figures 4 and 5. Since the same equipment and procedures were used, the variation in I is caused by random variation of ρ_w or ρ_s within the columns of moist soil. This explanation is supported by an analysis of variation and by the fact that the regression lines are not significantly different from a 1:1 relation.

Thus, an empirical calibration of the equipment in terms of I vs. $\rho_w + \rho_s$ is not only unnecessary, but also possibly misleading. Obviously, both I_0 and ρ_s should be determined with great precision. The same point is made by Davidson, et al. (1). However, our data show, in addition, that no significant error is made by neglecting the effect of

changing chemical composition. The data from Davidson, et al. (1) and our own give a value of 0.934 and 0.943, respectively, for μ_s/μ_w . Evidently, this is not significantly different from unity for the purpose at hand.

The accuracy of the method can be estimated from the errors in I_o , I , and μ_s as used in equation [3]. The precision is influenced only by the error in I . With the equipment used here the following standard errors for the measurement of $\rho_s + \rho_w$ are estimated:

$\rho_s + \rho_w$ g cm ⁻³	Accuracy g cm ⁻³	Precision g cm ⁻³
1.900	0.014	0.006
1.600	.013	.006
1.400	.012	.006
1.300	.011	.006
1.150	.010	.006

The above figures pertain to a total count of 20,000. The value of 0.002 g cm⁻³, as given by Davidson, et al. (1), presumably pertains to a precision and a total count of about 200,000. It is important to realize that the method may indicate changes in moisture content rather precisely, but that the absolute moisture content may be subject to a larger error.

The principal justification for using gamma attenuation for measuring the water content of soil in situ resides in the resolving power of the method, that is, the size of the soil body seen by the detector. Theoretically, it should be equal to the solid angle subtended by the scintillation crystal with reference to the radioactive point source. Previous work (5) using similar equipment has shown that the resolution of the method is on the order of 1 cm, as expected. This means that a soil profile could be scanned in one-centimeter layers.

Finally, attenuation is drawn to the undesirability of using large radioactive sources for field work. Thus, field observations will often require longer counting times and also have less precision

as compared to laboratory type experimentation. Nevertheless, a field version of the gamma attenuation method for moisture measurement can give results unattainable by any other method in terms of accuracy, resolution, and absence of time lag and site disturbance.

SUMMARY AND CONCLUSIONS:

Gamma-ray attenuation measurements of wet density were made with a 5-mc Cs¹³⁷ source over a pathlength of about 30 cm. Data were obtained for glass and water systems as well as for soil materials of varying water content.

The laboratory equipment was designed and constructed for use in the measurement of water content of soil in situ in 1-cm increments.

Experimental results verify theoretical considerations on the use of gamma attenuation for soil water measurement. For equipment calibration, only the unattenuated beam intensity and the attenuation coefficient for oven-dry soil need be determined to make use of the exponential inverse square law for calculating the water content, given the dry density. The data demonstrate that the difference in the attenuation coefficients of dry soil and water can be neglected without error.

Accuracy of the method, for a total count of 20,000, varies from 0.010 to 0.014 g cm⁻³ for wet densities of 1.150 to 1.900 g cm⁻³ respectively. For the same total count, a precision of 0.006 g cm⁻³ is demonstrated.

REFERENCES:

- (1) Davidson, J. M., Biggar, J. W., and Nielsen, D. R.
1963. Gamma-radiation attenuation for measuring bulk density and transient water flow in porous media. Jour. Geophys. Res. 68:4777-4783.
- (2) Grodstein, G. W.
1957. X-ray attenuation coefficients from 10 Kev to 100 Mev. NBS U. S. Circular 583.
- (3) Gurr, C. G.
1962. Use of gamma rays in measuring water content and permeability in unsaturated columns of soil. Soil Sci. 94:224-229.

- (4) Van Bavel, C. H. M.
1957. Transmission of gamma radiation by soils and soil densitometry. Soil Sci. Soc. Amer. Proc. 21:588-591.
- (5) Van Bavel, C. H. M.
1959. Soil densitometry by gamma transmission. Soil Sci. 87:50-58.
- (6) Van Bavel, C. H. M.
1962. Light-weight rate meter for neutron soil moisture measurement. Soil Sci. 94:418-419.

PERSONNEL: R. J. Reginato and C. H. M. van Bavel.

APPENDIX I—ELECTRONIC CIRCUITRY:

A schematic of the phototube and emitter-follower (preamp) is shown in Figure 9. Connections A, C, and E represent the numbered pins on a bayonet-type connector between the phototube and preamp. Connections A₁, A₂, and A₃ represent the external electrical leads. The construction of the detector tube is such that all parts (crystal, phototube, preamp, and exterior electrical leads) may be disconnected rapidly without having to unsolder connections.

The preamp was designed specifically for crystal scintillation counting. The gain of the preamp is adjustable by the magnitude of the fixed resistor, R. For example, a gain of 5x requires a 5K Ω resistor, a gain of 10x requires a 10K Ω resistor. Power for the preamp is supplied by four 5.4 v mercury batteries in series.

High voltage to the phototube is supplied from the circuit shown in Figure 10. The output voltage, 700 v, is quite stable, ± 0.5 v, if the high voltage to the phototube is on about 24 hours previous to the time of measurement. This is accomplished by connecting a laboratory transformer, 110 VAC to 6 VDC, to the phototube before a run is to be made. Then about one hour before the run, the 6 VDC lead is switched from the laboratory transformer to the two 5.4 VDC mercury batteries in parallel. This procedure is used to extend the useful life of the batteries for field use and to allow sufficient warm-up time for the phototube. The latter point was determined strictly from experience.

With 700 VDC applied to the phototube, the magnitude of the phototube output signal is on the order of 30 mv. This signal then goes to the preamp, amplified by a factor of five, and then feeds directly into the electronic counting equipment.

The complete representation of the detection and counting systems is shown in the block diagram, Figure 11. In actual practice the 700 VDC high voltage supply is incorporated directly into the modified Tempe rate meter.

able 1. Representative soils of the United States, their chemical composition^{1/} and theoretical mass attenuation coefficients at .662 mev.

Soil No.	Soil Type ^{2/}	Great Soil Group ^{2/}	Location	Depth
1	Caribou loam	Podzol	Houlton, Me.	1.5 - 4"
2	Miami silt loam	Grey-Brown Podzolic	Hancock Co., Ind.	5 - 12"
3	Norfolk sand	Red & Yellow soils	Mitchell Co., Ga.	13 - 24"
4	Cecil clay loam	Red & Yellow soils	Greenhill, N. C.	6 - 40"
5	Marshall silt loam	Prairie soils	Fremont Co., La.	0 - 10"
6	Houston black clay	Prairie soils	Reinhardt, Tex.	6 - 14"
7	Barnes silt loam	Chernozem	Moody Co., S. D.	8 - 23"
8	Dark Brown sandy clay	Brown soils	Gillette, Wyo.	9" +
9	Mohave loam	Grey Desert soils	Buckeye, Ariz.	6 - 14"

Element	$\mu\text{cm}^2 \text{g}^{-1}$	Soil Number								
		1	2	3	4	5	6	7	8	9
Composition of Oven-Dry Soil in % by Weight										
O	0.0775	52.2	50.7	53.3	52.0	50.5	49.8	51.9	50.6	49.6
Si	.0772	37.0	36.2	45.5	23.4	34.0	22.9	33.4	30.7	32.0
Ti		.5	.4	.1	.8	.4	.3	.4	.3	.4
Fe	.0732	.8	2.2	.2	6.5	2.2	2.8	3.2	2.8	3.7
Al	.0748	5.1	5.3	.6	14.1	6.4	5.7	6.2	6.5	7.3
Mn		.0	.1	.0	.0	.1	.1	.2	.0	.1
Ca	.0778	.1	.4	.0	.0	.6	10.4	.8	3.1	1.8
Mg	.0765	.3	.4	.0	.3	.5	.9	.6	.8	.9
K	.0756	1.1	1.8	.1	1.2	1.8	1.1	1.7	1.8	2.1
Na	.0741	.9	.9	.0	.3	1.0	.2	.9	1.1	1.4
P	.0750	.0	.0	.0	.0	.0	.1	.0	.1	.1
S	.0775	.0	.0	.0	.0	.0	.1	.1	.1	.0
N	.0774	.1	.1	.0	.0	.2	.2	.1	.1	.0
C	.0774	1.4	1.2	.2	.3	1.9	4.8	.8	1.5	.3
H	.1538	.5	.3	.0	1.1	.4	.6	.5	.5	.3
$\mu(\text{cm}^2 \text{g}^{-1})$		0.0775	.0773	.0773	.0776	.0774	.0776	.0780	.0774	.0772

Based upon data from "Atlas of American Agriculture," U. S. Department of Agriculture, Washington, 1936. The figure for H is obtained by subtracting $(20 \times N + \text{Carbonate } \text{CO}_2)$ from ignition loss, considering this as "bound water." To this amount is added $0.041 \times 20 \times N$, as an estimate of H in organic matter. C is found from Carbonate CO_2 and $0.58 \times 20 \times N$. The figures for H and C are estimates only. O is obtained by difference, all others are based upon actual analysis.

For reference purposes the names and classification of soils as used in the "Atlas" have been retained.

Table 2. Theoretical gamma attenuation coefficient at .662 Mev in $\text{cm}^2 \text{g}^{-1}$ of moist soil at varying dry density and volumetric moisture content.

Dry Density g cm^{-3}	Volumetric Moisture Content g cm^{-3}						
	0.00	0.10	0.20	0.30	0.40	0.50	0.60
0.90	0.0775	.0784	.0791	.0797	.0802	.0806	.0810
1.00	.0775	.0783	.0790	.0795	.0800	.0804	.0808
1.10	.0775	.0782	.0788	.0794	.0798	--	--
1.20	.0775	.0782	.0787	.0792	.0797	--	--
1.30	.0775	.0781	.0787	.0791	.0795	--	--
1.40	.0775	.0781	.0786	.0790	.0794	--	--
1.50	.0775	.0780	.0785	.0790	.0793	--	--
1.60	.0775	.0780	.0785	.0789	--	--	--
1.70	.0775	.0780	.0784	.0788	--	--	--

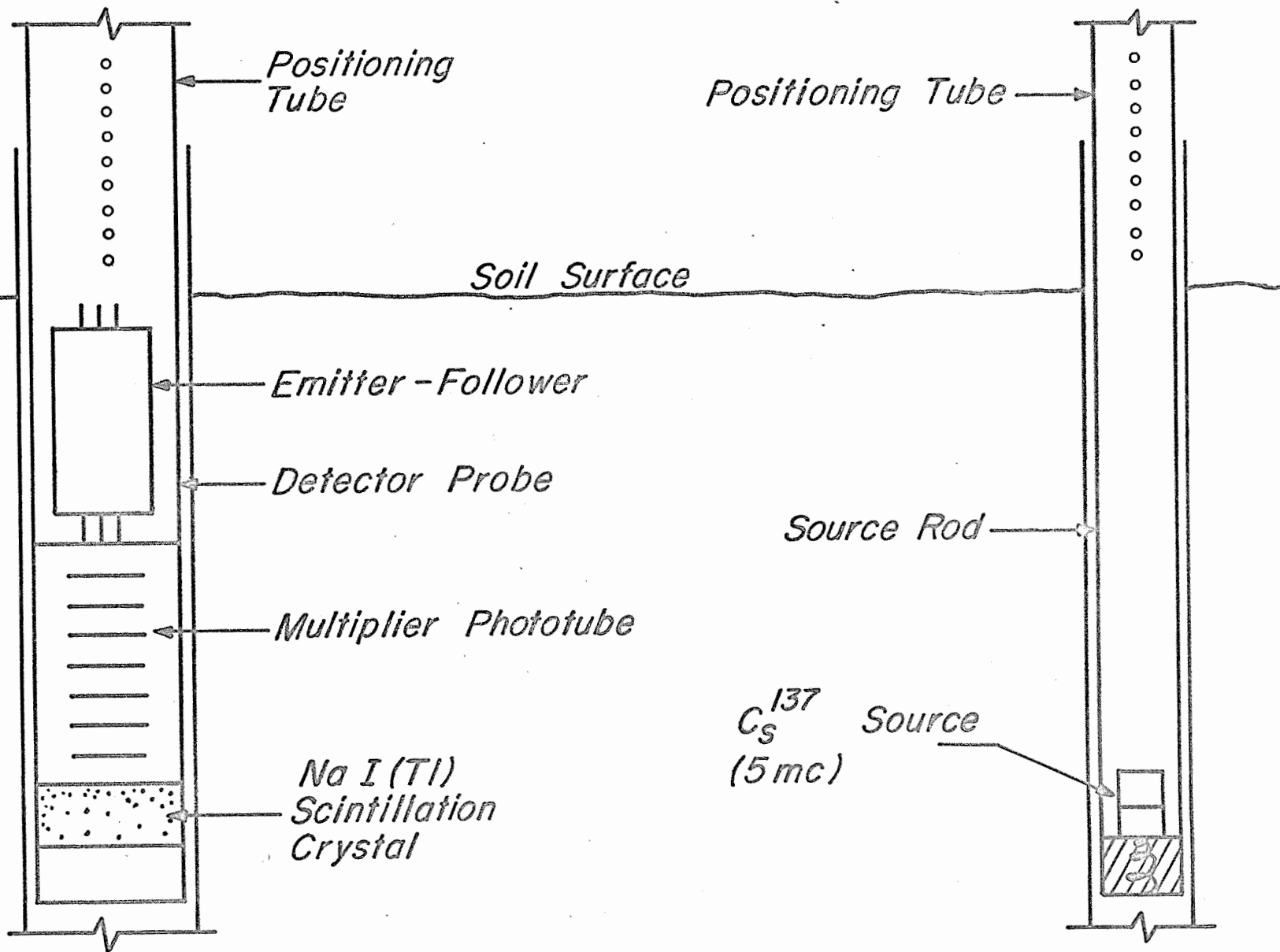


Figure 1. Source and detector probe arrangement for gamma transmission apparatus.

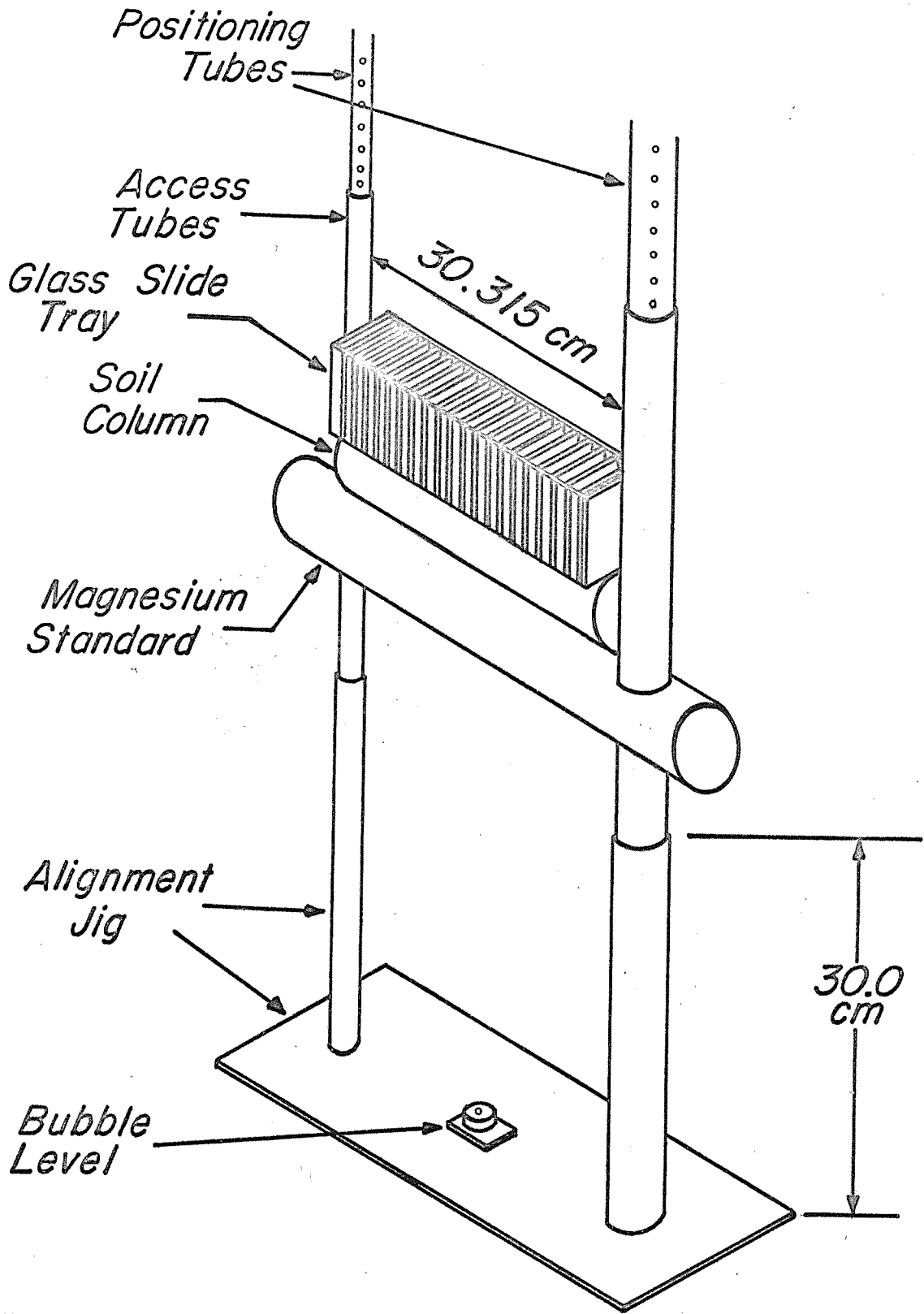


Figure 2. Laboratory setup for calibration of gamma transmission apparatus.

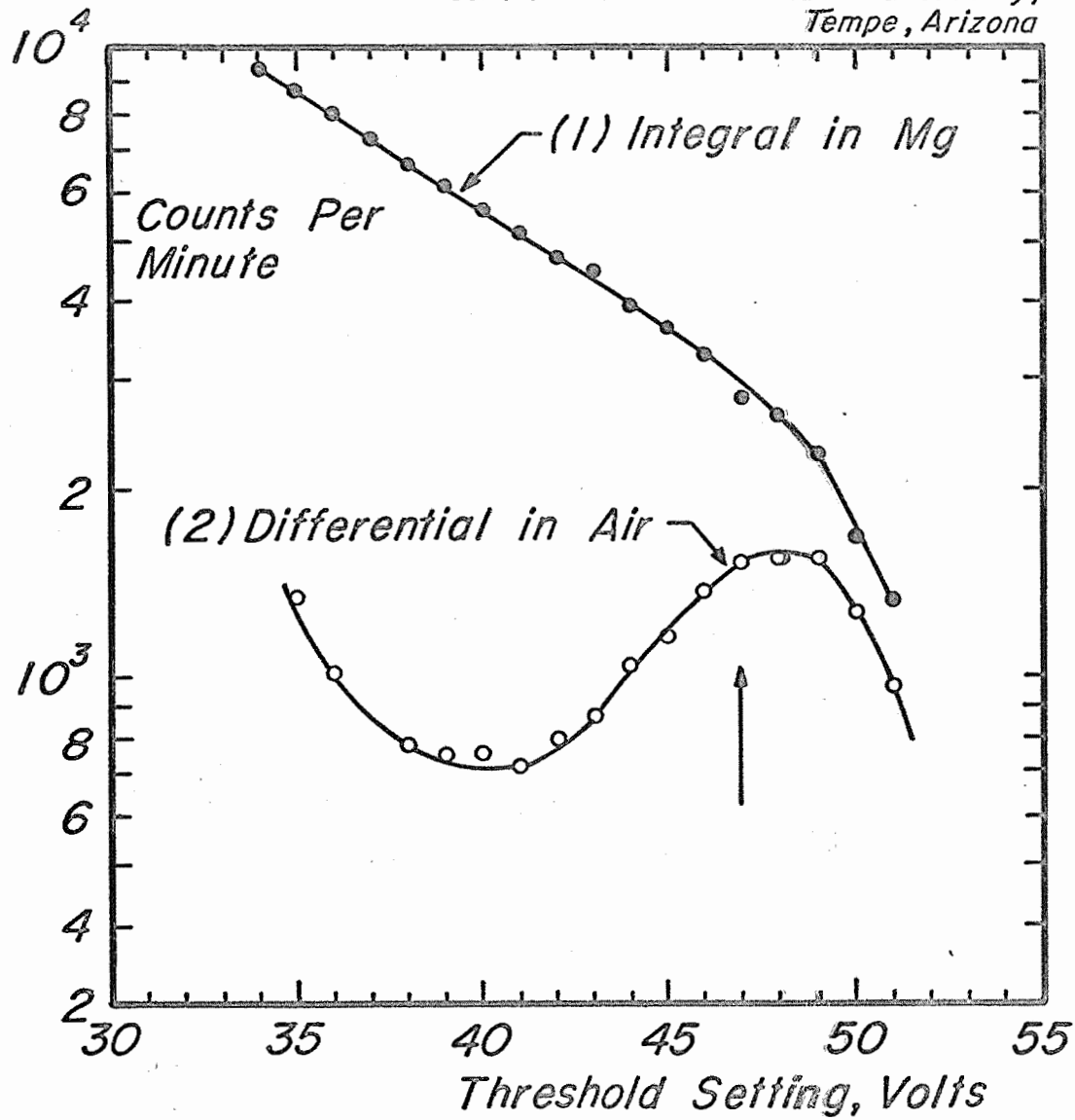
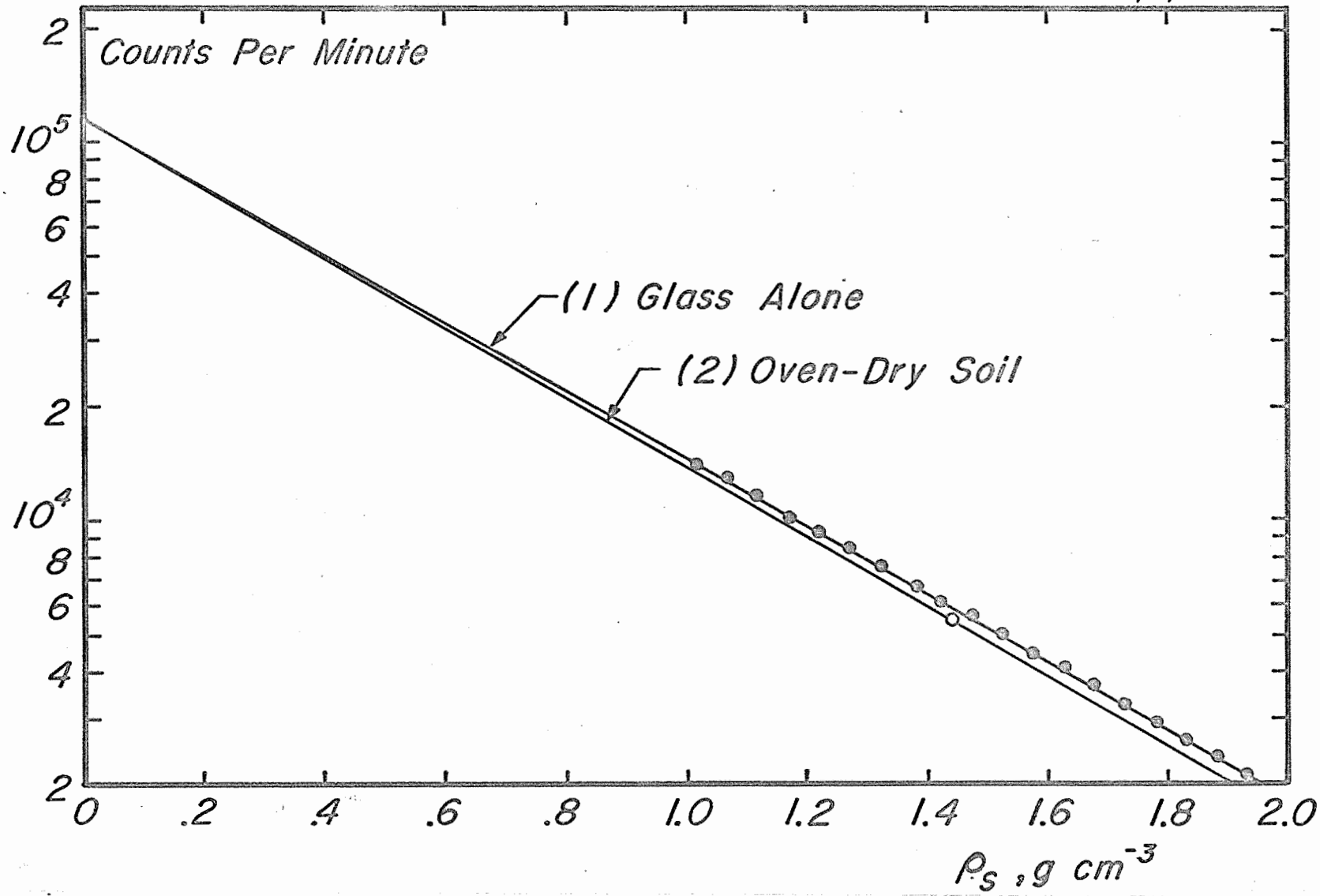
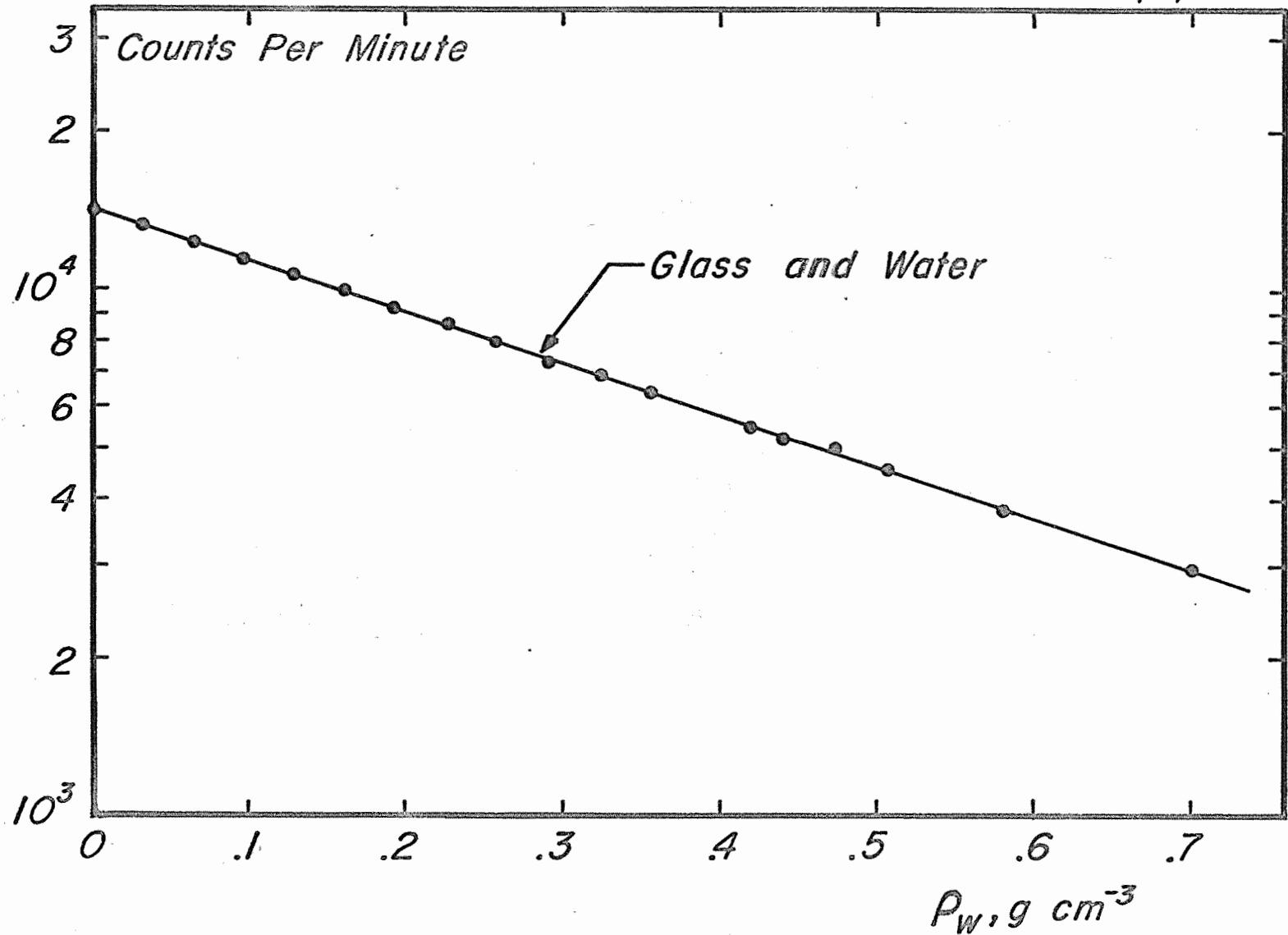


Figure 3. Energy spectrum for Cs¹³⁷; (1) integral count rate in Mg with a pathlength of 32 cm, (2) differential count rate in air with source and detector 1 m apart (arrow indicates threshold value).



20-17

Figure 4. Count rate versus density (g cm⁻³); (1) from plate angular report of the U.S. Water Conservation Laboratory soil point and intercept extrapolated from (1).



20-18

Figure 5. Count rate versus water content determined from fillings of glass with water. Annual Report of the U.S. Water Conservation Laboratory

20-19

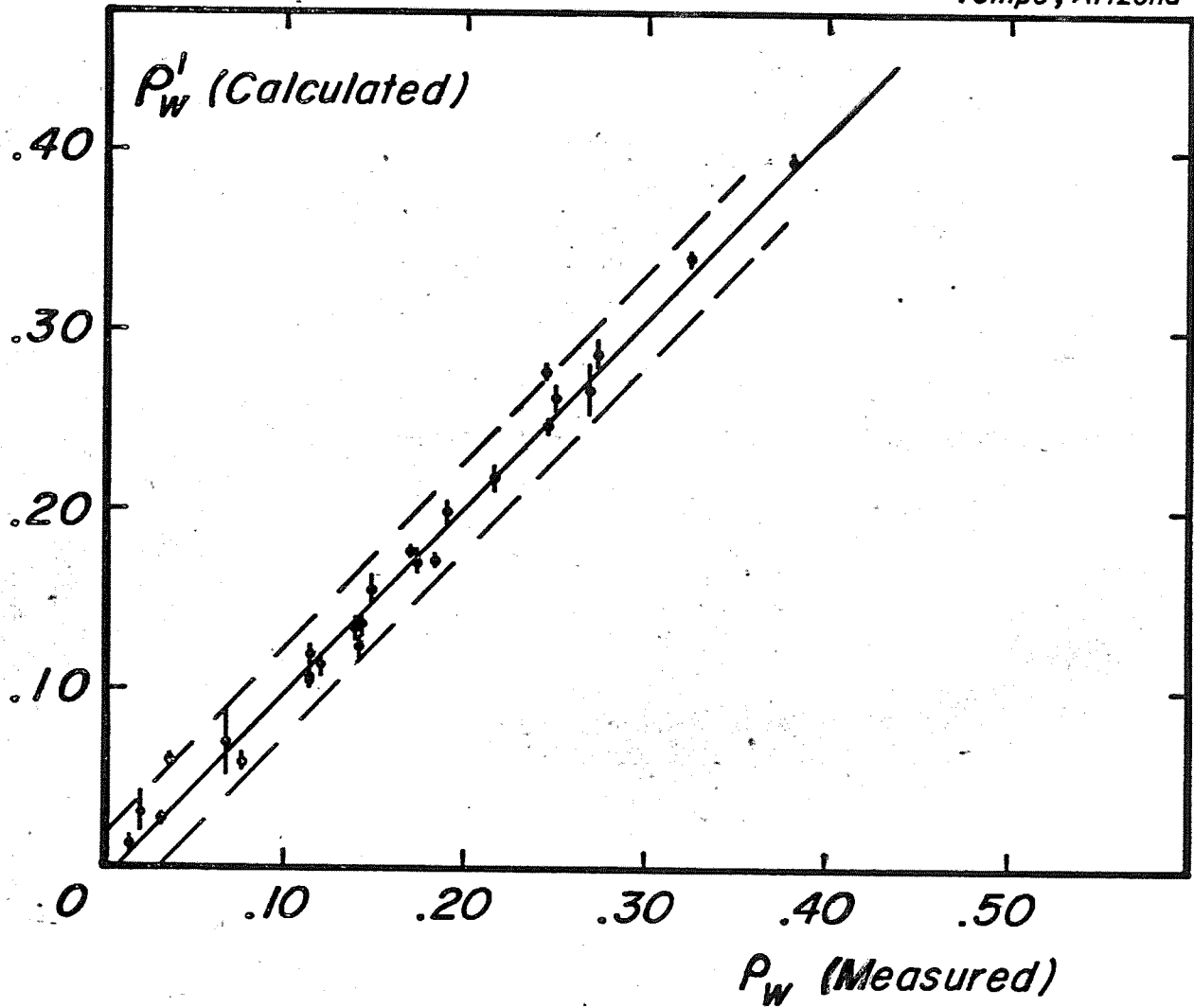
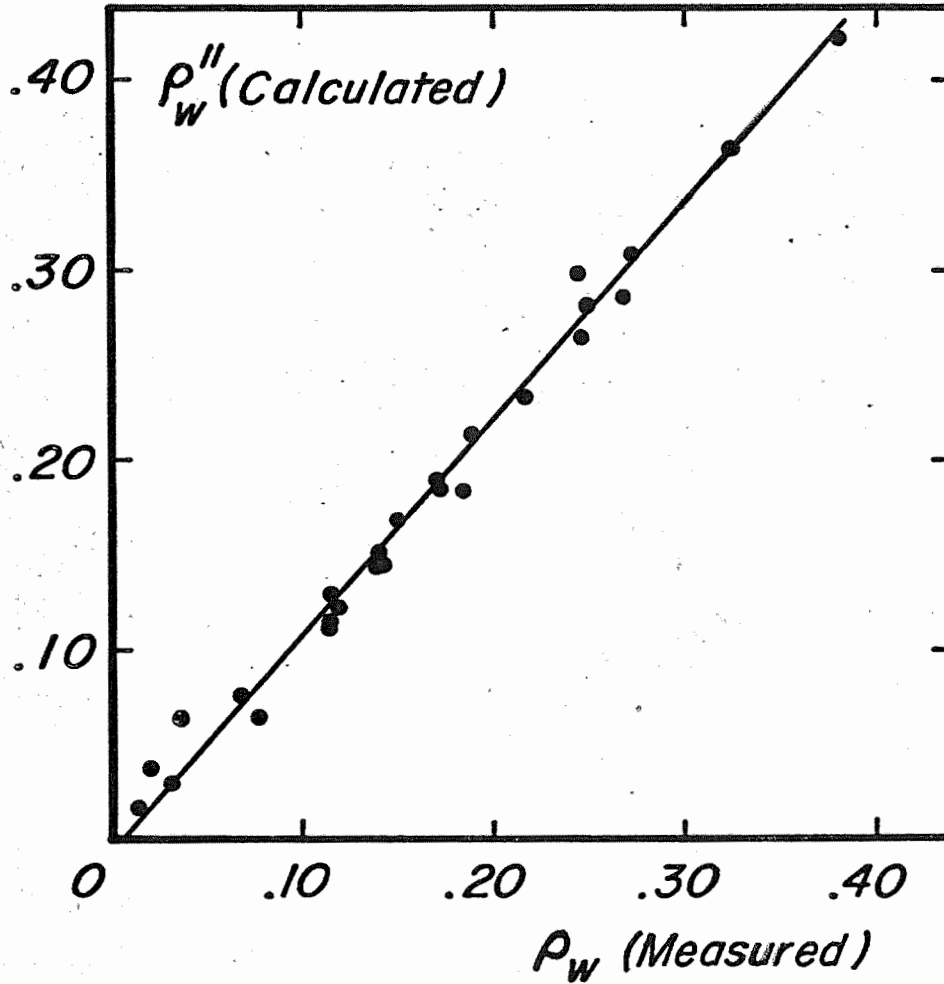


Figure 6. Water content calculated from $\rho_w' = \frac{\ln I_0 - \ln I - x \rho_s \mu_s}{\rho_w}$ versus measured water content, ρ_w .

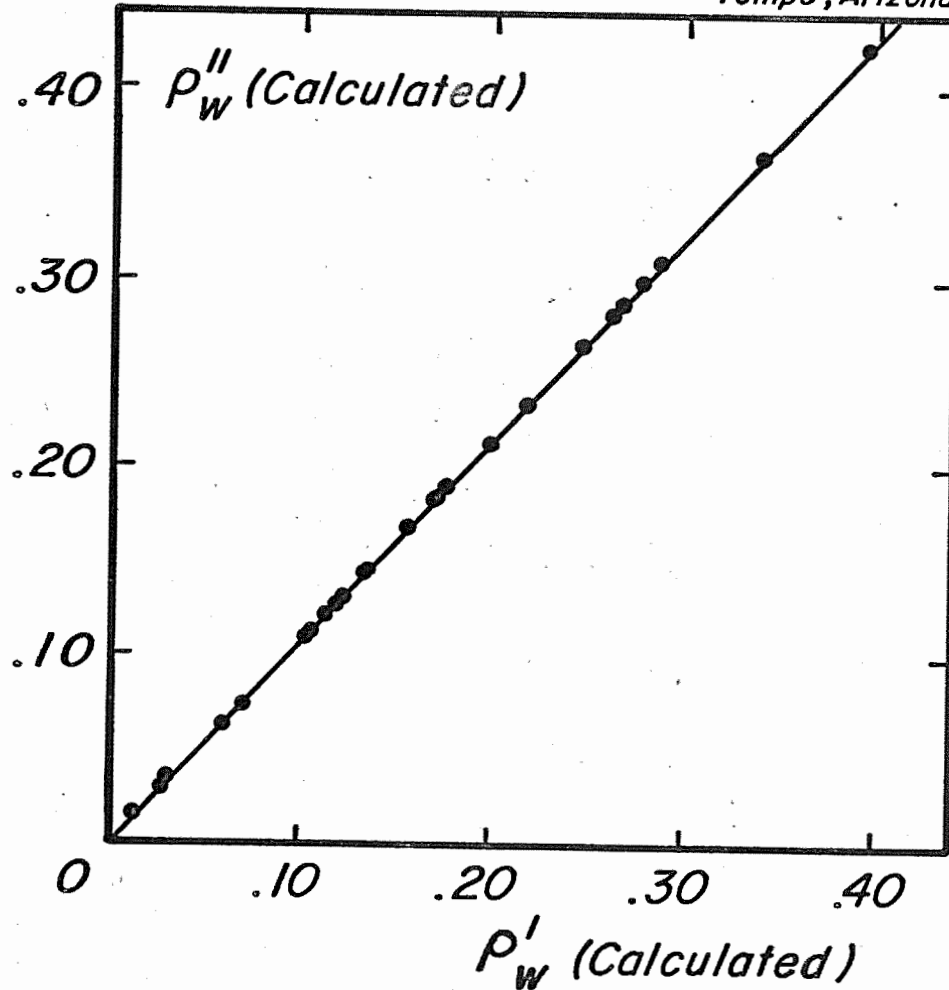
U.S. Water Conservation Laboratory,
Tempe, Arizona



20-20

Figure 7. Water content calculated from $\rho_w'' = \frac{\ln I - \ln I_s}{\ln I - \ln I_s}$ versus measured water content, ρ_w . Annual Report of the U.S. Water Conservation Laboratory, p. 115

U.S. Water Conservation Laboratory,
Tempe, Arizona



20-21

Figure 8. Water content ρ_w^{II} versus ρ_w^I . Annual Report of the U.S. Water Conservation Laboratory

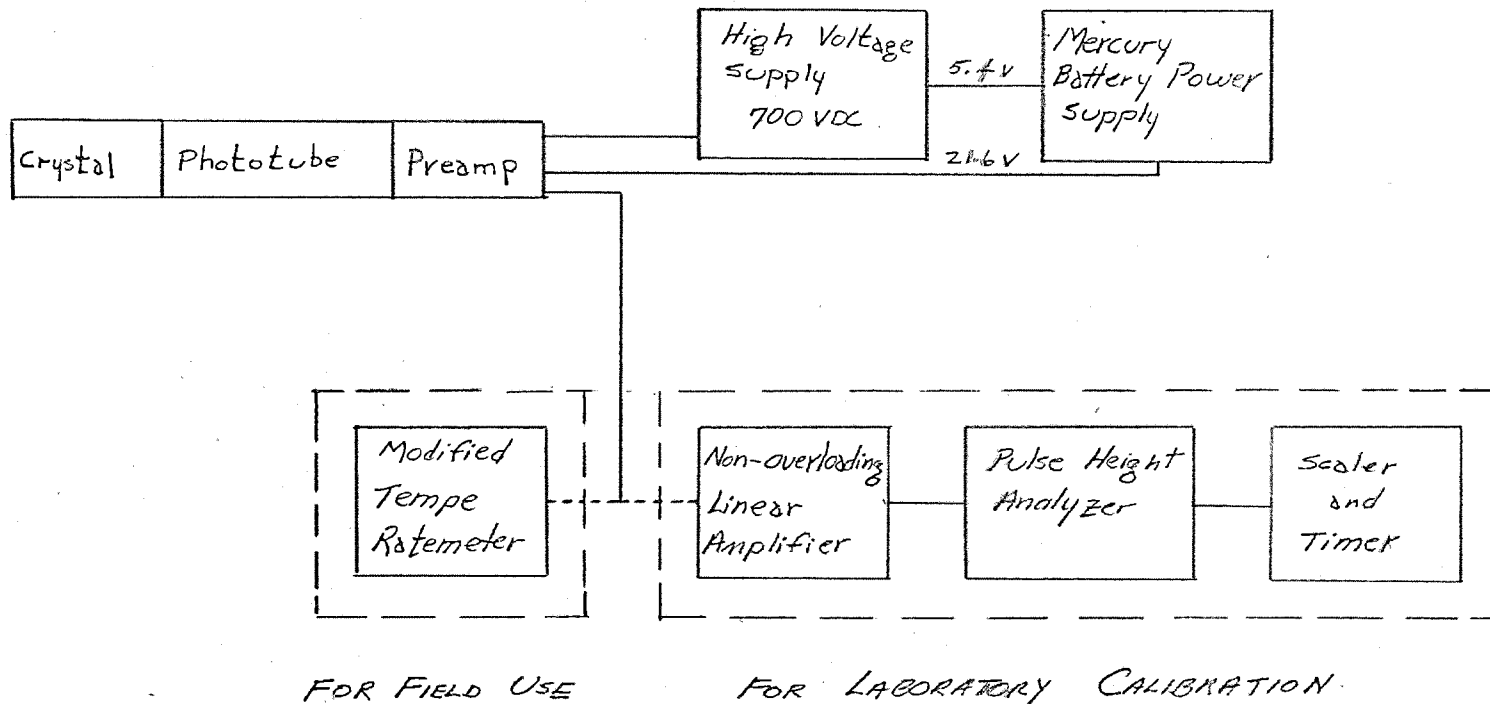
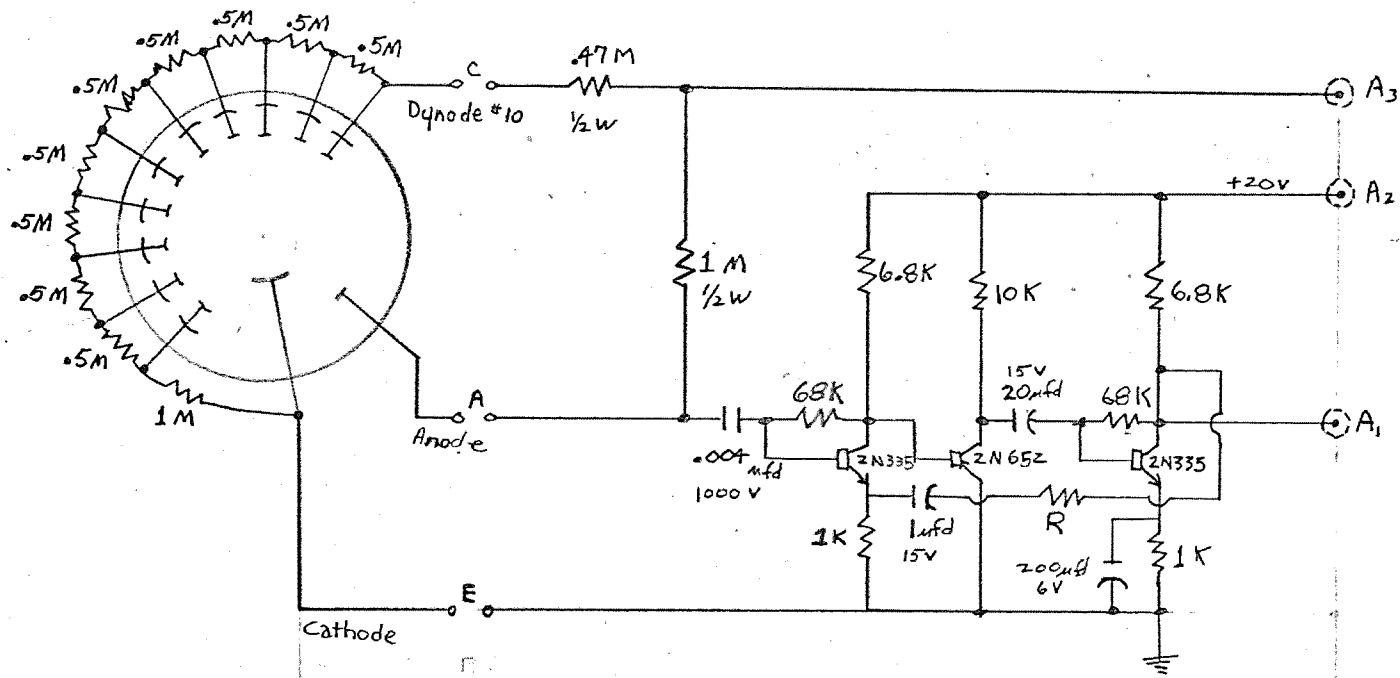


Figure 11. Block diagram of detection and counting systems for gamma transmission apparatus.
Annual Report of the U.S. Water Conservation Laboratory



NOTES:

A_1 : output signal

A_2 : preamp power (21.6 v)

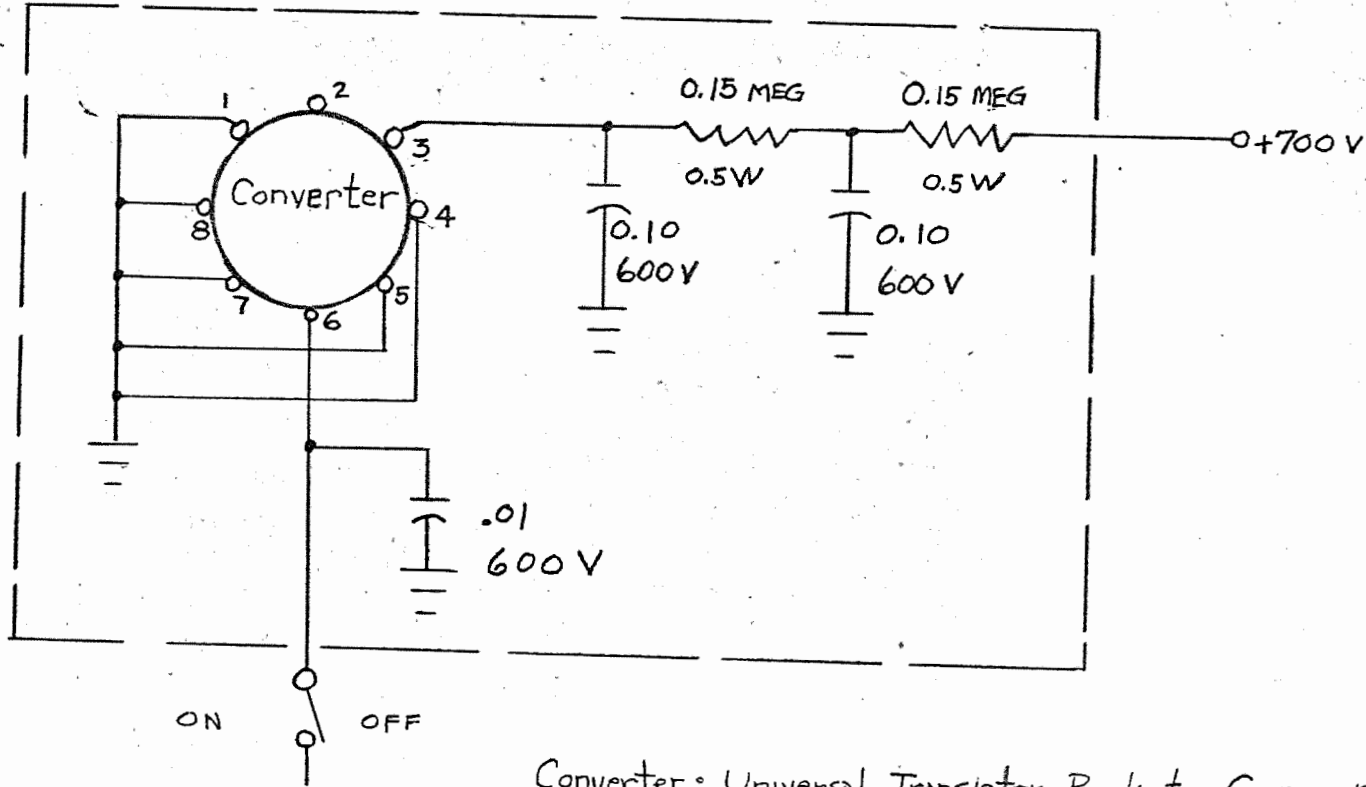
A_3 : high voltage input (700 v)

R: fixed resistor (gain proportional to magnitude)

All resistors, except as noted, are $\frac{1}{4}$ w and 5% tolerance.

Coaxial shields have common ground with circuit ground.

Figure 9. Schematic of multiplier phototube and preamplifier for gamma transmission apparatus.



Converter: Universal Transistor Products Corp. regulated high voltage DC-DC converter Model 350, (6v, 45 MA input ; 700v, 150 μ A output).

Figure 10. Schematic of high voltage supply for multiplier phototube.

TITLE: THE USE OF SALTY WELL WATER FOR THE PRE-PLANTING IRRIGATION
ON SILTY CLAY SOILS

LINE PROJECT: SWC 4-gG3

CODE NO.: Ariz.-WCL-22

INTRODUCTION:

For need of study see Annual Report 1958. The objective of the experiment is to determine the amount of water to apply at the pre-planting irrigation to maintain economic production. The experiment was initiated April 1, 1958. An investigative study on the use of saline water on the Price Ranch is included under WCL-22. Data will be found subsequent to the discussion on WCL-22.

PROCEDURE:

The experiment is located at the University of Arizona Experiment Farm, Safford Branch, Safford, Arizona. The experiment was conducted on Field "I" borders 1-18.

Plots were plowed in January 1963, and allowed to dry out. On March 25, 1963, the following amounts of pre-planting-leaching water (2596 ppm) were applied.

1. 8 inches of well water - plots 4, 6, 12, 17,
2. 12 inches of well water - plots 3, 8, 10, 16.
3. 18 inches of well water - plots 2, 7, 11, 14.
4. 19 inches of well water - plots 5, 9, 13, 15.

On April 11, 1963 all plots were planted to New Mexico 1517D (short staple) and Pima S-2 (long staple) varieties. Difficulty in proper placement of seed in moisture was noted at this time. A poor stand was obtained and the plots were disked, furrowed out, and replanted on May 12, 1963. Plots were then given a light irrigation on May 15, 1963.

Soil salt measurements were made on all plots previous to and after the leaching irrigation. A final soil-salt measurement was made just prior to harvest.

The application of water during the growing season was supervised. Only that amount necessary for consumptive use was given. Areas for yield measurements were marked off and thinned when plants were about 6 inches tall.

Irrigation dates. -- Leaching irrigation 3/25. Irrigations for consumptive use purposes. 6/27, 7/19, 8/17, 9/19. In addition, 4.43 inches of rain fell during the month of August.

RESULTS AND DISCUSSION:

A good stand of cotton was obtained after the second planting.

Yield Seed Cotton (1517D) in Pounds Per Plot

Reps.

<u>Trts.</u>	<u>1</u>	<u>2</u>	<u>3</u>	<u>4</u>	<u>Mean</u>
8"	21.0	18.0	20.0	17.0	19.0
12"	21.0	21.0	23.0	20.0	21.3
18"	19.0	25.0	27.0	28.0	24.8
19"	23.0	20.0	27.0	22.0	23.0

No. sig.

Yield Seed Cotton (Pima S-2) in Pounds Per Plot

Reps.

<u>Trts.</u>	<u>1</u>	<u>2</u>	<u>3</u>	<u>4</u>	<u>Mean</u>
8"	13.0	10.0	15.0	12.0	12.5
12"	11.0	12.0	17.0	16.0	14.0
18"	14.0	13.0	16.0	17.0	15.0
19"	18.0	12.0	17.0	18.0	16.3

No Sig.

A very salty soil existed previous to leaching (Figure 1). After leaching, soils were still in the 2900 to 3800 range, poor germination resulted, but mainly because of poor seed soil moisture contact. Where seeds and soil were in close contact and wet, good germination resulted. The late second planting date May 15 resulted in generally low yields especially in long staple cotton. The 4.4 inches of rain following the 8/17 irrigation probably accomplished some late season leaching.

SUMMARY AND CONCLUSIONS:

There was no significant difference in yield. However, the 8-inch leaching treatment was lowest on both varieties as in previous years. When both varieties are considered, average yield increases by treatments over the 8-inch treatment are:

12-inch treatment	12%
18-inch treatment	26.3%
19-inch treatment	24.0%

A. SALINE WATER USE INVESTIGATION ON THE PRICE RANCH

INTRODUCTION:

High saline water is being used in many areas in Arizona for irrigation purposes. One of these areas is the Price Ranch west of Chandler. Difficulties have been encountered on this ranch when producing cotton. Generally, it is difficult to obtain stands, maintain them, and realize high yields.

During the 1962 growing season observations, preliminary suggestions and small tests were conducted. It was found that good yields could be obtained by proper management during the production phase of the growing season. The major remaining problem was how to obtain and maintain stands. Changes in the planting operations, early season water management and asphalt mulches seemed to offer the greatest possibilities.

The quality of water in 1963 varied from 5000 to 7000 ppm. A water sample taken during the early part of the growing season contained 6400 ppm of salts. The sodium percentage was 64%, sodium-calcium ratio 1.37, sulphates 711 ppm, chlorides 3018 ppm, PH = 7.7 and an SAR value of 13.05. The PH of the soil was 8.0. The soil is a sandy loam containing 66% sand, 25% silt, and 9% clay.

No. 1 Investigation

A conventional vegetable planter was converted, such that it planted on the slope of a standard furrowed-out bed. Contact was made with an oil company to apply an asphalt emulsion as an 8-inch cap on plantings.

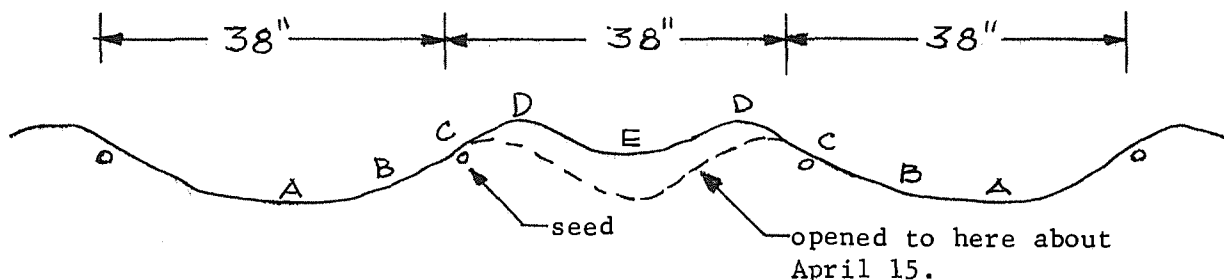
Four quarter-mile row plots were set up to study the use of the re-vamped vegetable planter as compared to the standard furrow planter. An asphalt emulsion cap (app. 8" wide) was applied over the planted seed on both types of initially wet and dry beds.

Soil-salt, temperature and soil moisture measurements were made on the 4-row plots starting at the soil preparation period and until plants were well established.

No. 2 Investigation

An additional set of plots was established in the field planting April 22 to follow the salt movement in the root zone during the growing season. Irrigations were applied on an every-other-row system until June 14, then irrigations were given in every row.

Soil-salt samples were taken at 5 locations, 2 samples at each location and each location duplicated. Samples were taken at depths of 0-6, 6-12, 12-24, and 24-36 inches.



A, B, C, D, E - refer to soil sampling locations.

RESULTS AND DISCUSSION:

No. 1 Investigation

1. After the first irrigation on initially dry soil on either type of planting bed in the 0-3 inch depth, mulched with a petroleum cap, the salts raised from less than 1000 ppm to about 1500 ppm. Where no cap existed, salts went up to about 2600 ppm. Subsequent irrigations increased salts mainly in the 0-3 inch depth.

2. On the initially wet soils on either type bed, a very desirable 0-3 inch depth, soil-salt zone existed (1380 ppm) until an irrigation was given, then the soil-salts increased to about 1900 ppm. The no-capped areas increased to 2900 ppm.

3. The amount of soil salts in the 0-3 inch soil profile progressively increased from the wetted perimeter to the top of the bed.

The soil-salt relationship at the 3-6 and 6-9 inch depths was desirable at all locations.

4. Soil-moisture depleted just as rapidly under a cap as without a cap.

5. Soil-temperature at the seed depth under a cap was considerably higher during the sunshine hours than without a cap.

6. Total soil-salts do not appear to be unusually high. This soil dries out quite rapidly, thus jeopardizing germination, causing the requirement of an irrigation, at which time the salts increase significantly, but still remain below the 3000 ppm range in the root zone during the early season.

7. Germination problems were most severe where seeds were planted too shallow or too deep, indicating the need for a more precision planting.

No. 2 Investigation

1. An analysis of variance showed significance at the 1% level between locations on the bed, and depths. The A and B locations were less toxic than the other locations. Both A and B were inundated when irrigation water was applied.

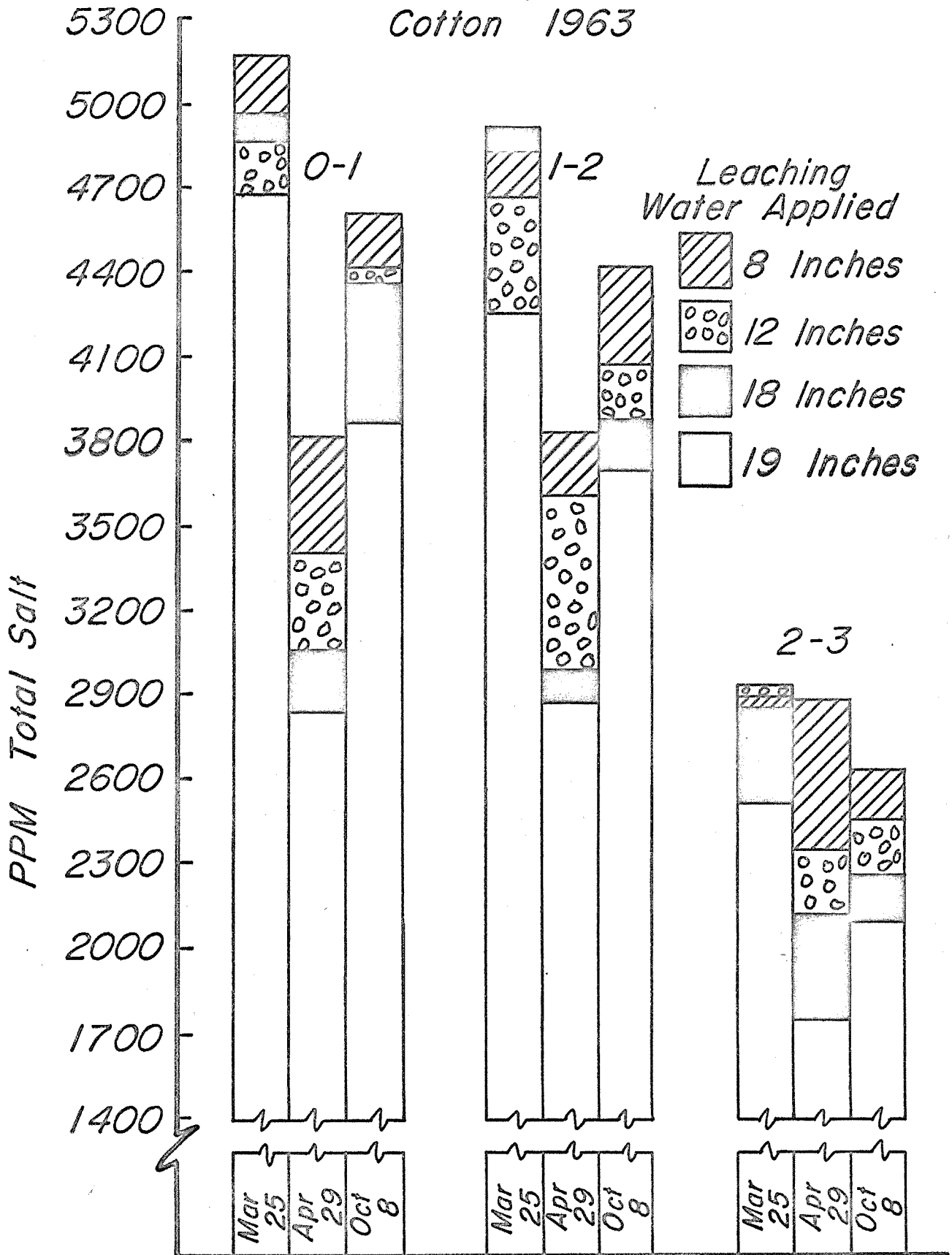
2. The 0-6 inch depth was the most toxic under the C, D and E locations. The soil-salt conditions at the A and B locations were quite homogeneous throughout the soil profile, averaging 1380 ppm. Salts were relatively low in the 12- to 36-inch soil profile (1600 ppm) under the C and D locations.

3. After converting to an every-row irrigation over an every-other-row system (middle of June) salts at the E location were significantly lowered. A trend upward at the C location occurred immediately after the irrigation change took place but returned to early season levels by the end of the year.

4. On the basis of past experience and the soil-salt measurements, it seems doubtful that soil-salts are the only problem affecting cotton production on this ranch. It would appear that more precision in planting must be achieved, nitrogen fertilizer applications must be increased, and the timing of the first irrigation after planting should be better managed.

PERSONNEL: Leonard J. Erie and Orrin F. French

Leaching Study - Soil Salts
Safford Experiment Farm
Cotton 1963



Annual Report of the U.S. Conservation Laboratory

TITLE: CONSUMPTIVE USE OF WATER BY CROPS IN ARIZONA

LINE PROJECT: SWC 11-gG1

CODE NO.: Ariz.-WCL-23

INTRODUCTION:

See previous Annual Reports.

PROCEDURE:

Consumptive use measurements were made at the following locations in 1963.

1. Alfalfa - Mesa Experiment Farm and Cotton Research Center.
2. Bermuda lawn - U. S. Water Conservation Laboratory.
3. Potatoes - Mesa Experiment Farm.
4. Safflower - Mesa Experiment Farm.
5. Grapes - Mesa Experiment Farm and Robert Frye Ranch, Litchfield Park, Arizona.

RESULTS AND DISCUSSION:

An exploratory study on the measurement of consumptive use by safflower planted at various row widths is included under WCL-23. Data will be found subsequent to the discussion on WCL-23. A field calibration of irrometers is also included under WCL-23 following the exploratory study on safflower.

Early irrigations on alfalfa were controlled to eliminate as much deep percolation as possible. By controlling these early irrigations, interpretations of measurements of consumptive use and soil moisture extraction patterns are simplified.

Frequency of irrigations on grapes were reduced from the 1962 schedule. Two irrigation schedules (2 & 4 week) were utilized at the Bob Frye Ranch on Thompson Seedless grapes. Soil moisture in the wet treatment in 1963 at the Frye Ranch was comparable to the dry treatment in 1962. Yield measurements indicate that reduced water applications within the limits of our study increased earliness and thus increased early picking yields. A suggested irrigation schedule was followed at the Mesa Experiment Farm on Cardinal grapes.

Tables 1 and 2 represent semi-monthly consumptive use and Blaney-Criddle "K" factors. In addition, seasonal "F" and "K" factors are included for each crop.

Figures 1 through 10 show the consumptive use curves for the various crops during the growing season. In addition, the percent water use by soil depth is included.

A. WATER USE BY SAFFLOWER

INTRODUCTION:

In the past 2 to 3 years, safflower has gained much importance economically in Arizona. There are several methods of planting as well as widths of row spacing. All previous consumptive use work was done on a 40" row spacing. The objective of this study was to determine the consumptive use of water by safflower at various row spacings.

PROCEDURE:

The experiment was located at the University of Arizona Mesa Experiment Farm, Mesa, Arizona. One border 27.5 x 275 feet was prepared for planting and a pre-planting irrigation was given about the middle of December. On January 1, 1963, the Gila variety of safflower was planted on the flat with a drill in 3-row spacings: 7, 21 and 42 inches. At the same time, 50 lbs to the acre of nitrogen was applied. Two more applications of nitrogen (50 lbs) were applied at the second and third irrigations.

Consumptive use measurements were made on the 3-row spacing treatments throughout the growing season.

RESULTS AND DISCUSSION:

Due to the excessive cold weather in January, the safflower did not get off to a good start. Uniform stands were noted in the 7- and 21-inch spacings. The 42-inch spacing was planted too deep and along with the cold weather, fell behind in initial growth and stand.

Irrigations were applied according to the best producing schedule developed from previous research.

SUMMARY AND CONCLUSIONS:

The consumptive use by safflower is increased as row widths are decreased. This increase in consumptive use is not in proportion to the increase in number of plants in the narrower row

spacings. The 7-inch spacing plots contained three times as many plants as the 21-inch spacing and used an additional 7 inches of water. The 42-inch spacing treatment used 8 inches less water than the 21-inch spacing treatment.

Because of a poorer stand and slow start in the 42-inch spacing, comparisons with the other spacings are not completely valid. The analysis of variance on yields indicated high significance in increased yield by the 7- and 21-inch over the 42-inch spacing. The 7-inch spacing outyielded the 21-inch by 8%. The 7- and 21-inch spacing plots averaged 5572 pounds per acre.

B. FIELD CALIBRATION OF IRROMETERS

INTRODUCTION:

Irrometers were installed on various fields at the Cotton Research Center. These irrometers were to be used to determine when to irrigate the various experiments. Readings were erratic and did not seem to correlate with the visual plant indications of moisture needs. The superintendent of the Cotton Research Center is responsible for determining when to irrigate. Since there was some doubt in the minds of the project supervisors about the validity of the irrometer readings it was decided to conduct a field calibration on some of them. This calibration phase was done in cooperation with Lloyd Patterson, University of Arizona.

PROCEDURE:

Irrometers were installed at depths of 12, 24 and 48 inches. It was decided to use irrometers at the 24-inch depth. Three soil-moisture samples (6 inches in length) were taken on three sides of the ceramic tip at various readings of the irrometer ranging from field capacity until the irrometer broke tension.

RESULTS AND DISCUSSION:

Figure 11 represents the comparison of actual soil moisture with the irrometer readings. Each entry on Figure 11 represents the mean of three separate samples of soil.

The tension would usually break before the irrometer read 80. It should be noted the limit of use is in the range of field capacity to where only 40 percent of the available water is used.

Very little change in reading occurs until about 20 percent of the available water is used, then the gage moves quite rapidly.

PERSONNEL: Leonard J. Erie and Orrin F. French.

Table 1. Semi-monthly use and "K" values for various crops in Arizona 1963

	<u>ALFALFA</u>		<u>ALFALFA</u>		<u>BERMUDA</u>		<u>POTATOES</u>	
	CU	MEF K	CU	CRC K	CU	K	CU	K
Jan 1-15								
Jan 16-31								
Feb 1-14								
Feb 15-28	1.05	.71	1.64	1.23				
Mar 1-15	2.10	.93	3.15	1.40			.11	.05
Mar 16-31	2.62	.99	4.10	1.54			.26	.10
Apr 1-15	2.81	.97	4.59	1.59			1.28	.44
Apr 16-30	3.35	1.25	4.91	1.84	1.80	.84	3.30	1.23
May 1-15	3.99	1.12	4.91	1.40	2.78	.79	6.15	1.73
May 16-31	4.85	1.22	5.10	1.30	3.42	.87	5.60	1.41
June 1-15	4.98	1.35	4.68	1.30	3.57	.99	3.02	.82
June 16-30	5.07	1.24	4.55	1.13	4.02	1.00	.82	.49
July 1-15	4.89	1.15	4.44	1.06	4.59	1.09		
July 16-31	4.94	1.05	4.78	1.03	5.33	1.15		
Aug 1-15	4.53	1.15	4.59	1.16	4.50	1.14		
Aug 16-31	4.69	1.14	4.99	1.22	3.87	.95		
Sept 1-15	4.20	1.16	4.47	1.25	2.85	.79		
Sept 16-30	3.84	1.11	3.95	1.14	2.21	.64		
Oct 1-15	3.15	1.04	3.38	1.12	1.13	.56		
Oct 16-31	2.69	.92	2.86	.99				
Nov 1-15	2.04	.88	2.37	1.03				
Nov 16-30	1.77	.88	2.18	1.09				
Dec 1-15	.98	.69	1.48	1.03				
Dec 16-31								
Total	68.5		77.1		40.1		20.5	
Seasonal "F"	63.05		62.43		43.18		23.82	
Seasonal "K"	1.09		1.23		.93		.86	

Table 2. Semi-monthly use and "K" values for various crops in Arizona 1963

	SAFFLOWER 7 inch		SAFFLOWER 21 inch		SAFFLOWER 42 inch		GRAPES MEF	
	CU	K	CU	K	CU	K	CU	K
Jan 1-15	.08	.05	.08	.05	.08	.05		
Jan 16-31	.32	.18	.32	.18	.32	.18		
Feb 1-14	.52	.24	.49	.23	.49	.23		
Feb 15-28	.84	.42	.76	.38	.81	.41		
Mar 1-15	1.79	.79	1.55	.68	1.42	.63		
Mar 16-31	3.66	1.39	3.57	1.35	2.48	.94		
Apr 1-15	5.40	1.85	4.88	1.68	3.52	1.21	.40	.20
Apr 16-30	6.67	2.49	6.27	2.34	4.68	1.75	1.42	.53
May 1-15	7.88	2.22	7.55	2.13	5.78	1.63	3.26	.92
May 16-31	9.12	2.30	8.93	2.25	7.10	1.79	3.40	.86
June 1-15	8.55	2.22	7.45	1.93	6.66	1.73	2.36	.64
June 16-30	7.95	1.95	6.66	1.63	5.55	1.36	1.95	.48
July 1-15	4.20	.99	1.23	.29	2.85	.67	1.80	.42
July 16-31	.15	.17	.14	.16	.18	.20	1.19	.36
Aug 1-15								
Aug 16-31								
Sept 1-15								
Sept 16-30								
Oct 1-15								
Oct 16-31								
Nov 1-15								
Nov 16-30								
Dec 1-15								
Dec 16-31								
Total	57.1		49.9		41.9		15.8	
Seasonal "F"	38.68		38.68		38.68		27.52	
Seasonal "K"	1.48		1.29		1.08		.57	

Table 3. Semi-monthly use and "K" values for various crops in Arizona 1963

	GRAPES		GRAPES	
	FRYE - WET		FRYE - DRY	
	CU	K	CU	K
Jan 1-15				
Jan 16-31				
Feb 1-14				
Feb 15-28				
Mar 1-15				
Mar 16-31	.24	.11	.24	.11
Apr 1-15	1.43	.49	1.04	.35
Apr 16-30	3.10	1.15	1.99	.72
May 1-15	4.05	1.12	2.73	.76
May 16-31	4.96	1.23	3.04	.76
June 1-15	3.23	.88	2.90	.79
June 16-30	2.10	.51	3.27	.80
July 1-15	4.17	.97	4.32	1.01
July 16-31	1.46	.61	.74	.31
Aug 1-15				
Aug 16-31				
Sept 1-15				
Sept 16-30				
Oct 1-15				
Oct 16-31				
Nov 1-15				
Nov 16-30				
Dec 1-15				
Dec 16-31				
Total	24.7		20.3	
Seasonal "F"	29.95		29.95	
Seasonal "K"	.83		.68	

CONSUMPTIVE USE - ALFALFA
MESA, ARIZONA 1963

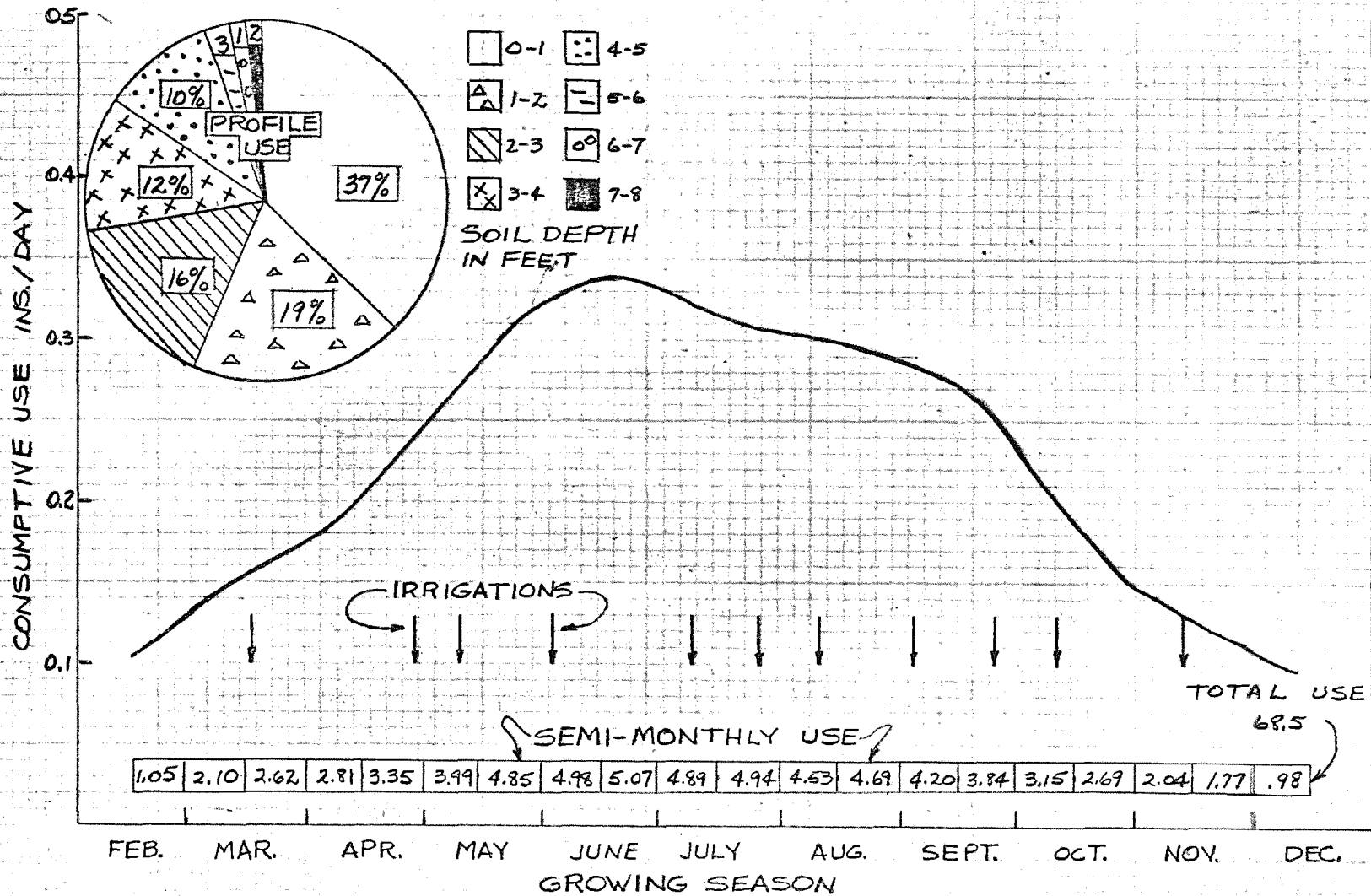


Figure 1.

CONSUMPTIVE USE - ALFALFA
 TEMPE, ARIZONA 1963

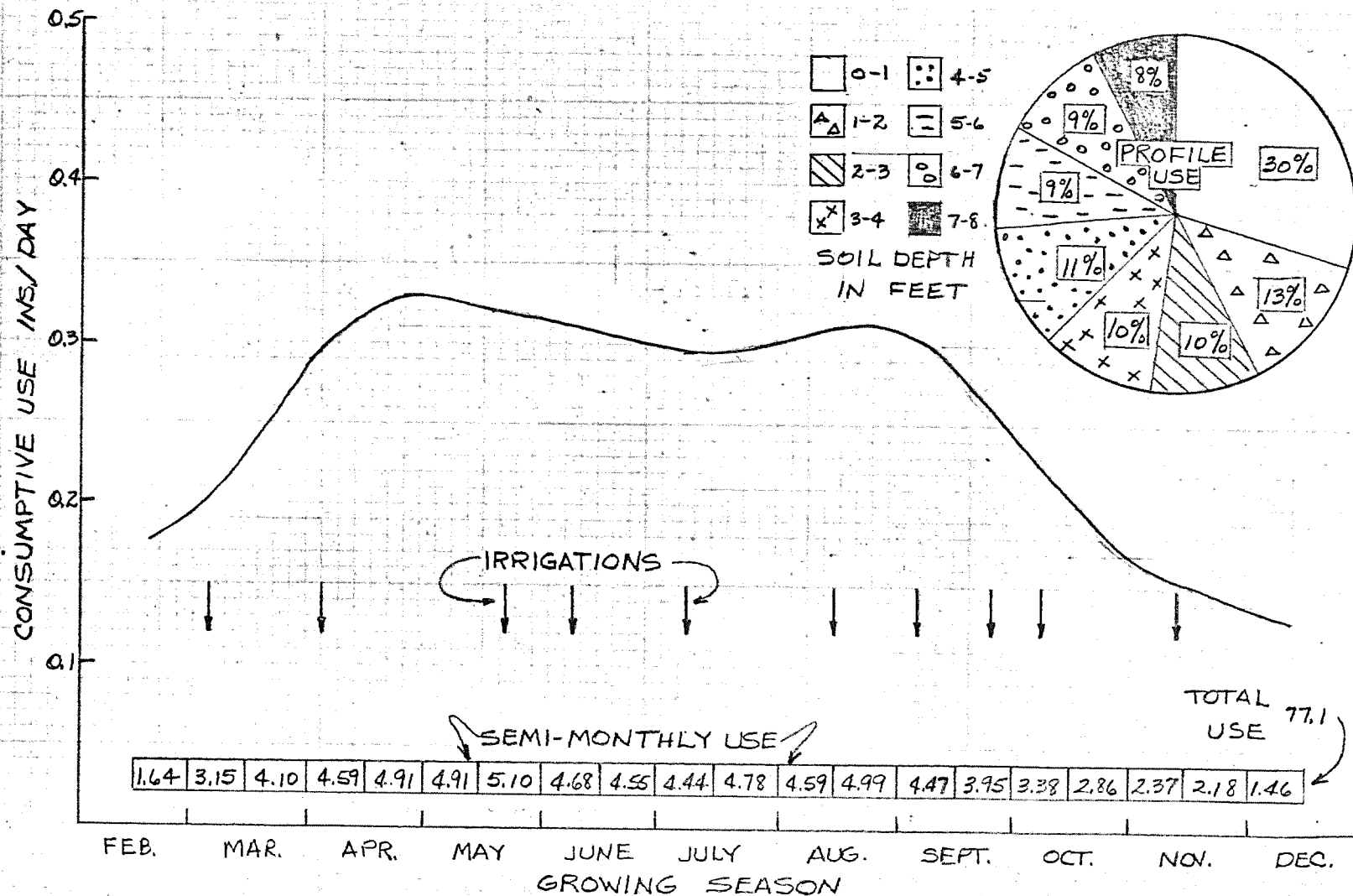


Figure 2.

CONSUMPTIVE USE - BERMUDA LAWN
 USWCL TEMPE, ARIZONA 1963

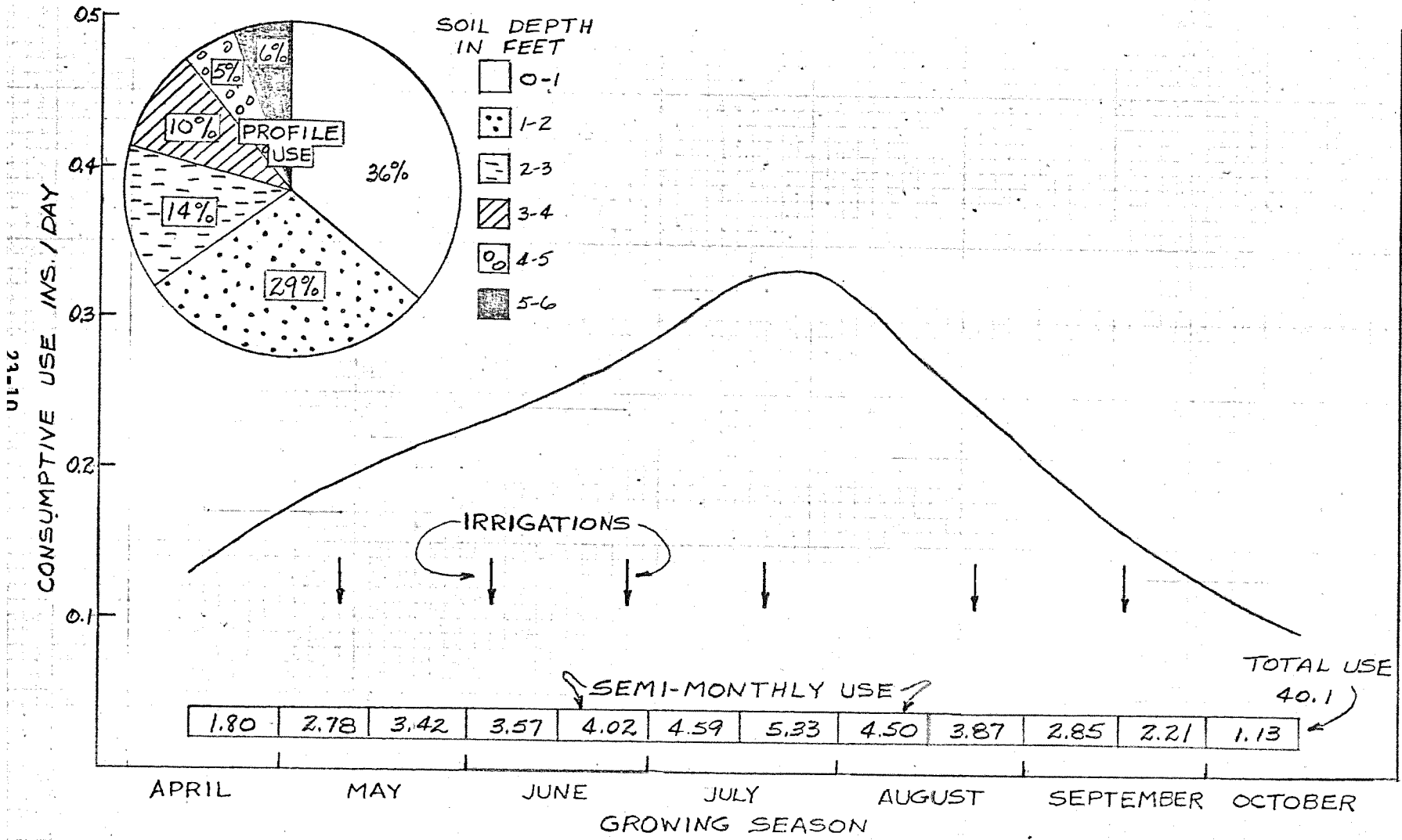


Figure 3.

CONSUMPTIVE USE - POTATOES
MESA EXP. FARM 1963

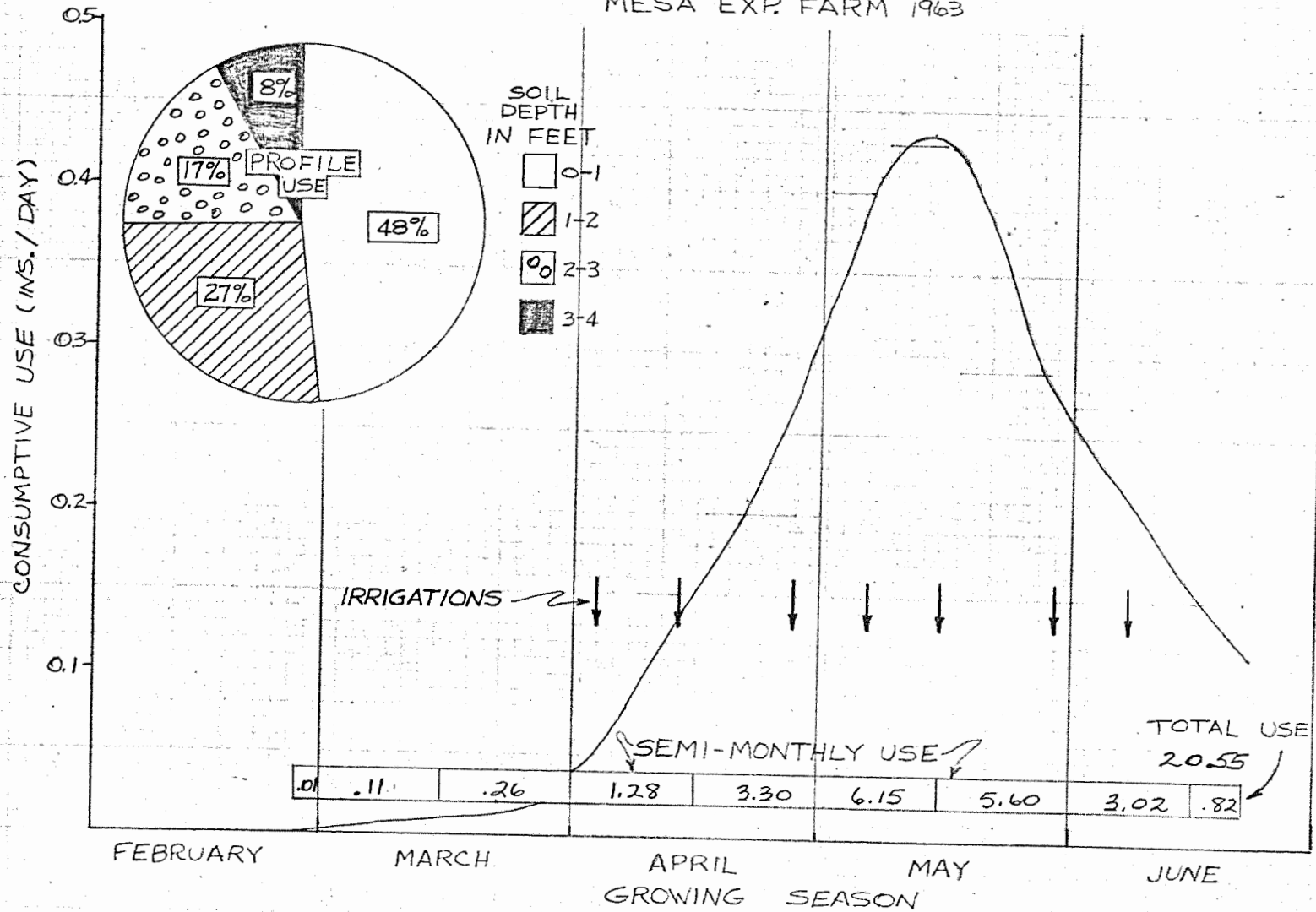


Figure 4.

23-11

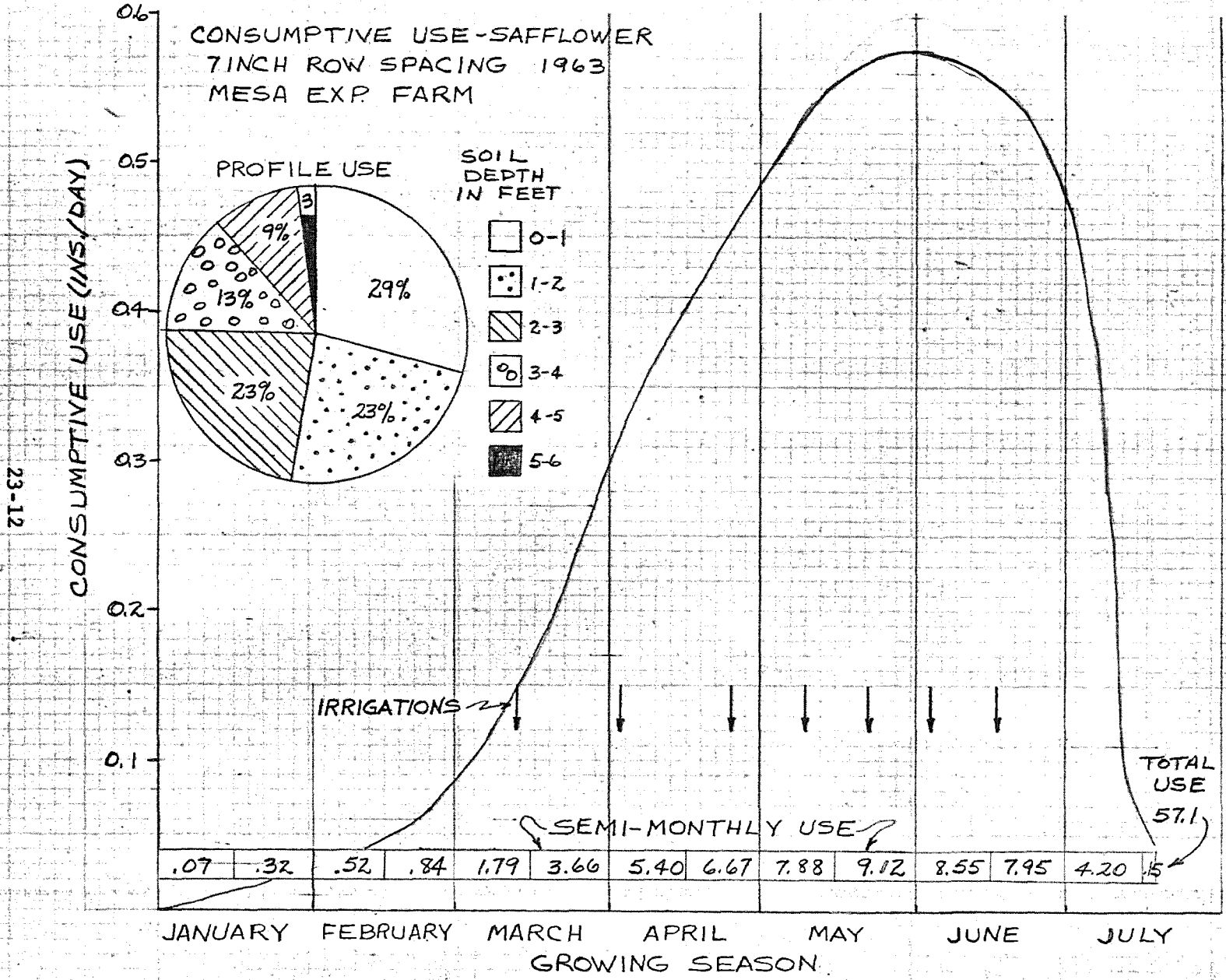


Figure 5.

23-13

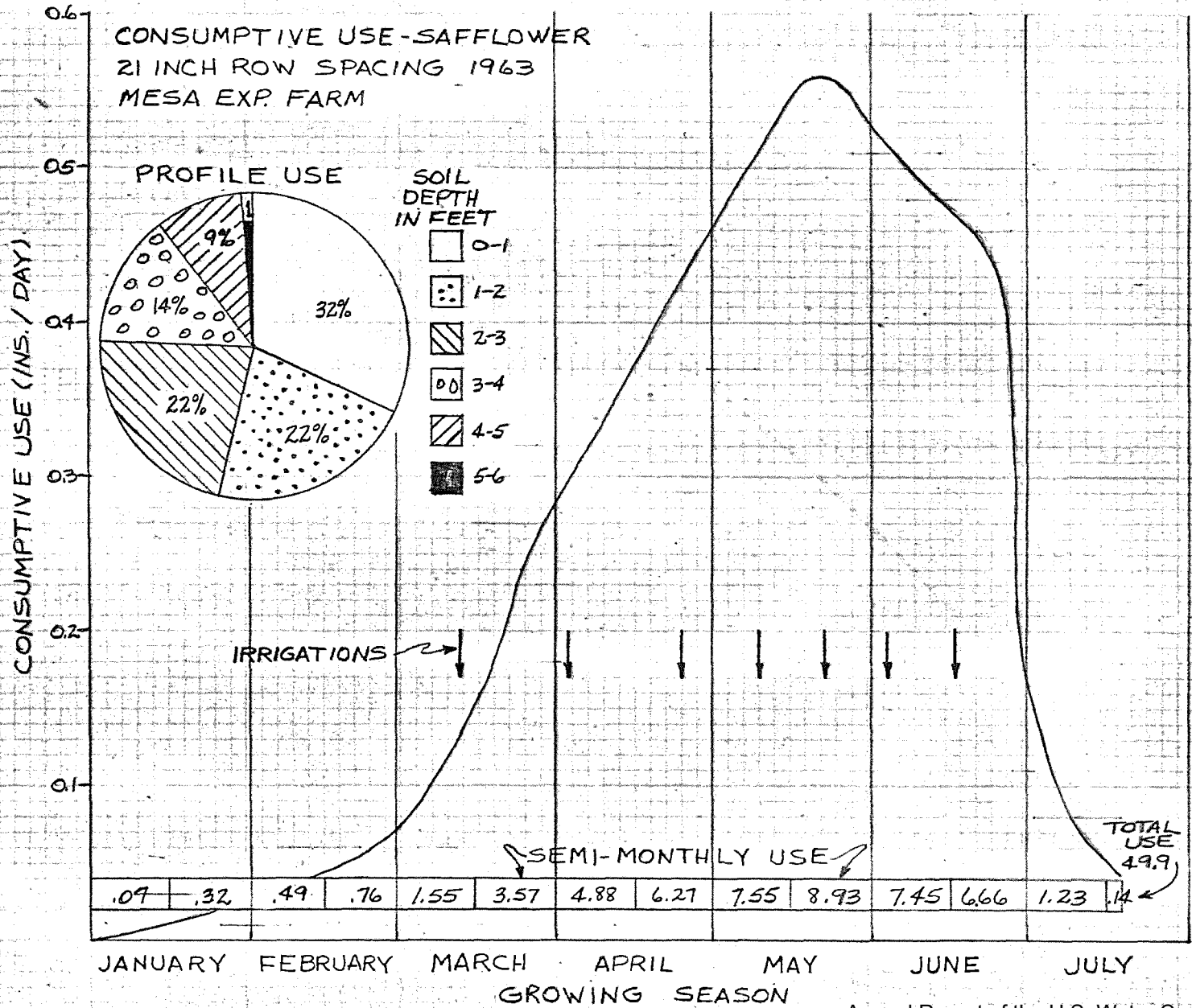


Figure 6.

CONSUMPTIVE USE-SAFFLOWER
 42 INCH ROWSPACING 1963
 MESA EXP. FARM

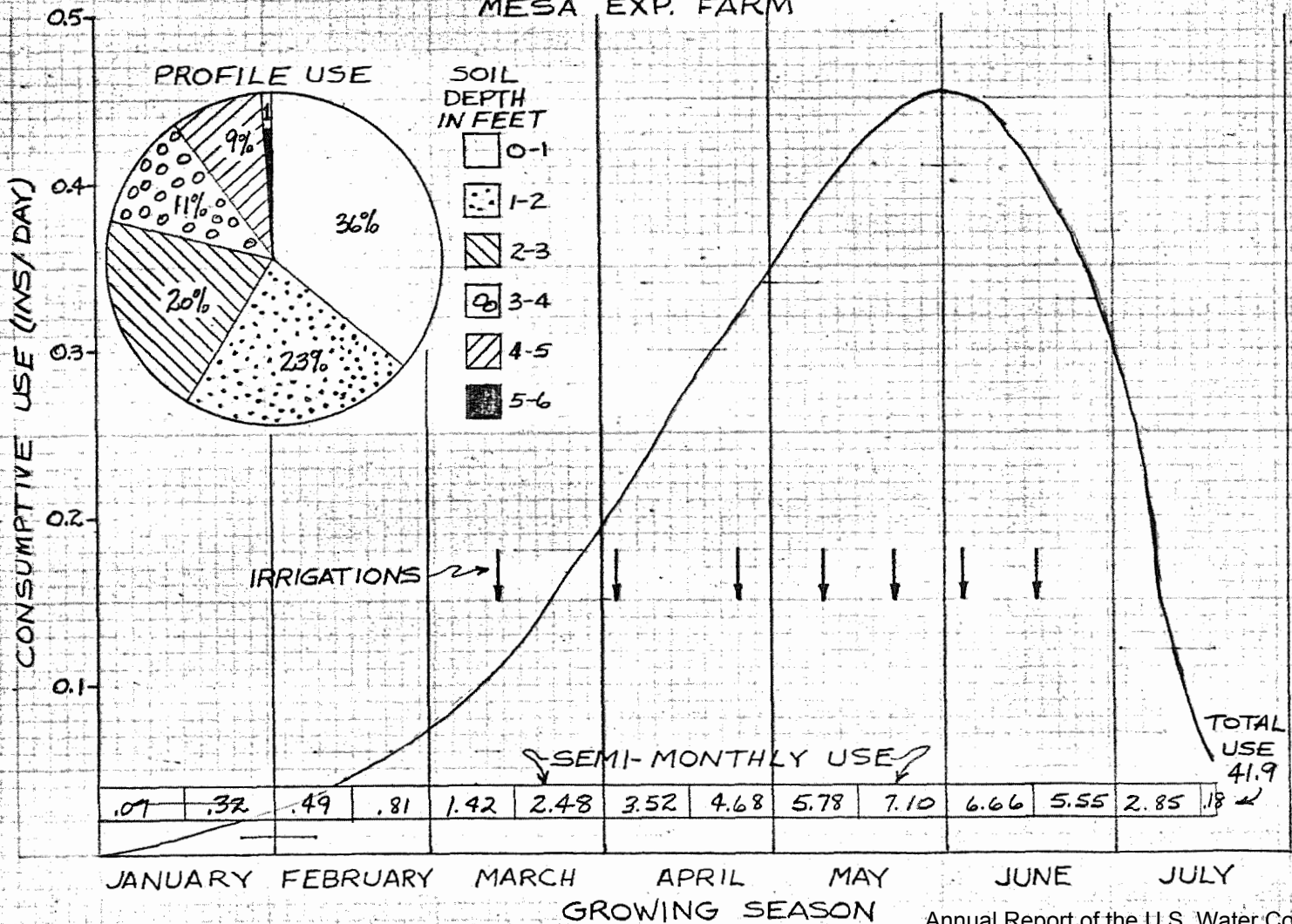


Figure 7.

CONSUMPTIVE USE - GRAPES
MESA EXP. FARM 1963

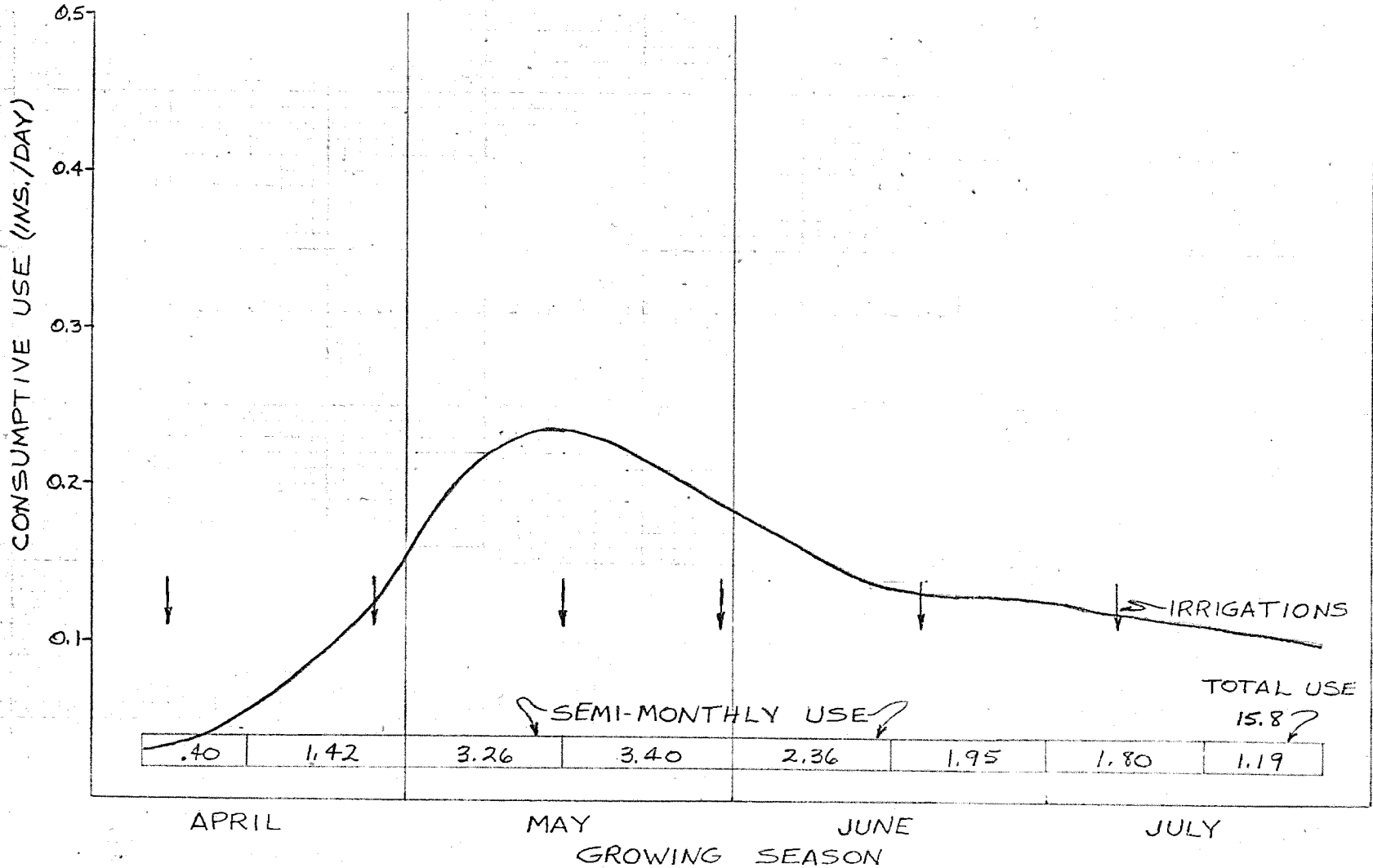


Figure 8.

23-15

CONSUMPTIVE USE (GRAPES)
WET TRT. FRYE RANCH 1963

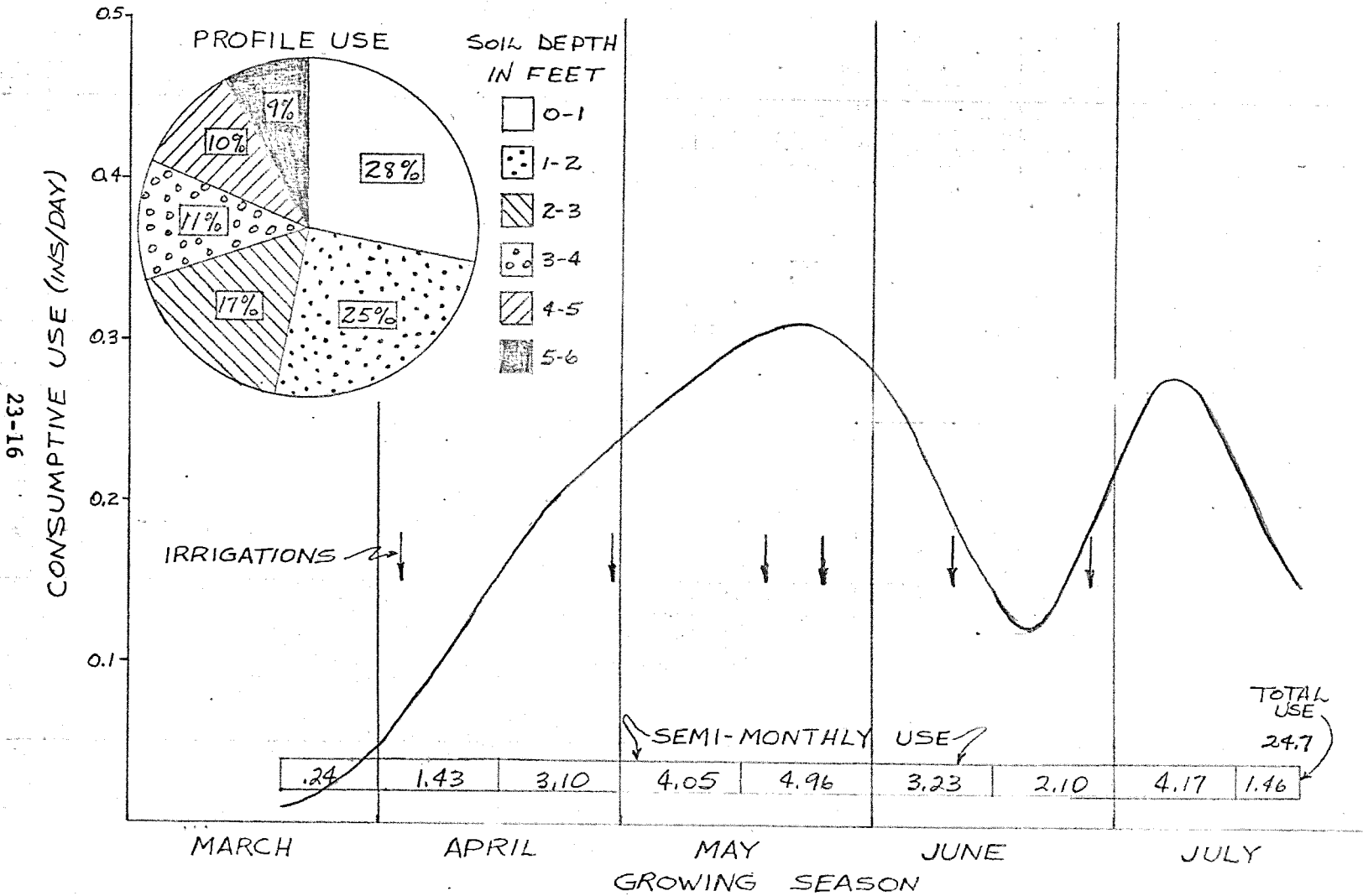


Figure 9.

CONSUMPTIVE USE - GRAPES
 DRY TRT. FRYE RANCH 1963

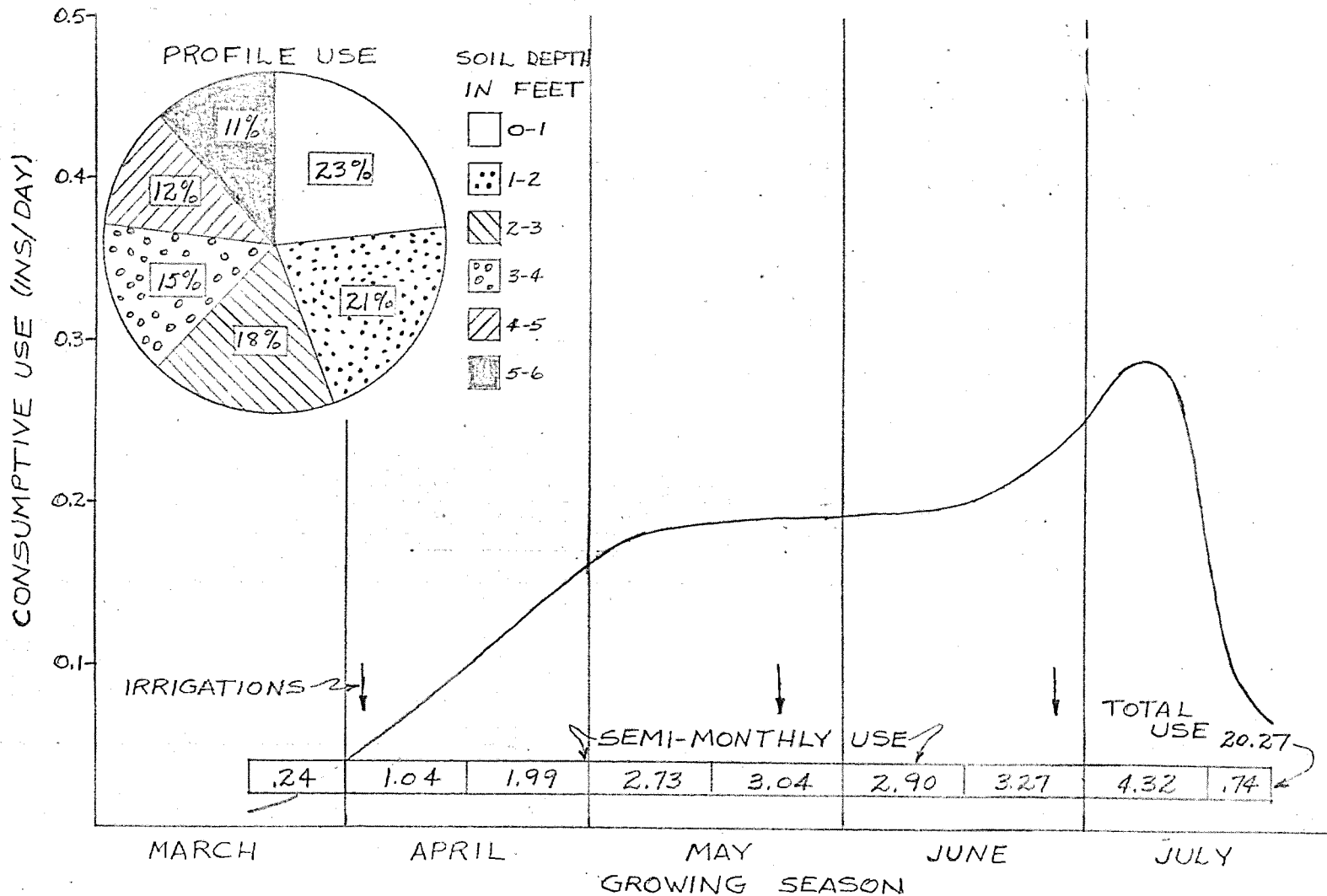


Figure 10.

23-17

COMPARISON OF IRROMETER READINGS
WITH SOIL MOISTURE PERCENTAGE
24 INCH DEPTH

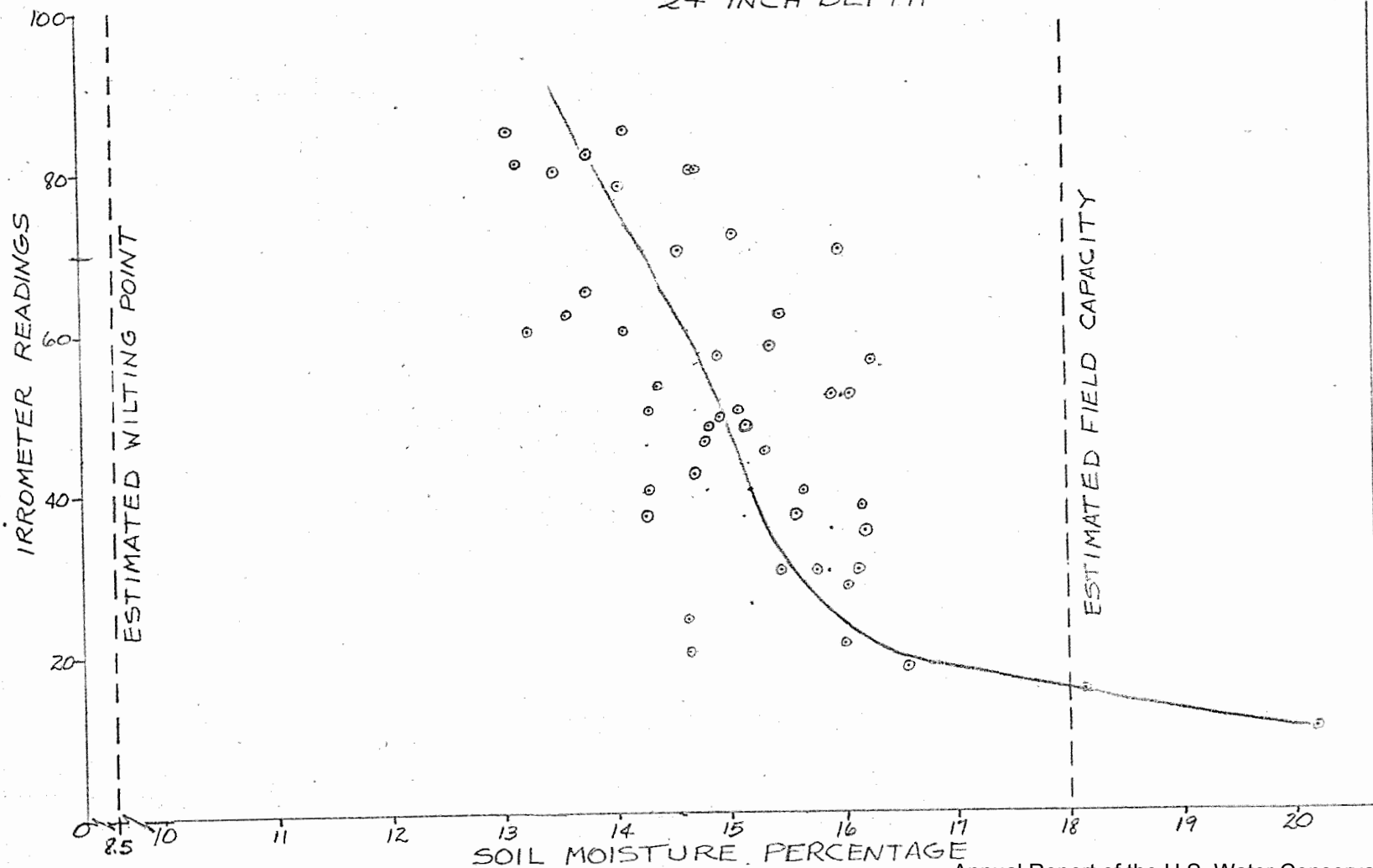


Figure 11.

TITLE: THEORETICAL EFFECT OF SOIL, WATER TABLE, AND CANAL CONDITIONS
ON SEEPAGE FROM CANALS

LINE PROJECT: SWC 4-gG1

CODE NO.: Ariz.-WCL-24

INTRODUCTION:

Analyses of canal seepage with the resistance network analog (R-analog) for various conditions of canal, soil, and water table, were continued in 1963. Part of the studies were reported in Annual Report 1962. The present report contains the complete results of the analyses for seepage into uniform soil underlain by very permeable or essentially impermeable material. The analyses of seepage to a free-draining permeable layer have been extended to cover a larger range of critical pressure-heads, after the validity of the use of a step function to describe hydraulic conductivity at negative pressure heads was demonstrated. The work on project WCL-24 is essentially completed and manuscripts for publication will be prepared in the first half of 1964.

PROCEDURE:

Conditions A and B. The general procedure was the same as described in Annual Report 1962. Geometry and symbols for seepage conditions A and B are shown in Figure 1. The condition of seepage into an infinitely deep soil with a water table at infinite depth is called condition ∞ . If, for condition A, $D_w \geq D_p + H_w$, the flow system is one of seepage into a horizontal, free-draining layer. This case is called condition A' and it is characterized by a lower boundary consisting of a horizontal contour of zero pressure-head (atmospheric pressure).

For relatively small D_i (condition B), the flow at some distance from the canal center will approach uniform, horizontal "Dupuit-Forchheimer" flow and the equipotentials will become essentially vertical. Thus, the lateral boundary of the flow system can be represented by a vertical equipotential. The distance of this equipotential from the canal center has arbitrarily been taken as $10W_b$.

For condition A, the water-table slope will continue to decrease with increasing distance from the canal until at infinite distance the slope has become zero. For practical purposes, however, the slope can already be taken as zero at a certain distance from the canal. This distance was also arbitrarily selected as $10W_b$ from the canal center.

Theoretically, seepage systems from individual canals should be treated with lateral boundaries at infinity. This condition, however, is almost never found in practice, where physical barriers, pumped wells, other seeping canals, or similar discontinuities make it impractical to use the water table at infinity as criterion for the water table position. Thus, for practical purposes, characterizing the water table at a finite specified distance seems preferable. Although D_w is taken at a specified distance of $10W_b$ from the canal center, it can be interpreted as characterizing the water table position at great distance from the canal where the immediate effect of the seepage flow system on the water table has become insignificant. Inspection of completed flow systems showed that $10W_b$ was sufficient distance for this characterization.

In practice, canal seepage is generally unsteady and subject to, among others, changing water levels in the channel as well as changing water tables in the soil. Thus, the steady state conditions covered by the analyses represent individual pictures of a system that in reality is in a continuous state of flux. It is assumed that the water table between the canal and a distance of $10W_b$ from the canal is sufficiently stabilized that any flow components across the water table for that reach can be ignored.

The results of the seepage analyses were expressed graphically in dimensionless parameters, relating seepage to the hydraulic conductivity and to the geometry of the flow system. In addition, the effect of water depth in the canal on seepage could be evaluated from these graphs. The effect of canal shape (triangular, trapezoidal, and rectangular) was also analyzed.

Unsaturated flow. In analyzing the effect of unsaturated flow, or rather negative-pressure flow, on canal or stream

seepage, distinction was made between what are called in this report the fringe effect and the divergence effect. The fringe effect occurs when there is a mildly sloping water table away from the canal. Inclusion of negative-pressure flow in the analysis of seepage in that case results in the presence of a capillary fringe above the water table with height numerically equal to the critical pressure-head, P_c . This fringe provides an extra path for the flow to take place. The divergence effect occurs when the water table is sufficiently deep to cause the streamlines below the canal to be initially in mainly vertically downward direction. Inclusion of negative-pressure flow in the analyses of seepage for this case yields an increased divergence of streamlines and consequently an increased width of the flow system below the canal.

The fringe effect was evaluated with the R-analog for condition B, using a P_c of $-W_b/12$. The validity of using P_c instead of the actual K-P relationship for this case can be demonstrated analytically. An approximate equation to account for the fringe effect for shallow systems (small D_i) was developed and checked against results of analog analyses.

The validity of using P_c instead of actual K-P curves to account for the divergence effect can not be as readily demonstrated analytically as for the fringe effect. Therefore, a comparison was made between a seepage solution for an actual K-P curve and for the equivalent P_c -value. The analysis for the actual K-P curve was made by Reisenauer (1) with a digital computer. The flow system was canal seepage to a relatively deep, free-draining layer. This comparison between the digital computer solution for the actual K-P curve and the analog solution for the equivalent P_c showed good agreement. An evaluation of the divergence effect of unsaturated flow on seepage was then made for a wide range in P_c . Analyses were performed with the R-analog for condition A' for five values of P_c ranging from 0 to $-0.75 W_b$. Other variables were H_w and D_p . The results were again expressed in the dimensionless ratios.

RESULTS AND DISCUSSION:

Conditions A and B. The results of the seepage analyses for conditions A, A', and B are shown in Figures 2, 3 and 4. Each figure applies to a certain water depth in the canal. The canal shape was taken as trapezoidal with 1:1 side slopes. The seepage is expressed as rate of fall of the water surface in the canal per unit hydraulic conductivity, or as \bar{I}_s/K . The dots in Figure 3 are results obtained with Dachler's method for estimating seepage for relatively shallow water tables and impermeable layers (see Annual Report 1962).

For condition A', the pressure head at the top of the free-draining layer was taken as zero. In actuality, this pressure-head depends on the K-P relationship of the underlying coarse material and it can be approximated by P_c , the critical pressure-head. Since the free-draining layer can, according to its definition, be expected to consist of relatively coarse material, P_c will only be slightly negative and it can be considered zero for most practical purposes. If \bar{I}_s/K needs to be estimated for $P_c < 0$, the curves in Figures 2, 3, or 4 for condition A can be extrapolated somewhat beyond the curve for condition A'.

An interesting aspect is the non-linearity between seepage and depth of water table, which is particularly evident at large D_w . If D_w is equal to approximately $4W_b$ to $6W_b$, depending on H_w , the seepage has essentially reached a maximum and further lowering of the water table will not significantly increase the seepage. This information will be of importance in assessing the effect of water tables on canal seepage, in predicting the effectiveness of locating well fields closer to recharging streams for accelerating natural recharge, in developing realistic input relationships for use with resistance-capacitance network analogs in analyzing hydrologic behavior of entire ground-water basins, in developing plans for integrated use of surface- and ground-water resources or storage facilities, etc.

If for new projects the hydraulic conductivity and other pertinent hydrogeological information are known, the seepage losses in the distribution system can be estimated from Figures 2, 3, and 4. These

losses should then be interpreted as maximum losses since "aging" (sedimentation, chemical and biological action, etc.) tends to reduce seepage. An analysis of seepage from clogged canals was presented earlier. (See Annual Report 1962.)

Effect of water depth. Figures 2, 3, and 4 permit evaluation of the effect of water depth in the canal on seepage. Such evaluation should be made for a constant water-table position. Therefore, the distance of the water table below the canal bottom, $D_w - H_w$, was used to describe the water table position, rather than D_w which refers to the canal water level. Furthermore, to eliminate the effect of H_w on \bar{I}_s through the effect of H_w on W_s , the seepage was expressed as loss per unit length of canal, per unit bottom width, and per unit K , or $\bar{I}_s W_s / K W_b$, which is a dimensionless term. The results of this evaluation, which was done for a relatively shallow, a medium, and a deep water table and different values of D_p or D_i , are shown in Figure 5. It appears that, in general, canal depth has its greatest relative effect on seepage for conditions A' and ∞ . For shallow and medium water tables, the relative effect of water depth in the canal on seepage decreases in the order of condition A with finite D_p , condition A or B with infinite D_i or D_p , and condition B.

For a complete evaluation of seepage at different water depths in the canal, the effect of water depth on discharge capacity should also be considered, so that the relative loss as a percentage of the total discharge can be determined. For water-conveyance purposes, relative discharge loss will be more significant than the absolute seepage loss. The dashed lines in Figure 5 show the discharge capacity per unit W_b of the canal, calculated according to Manning's equation as $AR^{2/3}/W_b^{8/3}$, where A is the cross section of the canal and R is the hydraulic radius. The dashed lines show that the discharge capacity of the canal generally increases much faster with depth than the seepage losses. Thus, for canals with uniform soil conditions along their wetted perimeter, deep canals will be more efficient conveyors of water than shallow canals.

To complete the picture of the effect of H_w on seepage, the condition of the clogged channel (condition C, see Annual Report 1962) has also been analyzed. The equation describing seepage from a clogged trapezoidal channel with 1:1 side slopes can be written as

$$\frac{\bar{I}_s W_s R_s}{W_b^2} = \left(\frac{H_w}{W_b} - \frac{P_c}{W_b} \right) \left(0.71 \frac{H_w}{W_b} + 1 \right) \quad (1)$$

where the term on the left side is a dimensionless parameter consisting of seepage \bar{I}_s , canal dimensions W_b and W_s , and hydraulic impedance R_s of the clogged layer. The relationship between this dimensionless seepage parameter and H_w/W_b for different values of P_c/W_b is shown in Figure 6. The effect of water depth on discharge capacity of the channel is again shown as a dashed line. The figure shows that the slope of the dashed line is much greater than that of the solid curves, so that also for condition C, deeper canals will give lower relative conveyance losses.

Effect of canal cross-section. To evaluate the effect of the cross-sectional shape of the channel on seepage, solutions were obtained with the R-analog for rectangular and triangular channels and for different conditions of soil and water table. The effect of channel shape on seepage can be expected to increase with increasing water depth in the canal. Therefore, the analyses were performed for the largest H_w -value employed for the trapezoidal channels ($H_w = 0.75 W_b$). To eliminate the effect of channel shape on the bottom width of the canal in the expression of results, all length dimensions in this study were expressed as ratios to the surface width W_s , which was held constant for the three cross-sections. The effect of channel shape on seepage for condition C was evaluated by means of the seepage equation for this case (see Annual Report 1962) assuming $P_c = 0$. The results (Table 1) show that canal shape has its greatest effect on seepage if a free-draining layer occurs at relatively small distance below the canal. Also, for the clogged canal of condition C, the seepage is considerably affected by canal shape. For condition B, the effect of shape is rather small. The effect of shape for condition A can be

expected to lie between that for condition B and condition A', or between that for B and ∞ , depending on the magnitudes of D_p and D_w .

To account for the effect of channel cross-section on the discharge capacity, the seepage losses were again divided by the discharge capacity of the channel to obtain expression for the relative seepage losses. In this comparison, the relative flow losses for the trapezoidal channels were arbitrarily set at 100. The results show, that rectangular cross-sections generally give the lowest relative seepage losses. For condition C, the relative loss for the rectangular shape was approximately the same as that for the trapezoidal shape.

Effect of unsaturated flow. The results of the analog analyses for the fringe effect are shown in Table 2, which applies to condition B with low, medium, and high values for H_w , D_w , and D_i . The P_c -value was arbitrarily selected as $-W_b/12$ (see Annual Report 1962).

The relative contribution to seepage due to the fringe effect can be quantitatively expressed as the ratio of the thickness of the fringe to the thickness of the saturated material below the water table. Since the thickness of the fringe will numerically be approximately equal to P_c , the relationship between the seepage with fringe effect and the seepage without fringe effect can be described as

$$\left(\frac{\bar{I}_s}{K}\right)_{P_c} = \left(\frac{\bar{I}_s}{K}\right)_{P_c=0} \left(1 + \frac{-P_c}{D_i + H_w - 1/2 D_w}\right) \quad (2)$$

In this equation, $D_i + H_w - 1/2 D_w$ describes the average height of the saturated material below the water table. The minus sign at P_c is introduced because P_c is negative. If $-P_c$ is small compared to $D_i + H_w - 1/2 D_w$, the term between the brackets in equation (2) is very close to 1 and the fringe effect contributes little to the seepage. This is illustrated in Table 2, which shows that the difference between \bar{I}_s/K at $P_c = 0$ and \bar{I}_s/K at $P_c = -W_b/12$ is largest for small values of D_i and H_w . The table also shows that equation (2) estimates the fringe effect of seepage correctly for relatively small D_i

and D_w . If D_w is relatively large (for instance $D_w > 3W_b$), equation (2) underestimates the effect of negative-pressure flow on seepage because the flow below the canal is then already sufficiently downward for the divergence effect to become dominant.

The fringe effect on seepage for condition A with small D_w can be expected to be less than for condition B. This is because flow to the lower drainage layer causes the horizontal flow components to decrease with distance from the canal.

The divergence effect of negative-pressure flow occurs when D_w is relatively large, for instance $D_w > 3W_b$. The validity of using P_c instead of the actual K-P relationship in evaluating divergence effects was investigated for the case of seepage to a deep drainage layer. The K-P curve used in the digital computer solution by Reisenauer (1) is shown in Figure 7. From this curve, P_c was determined by planimeter as -45.4 cm. This value was then used in the analog analysis of the flow system. The results in Figure 8 show good agreement between the 0 and -45.4 cm pressure-head contours in the analog solution with P_c and in the digital computer solution with the actual K-P curve. The -45.4 cm pressure-head contour for the actual K-P curve corresponds to a K-value of $0.475 K_{\text{saturated}}$. Thus, in the digital computer analysis, K decreases from $K_{\text{saturated}}$ at the 0 pressure contour to $0.475 K_{\text{saturated}}$ at the -45.4 cm contour and continues to decrease beyond this contour. Because of the relatively low K outside the contour, most of the flow in the digital computer analysis takes place within the -45.4 cm contour. For the analog system with P_c , however, K is equal to $K_{\text{saturated}}$ for the entire system between the canal and the -45.4 cm pressure-head contour. In the analog system, the -45.4 cm contour acts as a solid boundary and no flow takes place beyond this contour.

Good agreement was also obtained between the \bar{I}_s/K -values for the digital computer analysis with actual K-P and the analog analysis with P_c , which were 2.20 and 2.27 respectively. Part of this 3% difference can probably be attributed to the fact that the node density was higher in the digital computer than in the analog

analysis. This conclusion is based on earlier comparisons between \bar{I}_s/K from analog solutions and exact solutions, which showed a difference of approximately 2 percent (see Annual Report 1962).

The agreement between the digital computer solution with actual K-P curve and the analog solution with P_c lends support to the validity of using the critical pressure-head for evaluating the divergence effect of negative-pressure flow.

To evaluate the divergence effect in relation to P_c , analyses for condition A' were performed with the R-analog for five values of P_c , ranging from 0 to $-0.75 W_b$. Other variables were H_w and D_p . The condition $D_p = \infty$ was simulated by assuming complete divergence and start of uniform vertically downward flow at a distance of $11 W_b$ below the canal bottom. Inspection of completed flow systems showed that this assumption was valid. The shape of the canal was again taken as trapezoidal with 1:1 side slopes.

The results of the analyses (Figure 9) can best be interpreted by considering the extra streamline divergence due to $P_c < 0$ in relation to the existing streamline divergence caused by the water depth alone and to the opportunity for additional divergence by letting $P_c < 0$. The existing divergence at $P_c = 0$ increases with increasing H_w and the opportunity or "room" for additional divergence by letting $P_c < 0$ increases with increasing D_p . Thus the greatest relative increase in \bar{I}_s/K due to $P_c < 0$ can be expected to occur where the existing divergence at $P_c = 0$ is the smallest and the opportunity for increased divergence is the greatest, or for relatively small H_w and large D_p . This is illustrated by Figure 9, where for a given D_p/W_b , the slope of the curves of \bar{I}_s/K versus $-P_c/W_b$ increases with decreasing H_w/W_b , and where, for a given H_w/W_b , the slope of the curves increases with increasing D_p/W_b . For the two higher values of D_p/W_b in Figure 9, the steeper slope of the curves with small H_w/W_b causes the trend of \bar{I}_s/K to increase with increasing H_w/W_b for low values of $-P_c/W_b$ to be reversed for the higher values of $-P_c/W_b$. This reversal does not occur when D_p/W_b is small, because of the dominating effect of H_w/W_b on the hydraulic gradients, and thus on \bar{I}_s/K , in that case.

An interesting picture is obtained when \bar{I}_s/K is plotted against D_p/W_b for each water depth and for different values of $-P_c/W_b$. To facilitate plotting $D_p = \infty$, the ratio W_b/D_p is used instead of D_p/W_b . The resulting graphs (Figure 10) clearly demonstrate the dependency of the divergence effect on the opportunity for divergence. If $P_c = 0$, \bar{I}_s/K decreases with increasing D_p . With increasing opportunity for divergence at the higher D_p -values, however, the introduction of $P_c < 0$ will cause a greater increase in \bar{I}_s/K when D_p is large. This causes some of the curves of $P_c < 0$ to show a midway "sag." Since the initial divergence at $P_c = 0$ increases with increasing H_w , the divergence effect due to $P_c < 0$ will be more pronounced at smaller values of H_w . Therefore, the P_c -value of the curves showing a midway sag is numerically less for the curves with lower H_w -values. For $H_w = 0.75 W_b$, the P_c/W_b curves of -0.25, -0.50, and -0.75 all show a sag. For $H_w/W_b = 0.5$, the only shown curve with a sag is for $P_c/W_b = -0.25$ and for $H_w/W_b = 0.25$, the only sagging curves must be between $P_c/W_b = -0.25$ and 0. For relatively large numerical values of P_c , \bar{I}_s/K increases with increasing D_p for the entire range of D_p .

Field data regarding K-P relationships and P_c -values are scarce to nonexistent. From K-P curves in the literature, which were obtained from disturbed soil samples, it appears that P_c may be of the order of -30 cm water for "medium" textured soils, -20 cm or more for light textured soils, and -40 cm or less for fine textured soils. Since seepage problems tend to be more severe in relatively coarse textured soils, P_c -values of -10 cm to -20 cm may be the prevailing range of values expected. Equation (2) and Table 2 show, however, that $-P_c$ must not be small compared to the term $D_i + H_w - 1/2 D_w$ if the flow in the capillary fringe is to contribute significantly to the seepage. If the water table is relatively deep ($D_w > 3W_b$) and the effect of negative pressure flow is due to the divergence effect, Figure 9 shows that $-P_c$ must approach the value of W_b before the extra divergence causes significantly higher \bar{I}_s/K values. At present, the conclusion therefore is, that the fringe effect only needs to be considered for

very shallow channels underlain at very small distance by impermeable material, and that the divergence effect only needs to be considered for narrow channels with bottom widths not exceeding one foot. As more information regarding P_c -values in the field becomes available, this conclusion may have to be changed.

Although a decreasing P_c -value will give increased ratios of \bar{I}_s/K , it should be remembered that soils with low P_c -values, i. e., fine textured soils, will also have low K -values. Therefore, although \bar{I}_s/K may increase with decreasing P_c , \bar{I}_s as such will generally decrease with decreasing P_c .

SUMMARY AND CONCLUSIONS:

The analyses with a resistance network analog of seepage from open channels for various conditions of canal shape and depth, soil and water table, were completed in 1963.

One series of solutions dealt with seepage from trapezoidal channels with 1:1 side slopes in uniform soil underlain by material of different permeability. This material was taken as either much less permeable, or much more permeable, than the overlying soil. Variables included in the analyses were the water depth in the canal, the position of the "unaffected" water table at large distance from the canal, and the depth of the impermeable, or very permeable, material. If, for the case of soil underlain by very permeable material, the water table is at or below the top of the permeable material, the condition is one of seepage through uniform soil to a free-draining layer. For each water depth in the canal, dimensionless graphs were prepared which show seepage as a function of water table position for different positions of the impermeable or very permeable layer. The graphs show that, except for the condition of seepage to a free draining layer, seepage increases with increasing depth of the water table. The rate of seepage increase, however, reduces with increasing depth of the water table. Maximum seepage rates are essentially obtained if the water table at large horizontal distance from the channel has dropped to a level of 4 to 6 channel-bottom widths (depending on the water depth in the channel) below

the water surface of the stream. This has important consequences in a number of problems concerning the relation between seepage from a stream or canal and the position of the water table.

From the dimensionless graphs, a new graph was constructed showing the effect of water depth in the canal on seepage. Increasing the water depth always results in an increase in seepage. However, the rate of increase in seepage can decrease, be constant, or increase with increasing water depth, depending on the soil and water table conditions. The rate of increase in seepage is generally less than the rate of increase in the hydraulic discharge capacity of the channel with depth. Therefore, the deeper the channel, the lower the seepage loss in relation to the discharge, and the more efficient the channel is as a conveyor of water.

Analyses relative to the effect of cross-sectional shape of the channel on seepage showed, that, for the same water depth and surface width, total seepage increases from triangular to trapezoidal to rectangular cross-sections. If the seepage losses are again expressed in relation to the hydraulic discharge capacity of the cross section, however, it appears that rectangular canals are the most efficient water conveyors, followed by trapezoidal and triangular canals.

In the analysis of the effect of unsaturated flow, or rather negative-pressure flow, on seepage, distinction is made between the fringe effect and the divergence effect. The fringe effect occurs when there is a shallow, mildly sloping water table away from the canal. In that case, the negative pressure flow results in a capillary fringe above the water table, which causes an increase in the seepage. An equation for calculating the effect of the capillary fringe, using the concept of critical pressure-head, was developed. The equation agreed with results from analog analyses.

The divergence effect occurs when the water table is sufficiently low for mainly vertical flow below the canal to occur. In that case, negative pressure flow results in an increased

divergence of the streamlines, and consequently, in an increase in seepage. The validity of the use of critical pressure-head to account for the divergence effect was demonstrated by the excellent agreement that was obtained between a digital computer analysis with an actual, S-shaped curve of hydraulic conductivity versus pressure-head and an analog analysis for the corresponding critical pressure-head. A more complete evaluation of the divergence effect was then made for the condition of seepage to a free-draining layer. In this evaluation, the water depth in the canal, the critical pressure-head, and the depth of the free-draining layer were taken as variables. The results showed that, for a given critical pressure-head, the divergence effect caused the greatest relative increase in seepage if the canal was shallow and the free-draining layer was at great depth.

Considering that the order of magnitude of critical pressure-head is approximately -1 ft of water, the analyses showed that the increase in canal seepage due to the fringe effect only tends to be significant for shallow channels with impermeable layers at small distance below the channel bottom. The increase in seepage due to the divergence effect is only significant for narrow, small channels with relatively deep water tables and/or drainage layers in the soil.

REFERENCES:

(1) Reisenauer, A. E.

1963. Methods for solving problems of multi-dimensional partially saturated steady flow in soils. Journal Geophysical Research 68, 5725-5735.

PERSONNEL: Herman Bouwer

Table 1. Effect of channel shape on seepage and on relative discharge reduction, $H_w/W_s = 0.3$.

Cross-section	Seepage Condition	D_w/W_s	D_i/W_s	\bar{I}_s/K	Index of relative flow reduction
Triangular	∞	∞	-	1.56	145
Trapezoidal	∞	∞	-	1.81	100
Rectangular	∞	∞	-	2.31	83
Triangular	A'	0.63	-	1.68	140
Trapezoidal	A'	0.63	-	2.03	100
Rectangular	A'	0.63	-	2.83	91
Triangular	B	0.37	0.2	0.064	171
Trapezoidal	B	0.37	0.2	0.063	100
Rectangular	B	0.37	0.2	0.066	68
Triangular	B	0.9	∞	0.93	156
Trapezoidal	B	0.9	∞	1.00	100
Rectangular	B	0.9	∞	1.13	73
Triangular	C	$\bar{I}_{R_s}/H_w = 0.58$			118
Trapezoidal	C	$= 0.82$			100
Rectangular	C	$= 1.30$			103

Table 2. Effect of P_c on \bar{I}_s/K for condition B.

H_w/W_b	D_i/W_b	D_w/W_b	\bar{I}_s/K		
			$P_c = 0$ ^{1/}	$P_c = -W_b/12$ ^{1/}	$P_c = -W_b/12$ ^{2/}
0.75	0.5	0.92	0.063	0.070	0.070
0.75	2.17	2.25	0.32	0.34	0.34
0.75	4.83	4.25	0.90	0.93	0.92
0.50	0.5	0.67	0.048	0.054	0.054
0.50	2.17	2	0.33	0.35	0.34
0.50	4.83	4	0.97	1.01	0.99
0.25	0.5	0.42	0.032	0.037	0.037
0.25	2.17	1.75	0.34	0.35	0.35
0.25	4.83	3.75	1.06	1.11	1.08

^{1/} Analog results

^{2/} Calculated with eq (2)

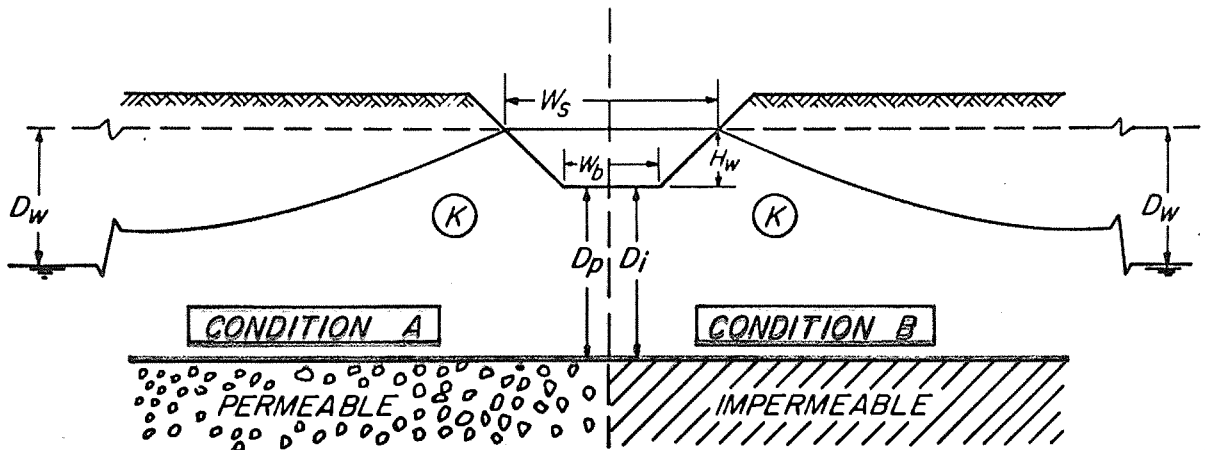


Figure 1. Geometry and symbols for seepage conditions A and B.

Figure 2. Results of seepage analyses for trapezoidal canal with $H_w = 0.75 W_b$.

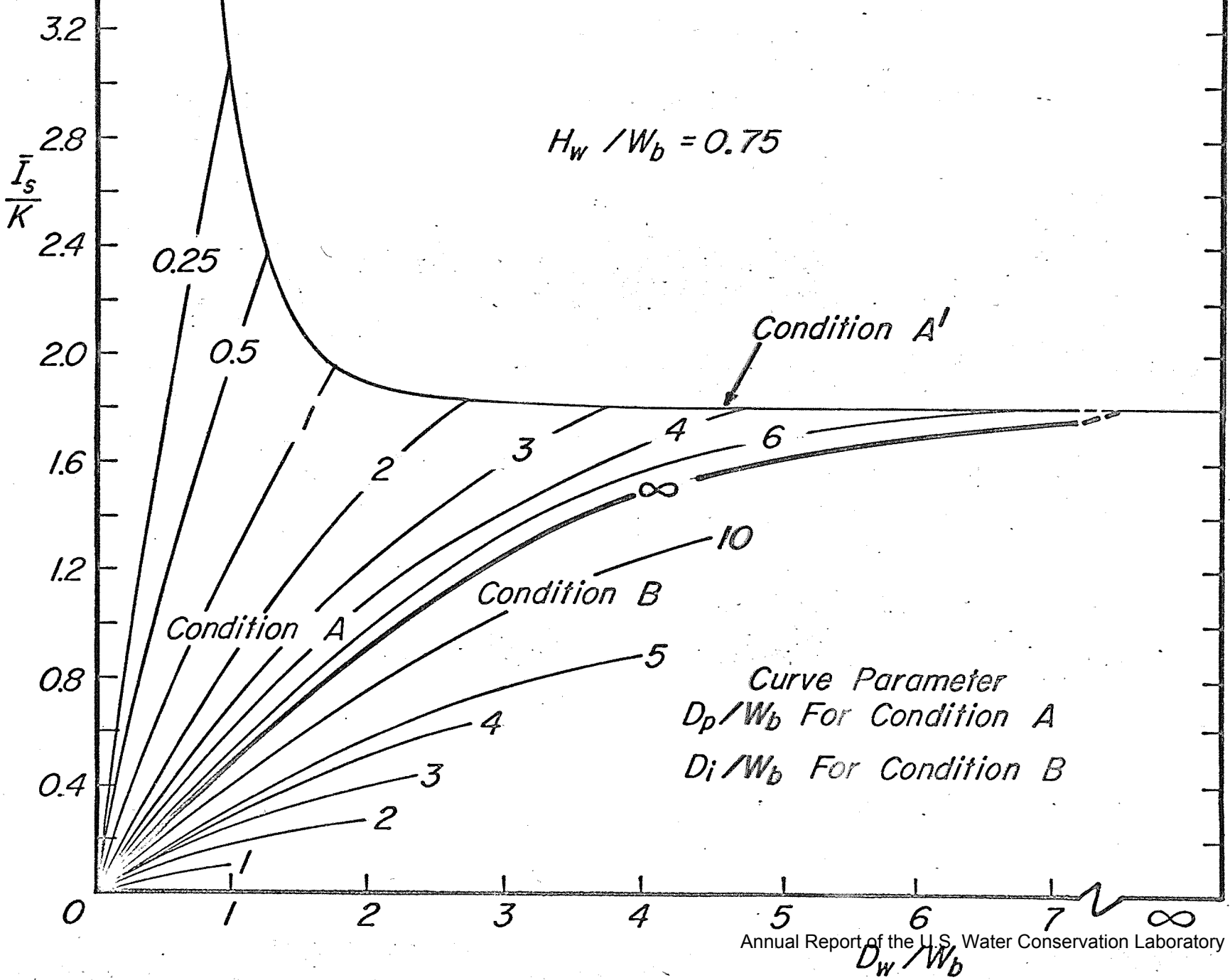


Figure 3. Results of seepage analyses for trapezoidal canal.
 with $H_w = 0.5W_b$.

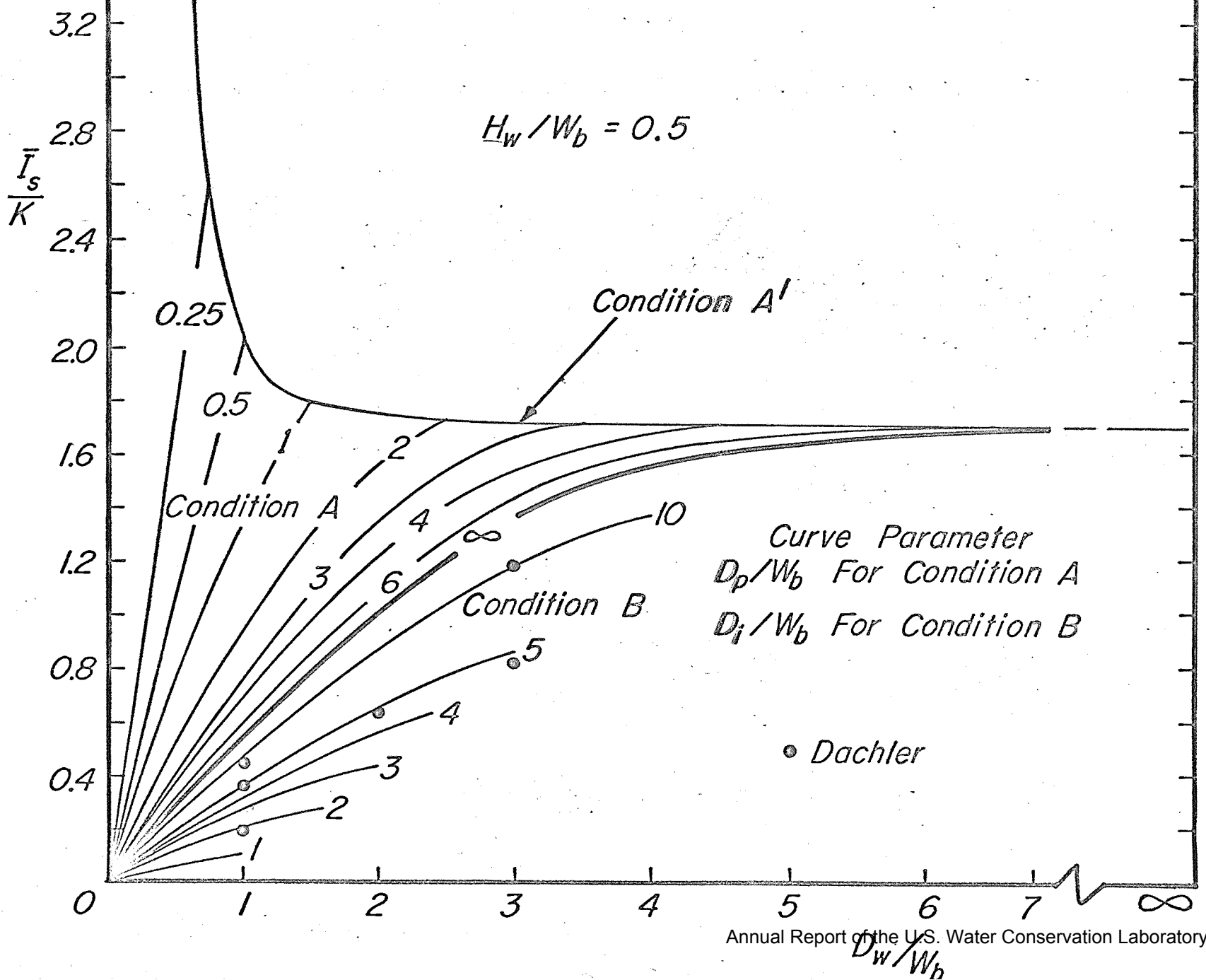
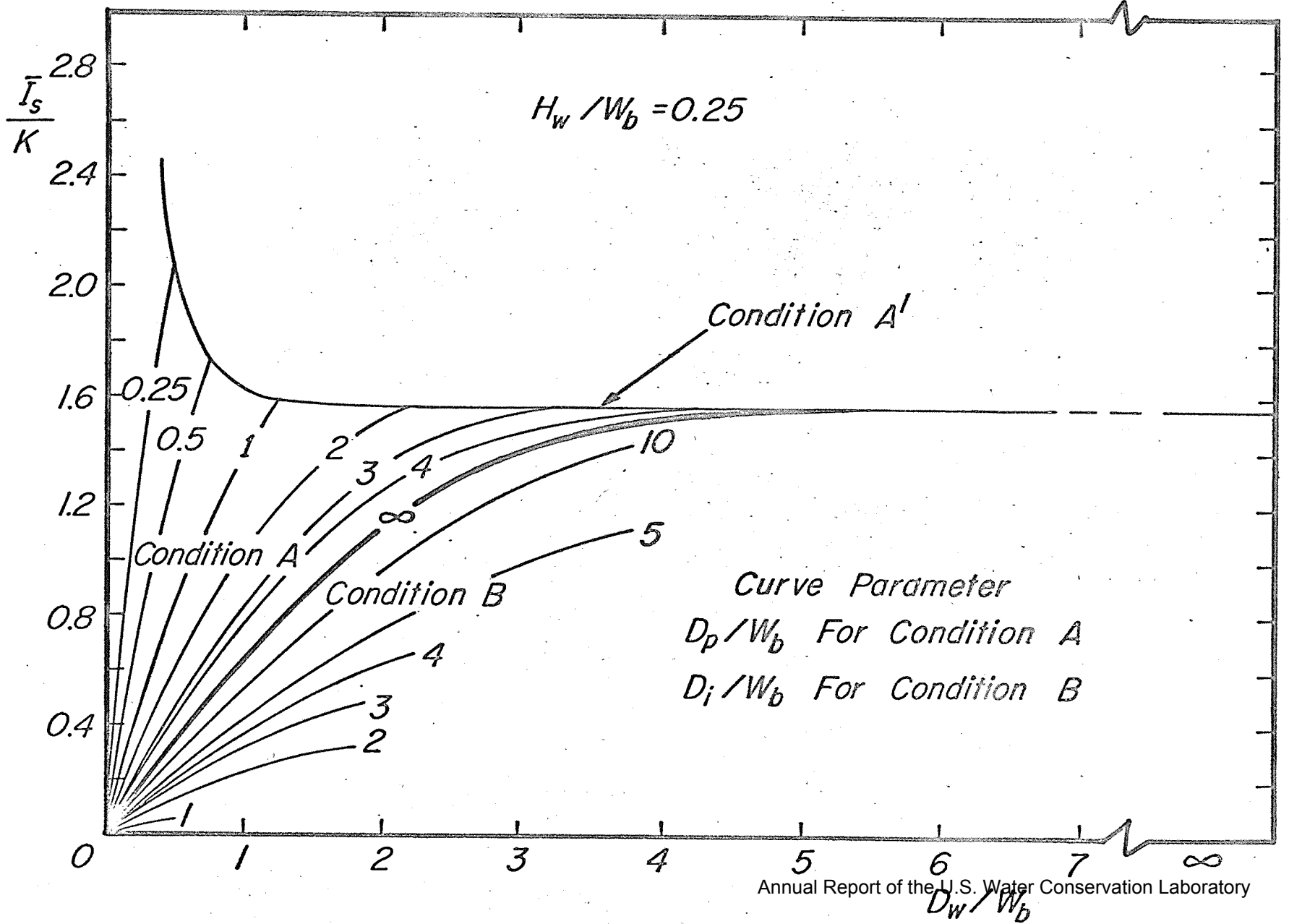


Figure 4. Results of seepage analyses for trapezoidal canal with $H_w = 0.25W_b$.



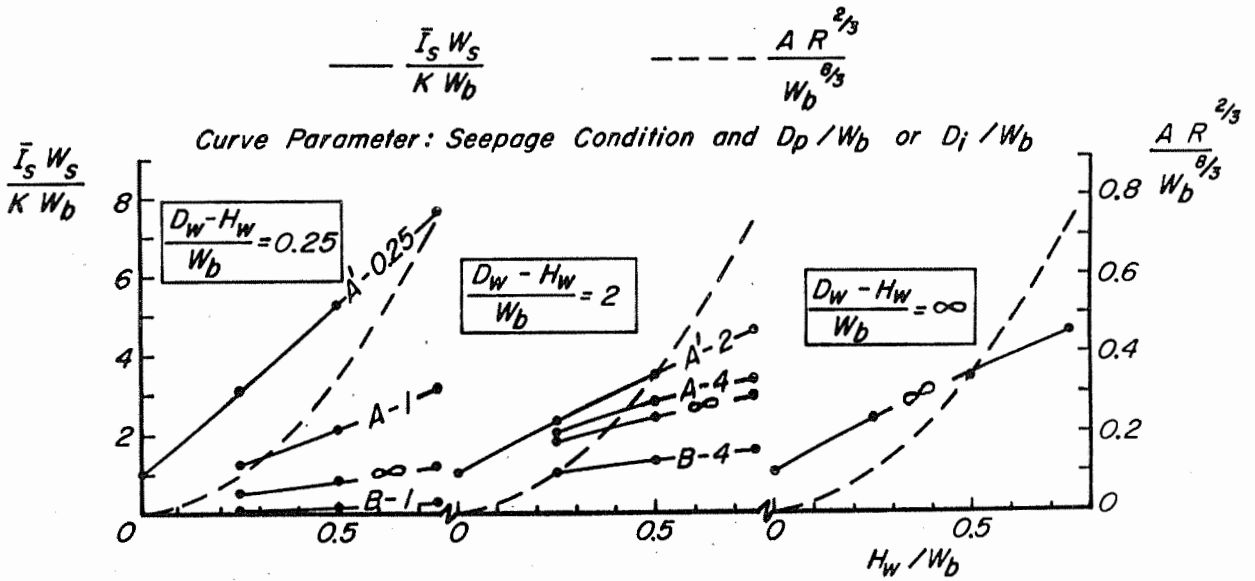


Figure 5. Effect of water depth on discharge capacity and seepage for a trapezoidal canal and different conditions of soil and water table.

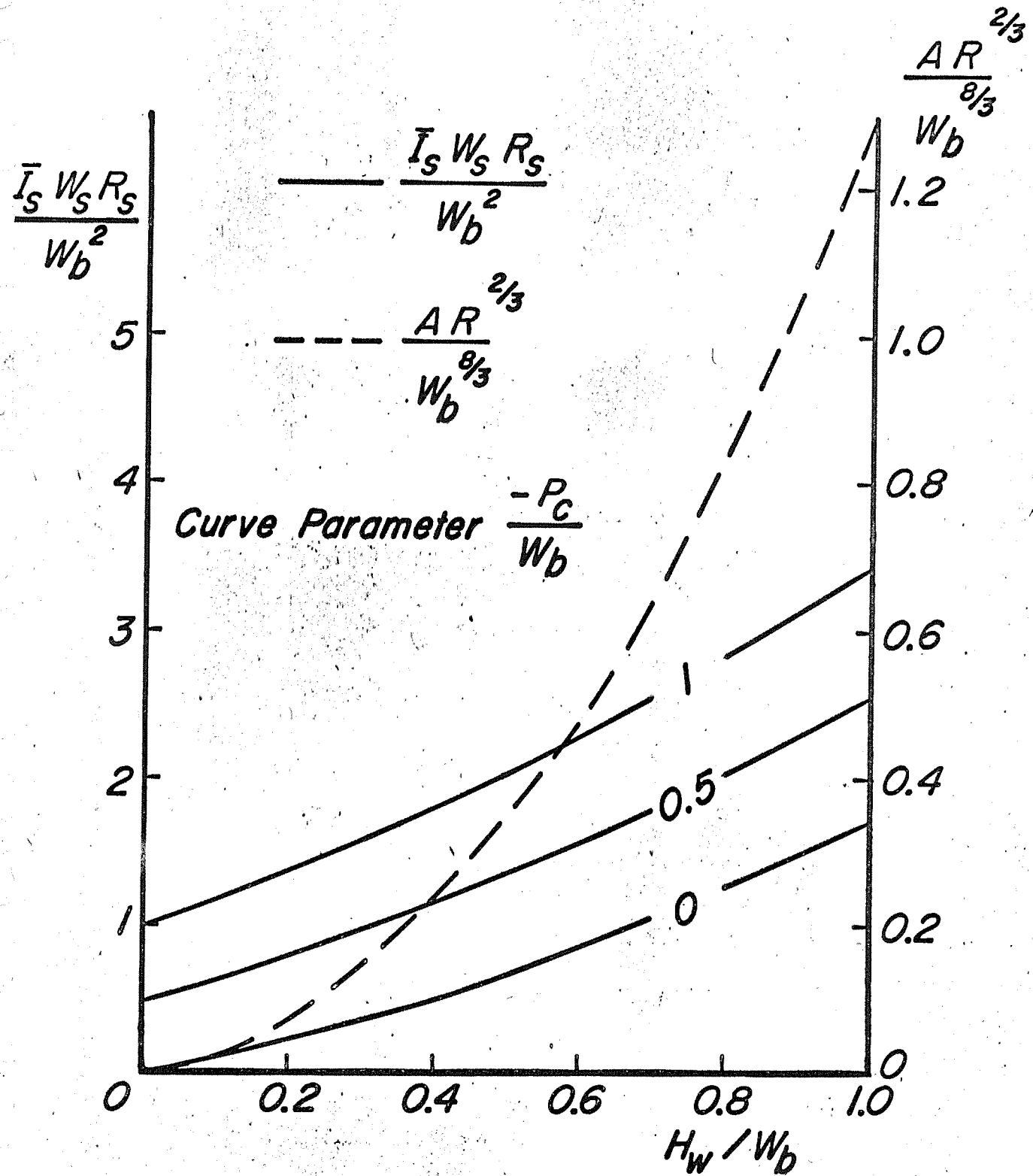


Figure 6. Effect of water depth on discharge capacity and seepage in a trapezoidal canal with clogged perimeter.

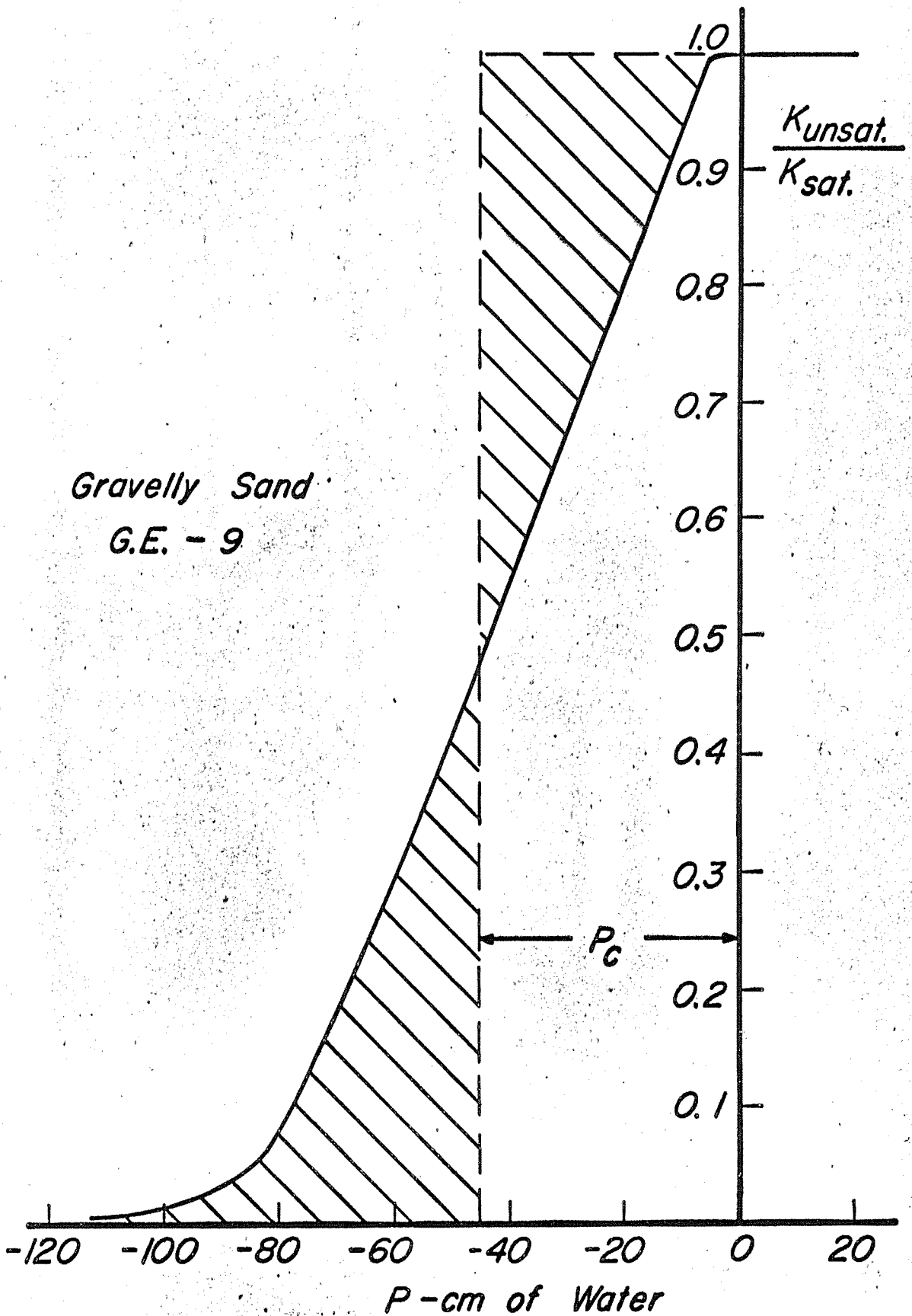


Figure 7. Relationship between K and P used in the digital computer analysis of canal seepage and evaluation of P .

Annual Report of the U.S. Water Conservation Laboratory

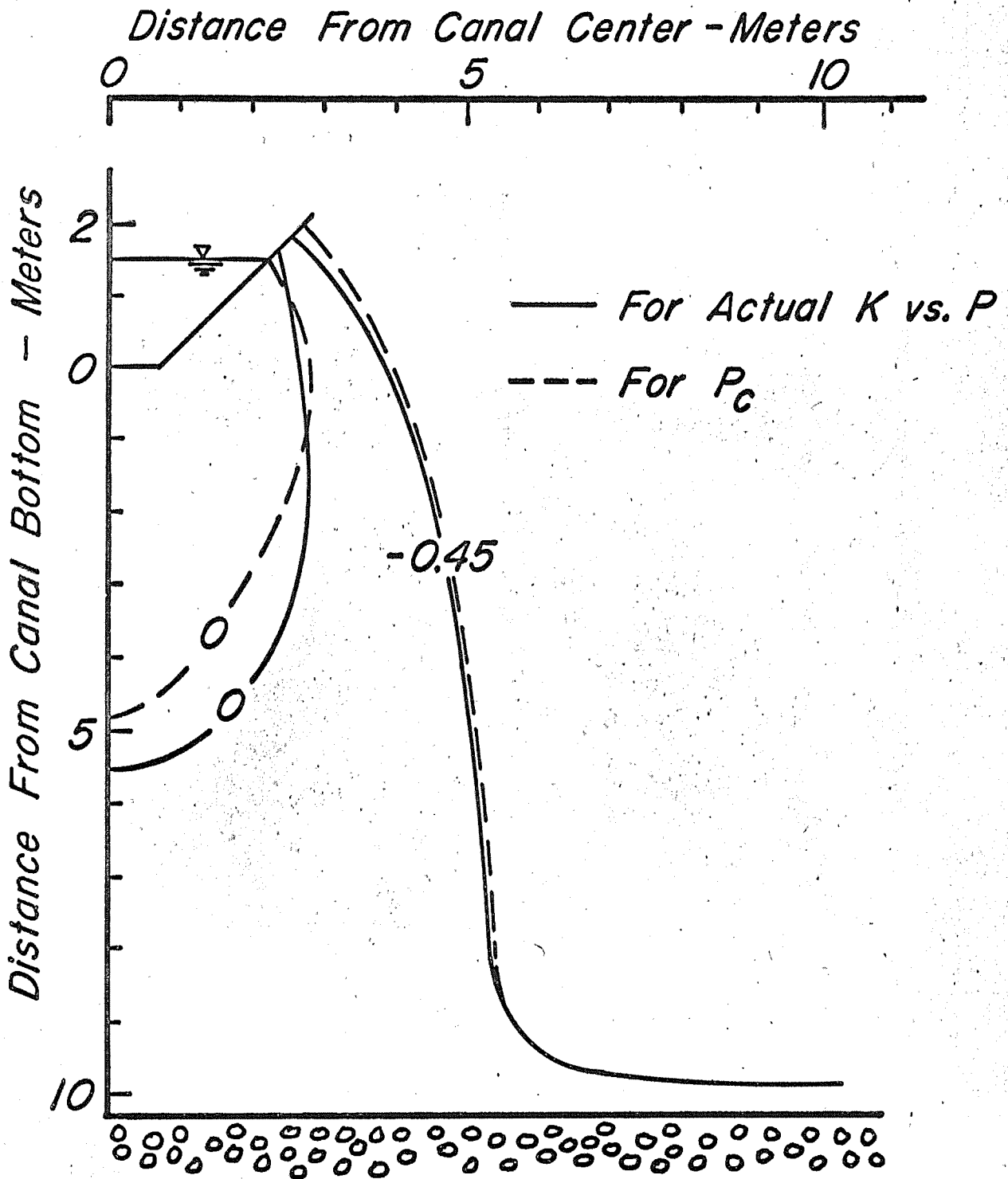


Figure 8. Flow system with contours of 0 and -45.4 cm pressure head obtained by digital computer and by resistance network.

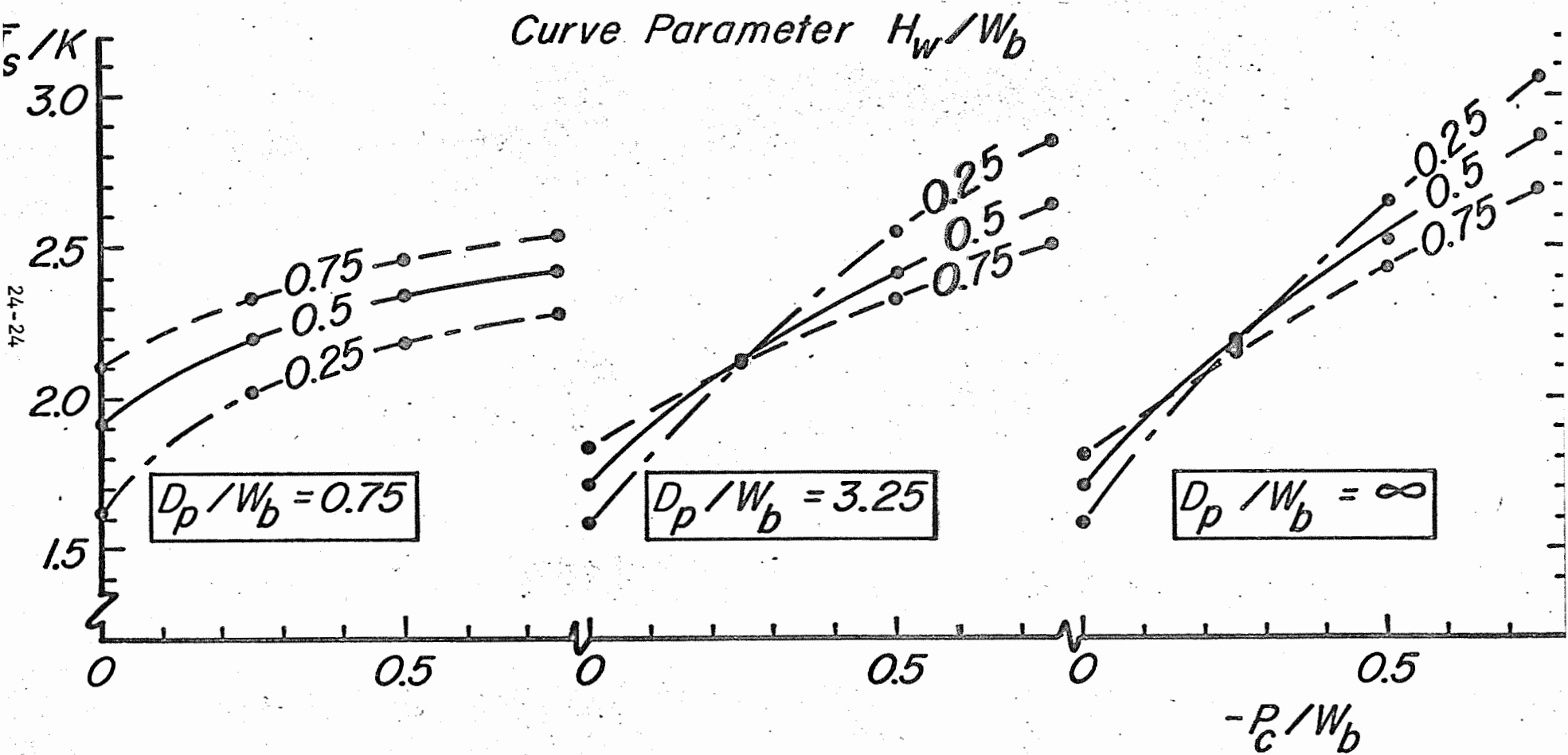


Figure 9. Relation between \bar{I}_s/K and P_c/W_b for condition A' for different values of D_p and H_w .
Annual Report of the U.S. Water Conservation Laboratory

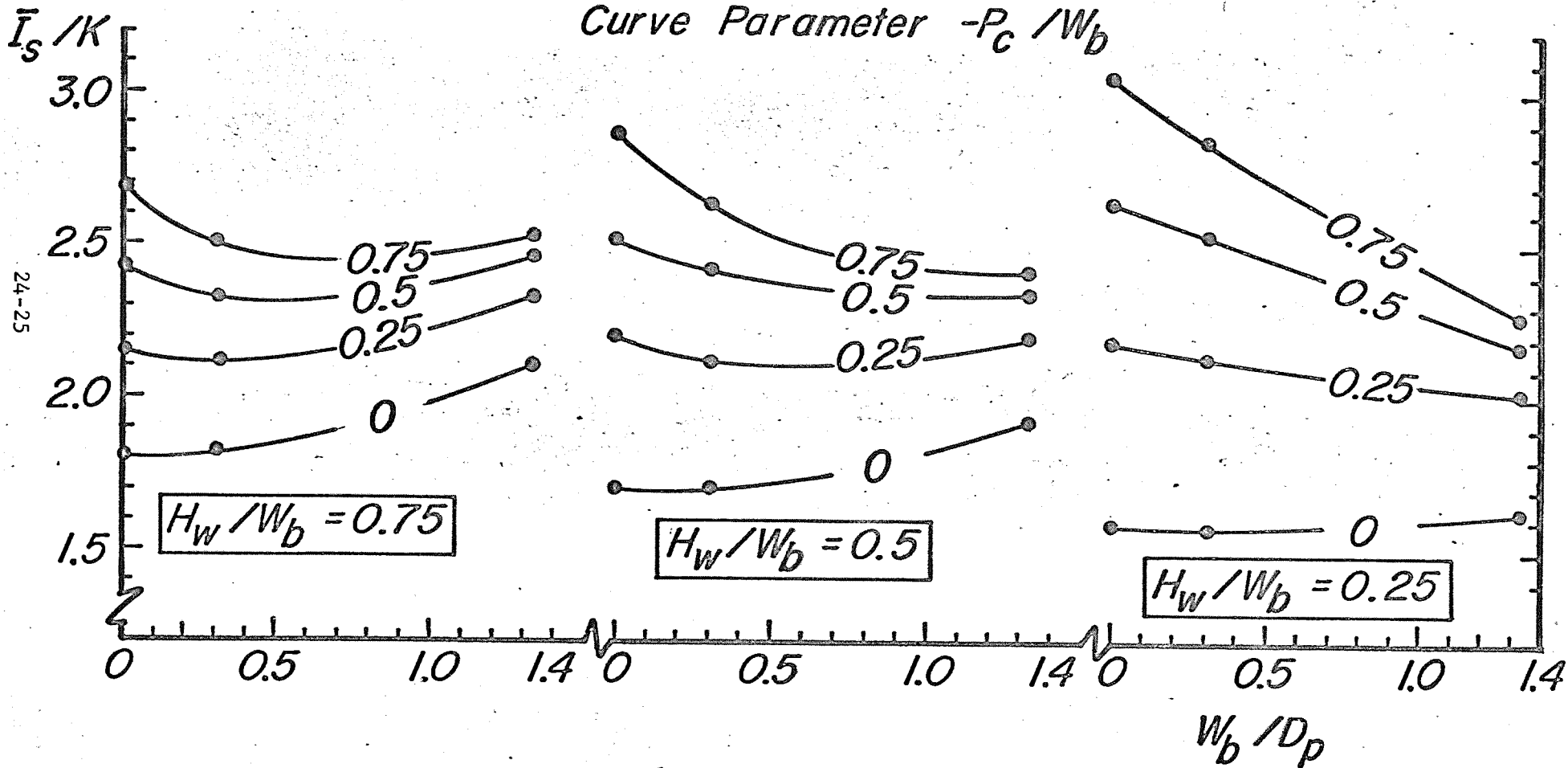


Figure 10. Relation between \bar{I}_s / K and W_b / D_p for different values of H_w and P_c .

TITLE: MEASURING HORIZONTAL AND VERTICAL HYDRAULIC CONDUCTIVITY OF
SOIL WITH THE DOUBLE-TUBE METHOD.

LINE PROJECT: SWC 4-gG1

CODE NO.: Ariz.-WCL-25

INTRODUCTION:

The work in connection with the double-tube method for measuring in-place hydraulic conductivity of soil in the absence of a water table was continued with field testing of the procedure for determining horizontal and vertical hydraulic conductivity, K_h and K_v , of anisotropic soil (see Annual Report 1962). In the course of these field tests, the need for a fast reacting device for measurement of the piezometric heads for K_v determination, became apparent. This need was confirmed by laboratory studies, and a minimum-flow pressure measuring system was developed and tested in the laboratory.

PROCEDURE:

Following the procedure discussed in Annual Report for 1962, tests for measurement of K_v and K_h were conducted at five locations in the Salt River bottom area, approximately 260 ft east of 35th Ave. The soil ranged from fine sand to sandy loam and was underlain by gravelly deposits. The piezometers were read with 1 mm manometer tubes.

Since infiltration rates from the inner tube are not constant, the piezometers for measuring K_v must be read with a fast-response device. Such a device will also make it possible to complete the test in a reasonable period of time. The relationship between the response time of the piezometers with the 1 mm manometer tubes and K of the soil, was determined in the laboratory on glass beads with K ranging from 0.039 to 1.77 cm/min. This study showed that the 1 mm manometer tube would only be suitable for field use in case of pervious soils. For medium or slowly permeable soils, a device with less response time would be required. For this purpose, a null-type pressure cell developed by the Bureau of Reclamation was modified and constructed (1). A vertical cross-section of this cell is shown in Figure 1. A thin, brass diaphragm rests flat against a rigid surface in which an electrode is imbedded. The chamber above the diaphragm is

connected to the piezometer. The pressure in this chamber is measured by increasing the back pressure below the diaphragm until the electrical contact between the diaphragm and the electrode is broken. At that instant, which is indicated by a current meter, the back pressure is measured with a U-tube manometer. This pressure is then equal to the piezometer pressure on the opposite side of the diaphragm.

RESULTS AND DISCUSSION:

The results of the five field tests with the double-tube method are shown in Table 1. The graphs of h versus z for the piezometer readings are shown in Figures 2 and 3. The K_{dt} -values for tests 1, 2, 3, and 5 were calculated using the standard and the simplified procedure (see Annual Report 1962). Both procedures gave the same K_{dt} -values. The K_{dt} -value for test 4 was calculated from the double-tube equation based on H_b -measurement. The K_v -values were calculated from the piezometer data in Figures 2 and 3. Tests 2, 3 and 4 yielded good, straight lines for all of the piezometers. In tests 1 and 5, the lines showed a break and representative K_v -values could not be calculated. The high gradient of 40 in the first centimeter of penetration for test 5 indicated the presence of a surface seal. This seal was probably a result of insufficient cleaning of the auger hole when the double-tube equipment was installed. The gradient below the first centimeter is 8, which is approximately the same as that for tests 2, 3 and 4. In test 1, the gradient for the first 6 cm is 2.2, which increases to 20 for the next 3 cm. The high gradient at the lower depth could be due to the presence of a silt layer of lower hydraulic conductivity which is frequently observed in the area of the tests. Thus, eliminating tests 1 and 5 as inconclusive, tests 2, 3 and 4 gave ratios of K_h/K_v of 3.0, 0.70, and 0.42, respectively.

The relationship between response time of the piezometer with the 1 mm glass-tubing manometer and the hydraulic conductivity of the glass beads in which the piezometer was placed, is shown in Figure 4. The response time is the time in which 63.2% of the pressure difference applied between the piezometer and the glass beads is registered by the manometer. A representative K -value

of medium to less permeable soils is approximately 0.01 cm/min. Figure 4 shows that the time constant for this K-value is approximately 30 to 40 minutes. Since the time for the manometer to reach equilibrium is a multiple of the time constant, it can readily be seen that the 1 mm glass tube was not a suitable device for measuring the piezometers in the field.

The minimum-flow pressure cell constructed for rapid measurement of the piezometric levels was first calibrated using air pressure. The air pressure was applied using a compressed air supply and a pressure regulator. The applied pressure was measured with a water manometer. After this test, which showed excellent agreement between the measured and the applied pressure, the pressure cell was filled with water and calibrated again. The results of this calibration are shown in Figure 5. It appears that the pressure cell is linear with an accuracy of ± 0.5 cm of water. There is a zero-shift in the calibration curve because of the difficulty in setting the contact rod flush with the rigid surface on which the diaphragm rests. The zero-shift can be checked at any time by measuring the pressure of a known reference level. In most cases, the magnitude of the zero-shift is unimportant because pressure differences must be measured to obtain piezometric gradients.

Care should be taken to keep the contact points on the electrode and the diaphragm clean and dry. When this is done, the pressure differential required to make or break the electrical circuit is less than 1 cm of water. The maximum volume displacement that occurs while taking a measurement of $1.1 \times 10^{-3} \text{ cm}^3$. However, this volume displacement occurs just after the diaphragm moves and the measurement is taken.

SUMMARY AND CONCLUSIONS:

Field tests of the double-tube method for evaluating horizontal and vertical hydraulic conductivity, K_h and K_v , in anisotropic soils were performed in the Salt River Bottom on fine sand to sandy loam. The piezometers for measuring vertical hydraulic gradients below the hole bottom were measured with 1 mm glass-tube manometers.

Of the five tests performed, three gave reliable measurement of K_v with the piezometers. The other two showed a break in the vertical hydraulic gradient below the hole bottom, indicating discontinuities within the soil region "sampled" by the method. The resulting values of K_h and K_v for the three successful tests were 1.34 and 0.44, 0.069 and 0.098, and 0.97 and 2.3 cm/min, respectively.

Since the infiltration rate at the auger-hole bottom is not constant, the piezometers for measurement of K_v must be read with a fast-response device. Laboratory studies regarding the relation between response-time and hydraulic conductivity of the soil showed that the 1 mm manometer tubes would be much too slow in medium to slowly permeable soils. Therefore, a null-type pressure cell developed by the Bureau of Reclamation was modified, constructed and tested. The cell utilizes a diaphragm separating an upper chamber connected to the piezometer and a lower chamber connected to a pressure regulating device with U-tube manometer. At incipient movement of the diaphragm, which is electrically indicated, the pressures are essentially the same and the pressure in the lower chamber is read with the manometer. Calibration of the cell in the range of -0.55 to +0.55 cm of water showed that the device was linear with an error not exceeding ± 0.5 cm water. The volume displacement of water in the cell is approximately 1 mm^3 . Movement of the diaphragm takes place after the electrical contact is broken, however.

REFERENCE:

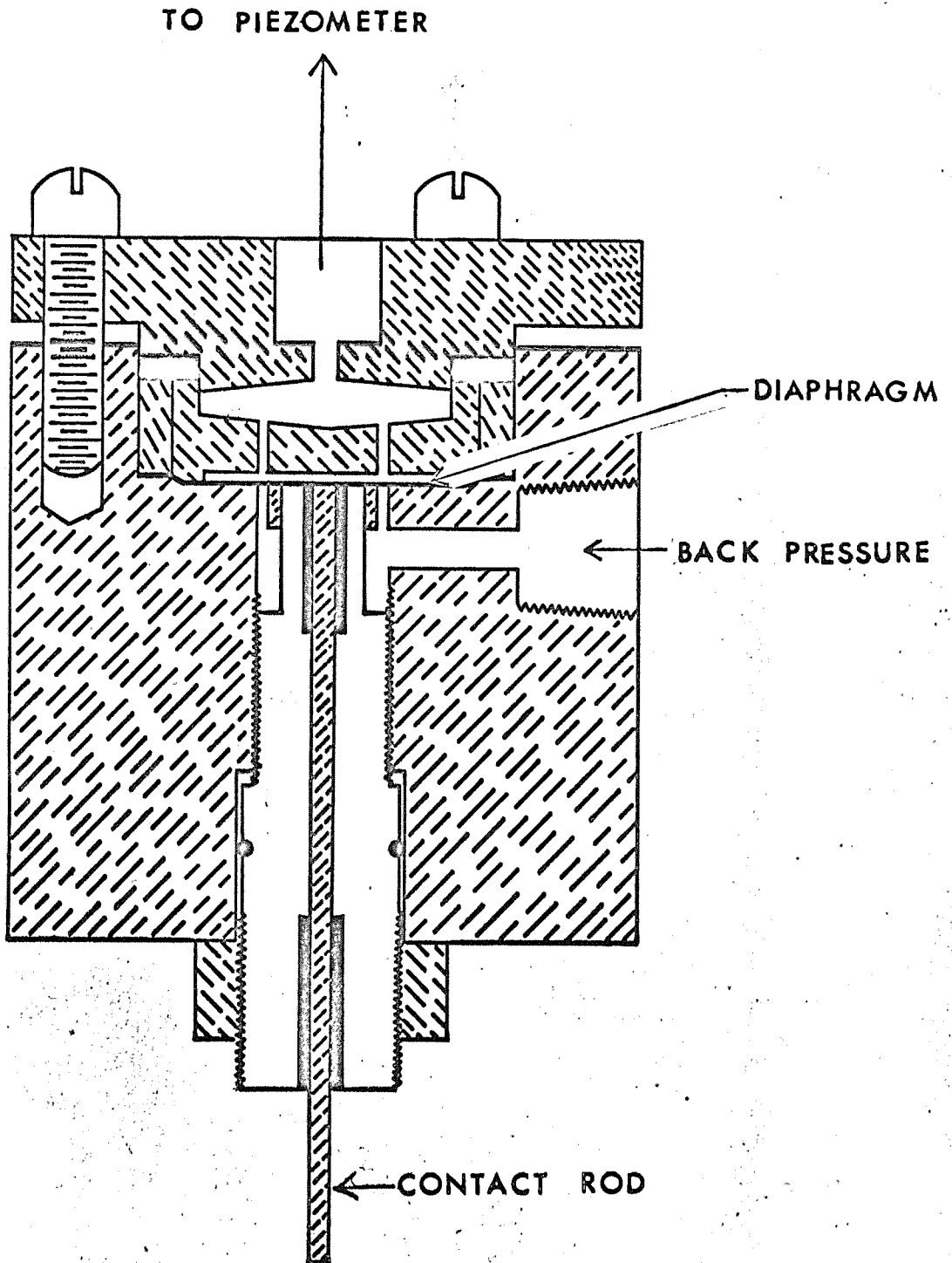
- (1) Gibbs, H. J., and Pettibone, H. C.

July 30, 1962. Development of earth pressure cell and test installation for the study of earth pressures on buried, rigid pipe. Soils Engineering Report No. EM-657. U. S. Bureau of Reclamation, Denver, Colorado.

PERSONNEL: Herman Bouwer and R. C. Rice.

Table 1. Results of double-tube tests in anisotropic soil.

Test	Soil Type	d/R_c	F_f	K_{dt} cm/min	$\frac{dh}{dz}$	$\left(\frac{dH}{dt}\right)_{H=0}$ cm/min	K_v cm/min	$\frac{K_{dt}}{K_v}$	$\frac{K_h}{K_v}$	K_h cm/min
1	Silty Loam	0.5	0.95	0.032						
2	Sand	0.43	1.04	0.58	11.7	5.2	0.44	1.3	3.0	1.34
3	Silty Loam	0.61	0.86	0.089	13	1.28	0.098	.91	0.70	0.069
4	Sand	0.31	1.23	1.87	8	18.6	2.3	.81	0.42	0.97
5	Sand	0.31	1.23	0.39						



NO FLOW PRESSURE CELL

Figure 1. Cross section of minimum-flow pressure cell.

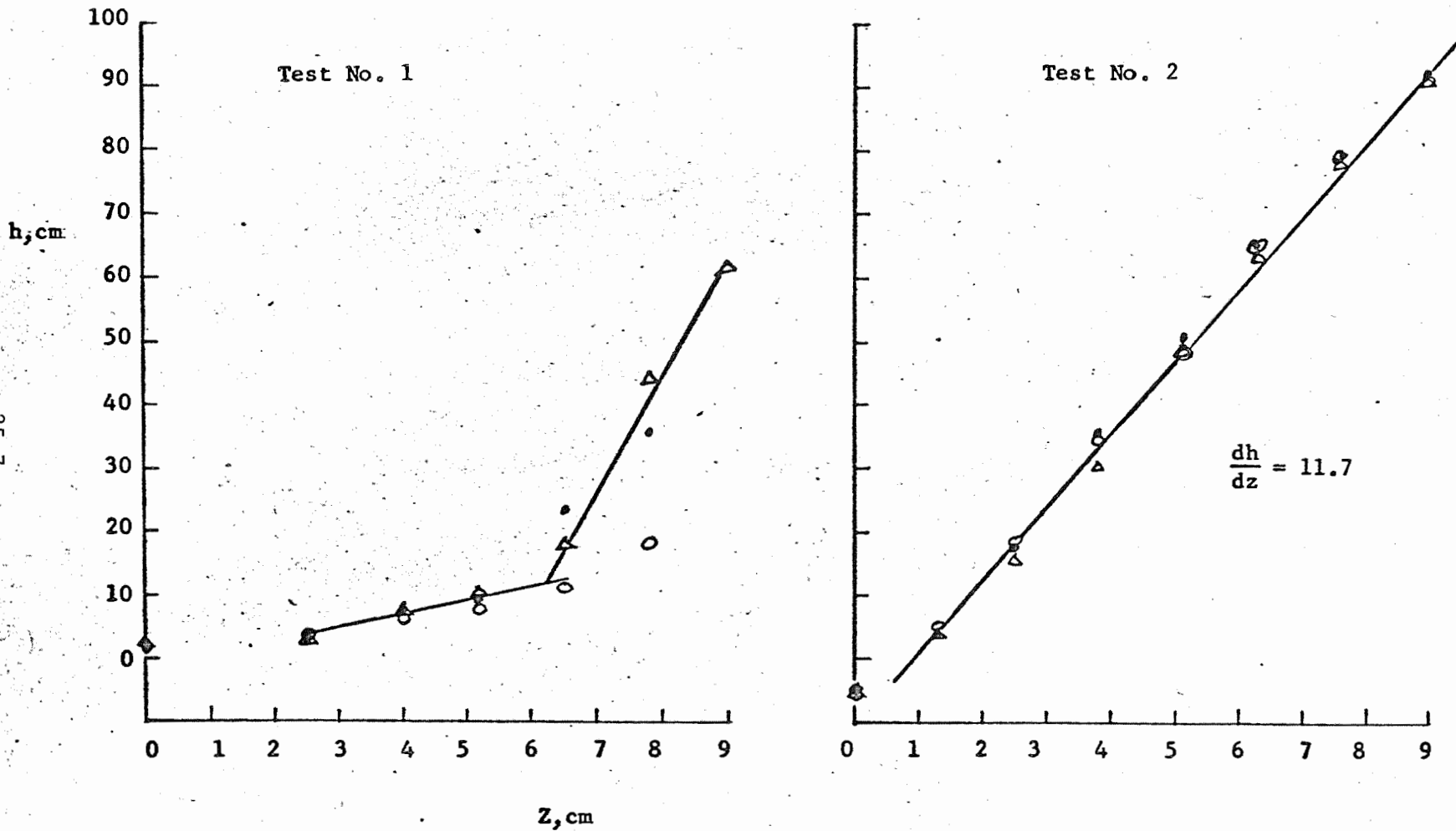


Figure 2. Piezometric head versus penetration of the three piezometers inside the inner tube.

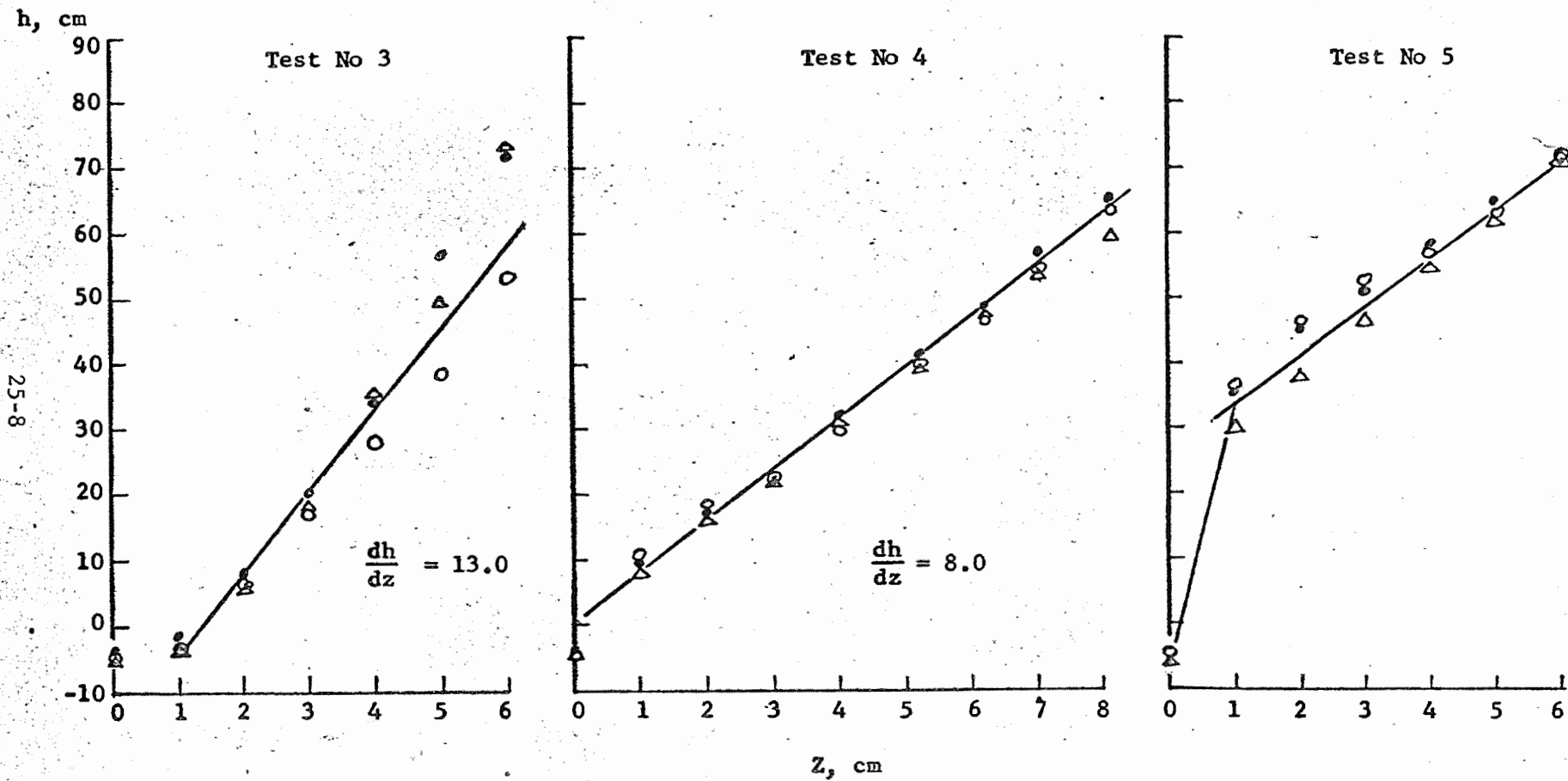


Figure 3. Piezometric head versus penetration of the three piezometers

inside the inner tube.

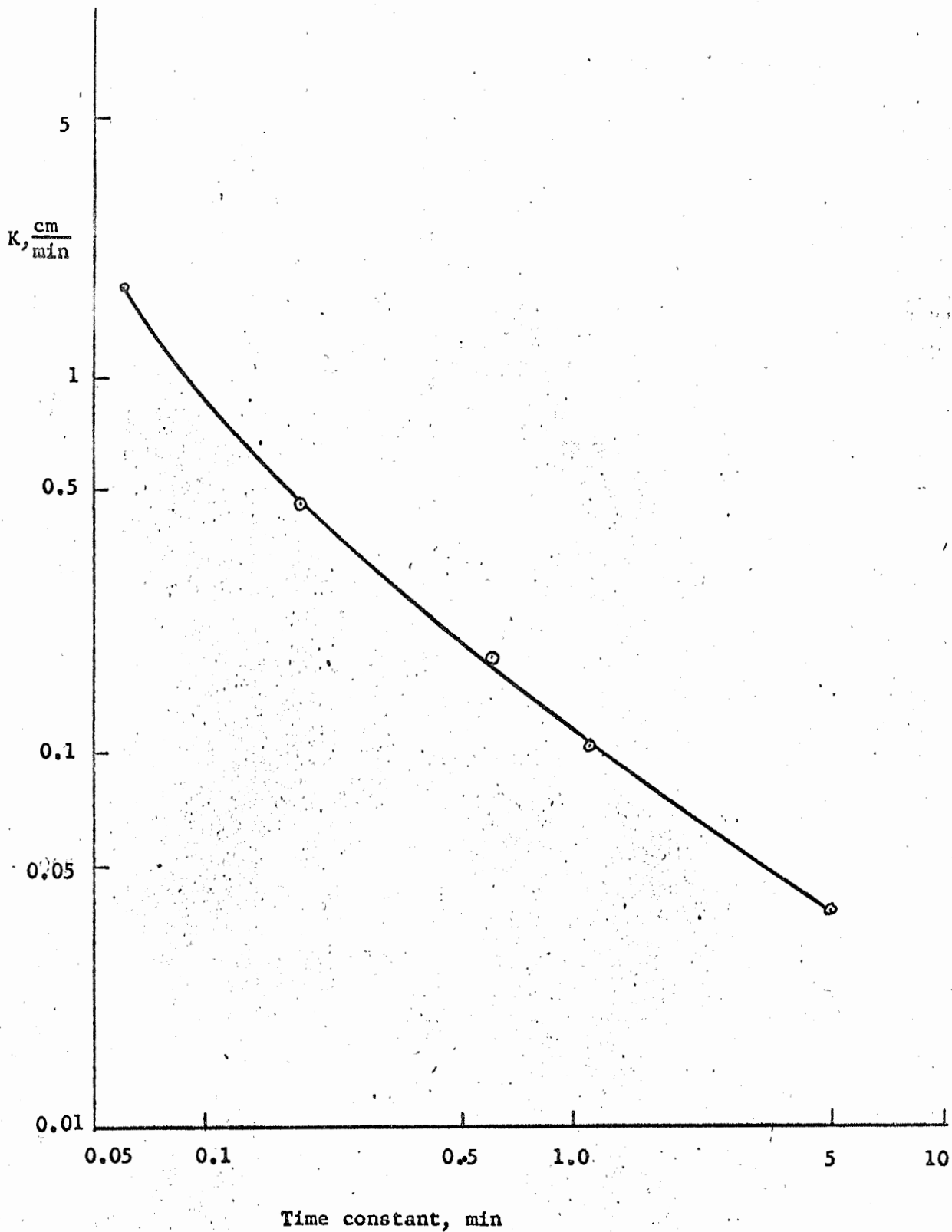


Figure 4. Relation between response time and soil hydraulic conductivity for the piezometers.

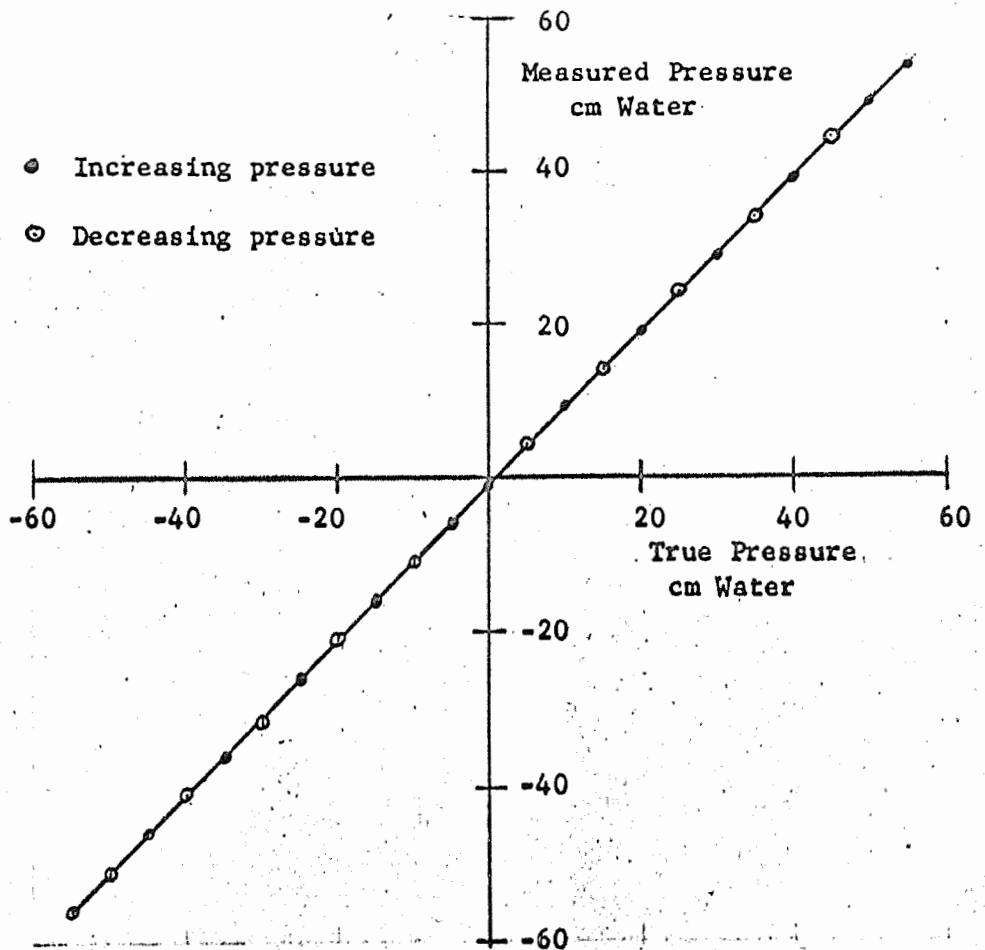


Figure 5. Results of calibration test of minimum-flow pressure well.

TITLE: NONDESTRUCTIVE BETA RAY TRANSMISSION METHOD FOR MEASURING WATER
CONTENT IN PLANTS

LINE PROJECT: SWC 11-gG1

CODE NO.: Ariz.-WCL-26

INTRODUCTION:

The objectives and portions of the theory, construction details, and procedure in the use of the beta ray gauge have been presented in the Annual Report of 1962.

I. CHOICE OF RADIOISOTOPE.

RESULTS AND DISCUSSION:

The method for choosing the proper radioisotope for the beta ray gauge was presented in a qualitative manner in the Annual Report for 1962. A quantitative method for choosing the radioisotope which will yield the maximum accuracy was further developed.

The attenuation of beta rays follow the exponential type relation

$$I = I_0 e^{-\mu x} \quad [1]$$

where

I = intensity of the transmitted radiation (cpm)

I_0 = intensity of the incident radiation (cpm)

μ = mass absorption coefficient ($\text{cm}^2 \text{mg}^{-1}$)

x = absorber thickness (mg cm^{-2})

The sensitivity, the change in count rate per unit change in absorber thickness, is defined as

$$\frac{dI}{dx} = - I_0 \mu e^{-\mu x} \quad [2]$$

and we see qualitatively that increased sensitivity can be obtained by increasing both the values of the incident radiation I_0 and the mass absorption coefficient μ . Since μ is inversely related to the maximum energy, greater sensitivity is possible for the lower energy beta ray emitting radioisotopes. The choice of the radioisotope based on the largest value of μ , however, cannot be made indiscriminately in practice because the range of the beta particle in the absorber must be considered, that is, there must be some measurable transmitted

radiation. Although the absolute value of the leaf absorber thickness is of interest, the more important item is the changes in thickness which the leaf undergoes. The relative error of measurement of changes in x for a given absorber thickness can be developed from equation [2] as

$$\frac{\Delta x}{x} = - \frac{e^{-\mu x} \Delta I}{\mu x I_0} \quad [3]$$

where the relative error, $\Delta x/x$ is associated with the error in the measuring equipment (1).

Because we are dealing with a radioactive material having random emission of radiation, the statistical fluctuation associated with the radiation source is

$$\frac{\sigma_I}{I_0} = \frac{(I)^{1/2}}{I_0} = \frac{(I_0 e^{-\mu x})^{1/2}}{I_0} \quad [4]$$

Thus, the relative error of the thickness, taking into account the natural fluctuation in the source from [3] and [4] is:

$$\frac{\sigma_x}{x} = - \frac{e^{-\mu x/2}}{\mu x (I_0)^{1/2}} \quad [5]$$

From equation [3] minimum error is obtained when $x = 1/\mu$ and when instrumental error is negligible in respect to the statistical fluctuation of source radiation, minimum error is present when $x = 2/\mu$.

The absolute values of $\Delta x/x$ were calculated for the radioisotopes C^{14} , Pm^{147} , Tc^{99} , and Tl^{204} using equation [5] and values of $I_0 = 10,000$ cpm for a one-minute counting period. These are plotted in Figure 1. Fortunately, the change in error at the minimum-error absorber thickness is gradual so that a given radioisotope is useful over a range of thicknesses instead of being restricted to a single thickness. The values of $2/\mu$ (the absorber thickness at minimum error) for C^{14} , Pm^{147} ,

Tc⁹⁹, and Tl²⁰⁴ are 7.6, 12.3, 17.5, and 64.5 mg cm⁻², respectively. Carbon-14 should be a good beta ray source for absorber thicknesses from 5 to 20 mg cm⁻², Pm¹⁴⁷ and Tc⁹⁹ useful from 10 to 40 mg cm⁻², and Tl²⁰⁴ from 15 to at least 70 mg cm⁻².

II. BETA RAY STEM GAUGE.

PROCEDURE:

An exploratory study was conducted to determine the applicability of the beta ray gauge presently used for leaf thickness investigation for measuring stem thickness changes. The Pm¹⁴⁷ source was replaced with a one-inch diameter 2 μ c Tl²⁰⁴ beta ray source. A one-quarter-inch diameter collimator was placed over the one-inch source. The source was located on one side and the end-window GM detector directly opposite on the stem of an eight-week old cotton plant. The experiment was conducted in the Controlled Environment Growth Chamber at 25.5 C and vapor deficit of 30 mb. Light intensity was variable at 0 and 1900 ft-c. Periodic one-minute counts were taken during the alternate dark and light conditions. The results are presented in Figure 2.

RESULTS AND DISCUSSION:

The count rate in the light ranged from 10,000 to 11,000 cpm. Within six minutes after the lights were turned off the count rate dropped to a minimum of 9280 cpm, indicating a rapid change in stem geometry. When the lights were turned on, the count rate increased indicating a decrease in stem thickness, and again when the lights were turned off, the count rate increased. The response to light and dark for the stem is similar to that previously noted with the plant leaves. Under the conditions of the experiment the cotton plant is apparently acting as a unit in respect to water balance.

III. WATER BALANCE IN COTTON PLANTS.

RESULTS AND DISCUSSION.

The beta ray gauge has been used in conjunction with water balance in cotton plants and the data is included in project WCL-29 (Water Absorption, Transpiration, and Internal Water Balance of Cotton Plants as Affected by Changes in Evaporative Demands). For current

studies, the count-rate data for the leaves are converted into equivalent aluminum thickness using calibration curves of the type presented in Figure 3. This method of data presentation was simpler and more reliable than those used previously such as relative turgidity. One of the difficulties encountered with relative turgidity was in the choice of the 100 percent value in the calibration procedure. The instrument was of such a sensitivity that the degree of wiping-off of the "excess" water from the leaf floated in water affected the turgidity value.

SUMMARY AND CONCLUSIONS:

A quantitative procedure for the selection of a radioisotope for the beta ray gauging of plant leaves was developed. Carbon-14 was calculated to work best for leaf absorber thicknesses of 5 to 20 mg cm⁻², Pm¹⁴⁷ and Tc⁹⁹ for absorbers of 10 to 40 mg cm⁻², and Tl²⁰⁴ from 15 to at least 70 mg cm⁻². The beta ray gauge has been used successfully in water balance studies of cotton plants in which the leaf water content is followed continually under varying environmental conditions. By use of a 2 μc Pm¹⁴⁷ source which is normally used in the beta leaf gauge, it was possible to monitor changes which occurred in the stem of the young cotton plant. The data showed that measurable and rapid changes in stem thicknesses occurred during transitions of dark and light periods.

REFERENCES:

- (1) Zumwalt, L. R.
1954. The best performance for beta gages. *Nucleonics*
12 (1):55-58.

PERSONNEL: F. S. Nakayama, W. L. Ehrler

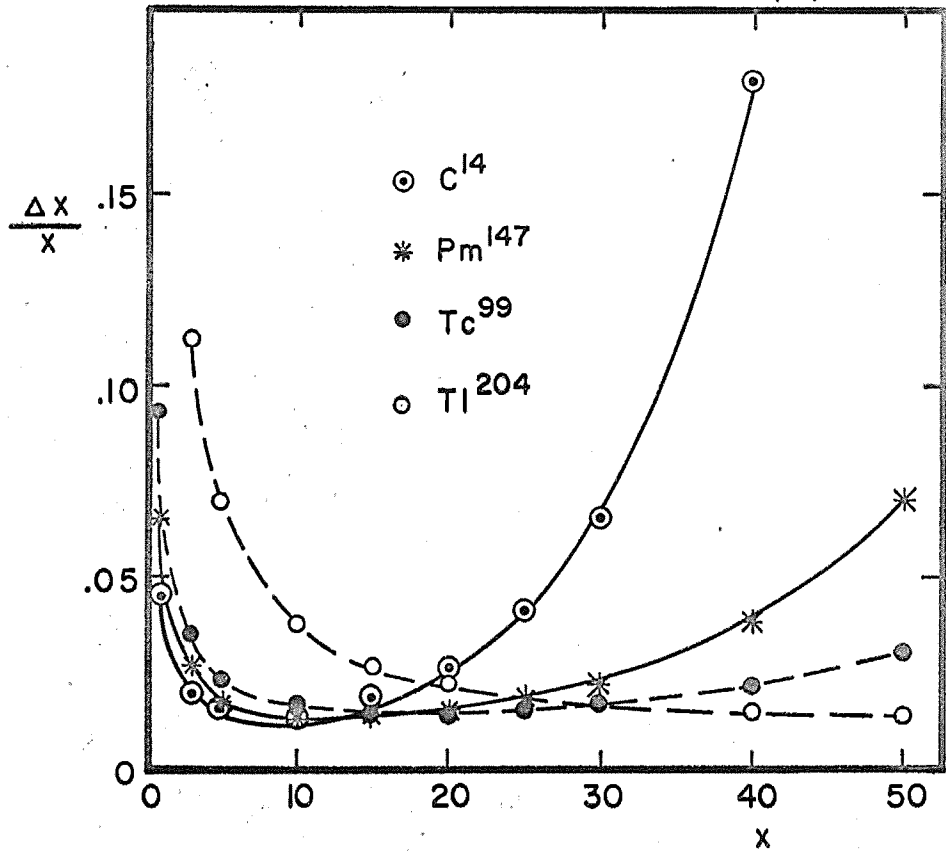


Figure 1. Relative errors for C^{14} , Pm^{147} , Tc^{99} , and Tl^{204} at various absorber thicknesses.

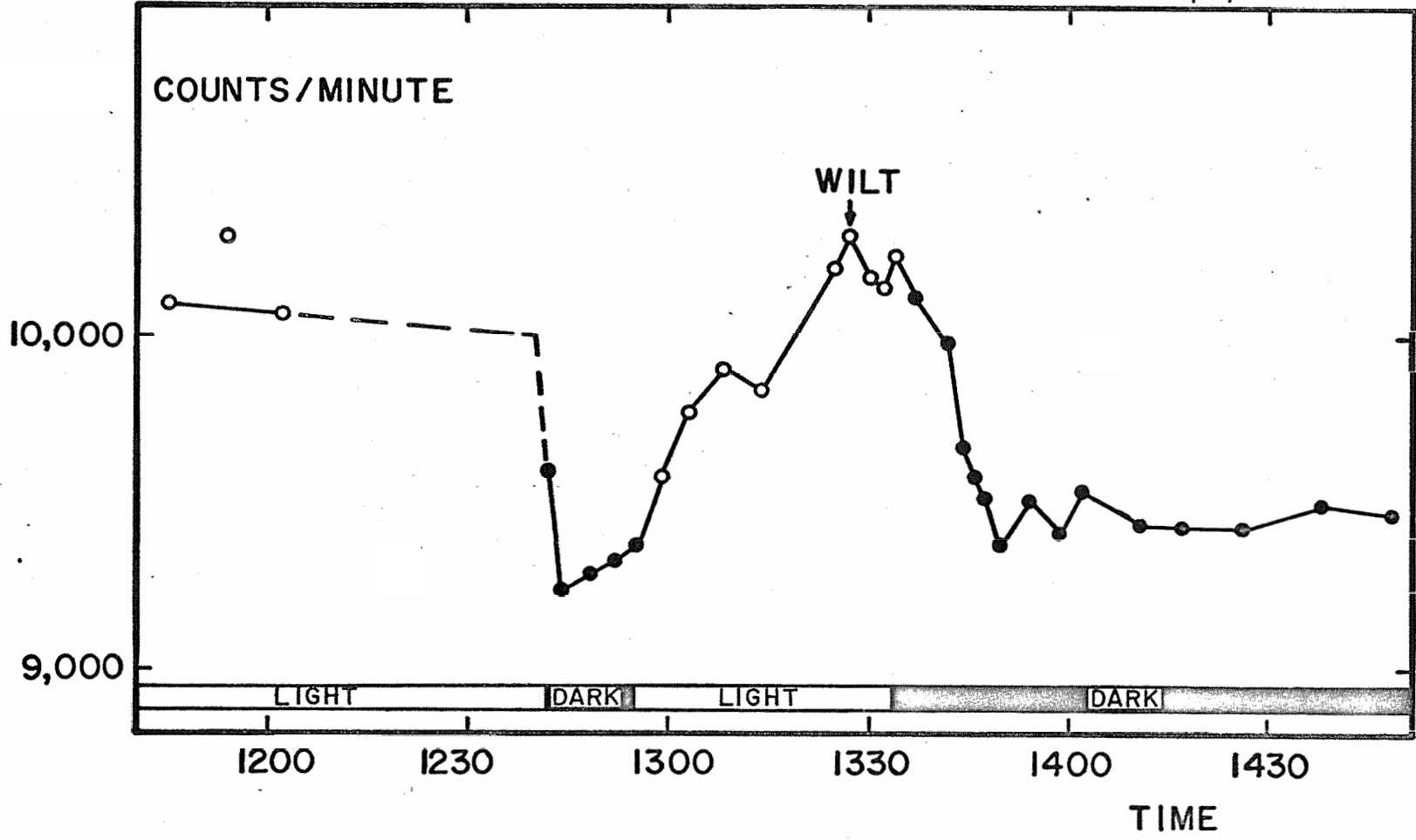


Figure 2. Response of cotton stem to variable light conditions as measured with the beta ray gauge.

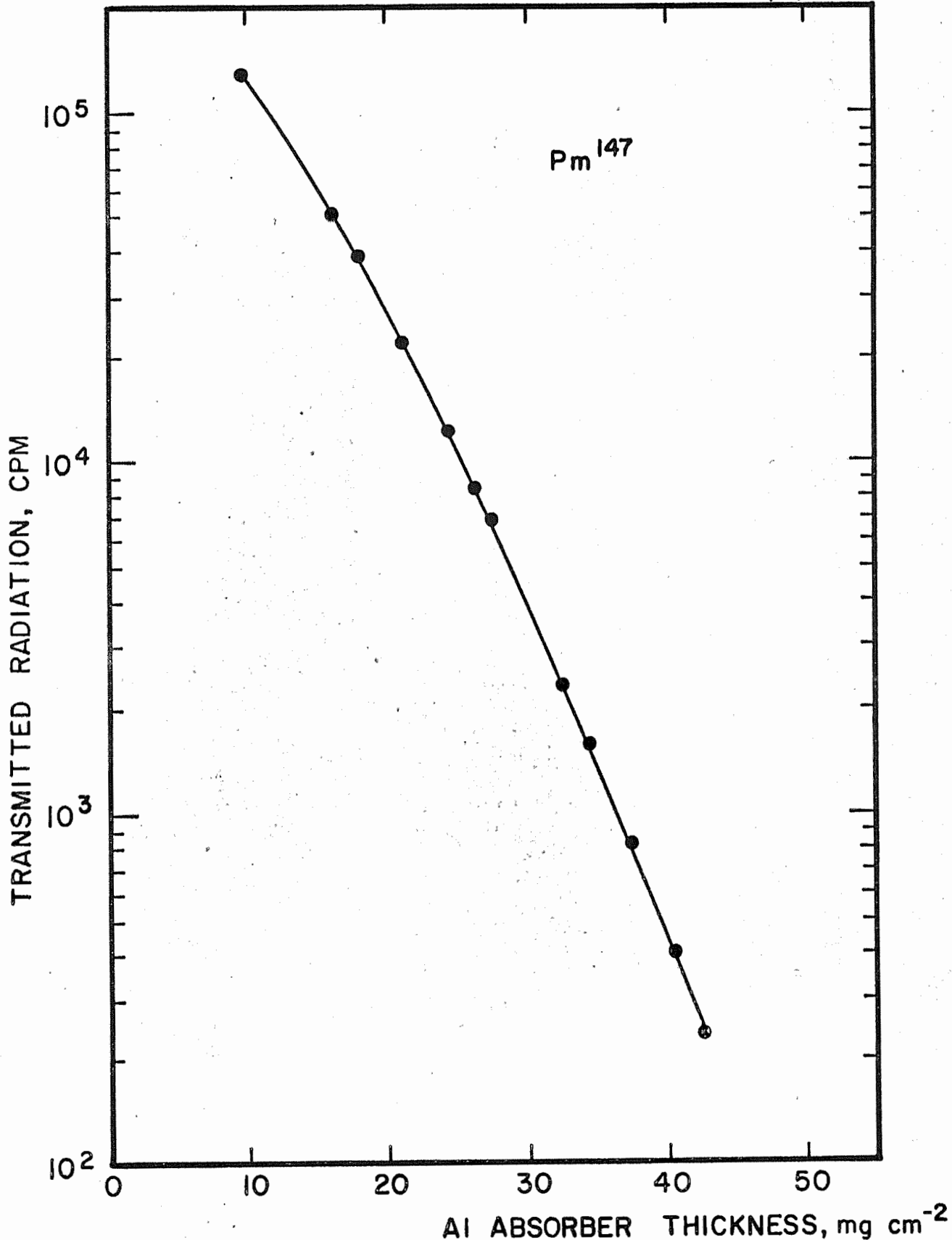


Figure 3. Calibration curve of beta ray gauge with aluminum for use in converting leaf count-rates to equivalent aluminum thickness.
Annual Report of the U.S. Water Conservation Laboratory

TITLE: WATER ABSORPTION, TRANSPIRATION, AND INTERNAL WATER
BALANCE OF COTTON PLANTS AS AFFECTED BY CHANGES
IN EVAPORATIVE DEMANDS

LINE PROJECT: SWC 11-gG1

CODE NO.: Ariz.-WCL-29

PART I. DIRECT AND INDIRECT MEASUREMENTS OF WATER BALANCE
OF COTTON PLANTS IN 1963

INTRODUCTION:

Since wilting, either incipient or visible, is extremely common among terrestrial plants during bright, warm days, internal water balance plays an important role in regulating the passage of water through plants. This loss of turgidity occurs because of an appreciable resistance to water movement through roots. Therefore, when transpiration is accelerated rapidly by increased evaporative demand, the rate of water absorption rises less rapidly, with a resultant net water deficit. A plant's ability to regulate the flow of water from soil to atmosphere must be understood as an integral part of the evapotranspiration process before intelligent efforts to conserve water can be made in the plant sphere. Therefore, last year a comprehensive study was begun on short-term water balance. The data in this report confirm what was learned before, and extend the range of information by a change in emphasis in the water-balance research. It should be re-emphasized at the outset that an assumption underlying the investigations conducted in the Climate Chamber is that transpiration is proportional to the saturation deficit of the air, and that leaf temperature under normal conditions in this room is quite close to air temperature. Therefore, the saturation deficit of the air is used as a substitute for the leaf value.

PROCEDURE:

In the first phase, summarized in the Annual Report for 1962, a predetermined saturation deficit (SD) of the air was maintained both during the overnight equilibration period and throughout the experiment proper, the only change being turning the lights on or off. Thus, transpiration was accelerated by a light-induced, fast stomatal opening in proportion to the SD. This led to a temporary

loss of turgidity, which was measured directly (by simultaneous transpiration and water absorption) and indirectly (by a beta ray leaf-thickness gauge). Three experiments covering the range from low to moderately high SD were summarized last year. A repetition of the experiment at the low SD confirmed the earlier data, and a later experiment extended the range to a very high SD, both experiments making use of the same technique as before. The rapid transpiration rates in the dark at predetermined values of high SD made it possible that plant hydration was not optimum at the beginning of the experiment. Therefore, in later experiments the SD was generated by a method permitting uniform initial conditions for all experiments, i.e., an equilibration period in the dark at a low SD, conducive to low transpiration and a fully turgid plant at the start of the experiments. To dehydrate the plant, the SD was generated by a method similar to that occurring in nature - although much faster, by maintaining a constant vapor pressure, but raising both dry-bulb and wet-bulb temperatures. In another set of experiments direct measurement of water balance was supplanted by an intensive investigation of the indirect method, by use of two beta ray gauges on one plant, near both the top and base. In both of the latter series of experiments illumination was a factor in addition to the increased SD, except for one experiment in darkness. The lights came on either in conjunction with the rapidly increasing SD, or after the SD had been raised and then stabilized at a high value. The lights were turned off before the SD was lowered to its initial value. The data from each beta ray gauge, obtained directly in counts min^{-1} , were converted into the equivalent leaf thickness in terms of aluminum by a suitable calibration (see WCL-3). These thickness values were plotted against time, the equivalent leaf-thickness characteristic of the equilibration period being considered the reference value, one representing full hydration.

RESULTS AND DISCUSSION:

Direct determination of water balance by measurement of transpiration and absorption

A. At a constant saturation deficit and with sudden illumination.

1. Saturation deficit 4.4 mb. This experiment (A-8) is comparable to that at a SD of 6 mb, presented in last year's report. Transpiration accelerated slowly when the lights were turned on, requiring four 30-minute periods to reach a peak rate. However, even this slow rate of transpiration rise was not equaled by the rate of water absorption, with a consequent water deficit. Only once in seven periods of light did absorption equal transpiration. This led to a cumulative deficit that at its worst was 6 g plant^{-1} . After the lights went out, absorption slightly exceeded transpiration, but this gain was not nearly enough to make up for the previous imbalance. As a result, at the end of the experiment the plant had a 4-gram water deficit, as determined by direct measurement. A beta ray gauge on a separate plant confirmed these results. Initially well hydrated, as indicated by a horizontal line plot of leaf thickness against time, the leaf became thinner when the lights came on. This is indicative of greater transpiration than absorption. The leaf became progressively thinner, at the worst being 2.5 mg cm^{-2} thinner than in the well-hydrated condition. In darkness there was some regaining of the lost water. However, at the end of the experiment, there still was a net water deficit, in qualitative agreement with the above results, amounting to 1.25 mg cm^{-2} .

2. Saturation deficit 52.9 mb. This experiment (A-9) was analogous to that having a SD of 29 mb in last year's report, except for the much higher SD this time (maintained throughout the whole experiment). The high transpiration in the dark preceding the light was noteworthy, being $1.4 \text{ g m}^{-2} \text{ hr}^{-1} \text{ mb}^{-1}$, compared to 0.43 from an analogous experiment at a lower SD. After the lights went out, the steady transpiration rate in the dark was considerably lower than it had been at the beginning of the experiment. This may indicate partial stomatal opening during the initial dark period.

B. At a rapidly increased saturation deficit, but constant vapor pressure.

1. Enhancement of darkness-induced rehydration by a return to the initial low saturation deficit. In Experiment A-10, the SD was raised from 8 mb to 24 mb in the light, and remained at the high value. The lights were turned off later to bring about rehydration of the plant. In Experiment A-11, almost identical conditions were employed to dehydrate the plant, an increase in SD from 8 to 22 mb, but to bring about rehydration the SD was lowered to 9 mb in addition to turning off the lights.

Transpiration was affected in an almost identical manner in both experiments A-10 and A-11 (Figure 1), being low in the dark at a low SD and accelerating rapidly to a primary peak, decreasing momentarily due to wilting and then reaching a higher peak before sharply decreasing to a low value when the lights went out. Differences in plant size (leaf area) account for the somewhat different magnitude of transpiration at all points prior to the second dark period. After the lights were turned off, however, transpiration in Experiment A-11 decreased to a lower value than that of Experiment A-10, on a plant basis, and even more so on a leaf-area basis - $13 \text{ g m}^{-2} \text{ hr}^{-1}$ for A-11, versus $25 \text{ g m}^{-2} \text{ hr}^{-1}$. This is attributed to the effect of a lowered SD during the second period after the lights went out added to that due to darkness only. In both experiments A-10 and A-11 (Figure 2) transpiration and water absorption initially were essentially in balance, as shown by the alignment of the data points near the zero reference line. The sudden sharp increase in evaporative demand, in conjunction with stomatal opening, induced an appreciable water deficit during the first half-hour after time zero in both experiments. However, in both experiments water absorption exceeded transpiration in the next half-hour and was at least equal to transpiration in the remaining periods of light, despite the continued high transpiration rate brought about by a SD of 22 to 24 mb. After the lights went off, absorption exceeded transpiration by a considerable amount in the

first half-hour in both experiments, and slightly in the two remaining dark periods in Experiment A-11. The difference between the two experiments was that in Experiment A-10 water absorption was less than transpiration in the second period after the lights went off, but slightly exceeded transpiration in Experiment A-11 at the same time. The cumulative effects (Figure 3) show that in both experiments the initial exposure to light and a rapid increase in SD induced a water deficit that was made up only gradually and at a different rate in the two experiments. However, 150 minutes after time zero, plant hydration in both experiments was essentially as good as the initial value before the change in evaporative demand took place. The difference is in the excess hydration (over the initial value) of plants in Experiment A-11, compared to the slightly poorer hydration (than initial value) of those in Experiment A-10. The better hydration is attributed to the return to the initial low SD, in addition to turning off the lights. The data from the beta ray gauge (Figure 4), in general, confirm the trends shown for the cumulative water balance of Figure 3, in that the plants in both experiments experienced an internal water deficit during exposure to light and an increased evaporative demand, after having started out in water balance. One discrepancy was that the extent of dehydration shown by the beta ray gauge was greater in Experiment A-11 than A-10, in contrast to the equal dehydration of both experiments shown in Figure 3. There is further agreement between the two methods in the response after the lights went off. As in the cumulative data of Figure 3, in the dark the beta ray gauge showed a somewhat better plant rehydration when the SD was returned to the initial low value, than when the SD was maintained at a high level.

2. Effect of a suddenly increased saturation deficit occurring in light, as compared to darkness. Transpiration before time zero was low in both Experiments A-11 and A-12 (Figure 1), since the plants were in the dark and at a low SD. As already discussed, transpiration accelerated rapidly in Experiment A-11 in response to both light and a rapid increase in SD. In contrast, transpiration in

Experiment A-12 showed only a slow acceleration in the dark in response to a similar change in SD; the peak was not attained until the second measurement period after the change, although the time taken to generate the higher evaporative demand was the same in both experiments (about 30 minutes). The maximum transpiration rate of $6 \text{ g plant}^{-1} \text{ hr}^{-1}$ occurring in the dark at a SD of 28 mb (Experiment A-12) was only one-fourth as much as that in the light in Experiment A-11.

In both experiments, if the change in evaporative demand had occurred in the light, transpiration might have been greater in Experiment A-12 by the ratio of the SD values; i. e.,

$$\frac{A-12}{A-11} = \frac{28}{22} \text{ or } 1.27 .$$

Instead, it was only one-fourth as much. On a leaf-area basis, transpiration was 0.22 as great in Experiment A-12 as in A-11. This comparison clearly indicates the pronounced effect of stomatal aperture on transpiration rate. As shown in Figure 2, in Experiment A-12 water absorption somewhat exceeded transpiration before time zero, but was less than transpiration when the SD was raised from 10 to 28 mb. This internal water deficit developed after a lag of one period, due to the delay in acceleration of transpiration mentioned above. The lowering of the SD to 9 mb (120 minutes after time zero) brought about equality in transpiration and absorption (the last five points representing data obtained after the lowering of the SD). Thus the responses were similar to those in Experiment A-11, but of smaller amplitude. The cumulative data in Figure 3 show only a very mild dehydration due to the increased SD in Experiment A-12, whereas the data from the beta ray gauge demonstrate a more severe and longer lasting dehydration (Figure 4). However, these two sets of data agree to the extent of showing an initial water balance, followed by a plant water deficit, which eventually was made up. As mentioned above, in Experiment A-11 the effect of light added to that of increased SD brought about not only greater dehydration, but also

a somewhat greater "superhydration" at the end of the experiment than did an increased SD alone.

3. Effect of magnitude of a suddenly increased saturation deficit, occurring in light, on internal water balance. Transpiration accelerated rapidly in both Experiments A-11 and A-13 (Figure 5), reaching a peak value, and then decreasing somewhat. As might be expected, transpiration was much more rapid at a SD of 45 mb than at 22 mb. On a leaf-area basis, the increased transpiration was almost directly proportional to the increase in SD. In both experiments transpiration rapidly fell to the initial rate when the lights went off and the SD was lowered to 9 mb. In both experiments the sudden increase in SD in the presence of light brought about excess transpiration over water absorption during the first period following the change, but excess absorption over transpiration in the second period (Figure 6). In succeeding periods of light the two processes were in balance in both experiments. With a return to the initial SD in the dark, water absorption exceeded transpiration by quite a bit for the first period, and then only slightly, in both Experiments A-11 and A-13. Both experiments also show quite similar responses for the cumulative water balance (Figure 7). A positive water balance was changed to a negative one during the time of the increased SD in the light, and back to a positive balance when the SD was lowered in the dark. Experiment A-13 was noteworthy for the extent to which "superhydration" occurred, i.e., the plants being considerably better hydrated at the end of the experiment than at the beginning. To a lesser extent this phenomenon occurred in Experiment A-11. The beta ray gauge data of Figure 8 confirm the cumulative data from direct measurements in all essentials. The plants of both experiments began in a well-hydrated condition, became partially dehydrated upon sudden exposure to a high evaporative demand in the light, partially overcame this negative water balance even in the light at a high SD, then made up the water deficit, and even "superhydrated" when the SD was lowered to the initial value in the dark.

4. Low-temperature preconditioning effects on the response to an increased SD. In four experiments described in Section 2 of this report the initial dry-bulb temperature was 21C; however, in Experiment 14, equilibrium conditions were: dry-bulb 12C, vapor pressure held at 9 ± 1 mb instead of the constant 17-mb characteristic of the other four experiments described in Section 2. Thus, Experiments A-11 and A-14 are closely comparable in the increase in evaporative demand, but are different primarily in the equilibrium temperature conditions. The major difference in response is in the pronounced lag in transpiration rise occurring in Experiment A-14, as compared to Experiment A-11 (Figure 5). In Experiment A-11 transpiration showed the normal rapid acceleration in response to light and an increased evaporative demand, rising fivefold, while the SD approximately doubled in the first 30 minutes. In contrast, in Experiment A-14 transpiration was more nearly proportional to the SD, both transpiration and the SD approximately doubling in the same period. The fast rise in transpiration was postponed for one whole period in A-14. By the early part of the second period after time zero, the ultimate value of SD had already been attained (25 mb), but transpiration continued to rise. After reaching a peak, it fell in the next period, due probably to temporary wilting, and then rose slightly. The peak transpiration rate in Experiment A-14 was only one-half that in Experiment A-11, even though the values of SD were essentially the same in both experiments (25 and 22 mb, respectively). This was true both on a plant and leaf-area basis. It may be that a lag in the rate of leaf-temperature rise for the plant equilibrated at 12C was responsible for the slow acceleration of transpiration. If so, the saturation vapor pressure of the water inside the leaf would be lower than anticipated, and hence would result in a lower effective SD, which in turn would result in lower transpiration. However, the thinness of leaves makes any significant lag in temperature equilibration doubtful. Conceivably, persistence of a lag would be enhanced by the direct effect of the cold water entering the roots and translocating to the shoots; this water, initially at 12C, definitely did not heat up rapidly, rising from

12C to 18C in 30 minutes. Whatever the cause, the effect of the delayed rise in transpiration can be seen in Figure 6, where the plant of Experiment A-14 had a negative water balance in the second period after time zero, rather than the first, as in Experiment A-11. Both experiments were similar in the response following the water deficit, in that absorption equaled or was greater than transpiration. The cumulative effect (Figure 7) was anomalous for Experiment A-14, since the points lie above rather than on the base line at the beginning of the experiment. Thus, subtracting the amount of water lost during the single period showing negative water balance from the preceding cumulative data results in only a slight dip below the reference line for one period. If the data points had been on the reference line before time zero, which is a more normal alignment (showing a balance between transpiration and water absorption), the single sharp drop in absorption minus transpiration (shown in Figure 6) would have resulted in a more noticeable decrease in the cumulative water balance (in Figure 7), as is true of the data from the beta ray gauge (in Figure 8). It is likely that the direct-measurement data are less reliable here than the data from the beta ray gauge, since the very low gains and losses of water characteristic even of large plants at low SD in the dark make direct measurements subject to a larger-than-normal proportional error. After the re-establishment of a low SD in the dark in Experiment A-14, considerable "superhydration" occurred, as shown by direct measurements, but not confirmed by beta ray gauge readings, which show only that the plant was as well hydrated at the end of the experiment as at the start.

Indirect determination of water balance by means of two beta ray gauges.

A. A higher saturation deficit generated by an increased dry-bulb temperature.

1. Increased saturation deficit occurring before illumination.

To be sure that the standard equilibrating conditions (16 hours in the dark at a low SD with the plant roots in aerated nutrient solution) resulted in a well-hydrated plant, attempts were made to enhance hydration by use of humidity chambers around the plant during the

equilibration period. Both short and long exposures of the plant to a chamber at or near 100-percent relative humidity had only a small and momentary effect on plant turgidity, as evidenced by leaf thickness determined from beta ray gauges near the top and base of the plant. Therefore, in succeeding experiments it was assumed that "standard" equilibration conditions with the SD preferably 12 mb or less would bring about conditions conducive to well-hydrated plants in repeated experiments.

In Experiment B-5 the initial and final conditions were: darkness, dry-bulb 25C, SD 10 mb; the intervening conditions were: dry-bulb 35C, SD 40 mb, first in the dark and later in the light. Figure 9 shows the time course of leaf thickness for two leaves of a cotton plant. In the time rectangles at the bottom of the graph the clear area represents an illumination period, while the cross-hatched areas represent dark periods; the saturation deficit (SD) is indicated in each rectangle. The initial equivalent thickness for the upper leaf, 21.75 mg cm^{-2} , represents a well-hydrated leaf, which, in turn, is representative of the whole plant. During the first part of the experiment there was no essential change in leaf thickness — either upper or lower — which indicates a balance between transpiration and water absorption. At 0845 the SD was increased from 10 to 40 mb, the whole change necessitating about 30 minutes. The negative water balance of the plant as a whole in response to the greater acceleration of transpiration than absorption resulted in a downward trend in leaf thickness soon after 0845. Shortly thereafter the plant began to recover, as shown by the regaining of leaf thickness. The upper leaf went through minor fluctuations during the remainder of the time at the 40-mb SD, but had regained turgidity by the time the lights came on at 1030. Then stomatal opening led to a greater loss than gain of water by the plant, which resulted in the second period of turgor loss, with the minimum leaf thickness 15 minutes after the lights came on. In this experiment, visible wilting of the plant corresponded with the times of minimum leaf thickness, the plant repeatedly wilting and recovering in phase with the fluctuations of leaf thickness shown

in Figure 9. The cycle length was one-half hour. The total decrease in leaf thickness was not very great, 0.35 mg cm^{-2} , but this amount of loss represented the difference between a turgid and a wilted plant. Turning off the lights was very effective in rapidly depressing transpiration. This, in turn, led to a fast recovery of the plant. In fact, there was a slight indication of excess hydration, which became more definite when the SD was returned to 10 mb. The "superhydration" (gain in leaf thickness over the initial well-hydrated value) amounted to 0.20 mg cm^{-2} in the upper leaf. The lower leaf went through approximately the same fluctuations and responses as the upper, but lost more water, 0.63 mg cm^{-2} , upon dehydration. It too was somewhat better hydrated at the end of the experiment than the beginning. It is significant that the peaks and troughs of the leaf-thickness curves coincided for upper and lower leaves, indicating unity of the bulk water within the plant.

2. Increased saturation deficit occurring along with sudden illumination. In Experiment B-3 the temperature range and humidity conditions were the same as those for B-5 during the bulk of the experiment, but not at the very beginning, where an attempt was made to get even better initial hydration than the "standard" procedure gave. With the Climate Chamber maintained at 25C, and a SD of 10 mb, the plant, which had been overnight under these conditions, was placed in a box with relative humidity at or near 100 percent. Figure 10 shows a slight loss of leaf thickness due to removal of the plant from the high humidity chamber and exposure to 10-mb SD in the dark. Then the leaf-thickness values (upper leaf) were steady at 17.1 mg cm^{-2} , instead of 17.25 mg cm^{-2} characteristic of the humidity chamber. The base line drawn at 17.25 could have been drawn just as appropriately at 17.10 mg cm^{-2} . Both leaves showed the slight lessening in thickness due to removal from a very low SD and exposure to the higher SD of 10 mb. When the values became stable at 10 mb, the lights were turned on at the same time as the SD was raised to 40 mb (dry-bulb going from 25 to 35C). The extreme decrease in leaf thickness in both

leaves is to be contrasted with the much milder dehydration occurring in Experiment B-5.

An increased SD coincident with sudden illumination was much more effective than the same increase in SD in darkness, followed by sudden illumination. However, the time to attain the greater dehydration was about the same - 15 minutes. Considerable recovery occurred in both leaves even in the light under the high evaporative demands. Turning off the lights had a rapid but slight effect in increasing leaf thickness in the upper leaf, and somewhat more effect in the lower leaf. Full rehydration was not attained, however, until the SD was lowered to 10 mb in the dark. At this point both leaves had achieved the same thickness as their initial well-hydrated value, but showed no evidence of "superhydration."

It seemed of great importance to understand the significantly different response of the cotton plant to increased evaporative demand, depending on the presence or absence of light during the change in SD. Therefore, in order to exclude the possibility that the direct effect of increased air temperature in some manner might be responsible for the cycling in leaf thickness, rather than the increased SD per se, it was decided to maintain a constant dry-bulb temperature, and raise the SD by lowering the vapor pressure.

B. Isothermal experiments in which higher values of saturation deficit were generated by a lowered vapor pressure.

1. Increased saturation deficit occurring before illumination.

In Experiment B-7 air temperature was maintained at 30C continuously. The initial and final values of SD were 12 mb; the intervening SD was 30 mb, generated by lowering the vapor pressure, the change occurring in the dark. Both upper and lower leaves began the experiment in a hydrated condition, as indicated by the very small fluctuations in the curves for leaf thickness (Figure 11). The increase in SD from 12 mb to 30 mb began at 1005, and was completed in 30 minutes, as in other experiments. Both leaves responded promptly to the increased evaporative demand by decreasing in thickness. They reached the point of greatest dehydration in about 20 minutes, and then made a partial

recovery. Later, when fairly steady values were being recorded, the lights were turned on. This again dehydrated the leaves to about the same extent as before, and in about the same time. Partial recovery occurred again in each leaf, but the stable level attained still represented a dehydration, in comparison to the initial value, of about 0.5 mg cm^{-2} and 0.35 mg cm^{-2} for the upper and lower leaf, respectively. No visible wilting could be detected at this time, however. When the lights were turned off, both leaves immediately started to regain thickness and in 20 minutes leveled off at a thickness somewhat less than the starting value. When the SD was returned to 12 mb, a slight additional hydration occurred, which brought the thickness essentially back to that characteristic of the well-hydrated plant. There is some indication of a cycling in leaf thickness, but it is not as clear as before in the analogous experiment. It is pertinent to point out that continuous analyses of carbon dioxide in the Climate Chamber were made with an infrared analyzer and recorded on a strip chart. These data show that CO_2 was at or above 300 ppm in the room at all times during the experiment. This would seem to rule out a periodic deficiency of CO_2 as the cause of periodic opening of stomates in the dark. Nevertheless, the CO_2 measured was the content of the bulk air — not that within the leaves. At present the relationship of CO_2 supply to the measured fluctuations in leaf thickness is obscure.

Preliminary results in measuring stomatal aperture on a sister plant to that with the gauges are extremely interesting (WCL-34A). These stomatal impressions of the upper leaf demonstrated a definite opening of stomates in the dark engendered by the suddenly lowered vapor pressure. In other respects the stomates acted predictably, being closed in the dark at a low SD, open in the light, and closed again at the end of the experiment (in the dark at a low SD).

2. Increased saturation deficit occurring along with sudden illumination. In Experiment B-6, again carried out at a constant air temperature of 30C, the SD was increased from 12 to 30 mb, and later returned to 12 mb. Occurrence of sudden illumination at the same time

the SD was increased brought about a greater dehydration of both leaves, especially the lower, than when an equal increase in SD occurred in the dark. Consequently, the time to reach maximum dehydration was longer when the dehydration took place in the light than in the dark. In contrast to the previous experiments, the upper and lower leaves in this last experiment were not quite in phase for the time of maximum dehydration (minimum leaf thickness), the lower leaf being delayed. The two leaves recovered from dehydration at the same rate, however. Considering the extent of dehydration, the degree of recovery of both leaves while the plant still was in the light exposed to 30-mb SD is significant. One hour after having reached its least thickness, the upper leaf regained its original thickness value. Turning off the lights caused a moderate "superhydration" which was not enhanced by lowering the SD to 12 mb. Fifty minutes after the lower leaf had reached its least thickness, it too had recovered, but not completely. It did not regain its original thickness until the lights were turned off. As with the upper leaf, lowering the SD to 12 mb in the dark brought about no enhancement of leaf hydration over that which was due to darkness alone.

In this experiment stomatal aperture measurements determined on both leaves showed the stomates to be closed in the dark and open in the light, with a very short response time, less than 5 minutes for a change from closed to fully open stomates.

SUMMARY AND CONCLUSIONS:

The internal water balance of cotton plants was altered by manipulation of evaporative demand under controlled conditions. Direct and indirect measurements showed the development of a temporary internal water deficit as transpiration accelerated faster than water absorption, in response to a rapid increase in the saturation deficit (SD). Transpiration was accelerated rapidly in two ways: (1) by imposition of sudden full-intensity illumination at a series of predetermined values of SD, and (2) by a rapid increase in the SD after the plants had been equilibrated in the dark at a low SD. In the latter method an increased SD was generated either by raising

dry- and wet-bulb temperatures, keeping the vapor pressure constant, or by lowering the vapor pressure, keeping temperature constant. The rapid increase in SD took place either in the presence or absence of full-intensity illumination.

It is significant that even in the dark, where stomatal aperture presumably is minimal, the response in transpiration to a rapidly increased evaporative demand was sufficiently more rapid than absorption to induce temporary plant dehydration. However, in the light a given increase in SD was much more effective in dehydrating a plant than in the dark, because of the difference in stomatal aperture. The magnitude of transpiration rate was closely correlated with the SD, but a moderately high evaporative demand was about as effective as a very high value in causing partial plant dehydration. Low temperature during the preconditioning period (darkness at a low SD) brought about a definite delay in the acceleration of transpiration rate. As a consequence, with the SD raised to a given value, turgor loss was not so severe after low temperature preconditioning as it was when normal temperature prevailed during preconditioning. The cause of this phenomenon may be a slower warming of the leaf and a consequent lesser effective SD than indicated by ambient conditions.

Usually, turning off the lights was sufficient to bring about recovery from a negative water balance, due to the effective suppression of stomatal transpiration. However, an early experiment gave evidence of enhanced recovery by a lowering of the SD to the initial value, in addition to turning off the lights. This enhancement is interpreted as a lowering of cuticular transpiration. Later experiments ended with provision of a low SD and darkness as a standard procedure.

That the isothermal method gave the same results as the constant vapor-pressure method of creating a higher SD indicates the negative water balance is due to the difference in relative rates of transpiration and water absorption, uncomplicated by some sort of direct effect of temperature rise occurring in the latter method.

Although a loss in turgidity could be induced quickly by increasing the evaporative demand, the plants partially recovered in the light and under the increased SD that had caused the internal water deficit. Two factors contributing to the regaining of turgor were (1) a reduction in transpiration due to partial stomatal closure, and (2) an increased water absorption rate, presumably due to a higher diffusion pressure deficit in the partially wilted leaves, which steepened the gradient in DPD from root to leaves.

The direct measurement of transpiration and absorption was confirmed and amplified by indirect measurements with two beta ray gauges, one near the tip, and one near the base of the plant. The principle underlying their use is a decrease in leaf thickness when transpiration exceeds absorption, and an increase when absorption is greater than loss of water. The two gauges responded at the same time to changes in evaporative demand, demonstrating the unity of the water system in plants. When the SD was increased from threefold to fivefold in the dark, plant turgidity decreased slightly, reaching a low point in about 15 minutes, but then increased in a somewhat longer period, under unchanged ambient conditions. Significantly, there was a considerable degree of stomatal opening in the dark in response to the suddenly increased evaporative demand, as evidenced by silastic rubber stomatal impressions. The stomatal measurements also showed closure in the dark previous to the increased evaporative demand, a partial closure after the opening and a wide opening in the light (see WCL-34A). When the lights came on, loss of turgidity occurred again, which coincided with visible wilting symptoms. This in turn was followed by recovery of turgidity and disappearance of wilting symptoms. A definite cycling in wilting and recovery occurred with a frequency of one-half hour.

The actual change in equivalent leaf thickness between peaks and troughs was small, 0.30 mg cm^{-2} in the upper leaf (0.50 mg cm^{-2} in the lower), but was sufficient to bring about wilting or recovery. After several cycles the lights were turned off, whereupon total

recovery of hydration was followed by a small amount of "superhydration." This chain of events occurred, regardless of whether the SD was increased by raising the temperature or lowering the vapor pressure.

In contrast to the rather small amount of dehydration associated with increased evaporative demand occurring in darkness, followed later by illumination, loss of turgidity was considerable when the lights came on simultaneously with the increased evaporative demand. This loss was about 1 mg cm^{-2} for the upper leaf, and 4 mg cm^{-2} for the lower leaf. As before, a considerable degree of recovery in turgidity occurred before the lights were turned off. Complete recovery depended on turning off the lights, however. The tendency for superhydration was not so pronounced as in the previous example.

Both direct and indirect measurements are in agreement in demonstrating the excess of loss over gain of water by plants exposed to a sudden increase in evaporative demand. With these methods, water balance can be followed over very short intervals, permitting precise characterization of the loss of turgor as well as the subsequent recovery of turgor as affected by light and saturation deficit.

PART II. IMPROVEMENTS IN THE PERFORMANCE OF THE CLIMATE CHAMBER

INTRODUCTION:

The investigation of water balance as affected by evaporative demand depends primarily on the adequacy of environmental control. Therefore, efforts were made to bring about even better performance of the Climate Chamber than before by the following improvements.

PROCEDURE:

Installation of new equipment. On 18 July two Leeds & Northrup Speedomax recorder-controllers were installed in the wall of room 143, facing the hall, using the thermohms already in use for recording dry- and wet-bulb temperatures. The new control system, substituted for the old Minneapolis-Honeywell mechanical controller, consists of two sets each of a current-adjusting type controller, a Speedomax recorder, and an electro-pneumatic converter. The same L & N dry- and wet-bulb thermohms as used previously each lead to one unit of the above control system. The dry- and wet-bulb sensors were moved from their former position in the return-air duct above and just behind the refrigeration coil back-pressure valve to a ledge immediately behind return-air register 4 in the Climate Chamber (room 145). In response to the dry- and wet-bulb thermohms, current from the controller determines the operating air pressure on steam valves through the converter. As before, two steam valves supply heat in response to the dry-bulb sensor, and one valve supplies live steam in response to the humidity sensor. Different springs were installed in all three valves to change the operating range from 7 to 12 psi to a more sensitive range of 5 to 11 psi. In an attempt to facilitate attainment of a controlled low temperature, insulation was applied to the bottom part of the air duct leading from the air handler to the intake registers of the Climate Chamber. After the new equipment had been tested adequately, a dew probe (Minneapolis-Honeywell SSP129A) was substituted for the wet bulb. This change avoids certain problems such as the need for a well-regulated constant supply of pure water, the possible complications of dirt

and other foreign material on the wet-bulb jacket, or frequent changes of jackets needed for optimum wet-bulb operation.

Checking-out procedures. In order to achieve better control than the $\pm 0.5\text{C}$ deviations from the set point, which were obtained in preliminary trials, attention was focused on the heating and cooling sources. Previous attempts to control pulsations in steam pressure originating at the boiler had been made by installation of a pressure-control device. Since the device did not work satisfactorily, it was decided to remove it, and to use only the 0.5-inch steam valve for heating, which helps eliminate much of the pressure variation. Temperature control in the Climate Chamber arises from the bucking of a given amount of refrigerating capacity against a variable amount of steam heat, the heating being proportional in response to deviations from the set point. Refrigerating capacity is not proportional -- being either on or off. However, some flexibility could be achieved if there were various fixed levels of refrigeration, as represented by refrigerant pressure within the coils. It was found that proper setting of the back-pressure regulators did result in a good control of refrigerant pressure and temperature. Regulation of the refrigerant temperature at the proper value thus permits just enough counteractive steam heat to have the controlling air pressure at the steam valve at 8 psi, the optimum pressure for good control. Although the back pressure can be regulated only within certain limits, a considerable range is feasible, especially at high temperatures. For example, good control was achieved at a dry-bulb temperature of 45C with the back pressure on coil 1 set as high as 80 psi, corresponding to a refrigerant temperature of 80F . The lower limit for back pressure seems to be 30 psi (31F). Lower pressures at the coil and therefore, lower coil temperatures can be obtained by opening the bypass; however, under such conditions there is no control. Another alternative for operating at low temperatures that would maintain control is to open both coils 1 and 2, with the back pressure set at the lowest possible limit in each coil.

The appropriate setting of the controller adjustments appears to be the same for all temperatures, whether dry bulb or dew probe. A proportional band of 5 percent seems appropriate for the dry-bulb control and of 10 percent for the dew probe control. In both instances, satisfactory results were obtained with a rate time of 0.1 and a reset of 0.2. A general principle is that if the rate time becomes excessive, oscillations of about four per 10 minutes will appear. If reset is excessive, the oscillations will be about two per 10 minutes. If proportional band is too narrow, oscillations will appear of about one per 10 minutes.

RESULTS:

Control limits and precision. An attempt was made to evaluate the lower limit of temperature, both under control and without control. Before the insulation was installed on the underside of the air duct, the lowest temperature achieved was 7.5C. Afterwards, the result of another attempt using the same settings was the same final temperature. In both instances coils #1 and #2 were open to bypass, but the low-temperature limit switch was set not to let the air temperature behind the coils drop below 1C in order to prevent freezing. Another change which had been made to facilitate obtaining of a low temperature was the reduction in speed of the air handler for the room. This lowered the heat input of the air-handler motor from about 5.5 kw to 3.6 kw. These efforts did not succeed in achieving a lower temperature. The lowest controlled temperature attainable was 10C.

The table lists the temperatures investigated for limits and precision of control, giving the vapor pressure and the saturation deficit for a wide range of conditions. Although 10C is the lowest controlled temperature, the upper limit of control (45C) is high enough to allow a tremendous evaporative demand to be developed.

SUMMARY AND CONCLUSIONS:

Precision of control was improved in the Climate Chamber by substitution of electro-pneumatic controllers for the mechanical-pneumatic type used formerly. Two Leeds and Northrup Speedomax recorder-controllers were installed, which operate through electro-pneumatic converters to determine the controlling air pressure on

steam valves for heating and humidifying. As before, Leeds and Northrup thermohms are used as temperatures and humidity sensors, but their location has been changed to the upper return-air duct in the Climate Chamber. Also, a dew probe has been substituted for a wet bulb to monitor vapor pressure. Another change was in the spring tension in the steam valves; the more sensitive range from 5 to 11 psi replacing the former range of 7 to 12 psi. The duct work under the air handler was insulated, and the speed of the air-handler motor was decreased from an equivalent of 5.5 to 3.6 kw, in an attempt to achieve lower temperature limits than before.

Careful checking-out procedures and testing established the optimum settings to use for precise control. These included a limitation on use of steam to a 1/2-inch valve over a wide range of temperatures, the regulation of refrigeration by control of the refrigerant back pressure, and appropriate setting of controller adjustments, including the proportional band, the rate time, and the reset.

These improvements made possible the attainment of precise temperature and humidity control from 10C to 45C. The low temperature limit was 7.5C, the same low limit as before the changes. Precision of the dry-bulb control was $\pm 0.2C$, and of humidity control, ± 2 mb at the greatest deviation. The increased refinement in control facilitates the creation of a specific evaporative demand, and thereby promotes the investigation of water balance under a controlled environment. Present controls also permit automatic programming of environment variables.

PART III. MEASUREMENT OF THE DIFFUSION PRESSURE DEFICIT OF PLANT MATERIAL BY THE SHARDAKOV METHOD

INTRODUCTION:

The results obtained by direct measurement of transpiration and water absorption demonstrated the rapidity with which cotton plants can recover from a temporary wilt even in the presence of light and the continued high SD that first induced wilting. As shown by the transpiration curves of Figures 1 and 5, part of the recovery is due to a sharply diminished transpiration rate, undoubtedly brought about by a reduced stomatal aperture. The direct measurement of water absorption showed it to be increased just after wilting, which would be another factor promoting rapid recovery from wilting. However, the rate of water absorption usually is determined by the rate of transpiration. Therefore, to have the absorption rate increase while the transpiration rate simultaneously decreases, presupposes another mechanism for the noted greater increase in water absorption. An increased DPD in the leaves would explain this phenomenon. When leaves wilt, the DPD increases; thus the gradient from roots to shoot is steepened, and the rate of water absorption correspondingly increased. Direct determination of the DPD would permit verification of the hypothesis. For this purpose relative turgidity was measured in leaves in several previous experiments. Although relative turgidity has been related to DPD by direct calibration, the relationship between the two determinations probably is not constant in different sets of plants; hence, relative turgidity has not proved to be useful in the above problem. A direct measurement of DPD in each experiment would be desirable. Therefore, a relatively new method for direct measurement of DPD has been tested — the Shardakov method (2).

PROCEDURE:

Description of method. The Shardakov or Russian dye method — more appropriately, the sucrose specific gravity method — is based on a difference in specific gravity between two sucrose solutions, initially at the same osmotic pressure (OP), one of which, the control, has been unaltered except for the addition of a minute

amount of powdered dye, and the other, the test solution, which has been used to extract a bit of plant tissue. Three alternatives result from extraction: (1) the sucrose solution loses water because it is hypotonic with respect to the DPD of the plant tissue; (2) the solution gains water because it is hypertonic with respect to the DPD of the tissue; or (3) no net exchange of water occurs due to an identity of DPD of the tissue and OP of the sucrose solution. A difference in specific gravity is detected by observing the direction of movement of a droplet of the colored control solution carefully pipetted into the colorless test solution (after removal of the extracted plant material). The first alternative would cause the droplet to rise because the loss of water by the solution increased its specific gravity in relation to that of the control solution.

Alternative No. 2 would cause the droplet to fall, whereas in alternative No. 3 the droplet would not move up or down, but rather diffuse outwards. In this third case, the DPD of the plant material would equal that of the sucrose solution showing no drop movement. In the two other alternatives, the DPD of the plant material is assumed to lie between the OP values represented by sucrose solutions in which the drop rises and falls. Use of a series of solutions permits bracketing the unknown DPD.

Accuracy check. Tests of the specific gravity method were made, and it then was used with field alfalfa and cotton plants in the field and greenhouse. A preliminary semi-quantitative accuracy check was run. Two similar cotton leaves were brought to 100-percent relative turgidity by the standard procedure (floating on water under weak light). Then one leaf was brought to a quasi-equilibrium over a saturated CaSO_4 solution in a room at $25 \pm 1\text{C}$. The 98-percent relative humidity partially dehydrated the leaf and in four days its weight had stabilized. The Shardakov test for DPD of this leaf indicated >27.3 atm, compared to <0.5 atm for that at 100 percent relative turgidity. Two repetitions of the test taking from 2 to 8 days and using saturated CaSO_4 gave a DPD of 27.3 - 30 atm, in good agreement with the calculated equilibrium value. Likewise,

the other value, <0.5 atm is suitably low for a leaf at maximum turgidity. Later tests, however, made use of a series of sugar solutions having 3 atm as the lowest OP level, for reasons given by Kramer (1) recently.

Sampling procedure. No difference in DPD was obtained by varying the volume of extracting solution from 2 to 4 ml. Three milliliters was chosen as a convenient volume. Extraction times of 1/2, 1, 2, and 3 hours with 3 ml of sucrose showed no differences in DPD value. One hour was selected as the routine time. At first, leaf disks with an area of 4.71 cm^2 were used; later those with an area of 2.83 cm^2 were decided on, since that size adapted better to the vials used in extraction. One disk taken from each of six different leaves comprised a unit sample weighing from 0.2 to 0.5 g. Five locations on a single leaf gave a total of five 6-disk samples. Thus, there could be five OP values to bracket the unknown DPD. The sampling location was the tip of each of the five lobes, astride the vein. Occasionally two more disks were taken for the correlation of relative turgidity with DPD values.

Adaptation of the specific gravity method for DPD to OP determination.

One of two series of 6-disk samples taken from 12 cotton leaves on the same plant was tested for DPD directly, giving a value of 5 to 7 atm. The other series was frozen over dry ice, thawed, and then tested for DPD in the standard manner. Its DPD of 10 to 12 atm shows that the cell solutes diffusing out through the killed cell membranes contributed to a higher value than before. This value can be considered the OP of the cell. At any time other than during complete wilting (zero turgor pressure), the OP will be greater than the DPD. Therefore, the experimental value obtained was qualitatively correct. However, there is a possibility that upon freezing, the solutes that diffuse out of the cell and mix with the sucrose might have the same total osmotic pressure as the extracting sucrose solution, but a different specific gravity. This could cause the test drop to move up or down when it actually should not have moved. Calculations show that at an OP of 11.1 atm (at 25C) the specific gravity of sucrose is 1.0507,

whereas that of several salts is as follows: CaCl_2 , 1.0148; NaCl , 1.0092; Na_2SO_4 , 1.0234; MgCl < 1.0146; and MgSO_4 , 1.0390.

Since leaf tissue contains the above inorganic solutes, determination of OP by killing the cell membrane would be complicated according to the above considerations. Therefore, use of the Shardakov method for OP determination was abandoned.

RESULTS:

Diurnal course of DPD in cotton plants. On eight occasions the DPD of cotton in the field was measured throughout the day in an attempt to establish a diurnal rhythm. In general, the field was watered frequently enough that DPD did not build up to very high values, even under the extremely high evaporative demand characteristic of midsummer in central Arizona. An example of one test follows:

<u>Time</u>	<u>Plant Symptoms</u>	<u>DPD (atm)</u>	<u>Relative turgidity (percent)</u>
0600	turgid	5	83.9
0830	turgid	8	74.6
1100	s1 wilted	< 10	67.9
1330	s1 wilted	15 - 17	67.4
1610	s1 wilted	8 - 12	74.1
1800	some recovery	8 - 10	81.0

The test occurred 3 October 1963, 18 days after irrigation when the soil water content in the zone ranging from 10 cm to 140 cm below the surface was 28 percent by volume (field capacity, 31 percent by volume). Both relative turgidity and DPD demonstrated the negative water balance developed in the cotton leaves during midday, as contrasted with the turgid conditions at dawn and near dusk.

SUMMARY AND CONCLUSIONS:

With sufficient allowance given to plant variability and the consequent difficult sampling problem, the Shardakov method is adequate to give a direct, fast determination of DPD, both in the field and laboratory. It is planned to utilize the method to measure the DPD at both the equilibrium period before wilting and at peak wilting of cotton plants in a controlled environment.

REFERENCES:

(1) Kramer, P. J.

Measurement of the diffusion pressure deficit of plant material by the Shardakov method.

(mimeographed).

(2) Shardakov, V. S.

1957. The water regime and timing of irrigation in cotton.

From the collection: The Biological Bases of Irrigated Agriculture, Moscow.

PERSONNEL: W. Ehrlner, C. H. M. van Bavel, F. S. Nakayama

Table 1. Temperature control limits and precision of control in the Climate Chamber.

Point	Dry-bulb temperature	Lowest vapor pressure	Saturation deficit	Lowest controlled vapor pressure	Saturation deficit	Highest controlled vapor pressure	Saturation deficit
	← centigrade →	← millibars →		← millibars →		← millibars →	
Set	10.0						
Pen	9.8 ± 0.2	7.0 ± 0.2	5.1 ± 0.2	8.6 ± 0.3	3.5 ± 0.3	10.9 ± 0.6	1.2 ± 0.6
Set	20.0						
Pen	20.0 ± 0.3	4.2 ± 0	19.2 ± 0	7.9 ± 0.1	15.5 ± 0.1	18.0 ± 0.3	5.4 ± 0.3
Set	30.0						
Pen	30.0 ± 0.2	15.1 ± 0.8	27.3 ± 0.8	16.5 ± 0	25.9 ± 0	23.7 ± 0.5	18.7 ± 0.5
Set	35.0						
Pen	34.8 ± 0.2	18.9 ± 0.6	36.7 ± 0.6	22.2 ± 0.2	33.4 ± 0.2	36.8 ± 1.0	18.8 ± 1.0
Set	40.0						
Pen	39.8 ± 0.2	36.6 ± 0.4	36.4 ± 0.4	25.7 ± 0.6	47.3 ± 0.6	40.8 ± 2.3	32.2 ± 2.3
Set	45.0						
Pen	45.0 ± 0.2	22.1 ± 0.2	73.8 ± 0.2	24.7 ± 0.3	71.2 ± 0.3	54.9 ± 0.2	41.0 ± 0.2

29-27

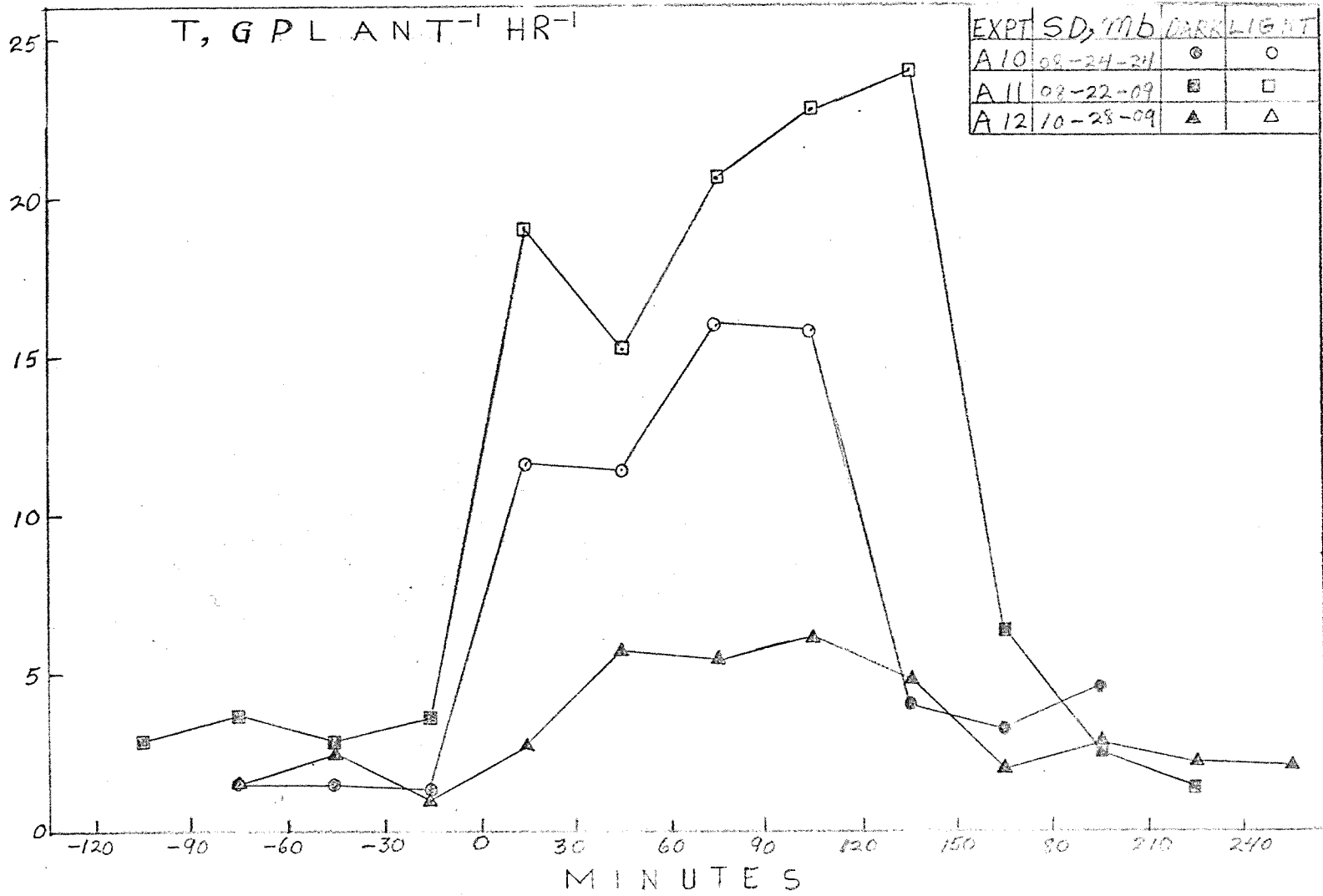


Figure 1. Transpiration as affected by light and a change in saturation deficit.

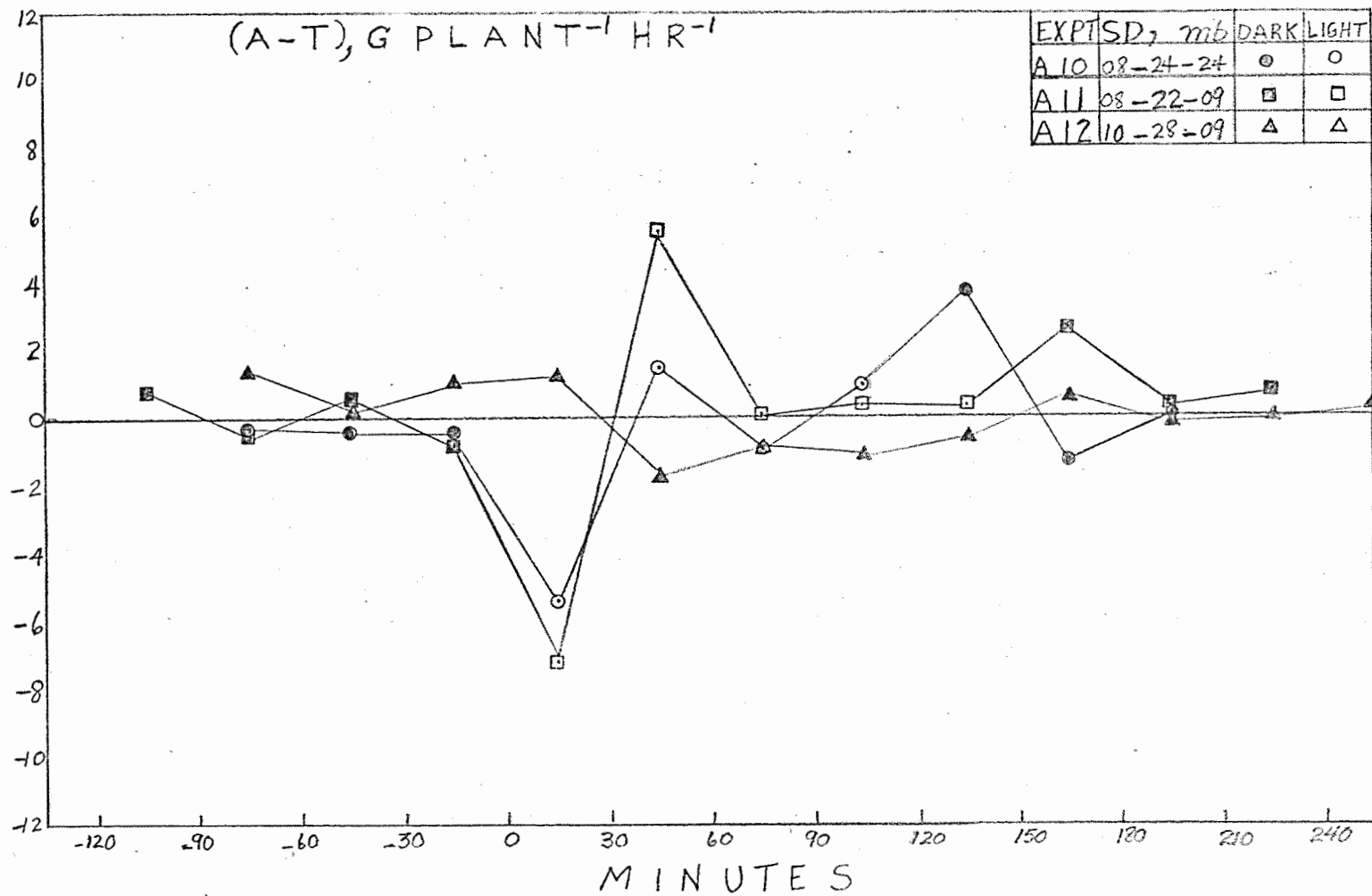


Figure 2. The difference between water absorption and transpiration as affected by light and a change in saturation deficit.

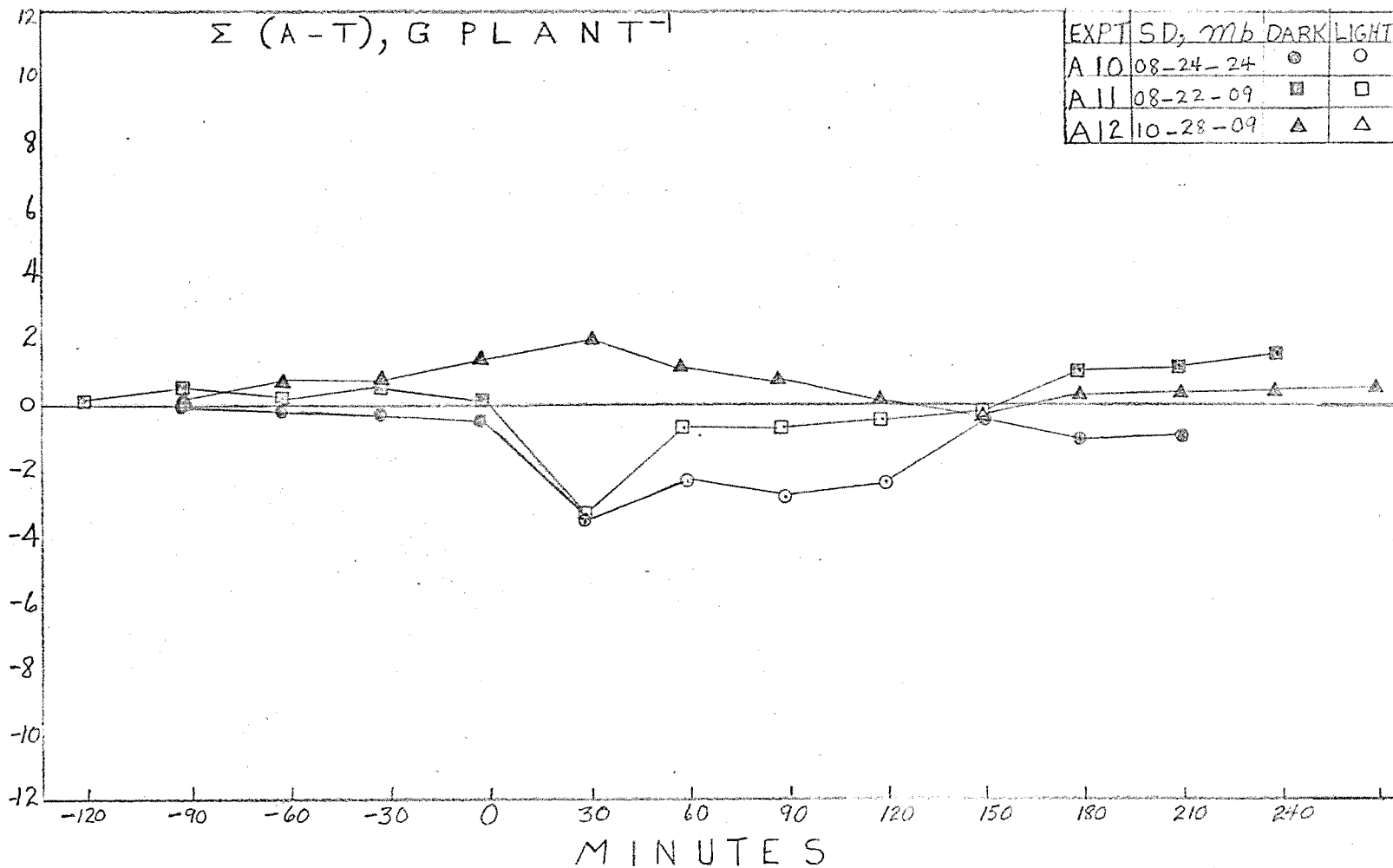


Figure 3. Cumulative water balance as affected by light and a change in saturation deficit.

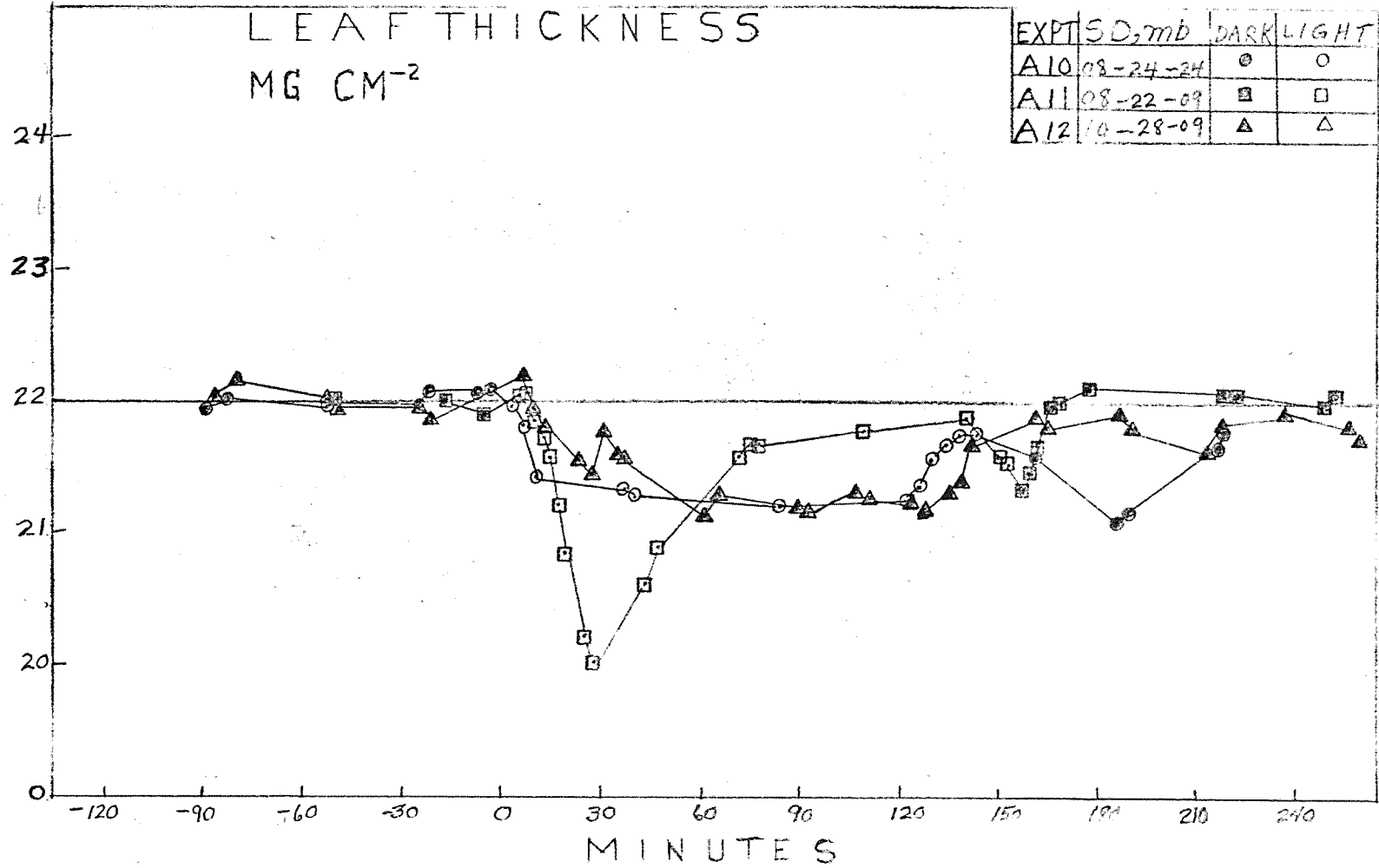


Figure 4. Time course of leaf thickness as determined by beta ray gauging.

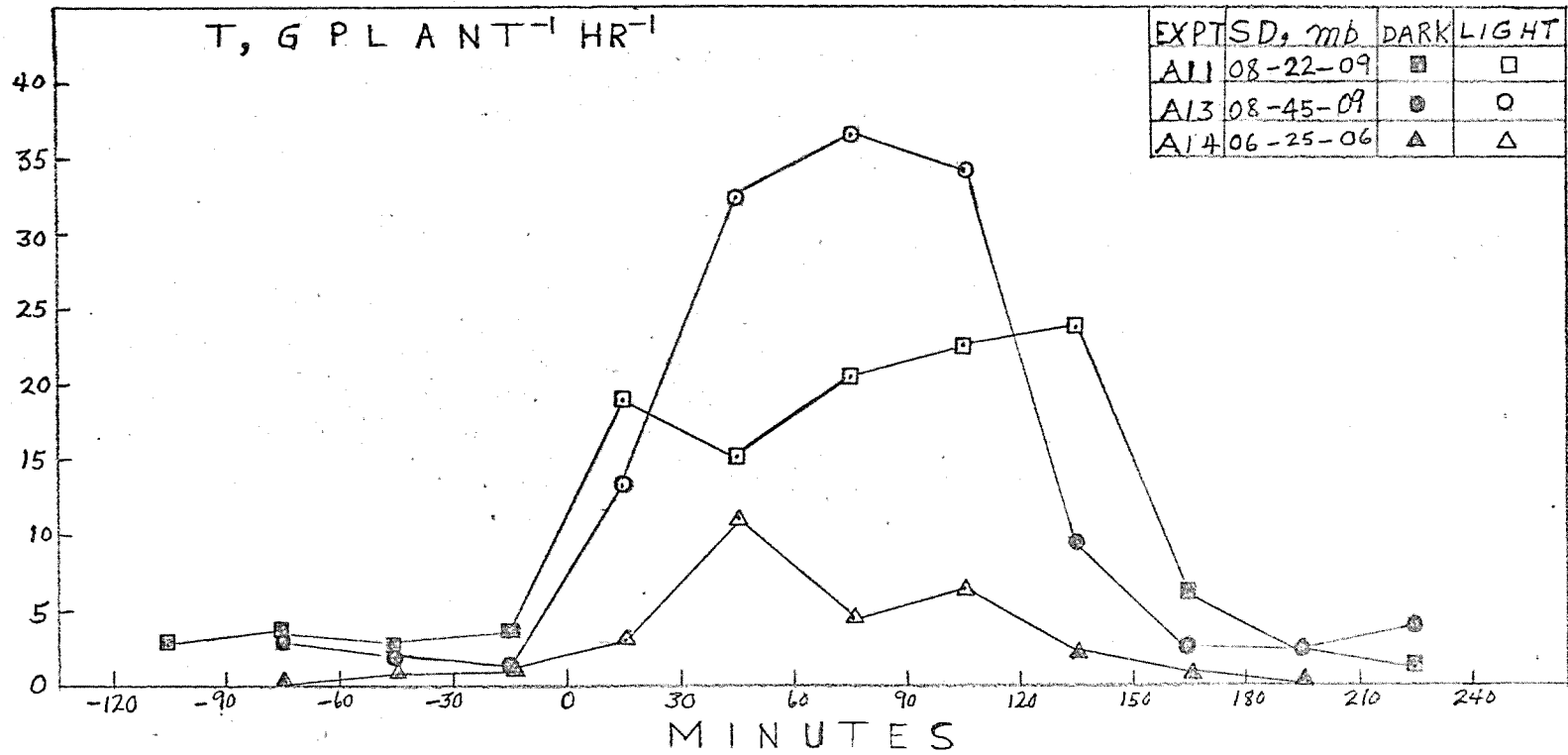


Figure 5. Transpiration as affected by light and a change in saturation deficit.

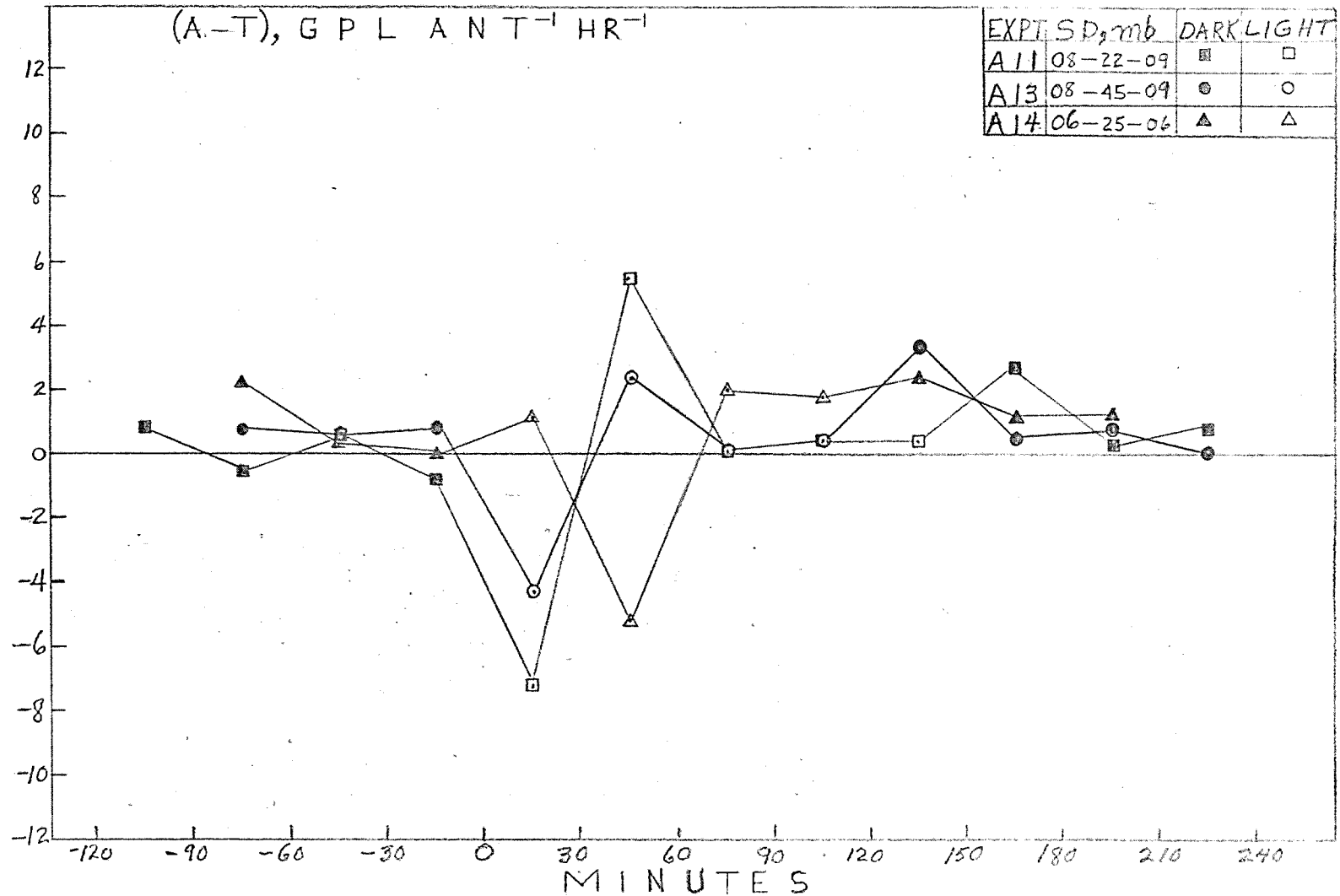


Figure 6. The difference between water absorption and transpiration as affected by light and a change in saturation deficit.

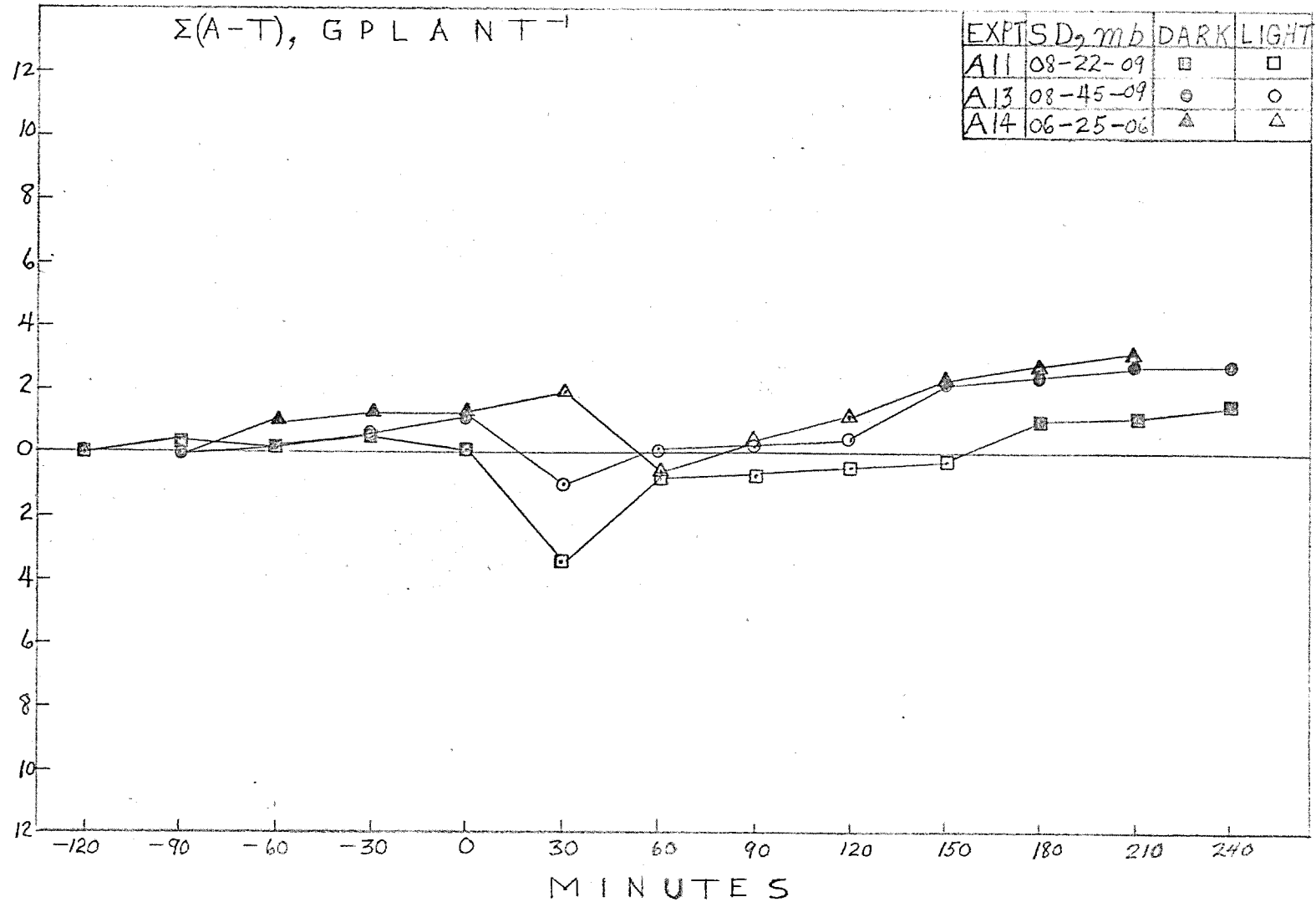


Figure 7. Cumulative water balance as affected by light and a change in saturation deficit.
Annual Report of the U.S. Water Conservation Laboratory

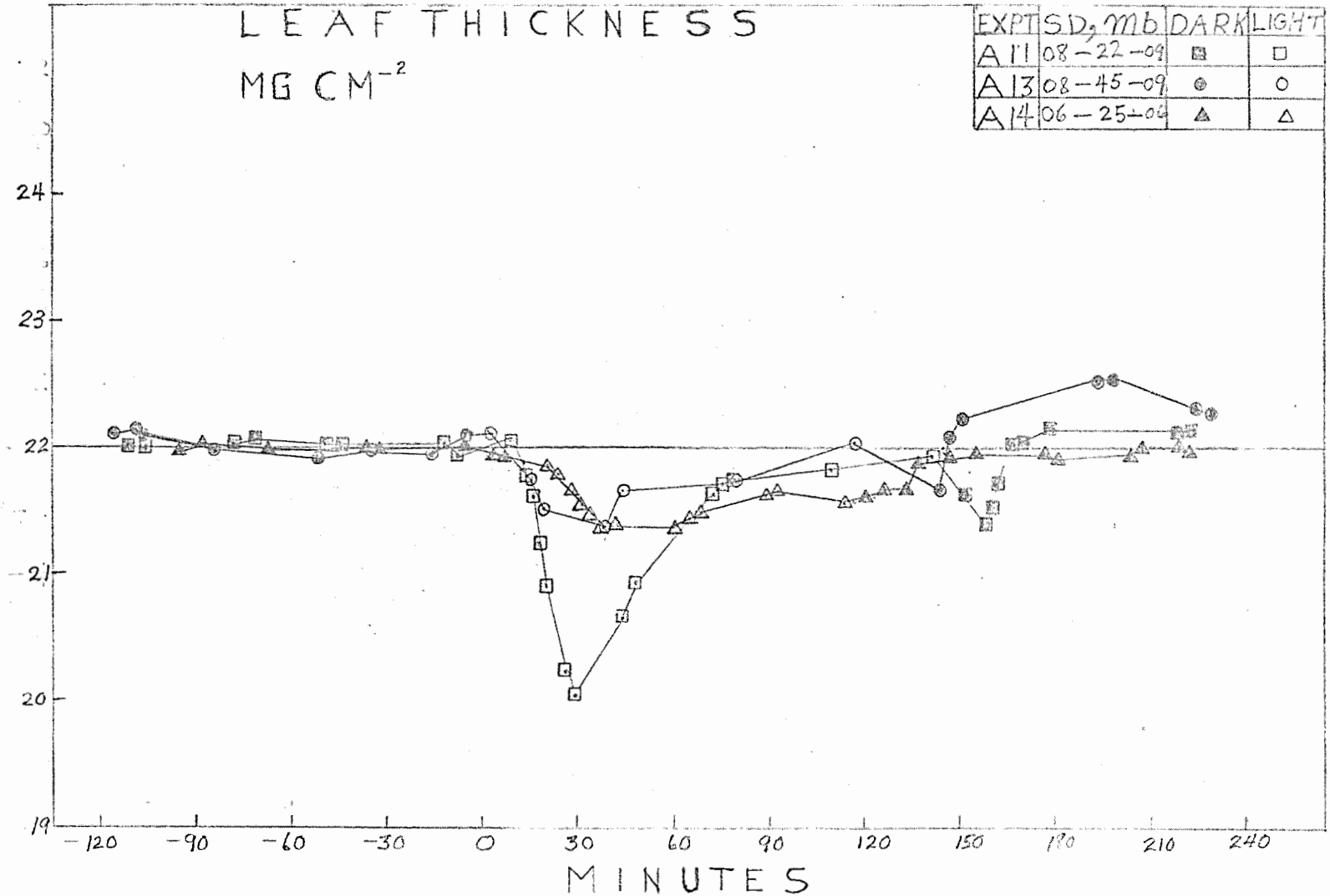


Figure 8. Time course of leaf thickness as determined by beta ray gauging.

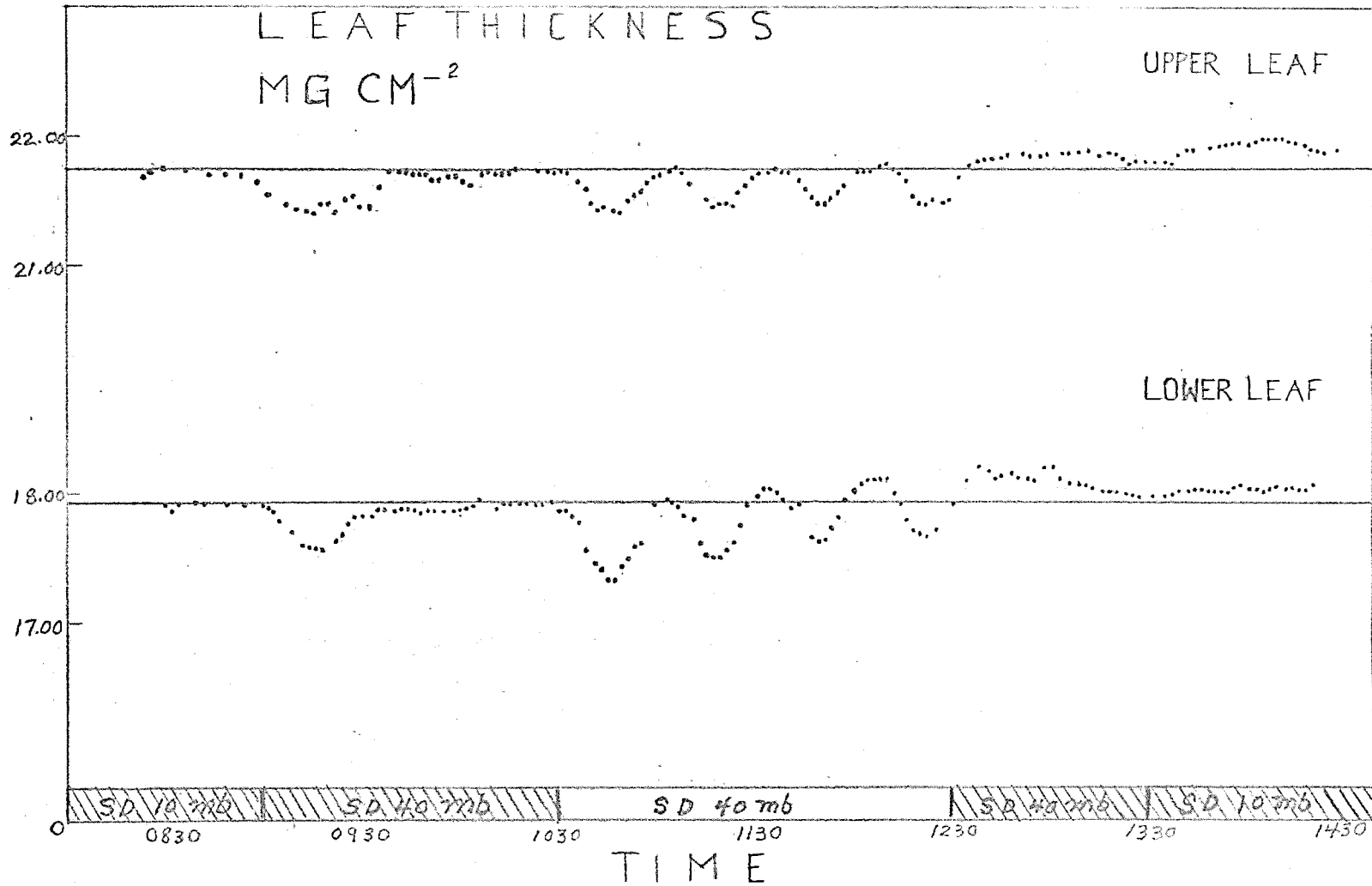


Figure 9. Continuous beta ray gauge measurements of leaf thickness at upper and lower levels of a cotton plant as affected by an increased saturation deficit, followed by sudden illumination.

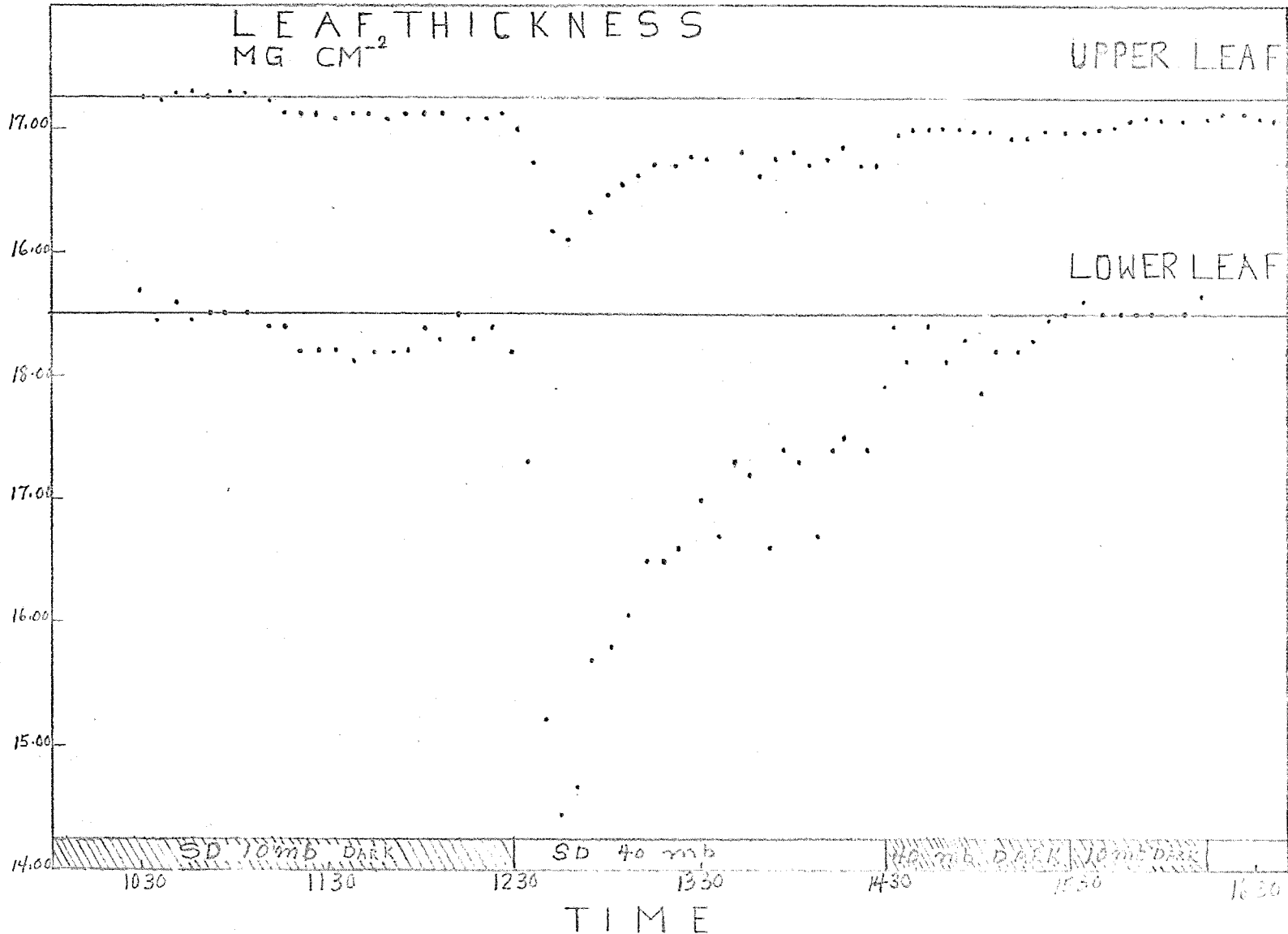


Figure 10. Continuous beta ray gauge measurements of leaf thickness at upper and lower levels of a cotton plant as affected by an increased saturation deficit and coincident sudden illumination.
 Annual Report of the U.S. Water Conservation Laboratory

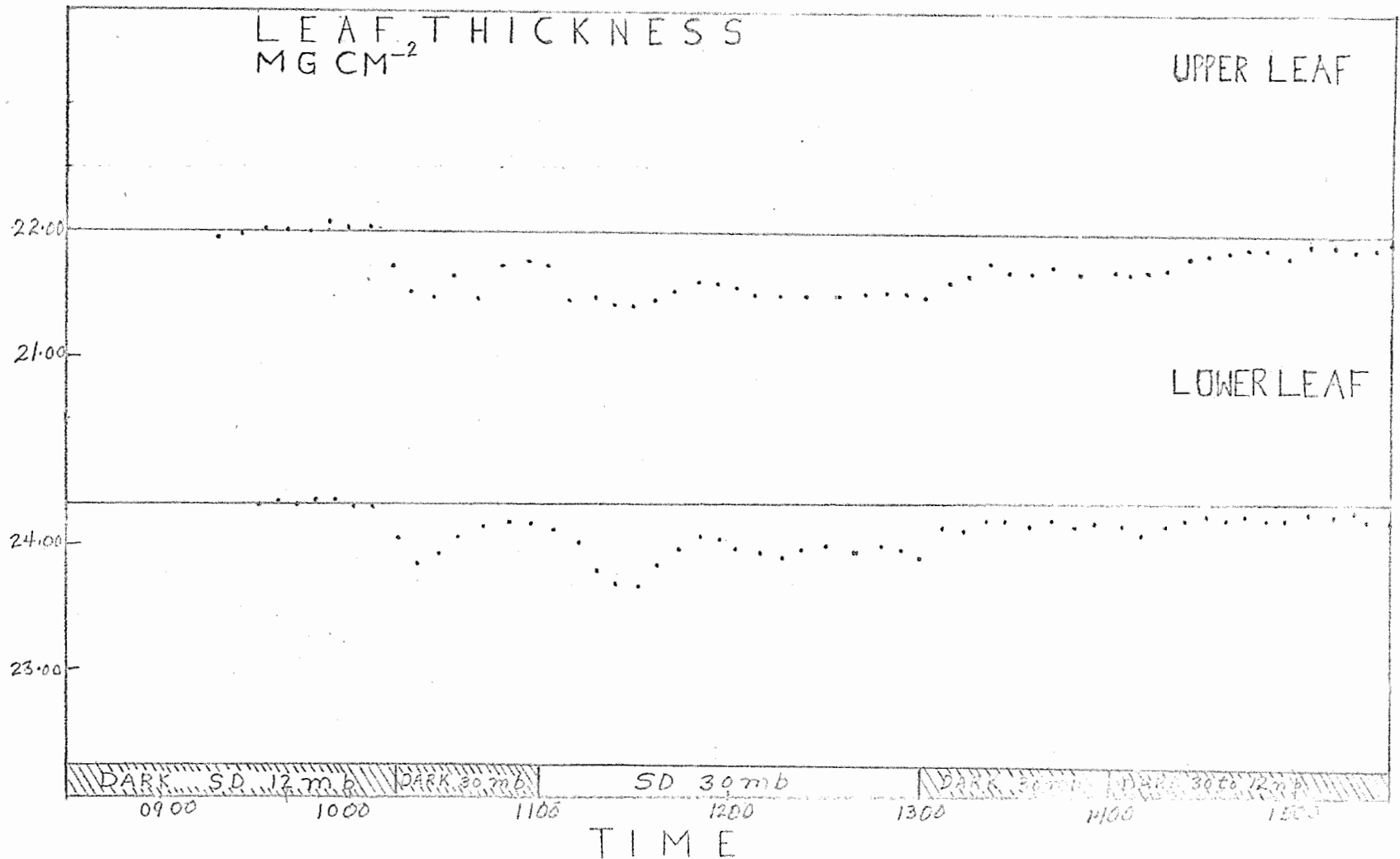


Figure 11. Continuous beta ray gauge measurements of leaf thickness at upper and lower levels of a cotton plant as affected by an isothermally increased saturation deficit, followed by sudden illumination.

29-39

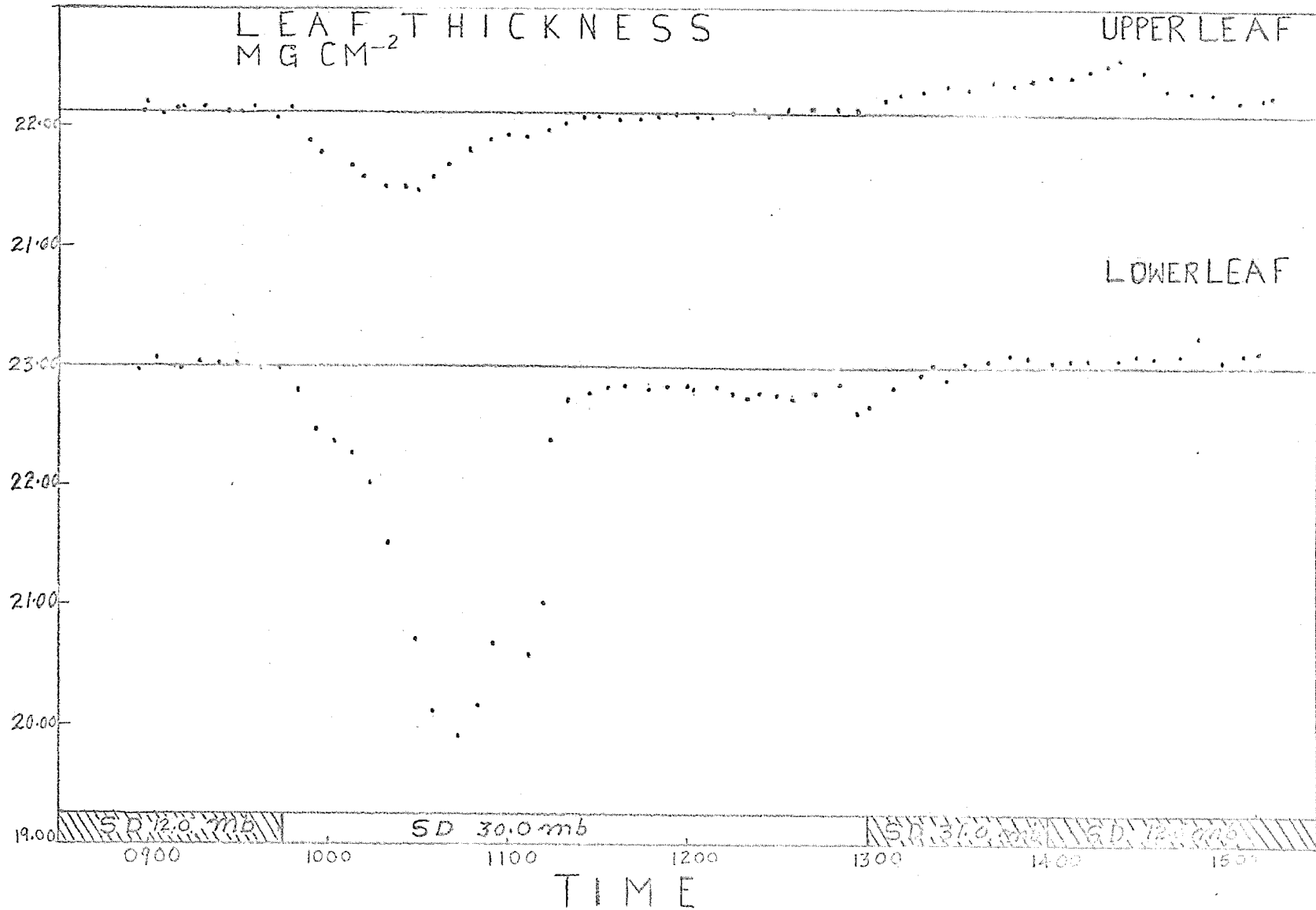


Figure 12. Continuous beta ray gauge measurements of leaf thickness at upper and lower levels of a cotton plant as affected by an isothermally increased saturation deficit and coincident sudden illumination. Annual Report of the U.S. Water Conservation Laboratory

TITLE: QUANTITATIVE MEASUREMENT OF WATER FLOW WITH CHEMICAL TRACERS

LINE PROJECT: SWC 4-gG5

CODE NO.: Ariz.-WCL-30

INTRODUCTION:

Field equipment and techniques for quantitative measurement of dilute fluorescent tracer concentrations had been developed previously so that concentrations in the 10 to 100 parts per billion range could be measured with less than 1 percent error. (See Annual Report for 1962.)

During March of 1963 the Bureau of Reclamation made isotope tracer measurements in two large Salt River Project canals. This offered an opportunity to evaluate the fluorescent tracer system for measuring quantitative flow in excess of 500 cfs in a channel having no mixing length restrictions.

PROCEDURE:

The first tracer measurements were made in the Arizona Canal about 1 mile east of Scottsdale. The isotope and fluorescent tracers were dropped near the center of the canal, 1 mile upstream from the sampling station. The isotope tracer flow measurements were determined using the "Total Count" method. Fluorescent tracer measurements were determined by the integrated sample method using continuous sampling from two different locations in the measurement cross section as described in "Annual Report of 1962."

Flow measurements were also made in the South Canal below Granite Reef Dam. Isotope and fluorescent tracers were not coordinated in these measurements. The fluorescent tracers were dropped near the center of the canal, 1.2 and 2.9 miles upstream from the sampling station. Three drops were made at the 1.2 mile station and one drop made at the 2.9 mile station. Two integrated samples, one near the canal bank and one near the canal center, were used in calculating the flow.

RESULTS AND DISCUSSION:

Attempts to coordinate the fluorescent tracer and isotope tracer measurements were not successful apparently because of operational problems with the isotope counting equipment. The only coordinated drop was found to have too short a mixing length for complete mixing

so that direct comparison of the two tracer measuring methods was impossible. However, discharges during the measuring periods were obtained with current meters and calibrated gates by personnel of the Salt River Project. A comparison of fluorescent tracer and Project flow measurements is presented in Table 1. Their measurements did not include the seepage losses and unmeasured diversions occurring between their gaging stations and the tracer measuring stations. The accuracy of their measurements is also unknown. Accordingly, the comparison is presented as a matter of interest only and cannot be used to evaluate the accuracy of the fluorescent tracer method.

The fluorescent tracer discharge measuring results are given in Table 2. Drop number 1 did not have sufficient mixing length as indicated by the deviation of ± 3.2 percent between the two integrated samples. Drops 2, 3, and 4, made at the same location, indicate that the flow rate was decreasing during the measuring period. Drop 5 was made 1.7 mile further upstream and resulted in a 1.9 percent increase in calculated discharge. This increase is greater than the deviation at drops 2, 3, and 4 and could be explained by seepage loss, tracer adsorption, or both.

An indication of the potential accuracy of the fluorescent tracer method may be obtained by comparing the deviation between integrated samples of the same drop. Maximum deviation from the average for the drop was ± 1.0 percent. Part of this deviation may be due to non-uniform mixing of tracer in the canal flow. Future tests will be conducted with a minimum of four samples per drop to evaluate the influence of mixing on measurement accuracy.

Adsorption of the Rhodamine B on the channel boundaries was suspected, based on adsorption tests made by filtering the dye through columns of fine sand. Another dye, Pontacyl Brilliant Pink B, exhibited about one-tenth the adsorption rate of Rhodamine B and should correspondingly reduce any errors due to adsorption on the canal bed.

The equipment and techniques developed in 1962 performed perfectly under the actual field conditions of this test. Accurate measurements

of dye concentrations in canal water samples were made without difficulty. The present system is quite adequate for evaluating and solving problems resulting from nonuniform mixing and dye adsorption. Only one serious problem remains and that is the verification of fluorescent tracer measurement accuracy with an alternate method of measurement. The problem arises from the fact that the tracer method is potentially capable of performing at the 1 percent error level while presently used rated structures and current meter measurements may be in error by 5 to 10 percent. Means of solving this verification problem are currently under study.

SUMMARY AND CONCLUSIONS:

Equipment and techniques developed for measuring flow rates with fluorescent dyes were tested on two different 1,000 cfs Salt River Project canals during March 1963. The system and methods worked very well under these actual field conditions. Accurate measurement of dye concentrations of 16 to 26 parts per billion in the canal water samples were made without difficulty. Problems were encountered in verifying tracer flow measurements with other independent measurements. Complete mixing of dye with the canal flow did not occur in a reach of 1 mile. Separate samples taken from the center and side of the canal showed that good mixing did occur in a reach of 1.2 miles. Comparison of tracer measurements with flow rates reported by the Project showed differences as high as 8 percent. Part or all of this difference could be accounted for by channel losses between the two points of measurement, dye adsorption by the canal bed, and changes in flow rate which occurred during the measurement period. Potential accuracy of the tracer method is indicated by a maximum deviation of 1.0 percent between paired samples taken for each of three separate dye applications made at the same measurement location. The present system proved that it is adequate for evaluating and solving problems resulting from nonuniform mixing and dye adsorption. Verification of tracer measurement accuracy remains the only serious problem under study. The tracer method is potentially capable of measurement at the 1 percent error

level and other measurement methods capable of this accuracy are not readily available.

PERSONNEL: L. E. Myers, K. J. Brust, J. A. Replogle

Table 1. Fluorescent tracer and Salt River Project discharge comparison.

Canal	Drop No.	Discharge measured by		Discharge deviation
		Salt River	Fluorescent tracer	
		cfs	cfs	%
Ariz.	1	675	618	-8.4
South	2	945	1026	+8.6
South	3	945	1022	+8.1
South	4	945	992	+5.0
South	5	945	1032	+9.2

Table 2. Fluorescent tracer discharge measurements in two large canals.

Canal	Drop No.	Mixing length	Tracer added	Integrated sample <u>1/</u>	Sampling time	Calculated discharge	Average discharge	Deviation
		miles	grams	ppb	min	cfs	cfs	%
Ariz.	1	1.0	940.8	24.8 26.4	35.00	638 599	618	3.2
South	2	1.2	470.4	15.9 15.7	17.07	1020 1033	1026	0.6
South	3	1.2	470.4	15.8 15.8	17.15	1022 1022	1022	0.0
South	4	1.2	470.4	16.0 16.3	17.30	1001 982	992	1.0
South	5	2.9	1411.2	26.4 26.1	30.65	1026 1038	1032	0.8

1/ First sample from center of canal and second sample 5 feet from canal bank.

30-5

TITLE: WATER VAPOR DIFFUSION IN SOILS

LINE PROJECT: SWC 4-gG4

CODE NO.: Ariz.-WCL-31

INTRODUCTION:

Theories proposed to describe water losses from soils by surface evaporation have, for the most part, been based on the assumption that water movement is predominantly in the liquid phase. This assumption is probably valid for the early and intermediate stages of drying, but when the first few centimeters of the soil surface become dry, vapor diffusion plays a more prominent role. In the intermediate water content regions, vapor diffusion and liquid flow occur simultaneously. It is very difficult to assess the relative roles of the two different mechanisms of flow. In the relatively dry water content regions, vapor diffusion should be the predominant mechanism. At these water contents liquid flow is either very low or nonexistent.

Actually water movement in relatively dry soils is not a simple vapor diffusion process. The diffusion of vapor is coupled with the exchange of water between liquid and vapor phases (evaporation and condensation), and the adsorption of water molecules on solid surfaces. Liquid flow, if it occurs, is by diffusion and perhaps some viscous flow. The mathematical description of water flow at these relatively low water contents must account for the diffusion of water vapor, the exchange of water between liquid and vapor phases, and liquid diffusion. The mathematical development will be given below under the subheading Theoretical Considerations.

The measurement of water vapor diffusion coefficients can be made in three ways - the transient method, steady-state method, and calculated from adsorption isotherms. In each of the three cases diffusion coefficients may be different for the wetting phase and for the drying phase. A difference between diffusion coefficients measured during wetting and during drying is expected because of the well-known hysteresis of the adsorption isotherms. As will be shown in the mathematical development, the water vapor diffusion coefficients are closely related to the slopes of the adsorption isotherms. Diffusion coefficients measured by transient or steady-state methods will include

flow in both the vapor and liquid phases. Diffusion coefficients calculated from adsorption isotherms are, theoretically, based solely upon vapor diffusion. Therefore, a comparison of diffusion coefficients measured by transient and steady-state methods and those calculated from adsorption isotherms may yield qualitative information about the water content at which liquid flow becomes noticeable.

If blind or dead-end pores are present in the system, a difference between steady and transient states of flow may occur. Dead-end pores would serve as sources or sinks during transient flow, but would not appreciably influence the steady-state flux through the medium. Thus, if appreciable numbers of dead-end pores are present in the medium, they should manifest themselves by causing a difference between steady and transient diffusion coefficients.

From the foregoing discussion it is evident that it is necessary to study water vapor diffusion in transient and steady-state cases, measure adsorption isotherms for the same soil materials, and calculate the diffusion coefficients from those isotherms in order to evaluate the various factors involved in water flow at these low water contents.

Theoretical considerations.

Symbols.

- D_v = vapor diffusion coefficient, $\text{cm}^2 \text{sec}^{-1}$
 D_θ = liquid water diffusion coefficient, $\text{cm}^2 \text{sec}^{-1}$
 $D_{\theta v}$ = combined liquid and vapor diffusion coefficient, $\text{cm}^2 \text{sec}^{-1}$
 q_v = vapor flux density, $\text{g cm}^{-2} \text{sec}^{-1}$
 q_θ = liquid flux density, $\text{g cm}^{-2} \text{sec}^{-1}$
 $q_{\theta v}$ = combined liquid and vapor flux density, $\text{g cm}^{-2} \text{sec}^{-1}$
 S = source function, $\text{g cm}^{-3} \text{sec}^{-1}$
 t = time, sec
 x = distance, cm
 e = air filled porosity, $\text{cm}^3 \text{cm}^{-3}$
 θ = volumetric water content, g cm^{-3}
 λ = $xt^{-1/2}$ is the Boltzmann transformation $\text{cm sec}^{-1/2}$
 ρ = vapor density, g cm^{-3}

The isothermal steady state diffusion of water vapor can be described by the equation

$$q_v = - D_v \frac{\partial \rho}{\partial x} , \quad [1]$$

where D_v is a concentration dependent diffusion coefficient which includes factors such as porosity, tortuosity, mass flow factor, and the coefficient of water vapor diffusion in air. For convenience, all equations will be written in one dimension and the effect of gravity will be assumed negligible.

Using the relation

$$\frac{\partial \rho}{\partial x} = \frac{\partial \rho}{\partial \theta} \frac{\partial \theta}{\partial x} , \quad [2]$$

equation [1] becomes

$$q_v = - (D_v \frac{\partial \rho}{\partial \theta}) \frac{\partial \theta}{\partial x} . \quad [3]$$

For liquid diffusion we have

$$q_\theta = - D_\theta \frac{\partial \theta}{\partial x} . \quad [4]$$

Summing [3] and [4],

$$q_{\theta v} = - D_{\theta v} \frac{\partial \theta}{\partial x} , \quad [5]$$

where

$$D_{\theta v} = D_\theta + D_v \frac{\partial \rho}{\partial \theta} . \quad [6]$$

Water transfer at steady state is described by equation [5]. Equation [6] shows that it may be possible to partition liquid and vapor flux by measuring $D_{\theta v}$, calculating $D_v \partial \rho / \partial \theta$ and obtaining D_θ by difference.

For transient conditions we employ the continuity condition and equation [1] to obtain

$$\frac{\partial \rho}{\partial t} = \frac{\partial}{\partial x} \left(\frac{D_v}{\epsilon} \frac{\partial \rho}{\partial x} \right) . \quad [7]$$

Equation [7] holds only for nonadsorbing media. Water in a soil system is continuously evaporating and condensing and, in a transient system, the liquid water content, in addition to the vapor concentration, changes with time and distance. To account for this we add a source term to [7]

$$\frac{\partial \rho}{\partial t} = \frac{\partial}{\partial x} \left(\frac{D_v}{\epsilon} \frac{\partial \rho}{\partial x} \right) + S, \quad [8]$$

where $S = -\frac{1}{\epsilon} \frac{\partial \theta}{\partial t}$. We can now write, assuming ϵ to be constant,

$$\epsilon \frac{\partial \rho}{\partial t} + \frac{\partial \theta}{\partial t} = \frac{\partial}{\partial x} D_v \frac{\partial \rho}{\partial x} \quad [9]$$

Since the vapor density ρ is less than $2.5 \times 10^{-5} \text{ g cm}^{-3}$ at 27 C and is a decreasing function of θ , θ exceeds ρ by 10^3 or more, and hence $\epsilon \partial \rho / \partial t$ can be considered negligible compared to $\partial \theta / \partial t$, except perhaps in exceedingly dry systems where θ is on the order of 0.0001 g cm^{-3} .

If we therefore assume that $\partial \theta / \partial t \gg \epsilon \partial \rho / \partial t$ and using [2] in [9] we obtain

$$\frac{\partial \theta}{\partial t} = \frac{\partial}{\partial x} \left[(D_v \frac{\partial \rho}{\partial \theta}) \frac{\partial \theta}{\partial x} \right], \quad [10]$$

an equation which describes vapor diffusion and associated evaporation and condensation, expressed in terms of liquid water content. An analogous equation for liquid diffusion is

$$\frac{\partial \theta}{\partial t} = \frac{\partial}{\partial x} (D_\theta \frac{\partial \theta}{\partial x}), \quad [11]$$

which we can sum with [10] to obtain

$$\frac{\partial \theta}{\partial t} = \frac{\partial}{\partial x} (D_{\theta v} \frac{\partial \theta}{\partial x}) \quad [12]$$

where $D_{\theta v}$ is given by [6].

Equation [5] and [12] are the pertinent equations for use with steady- and transient-state diffusion experiments, respectively. For the steady state $q_{\theta v}$ and $\partial \theta / \partial x$ are evaluated experimentally. For the transient case [12] can be solved by assuming the Boltzmann transformation ($\lambda = xt^{-1/2}$) and using the boundary conditions

$$\begin{aligned} \theta &= \theta_i, \quad x > 0, \quad t = 0 \\ \theta &= \theta_s, \quad x = 0, \quad t > 0, \end{aligned} \quad [13]$$

to give

$$D_{\theta v} = -\frac{1}{2t} \frac{dx}{d\theta} \int_{\theta_i}^{\theta} x d\theta, \quad [14]$$

from which $D_{\theta v}$ is evaluated by graphical integration and differentiation of the transient water content distribution curve.

Equations [13] and [14] are valid for both sorption and desorption if the definition $\theta_s > \theta_i$ is made for sorption and $\theta_i > \theta_s$ for desorption.

In the second order equations ([9] through [14]) the water content θ can refer either to a weight or volume basis since the conversion factor (bulk density) cancels. For the first order equations, specifically [5], θ must refer to a volume basis to make the diffusion coefficients dimensionally consistent. Some graphs in the Results and Discussion section will be on a weight basis and some on a volume basis.

PROCEDURE:

Transient-state experiments. The soil materials used were Adelanto loam, Pachappa loam, and Pine silty clay. The particle size data for these soil materials are given on page 221 of the 1962 Annual Report. The air dry soil materials were passed through a 2-mm sieve and packed into columns with a mechanized soil column packer. The columns were constructed from 3.2cm i.d. acrylic plastic cylinders cut into 1-cm sections. To obtain water contents less than air dry, yet maintain the same bulk densities, columns were placed into a chamber containing a desiccant and evacuated. To obtain water contents greater than air dry, the columns were placed into a chamber containing beakers of saturated K_2SO_4 solution and evacuated. The columns were weighed periodically to determine when equilibrium was obtained. Under evacuation, equilibrium was obtained in one to two weeks for the drying and two to three weeks for the wetting.

Since the columns were constructed of sections held together by three strips of 1/2-inch masking tape, gaseous interchange between soil material and the external atmosphere could take place between the sections. This pathway for interchange facilitated the wetting or drying under vacuum, but posed a problem of completely sealing all of the column except one end prior to placing it into the diffusion chamber. For the sorption experiments the columns were sealed by encapsulating them in a pliable vacuum sealing wax. For the desorption experiments it was necessary to encapsulate the columns with mercury.

The mercury encapsulation was accomplished by inserting the column, previously equilibrated over a saturated K_2SO_4 solution (yielding water content in equilibrium with 0.97 relative pressure) into an acrylic plastic cylinder open on one end having an i.d. about 6 mm greater than the o.d. of the plastic sections of the column. An O-ring was placed on the end of the column which protruded about 0.5 cm from the end of the cylinder. The O-ring was held tightly to the cylinder by a bracket, forming a seal. The space between the column and the outer cylinder was filled with mercury to prevent water vapor from diffusing to the sides of the soil column.

The diffusion chamber for the transient experiments is illustrated by Figure 1. The chamber was an acrylic plastic container in which the water vapor density was controlled by saturated salt solutions. A small pump was used to bubble air through a saturated salt solution in a flask and then through the diffusion chamber. For the desorption experiments, the flask and the diffusing chamber were filled with a desiccant in place of the saturated salt solutions used for the sorption experiments. The apparatus, with the exception of the pump, was placed in an insulated box. The system was located in a room in which the temperature was controlled to 27 ± 1 C. The temperature within the box was monitored and found to vary less than 0.1 C during the 24-hour period. To initiate a diffusion run a column, sealed everywhere except at one end, was placed in the diffusion chamber and the time noted. After a predetermined number of days, the column was removed from the chamber; the sealing compound or the mercury removed;

the column sectioned into 1-cm sections; and the soil material placed into weighing cans. This operation required 3 to 5 minutes. The water contents were determined gravimetrically after drying at 110 C for 24 hours. Plots of water content versus distance from the source were made from which the diffusivity function in equation [14] was calculated.

There are several critical assumptions in this experimental procedure. They are: 1. The water content at the plane $x = 0$ is maintained at the constant value θ_s for all $t > 0$. 2. Flow is in one dimension, i.e., no movement of vapor takes place through the sides of the column and the sealing compound. 3. The temperature of the medium is constant.

Steady-state experiments. For the steady-state experiments the soil materials were prepared in identical manner as enumerated above for the transient experiments. That is, with the exception that only two of the soil materials, Adelanto loam and Pachappa loam, were used. One 10-cm and one 15-cm column of each soil material were used for the steady-state measurements. A wire screen at each end held the soil in place. Columns to be used for sorption measurements were dried over a saturated LiCl solution in a vacuum desiccator. Columns to be used for desorption measurements were wetted over a saturated K_2SO_4 solution in a vacuum desiccator. The steady-state diffusion cell, illustrated by Figure 2, consisted of two brass cylinders 6.4 cm in diameter and 10 cm high with a 3.2-cm diameter hole cut into a side. To receive the soil columns, one cylinder was placed at each end of the column so that the column provided a diffusion path from one brass cylinder to the other. The entire column and the junction between the column and the brass cylinders were covered with a vacuum sealing wax to minimize the vapor losses. In each brass cylinder a 50-mm beaker containing a saturated salt solution was placed. One solution was K_2SO_4 (0.97 relative pressure); the other was LiCl (0.11 relative pressure). In all cases salt crystals were present in the beakers, insuring the saturated solution. A hole of sufficient diameter to accomodate a 00 rubber stopper was drilled in the top of each

cylinder cap. A brass rod was forced through the rubber stopper and down to a wire handle on a beaker. This arrangement enabled a diffusion cell to be set inside an analytical balance; the rubber stopper, and hence the beaker, raised; and the brass rod hooked onto the weighing pan. The beakers could be weighed accurately with very little water loss to the atmosphere since only a small opening to the surrounding room was exposed for about 30 seconds. The diffusion cells were kept in an insulated box in a controlled temperature room. The temperature in the box was 27 ± 0.1 C.

Diffusion was allowed to proceed until the rate of water loss from the K_2SO_4 solution equalled the rate of gain of the LiCl solution. This provided the direct measure of the flux q . After steady state had been achieved, the diffusion cell was disassembled and the columns were sectioned into 1-cm sections and the water content determined by weighing after drying at 110 C for 24 hours. Plots of volumetric water content versus distance were made from which the slope was determined at particular water contents for calculation of the diffusion coefficient using equation [5]. The averages of the diffusivities obtained from the 10-cm and the 15-cm columns, at a given water content, are reported in the Results and Discussion.

Adsorption isotherms. Adsorption isotherms were determined on the two soil materials by placing approximately 5 grams of air dry soil into weighing bottles. Three replications of each soil material were used for adsorption; and three replications of each for desorption. The beakers were placed in vacuum desiccators containing a saturated salt solution, evacuated, and let stand for a period of 2 to 5 days. A magnetic stirrer beneath each desiccator was energized for 30 seconds every 5 minutes to stir the salt solution. Periodic stirring was used to minimize temperature fluctuations. The bottles were weighed daily until two consecutive readings indicated that equilibrium was essentially obtained. At the conclusion of the measurements, the samples were dried in an oven at 110 C for 24 hours and the oven dry weight used as a basis for determination of water contents at all relative pressures. Plots were made of water content

versus relative pressure from which the slopes of the lines were taken for the calculation of diffusion coefficients. Since the bulk density of the soil in the weighing bottles was unknown, the relative vapor pressure was plotted versus gravimetric water content. The bulk densities of the packed columns (1.42 g cm^{-3} and 1.40 g cm^{-3} for Adelanto and Pachappa, respectively) were used to convert to the volumetric basis for the calculation of diffusion coefficients. This calculation assumes that the bulk density differences would have a negligible effect on the adsorption isotherms.

RESULTS AND DISCUSSION:

Transient-state experiments. For a particular set of initial and boundary conditions a test of the applicability of diffusion theory can be made by subjecting replicate soil columns to different diffusion time periods and plotting the resulting water contents as a function of $xt^{-1/2}$. If the plots of the data from different time periods are identical, the assumptions made in the theory may be considered valid for these conditions and the theory applicable. A more conclusive test can be made by comparing diffusivities calculated from θ versus $xt^{-1/2}$ data for different boundary and initial conditions. If the diffusivities are identical for the different conditions, the theory will describe the experimental results.

Plots of θ versus $xt^{-1/2}$ for Adelanto loam are shown in Figure 3. Three sets of data are shown, each set corresponding to different initial and boundary conditions. Each set consists of data from two columns; each column was subjected to a different diffusion time period. The time periods are shown in the figure. The plots of θ versus $xt^{-1/2}$ for Pachappa loam and Pine silty clay are shown in Figure 4. One set of initial and boundary conditions is shown for each soil material.

Desorption water content distribution curves for Adelanto loam are shown in Figure 5. Curves for two sets of initial conditions are shown. Desorption water content distribution curves for Pine silty clay and Pachappa loam are shown in Figure 6. In all cases, each set consists of data from two columns; each column was subjected to a different diffusion time period. The diffusion times for each column are shown in the figures.

The agreement between the θ versus $xt^{-1/2}$ plots of data from columns subjected to different time periods at several different initial and boundary conditions for both sorption and desorption meets the criteria set forth earlier for determining the applicability of diffusion theory. Additional, more conclusive, evidence of the applicability of diffusion theory is shown in Figures 7 and 8. In Figure 7 the sorption diffusion coefficients for Adelanto loam measured for three sets of initial and boundary conditions are shown. The data for the three sets of conditions overlap and are in good agreement. Figure 8 shows desorption diffusivity data with the sorption diffusivities shown as a broken line. The data for two sets of initial conditions for desorption of Adelanto again overlap and are in good agreement.

In Figure 8 the desorption diffusivity curve, in contrast to sorption, reaches a maximum gradually; is smaller in magnitude; and occurs at a higher water content. The dependence of diffusivity on water content is much less for desorption than for sorption over the same water content range, a fact that can be qualitatively ascertained from the water content distribution curves.

Figures 9 and 10 show sorption and desorption diffusion coefficients for Pachappa loam and Pine silty clay, respectively. In all cases the symbols are the averages of two measurements. With increasing water content the sorption diffusivities increase to a maximum and then decrease. For desorption, the diffusion coefficient water content curve has the same general shape, but the maximum is of lesser magnitude and the overall dependence of the diffusivities on water content is considerably less for desorption than for sorption.

In a field soil with a dry surface layer water loss through the dry layer is largely by vapor diffusion. The water content of the layer fluctuates diurnally, alternately drying during the day and wetting at night. At a given time a portion of the layer may be drying while another portion may be wetting. Because of the difference between sorption and desorption diffusivities, the diffusivity water content relation applicable in this situation could only be expressed

as a range of diffusivities. For Adelanto and Pine, the two soil materials whose desorption diffusivities exhibit a relatively small change of water content, a range in diffusivities of 2 to 4×10^{-5} $\text{cm}^2 \text{sec}^{-1}$ would include both sorption and desorption diffusivities, and an assumed constant diffusivity of 3×10^{-5} $\text{cm}^2 \text{sec}^{-1}$ would be sufficient for some applications. For Pachappa the sorption and desorption diffusivities differ by about a factor of 2, but the dependence upon water content is much more pronounced and the use of a constant diffusion coefficient in attempts to describe the diurnally fluctuating system could cause serious errors.

Steady-state experiments. The steady-state water content distribution curves for Adelanto loam and Pachappa loam are shown in Figure 11. The data are for the 15-cm columns. For Adelanto loam the distribution curve for sorption is definitely nonlinear, whereas for desorption a linear relation obtains. Therefore, the sorption diffusivities are concentration dependent, whereas the desorption diffusivities are constant over this range of water contents. The data for Pachappa show that both sorption and desorption water content distribution curves are nonlinear. This indicates that both sorption and desorption diffusivities are concentration dependent for this soil material.

Adsorption isotherms for Adelanto loam and Pachappa loam are shown in Figure 12. The sorption and desorption branches are indicated by arrows. A marked hysteresis loop is evident for both soil materials. The slope of the lines were obtained at several water contents for each soil material and for desorption and sorption branches of each. The slopes, multiplied by D_v and divided by the bulk density, yielded theoretical values for water vapor diffusion coefficients. The values of D_v were calculated from the relation $D_v = D_a \alpha(\epsilon - \theta)$ where $D_a = 0.261 \text{ cm}^2 \text{sec}^{-1}$ is the coefficient for water vapor diffusion in air at 27 C; $\alpha = 0.66$ is the tortuosity; ϵ is the total porosity; and θ the volumetric water content. The term $(\epsilon - \theta)$ was different for each soil material and each water content. The values for the diffusion coefficients obtained in this manner are indicated by the triangular symbols in Figures 13 through 16.

The calculation of diffusion coefficients by the three methods used in these studies requires the graphical measurement of slopes at water content distributions and adsorption isotherms. The transient water content distributions were better defined with more data points than were the steady-state measurements and adsorption isotherms, allowing more precise slope measurements for the former. The measurement precision is in the order transient > steady state > calculation from adsorption isotherms. The transient diffusion coefficients will therefore be considered as a basis for comparison of the coefficients obtained from steady-state measurements and adsorption isotherms. The transient coefficients are indicated by dashed lines in Figures 13 through 16. Diffusion coefficients for Adelanto loam are shown in Figure 13 for sorption and in Figure 14 for desorption. For Pachappa loam, diffusion coefficients are given in Figure 15 for sorption and in Figure 16 for desorption. The steady-state sorption diffusivities for both Adelanto (Figure 13) and Pachappa (Figure 15) shown by circular symbols, fall on or close to the transient curve. The agreement between the steady and transient data confirm the maximum in the diffusivity water content function for sorption.

The steady-state desorption diffusivities for Adelanto (Figure 14) are shown by a solid straight line. No data points are shown because only one value of diffusivity was obtained from the linear water content distribution curve (Figure 11). Neither the steady-state nor the transient desorption curves exhibit the large diffusivity changes with water content that sorption diffusivity curves do. The desorption diffusivities for Pachappa (Figure 6), however, show marked diffusivity changes with water content as do the sorption curves.

The close agreement between steady and transient diffusivities for sorption and desorption for both soil materials indicates that the volume of dead-end pores in these materials is too small to cause measurable difference between steady and transient flow of water vapor. This may not be true at higher water contents, because the relationship

between air- and liquid-filled pores increases in complexity as the water content increases.

The least precise of the three measurements, the diffusivities calculated from adsorption isotherms, yield values remarkably close to the steady and transient diffusivities. For Adelanto desorption (Figure 14) the adsorption isotherm diffusivities exhibit a maximum at about the same water content as the sorption diffusivity maximum with the overall shape of the curve different than the steady and transient curves. If the difference between sorption and desorption diffusivities could be explained on the basis of hysteresis of the adsorption isotherms, the adsorption isotherm diffusivities should be the same as the steady and transient values for both sorption and desorption. For Pachappa the adsorption isotherm diffusivities are somewhat higher than the steady and transient values, but in general, have the same shape. Thus, for Pachappa, the difference between sorption and desorption diffusivities can largely be explained on the basis of hysteresis of adsorption isotherms. It appears that, for the finer textured Adelanto, the rate of movement of water molecules between and among the clay platelets is different for sorption and desorption, causing a hysteresis effect in addition to the difference in the amount of water retained at a particular relative pressure (as measured by adsorption isotherms).

Adsorption isotherm diffusivities are, theoretically, based only on vapor flow, whereas the measured steady and transient diffusivities include both vapor and liquid diffusion. The contribution of the liquid diffusion would cause the diffusion coefficient to be larger than that which would occur if vapor diffusion were the only mechanism. We can, therefore, hypothesize that the water content at which adsorption isotherm diffusivities fall below the steady and transient diffusivities is the water content at which liquid flow begins. For Adelanto sorption (Figure 13) this point occurs at about 0.72 relative pressure and for desorption (Figure 14) at about 0.50. At water contents of about 0.07 to 0.08 the vapor and liquid diffusivities for Adelanto were of about the same magnitude. At higher

water contents the vapor flow can be expected to decrease and liquid flow to increase.

For Pachappa, the water content at which the diffusivities curves cross is not well defined. It appears that this point occurs at about 0.90 and 0.80 relative pressure for sorption and desorption, respectively. At these water contents, the magnitude of liquid flow apparently is greater for desorption than for sorption.

SUMMARY AND CONCLUSIONS:

Water transfer in relatively dry soils consists of three mechanisms: diffusion of water vapor in the air-filled pores, continuous exchange of water molecules between the liquid and vapor phases, and diffusion in the liquid phase. The three combined mechanisms can be described by diffusion equations with concentration dependent diffusion coefficients.

Diffusion coefficients were obtained by three methods: transient-state, steady-state, and calculated from slopes of adsorption isotherms. All measurements were made at a controlled temperature of 27 C. For the three methods, diffusion coefficients were obtained for both wetting and drying. Comparison of data obtained from the various methods lead to the following observations and conclusions.

1. Diffusion theory (in particular, the use of the Boltzmann transformation for solving the nonlinear diffusion equation) is valid for both sorption and desorption of water by soil at relatively low water contents.

2. With increasing water content the diffusion coefficients increase to a maximum and then decrease. For wetting, the maximum occurs at about the water content where one molecular layer is formed. For desorption, the maximum diffusivity is smaller in magnitude, occurs at a higher water content, and is approached more gradually than for sorption.

3. Diffusion coefficients measured at steady and transient states compare remarkably well. Agreement of data from the two completely different methods further confirms the validity of diffusion theory and the use of the Boltzmann transformation for these systems.

The agreement between the two methods indicates that the volume of "blind" or "dead-end" pores is negligibly small for these soil systems.

4. Diffusion coefficients calculated from adsorption isotherms compare favorably with transient and steady-state values except at the higher water contents. Since the coefficients from adsorption isotherms are, theoretically, based solely on vapor diffusion, the fact that these coefficients fall below those measured by steady and transient methods at higher water contents is taken as an indication that liquid flow becomes noticeable at these water contents. In particular, for Adelanto sorption, liquid diffusion may begin at a volumetric water content of 6 percent, for Pachappa at about 3 percent.

PERSONNEL: R. D. Jackson

31-16

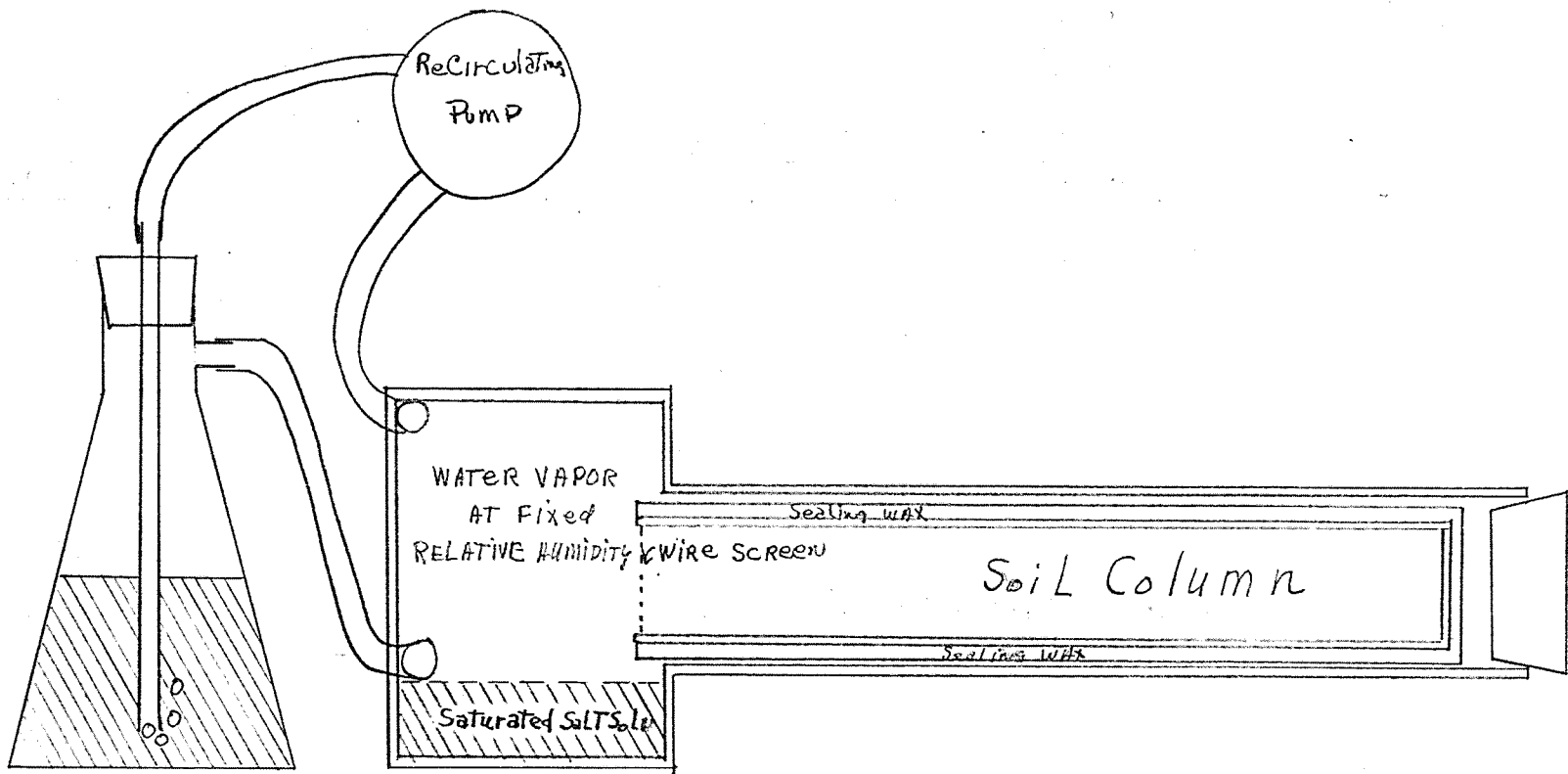


Figure 1. Transient-state water vapor diffusion apparatus.

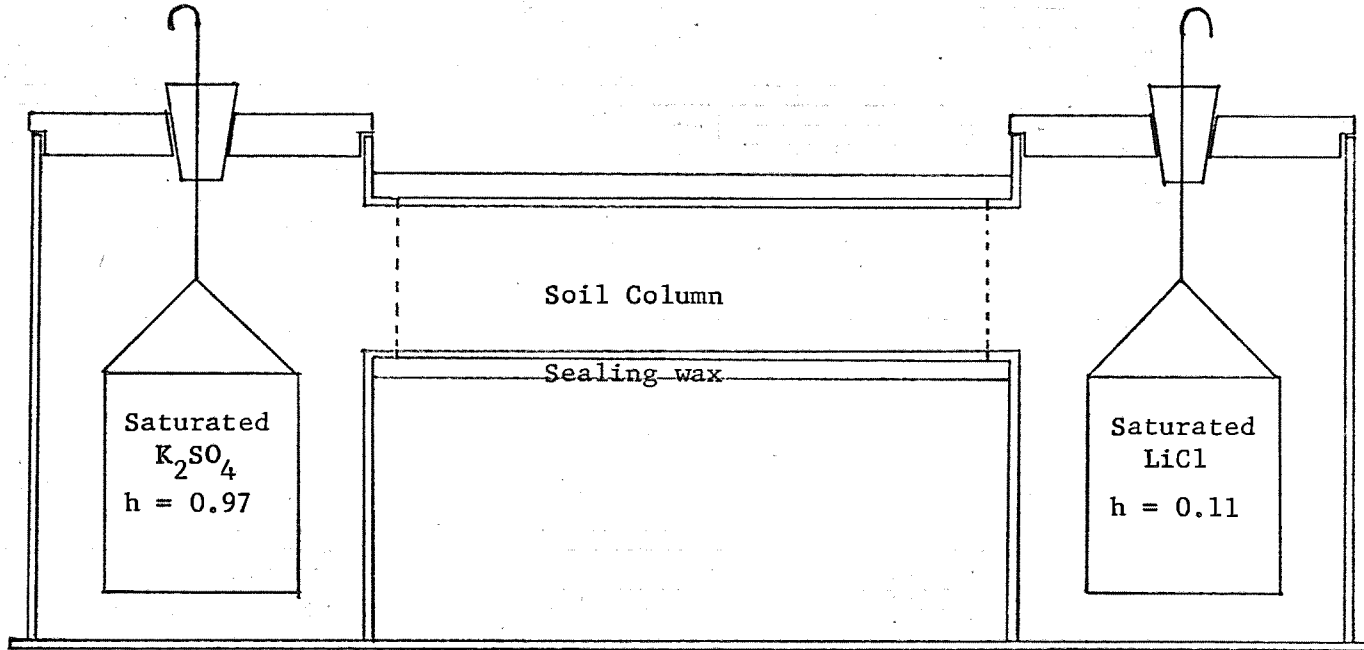


Figure 2. Steady-state water vapor diffusion apparatus.

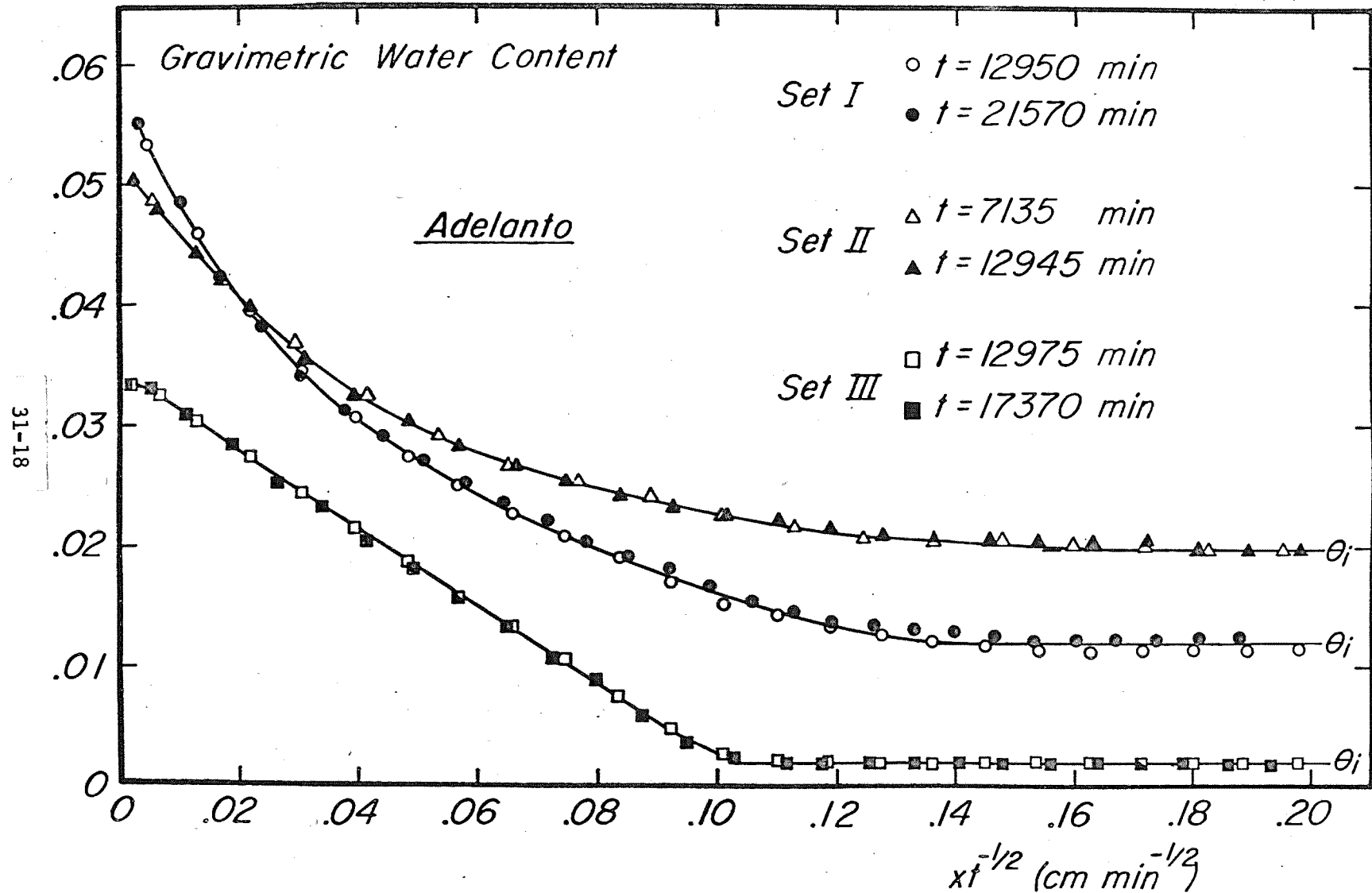
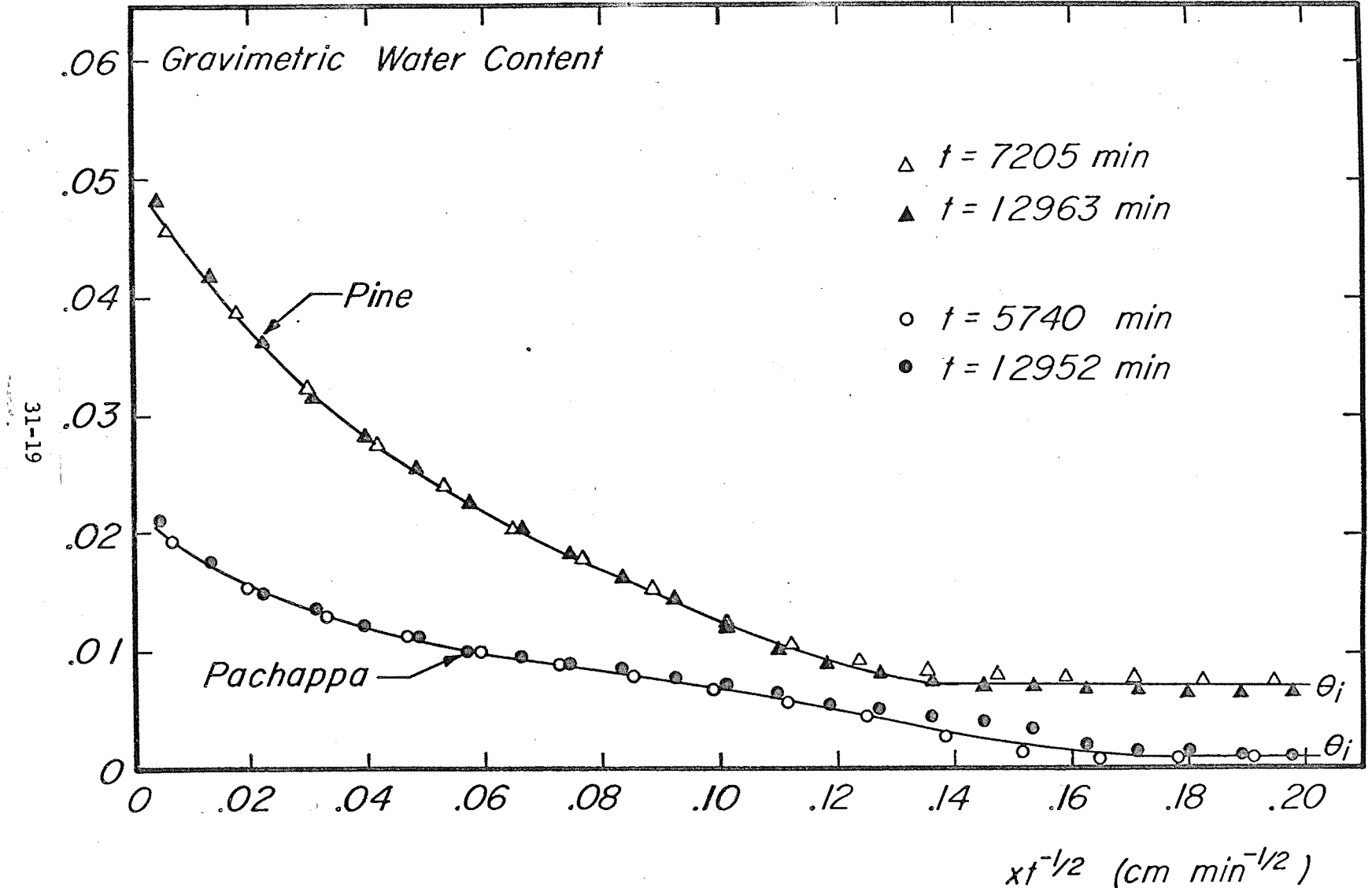
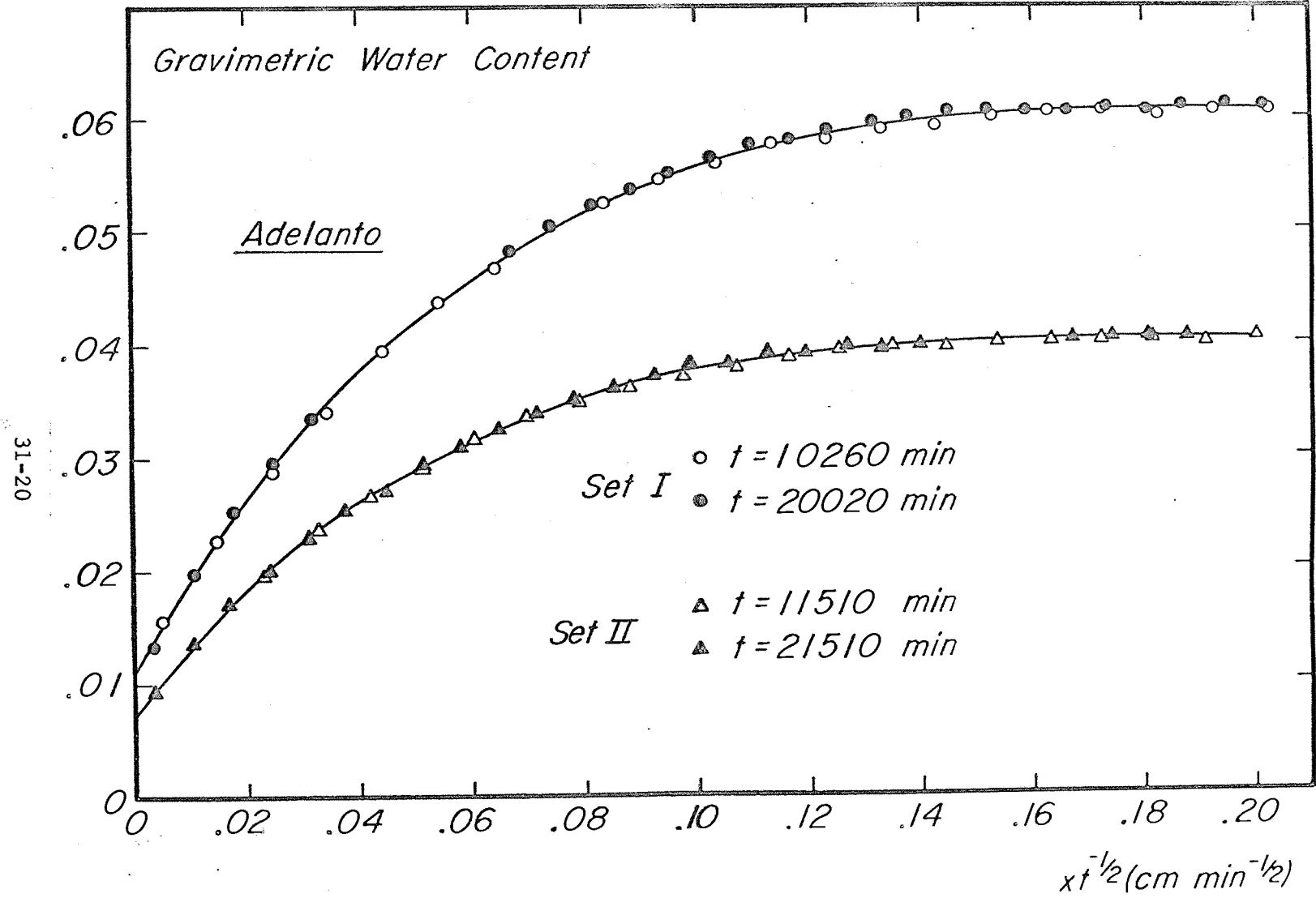


Figure 3. Sorption water content distributions for ~~Annual Report of the U.S. Water Conservation Laboratory~~ and initial conditions.



Annual Report of the U.S. Water Conservation Laboratory
Figure 4. Sorption water content distributions for Pine silty clay and Pachappa loam.



Annual Report of the U.S. Water Conservation Laboratory
Figure 5. Desorption water content distributions for Adelanto loam.

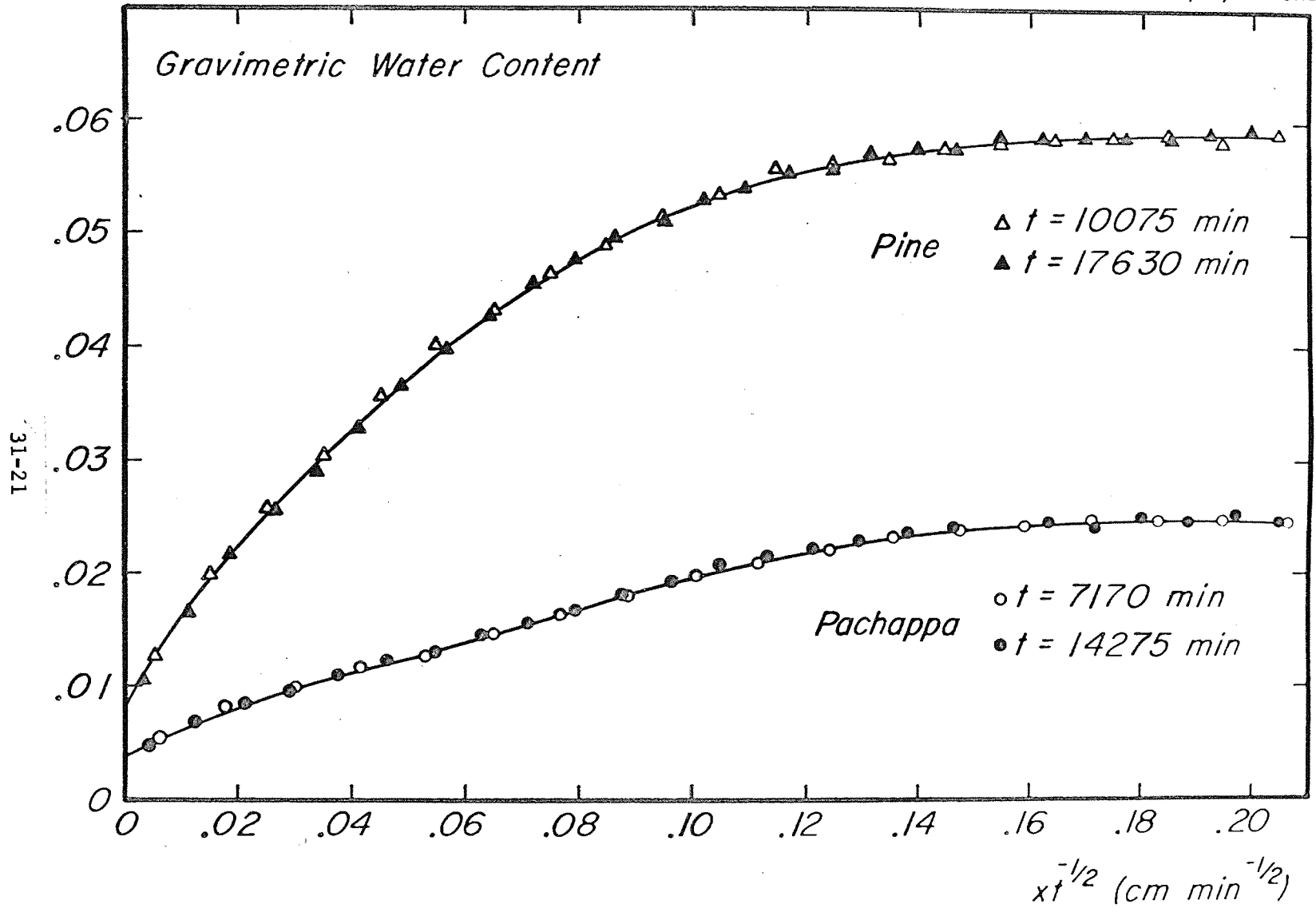
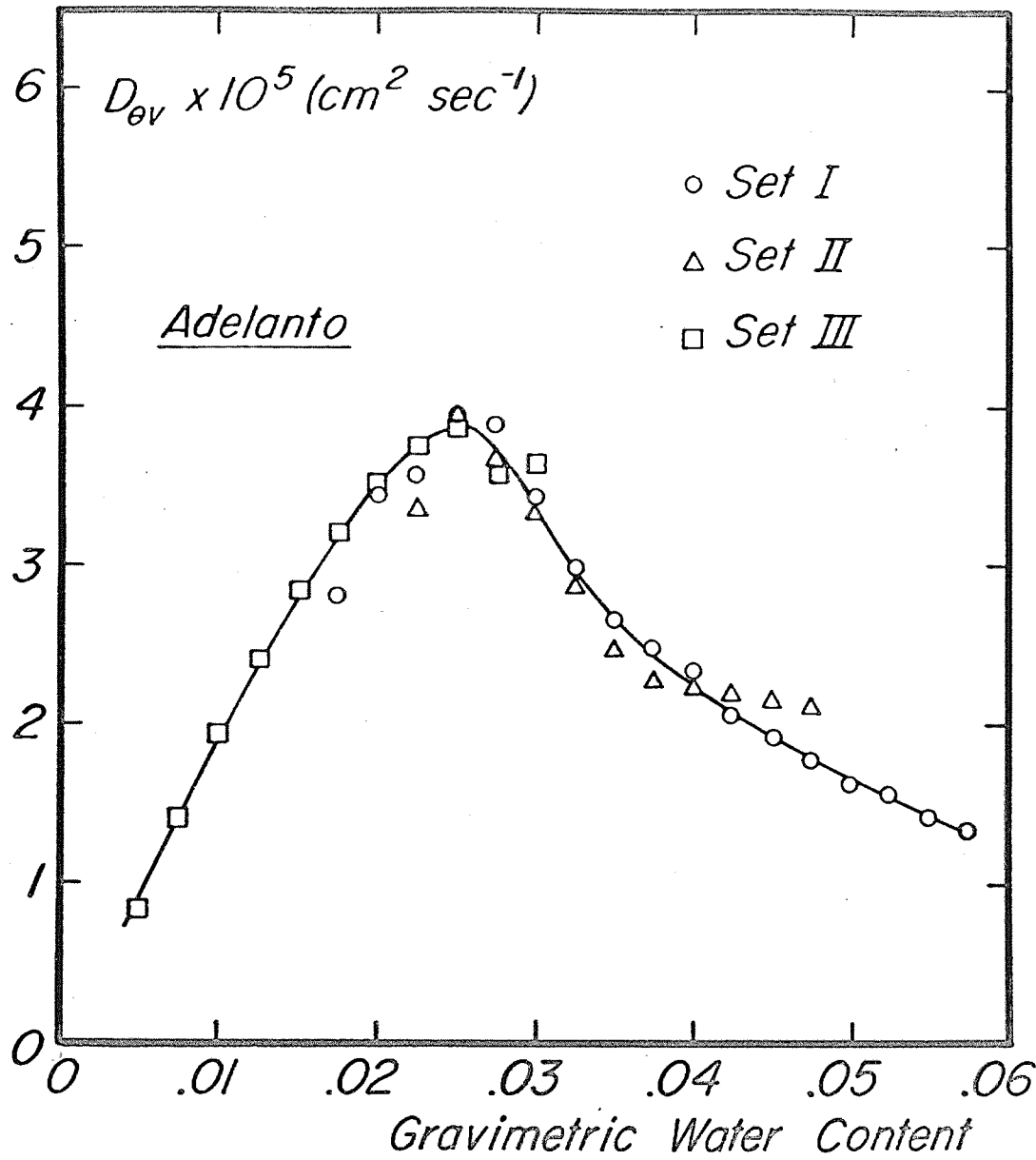


Figure 6. Desorption water content distributions for Pine silty clay and Pachappa loam.



31-22

Figure 7. Sorption diffusion coefficients for Adelanto loam at three sets of boundary and initial conditions. Annual Report of the U.S. Water Conservation Laboratory

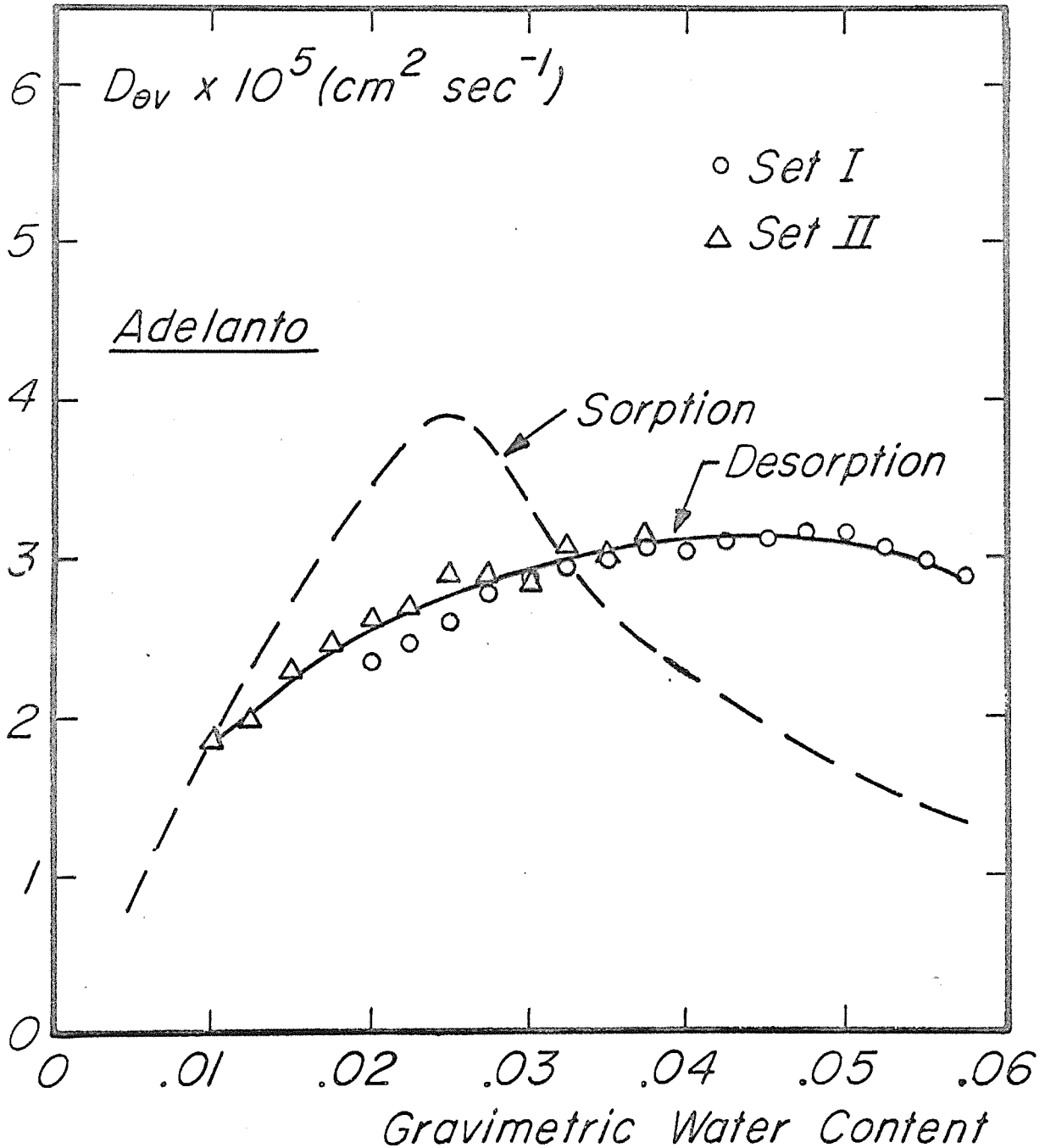


Figure 8. Diffusion coefficients for Adelanto loam.

U.S. Water Conservation Laboratory,
Tempe, Arizona

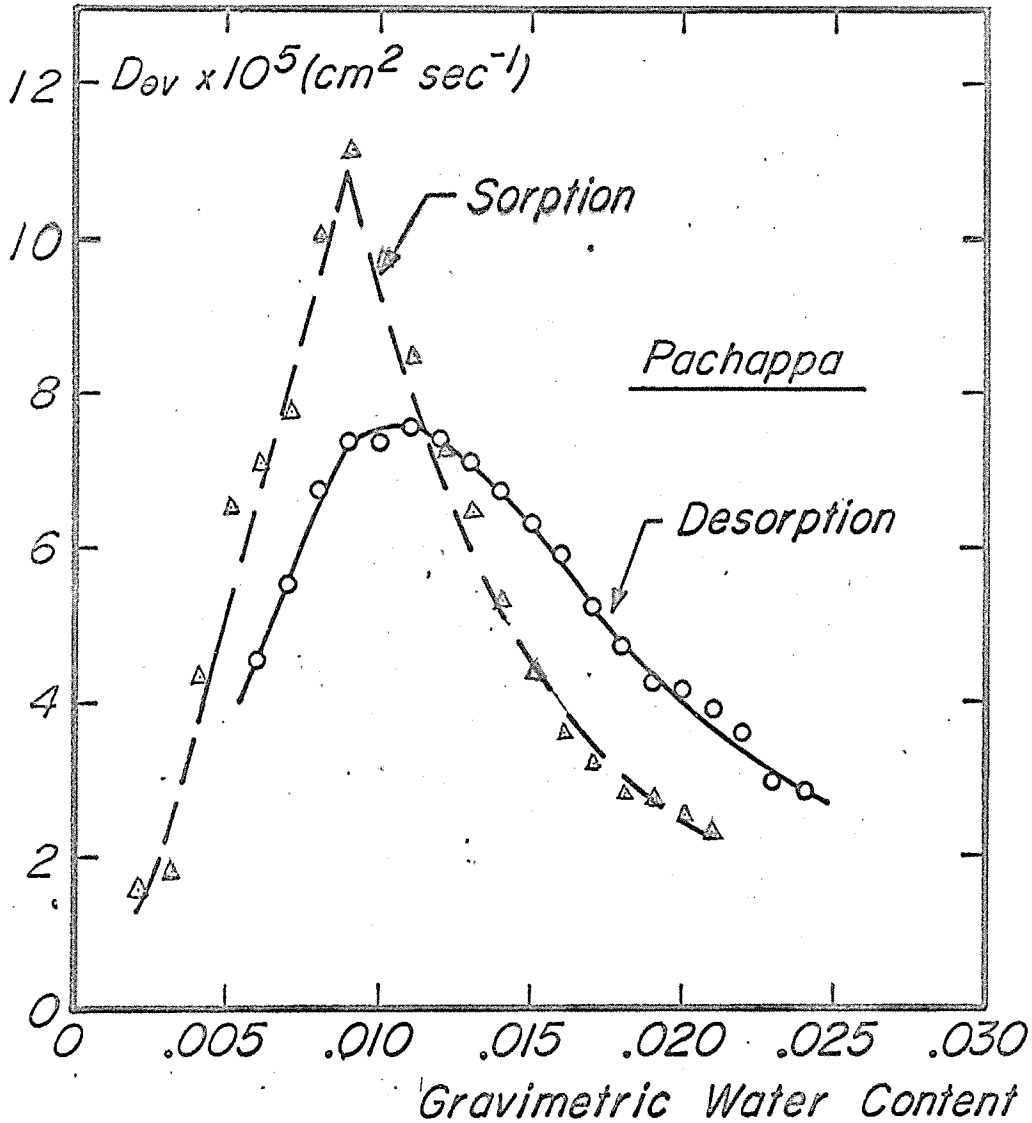


Figure 9. Sorption and desorption coefficients for Pachappa loam.

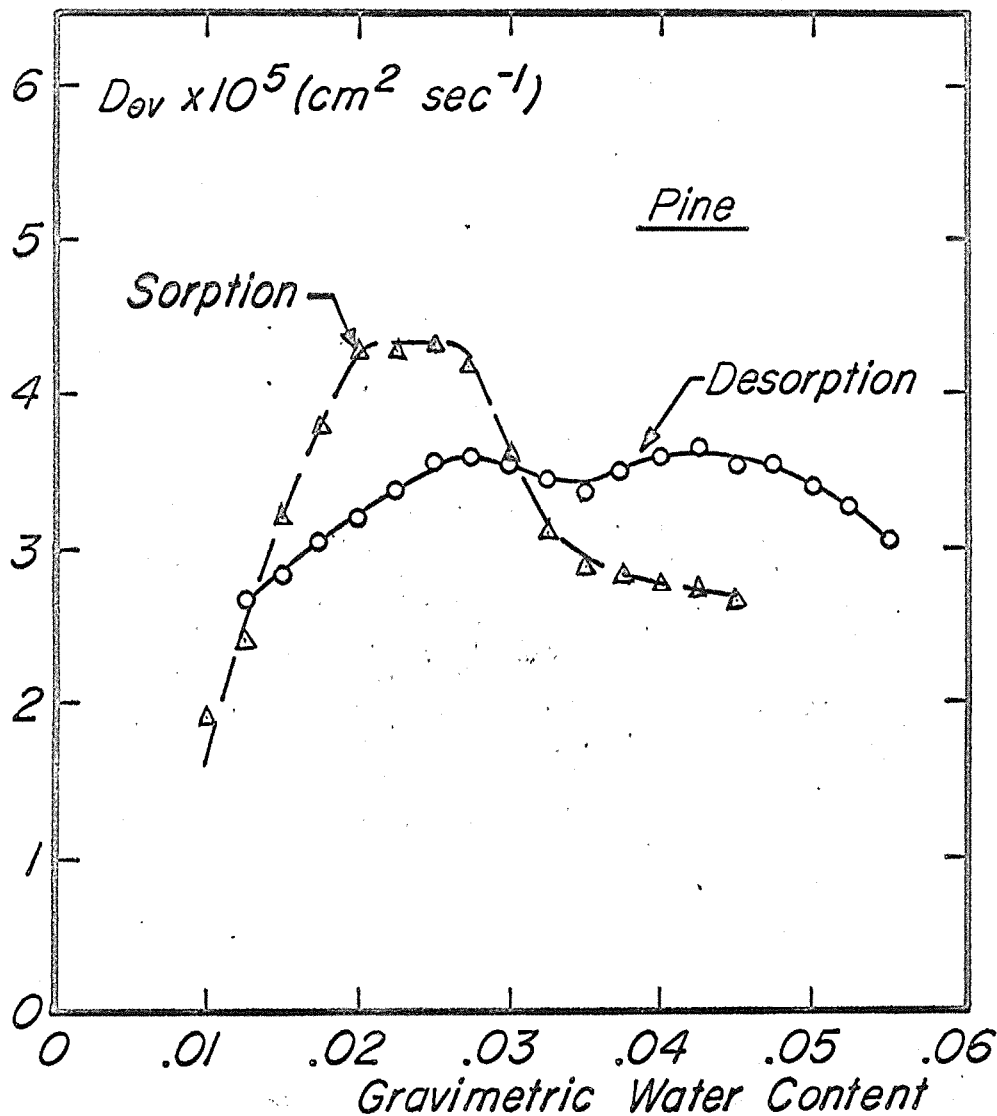


Figure 10. Sorption and desorption coefficients for Pine silty clay.

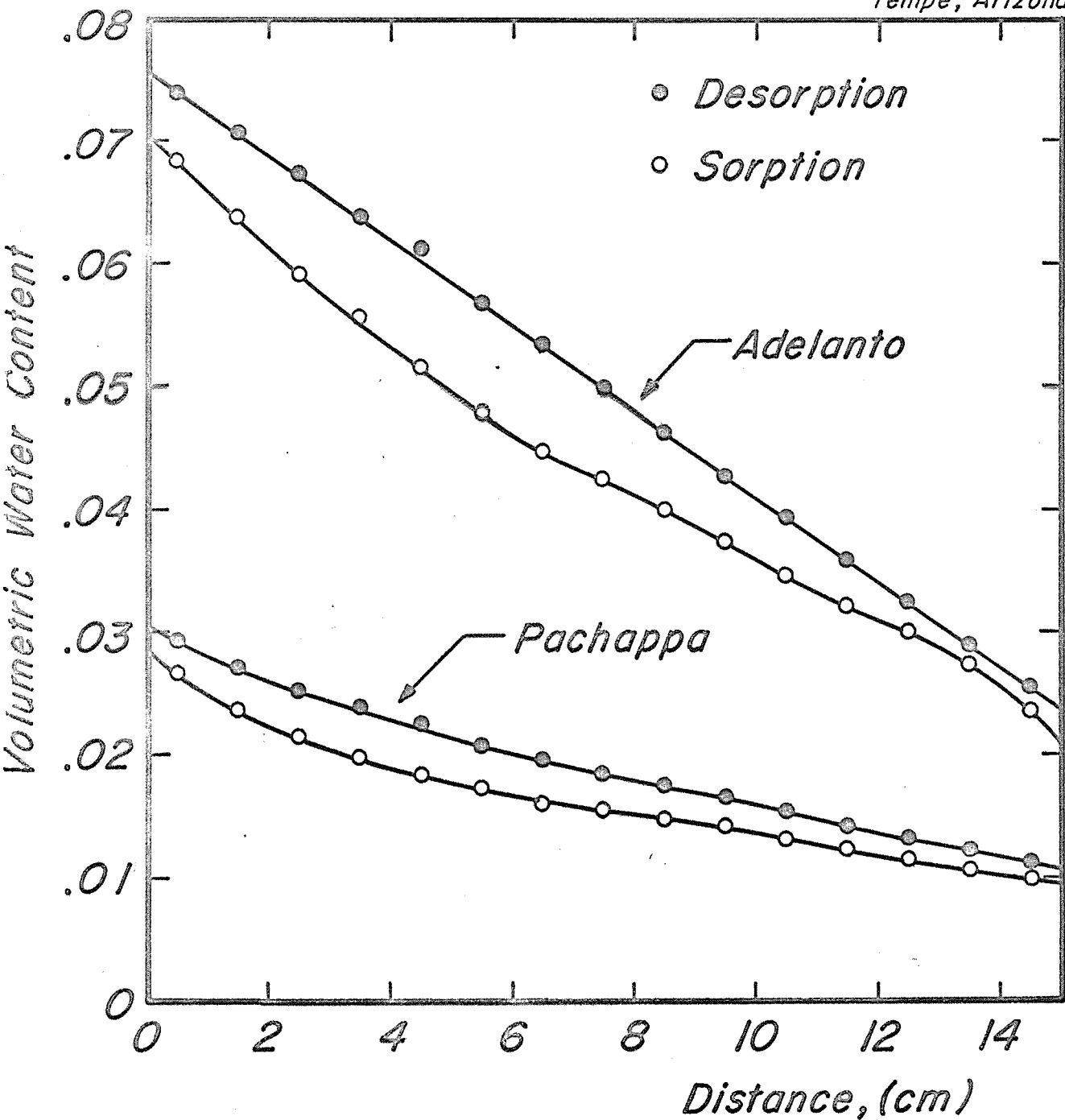


Figure 11. Steady-state water content distribution curves for Adelanto loam and Pachappa loam.

U.S. Water Conservation Laboratory,
Tempe, Arizona

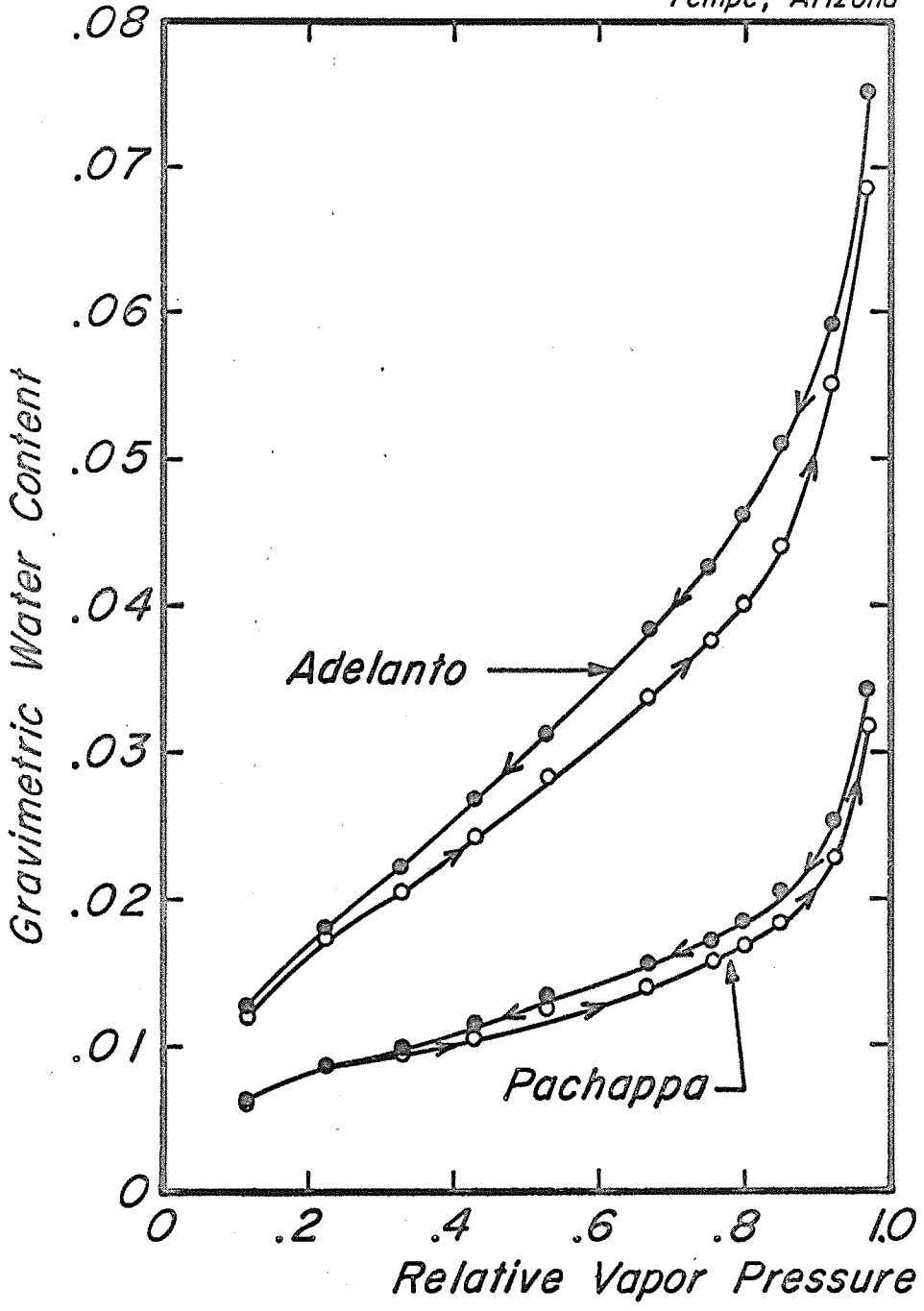


Figure 12. Adsorption isotherms for Adelanto and Pachappa soils. U.S. Water Conservation Laboratory

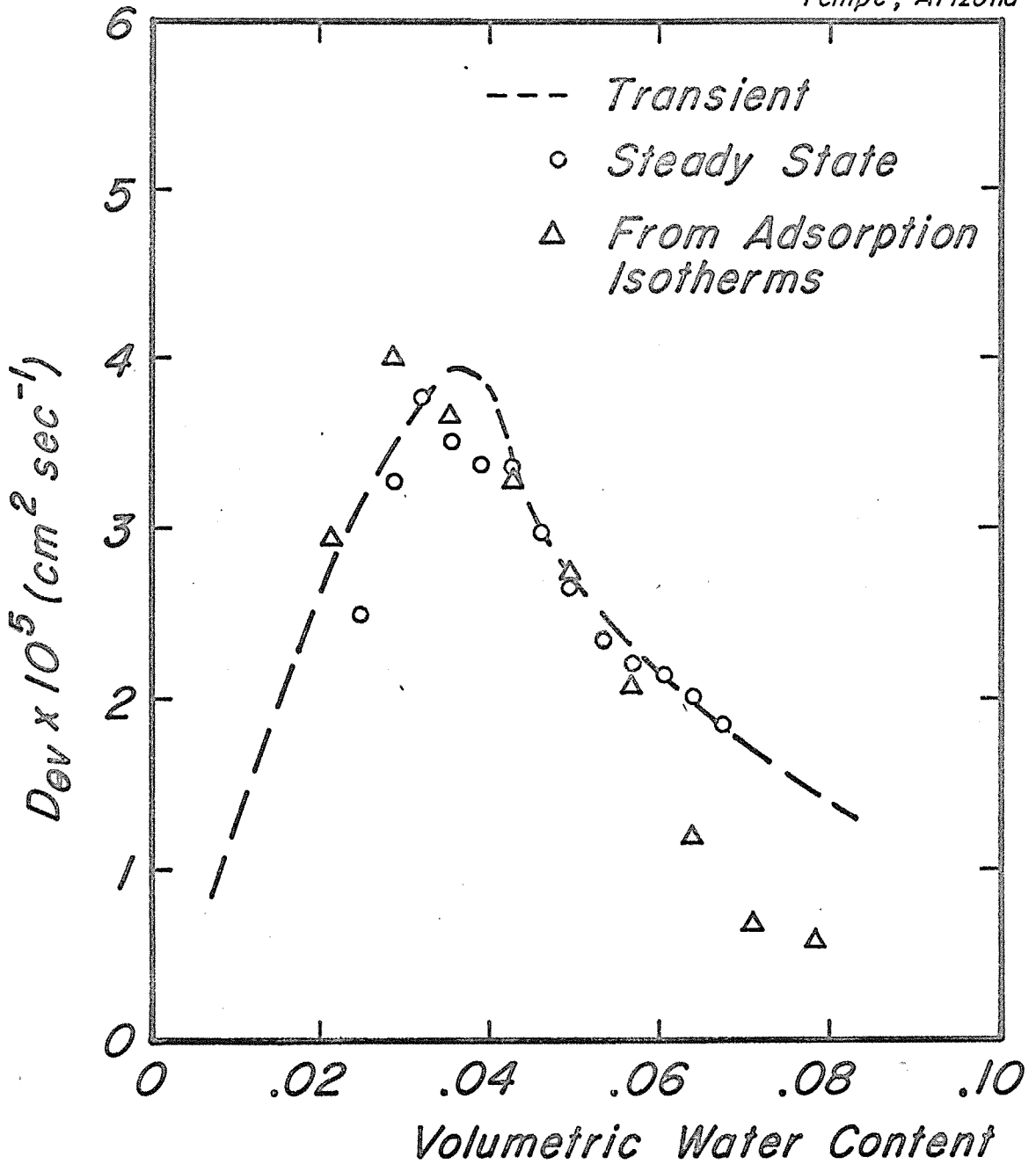


Figure 13. Sorption diffusion coefficients obtained by three methods

for Adelanto loam.

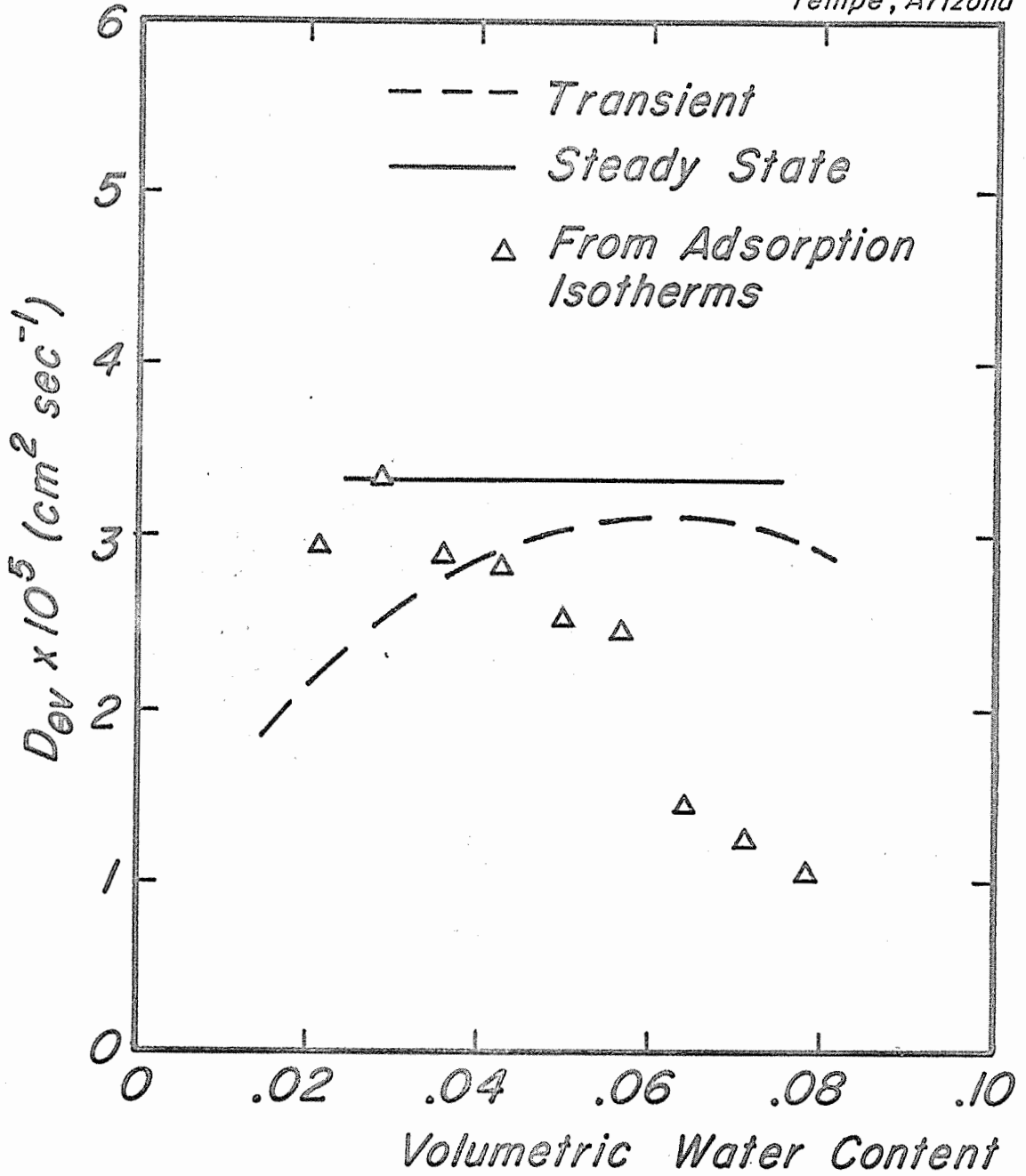


Figure 14. Desorption diffusion coefficients obtained by three methods for Adelanto loam.

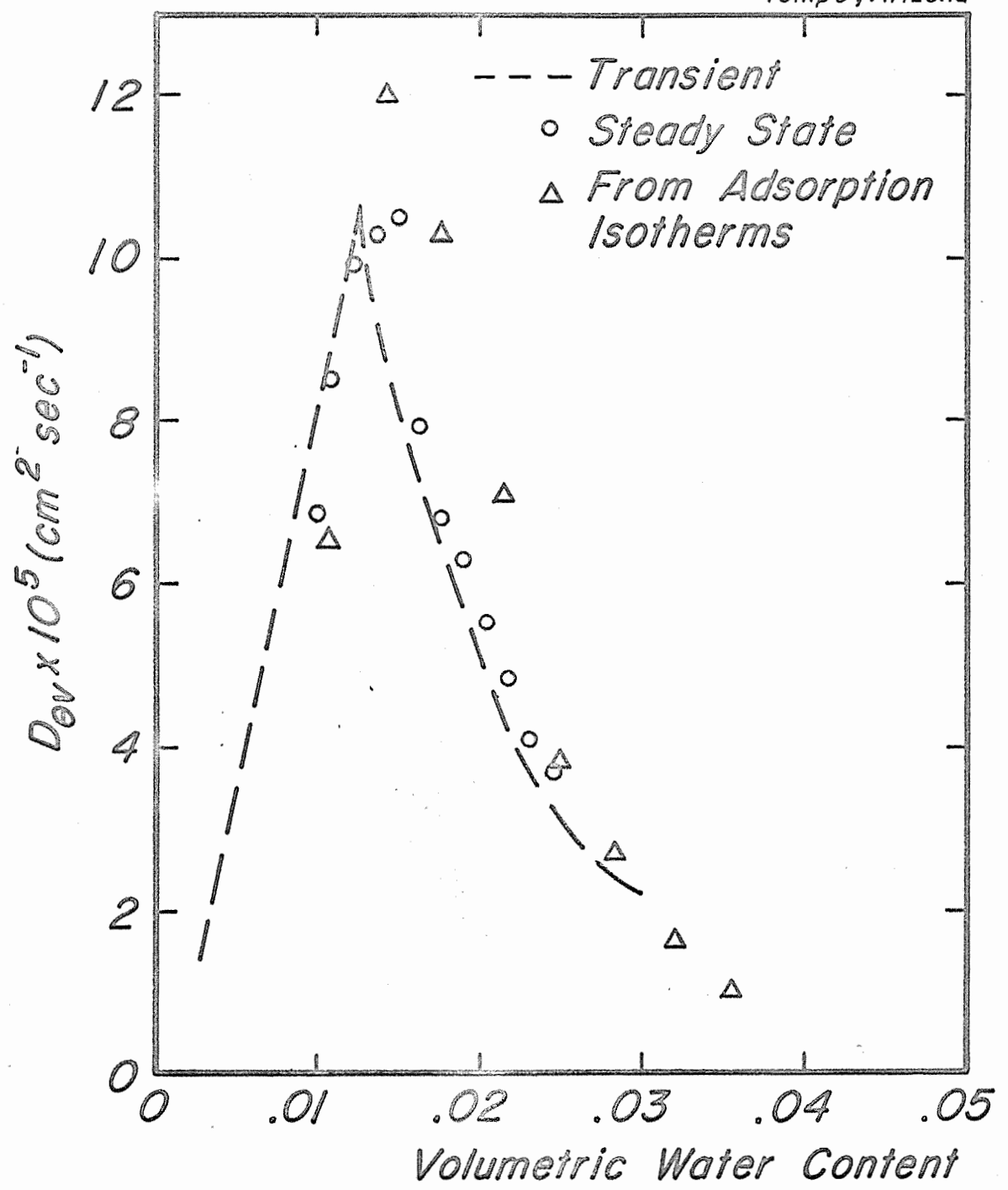


Figure 15. Sorption diffusion coefficients obtained by three methods for Pachappa loam.

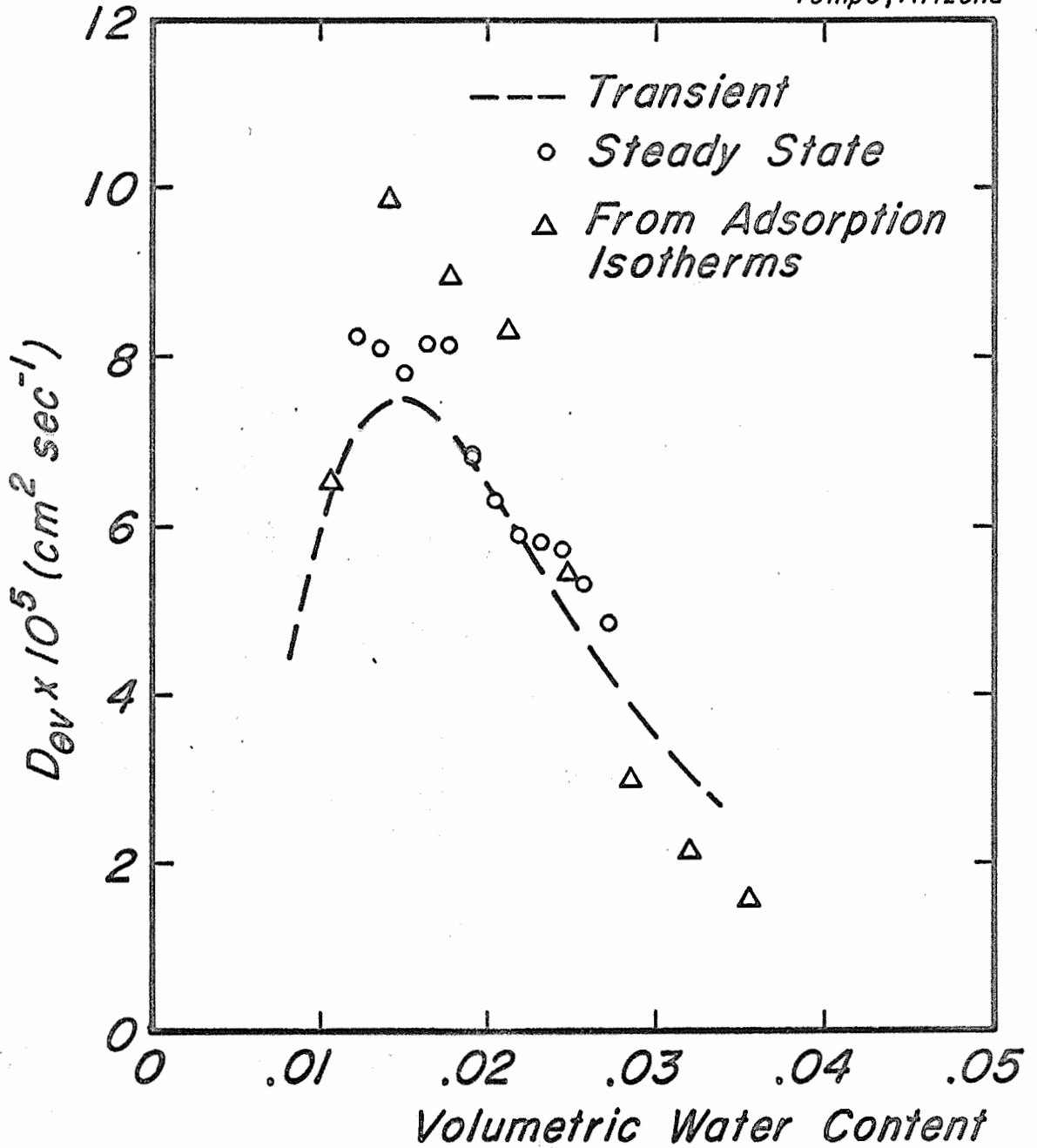


Figure 16. Desorption diffusion coefficients obtained by three methods
for Pachappa loam.

TITLE: DIRECT MEASUREMENT OF EVAPOTRANSPIRATION AND THE ENERGY
BALANCE OF IRRIGATED CROPS

LINE PROJECT: SEC 4-gG2

CODE NO.: Ariz.-WCL-33

INTRODUCTION:

This Annual Report is presented in six parts as follows:

	PAGE
PART 1. Evapotranspiration and energy balance of irrigated alfalfa	33-2
PART 2. Routine measurement of standard weather data in 1963	33-25
PART 3. Test of a prediction method: the combina- tion approach.	33-41
PART 4. Evaporation from a lawn in 1963.	33-53
PART 5. Lysimeter study of the salt balance of an irrigated soil over a three year period.	33-66
PART 6. Construction and evaluation of a simple hydraulic lysimeter.	33-81

PART 1. EVAPORATION AND ENERGY BALANCE OF ALFALFA.

INTRODUCTION:

In late 1962 alfalfa was planted in the lysimeter field. This cover was maintained to date. The purpose of the investigations carried out with this cover was, in the main, threefold: (1) To obtain accurate data on the long-time and short-time consumptive use of alfalfa at different conditions, (2) to systematically collect information on the relationship between gross meteorological variables and the consumptive use of the alfalfa, (3) to use the alfalfa cover as a detailed study object for micrometeorological investigations. Whereas the first two objectives were continually pursued throughout the year, the third one, because of the complexity of the measurement equipment and the necessity for having near-ideal conditions, was limited to a series of 1-, 2-, or 3-day experiments carried out throughout the year. These experiments, coded with the name Alfalfa-63, were 14 in total and took place on 28, 24-hour periods. They are reported in greater detail in WCL-17 and, where an evaluation was made of the combination method for estimating evaporation, in Part 3 of the present experimental outline report.

The purpose of the present section is to give general information on the management of the crop and on the methods of measurement used to obtain a continuous energy balance. Further, the report gives a condensation of the data obtained from continuous observation of the field during 1963.

General Management. Alfalfa was planted on 12 October 1962 and the field irrigated on 12 October. An excellent stand was obtained and by January 1963 the crop had a height of about 25 cm. Heavy frost occurred on 12, 13, and 14 January whereby the crop was damaged and reduced to a height of about 10 cm continuing through the remainder of January. Regrowth started in the first week of February following which the crop was regularly irrigated and trimmed, when necessary, to a height of about 15 cm by means of rotary mower. The date of individual operations such as mowing, irrigation, and of rains may be seen in Table 1. This table refers to check number 4 and lysimeter 2 of

the field since this was the area over which the routine weather observations were made (see Part 2). At times, as will be noted below, the treatment of lysimeters 1 and 3 was different from that of 2.

In order to be able to simultaneously study three different heights of alfalfa, a schedule of differential mowing was followed starting on 1 April. That is to say, lysimeter 3 and checks 5, 6, and 7 of the field were left alone whereas the others were mowed. On 16 April only lysimeter 1 and associated checks 1, 2, and 3 were mowed to a height of 10 cm so that on 22 and 23 April three different heights could be investigated simultaneously (Alfalfa 63-4). Following these observations, on 30 April, the crop on lysimeters 2 and 3 and checks 4, 5, 6, 7, and 8 was mowed to the ground with sickle bar mower. The field was then allowed to become uniform, which was attained by 10 May.

A similar procedure was followed starting 24 June, a three-level cover existing by 8 July. This was studied on the 17 and 18 July (Alfalfa 63-8). The field was then mowed to the ground and became uniform by 5 August.

No further irrigation was applied after 29 July, immediately following the mowing of the field to the ground with the sickle bar mower. This was done in an effort to gradually allow the soil moisture reserves to be depleted and to reduce evaporation for lack of available soil moisture. Not until the second week of September did the alfalfa show signs of distress and did evapotranspiration rates reflect clearly the lack of soil moisture. By the last of September the crop had declined severely and was shedding leaves in many places in the field. Measured evaporation was down to 1 mm day^{-1} .

In the first week of October the crop was mowed to the ground with a sickle bar mower, the field harrowed, fertilized with superphosphate and lightly seeded over. By two heavy irrigations during the latter part of October the stand in the field was successfully re-established and by the middle of November an excellent stand was again obtained which continued through December. The tops of the plants, however, were slightly damaged by frost in the third week of December.

The most pertinent events during 1963 are summarized in Table 1. This table gives by decades, the measured evaporation rate in mm day^{-1} . For those decades where the cover was not uniform, the evaporation is given for lysimeter 2 and in two cases only for a part of a decade since during the remainder the crop was a stubble as a result of mowing. Table 1 also gives the date and the amount of significant rainfall, irrigation and height of the crop. At the beginning of the decade, the date of mowing, and the height to which the field was mowed ^{is shown} as well as a few other pertinent events. It will be seen from Table 1 that, except during periods of recovery after close mowing or frost, the height of the field was around 25 to 30 cm. A notable exception to this is the second and third decades of July where the crop was allowed to grow to a height of 48 cm.

During the early part of the year symptoms of salinity were noted in spots in the field and also in and around the lysimeters. Heavy irrigations during May and June alleviated this problem (see also Part 5). Salinity effects on alfalfa can be noted from a stunted growth, narrowing and thickening of leaves and a dark green to bluish color of the foliage. Young plants may die if conditions persist too long. During the period January through November 1963 about 2200 mm of water were applied to the lysimeters whereas about 1800 mm were lost by evaporation, giving an excess of 300 mm which was available for leaching. The actual measured amount of leachate was 340 mm.

As a general rule, the irrigation schedule was such that the soil moisture content was high and never could have limited water absorption by the plants except during the month of September. Measurement of the moisture content of the soil was done with the neutron method every week until 1 October at 8 depths and 4 locations in the field. Moisture contents generally ranged between 20 and 30 percent by volume. Other than in September, moisture content fell to its lowest level by 18 February, the last irrigation having taken place in the previous October. Moisture content then ranged from about 20 percent at 30 cm to 26 percent at 120 cm depth. The moisture characteristic of the lysimeter soil is given in Figure 1.

At the end of the drying-out period on 1 October, the moisture content was about 16 percent throughout the profile down to 120 cm depth. It was still as high as 24 percent at a depth of 140 cm.

Meteorological Measurements. As indicated above, simple, routine-type meteorological measurements were made continuously over the field in check number 4, in which lysimeter 2 is located. They consisted of a measurement of solar radiation, of net radiation, of air temperature and humidity at 2 m above the surface, and of wind speed at 2 m above the surface. Also, soil temperature at 1 m depth was measured. These data are reported in detail in Part 2.

In addition, on special occasions, detailed micrometeorological studies were made. Generally, these would consist of measurements of net radiation and soil heat flow over all lysimeters, a measurement of reflected short-wave radiation, and sometimes a measurement of incoming and outgoing long-wave radiation. Further, a wind profile would be obtained as well as a measurement of the temperature differential between two levels close to the surface of the air temperature and air humidity. These data are collectively reported in a series of observations coded Alfalfa 63. They are discussed in detail under WGL 17 and they are listed here for reference.

Alfalfa 63-1	08, 13, 14	FEB	Short alfalfa cover in wintertime.
Alfalfa 63-2	26, 27	MAR	Short alfalfa cover in spring.
Alfalfa 63-3	10	APR	Comparison of a long and a short alfalfa cover.
Alfalfa 63-4	22, 23	APR	A comparison of 3 different heights.
Alfalfa 63-5	28, 29	APR	Study of 2 isolated plots, 1 m ² in area, the surroundings having been mowed.
Alfalfa 63-6	20, 21	JUN	Short crop of alfalfa in summertime.
Alfalfa 63-7	03, 04	JUL	Comparison of a long and a short cover of alfalfa.
Alfalfa 63-8	17, 18	JUL	Comparison of 3 heights of alfalfa.
Alfalfa 63-9	25, 26	JUL	Study of an alfalfa stubble.
Alfalfa 63-10	08, 09	AUG	Short alfalfa cover in the late summer.
Alfalfa 63-11	12, 13	SEP	An alfalfa cover subject to limited soil moisture supply.

Alfalfa 63-12	24, 25	SEP	Alfalfa crop with severely limited soil moisture supply.
Alfalfa 63-13	15, 16	OCT	A dry alfalfa stubble.
Alfalfa 63-14	18, 19	OCT	A recently irrigated alfalfa stubble.

RESULTS AND DISCUSSION:

Decade Values of Evapotranspiration. Table 1 gives, in mm day^{-1} the decade averages of evapotranspiration for all three lysimeters or, if the three were not treated equally, for lysimeter 2 only. The latter values are indicated with an asterisk. It can be seen that the decade average for a crop undamaged by freezing may go down to 1.6 mm in the wintertime. On the other hand, the decade average may range as high as 12.4 mm, as in the second decade of July. This decade value undoubtedly reflects to a certain extent the fact that the crop was allowed to grow as high as 35 cm in comparison with an overall height of about 25 cm during the remainder of the year. The effect of height itself will be discussed later on.

The decade values show that evapotranspiration is a relatively conservative quantity, affected only in a minor way by such incidences as the freezing of the crop during the second decade of January and the mowing to a ground stubble as happened during the third decade of April and of July. It will be noted that during the decade following the mowing, the rate of evapotranspiration was not very different from a normal value, reflecting the rapid regrowth of the crop. During the second and third decades of September the consumptive use reflects the limiting influence of soil moisture content, and during the first and second decade of October the incompleteness of the cover. The total actual consumptive use of water by the alfalfa crop for the calendar year 1963 was around 1870 mm. If the crop had been supplied with water during September and October, this value would probably have been somewhat in excess of 2000 mm.

A study was also made of the maximum daily values of evapotranspiration by decades. These are reported in Table 3. The first column in this table gives the average decade value and is the same as the first column in Table 1. In the second column, the maximum daily evapotranspiration during each decade is shown. If decades

during which irrigation of a bare stubble are excluded (first decade of May and second decade of October it will be seen that evapotranspiration never exceeds the average decade value by a very large fraction. Thus the highest amount ever measured, 13.9 mm in the second decade of July, was only 1.5 mm in excess of the average for the same period. Actually, percentage or fractional deviation of the maximum values seem to be greater during the winter period than at any other time of the year. This is in keeping with the idea suggested by the combination approach (see Part 3), which is that advective effects should dominate during the cool periods rather than during the warm periods. In absolute terms, however, the deviation of the maximum from the average values are no greater in winter than they are in the summer.

The following pertains to the effects of individual management practices on consumptive use. Though the detailed data are not given here, it is very clear that the irrigation of a full-grown stand of alfalfa has no measurable effect whatever upon the rate of evapotranspiration, unless soil moisture had been inadequate. The foregoing statement applied on 19 February when the last irrigation was four months previous. It also applied on April 4 when 30 days had elapsed since the last irrigation and on 29 May when the previous irrigation had been 24 days earlier. The only irrigation that had a measurable effect on consumptive use was the one that took place on 17 October after the crop had been permitted to dry out the soil since 29 July. Thus we may conclude, that as long as soil moisture levels are held at an adequate level, the frequency of irrigation of alfalfa will have an insignificant effect on consumptive use.

Another important management factor is mowing the crop. Reducing the height of alfalfa either by a trim cut or cutting to the ground always has a significant effect upon consumptive use. The day following a trim, evaporation is often cut to one-half or the original value. However, within four to five days, the original level may be attained. Cutting the crop to the ground reduces evapotranspiration to low values, around 2 mm day^{-1} . Recovery may require up to 7 days during which the

evapotranspiration varies with height almost linearly. It is also of considerable interest to note that the evaporation from a recently irrigated stubble is always less than that from a fully grown crop. This is in accord with the studies of evaporation from bare soil in previous years, that have indicated that these values are by no means the maximum possible ones.

Energy Balance Studies by Decades. Using the routine data on net radiation and ignoring, for daily and decade values, the soil heat flux, an energy balance was calculated for each decade and reported in Table 2. This table gives in column 1 the actual measured decade average of evaporation, and in column 2 the measured decade value of net radiation. Column 3 gives the evaporative energy flux and column 4 the energy derived from or given off to the air, computed as a difference. Column 5 gives the ratio of the latent heat flux to the net radiation.

The significant information in Table 2 is that with the exception of those periods during which the crop was damaged by frost (decades 2 and 3 of January) and during which moisture was limiting either by low moisture content or by the fact that the cover was incomplete (decade 2 of September through decade 1 of November) the value of A is positive. That is, as a general rule, a fully grown crop of alfalfa that has a non-limiting supply of soil moisture will evaporate in excess of the available net radiation at our location. This excess amount, on a fractional basis, may be as much as 50 percent in both the winter and in the summer, but will average less, around 20 percent. Looking at the column for A, it is obvious that the effect of advection on consumptive use in absolute terms is by far the greatest during the months of June and July.

In Part 3 it has been demonstrated that the effect of ambient weather conditions is rather accurately taken into account by the combination method. This, then, leads us to recognize that the large advective effects, in terms of absolute quantities of water involved, occurring during the latter part of May, June and July are directly associated with the high vapor pressure deficits. Since radiation is also highest during this same period, it is no surprise that

consumptive use during this period is exceedingly high. If water is to be saved in significant quantities, alfalfa should not be maintained in a vegetative condition during the months of June and July which would mean that a final irrigation should be applied in the latter part of April, with the following irrigation to take place around 15 August.

On individual days the advective effects can, of course, be much greater than those noted for decades. The extent to which this happens can be seen in Table 3, already referred to earlier. In this table, a value for the highest daily evapotranspiration in each decade is given in the second column, whereas the third, fourth and fifth columns give the energy balance, also for that same day. Generally, the fractional amount to which evaporative flux exceeds net radiation on days of maximum evaporation is around 50 percent and does not seem to differ significantly between the wintertime and summertime. Again, the excursions from the average represent much larger absolute quantities of water in the summertime than in the wintertime. We find that on at least one day in June an amount of water, almost equal to that of the net radiation received, was lost as a result of sensible heat inflow, to a total amount of approximately 6.5 mm.

The maximum daily figure for water loss caused by advective effects alone can be put between 1 mm in the wintertime to about 5 mm for the summertime. The days of maximum advection are invariably associated with days of high wind speed. Thus, in the prognostication of climatological evaluation of possible or potential amounts of evapotranspiration, wind speed must definitely be taken into account. It appears that the combination approach (Part 3) does this accurately.

From Tables 2 and 3 we can conclude that the evapotranspiration from alfalfa may occasionally exceed the amount of energy available from net radiation very significantly in individual days. On the average, it will exceed net radiation measurably but not drastically, a typical figure being around 20 percent. From this broad statement, we can arrive at a very approximate evaluation of the maximum potential evapotranspiration from alfalfa in the Phoenix area. This rough estimate given in table 4, is obtained by taking during each decade of the

year, the maximum value for net radiation and converting it to millimeters of water, adding 20 percent to account for the average sensible heat input. Thus, monthly totals in Table 4 are obtained in millimeters, giving a total for the year of 2018 mm. The total of 2018 mm is not much higher than the actual measured value of about 1870 mm during 1963. When the latter total is adjusted for the period of drought during September and part of October, a figure very close to 2,000 mm is obtained as noted earlier. This would indicate that the maximum potential evapotranspiration is closely reached year in and year out, provided moisture is available for evapotranspiration. The reason for this is primarily that the Phoenix climate has near maximum radiation every year. A detailed and critical examination of this proposition must be based on climatological studies of radiation, wind speed, and vapor pressure deficit, but it is not likely to reveal anything very much different from what has been stated here.

For reference purposes, Table 4 also gives the equivalent amount of evapotranspiration in inches. It is of interest to compare these values with previously reported measured values for consumptive use using soil moisture measurements. Column 3 gives values as reported by Harris in a provisional supplement to SCS-TP-96. Actually, two sets of values were obtained, one between 1931 - 1954 and the other between 1945 - 1946. During August and the first half of September the alfalfa was "resting" and evidently it was assumed that there would be no consumptive use during that period. When the values computed here as maximum amount of consumptive use are similarly adjusted by subtracting the entire amount for August and half of that for September, a total of 66.1 inches is obtained as compared to the figures of 56.5 and 51.0 reported by Harris. It will be seen that the discrepancy occurs principally during the winter and early spring months

Inasmuch as the figures obtained in 1963 are in agreement with micrometeorological estimates (see Part 3), the values reported by Harris during the winter and spring months must be too low. Although it is not known what the cause for this might be, it is unrealistic to assume that the consumptive use during the months of August and

the first half of September is zero, even though the alfalfa is not irrigated. For two reasons, then, the figures given on the measured annual use of well-watered alfalfa, as supplied by Harris, seem to be on the low side, some 20 to 30 percent too low. Since the so-called Blaney-Criddle coefficients are computed by using actually measured values, all estimates of consumptive use based on the Blaney-Criddle method, as applied to alfalfa are too low by the same amount.

One objection that may be raised against the field applicability of the data on alfalfa reported here, is that the size of the field is such that an alfalfa field of, say, 10 or 20 times the experimental field would, on the average, show lower figures for consumptive use. The fact that a meteorologically based estimate of evapotranspiration comes very close to the actually measured ones, would speak against any significant role of the size of the field. Additional evidence must be obtained, however, before the argument concerning the size of the field can be fully refuted.

The Effect of Height of Alfalfa on its Evapotranspiration. During five periods in 1963 different heights of alfalfa were maintained on the three lysimeters by mowing either 1 or 2 of them and not the other 2 or 3, (see Table 5). During period A, two different heights were thus maintained and during period B three different heights. It may be seen in Table 5 that during periods A and B the average daily evaporation was obviously related to the height of the crop. In all instances the crop was in a vegetative stage and the cover was very complete.

Another differential mowing experiment was started on 24 June which can be studied in three periods, also given in Table 5. During this experiment the stand was somewhat less dense. Bare soil and trash was visible through the canopy when it was mowed to the trimming height of roughly 16 cm. During period C the effect of height is again noticeable though there was also a difference between lysimeters 1 and 2 which were at the same height. During period D the fact that lysimeter 2 was now higher than 1 was not noticeable but lysimeter 3, which was the tallest, showed a definitely higher evaporation rate. During this period, flowers appeared on lysimeter 3.

In contrast to the previous two periods, period E gives again a very clear-cut demonstration of the effect of height in spite of the fact that the crop on lysimeter 3 was now in almost full bloom and a number of blossoms had appeared on lysimeter 2.

Generalizing the results given in Table 5 we can see that the height of alfalfa generally has a substantial influence on the evaporation rate. This is in keeping with the fact that throughout the entire year heat was derived from the overlying air in the evapotranspiration process. Obviously, through a greater roughness, crop height and possibly canopy flow the interchange of the overlying air mass with the crop is more vigorous for a taller crop than a shorter one. Another conclusion reached from this data is that the appearance of flowers in the alfalfa does not seem to have had any noticeable effect on its transpiration. In this respect, the data are in sharp contrast with those obtained for sudangrass in 1962.

Several detailed energy budget and micrometeorological comparisons were made over the three different heights. These are reported under WCL 17.

Effect of Declining Soil Moisture Content and Availability on Evapotranspiration from Alfalfa. One of the most frequently asked questions concerning the relationship of water management and water use by crops is to what extent soil moisture content has an influence on consumptive use. A number of recent investigations have made it clear that there is no single or simple answer to this question because the moisture holding properties of the soil, the nature of the crop, and the atmospheric demand for transpiration must all be considered and for any given combination may give rise to a different answer.

In the case of the alfalfa field in 1963 the matter is simplified to a situation where the soil is homogeneous and yields moisture gradually as soil moisture tension increases (see Figure 1). Furthermore, there was a well-established stand with a deep and presumably homogeneous root system. Finally, the atmospheric demand, with minor exceptions, is near constant from day to day and shows only a gradual change with the progress of the season. Probably, the best answer as

to how a declining moisture supply affects transpiration by alfalfa could be had from a continuing computation of the potential evaporation from the alfalfa cover using a combination formula (see Part 3) and to note the difference between actual and potential evapotranspiration. At this time there is no complete analysis of the data available to this end. Therefore, a simplified analysis is given in the present report in anticipation of a more complete one currently under preparation.

It will be recalled that on 23 July the entire lysimeter field was mowed to the ground, at an approximate crop height of 4 cm and that on 29 July following the entire field was irrigated so as to bring the soil to the maximum field moisture content. For a rooting depth of 1.5 m this would represent an available moisture reserve, between the 15 atmospheric percentage and the maximum moisture content, of approximately 300 mm. The crop recovered rapidly from the mowing and an analysis of data for 9 August indicated that on that day the crop was transpiring at the potential rate, as calculated from net radiation and other standard weather data. The amount of heat derived from the air for evaporation was about 50 ly day⁻¹ and this level of advection was maintained for the duration of the entire month of August and the first part of September.

The changing nature of the energy balance during the period of moisture depletion is indicated in Figure 2, in which the daily amounts of evaporative flux, net radiative flux, and the sensible heat exchange between surface and the air are given. Pending more detailed analysis, we conclude that until about 4 or 5 September, that is, the first 36 days of the period of moisture depletion, the declining moisture content of the soil had no measurable effect on the transpiration rate. By the last day of August, the total amount of loss by evaporation was 250 mm but, also, 70 mm of rain had fallen. Thus, the available moisture was depleted to about 120 mm. By 5 September, an additional 30 mm had been lost, reducing the moisture reserves to approximately 90 mm.

After 5 September the sign of A began to change from positive to negative and a steep decline in the evaporation rate was noted beginning with 10 September. An analysis of the actual and potential

evapotranspiration for 12 September indicated that the actual evaporation was .63 of the potential rate, indicating a substantial resistance to moisture loss in the leaves, presumably by partial closure of stomates. The crop itself also showed definite signs of stress by a change of color and partial wilting during the afternoon. On 12 September the available soil moisture reserves had declined further to approximately 50 mm. During the last decade of September the crop showed definite signs of moisture stress, growth had ceased completely, and dead leaves appeared on the branches. By 2 October the evaporation rate had declined to about 1.4 mm day^{-1} and a large portion of the net radiation received was returned to the air as sensible heat. If the estimate of 300 mm of the original moisture reserves is correct, then these were entirely depleted by the end of September and the experiment was considered to have come to an end.

An approximate evaluation of the data shows that transpiration proceeded at a potential rate for as long as moisture had not depleted to less than one-third of the original amount. By the time the actual evapotranspiration rate was one-half the potential rate, moisture reserves had probably declined further to about one-fifth of the original amount and the remainder was slowly extracted at very much reduced rates until the crop had become virtually dormant. Even under those conditions, moisture loss continued at a rate of approximately 1 mm day^{-1} . This however, is not necessarily related to transpiration but has also been found to occur on dry bare soil (see Annual Report for 1961).

It is further worthy of note that the records of the crop height indicated that appreciable growth rates persisted through the first week of September but that very little growth was noted after that time.

Our observations definitely refute two extreme views, often held, the first one being that transpiration would decline more or less in proportion to the moisture reserves available to the plant and the other being that transpiration goes on unabated until the entire supply of available soil moisture is exhausted. If the two months' period, August through September, is considered as a single irrigation

cycle, it will be seen that potential rates of transpiration prevailed for the better part of this cycle. There would seem to be little agronomic advantage in protracting the cycle to the length of time that we carried it since there was virtually no growth after approximately 15 September. Thus it appears on superficial analysis that during the time the crop was making appreciable growth and accumulating dry matter, transpiration proceeded at the potential rate. It is of further interest to observe that the period of desiccation had no apparent harmful effect on the alfalfa crop since it made an excellent recovery after it was irrigated on 17 October.

SUMMARY AND CONCLUSIONS:

A crop of alfalfa was observed continuously during the calendar year 1963 as to its hourly and daily rate of moisture loss to the atmosphere. From the required meteorological observations, a continuous daily energy balance over the crop was obtained. With the exception of a period immediately following a damaging frost, and a period of approximately three to four weeks during which soil moisture had been depleted close to the limit of availability to the plants, the water losses from the crop proceeded at a rate which can be arrived at from meteorological variables as the potential rate. This implied that the ability of the crop to absorb, conduct, and transmit water through the leaves to the atmosphere did not significantly determine the rate of water loss. Rather, this rate was determined by external factors.

Under the conditions prevailing at the site of observation, significant amounts of sensible heat were extracted from the air on behalf of the evaporation process. As a general rule, this amount of energy was equal to about 20 percent of the net radiation received at the surface. This figure would apply during the winter as well as during the summer, but obviously during the summer much larger absolute quantities of energy were involved than in the wintertime.

The evaporation losses from the alfalfa varied from approximately 1.5 mm day^{-1} in December and January to a maximum of 12.5 mm day^{-1} which was observed during a 10 day period in July. The total amount of water lost by the crop was about 1850 mm, which amount would probably have been slightly in excess of 2000 mm if water had not been

withheld from the crop during the entire month of August and September. The consumptive use rates as measured are significantly in excess of those based on soil moisture measurements and reported earlier in the literature. The earlier values, and the empirical estimated of consumptive use of alfalfa based thereon, seem to be too low primarily during the winter months. It also seems in error to assume that consumptive use would be zero during the latter part of the summer when alfalfa is not irrigated (1 August through 15 September) in the central Arizona area.

Though the evaporative losses from alfalfa are meteorologically determined, the nature and, in particular, the height of the cover has a significant influence on the evaporation rates. Two separate experiments demonstrated that a factor 2 in the height of the alfalfa stand would result in an increase in rate of water loss anywhere from 25 to 35 percent. This effect is attributed to differences in the roughness parameter of the respective covers and the resultant increase in efficiency with which the overlying air can exchange heat with the evaporating crop surface.

A preliminary analysis of the effect of declining soil moisture supplies on the evaporative losses from alfalfa cover indicated that the latter proceed at a potential rate until at least two-thirds of the soil moisture reserves had been depleted. When four-fifths of the total reserves had disappeared, the growth of the crop came virtually to a standstill and the evaporation rate declines to about one-half of the potential rate.

These observations tentatively suggest that, as long as agronomically desirable moisture conditions are maintained in the root zone, the moisture losses from alfalfa proceed at a rate which is determined by meteorological factors.

Furthermore, the data indicate that irrigation of a well developed stand of alfalfa has no measurable effect on its evaporation rate as long as soil moisture reserves are not considerably depleted.

Table 1. Evaporation, rain, irrigation, and management of alfalfa by decades in 1963.

Month	Decade	Evap. mm/day	Irrigation or Rain	Crop Ht.** (cm)	Day	Events & Remarks	
Jan	1	1.64	R 03,10	18 mm	25	02	Mowed to 20 cm.
	2	1.14			18	12-14	Freezing-crop damaged.
	3	1.33			10		
Feb	1	2.70	R 10,11	21 mm	9		
	2	2.48	I 19	130 mm	11		
	3	4.43			15		
Mar	1	4.65	I 07	90 mm	25		
	2	4.09	R 17,18	8 mm			
	3	4.99	I 19	100 mm	28	14-15	Mowed to 10 cm.
Apr	1	* 5.09	I 04	91 mm	13	05	Mowed to 13 cm.
	2	* 6.54			15	16	
	3	* 7.84 ^{1/}	R 25	6 mm	28	24-30	Mowed to ground
May	1	* 6.02	I 02,03				
	2	8.48	07	218 mm	5	10	Mowed to 18 cm.
	3	8.28	I 29,31	250 mm	20	16 24	Mowed to 16 cm. Mowed to 16 cm.
Jun	1	10.16			30	04	Mowed to 16 cm.
	2	10.40	I 11	140 mm		10	Mowed to 16 cm.
	3	*10.97	I 18 I 28	130 mm 100 mm	16 30	14 24	Mowed to 16 cm. Mowed to 16 cm.
Jul	1	*10.93	I 05	100 mm	20		
	2	*12.42	I 16	140 mm	35		
	3	*11.82 ^{2/}	R 22,27 I 29	5 mm 140 mm		48	23
Aug	1	7.63	R 01,04				
	2	7.92	06	6 mm	23	05	Mowed to 19 cm.
	3	6.80	R 12,14 16,17 R 21,22 25,30,01	14 mm 49 mm	34 20	14	Mowed to 19 cm.
Sep	1	6.22			25		
	2	3.74	R 13	1 mm	33		
	3	1.90			36		Crop is drying up & has dead leaves
Oct	1	0.71			35	02	Mowed to ground.
	2	1.75	I 17	140 mm		03-10	Work up and seed
	3	2.62	I 28	140 mm	3		

Table 1. Continued.

Month	Decade	Evap. mm/day	Irrigation or Rain	Crop Ht. (cm)	Day	Events & Remarks
Nov	1	2.60	R 01,07	8 mm	20	
	2	3.08			30	
	3	2.43	R 21	9 mm	32	29 Mowed to 16 cm.
Dec	1	2.00			16	
	2	1.28			18	
	3	1.49			15	Periodic night frosts

**Crop heights are on the nearest date of the beginning of each decade and also for lysimeter 2 only.

*Value for lysimeter 2 only, since three different treatments were in effect.

1/ Value for first 4 days only.

2/ Value for first 2 days only.

Table 2. Evaporation and energy balance over alfalfa by decades in 1963

Month	Decade	E	R _n	-LE	A	-LE/R _n
		mm	ly	ly	ly	
Jan	1	1.64	59	96	37	1.62
	2	1.14	94	66	- 28	.70
	3	1.33	122	78	- 44	.64
Feb	1	2.70	132	157	25	1.19
	2	2.48	163	145	- 18	.89
	3	4.43	179	258	79	1.44
Mar	1	4.65	205	271	66	1.32
	2	4.09	234	238	4	1.02
	3	4.99	246	291	45	1.18
Apr	1	* 5.09	*270	297	27	1.10
	2	* 6.54 _{1/}	*301 _{1/}	381	80	1.27
	3	* 7.84 _{1/}	*340 _{1/}	457	117	1.34
May	1	* 6.02	*377	351	- 26	.93
	2	8.48	403	494	91	1.23
	3	8.28	372	483	111	1.30
Jun	1	10.16	417	592	175	1.42
	2	10.40	447	606	159	1.36
	3	*10.97	*476	640	164	1.34
Jul	1	*10.93	472	637	165	1.35
	2	*12.42	473	724	251	1.53
	3	*11.82 _{2/}	347 _{2/}	689	342	1.98
Aug	1	7.63	376	445	69	1.18
	2	7.92	375	462	87	1.23
	3	6.80	329	396	67	1.20
Sep	1	6.22	323	363	40	1.12
	2	3.74	301	218	- 83	.72
	3	1.90	294	111	-183	.38
Oct	1	0.71	211	41	-170	.19
	2	1.75	192	102	- 90	.53
	3	2.62	201	153	- 48	.76
Nov	1	2.60	162	152	- 10	.94
	2	3.08	145	180	35	1.24
	3	2.43	124	142	18	1.14
Dec	1	2.00	121	117	- 4	.97
	2	1.28	109	75	- 34	.69
	3	1.49	107	87	- 20	.81

*Evaporation E and R_n data is for lysimeter 2 and check 4 only due to inhomogeneous crop cover on field.

1/ Value for first 4 days only, due to mowing to ground.

2/ Value for first 2 days only, due to mowing to ground.

Table 3. Maximum daily evaporation by decades and energy balance on day of occurrence over alfalfa, 1963.

Month	Decade	E	E _{max}	R _n	-LE	A	-LE/R _n
		mm	mm	ly	ly	ly	
Jan	1	1.64	3.04	88	177	89	2.01
	2	1.14	2.76	82	161	79	1.96
	3	1.33	1.86	117	108	- 9	.92
Feb	1	2.70	3.54	153	206	53	1.34
	2	2.48	3.68	182	214	32	1.18
	3	4.43	4.90	210	286	76	1.36
Mar	1	4.65	6.90	198	402	204	2.03
	2	4.09	6.26	233	365	132	1.57
	3	4.99	6.21	265	362	97	1.37
Apr	1	* 5.01	7.07	280	412	132	1.47
	2	* 6.54 ^{1/}	7.55	323	440	117	1.36
	3	* 7.84 ^{1/}	9.51	349	554	205	1.59
May	1	* 6.02	9.01	360	525	165	1.46
	2	8.48	9.71	409	566	157	1.38
	3	8.28	9.43	416	550	134	1.32
Jun	1	10.16	13.83	417	806	389	1.93
	2	10.40	11.80	468	688	220	1.47
	3	*10.97	13.40	453	781	328	1.72
Jul	1	*10.93	12.41	499	724	225	1.45
	2	*12.42	13.92	465	812	347	1.75
	3	*11.82 ^{2/}	13.23	465	771	306	1.66
Aug	1	7.63	9.70	393	566	173	1.44
	2	7.92	9.50	423	554	131	1.31
	3	6.80	8.22	390	479	89	1.23
Sep	1	6.22	7.12	359	415	56	1.16
	2	3.74	5.47	345	319	- 26	.92
	3	1.90	2.45	304	143	-161	.47
Oct	1	0.71	1.12	272	65	-207	.24
	2	1.75	4.79	208	279	71	1.34
	3	2.62	2.84	214	166	- 48	.78
Nov	1	2.60	3.86	204	225	21	1.10
	2	3.08	4.08	146	238	92	1.63
	3	2.43	3.26	138	190	52	1.38
Dec	1	2.00	2.31	114	135	21	1.18
	2	1.28	1.69	94	99	5	1.05
	3	1.49	2.25	97	131	34	1.35

^{1/} Value for first 4 days only.

^{2/} Value for first 2 days only.

Table 4. Estimated maximum consumptive use from alfalfa in the Phoenix area (columns 1 and 2) and consumptive use data by Harris (columns 3 and 4).

Month	1	2	3	4
	mm	in.	in.	in.
Jan	57	2.2	1.5	1.0
Feb	108	4.2	2.5	2.0
Mar	140	5.5	4.0	3.5
Apr	190	7.5	6.0	5.0
May	239	9.4	7.5	6.5
Jun	268	10.6	10.0	9.0
Jul	286	11.3	12.0	12.0
Aug	241	9.5	--	--
Sep	202	8.0	3.5	3.0
Oct	139	5.5	4.5	4.0
Nov	98	3.9	3.0	3.0
Dec	50	2.0	2.0	2.0
Year	2018	79.6	56.5	51.0
Adjusted for "rest"		66.1		
1 Aug - 15 Sep				

Table 5. Height (in cm) of alfalfa and daily evapotranspiration (in mm) during 5 periods in 1963.

Period		Lysimeter	Height	Evaporation
			cm	mm
A	[Cut 1 and 2 on 1 Apr]	1	12 - 25	5.12
	2 Apr - 15 Apr	2	12 - 25	5.45
		3	33 - 46	7.71
B	[Cut 1 on 16 Apr]	1	10 - 12	4.62
	17 Apr - 23 Apr	2	25 - 28	6.80
		3	46 - 47	7.92
C	[Cut 1 and 2 on 24 Jun]	1	16 - 20	9.39
	3 Jul - 7 Jul	2	16 - 20	10.68
		3	38 - 50	12.80
D	[Cut 1 on 2 Jul]	1	16 - 22	11.35
	3 Jul - 7 Jul	2	20 - 30	11.42
		3	50 - 57	13.82
E	[Cut 1 on 8 Jul]	1	16 - 42	9.90
	9 Jul - 22 Jul	2	30 - 50	11.90
		3	57 - 63	12.90

33-23

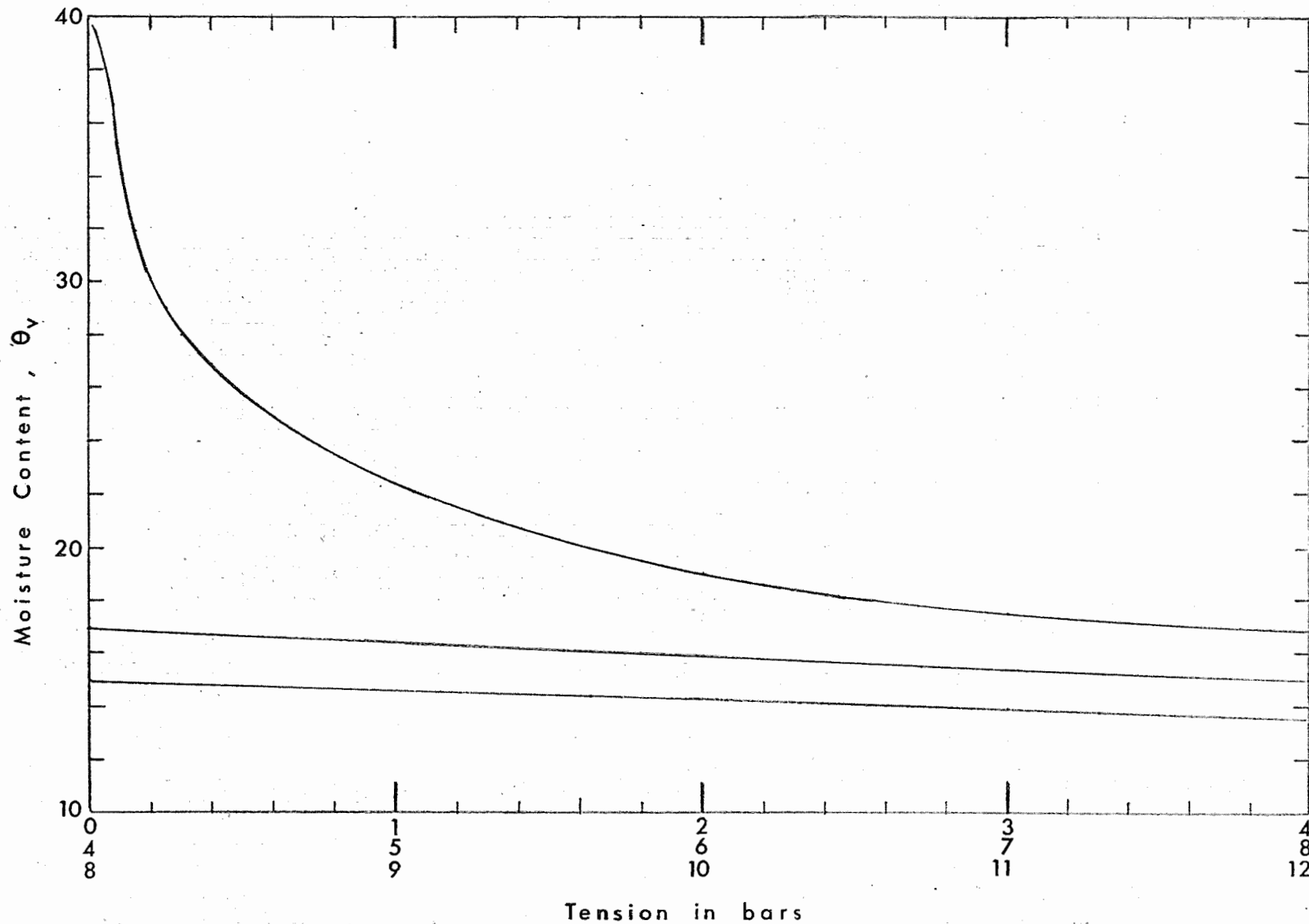


Figure 1. Moisture characteristic of Adelanite. Annual Report of the U.S. Water Conservation Laboratory

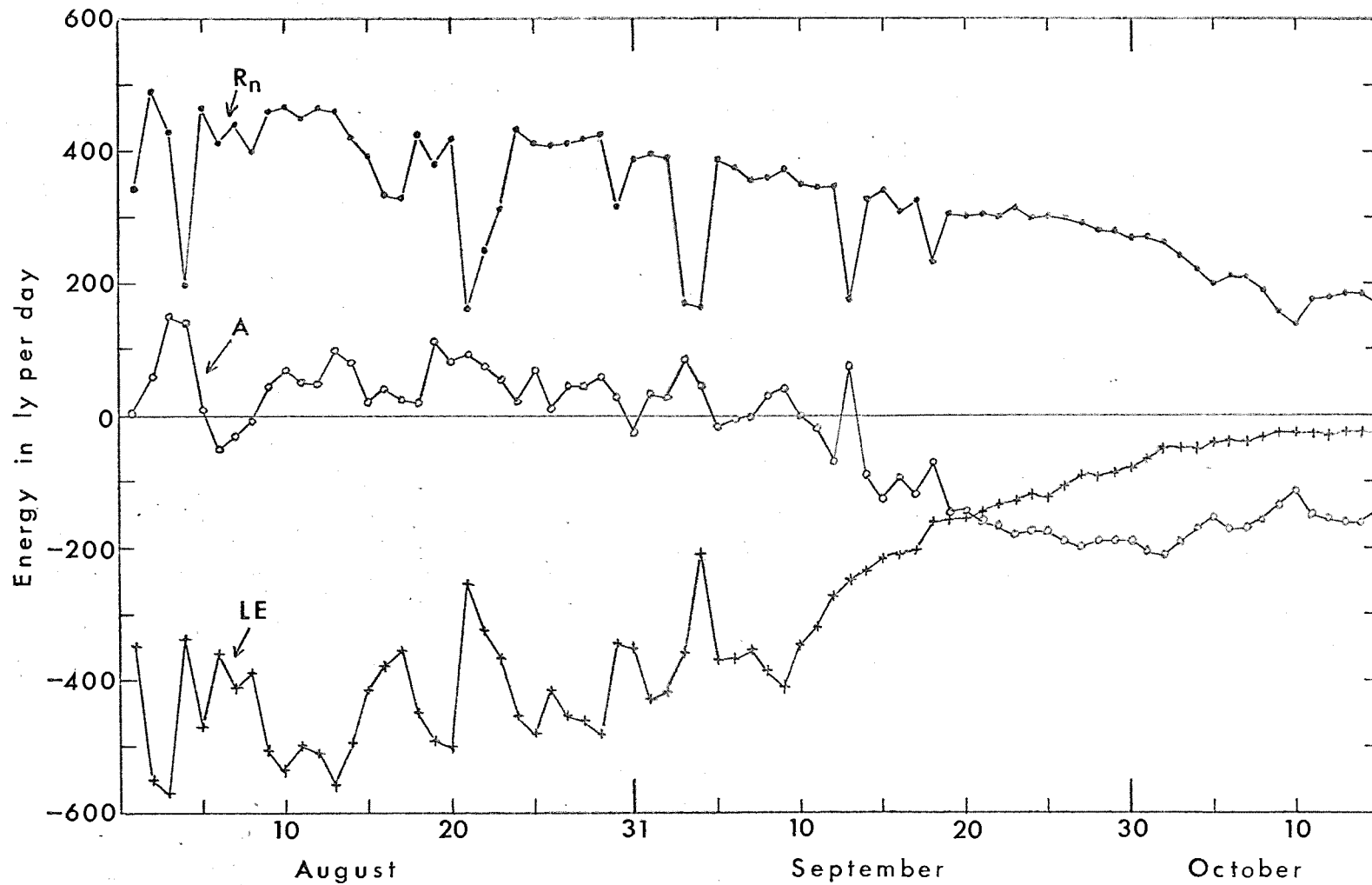


Figure 2. Daily evaporation rate and energy balance components of alfalfa during moisture depletion period starting 29 July 1963.

PART 2. ROUTINE MEASUREMENT OF STANDARD WEATHER DATA IN 1963.

INTRODUCTION:

Starting with late 1963 a program of half-hourly observations of air temperature, air humidity, solar radiation, net radiation, and windspeed has been put in operation. Principally, these data are taken and recorded on behalf of meteorological and climatological studies (see Parts 1, 3, and 4, and also outlines WCL 16, 17, 18, and 19). However, a permanent record is maintained for general reference purposes.

During 1963 the final transducer system has been evolved but the recording system was still temporary, an automatic, digital recorder to be installed as soon as received. This report will serve mainly to describe current methods of measurement and to present a summary of the data.

PROCEDURE:

Air Temperature Measurement. Air temperature was measured at 2 m above the ground, beginning on 18 January 1963. A 30-gage (.25 mm diameter) nylon-covered, copper-constantan thermocouple was used. The thermocouple was tested with a Leeds and Northrup type-K-3 potentiometer and found to be within 0.2 C of the true temperature, a value within the calibration of the wire.

The thermocouple was housed in a 3 cm diameter, thin walled, brass tube 30 cm long that was within a nickel-plated, copper shield. This assembly was also the housing for the wet bulb thermocouple of the psychrometer. Air was drawn over the thermocouple by a blower at one end of the tube. A diagram of this system is discussed in section 2 on humidity measurements.

A soil probe containing a thermocouple and a resistance thermometer was constructed to provide a reference junction at 1 m below the ground level. This probe was originally made from 1.2 cm diameter electrical conduit but changed to a similar lucite tube on 7 March 1963.

Soil temperature measurements were made at least weekly. A compensator was constructed and set at the measured soil temperature so as to give a millivolt signal equivalent to the actual air temperature.

On 8 November 1963 a new housing for air temperature measurements was installed. This contained a self-powered reference junction set at 0 C, thereby eliminating the need for soil reference junction and compensator. The copper-constantan thermocouple remained the same. A diagram of this system is shown in Figure 1.

Air Humidity Measurement. Measurement of air humidity began on 18 January 1963. The housing, measurement circuit, and recording was developed concurrently with that for air temperature measurement. The transducer consisted of a nylon-covered, copper-constantan thermocouple inside a water saturated nylon wick. Air is drawn continually over the wick by a fan at the end of the tube, see Figure 2.

The constantan wire of the wet bulb thermocouple is joined to the constantan of the dry bulb (air temperature) thermocouple. Thus the depression of the wet bulb is found directly.

Operational tests were made with the psychrometer comparing its performance to that of Aminco elements and a Bendix psychrometer. Results were satisfactory. A heat lamp was used in a laboratory test of the psychrometer to evaluate the effectiveness of the radiation shield. Acceptable results were obtained under radiation intensities of 2 ly min^{-1} .

Beginning on 6 June 1963, air humidity was measured with a Minneapolis-Honeywell dew probe, model SSP-129A. This is a lithium-chloride bobbin wound with a silver bifilar wire. A temperature equilibrium will develop corresponding to the hydration balance of the bobbin. The temperature reading is obtained by a thermocouple inserted into the cavity of the dew probe bobbin. An aluminum rod 1.2 cm in diameter and 7.5 cm long was connected to an 18 cm long lucite tube. A thermocouple was potted in the aluminum rod near the joint. This thermocouple positioner places the thermocouple in the center of the dew probe bobbin and favors the conduction of heat of the dew probe bobbin to the thermocouple.

Readout of the dew probe thermocouple was obtained by connecting the constantan wire of the dew probe thermocouple to the constantan of the soil probe thermocouple. The voltage obtained corresponds to the temperature of the dew probe above that of the soil. The known soil

temperature was then added to this value to obtain the dew probe temperature.

From 8 July 1963 on, the dew probe was used exclusively to measure air humidity. On 8 November 1963 the wet bulb psychrometer was removed. The soil probe was disconnected and the dew probe and air temperature thermocouples were connected to a self-powered reference junction (Model JR114B, serial number 42, 0 C, manufactured by Consolidated Ohmic Devices Company).

Solar Radiation. Measurement of solar radiation began 7 December 1962. The instrument is located on a pipe stand 3.25 m above the ground, and midway between the north side and the center of the lysimeter field. This site is free of any significant obstruction above the plane of the sensing element.

The sensing instrument is an Eppley Pyrheliometer. Readout of the pyrheliometer is obtained through the use of a voltage divider (2.5 k) across the input leads of the recorder. An emf from a portable millivolt source is adjusted to equal the output of the pyrheliometer at 1 ly min^{-1} . The pyrheliometer is disconnected at the field and the millivolt source is attached. The voltage divider is adjusted to give a readout at the recorder of 1 ly min^{-1} .

Net Radiation. The measurement of net radiation began 7 December 1962. The radiometer is mounted on a horizontal rod 1 m above ground level and approximately 1 m from the tripod support stand. The transducer is a miniature net radiometer as developed by Fritschen. It consists of a copper-constantan thermopile mounted between two hemispherical polystyrene windows. Details of construction and calibration of this instrument can be found in annual reports of 1960 and following.

The output of the net radiometer is matched to the recorder span by the use of a voltage divider (2.5 k). A portable millivolt source adjusted to the output and impedance of the transducer is taken into the field and plugged into the leads in place of the net radiometer. The voltage divider is adjusted to obtain a recorder reading equal to the unit output of the radiometer, in this case 1 mv on the recorder for 1 ly min^{-1} of net radiation.

Five net radiometers were used during the year of recording. Three were removed after being damaged either by exposure or by rain storms. Service life for the net radiometers has now been set at 90 days between October and April, and 60 each between April and October.

All measurements in 1963 were made over check 4 of the alfalfa field. For a more precise description of the condition of this field see Part 1.

Wind Speed. Continuous measurement of the wind speed began 5 March 1963. A Beckman & Whitley type F wind measuring system was used with the anemometer cups at 2 m above the ground and 1 m from the mast holding the solar radiometer. The Beckman & Whitley system was removed 2 July 1963.

The major components of the Beckman & Whitley system are the wind speed transmitter, translator, and recorder. The wind speed transmitter has a 3 cup anemometer mounted on a vertical housing. The anemometer drives a shaft connected to a circular light chopper. An exciter lamp is positioned above a slotted plate and a phototube is below. The pulse from the phototube is amplified and transmitted to the translator. The translator contains a power supply circuit and a clipper amplifier for amplifying and converting the signal from the wind speed transmitter and transmitting it to the recorder. The recorder used to measure the signal was a Leeds and Northrup AZAR (adjustable zero, adjustable range) millivolt recorder.

The recorder was adjusted for a 1 m sec^{-1} wind full scale. Reading was continuous at 3 inches hr^{-1} . The chart was read weekly, integrated "by eye" for half-hour periods to the nearest $.5 \text{ m sec}^{-1}$.

On 25 June 1963 an integrating, digital-to-analog system was installed. Wind speed is measured by a Casella 3-cup anemometer. The anemometer is mounted on a tripod stand with the cups at 2 m above the ground. The recording of wind speed is from a contact that is geared to the spindle of the anemometer. A contact is closed twice for every three revolutions of the anemometer cups.

Contact closures are registered on a set of four decade type stepping switches at 30-minute intervals. Switches 2, 3, and 4, which

register the tens, hundreds, and thousands, contain two banks of parallel gold-plated, bridging contacts each. Stepping switch number 2 advances through 10 half-ohm precision resistors each cycle. In the same manner, stepping switches 3 and 4 advance through 5-ohm and 50-ohm resistors respectively. Figures 3 and 4 give the circuits of the wind registration system.

A typical anemometer will produce 7970 contact closures in half an hour with a 10 m sec^{-1} wind. The stepping switches are manually advanced to this position and a voltage source from an Even-Volt current supply is adjusted to produce a full scale, or 2 mv signal at the recorder through this circuit. The zero is adjusted in the same manner. The wind speed system will then cover a range from zero to 10 m sec^{-1} in 797 steps.

Printout and resetting the counters are controlled by a timer mounted in the wind speed system chassis. The starting power comes from the main timer in the recorder. The wind speed timer is then self-powered and adjusted to stop the registering of contact closures for the channel printout, reset the counters to zero and begin the registering of contact closures after the printout. The period of count interruption is 30 seconds. The data obtained from this system is read to the nearest 0.1 m sec^{-1} .

Recording. The recorder used to register the weather data is a Minneapolis-Honeywell 6-point, multicolored dot recorder. The range is from -2 to +2 mv. Print time is 30 seconds and full scale, print wheel travel time is 24 seconds. A timer has been connected to the recorder to begin a printout cycle every 30 minutes. One point is identified for correct time each day and the record is evaluated weekly.

Solar radiation and net radiation are matched to the recorder scale by voltage dividers so that one millivolt equals one langley per minute. Air temperature and dew probe temperature are recorded directly on a scale of 2 mv approximately equal to 50 C. The dew probe has an offset of 20 C by means of a constant voltage supply adjusted to provide 0.790 mv, opposed to the dew probe output. The

wind speed system is calibrated to the scale of the recorded at 10 m sec⁻¹ wind speed equal to 2 mv. The wind speed printout also contains a zero offset since the anemometers cannot measure wind speeds below 20 cm sec⁻¹.

The voltage supply for both the dew probe temperature offset and the wind system is an Even-Volt DC current supply, Model 101.05, manufactured by Instrulab, Incorporated.

The recorder will be modified in the future to print the data on 8-channel punched tape. Figures 5 and 6 show, schematically, how the different transducers are connected to the recorder input.

RESULTS AND DISCUSSION:

Data are available for each half-hour and have been averaged by the day, and day-value tables have been compiled by months of the year (Data Books V25 and V30).

Decade values have been calculated also and are given here in Table 1 for solar radiation, net radiation, wind speed, vapor pressure, and maximum, minimum, and average air temperature. The wind data show generally lower values beginning with 1 July, as compared to prior data. This is attributed to erroneously high values obtained from the Beckman & Whitley system during periods of very low wind speed. Data prior to 1 July during periods that wind speed is less than 1 m sec⁻¹ should not be regarded as reliable.

Often, standard Weather Bureau data, obtained at Sky Harbor Airport, are used for reference purposes. To tie them to our data a comparison is made in Figures 7 and 8 of the decade maximum and minimum air temperatures. They show that, outside of the months of December and January, temperatures at the airport runway are 2 to 4 degrees higher, particularly at night. In using airport wind data, wind speeds are generally twice as high as the ones measured at the Laboratory at 2.0 m. The Weather Bureau wind speed is measured at 5.6 m. Since $\ln 5.6/\ln 2.0 = 2.5$, the difference is approximately accounted for by the difference in height of measurement.

SUMMARY AND CONCLUSIONS:

Half-hourly measurements of standard weather data were made continuously during 1963 over an alfalfa field at 2 m above the ground.

Solar radiation was measured with an Eppley pyrhelimeter, net radiation with a Fritschen polystyrene shield net radiometer, air temperature with a ventilated, shielded thermocouple with automatic self-powered reference junction, air vapor pressure with a lithium chloride dewcell and a compensated thermocouple, and wind speed with a sensitive cup anemometer and totalizing revolution counter with electrical analog readout. All signals were recorded on a self-recording voltmeter with a -2 to +12 millivolt span.

Data are available in tabulated form for half-hours, days, and decades of 1963.

Table 1. Weather data at 2 m over alfalfa, U. S. Water Conservation Laboratory, Tempe, Arizona, 1963

Month	Decade	R_g	R_n	Wind Speed	Vapor Pressure	Air Temp. Ave. Max.	Air Temp. Ave. Min.	Air Temp. Ave.
		ly day ⁻¹	ly day ⁻¹	m sec ⁻¹	mb	°C	°C	°C
Jan	1	225	59	-	-	-	-	-
	2	346	94	-	-	-	-	-
	3	337	122	-	6.0	20.3	2.3	11.3
Feb	1	347	132	-	8.2	26.9	9.1	18.0
	2	381	163	-	7.5	17.9	3.5	10.7
	3	454	179	-	7.6	24.4	5.4	14.9
Mar	1	482	205	-	5.8	20.1	2.8	11.5
	2	502	234	2.4 ^{1/}	7.0	20.2	4.6	12.4
	3	511	246	2.0	9.1	26.2	8.7	17.4
Apr	1	558	270	2.6	6.8	25.0	8.0	16.5
	2	607	301	2.5	7.7	25.2	6.8	16.0
	3	624	306	2.8	7.6	25.4	7.0	16.2
May	1	669	377	2.6	8.1	32.5	12.9	22.7
	2	684	403	2.3	7.2	34.4	14.3	24.3
	3	683	372	2.5	7.4	33.3	13.8	23.5
Jun	1	730	417	3.5	7.8	32.2	12.8	22.5
	2	740	447	3.0	10.6 ^{3/}	34.6	14.2	24.4
	3	739	476	2.4	9.6	35.9	14.0	25.0
Jul	1	655	472	1.6 ^{2/}	13.4	38.0	20.7	29.4
	2	663	473	1.5	21.0	38.6	22.7	30.7
	3	643	398	1.8	22.4	38.4	22.9	30.7
Aug	1	562	376	1.6	25.4	34.4	20.9	27.7
	2	578	375	1.4	26.0	36.3	22.8	29.6
	3	502	329	1.3	26.3	34.5	21.8	28.2
Sep	1	514	323	1.6	22.1	35.5	21.3	28.4
	2	483	301	-	18.2	35.4	20.1	27.2
	3	507	294	-	14.4	37.6	18.0	27.8
Oct	1	450	211	1.3	11.3	35.9	16.0	25.9
	2	406	192	1.7	11.3	29.8	12.8	21.3
	3	404	201	1.0	14.9	28.4	13.5	20.9
Nov	1	328	162	1.3	12.6	24.0	10.0	17.0
	2	320	145	1.4	9.9	24.0	8.4	16.2
	3	276	124	1.5	9.2	19.8	5.1	12.5
Dec	1	296	121	1.4	7.0	21.8	4.2	13.0
	2	280	109	1.2	5.6	17.7	4.2	9.0
	3	283	107	1.5	4.7	19.6	6.3	10.0

^{1/} Measured with B & W analog system until 1 July.

^{2/} Measured with Casella and digital system after 1 July.

^{3/} Earlier data based on psychrometer, later ones on dewcell.

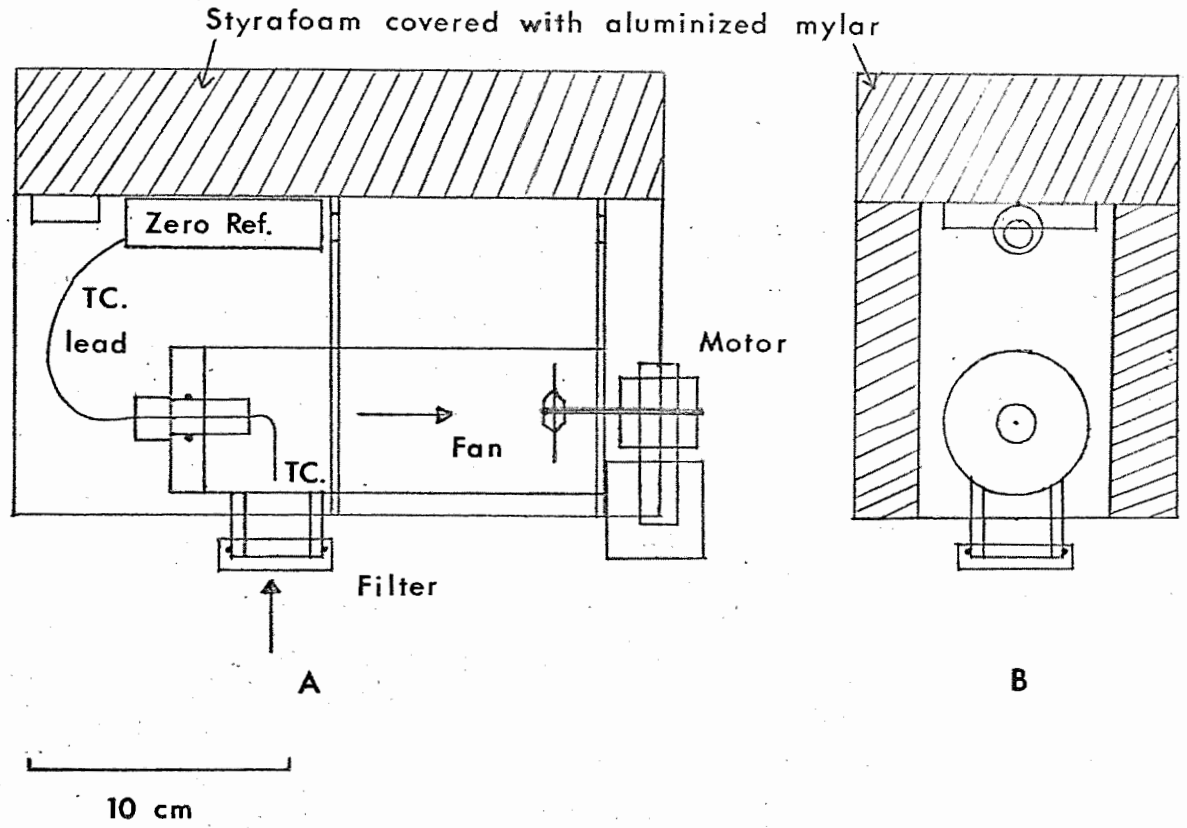


Figure 1. Thermocouple housing. Arrow shows direction of air flow. Construction is of lucite and styrofoam. A is lengthwise section. B is cross section, Annual Report of the U.S. Water Conservation Laboratory

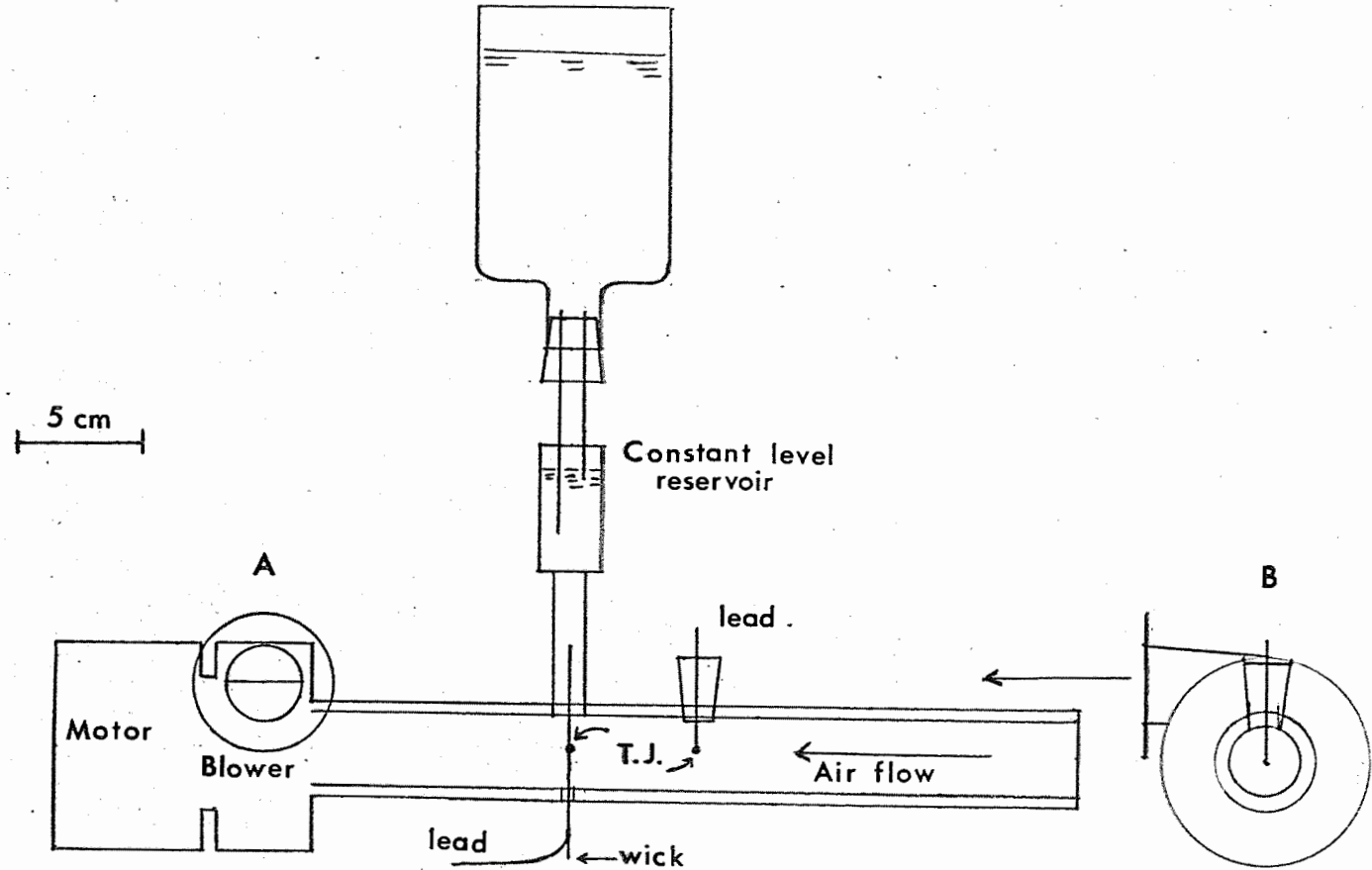


Figure 2. Lengthwise (A) section and cross section (B) of aspirated dry and wet thermocouple with double shield.

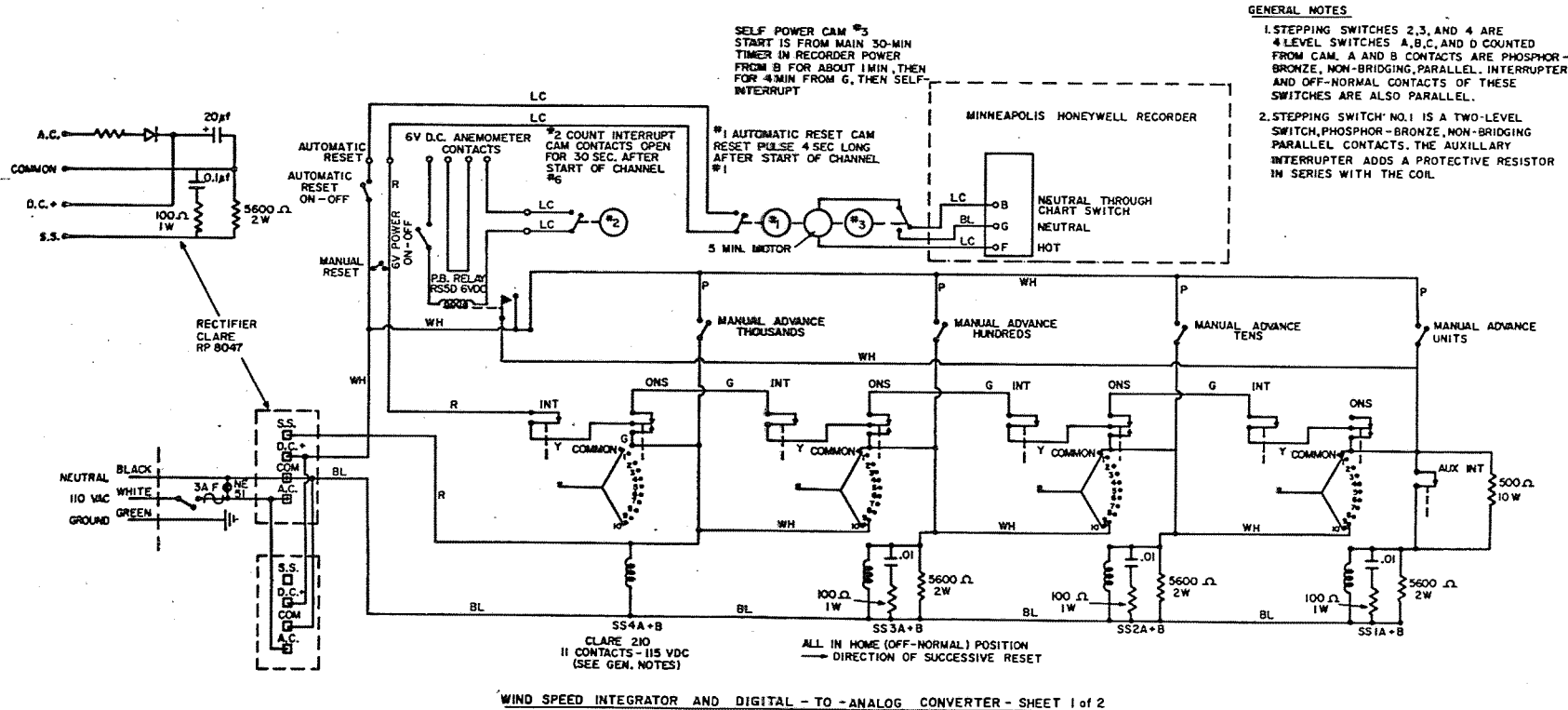
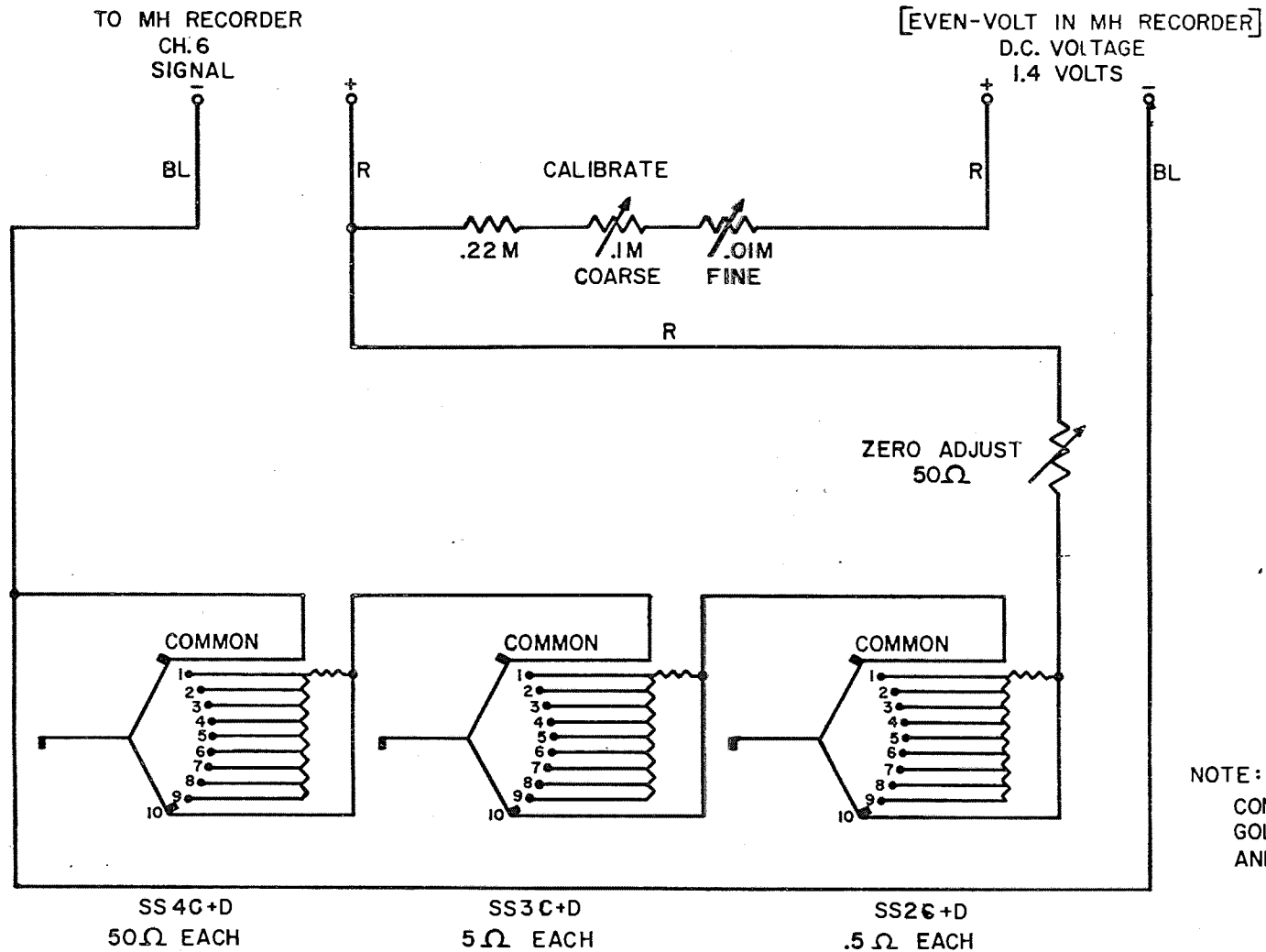


Figure 3. Wind recorder circuit, showing programmer and recording section.

33-36



NOTE:
CONTACTS C AND D ARE
GOLD-PLATED, BRIDGING
AND PARALLEL

WIND SPEED INTEGRATER AND DIGITAL-TO-ANALOG CONVERTER -- SHEET 2 of 2

Figure 4. Wind recorder circuit, showing readout section.

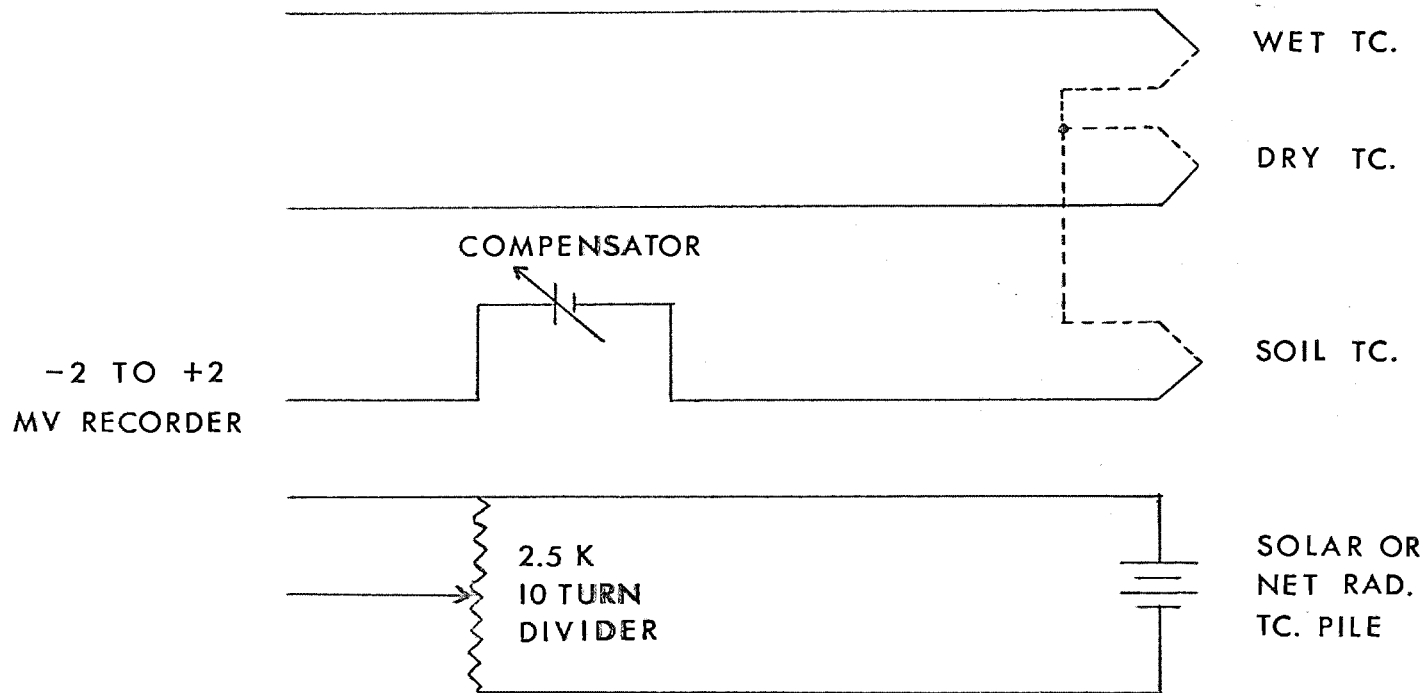


Figure 5. Method of connecting wet and dry bulb assembly, and radiometers to recorder.

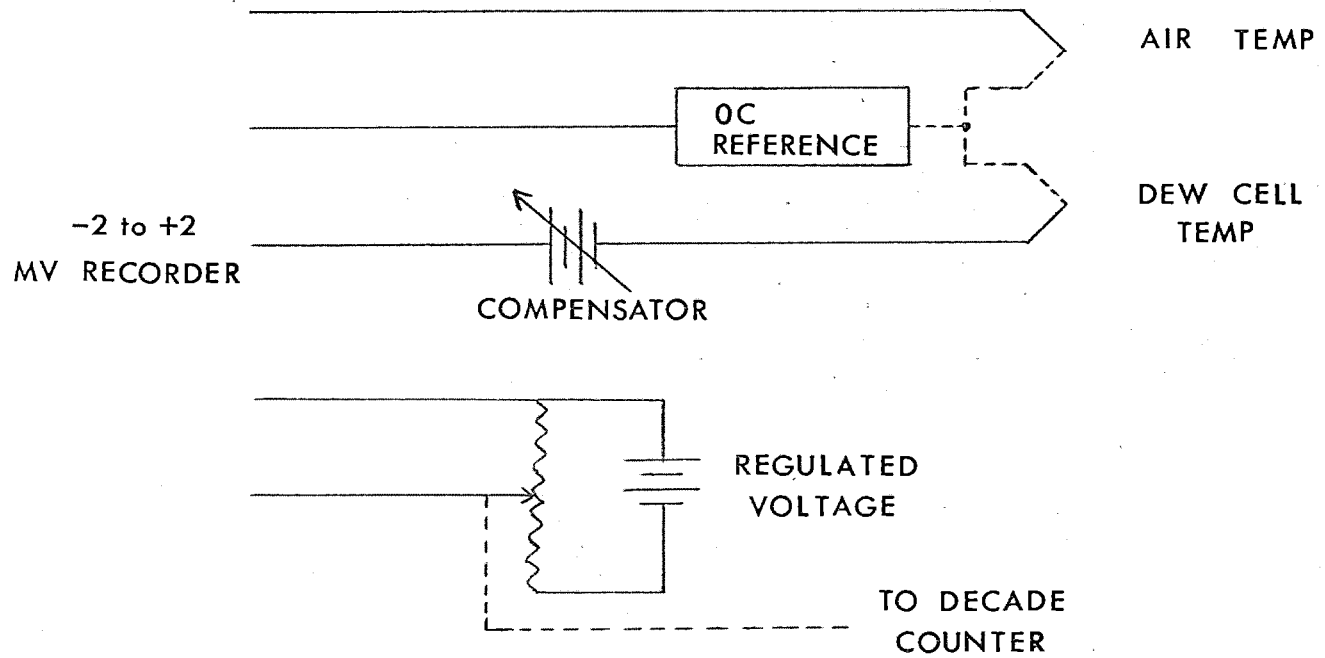


Figure 6. Method of connecting air and dewcell thermcouple, and wind counter readout device to recorder.

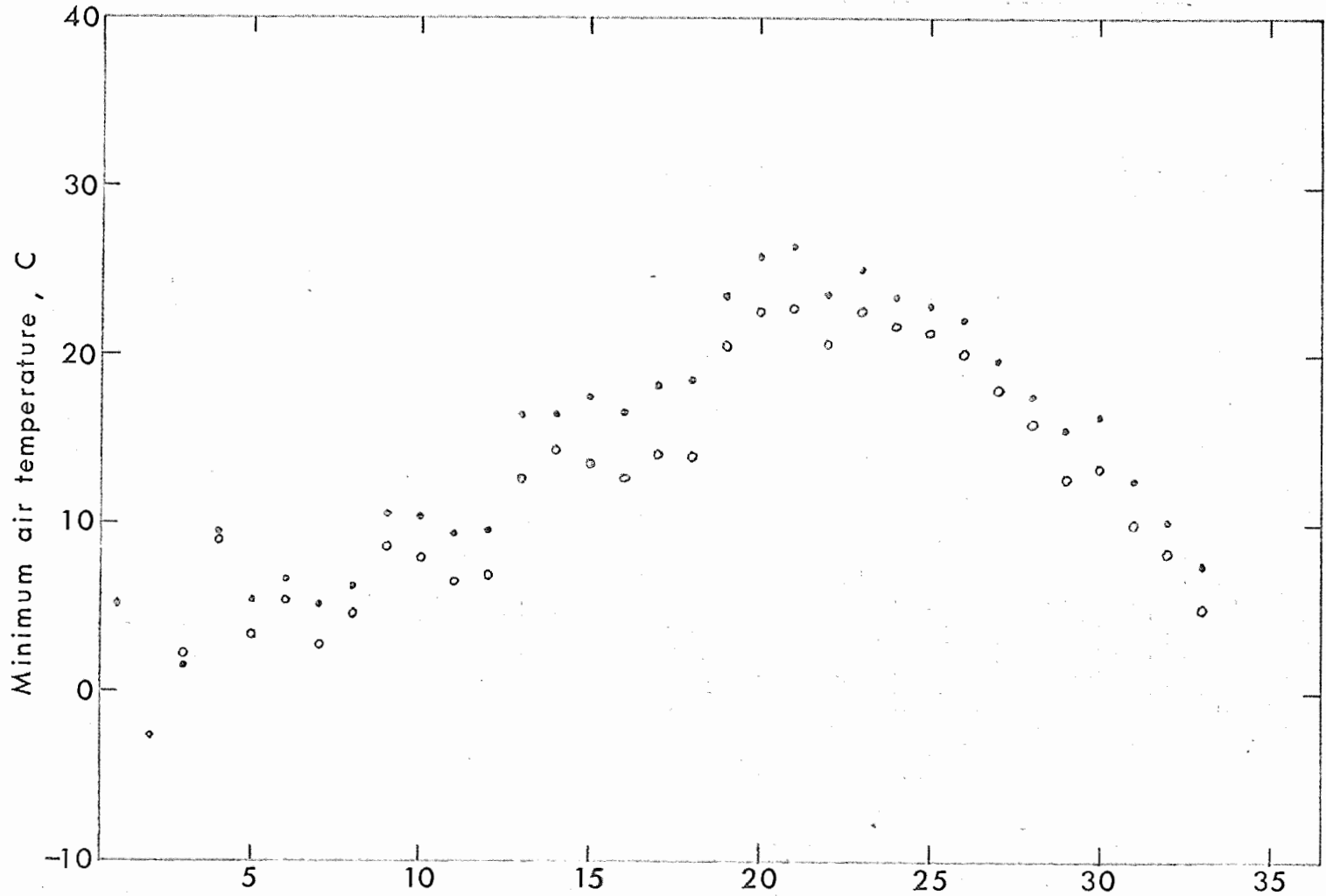


Figure 7. Decade averages of minimum daily air temperature at U. S. Water Conservation Laboratory (open dots) and Phoenix Airport Weather Bureau Site (solid dots).

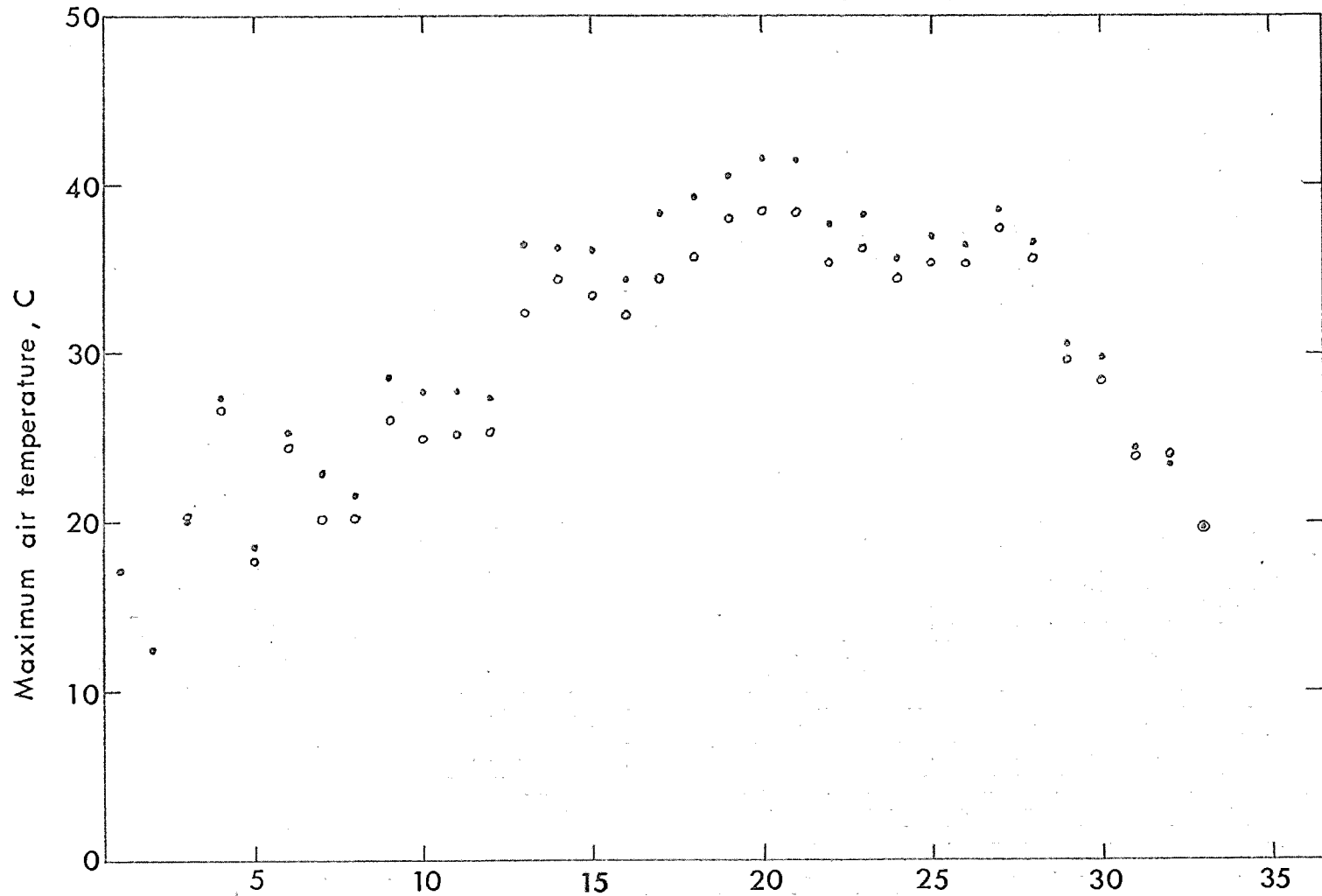


Figure 8. Decade averages of maximum daily air temperatures at U. S. Water Conservation Laboratory (open dots) and Phoenix Airport Weather Bureau. Annual Report of the U. S. Water Conservation Laboratory

PART 3. TEST OF PREDICTION METHOD: THE COMBINATION APPROACH.

SYMBOLS:

A	sensible heat flux in air - ly min^{-1}
B_v	transport coefficient for vapor - $\text{g cm}^{-2} \text{ min}^{-1} \text{ mb}^{-1}$
E	evaporation rate - $\text{g cm}^{-2} \text{ min}^{-1}$
K_a, K_v	eddy diffusivity - $\text{cm}^2 \text{ min}^{-1}$
L	latent heat of vaporization - cal g^{-1}
R_n	net radiation - ly min^{-1}
S	soil heat flow - ly min^{-1}
T	temperature - C
c	specific heat of air - $\text{cal C}^{-1} \text{ g}^{-1}$
d	vapor pressure deficit - mb
e	vapor pressure - mb
k	Von Karman's constant (.41)
p	ambient pressure - mb
u	windspeed - cm sec^{-1}
z	elevation - cm
z_o	roughness factor - cm
Δ	de/dT - mb C^{-1}
γ	psychrometer constant - mb C^{-1}
ϵ	water/air molecular weight ratio (1622)
ρ	density of air - g cm^{-3}
X	absolute humidity - g cm^{-3}

Subscript 'a' indicates elevation in air except in K_a .

INTRODUCTION:

The combination approach is a method of estimating evaporation (E) from combining the energy balance equation ($LE + R_n + A + S = 0$) with aerodynamic expressions for the flow of sensible heat ($A = K_a d(\rho C T)/dz$) and for the flow of vapor ($E = K_v dX/dz$).

The combination is carried out so as to obtain an expression in which the energy balance components, except A, and properties of the air at some standard height, including windspeed, are retained.

The following assumptions are involved in the derivation:

- a. Similarity of heat and vapor flow, e.e., $K_a = K_v$.

- b. The slope of the vapor pressure-temperature curve at air temperature is not significantly different from that at the temperature of the evaporating surface.
- c. At the evaporating surface, where the turbulent regime begins, the vapor pressure is substantially equal to the saturation vapor pressure at the temperature of that surface.

With these assumptions the following expression is obtained:

$$-LE = \frac{\Delta/\gamma (R_n + S) + LB_v d_a}{\Delta/\gamma + 1} \quad [1]$$

This expression has been developed in various steps and forms, primarily by Penman, and also by Ferguson. It is important to realize at the outset that during the daytime the first term is usually much larger than the second one. Only under conditions of high wind speeds, high vapor pressure deficits, or at night, does the second term become prominent or dominant. Further, high air temperatures, through the effect of Δ/γ , tend to increase the dominance of the first term. The latter is usually referred to as the radiation term and the second as the aerodynamic term. However, the two are not entirely independent and equation 1 should not be viewed as some form of an energy balance expression.

It is further important to appreciate the fact that [1] is, in essence, an instantaneous equation that applies only to periods over which all variables are substantially constant. It can be applied to periods of one hour or so without too much chance for error. However, it is in principle erroneous to apply it to 24-hour totals or averages.

The factor B_v is a turbulent transport factor for water vapor. It has often been derived from empirical relations between evaporation and wind speed. However, one may also obtain it from the log-height wind law, thereby assuming adiabatic conditions--a fourth assumption.

In that case we find

$$B_v = \frac{\rho c}{p} \frac{k^2}{[\ln(Z_a/Z_o)]^2} u_a \quad [2]$$

It is possible to make corrections for stability, or to otherwise develop expressions relating B_v to wind speed, as was done by Businger and Tanner. Expression [2] does not involve localized empiricism, though the roughness factor z_o of the surface must be measured or estimated.

Reiterating, in many cases the accuracy required in estimating the aerodynamic term is not comparable to that involved in finding the radiation term. Thus, some of the drastic assumptions concerning the transport coefficient are not fatal.

Strangely enough, expression [1] has been widely used in one form or another, but never stringently tested. Data were available at Tempe from 1961 and 1963 to carry out a test of the combination method under a variety of circumstances. This report gives a partial evaluation of the available data.

PROCEDURE:

Accurate hourly data on evaporation were available from the weighing lysimeter records, often in triplicate. In 1961 and 1963, during special observation periods, R_n and S were measured on each lysimeter as well as u , T and, in 1961, e (air vapor pressure). Also, from wind profiles, z_0 could be estimated.

In addition, during 1962, R_n was measured routinely as well as T , e , and u at a height of 2 meters above the surface. In one case z_0 was estimated from the height of the crop and by comparison with other situations. Six 24-hour periods were examined, the selection being more or less at random, except that all days were clear, and that irrigation had been recently applied so that soil moisture could not be limiting.

a. Big Splash 1, 25 April 1961. This was probably the most ideal situation - a shallow layer of ponded water over the entire field (slightly less than 1 ha). Air temperature varied from 5 to 24 C. Vapor pressure was around 3 mb, maximum solar radiation 1.5 ly min^{-1} . Winds were fairly strong, up to 4.6 m sec^{-1} in the afternoon. Roughness was measured as .001 cm.

b. Big Mud 1, 29 April 1961. This was the second day after flooding the field. Air temperature varied from 9 to 31 C, vapor pressure around 4 mb, maximum solar radiation 1.5 ly min^{-1} . Winds were again fairly strong, up to 3.8 m sec^{-1} in midafternoon. Roughness was measured as .02 cm.

c. Alfalfa 2, 26 March 1963. A good stand of young (6 months) alfalfa, 20 cm high, watered on 19 March. Air temperature was from

7 to 26 C, vapor pressure around 8 mb, maximum solar radiation 1.3 ly min⁻¹, wind speeds moderate up to 2.7 m sec⁻¹ in the afternoon. Windspeed was measured at 65 cm over the crop and air temperature and humidity at 200 cm over the surface. This introduces some ambiguity in the data, even though appropriate corrections were made. Roughness was measured at 1.0 cm.

d. Alfalfa 6, 21 June 1963. A good stand of mature alfalfa, 32 cm high, trimmed on 14 June and watered on 18 June. Air temperature from 12 to 33 C, vapor pressure around 6 mb, maximum solar radiation 1.5 ly min⁻¹. Windspeeds were quite high, up to 5 m sec⁻¹ for 30-minute periods. This day was chosen as a typical "advection" day. Roughness was measured as 0.7 cm.

e. Alfalfa 10, 9 August 1963. A good cover, 25 cm high, though open as a result of recent mowing to the ground on 23 July. Watered on 29 July, trimmed on 5 August. Air temperature from 22 to 38 C, vapor pressure around 21 mb, maximum solar radiation 1.3 ly min⁻¹ wind speeds moderate, up to 2.7 m sec⁻¹ for 30 minutes. Chosen as a typical central Arizona summer "monsoon" day. Roughness was measured as 3.0 cm, the high value possibly due to the open nature of the stand.

f. Alfalfa, 12 November 1963. A very complete cover of alfalfa 30 cm high. Renovated first week of October and last irrigated on 28 October. Air temperature from 12 to 28 C, vapor pressure around 11 mb, maximum solar radiation .9 ly min⁻¹. Wind was slight, during most of the day less than 1 m sec⁻¹ but for several hours around 2.5 m sec⁻¹ in the afternoon. A typical late fall day in central Arizona. Roughness estimated at 1.0 cm. Data on soil heat flow not available.

Calculations were made for each hour of the day using formula [1]:

$$LE = - \frac{\Delta/\gamma (R_n + S) + LB \frac{d}{v a}}{\Delta/\gamma + 1}$$

Using a table, the dimensionless quantity Δ/γ was found from the air temperature, rounded off to the nearest .5 C. R_n and S were expressed

in ly min^{-1} . Since d_a , the vapor pressure deficit, was expressed in mb, LB_v has the dimension $\text{ly min}^{-1} \text{mb}^{-1}$ and is found from:

$$\text{LB}_v = \frac{L_0 e}{p} \frac{k^2}{[\ln(z_a/z_0)]^2} u_a$$

For standard conditions (25 C, 1000 mb) we may write:

$$\text{LB}_v = \frac{4.27 \times 10^{-3} \times u_a}{[\ln(z_a/z_0)]^2}$$

in which u_a is in cm sec^{-1} , z_a the height of measurement of T_a , e_a , and u_a , and z_0 the roughness. Thus we calculate from hourly values as follows, for example:

$$\begin{aligned} R_n &= 1.06 \text{ ly min}^{-1} \\ S^n &= -0.20 \text{ ly min}^{-1} \\ R_n + S &= 0.86 \text{ ly min}^{-1} \\ T_a &= 23.3 \text{ C} \\ \Delta/\gamma &= 2.58 \\ \Delta/\gamma (R_n + S) &= 2.22 \text{ ly min}^{-1} \\ z_a &= 150 \text{ cm} \\ z_0 &= .001 \text{ cm} \\ \ln z_a/z_0^2 &= 1.42 \times 10^2 \\ u_a &= 260 \text{ cm sec}^{-1} \\ \text{LB}_v &= .0081 \text{ ly min}^{-1} \text{mb}^{-1} \\ d_a^v &= 25.4 \text{ mb} \\ \text{LB}_v d_a^v &= 0.20 \text{ ly min}^{-1} \\ \text{numerator}^v \text{ of } [1] &= 2.42 \text{ ly min}^{-1} \\ \Delta/\gamma + 1 &= 3.58 \\ \text{LE} &= -0.68 \text{ ly min}^{-1} \end{aligned}$$

The example demonstrates, first of all, that an order-of-magnitude value of z_0 can be sufficiently precise. Also, that, in this case, the accuracy requirement for d_a and u_a is about 10 times less than that for Δ/γ and for $(R_n + S)$. By and large, the brunt of the accuracy is borne by the measurement of R_n , then of T_a , with other factors on a secondary plant of importance.

Following the scheme outlined above, hourly calculations were made for the 6 days given above. Since for case F (12 November 1963) no values for S were available, $R_n + S$ was assumed to be zero for all hours where R_n was less than 0.05 ly min^{-1} . The total of measured R_n for those hours was then equally distributed over the remaining hours. Thus S for the day was assumed to be zero and negative hourly values

for $(R_n + S)$ were eliminated. For the daily total it makes no difference whether this or the regular procedure is followed, but hourly values of positive LE are thus avoided.

RESULTS AND DISCUSSION:

Detailed hourly results are given in Figures 1, 2, and 3 for the Big Splash, Alfalfa 6 and Alfalfa November data, respectively.

The Big Splash data are the most pertinent test of the combination approach since uniformity was ideal here, as was the condition for zero vapor pressure deficit at the surface. Also, the value for z_0 should be very reliable in this case.

Obviously, the agreement for the daily total is excellent, being well within the tolerance of measurement estimated to be around 10 ly. On this day, net radiation plus soil heat flux were 74 ly more than -LE. Heat was, therefore, not imported in spite of the wetness of the surface, the general aridity of the environment and the moderately high wind-speeds. This fact must be attributed to the low value of z_0 , which resulted in low values for B_v , the vapor exchange coefficient. Hourly agreement is fair, some lag of measured versus computed values being apparent.

Figure 2 affords a remarkable example of the power of the method for a well-developed leafy cover in an arid environment. In this case, net radiation plus heat flux was 264 ly less than (-LE), a case of strong advection of sensible heat. Yet the daily total of calculated values was within 3% of the actual measured value and hourly agreement was also good. Note, in particular, how the estimated value accurately reflects the late afternoon wind movement.

Another outstanding feature of the data for 21 June 1963 is that in no way the assumption of zero deficit at the evaporating surface is refuted. In other words, we must conclude that the contribution of leaf-associated diffusion impedance for water vapor is insignificant with respect to the atmospheric impedance.

The last conclusion, which should, of course, be limited to a well-watered, well-developed alfalfa cover, is sustained by the data for 12 November in Figure 3. Here, also, the value for A is positive - 52 ly for the day, advection playing a major role. The daily total is

fairly accurately predicted and so are the hourly values, bearing in mind the somewhat arbitrary correction for the absence of data for soil heat flow.

Table 1 summarizes the data on a 24-hour basis for all six cases. Though the available data material has not been exhausted for making further tests, the preliminary impression is that the combination method can provide a practically acceptable estimate of evaporation, with an apparent error of around 5 percent of the daily total. A bias seems to be absent since the total for the six days is within 2 percent of the measured value. The tests reported here were made for six widely varying conditions, including very strong advection of sensible heat. Thus, further testing and examination of the combination approach appears fully warranted.

SUMMARY AND CONCLUSIONS:

Hourly and daily estimates of evapotranspiration were made for six widely differing conditions occurring in 1961 and 1963 using the combination method, sometimes better known as the Penman method. Included were open water, bare soil, and well-watered alfalfa. Standard hourly weather data were used in addition to net radiation and an estimate of the surface roughness. The results were compared with highly accurate weighable lysimeter data.

For all cases agreement was good. Daily values were typically estimated within 5 percent, or around 1/2 mm. Strong advective effects were properly accounted for. Hourly estimates, though less precise, indicated the diurnal pattern of radiation, wind speed, and vapor pressure deficit correctly.

Though further tests with available data will be made, it appears that the combination method is basically sound and needs no empirical adjustment whatever. It also is evident that the method is applicable to an arid environment that is heterogeneous and where evaporation involves strong advection of sensible heat.

Results are summarized as follows, in which E is the daily evaporation and r the ratio of the estimated to the measured value.

April	Open Water	5.58 mm	.985
April	Bare Soil	6.89 mm	.975
March	Alfalfa	5.13 mm	1.110
June	Alfalfa	12.20 mm	.972
August	Alfalfa	7.88 mm	1.059
November	Alfalfa	3.39 mm	1.064

Table 1. Daily values for six comparisons of measures (LE) and computed (\hat{LE}) values of evaporative flux, together with other energy balance components and estimate of surface roughness.

DATE	NAME	z_o	$\Sigma(R_n + S)$	A	-LE	$-\hat{LE}$	r_1	r_2
25/04/61	Big Splash 1	.001	425	- 74	351	346	.985	.825
29/04/61	Big Mud 1	.02	413	+ 1	414	404	.975	1.000
29/03/63	Alfalfa 2	1.0	261	+ 47	308	342	1.110	1.180
21/06/63	Alfalfa 6	.7	468	+264	732	712	.972	1.563
09/08/63	Alfalfa 10	3.0	377	+ 97	474	502	1.059	1.257
12/11/63	Alfalfa	1.0	151	+ 52	203	216	1.064	1.343

z_o in cm, all others in ly.

r_1 is ratio of \hat{LE} to LE

r_2 is ratio of LE to $\Sigma(R_n + S)$

U.S. Water Conservation Laboratory,
Tempe, Arizona

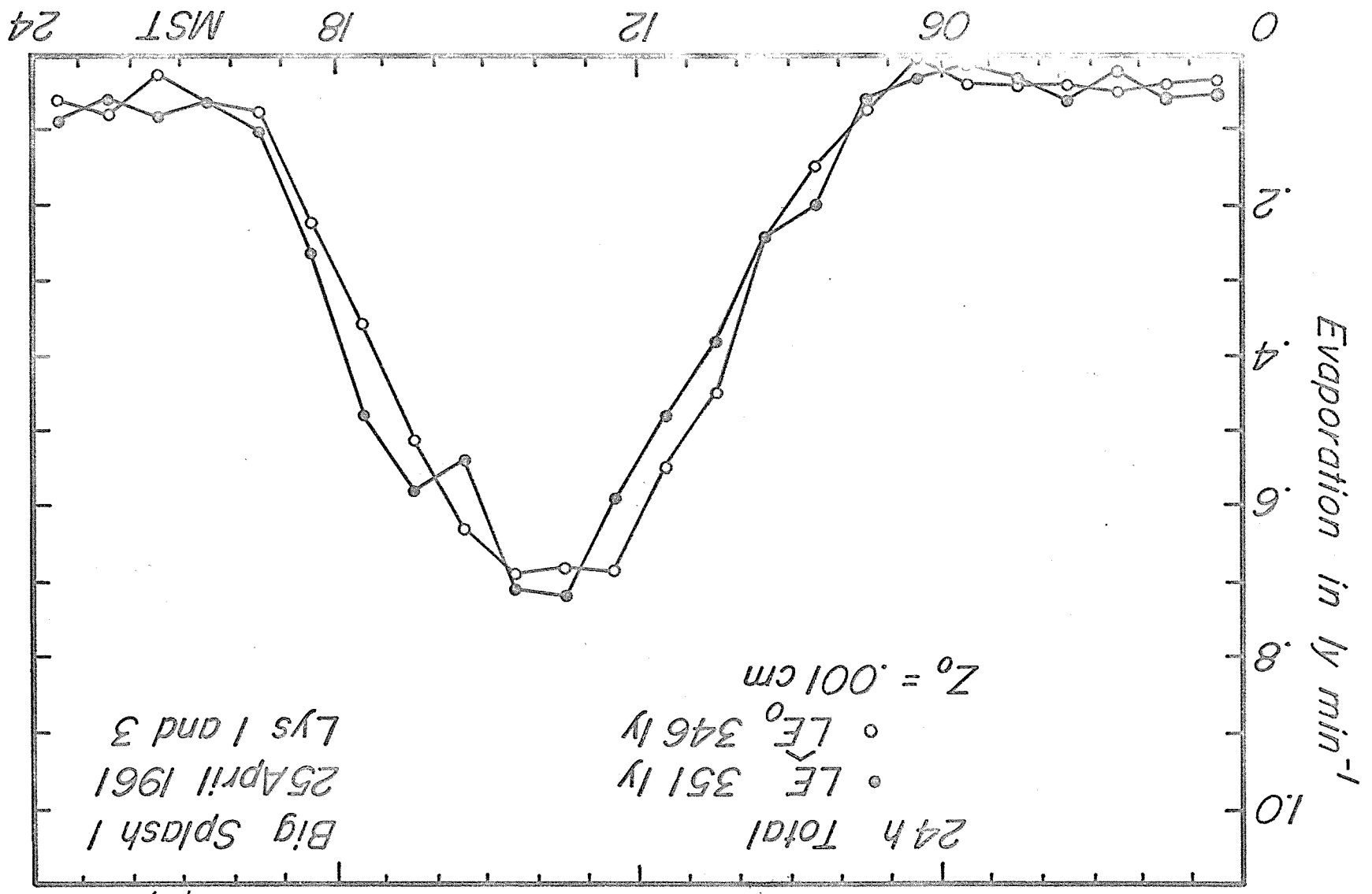


Figure 1. Measured and calculated value of hourly evaporative flux. Open, shallow water surface on 25 April 1961.

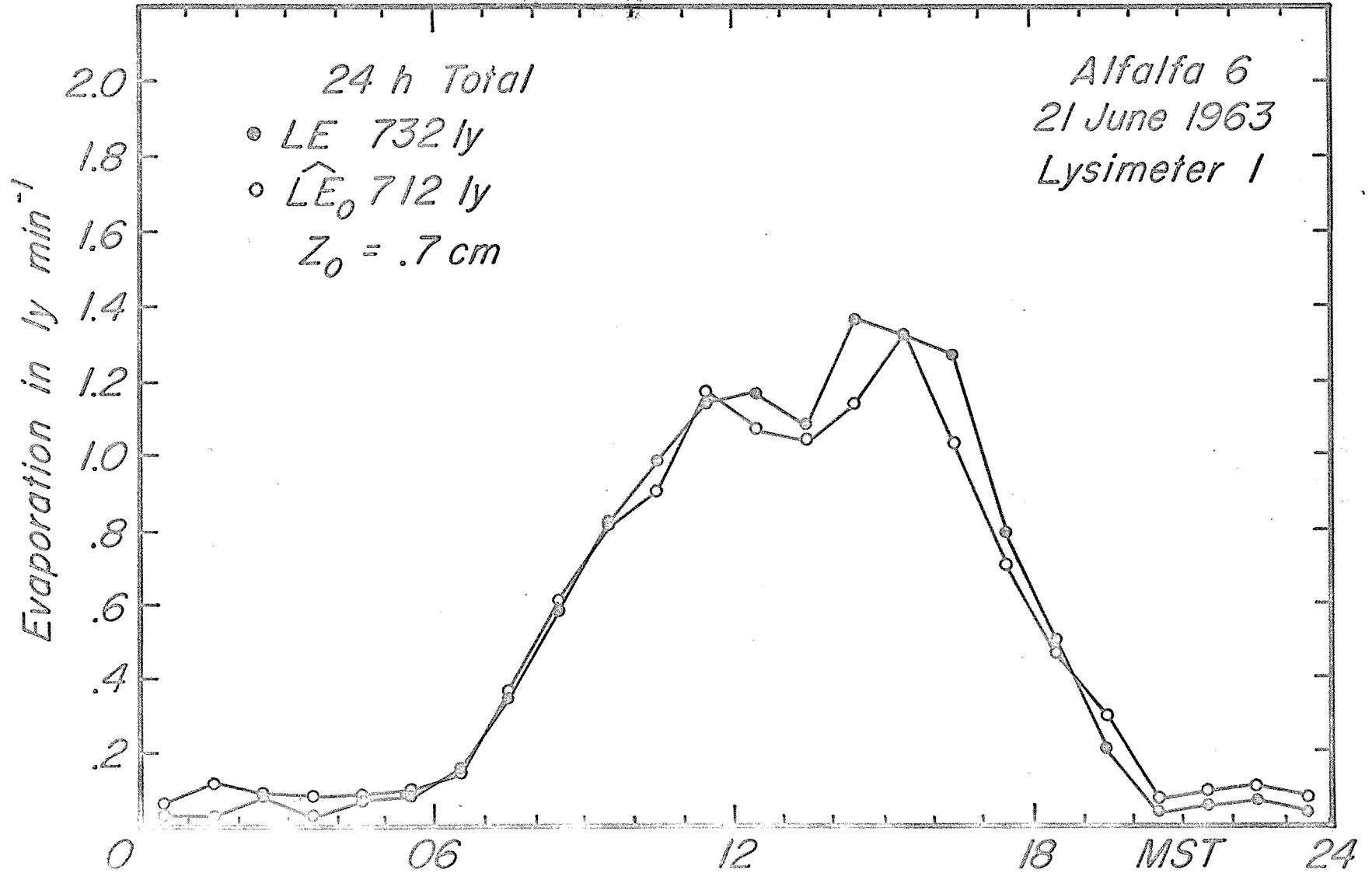
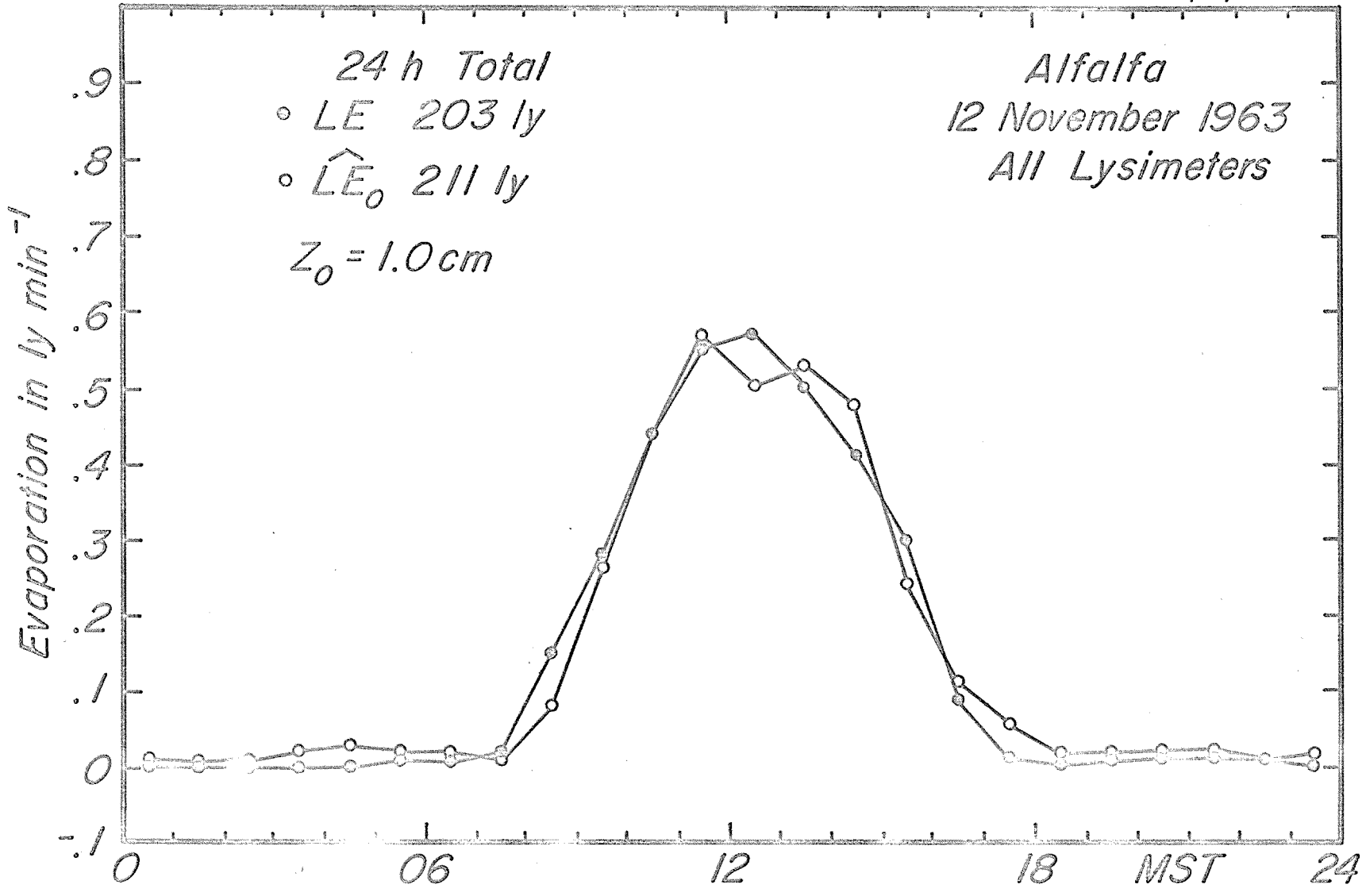


Figure 2. Measured and calculated value for hourly evaporative flux. A dense stand of alfalfa on 21 June 1963



33-52

Figure 3. Measured and calculated values for hourly evaporative flux. A dense stand of alfalfa on 12 November 1963. Annual Report of the U.S. Water Conservation Laboratory

PART 4: EVAPOTRANSPIRATION FROM A LAWN IN 1963.

INTRODUCTION:

In the Annual Report for 1962 a report was given on the construction and testing of a simple lysimeter supported by a single loadcell, suitable for the measurement of daily values of evaporative water loss. The present report gives data on the performance of this lysimeter through the calendar year 1963 and, at the same time, provides a complete series of observations on a typical lawn such as may be found around homes and buildings in the Phoenix area.

PROCEDURE:

Lysimeter Use and Maintenance. The single loadcell lysimeter has worked satisfactorily since October 1962. Occasional maintenance and adjustments were necessary since its installation, but in each instance, not more than one day's data was lost.

In March 1963 a small leak was detected in the gasket following an irrigation (see next section for irrigation method). Also, after 5 months of operation, the butyl gasket and butyl cemented corners started showing a slight deterioration. The gasket and fiberglass tape straps were removed. About 5 cm or 50 liters of water was pumped out of the bottom of the outer bin. This amount of water did not affect the operation of the lysimeter, since there is 25 cm clearance underneath the inner bin and the loadcell is hermetically sealed. New 7.5 cm x 2.5 cm fiberglass straps (Scotchbrand) were installed (three straps in three locations on each of the four sides).

A calibration check was made after the straps were installed by adding 5.0-kg and 12.5-kg increments up to 30.0-kg. The readings showed a change of 30.0-kg when the total amount was added and a change of 29.5-kg when taken off with a maximum error or ± 0.5 -kg at at the various increments. Strain indicator sensitivity was 0.5-kg.

The gasket was left off for one week to allow inside space to become air-dry. Instead of the butyl gasket, a waterproofed, cloth adhesive tape (Silver Permacel Brand) 9.5 cm wide and 0.4 mm thick was used. This tape was easier to install. Silastic RTV 891 was used to insure a waterproof seal at all the joints and corners of the tape.

A calibration check was made after the gasket was installed by adding 2.5-kg, 5.0-kg, and 12.5-kg increments up to 32.5-kg total load. At each of the increments, there was no error in the weight change and a sensitivity check gave 0.5-kg change, which is the sensitivity of the indicator.

In September 1963, the tape gasket showed some slight signs of deterioration and separation on one side, due to weather exposure. Also, the inner bin was tilting a little towards one corner, indicating that the fiberglass tape straps needed replacing. There was no water in the bottom of the outer bin, but the bottom and sides of both bins were moist due to condensation. After the gasket was removed, the bins were allowed to air-dry.

In order to prevent the bin from tilting to one corner, the number of tape straps was increased to five in three locations on the on the other two sides. The new gasket was installed and sealed as before. A calibration check was then made by adding 12.5-kg increments up to a 100.0-kg total load. The readings showed a change of 99.5-kg when the total weight was added and a change of 99.5-kg when taken off with a maximum deviation of ± 0.5 -kg at the various increments.

Up until December 1963 a Baldwin-Lima-Hamilton (BLH) Type "N" portable strain indicator was used to obtain the daily readings. After that time a BLH type 20 portable strain indicator will be used. The new indicator has a slightly greater readability.

Irrigation and Drainage. The lysimeter was irrigated whenever the lawn was irrigated (see Table 1 for irrigation schedule and amounts). The lawn and lysimeter would be flooded over periodically, depending on seedings, fertilizing, trimmings and consumptive use. On the day of irrigation, the lysimeter would be read at 0800 and the gasket checked for leaks. At 0800 on the day following the irrigation, any excess water still standing on the lysimeter would be drained off and the lysimeter read. The difference would be the amount of the water added minus the evapotranspiration for the irrigation day. The latter was estimated as the average of the

evapotranspiration on the day preceding and the one following the irrigation. The lysimeter edge is 4 cm above the soil level inside and outside the bin. As the water distributes and recedes in the lawn, it remains on the lysimeter at the 4-cm depth. This water is drained off before the lysimeter is read on the day following the irrigation.

The lysimeter was drained after each irrigation with one exception (see Table 1 for drainage schedule and amounts). The water was extracted from the bottom of the soil column through two filter candles (Selas) with a vacuum pump. The water from each filter candle was collected in a suitable container measured by placing the containers on the lysimeter and noting the difference in reading.

During the first half of the year, drainage took about 3 days. On these occasions the vacuum pump was regulated so that the water was extracted at a slow rate similar to the infiltration of water through the soil column. This proved to be time-consuming and too precise. During the remainder of the year, drainage took about 8 hours, usually 4 to 7 days following irrigation.

Lawn Management. The lysimeter was installed in a ryegrass lawn which had been in bermudagrass for two years. In October 1962, ryegrass was planted in the lysimeter. The rye lawn was kept until 14 May 1963. At that time bermuda plugs were added to the lysimeter and by the middle of June 1963, the lysimeter had a complete bermuda cover. From that time on, the lysimeter was seeded and fertilized whenever the whole lawn needed such attention. On October 22, 1963 the lawn was fertilized and seeded with ryegrass for the winter months.

The lawn was mowed with a multiple reel-type mower. At the same time the lysimeter and close surrounding areas not accessible to the mower were trimmed with hand clippers to the same height of about 4 cm. In October 1963 it was mowed close to the ground in order to plant the ryegrass. Dates of mowing are shown in Table 1.

Record Taking Method. Daily readings were started on 1 November 1962 and were taken on Monday through Friday at 0800. The data over weekends and holidays were taken at 0800 of the last work day before and at 0800 of the first day after each instance and averaged for the

appropriate number of days. The daily evaporation rates are for a 24-hour period extending from 0800 to 0800.

These daily readings were continued until December 2, 1963. At this time it was decided to collect data on a decade basis whereby readings are to be taken on the 1st, 11th, and 21st day of each month or the nearest working date to these dates.

The reading is found in microinches per inch and the difference between readings, when multiplied by 0.5, gives the change in kg or mm with the appropriate setting of the gauge factor dial.

EXAMPLE: 0800 01 APR - 0800 02 APR

14752 - 14740 = 12 x 0.5 = 6.0 mm evaporation

The rainfall data is taken from the data supplied by three automatic Bytrex lysimeters which record weight every hour. A recording rain gauge could also be used. The daily loss from the lawn lysimeter is corrected for the occasional periods of rainfall.

RESULTS AND DISCUSSION:

The daily measurements of evaporation from the lawn lysimeter are summarized in Table 2 which gives the decade averages in millimeters. In addition, Table 2 contains decade averages of net radiation measured over an adjacent field of alfalfa. The latter values may not be representative for the net radiation that prevails over the bermudagrass. However, the order of magnitude is certainly correct and the net radiation data serve as a basis of normalizing the evaporation data to a certain extent. The fourth column in Table 2 gives the energy equivalent of evaporation and the fifth column the ratio of evaporative flux to net radiation.

Bearing in mind the limitation on the applicability of the net radiation data, it is evident that as a whole, the evapotranspiration was less than the net radiation measured over the alfalfa. Another useful aspect of the ratio is that it demonstrates clearly when the condition of the lawn limited evaporation. This was the case during the last decade of May and the first two decades of June when the ryegrass was dead and the bermudagrass cover had not fully developed. Similarly, low ratios of ET over R_n were found during the months of

November and December when the bermudagrass bermudagrass became dormant and the ryegrass had, for the most, failed to develop a full stand.

In addition to average figures for periods of 10 days, there is often considerable interest in the maximum figures that are obtained for daily evaporation. These figures would have some bearing on the capacity of water delivery systems used for irrigating lawns. Maximum daily water use rates are given in Table 3 for each decade in the second column, again in millimeters. The day of the month and the corresponding net radiation over alfalfa on the same day are given in columns 3 and 4. The energy equivalent and the ratio of ET to R_n are given in columns 5 and 6. The values of ET/ R_n ratio run higher in Table 3 as compared to Table 2, indicating that the higher values for evaporation were not due solely to higher values of net radiation but were also associated with other factors, conceivably, irrigation, the height of the lawn and windspeed. Nevertheless, a comparison of Table 3 and Table 2 demonstrate that evaporation is a reasonably conservative phenomenon. The maximum excursion was found during the third decade of June and July where evaporation on one day was nearly double that for the corresponding decade. Generally, these high values are found on a day immediately following an irrigation or rain.

Both average and maximum daily rates of evaporation from the lawn are portrayed by decades in Figure 1. For the average values the figure shows a fairly steady rise until the first decade in May. Following this, there is a decline as the ryegrass dies and the bermudagrass slowly takes over, a full cover being formed by the first decade in July. The first decade in August shows a decline which is thought to be associated with an undue delay in irrigation following which the evaporation declines again particularly during the first part of October as the bermudagrass becomes dormant and rye is planted but does not as yet grow vigorously.

Table 4 gives a summary of the total amount of irrigation water applied and rain that fell on the area. Also shown are the monthly and annual amounts of evaporation as well as the amount of water

drained from the lysimeter. It is of interest to note that approximately 2,000 mm of irrigation (80 inches) were applied to the lawn in addition to about 200 mm (8 inches) of rain. At the same time, the total measured use of the lawn was about 1,400 mm (56 inches), indicating that the lawn was considerably over-irrigated at the point of measurement and that probably at all times conditions were maintained for maximum transpiration by the plants. Allowing for the period of partial cover in parts of May and June, a figure of 1,500 mm (60 inches) is a safe estimate for the typical maximum consumptive use of the lawn in question over an annual period. The figures in Table 4 demonstrate that the inefficiency and waste of irrigation water took place during the months of January, March, June, September and in December. During these periods the total amount of water applied to the lawn exceeded evaporation 2 or 3 times. Part of the inefficiency measured is undoubtedly due to poor leveling and, next, to an indiscriminate application of water whenever irrigation was scheduled.

SUMMARY AND CONCLUSIONS:

The consumptive use of water by a bermudagrass-ryegrass lawn adjacent to the Laboratory buildings was measured during the calendar year 1963. Data were obtained with a simple 1 m^3 steel lysimeter supported by a single loadcell. Daily values of water loss were obtained to the nearest .5 mm so that quite accurate weekly figures could be established.

Other than occasional replacement of a gasket and of the fiberglass tape flexures, the lysimeter did not require maintenance and worked within the limit of its reliability during the entire period.

The lysimeter was located in a lawn that was irrigated by flooding, in which process the lysimeter itself was flooded over. Excess water was removed by a pump and drainage system when necessary.

The data showed a minimum daily loss of about 1 mm day^{-1} during December and a maximum of 8 mm day^{-1} in July. Occasionally, a daily consumptive use of 11 mm for one day was measured. The consumptive use was appreciably depressed during the period of transition from one type of grass to the other. Total use of water for the year was

close to 1,400 mm where about 2,200 mm of water were applied as irrigation and rain. The customary irrigation procedure has resulted in considerable over-irrigation during December and January, the transition period in June, and also during September.

The experience and data obtained indicate that the single load-cell lysimeter is a reliable, trouble-free instrument that can give accurate data on consumptive use with a minimum of effort. The order of magnitude of consumptive use of a typical lawn in the Phoenix area was established as a conservative estimate of 1,500 mm for the year (60 inches) with a maximum use rate of 240 mm in July and a minimum use rate of 30 mm in December (9.8 and 1.6 inches, respectively).

Table 1. Irrigation and drainage of lawn lysimeter.

Irrigation		Drainage		Mowing	
Date	Amt	Date	Amt	Date	Cover
	mm		mm		
31 Dec 62	124	08-11 Jan 63	94	12 Feb 63	Rye
28 Jan 63	104	13-15 Feb 63	70	20 Mar 63	Rye
14 Mar 63	196			02 May 63	Rye
10 Apr 63	128	01-12 Apr 63	30	26 Jun 63	Bermuda (very little rye)
10 May 63	154	15-17 May 63	81	08 Jul 63	Bermuda
04 Jun 63	183	05-06 Jun 63	56	17 Jul 63	Bermuda
28 Jun 63	178	01 Jul 63	48	30 Jul 63	Bermuda
19 Jul 63	167	31 Jul 63	36	12 Aug 63	Bermuda
02 Aug 63	109	07 Aug 63	54	19 Aug 63	Bermuda
16 Aug 63	118	20 Aug 63	59	27 Aug 63	Bermuda
13 Sep 63	137	17 Sep 63	62	11 Sep 63	Bermuda
27 Sep 63	118	01 Oct 63	45	27 Sep 63	Bermuda
24 Oct 63	95	29 Oct 63	57	11 Oct 63	Bermuda) Close to ground) for rye grass
03 Dec 63	96	10 Dec 63	46	14 Oct 63	Bermuda) planting(22 Oct 63
17 Dec 63	<u>64</u>		<u> </u>	18 Nov 63	Rye (very sparse; some bermuda due to warm weather)
	1971		738		

Table 2. Decade averages of lawn evaporation in mm per day. Also, the net radiation as measured over alfalfa, the evaporative flux, and the ratio of the latter two, 1963.

Month	Decade	Evap. mm	R_n^* ly	-ET ly	$-ET/R_n$		Remarks Ryegrass since Nov. 62
Jan	1	1.20	59	70	1.19	01	Irr. 124 mm
	2	1.38	94	80	.85	02-03	Rain 16 mm
						10	Rain 2 mm
3	1.50	122	87	.71	13	Freezing temp.	
Feb	1	2.79	132	163	1.23	28	Irr. 104 mm
	2	2.29	163	134	.82	10-11	Rain 21 mm
	3	3.56	179	208	1.16	12	Trim
Mar	1	3.54	205	206	1.00		
	2	3.45	234	201	.86	15	Irr. 196 mm
	3	3.00	246	175	.71	17	Rain 8 mm
Apr	1	5.18	270	302	1.12	20	Trim
	2	5.90	301	344	1.14	10	Irr. 128 mm
	3	4.85	306	283	.92	25	Rain 6 mm
May	1	5.40	377	315	.84	02	Trim
	2	6.76	403	394	.98	10	Irr. 154 mm
						14	Bermuda plugs added
3	3.48	372	203	.55			
Jun	1	4.43	417	258	.62	05	Irr. 183 mm
	2	3.36	447	196	.44	26	Trim
	3	6.30	476	367	.77	28	Irr. 178 mm
Jul	1	7.16	472	417	.88	08	Trim
	2	7.08	473	413	.87	17	Trim
						19	Irr. 167 mm
3	7.27	398	424	1.06	22	Rain 4 mm	
Aug	1	4.82	376	281	.75	30	Trim
						02	Irr. 109 mm
	2	6.29	375	367	.98	04-05	Rain 11 mm
12						Trim	
3	4.55	329	265	.80	14,16,17	Rain 23 mm	
					16	Irr. 118 mm	
					19	Trim	
21,26	Rain	22 mm					
	27	Trim					
30,01	Rain	27 mm					
Sep	1	4.60	323	268	.83	11	Trim
	2	4.62	301	269	.89	13	Irr. 137 mm
	3	5.00	294	292	.99	27	Trim
						27	Irr. 117 mm

Table 2. Continued

Month	Decade	Evap.	R_n^*	-ET	$-ET/R_n$	Ryegrass since Nov. 62		
		mm	ly	ly				
Oct	1	4.16	211	242	1.15			
	2	2.29	192	134	.70	11,14	Trim	
	3	1.92	201	112	.56	18,19	Rain	38 mm
						22	Plant Rye	
							Irr.	95 mm
Nov	1	1.70	162	99	.61	01-02	Rain	5 mm
	2	1.61	145	94	.65	07	Rain	3 mm
	3	1.10	124	64	.52	18	Trim	
						20,21	Rain	9 mm
Dec	1	1.37		80				
	2	1.00				17	Irr.	64 mm
	3							

*Net radiation R_n measured over alfalfa field.

Table 3. Maximum hourly lawn evaporation in mm; also, net radiation over alfalfa on same day, the evaporative flux and ratio of latter two, 1963.

Month	Decade	Evap. max.	Day	R_n^*	$-ET_{max.}$	$-ET/R_n$
		mm		ly	ly	
Jan	1	1.5	7	88	87	.99
	2	1.5	15	120	87	.73
	3	2.0	27	123	117	.95
Feb	1	4.5	7	153	262	1.71
	2	4.0	13	220	233	1.06
	3	4.0	28	210	233	1.11
Mar	1	4.5	7	222	262	1.18
	2	4.0	19	192	233	1.21
	3	3.6	23	281	210	.75
Apr	1	6.1	5	312	356	1.14
	2	8.0	11	319	466	1.46
	3	6.5	30	348	379	1.10
May	1	6.5	6	402	379	.94
	2	8.8	12	420	513	1.22
	3	6.5	21	373	379	1.02
Jun	1	8.0	6	411	466	1.13
	2	3.7	16	457	216	.47
	3	11.5	30	510	670	1.31
Jul	1	8.5	1	504	496	.98
	2	8.5	15	480	496	1.03
	3	11.0	21	465	641	1.38
Aug	1	6.8	10	430	396	.92
	2	8.5	15	361	496	1.37
	3	6.5	28	384	379	.99
Sep	1	6.0	9	372	350	.94
	2	6.0	17	324	350	1.08
	3	5.5	25	302	321	1.06
Oct	1	5.0	1	272	292	1.07
	2	3.5	14	186	204	1.10
	3	2.5	29	173	146	.84
Nov	1	2.3	1	204	134	.66
	2	2.0	14	148	123	.83
	3	1.5	26	138	87	.63

*Net radiation (R_n) measured over alfalfa field.

Table 4. Monthly totals of irrigation, rain, evaporation, and drainage of a lawn as measured by a lysimeter, 1963.

Month	Irr.	Rain	Total Add.	Evap.	Drain	Total Loss
	mm	mm		mm	mm	
Jan	228	18	246	40	94	134
Feb	---	21	21	80	70	150
Mar	196	8	204	103	--	103
Apr	128	6	134	159	30	189
May	154	--	154	160	81	241
Jun	361	--	361	141	104	245
Jul	167	4	171	222	36	258
Aug	227	54	281	161	113	274
Sep	255	25	280	142	107	249
Oct	95	38	133	86	57	143
Nov	--	17	17	44	--	44
Dec	160	--	160	30	88	118
Total	<u>1971</u>	<u>+</u> <u>191</u>	<u>=</u> <u>2162</u>	<u>1368</u>	<u>+</u> <u>780</u>	<u>=</u> <u>2148</u>

33-65

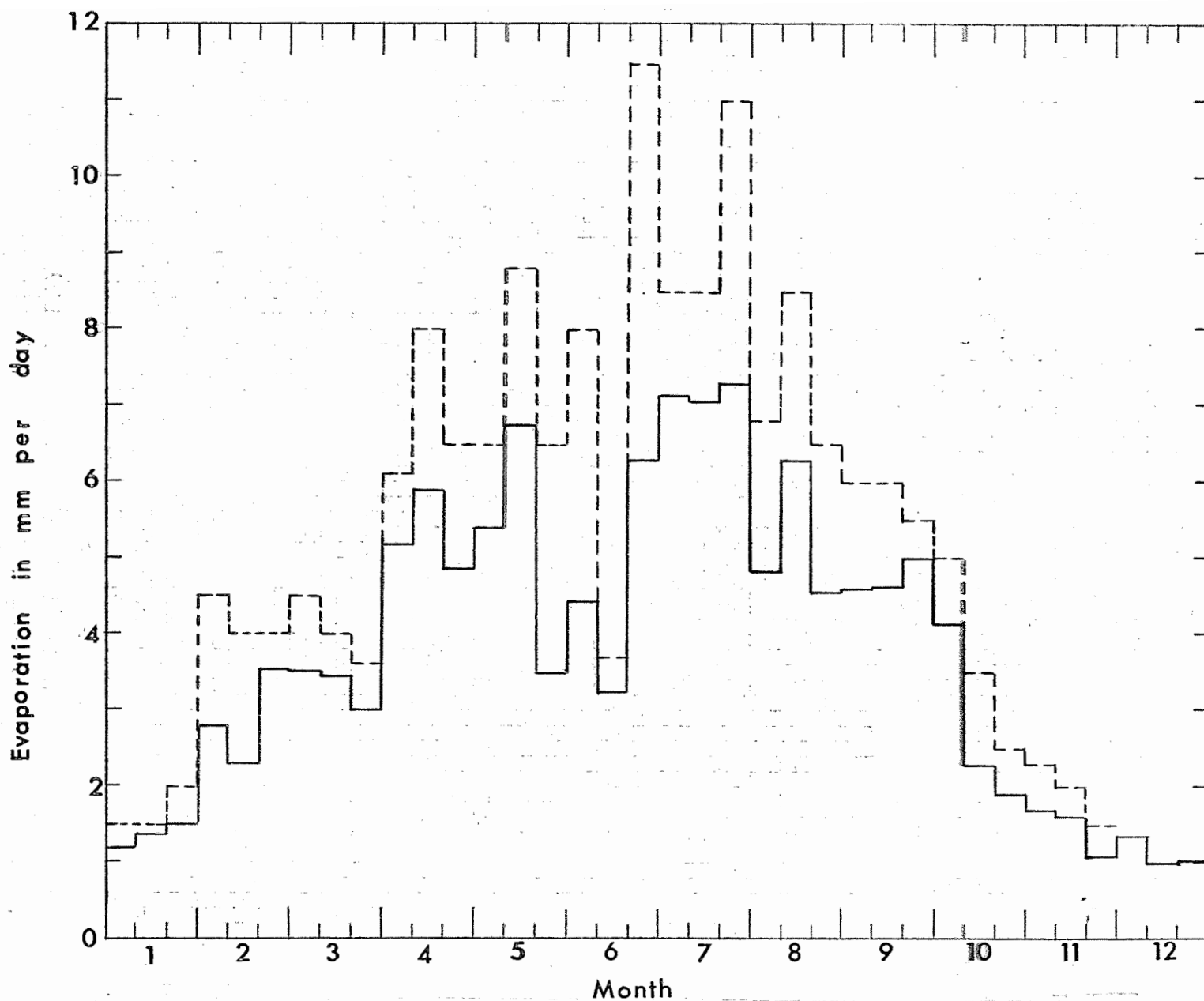


Figure 1. Average and maximum daily evaporation in mm by decades from a bermuda-ryegrass Annual Report of the U.S. Water Conservation Laboratory (solid line is average, interrupted line is maximum).

PART 5. LYSIMETER STUDY OF THE SALT BALANCE OF AN IRRIGATED SOIL
OVER A THREE-YEAR PERIOD.

INTRODUCTION:

The weighable lysimeter installation at the United States Water Conservation Laboratory was constructed for the purpose of getting reliable, direct measurements of evaporative flux. However, in the process of creating different surface conditions and growing crops on the lysimeters and the surrounding field, it was necessary to pay some attention to the salt balance of the soil in the lysimeter. The surface was irrigated and also, in order to maintain moisture conditions throughout the profile in the lysimeter identical to those outside of it, excess water was removed with a drainage installation provided for this purpose at the time of installation.

For details on the lysimeter construction and operation the reader is referred to the annual report for the calendar year 1960. It suffices to state here that both the evaporative losses and the amounts of water applied and removed could be determined with great precision. Also, that from the beginning, a policy was followed to determine the total salt and chloride content of the irrigation and the drainage water. Thus an opportunity arose to study the salt balance of the lysimeters. Interest in this matter was increased by the fact that in attempting to establish an alfalfa cover on at least one lysimeter, symptoms of excess salinity in the crop were noted.

PROCEDURE:

The lysimeters were installed in late 1960 and during the calendar year 1961 they were, for the most part, in bare soil. Early in 1962 an attempt was made to establish an alfalfa cover but, this being a failure, a crop of sudangrass was established during June and it was grown through the month of September. In October, the cover was changed to alfalfa in which it has been continually throughout the year 1963.

The irrigation schedule in 1961 was primarily dictated by the need to wet the surface from time to time for studies of evaporation from bare soil. By and large, the applications of water exceeded the evaporation loss only slightly. A similar policy was followed during 1962, however, during the summer period much greater losses of water took place

in consequence of the sudangrass cover, than occurred during 1961.

Originally, the alfalfa cover was treated rather in the same way as the sudan cover but by the end of the first half of 1963, it became apparent that in one of the lysimeters and in several spots in the field the alfalfa showed the result of excess accumulation of salts. Consequently, much greater applications of irrigation water were made and from the visual symptoms it soon became evident that the leaching treatment was successful. As stated above, the drainage water as well as the irrigation water was analyzed for total salts and chlorides. In addition, the complete chemical composition of the waters was analyzed during 1963. The methods for analysis were those recommended in Handbook 60 of the United States Department of Agriculture.

From the measurements of evaporation, a daily balance of total water content in the lysimeter soil column, 1 m^2 by 1.5 m could be calculated. In addition, periodic measurements of the volumetric moisture content of the soil was made by the neutron method in the center lysimeter (number 2). These data generally agree quite well with the direct determination of the water content of the column. Drainage took place intermittently, usually after heavy applications of the irrigation water. The soil was drained to a tension of approximately 100 mb. In one of the lysimeters, the soil moisture tension was continually monitored by means of a tensiometer at 1.4 m below the surface.

The data on moisture content, moisture distribution, soil heat flow, and soil temperature all indicate that the physical properties of the soil column under study were closely identical to those in the surrounding field where similar measurements were made.

No accounting has been made for the minerals removed as a part of the crop. Twice in 1962 a sudangrass crop was cut and removed and the same was done twice in 1963 with the alfalfa. For the most part, the cover was trimmed and the clippings were allowed to fall and decay. We believe that neglecting the mineral content of the crop is of no significant influence on the data.

RESULTS AND DISCUSSION:

The total amount of water applied to each lysimeter during the three-year period is given in Table 1. The amounts by year reflect the management practices discussed above. During 1961 and 1962 the irrigation water used was the laboratory tap water. A typical analysis of this tap water is given in Table 2. This water runs close to 2,000 ppm total salts. During 1963 the laboratory was connected to Phoenix city water which resulted in a rather different analysis also typified in Table 2. The field surrounding the lysimeters was irrigated with surface water or with well water, depending on its availability. The well water resembles closely the tap water applied during 1961-1962, whereas the surface water delivered by the irrigation project is similar in quality to the tap water used during 1963. In fact, the City of Phoenix drinking water is derived from the same surface water.

It may be seen in both cases that sodium chloride constitutes little better than half of the total salt level of the water. In Table 3, the total amount of salts in kilograms per square meter as based on the actual analysis of each individual application is given. The change in the quality of the irrigation water during 1963 is apparent. Evidently, during the three years a total of about 4.5 kg m^2 was applied, equivalent to some 45 metric tons per hectare (roughly 20 tons to the acre).

Evaporation on each lysimeter during each year is given in Table 4. There is some variation between lysimeters because they were not always identically treated, nor was development of the crop always identical as was desired. Nevertheless, the variation is well within 10 percent.

The total amount of water leached by drainage from the lysimeter, reflects the variability in the evaporation. It is given in Table 5. These data show that during 1961-1962 the drainage from the lysimeters was roughly equal to 10 percent of the amount of water applied. During 1963, this fraction was considerable greater, running approximately 20 percent. The removal of salts by drainage is given in Table 6. Again we can see here that during 1961-1962 the removal of salts was

nominal only, but that in 1963 a considerable amount of salts were leached out to a total average of 2.4 kg m^{-2} . The total for the three-year period is 3.22 kg m^{-2} which, when combined with the data in Table 3 would lead one to believe that there should be a positive salt balance of about 1.1 kg m^{-2} .

An additional illustration, in more detail, of the results as given above is available in Figures 1, 2, and 3 which refer to lysimeters 1, 2 and 3, respectively. The behavior of the three lysimeters is not too different but since they were not always treated the same, it was not considered correct to average the results for the three. Figures 1, 2 and 3 give, by months, the total water balance, the total salt balance, and the chloride balance of the three lysimeters.

Since differences between lysimeters are minor, the following discussion will refer to all three, and individual features may be verified by the data as given for individual lysimeters. During 1961 the water balance was first slightly negative and then positive during the second quarter. This was caused by an experiment in which the area was kept flooded for two days. For the remainder of the year, the water balance was slightly negative and as a result we see a slow accumulation of total salts and of chlorides in the lysimeter. During 1962, initially the same situation continued until the sudangrass started growing and evaporating large quantities of water. Accordingly, during quarters three and four of 1962 the water balance became negative and accumulation of salt proceeded rapidly, reaching about a maximum by the end of 1962, both in terms of total salts and chlorides.

During the first half of 1963, the irrigation schedule was stepped up, but still resulted in a largely negative water balance and a maintenance of the salt balance at the same level. During the second and third quarter, however, large amount of irrigation water were applied on purpose, resulting in a positive water balance during two months and an appreciable depletion of salts. In the third quarter, the alfalfa was allowed to wilt and a very low water balance was obtained. During this period, of course, there was no additional reduction of the total salt content. During the fourth quarter a normal operation was resumed.

A negative water balance of about 300 mm would correspond to a profile that was in its entirety at the 15 atmosphere percentage. Thus, it may be seen that at no time did the profile reach this point completely. Saturation of the profile would result in a positive water balance of somewhere around 175 mm.

The significant information in Figures 1, 2, and 3 is that, whereas at the end of 1963 the chloride balance had essentially returned to its starting point, this was not true of the total salt balance. It should be remembered that both are obtained by comparing the inflow with the outflow of salt and are not based on actual measurement. Thus, if a balance was made of total salts, one would conclude that the salinity of the soil was higher than it was at the beginning and that additional leaching might be required whereas, in fact, the chloride balance would give the opposed conclusion.

The explanation is suggested by the analysis of the drainage water, exemplified in Table 7. These data refer to 1963 and are separated into the first and second half of the year. The difference lies in the total concentration, being higher at first. The relative chemical comparison is not different. However, there is a difference in the relative chemical composition between the drainage and the irrigation water, as shown in Table 2.

Since the analyses in Tables 2 and 7 are exemplary only, an accounting of the total situation is given in tables 8 and 9. In Table 8 we see the ratio of chlorides to total salts in the irrigation water which runs about 35 percent during the first two years and about 44 percent during the last year, reflecting again the different source of irrigation water. Table 9 shows the same ratio in the drainage water which, during 1961-1962, runs slightly higher but is almost doubled in 1963, this being the year during which the greater part of the salts were removed (see Table 6).

Thus, it appears that in the process of concentration, leaching, and uptake of water by plants, the water applied as irrigation water undergoes a chemical change when it becomes a soil solution.

Actually, we must distinguish between the events of 1961-1962 and those of 1963. In the former period, the irrigation was local well

water and, in a sense, was already a natural drainage water. Thus, the chemical nature of the irrigation water reflects the processes taking place in the soil from which it is derived and it is merely reapplied to the surface. Accordingly, as may be seen in Tables 2 and 7, the chemical composition of the drainage water during 1961-1962 is not very much different from that of the irrigation water except that it is more concentrated. However, when surface water was being used as a source of irrigation water in 1963, there is a large difference between irrigation water and drainage water. The irrigation water is basically a sodium, magnesium, bicarbonate, and chloride mixture, whereas in the drainage water bicarbonate is much reduced and chlorides and sulfates increased. Also, we find nitrates from the fertilization and biological activity in the soil. As to the cations, sodium is enriched in the drainage water primarily at the expense of calcium and, to a lesser extent magnesium. Thus, during 1963 the leaching process seems to consist primarily of the removal of excess sodium chloride and sodium sulfate and the conversion of soluble bicarbonates to insoluble calcium carbonate.

The data presented here are probably not sufficiently complete, nor entirely conclusive. Nevertheless, since they were obtained on a controlled situation that closely resembled the processes resulting from irrigation and drainage of a natural soil profile, they suggest two principles of practical importance. The first of these is that it may not always be possible to obtain the salt balance of the soil by the mere consideration of the input and output of salt in the irrigation and drainage waters, respectively. In the case considered here, such a procedure would lead to a considerable overestimate of the rise in salinity and a consequent overestimate and waste of leaching water. A second conclusion is that when soil is irrigated with, what is in essence an equilibrium leachate, that the relative composition of the drainage water is quite similar to that of the irrigation water and that in such a case the salt balance can simply be obtained by addition and subtraction.

If we may assume that the chloride is not affected by any chemical reaction and moves through the soil column in a simple fashion, then we

may conclude that of the total amount of salts applied with irrigation water over a three-year period, about one-third was removed from the soil solution by becoming insoluble and thus did not contribute to the salt balance. However, it is likely that in actuality this statement could be made only to the salts applied during 1963 in which case we would have to say that out of the total amount of 4.42 kg m^2 applied in the irrigation water about 1.3 kg m^2 was precipitated. A similar favorable situation may not be expected if locally pumped irrigation water is used, though our data give no clue directly bearing on this issue.

SUMMARY AND CONCLUSIONS:

Three lysimeters filled with Adelanto loam and situated in a field of the same soil were observed over a three-year period as to the quantity and chemical composition of irrigation and drainage waters. In 1961 the field was bare, in 1962 it had a sudangrass crop, and in 1963, alfalfa. During 1961-1962 the irrigation water was locally pumped and relatively concentrated with an average salt load of 2,000 ppm. During 1963 surface-derived water was used for irrigation with a typical salt load of 700 ppm. Also, during 1963 rather large amounts of irrigation were applied to restore a favorable level of salinity in the soil. During 1961-1962, drainage and irrigation waters were alike in chemical composition though the former were much more concentrated, up to 10,000 ppm. During the same period, the drainage amounted to roughly 10 percent of the amount of water applied and, in consequence, a slow but persistent rise in salinity was observed until the total amount of salts accumulated in the soil profile was about 2.6 kg m^{-2} , the lysimeters having a depth of 1.5 m. During 1963, in consequence of irrigation with the less salty water in more copious quantities, salinity was reduced. At the end of 1963, the chlorides were back to the original level, indicating that salinity had been reduced to the level existing at the beginning of 1961. During this process the drainage waters differed materially in chemical composition from the irrigation water. The irrigation water was

basically a mixture of sodium, magnesium, calcium, bicarbonate, and chloride whereas the drainage water was predominately sodium chloride with marked reductions in bicarbonate and calcium, and an increase in sulfate.

It is believed that, besides the larger quantities of water applied, the decrease in salinity is also caused by the nature of the irrigation water, giving rise to the formation of insoluble calcium carbonate during the leaching process. This assumption is further substantiated by the fact that the total salt balance, as derived from the total salt load of the irrigation drainage waters at the end of 1963 showed a positive value of about 1.3 kg m^{-2} , whereas the chloride balance indicated that leaching had recreated the original situation. Thus, of the total amount of salts applied, 3.2 kg m^{-2} over the three-year period, one-third did not reappear in the drainage water.

It would be erroneous, then, to base an estimate of the salinity of the soil on a computation of input and output of salt only. Such a procedure may only be warranted if the soil is irrigated with what is essentially a drainage water to begin with. This was the case during 1961 and 1962. During 1963 a foreign water was used for irrigation and its chemical interaction with the soil resulted in the fact that a simple salt balance could no longer be obtained. In actuality, the salinity situation was much more favorable than would be indicated by a total salt balance sheet since of the total amount of salts applied during 1963 approximately one-half seemed to have been rendered insoluble.

Table 1. Total amount of water in mm applied to lysimeters, Jan 1961 through Nov 1963. Rainfall is not included.

	#1	#2	#3	Ave.
1961	574	569	557	567
1962	1484	1395	1402	1427
1963	1879	1931	1957	1922
Total	3937	3895	3916	3916

Table 2. Chemical composition of irrigation water. Local well water was used in 1961-1962; city water (surface water) in 1963. Analysis is average of several irrigations.

	1961-1962		1963	
	meq/l	%	meq/l	%
Carbonate	0.2	1	0.1	1
Bicarbonate	5.2	17	3.4	46
Chloride	20.7	66	3.4	46
Nitrate	0.7	2	0.1	1
Sulfate	4.5	14	0.4	6
Anions	31.3		7.4	
Sodium	19.3	62	3.6	46
Calcium	6.5	21	2.2	28
Magnesium	5.4	17	2.1	26
Cations	31.2		7.9	

Table 3. Total amount of salts applied to lysimeters in kg m^{-2} , Jan 1961 through Nov 1963.

	#1	#2	#3	Ave.
1961	1.02	1.01	.99	1.01
1962	2.46	2.31	2.31	2.36
1963	.97	.99	1.06	1.01
Total	4.45	4.31	4.36	4.38

Table 4. Total amount of evaporation in mm from lysimeters, Jan 1961 through Nov 1963.

	#1	#2	#3	Ave.
1961	657	637	360	641
1962	1550	1447	1455	1484
1963	1701	1862	1869	1811
Total	3908	3946	3954	3936

Table 5. Total amount of drained water in mm from lysimeter, Jan 1961 through Nov 1963.

	#1	#2	#3	Ave.
1961	90	107	86	94
1962	112	142	124	126
1963	375	352	292	340
Total	577	601	502	560

Table 6. Total amount of salts in kg m^{-2} removed by drainage from lysimeters Jan 1961 through Nov 1963.

	#1	#2	#3	Ave.
1961	.27	.27	.23	.26
1962	.56	.59	.46	.54
1963	2.42	2.23	2.62	2.42
Total	3.45	2.99	3.31	3.22

Table 7. Chemical composition of drainage water during first and second half of 1963, based on all available data.

	First Half		Second Half	
	meq/l	%	meq/l	%
Carbonate	--	--	--	--
Bicarbonate	13.6	9	12.9	14
Chloride	108.8	75	62.8	66
Nitrate	7.8	5	1.7	2
Sulfate	15.4	11	17.7	18
Anion	145.6		95.1	
Sodium	76.4	52	54.0	58
Calcium	27.5	19	15.3	16
Magnesium	41.9	29	23.8	26
Cation	145.8		93.1	

Table 8. Ratio of ppm chloride to ppm total salts in irrigation water of lysimeters.

	#1	#2	#3	Ave.
1961	.34	.34	.34	.34
1962	.37	.35	.36	.36
1963	.24	.24	.25	.24

Table 9. Ratio of ppm chloride to ppm total salts in drainage water of lysimeters

	#1	#2	#3	Ave.
1961	.34	.35	.33	.34
1962	.47	.43	.39	.43
1963	.44	.43	.45	.44

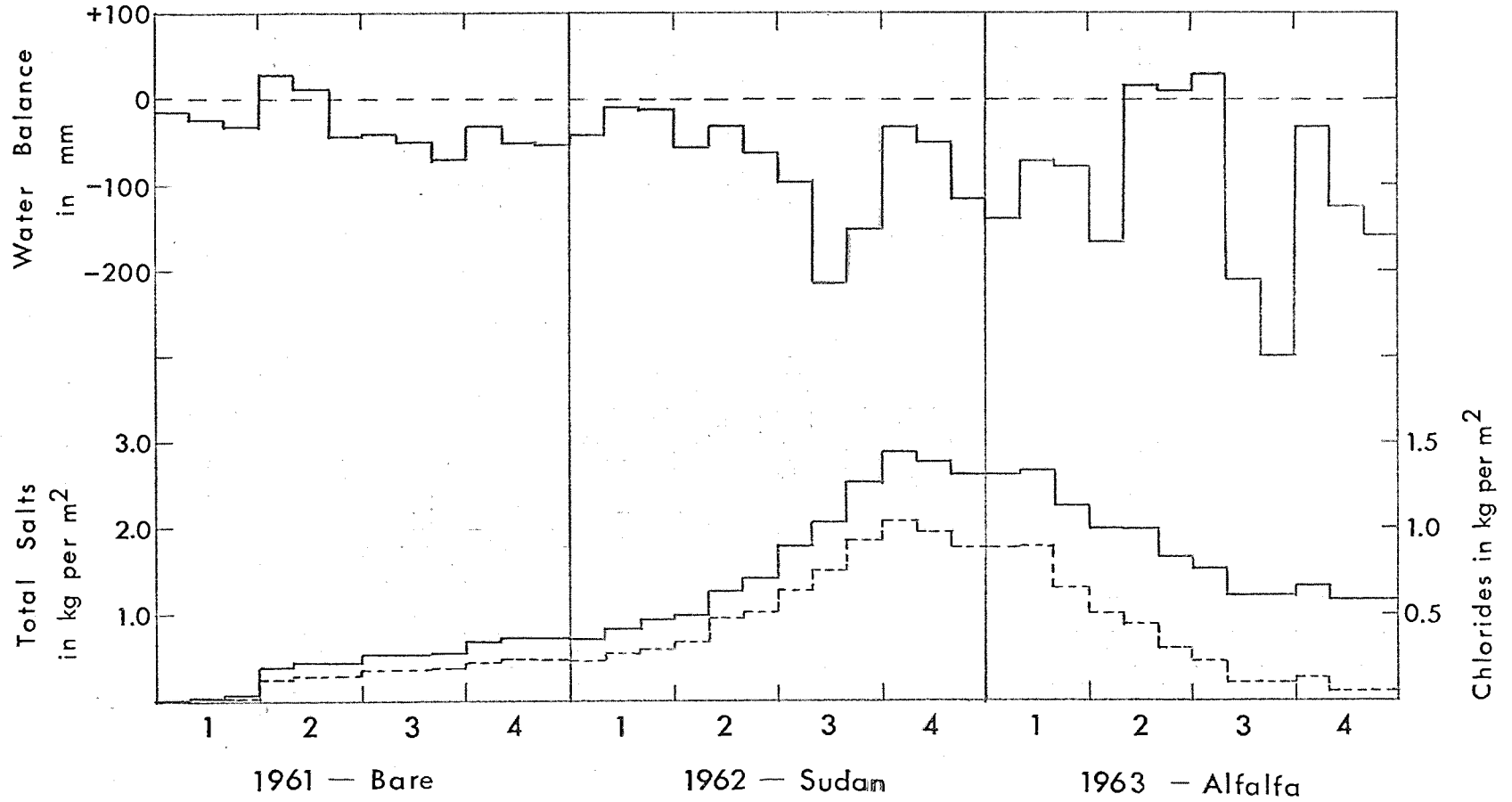


Figure 1. Monthly balance of water, total salts and chlorides for lysimeter 1.

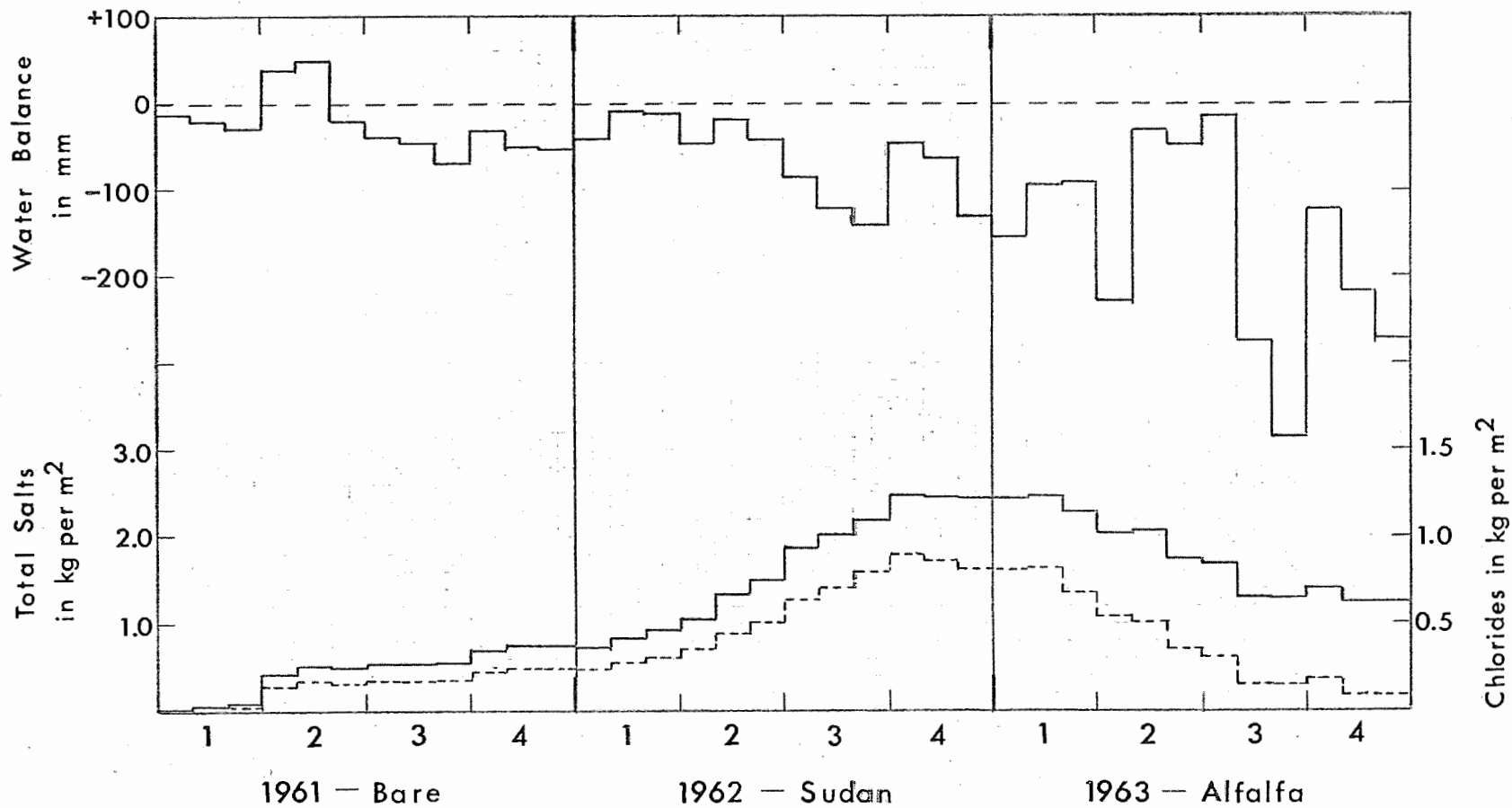


Figure 2. Monthly balance of water, total salts and chlorides for lysimeter 2.

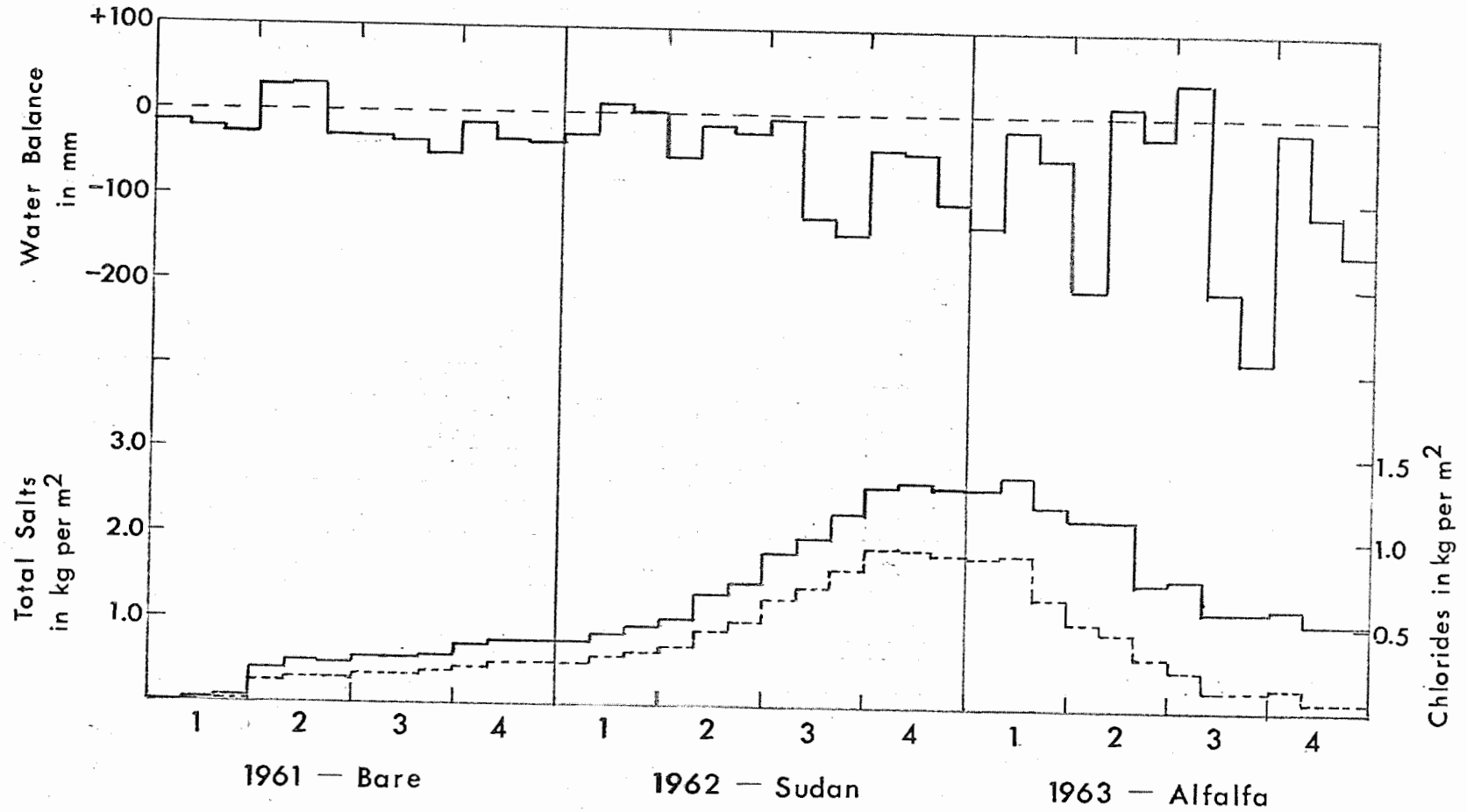


Figure 3. Monthly balance of water, total salts, and chlorides for lysimeter 3. Annual Report of the U.S. Water Conservation Laboratory

PART 6. CONSTRUCTION AND EVALUATION OF A SIMPLE HYDRAULIC LYSIMETER.

INTRODUCTION:

The purpose of this investigation is to determine whether or not it is possible to construct a simple, weighable lysimeter that can be used in the field for the routine determination of consumptive use. The lysimeter should be sufficiently accurate to get a reasonable estimate of daily values and should be more than sufficient to give accurate values over periods of several days. The lysimeter should be reasonable in cost, for example, close to \$100, and require no special materials, tools, or skills in construction and operation.

A hydraulic lysimeter was chosen because even a fairly simple balance-type mechanism would probably be too expensive and, also, the literature mentions at least 3 instances where a simple solution was found by taking an inner tube or similar flexible container, filling it with water and letting it be the support for a container filled with soil. The only instance in which an accurate description was given was in work by Winter in England which referred to garbage can-size containers that were supported by a small inner tube. No exact data on performance, stability, and drift were available, however.

We decided to continue with a 1 m^3 lysimeter as a standard size (see Annual Report for 1962). Such a lysimeter, when filled with moist soil, will have an approximate weight of 1700 kg at a moisture content of 0.4 volume fraction and 1500 kg at a moisture of 0.2 volume fraction, depending on the density of the soil and the nature of the material out of which the soil container is made. It was decided to support this weight, distributed over an area of 1 m^2 , with a water container made out of some form of tubing, after several experiments with diverse size inner tubes had failed. The difficulty with the latter was primarily that the stretching of the rubber caused instability and made the container lean toward one side or the other. In previous work along the same lines reported in the literature, the soil containers were much less deep than 1 m and the pressures and consequent stretching of the rubber did, obviously, not create any problems.

First attempts were made with 5 cm diameter lay-flat green polyethylene tubing of 1 mm wall thickness, layed out in back-and-forth-loops giving a support area of roughly 0.5 m^2 . This material was not satisfactory because, evidently, the polyethylene tubing leaked water sufficiently so as to cause a continuous drift in the readings of a manometer connected to the tubing.

Another material which was not satisfactory was a nylon reinforced butyl tubing 5 cm in diameter. This tubing was made with a seam, which appeared to leak in spite of efforts to obtain a perfect sample from the manufacturer. Even when no visible leaks were present, the tubing would lose water continually under pressure and was considered unsuitable.

Finally, as an acceptable material we found ordinary, 5 cm diameter lay-flat butyl tubing which is a standard item in the construction industry. Its use will be described in further detail below.

CONSTRUCTION DETAILS:

The soil container is 1 m^3 on the inside and is made out of .75-inch marine plywood, reinforced with steel corner braces where necessary (see Figure 1). The outside container is made to provide a clearance of 2.5 cm all around and is also made out of .75-inch marine plywood, reinforced in the corners with steel. In the bottom, a strip of wood extends about 5 cm from the sidewalls so as to make sure that the tubing, when laid down, will fully support the soil container. The height of the outer container is so dimensioned that, when supported, the edges of the inner container and outer container will be level so that the gap can be sealed with a flexible tape that adheres to the horizontal rims of inner and outer container. All wood parts are given a double coating of coaltar epoxy paint.

The 5 cm diameter butyl tubing is placed on the bottom in a spiral with square sides which requires approximately 15 m of tubing (the tubing is sold in 17 m [50 foot] lengths). The ends of the tubing are vulcanized and clamped with a flat clamp made out of two metal pieces bolted together. The outside end of the tubing is provided with a standard inner tube valve stem, which is vulcanized in. To the valve stem is connected a sufficient length of .5 cm inner diameter

tubing (butyl rubber or polyvinylchloride) which ends at the bottom of a standard laboratory burette. For the latter, the cheapest type burette without valve and with 500 divisions is sufficient.

In assembling the lysimeter, the tubing is first evacuated to get rid of most of the air and, then, water is admitted to the tubing under pressure. The tubing should be filled to a relatively low pressure; the exact amount is not easy to predict. Roughly the pressure should be about $.025 \text{ kg cm}^{-2}$ (.35 psi). The tubing is then closed off and is coiled in the bottom of the outer container. When fully loaded, the support area will be about 0.7 m^2 thus resulting in an amplification of the pressure by about 1.3.

Following the installation of the tubing, the empty inner container is put in place and centered as well as possible. It is probably advisable to use some removable spacers at the top rim for this purpose. Soil can then be filled into the container. In our tests, the load was obtained by using concrete blocks. A base load of 1400 kg was used, which was increased in small steps to a maximum of 1700 kg and decreased again.

The manometer is mounted so that the middle of the range (250 divisions) comes at about eyelevel for the average person, 1.5 m. Accordingly, at average load the amount of water in the tubing should be such that a pressure of approximately 2.5 m of water of $.25 \text{ kg cm}^{-2}$ results. Since the divisions on the burette are roughly equal to mm we can see that the manometer will change by about 1.3 mm if one kg is added to the lysimeter or 1.3 mm for each mm of surface water depth. Accordingly, we should have a lysimeter with a readability of somewhere between 0.5 and 1.0 mm of water since the burette can easily be read to the nearest division. After a number of preliminary tests the final assembly was examined by a static test at constant load over several days to detect any drift in the system and by some 20 cycles of loading and unloading the lysimeter, the process requiring roughly a day per cycle. This procedure provides also a test for drift, repeatability, and linearity of the system. All tests were carried out in the hydraulics laboratory where temperature is controlled to the nearest 2 C or 3 C.

RESULTS AND DISCUSSION:

The butyl tubing proved to be entirely satisfactory. Static tests showed that after an initial period of equilibration, possibly related to temperature adjustment and adjustments of the corner foldings of the butyl tubing, there was no more than 1 division drift in the manometer reading over a period of many days. Also, the assembly as used is very stable, that is the inner container has no tendency to lean one way or the other and has a very firm feel, almost as if it were seated on a solid footing.

The results of the loading tests were also satisfactory. Usually, on the first loading and unloading cycle a marked amount of hysteresis was found, that is, the loading and unloading curves did not agree but were several manometer divisions different. However, all following loading and unloading cycles were very close, within the readability of the manometer. Also, the end points, that is, minimum and maximum load, were reproduced day in, day out, in many cycles. An example of a typical loading and unloading experiment is shown in Figure 2. Each successive point is obtained by adding or removing a concrete block, the weight of which is approximately 8.5 kg each. The blocks were individually marked and weighed to obtain maximum precision in the calibration procedure. Figure 2 not only indicates that increasing or decreasing the weight has the same effect but also that the relationship between manometer reading and load is linear. No deviations from linearity are greater than the readability of the manometer.

The next step in the evaluation will be to test the performance of the system under actual field conditions. It is recognized that any type of hydraulic weighing device is subject to temperature effects, related to the expansion of the liquid and the changes in its density. With water, these changes are minimal and it is not believed, with the principal part of the system deep in the ground, that these will give serious difficulty. Certainly they should not affect weekly readings of a simple hydraulic lysimeter as described and probably not even daily readings. Winter in his evaluation also writes that no special precautions were necessary in England to shield the manometer against extremes in temperature. This may not prove to be

true in our climate. In an actual installation outdoors it will be necessary to have a drainage system in the lysimeter. This will be done following a scheme similar to that in the single load cell lysimeter which is described in the Annual Report for 1962. However, it is thought that for a low-cost installation a single filter candle will probably be sufficient since it proved possible to drain a 1 m^3 lysimeter rather rapidly with two filter candles.

Figure 1 indicates diagrammatically the nature of the field installation with the rim of the lysimeter just barely protruding from the ground and the manometer at eye level. Since the inner and outer containers are connected by a moisture proof seal there is no reason why this type of installation could not be flooded over. Even if water would get in the space between the inner and outer container, no damage could result and it would be merely necessary to pump this water out.

SUMMARY AND CONCLUSIONS:

A description is given for the design of a 1 m^3 hydraulic lysimeter with a direct readout using a water manometer. The purpose of the investigation is to arrive at a low cost (\$100) instrument that can be used for the routine measurement of consumptive use in the field for periods of several days down to one day.

Successful tests were completed in the laboratory with a design in which the containers are made out of standard plywood and the support for the soil container out of 5 cm collapsible butyl tubing that is filled with water to a pressure of approximately $.25 \text{ kg cm}^{-2}$ (3.5 psi). The tests showed drift, non-linearity, and hysteresis to be all less or equal to the readability of the manometer which is about 1 mm. Accordingly, the accuracy of the device is judged to be between 0.5 and 1 mm surface depth of water. A field installation is now under test.

PERSONNEL: (applied to entire research outline).

C. H. M. van Bavel, L. J. Fritschen

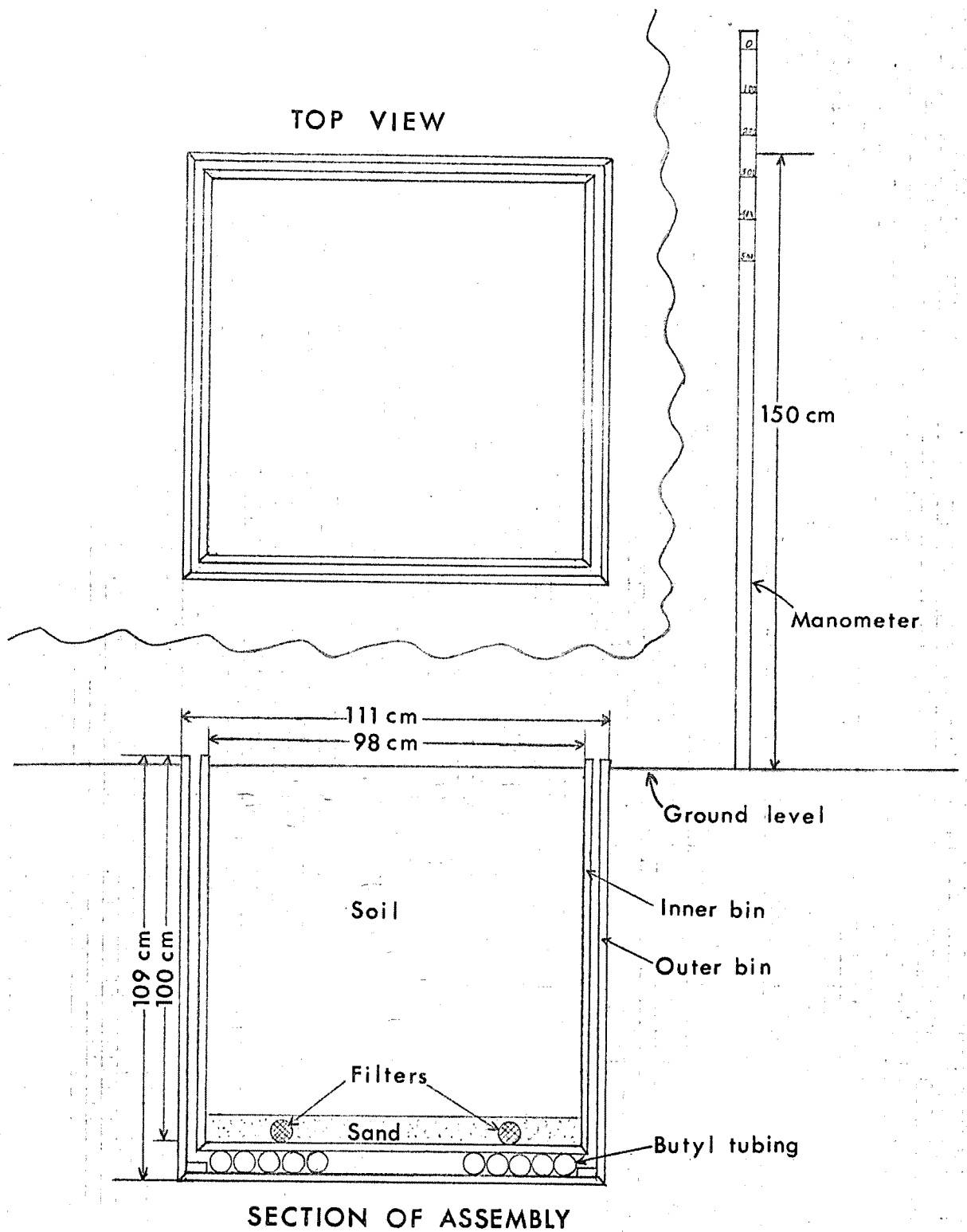


Figure 1. Top view and vertical section of simple hydraulic lysimeter.

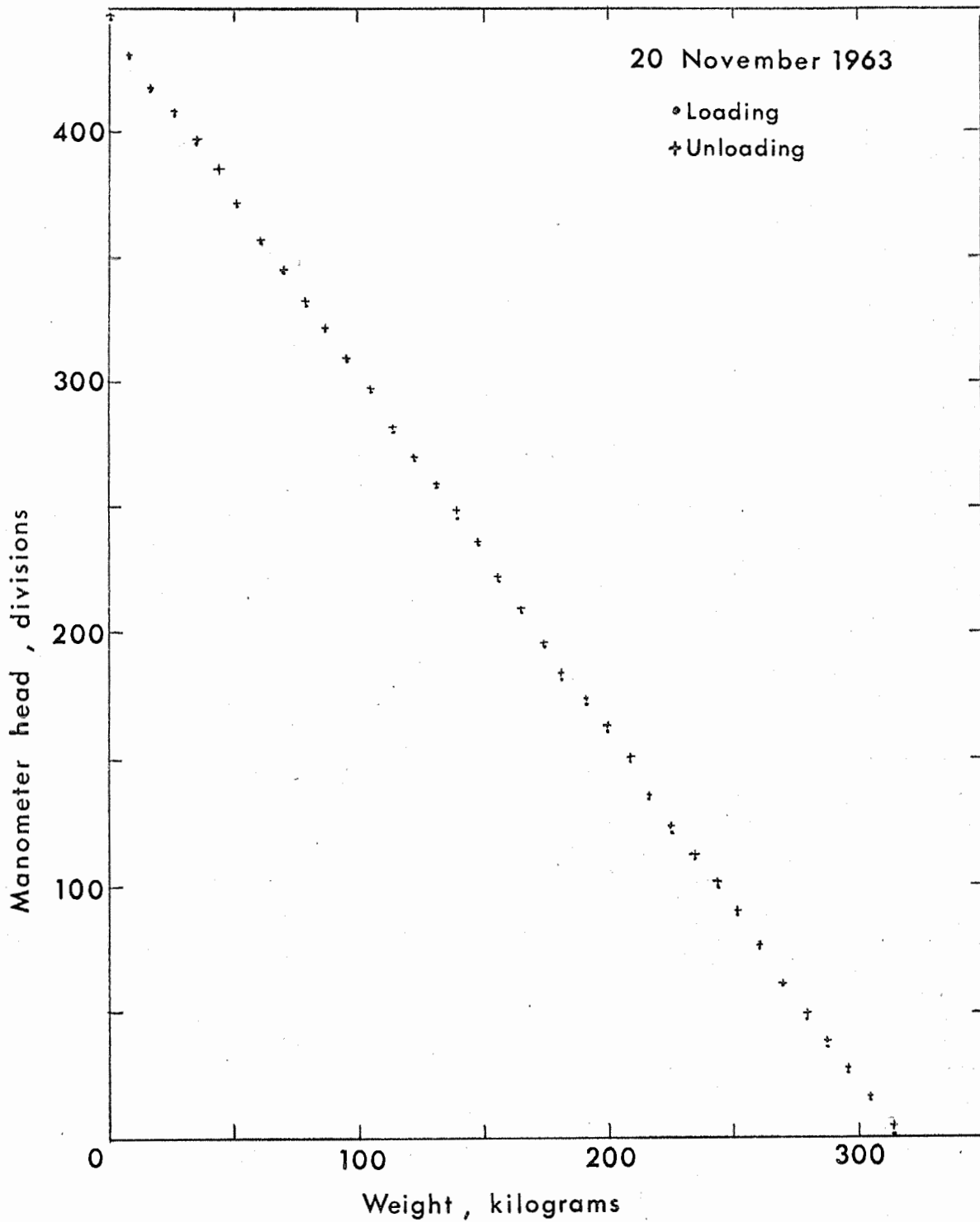


Figure 2. Linearity and drift test results of simple hydraulic lysimeter.

TITLE: EXCHANGE OF WATER VAPOR WITH PLANT LEAVES AND ITS RELATION TO
STOMATAL DIFFUSIVE RESISTANCE

LINE PROJECT: SWC 11-gG1

CODE NO.: Ariz.-WCL-34

INTRODUCTION:

The objectives and some of the introductory material have been presented in the exploratory report of 1962 entitled "Water Loss from Plants as Related to Stomatal Diffusive Resistance."

Transpirational water losses have been assumed to follow the relationship

$$E_{H_2O} = \frac{DA (C_i - C_o)}{L} \quad [1]$$

where

E_{H_2O} = water vapor loss, $g\ cm^{-2}\ min^{-1}$

D = diffusion coefficient of water vapor in air, $cm^2\ min^{-1}$

A = stomatal pore area, cm^2

L = diffusion path length, cm

C_i = water vapor concentration in the substomatal cavity,
usually assumed to be at 100 percent relative humidity,
 $g\ cm^{-3}$

C_o = water vapor concentration outside and adjacent to the
leaf surface, $g\ cm^{-3}$

The use of tritiated water vapor (THO) as a tracer for ordinary water vapor was considered as a means of evaluating the transpirational behavior of a leaf. When a leaf is exposed to a THO vapor atmosphere, the leaf will gain THO, and it is presumed that any physical and physiological factor involved in this gain is similar to those involved in the loss of water vapor. An important built-in advantage to the use of THO is that the process of interchange of THO for leaf water results in a negligible temperature change. The process of the loss of water vapor, on the other hand, results in leaf temperature changes which consequently alters the values of D , C_i , and C_o .

Two approaches can be considered in the evaluation of equation [1]. An apparent diffusion coefficient of tritiated water vapor in the leaf (D_{THO}) can be evaluated such that $D_{\text{THO}} = D_o k$, where D_o is the diffusion coefficient of THO vapor in air and k is a complexity factor which includes the porosity of the leaf, the tortuosity of the diffusion path, and any interaction of the tracer molecules with the leaf water. Equation [1] can be used to define the gain in THO when the leaf is exposed to the tracer vapor as

$$E_{\text{THO}} = D_{\text{THO}} \frac{A'}{L'} (C_o - C_i)_{\text{THO}} \quad [2]$$

For this case A' is the actual leaf area, and L' is the half-thickness of the leaf.

An alternative method when dealing with water vapor loss is to define a resistance term such that $R, \text{cm}^{-1} \text{min} = L/DA$ and, thus, we avoid the necessity for knowing both L and A in evaluating equation [1]. By using this relation, equation [1] can be written as

$$E_{\text{THO or H}_2\text{O}} = \frac{(C_i - C_o)_{\text{THO or H}_2\text{O}}}{R_{\text{THO or H}_2\text{O}}} \quad [3]$$

and as stated earlier, it is assumed that the measured R_{THO} will be the same as $R_{\text{H}_2\text{O}}$.

The total resistance to water vapor loss in the transpiration process is made up of a series of different types of resistance, which by analogy to Ohm's law is additive. For the situation under consideration, these include the resistance of the layer immediately adjacent to the external leaf surface (R_A), the resistance in the stomatal pore (R_S), and the resistance in the mesophyll tissue (R_M), which in our case will be considered to be negligibly small in comparison to R_A and R_S . Thus equation [3] can be written in the more inclusive form

$$E_{\text{THO or H}_2\text{O}} = \frac{(C_i - C_o)_{\text{THO or H}_2\text{O}}}{(R_A + R_S)_{\text{THO or H}_2\text{O}}} \quad [4]$$

PART I. EXPOSURE OF BLOTTER PAPER AND PLANTS TO THO VAPOR AND THE MEASUREMENT OF EXCHANGE

PROCEDURE:

At least four different types of chambers were designed and built so that the plants could be properly exposed to THO vapor. Difficulties encountered were problems such as leakage, improper air circulation, and heating of the chamber air, all causing poor results. The final model was made from 1/4-inch plexiglass (20" wide × 10" deep × 20" high) with a 60 cfm squirrel cage type blower. The motor was mounted outside the chamber and a drive shaft arrangement provided to operate the fan placed inside the chamber. The motor was equipped with hose connections so that cooling air could be forced over the motor coils. The doors were made demountable and arranged in such a way that they were clamped to the chamber against rubber gaskets.

In the exposure procedure, the blotter was placed in the chamber for 15 minutes together with 100 cc of tritiated water contained in an ointment jar. The chamber was sealed tight and the blower air stream directed over the tritiated water. After the materials were exposed to the THO vapor, they were analyzed for THO using the techniques described in the Annual Report for 1960.

Corn plants were exposed to the tritiated water vapor in a similar manner. In one set of treatments, three-week old corn plants at soil moisture contents of 17.5 to 19.2 percent were treated with 0.02 percent tergitol, tergitol + 0.001 M phenylmercuric acetate (antitranspirant). Six plants and six moist blotters were placed in the treatment chamber and exposed to tritiated vapor for 15 minutes. Two sets of experiments were conducted in the greenhouse on two separate days. Light intensity was 800 ft-c and temperature at 26 C.

Concurrent with the study on the effect of antitranspirant on THO exchange, the effect of the soil moisture content on THO exchange

was also investigated. In this case, the soil media of the three-week old corn plants were brought to predetermined moisture levels the day prior to the THO exposure either by withholding irrigation or adding varying quantities of water. Plant exposure to THO was for 15 minutes under similar conditions described in the preceding section. The same experiment was conducted, but this time the plants were exposed to the THO vapor in the dark.

RESULTS AND DISCUSSION:

The THO activities of moist blotter papers exposed to THO vapor in the specially constructed treatment chamber are presented in Table 1. The activities within a replicate and between treatments are comparable. The results for the THO exposure of moist blotter paper and corn leaf in which the plant was treated with tergitol and phenylmercuric acetate are presented in Tables 2 and 3. The activities of THO in the blotters were similar in the different treatments indicating that valid comparison could be made among the different exposures. Statistical analysis shows no significant effect of the antitranspirant or the tergitol upon the amount of THO exchange under the experimental conditions described.

The data for the THO exchange for the corn plants exposed to THO vapor at the different water contents are presented in Figure 1. The open circle represents treatment data in light, and the solid dot signifies treatment in the dark. The THO activity is presented in terms of the μc per unit area of leaf surface which includes both the upper and lower surfaces. It is evident that the soil water content has no effect on the degree of exchange between the leaf water and external THO vapor under dark conditions. That exchange is present in the dark suggests that the stomates are not completely closed. There is also the possibility of some exchange occurring through cracks in the cuticle and the cuticle itself, but the magnitude of this exchange cannot be assessed.

In the presence of light, however, THO exchange between the atmosphere and the leaf water decreases with the soil water content. Apparently the closing of the stomates at the lower water contents is

responsible for this behavior. In terms of soil water potential (by using the soil moisture characteristic of the substrate) the changes occur below the one-bar moisture potential. Even by use of carefully controlled environment and selection of plants there is great variability in the results for the light-exposed plants. The leaves at the 5 percent soil water content and lower were badly wilted (permanent wilt at 3.6 percent water content), and yet there was measurable exchange occurring. It is apparent that the stomates were still partially open even at wilt.

PART II. EVALUATION OF D_{THO} AND R_{THO} .

PROCEDURE:

The amount of THO moving into the leaf was measured at different time intervals from 0.25 to 30 minutes under conditions where the vapor THO was in direct contact with the leaf surface. In the case of the liquid THO treatment, the three-week old corn leaf was immersed into the THO solution in a 250-ml graduate cylinder for a predetermined time period. Surface moisture was wiped off the leaf and the leaf water analyzed for THO. The tritiated water did not seem to wet the leaf surface. Also, little, if any, liquid THO was observed to cling to the leaf. These could be easily removed by shaking the leaf sharply or by absorbing it with a soft absorbent paper. The experiment was conducted at 26 C, both in the dark and light at several different soil moisture levels. Light intensity was 50 ft-c.

For the THO vapor treatment, the corn leaf was inserted into a 1 1/2" x 15" lucite cylinder. The tritiated vapor was recirculated through the bubbler and the cylinder by a diaphragm pump at a rate of 200 cc per minute.

RESULTS AND DISCUSSION:

Typical data for THO activity in corn leaf exposed to liquid and vapor THO at different time periods are presented in Tables 4 and 5, respectively. The duplicate samples compare favorably with each other. As expected, the exchange of THO was greater in the leaves exposed directly with the liquid THO than the vapor. Such data were tested statistically to see whether the nonsteady-state or the

steady-state condition as represented by equation [1] was fulfilled in the experiment. In the transient case a linear relation should exist between C/C_0 and $t^{1/2}$, and also the curve should pass through zero. In the steady-state case, the linear relationship is for the total gain in THO activity and t . The calculated data are presented in Table 5. Data of columns 4, 5, and 6 showed a linear relation between C/C_0 and $t^{1/2}$, however, the null hypothesis test (column 6) indicated that the linear curve will not intercept the origin. The data of columns 7, 8, and 9 showed that the experimental data fitted the steady-state case. Thus, by a knowledge of the rate of gain of THO (E) and the THO vapor concentration, the stomatal resistance R_{THO} can be estimated using equation [3] or [4]. Sufficient data were not available to make the calculation R_{THO} at this time.

SUMMARY AND CONCLUSION:

Three-week old corn plants were exposed to tritiated water vapor in a controlled environment. Under dark condition the exchange was lower than in the light and was also independent of the water content of the soil material. The presence of exchange even in the dark suggests that the stomates are not completely closed. In the presence of light, the amount of THO exchange decreased with decreasing soil water content and exchange occurred even when the plants were badly wilted. The quantity of exchange was directly proportional to the exposure period.

PERSONNEL: F. S. Nakayama

Table 1. THO activity of moist blotter paper exposed to THO water at 26 C for 15 minutes.

Replicate	Sample	Blotter Total activity, $\mu\text{c cm}^{-2} \times 10^4$
A	1	29.8
	2	28.6
	3	26.6
	4	26.5
	5	29.2
	6	26.8
	7	28.5
	8	27.4
		<hr/> 27.9 \pm 1.2
B	1	28.1
	2	28.5
	3	28.2
	4	29.2
	5	29.6
	6	28.9
	7	28.5
	8	28.4
		<hr/> 28.7 \pm 0.5

$$C_o = 0.96 \mu\text{c ml}^{-1}$$

Table 2. THO activity in moist blotter paper and corn leaf in which the plant was treated with tergitol and phenylmercuric acetate.

Treatment		Plant, Total activity $\mu\text{c cm}^{-2} \times 10^4$	Blotter, Total activity $\mu\text{c cm}^{-2} \times 10^4$
Control ($\text{H}_2\text{O} = 19.1\%$)	1	7.72	294.6
	2	8.59	308.2
	3	6.50	267.7
	4	5.88	265.8
	5	6.01	230.9
	6	6.45	294.8
		6.86 ± 1.14	277.0 ± 25.6
Tergitol + Phenylmercuric acetate ($\text{H}_2\text{O} = 19.2\%$)	1	6.00	263.2
	2	7.34	250.1
	3	4.21	245.0
	4	4.28	240.8
	5	5.66	289.3
	6	5.76	265.1
		5.54 ± 1.37	258.9 ± 17.8
Tergitol ($\text{H}_2\text{O} = 18.0\%$)	1	7.41	318.9
	2	8.53	266.4
	3	8.13	292.2
	4	8.73	261.8
	5	5.98	249.4
	6	5.86	271.6
		7.44 ± 1.34	276.7 ± 25.0

$$C_{\text{THO}} = 7.15$$

Table 3. THO activity in moist blotter paper and corn leaf in which the plant was treated with tergitol and phenylmercuric acetate.

Treatment		Plant, Total activity $\mu\text{c cm}^{-2} \times 10^{+4}$	Blotter, Total activity $\mu\text{c cm}^{-2} \times 10^4$
Control (H ₂ O = 18.1%)	1	6.33	361.1
	2	5.95	276.7
	3	7.77	299.4
	4	8.22	307.4
	5	6.28	245.9
	6	7.58	266.5
			7.02 ± 0.95
Tergitol + Ø HgAc (H ₂ O = 17.5%)	1	6.13	329.7
	2	6.36	308.8
	3	7.72	313.8
	4	6.91	314.8
	5	8.24	283.8
	6	6.36	287.4
			6.97 ± 0.85
Tergitol (H ₂ O = 19.0%)	1	5.23	277.1
	2	4.72	331.0
	3	7.67	313.2
	4	7.67	258.8
	5	8.01	291.9
	6	6.87	259.9
			6.70 ± 0.39

$$C_o = 7.15 \mu\text{c ml}^{-1}$$

Table 4. THO activity in corn leaf exposed to liquid THO solution at different time periods.

	Time	C/C _o	THO activity μc cm ⁻² × 10 ⁴
4.6% H ₂ O	1	0.0134	0.94
		.0093	.78
	5	.0291	2.04
		.0352	1.95
	10	.0409	2.58
		.0368	2.57
	15	.0666	4.57
		.0686	4.25
	30	.1337	10.51
		.1394	10.29
10.7% H ₂ O	1	.0120	1.05
		.0111	.88
	5	.0416	2.71
		.0448	2.80
	10	.0557	4.06
		.0673	4.21
	15	.0750	5.57
		.0732	5.52
	30	.1671	13.66
		.1594	10.99

$$C_o = 0.879 \mu\text{c ml}^{-1}$$

Table 5. THO activity in corn leaf exposed to vapor THO at different time periods.

	Time, min	$C/C_o \times 10^3$	THO activity $\mu\text{c cm}^{-2} \times 10^4$
4.8% H ₂ O	0.25	0.0795	0.04
		.131	.07
	.50	.253	.10
		.170	.07
	1	.366	.17
		.346	.22
	2	1.48	.60
		1.62	.77
	4	1.91	.91
		2.15	1.03
	8	3.60	1.98
		3.54	1.78
	16	4.28	1.79
		4.18	1.53
11.8% H ₂ O	.25	.211	.14
		.138	.06
	.50	.964	.57
		.806	.39
	1	1.22	.63
		1.03	.51
	2	3.08	1.50
		2.03	.92
	4	4.71	1.82
		4.51	1.77
	8	9.99	4.75
		9.55	5.22
	16	18.8	10.28
		18.4	11.93

$$C_o = 9.34 \mu\text{c ml}^{-1}$$

Table 5. Summary data for leaf treated with liquid and vapor THO at different exposure periods.

Trial	Experimental condition	Soil water content	Transient case			Steady-state case		
			Slope $\frac{C/C_0}{\sqrt{t}}$	r	"Student" t H: $\alpha = 0$	Slope $\mu\text{c cm}^{-2} \text{min}^{-1} \times 10^4$	r	"Student" t H: $\alpha = 0$
A	THO liquid, light	4.6	.0275	.95	-2.71*	.331	.99	1.01
		10.7	.0325	.96	-2.83*	.384	.99	1.68
B	THO liquid, light	5.6	.0254	.94	-3.30**	1.28	.98	- .22
		9.3	.0222	.96	-5.20**	1.04	.99	-6.61**
C	THO liquid, light	6.2	.0275	.96	-4.12**	2.08	.99	- .37
		15.2	.0273	.98	-6.12**	1.77	.99	2.14
D	THO liquid, dark	5.2	.00991	.99	-7.63**	.594	.98	1.34
		18.2	.01190	.96	-4.33**	.760	.98	2.53*
E	THO vapor, light	4.8	.00129	.98	-3.50**	.111	.85	2.47*
		11.5	.00516	.98	-3.38**	.696	.99	-1.93
		17.7	.00666	.96	-4.33**	.814	.99	-1.93

34-12

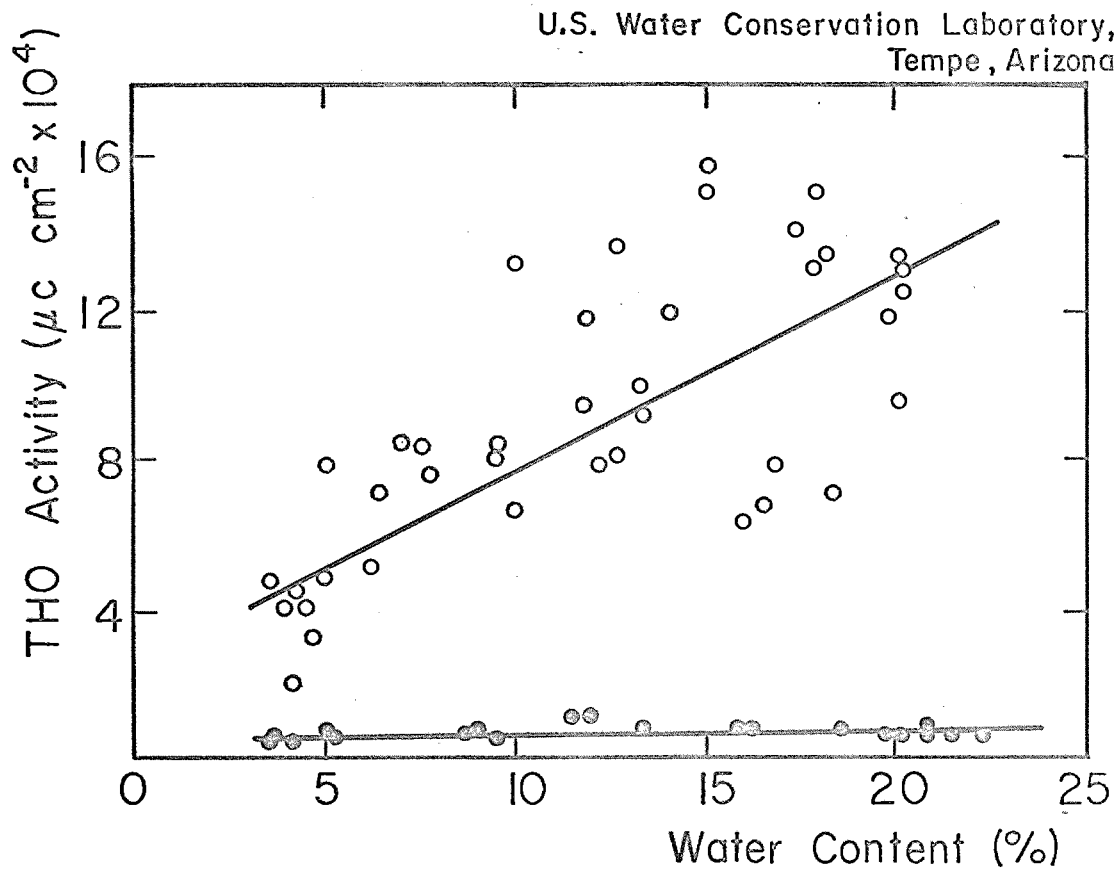


Figure 1. Exchange of tritiated water vapor with corn leaf in the dark and light under varying soil water contents. Annual Report of the U.S. Water Conservation Laboratory

TITLE: STOMATAL BEHAVIOR OF COTTON PLANTS UNDER CONTROLLED ENVIRONMENTAL
CONDITIONS

LINE PROJECT: SWC 11-gG1

CODE NO.: Ariz.-WCL-34A

INTRODUCTION:

A more comprehensive picture of plant water exchange (WCL-34, Exchange of Water Vapor with Plant Leaves and Its Relation to Stomatal Diffusive Resistance) and water balance (WCL-29, Water Absorption, Transpiration, and Internal Water Balance of Cotton Plants as Affected by Changes in Evaporative Demands) processes can be arrived at by an independent and reliable method for determining stomatal behavior. Thus, the method can substantiate or help to explain by experimental measurement rather than indirect inference some of the results observed previously in plant-soil-water relationships. A new technique has been described by Zelitch (1) for measuring stomatal apertures of tobacco plants. The purpose of the study was to investigate the applicability of the method for studying the behavior of cotton stomates under controlled environmental conditions.

PROCEDURE:

Leaf impressions. A rapid setting silicone rubber compound was prepared by thoroughly mixing 5 ml of a rubber base (RTV-11, General Electric Co.) and 3 drops of catalyst (Silicure T-773 or Nuocure 28, Heyden Newport Chemical Corp.). The paste material was spread over the upper surface of the leaf within 40 seconds after the catalyst was added and allowed to harden on the plant for 3 minutes. After stripping the hardened impression from the leaf and drying in air, a cellulose acetate-acetone mixture was painted over the rubber and allowed to dry. The acetate strip was placed on the microscope slide and studied under magnification of 600 and 1500 X.

Stomatal aperture index. The work of evaluating the size of the stomatal aperture was simplified by setting up a stomatal aperture scaling index as shown in Figure 1. The value of 10 was designated for the fully open and that of 0 for the fully closed stomate. The indexing was arbitrary and general geometric form was the primary criterion considered in the selection of the scale. A leaf impression

was observed with the microscope and each stomate assigned an index number and the average stomatal index value for the particular impression was calculated.

Plant. Stomatal impressions were made at varying intervals on two sets (A and B) of 10-week old cotton plants (Pima S-2, long staple), Set A being exploratory in nature. Plants grown in 1/2- Hoagland solution in the greenhouse were preconditioned for 24 hours in the Controlled Growth Chamber under 12 hours of light and dark. The experiments were conducted in the environmental chamber at 30 C under variable humidity and light conditions.

The environmental conditions during the progress of the experiments were as follows:

Set A	12 mb	→	30 mb	→	30 mb	→	12 mb		
	<u>dark</u>		light		<u>dark</u>		<u>dark</u>		
Set B	12 mb	→	30 mb	→	30 mb	→	30 mb	→	12 mb
	<u>dark</u>		<u>dark</u>		light		<u>dark</u>		<u>dark</u>

RESULTS AND DISCUSSION:

The results of the stomatal aperture measurements for the two sets of experiments are presented in Figure 2. The amount of chemical for making the impressions in Set A was limited so that fewer impressions were made in this series. In Set A a large increase in stomatal index value occurred when the light was turned on. The vapor deficit was changed from 12 to 30 mb at the same time but the final 30 mb deficit was reached approximately 15 minutes after the initial light change. The responses in opening the stomates to light for these plants were rapid. Simultaneous beta ray gauging technique (WCL-26) on another plant showed a rapid change in leaf thickness when light was imposed on the previously dark adapted leaf. Similarly, transpiration rate increased rapidly (WCL-29) in the change in environment from light to dark. The stomatal index measurements are thus further confirmation regarding the behavior of the stomates. The stomatal index decreased upon the onset of darkness.

The dimensions of the fully opened elliptically shaped stomate from the cellulose acetate impressions are $12 \mu \times 5 \mu$ in the major and minor axis, respectively.

In Set B, the stomatal index increased significantly in the change from 12 to 30 mb vapor deficit even under the dark condition. The beta ray gauge also showed a net loss of leaf water. There is thus an opening of the stomates during the imposition of the drying environment upon the leaf. A good explanation for this behavior is lacking at present although the stomatal behavior is apparently related to the turgor properties of the guard and accessory cells. The stomates opened further when the lights were turned on and quickly closed when the light source was removed similar to that in condition A.

SUMMARY AND CONCLUSIONS:

The silicone rubber impression technique was found to be useful for evaluating the stomatal aperture of cotton plants. A stomatal aperture index system was designed which was based on the geometric shape of the stomate for the rapid evaluation of stomatal aperture of test samples. Preliminary studies on plants grown under controlled environmental conditions indicated the applicability of the method for explaining some of the water-loss behavior of plants during changes in light and water vapor deficits. Increases in water-loss rate were associated with an increase in the stomatal aperture index, and, similarly, the decreases to decreases in the index.

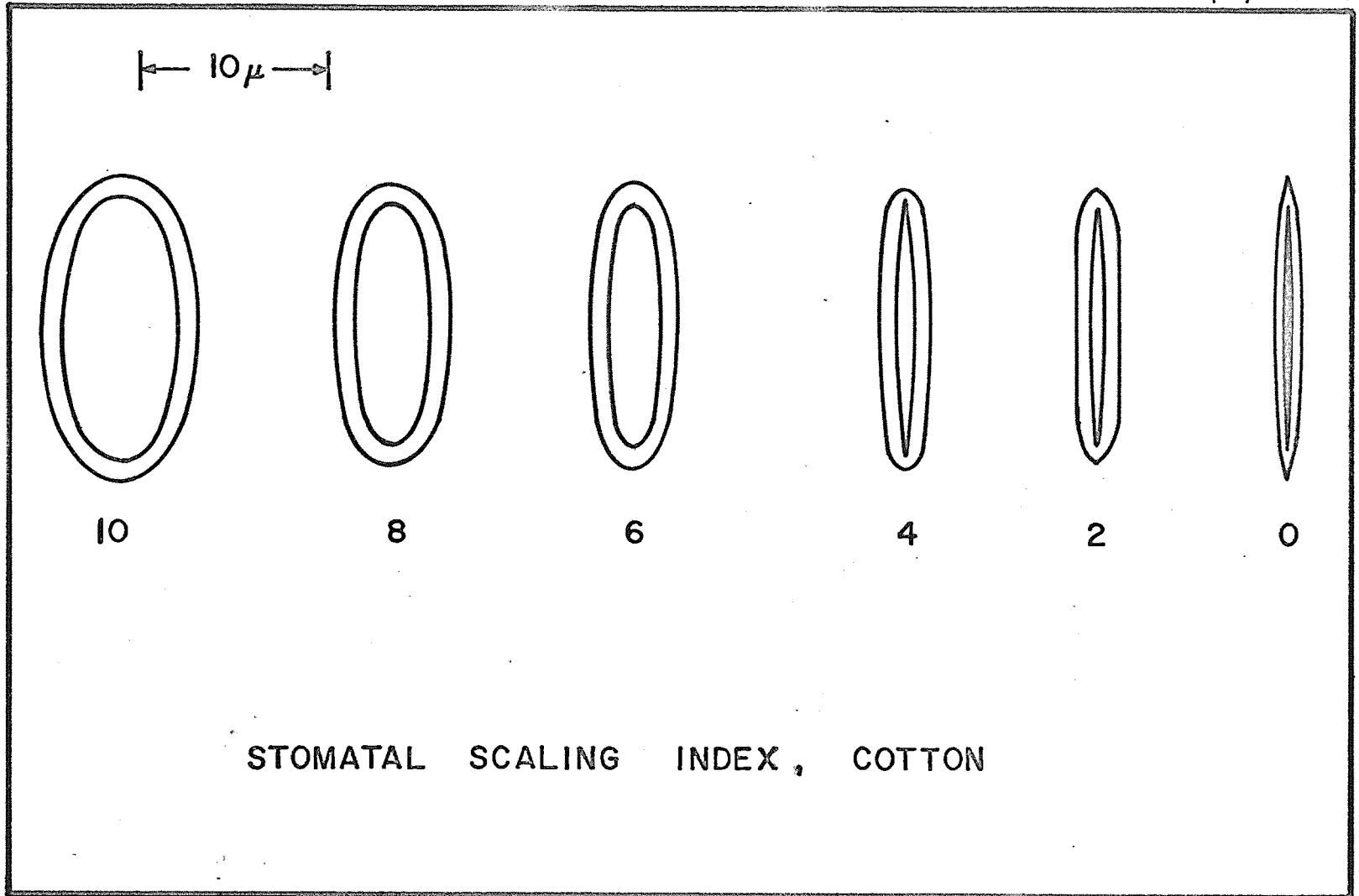
REFERENCES:

(1) Zelitch, I.

1961. Biochemical control of stomatal opening in leaves, Proc. Natl. Acad. Sci. 47:1423-1433.

PERSONNEL: F. S. Nakayama, W. L. Ehrler

34A-4



Annual Report of the U.S. Water Conservation Laboratory
Figure 1. Stomatal scaling index for cotton stomates.

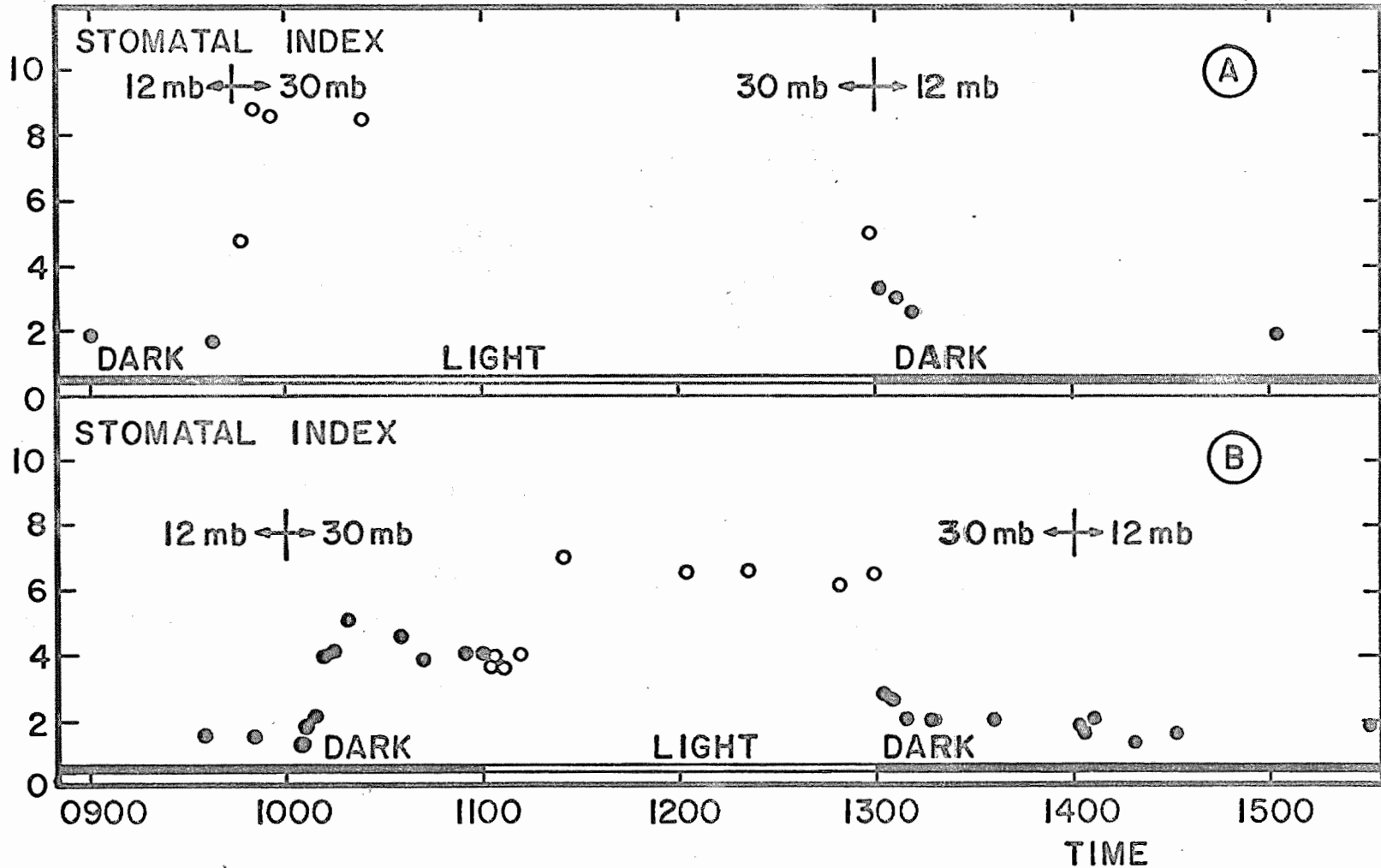


Figure 2. Stomatal aperture index values for cotton plant under variable light and vapor pressure deficit conditions. Annual Report of the U.S. Water Conservation Laboratory

34A-5

APPENDIX I

ANALYTICAL LABORATORY

PROGRESS:

The work performed by the Analytical Laboratory during 1963 included 950 chemical and physical analyses of 123 soil and 93 water samples. A breakdown of the analyses is given in Table 1.

Table 1. Analyses performed by Analytical Laboratory 1963.

Analysis	Number of determinations
Particle size	
a. Hydrometer	80
b. Sieve	11
Moisture characteristics	
a. Pressure cooker	28
b. Pressure membrane	7
pH and total salts	234
Calcium and magnesium	116
Sodium and potassium	117
Carbonate and bicarbonate	68
Chlorides and sulfates	198
Cation exchange capacity	19
Nitrates	66
Surface area	5

The operation of the Analytical Laboratory was suspended in November 1963.

PERSONNEL: J. Bennett Miller, F. S. Nakayama, R. D. Jackson

APPENDIX II
MANUSCRIPTS APPROVED AND PUBLISHED, 1963

	<u>MS Number</u>
Bouwer, Herman, Theoretical effect of unequal water levels on the infiltration rate determined with buffered cylinder infiltrometers. J. Hydrol., Netherlands, 1:29-34. 1963.	26
Bouwer, Herman, The flow system below a water spreading basin. Proc., 5th Cong. of Internatl. Com. Irrig. & Drain., Tokyo, 1963. Quest. 18, (Pp. 18.89-18.106)	73
Bouwer, Herman, and Rice, R.C., Seepage meters in seepage and recharge studies. J. Irrig. and Drain. Div., Proc. Amer. Soc. Civ. Engin. 89(IR 1):17-42, 1963.	82
Bouwer, Herman, In-place measurement of soil hydraulic conductivity in the absence of a water table. Proc. Internatl. Soc. Soil Mechanics and Found. Engin., 2nd Asian Region. Conf., Japan, 1963. Vol. I, pp. 130-133.	85
Bouwer, Herman, and Van Schilfgaard, J., Simplified method of predicting fall of water table in drained land. Trans. Amer. Soc. Agr. Engin., 6:288-291, 296, 1963.	87
Bouwer, Herman, Applications of seepage meters. Proc. Seepage Symp., U.S. Water Conserv. Lab., Tempe, Ariz. 1963. USDA ARS 41-90 (In press).	93
Bouwer, Herman, Theory of seepage flow systems. Proc. Seepage Symp., U.S. Water Conserv. Lab., Tempe, Ariz. 1963. USDA ARS 41-90 (In press).	94
Bouwer, Herman, Measuring horizontal and vertical hydraulic conductivity of soil with the double-tube method. Soil Sci. Soc. of Amer. Proc. (In press).	96
Bouwer, Herman, and Rice, Robert C., Simplified procedure for calculation of hydraulic conductivity with the double-tube method. Soil Sci. Soc. Amer. Proc. (Note). (In press).	97
Bouwer, Herman, Closure: Analyzing ground-water mounds by resistance network. J. Irrig. & Drain. Div., Proc. Amer. Soc. Civ. Engin., 89(IR 2):89-93. 1963.	98

	<u>MS Number</u>
Bouwer, Herman, Limitations of Dupuit-Forchheimer assumption in recharge and drainage. Proc., Symp. on Transient Ground-water Hydraul., Colorado State U. 1963.	110
Bouwer, Herman, and Rice, R.C., Seepage meters in seepage and recharge studies. Trans., Amer. Soc. Civ. Engin. (In press).	118
Bouwer, Herman, Resistance network analogs for solving ground-water problems. Ground Water. (J. of Natl. Water Well Assoc.) (In press)	120
Bouwer, Herman, Discussion of "Seepage from trapezoidal channels", by El Nimr. J. of Engin. Mech. Div., Proc. Amer. Soc. Civ. Engin. (In press)	121
Ehrler, William L., Water absorption of alfalfa as affected by low root temperature and other factors of a controlled environment. Agron. J., 55:363-366. 1963.	80
Ehrler, W.L., Van Bavel, C.H.M., and Nakayama, F.S., Water balance of cotton plants as affected by sudden illumination in a controlled environment. Proc. West. Sect. Amer. Soc. Plant Physiol., Pacific Div. of Amer. Assoc. Advn. Sci., Stanford, Calif., 1963.	101
Erie, Leonard J., Irrigation management for optimum cotton production. Proc. Beltwide Cotton Prod.-Mech. Conf., Dallas, Texas, Jan. 1963. Published in the Cotton Gin & Oil Mill Press, Jan. 19, 1963. Pp.30-32.	89
Erie, Leonard J., and French, Orrin F., Irrigation water management on safflower. Presented, Oilseed & Industrial Crops Res. Br., Safflower Planning Conf., Tucson, Arizona, 1963. 6 pp., illus. (Multilithed)	104
Fritschen, Leo J., Construction and evaluation of a miniature net radiometer. J. Appl. Met., 2:165-172. 1963.	50
Fritschen, Leo J., and Van Bavel, C.H.M., Evaporation from shallow water and related micrometeorological parameters. J. Appl. Met., 2:407-411. 1963.	63
Fritschen, Leo J., and Van Bavel, C.H.M., Micrometeorological data handling system. J. Appl. Met., 2:151-155. 1963.	67
Fritschen, Leo J., Condensation on shielded net radiometers. J. Appl. Met. 2:308-310. 1963. (Note)	75

MS Number

Fritschen, Leo J., and Van Bavel, C.H.M., Experimental evaluation of models of latent and sensible heat transport over irrigated surfaces. Pub. No. 62, Internatl. Assoc. Sci. Hydrol. Sect., Com. for Evaporation, Internatl. Union Geod. and Geophys. Gen. Assembly, 1963. Pp. 159-171.	90
Fritschen, Leo J., and Van Bavel, C.H.M., The energy balance as affected by height and maturity of Sudangrass. Agron. J. (In press).	102
Harris, Karl, and Erie, Leonard J., Minimum tillage pays in the Southwest. (Submitted for pub.)	107
Jackson, Ray D., and Taylor, Sterling A., Heat transfer. Chap. 26 of monog., "Methods of Soil Analysis", sponsored by Amer. Soc. of Agron. and Amer. Soc. for Testing & Mater. (In press).	33
Jackson, Ray D., Porosity and soil-water diffusivity relations. Soil Sci. Soc. Amer. Proc. 27:123-126, 1963.	64
Jackson, Ray D., Temperature and soil-water diffusivity relations. Soil Sci. Soc. Amer. Proc. 27:363-366, 1963.	77
Jackson, Ray D., Van Bavel, C.H.M., and Reginato, R.J., Examination of the pressure plate outflow method for measuring capillary conductivity. Soil Sci. 96:249- 256. 1963.	86
Jackson, Ray D., Nielsen, D.R., and Nakayama, F.S., On diffusion laws applied to porous material. USDA ARS 41-86, 11 pp. 1963.	91
Jackson, Ray D., Water vapor diffusion in relatively dry soil: I. Theoretical considerations and sorption experiments. Soil Sci. Soc. Amer. Proc. (In press)	105
Jackson, Ray D., Water vapor diffusion in relatively dry soil: II. Desorption experiments. Soil Sci. Soc. Amer. Proc. (Submitted for pub.)	116
Jackson, Ray D., Water vapor diffusion in relatively dry soil: III. Steady-state experiments. Soil Sci. Soc. Amer. Proc. (Submitted for pub.)	119

	<u>MS Number</u>
Kramer, P.J., Biddulph, O., and Nakayama, F.S., Water absorption, conduction and transpiration. Chap. 17, Irrigation Monograph, sponsored by Amer. Soc. Agron. (Submitted to Editor)	92
Myers, Lloyd E., Potential low-cost treatments to reduce seepage losses. Soil Conservation (Sub- mitted for pub.)	52
Myers, Lloyd E., and Van Bavel, C.H.M., Measurement and evaluation of water table elevations. Proc., 5th Cong. of Internatl. Com. Irrig. & Drain., Tokyo, 1963.	74
Myers, Lloyd E., Water conservation -- a research challenge. J. of Soil and Water Conserv., 18:31-34, 1963.	78
Myers, Lloyd E., Harvesting precipitation. Trans., Internatl. Union Geod. & Geophys. Gen. Assembly, Berkeley, Calif., 1963.	84
Myers, Lloyd E., The conservation and beneficial use of water. Proc., 7th Ann. New Mexico Water Conf., 1962.	88
Myers, Lloyd E., Water harvesting by catchments. Proc., 7th Ann. Watershed Symp., Phoenix, Arizona, 1963.	111
Myers, Lloyd E., Discussion: Water harvesting, by H.J. Geddes. Proc., Natl. Symp. on Water Resources, Use and Management, Canberra, Australia, 1963.	122
Myers, Lloyd E., Discussion: The gain, transfer and loss of soil-water, by J.R. Philip. Proc., Natl. Symp. on Water Resources, Use and Management, Canberra, Australia. 1963.	123
Myers, Lloyd E., Discussion: Australian policy for hydrologic education, by C.H. Munro. Proc., Natl. Symp. on Water Resources, Use and Management, Canberra, Australia, 1963.	124
Nakayama, F.S., and Jackson, R.D., Diffusion of tritiated water in soils. Soil Sci. Soc. Amer. Proc., 27:255-258. 1963.	72

- Nakayama, F.S., and Van Bavel, C.H.M.,
Root activity distribution patterns of sorghum
and soil moisture conditions. Agron J., 55:271-274,
1963. 79
- Nakayama, F.S., and Jackson, R.D., Diffusion of
tritiated water ($\text{H}^3\text{H}^{16}\text{O}$) in agar gel and water.
J. Phys. Chem., 67:932. 1963. 81
- Nakayama, F.S., and Ehrler, W.L., Beta ray gauging
technique for measuring leaf water content changes
and moisture status of plants. Plant Physiol.
(In press). 100
- Nakayama, F.S., Exchange of tritiated water (THO)
vapor with plant leaves. Science (Approved for
pub.) 113
- Penman, H.L., Angus, D.E., and Van Bavel, C.H.M.,
Microclimatic factors. Chap. 27, Irrigation
Monograph, sponsored by Amer. Soc. Agron. (Sub. to Ed.) 115
- Reginato, R.J., and Van Bavel, C.H.M., Soil-water
measurement with gamma attenuation. Soil Sci.
Soc. Amer. Proc. (Submitted for pub.) 112
- Stanberry, C.O., Schreiber, H.A., Lowrey, M., and
Jenson, C.L., Sweet corn production as affected
by moisture and nitrogen variables. Agron. J.,
55:159-161. 1963. 48
- Taylor, Sterling A., and Jackson, Ray D.,
Heat capacity and specific heat. Chap. 25 of
monog., "Methods of Soil Analysis", sponsored
by Amer. Soc. of Agron. and Amer. Soc. for
Testing and Mater. (In press). 31
- Taylor, Sterling A., and Jackson, Ray D., Temperature.
Chap. 24 of monog., "Methods of Soil Analysis",
sponsored by Amer. Soc. of Agron. and Amer. Soc.
for Testing and Mater. (In press). 32
- Van Bavel, C.H.M., Composition of the soil atmosphere.
Chap. 22 of monog., "Methods of Soil Analysis",
sponsored by Amer. Soc. of Agron. and Amer. Soc. for
Testing and Mater. (In press) 40
- Van Bavel, C.H.M., Fritschen, L.J., and Reginato, R.J.,
Surface energy balance in arid lands agriculture.
USDA ARS Prod. Res. Rpt. 76, 1963. 46 pp., illus. 59

MS Number

- Van Bavel, C.H.M., and Reginato, R.J., Precision lysimetry for direct measurement of evaporative flux. Proc. Symp. on Methodology of Plant Eco-Physiology, Montpellier, France, 1962. (In press). 65
- Van Bavel, C.H.M., and Fritschen, L.J., Energy balance of bare surfaces in an arid climate. Proc. Symp. on Methodology of Plant Eco-Physiology, Montpellier, France, 1962. (In press). 66
- Van Bavel, C.H.M., Nixon, P.R., and Hauser, V.L., Soil moisture measurement with the neutron method. USDA ARS 41-70. 1963. 39 pp., illus. 71
- Van Bavel, C.H.M., and Fritschen, L.J., Transpiration by sudangrass as an externally controlled process. Science, 141(3577):269-270. (Note) 1963. 95
- Van Bavel, C.H.M., A further note on the efficiency of soil moisture neutron probes. Soil Sci. Soc. Amer. Proc. 27:604. (Note). 1963. 99
- Van Bavel, C.H.M., Triennial report of the Committee on Physics of Soil Moisture of the Amer. Geophys. Union. Trans., Amer. Geophys. Union, 44:571-579. 1963. 103
- Van Bavel, C.H.M., Neutron scattering measurement of soil moisture: Development and current status. Proc. Internatl. Symp. on Humidity and Moisture, Washington, D.C., 1963. 106
- Van Bavel, C.H.M., Water and weather. Special series on Water in Agriculture, by Soil Sci. Soc. Amer. (In press). 114
- Van Bavel, C.H.M., Letter to the editor of Scientific American. Sci. Amer. (In press). 117